

Dissertation zur Erlangung des Doktorgrades
der Fakultät für Chemie und Pharmazie
der Ludwig-Maximilians-Universität München



**Reactivity Parameters for Nitrogen Nucleophiles:
From the α -Effect to Applications as
Organocatalysts and Photo-leaving Groups**

Tobias Alexander Nigst

aus

Freising

2012

Erklärung

Diese Dissertation wurde im Sinne von §7 der Promotionsordnung vom 28. November 2011 von Herrn Prof. Dr. Herbert Mayr betreut.

Eidesstattliche Versicherung

Diese Dissertation wurde eigenständig und ohne unerlaubte Hilfe erarbeitet.

München, 03.09.2012

.....
Tobias Alexander Nigst

| | |
|-----------------------------|-------------------------|
| Dissertation eingereicht am | 14.09.2012 |
| 1. Gutachter | Prof. Dr. Herbert Mayr |
| 2. Gutachter | Prof. Dr. Hendrik Zipse |
| Mündliche Prüfung am | 11.10.2012 |

FÜR MEINE ELTERN

Danksagung

In erster Linie möchte ich mich herzlich bei Prof. Dr. Herbert Mayr dafür bedanken, dass er mir die Möglichkeit zur Durchführung meiner Arbeit auf so interessanten wie auch diversen Themengebieten gegeben hat. Seine beispielhafte Betreuung durch geduldige Hilfs- und Diskussionsbereitschaft sowie die exzellenten Arbeitsbedingungen haben maßgeblich zum Gelingen dieser Arbeit beigetragen.

Besonderer Dank gilt Dr. Andrew Smith für die Möglichkeit drei Monate in seinen Laboren in St. Andrews forschen zu dürfen und dabei ein völlig anderes Arbeitsgebiet kennenzulernen.

Seinen Mitarbeitern, besonders Dr. Caroline Joannesse und Dr. Eoin Gould danke ich für die überaus freundliche Aufnahme in die Gruppe, ihre Kollegialität und Hilfsbereitschaft. Mit freudigen Erinnerungen blicke ich auf die schöne Zeit zurück, in der ich so viel erleben durfte.

Dem Fonds der Chemischen Industrie gebührt mein Dank für die zweijährige Finanzierung meiner Doktorarbeit. Weiterhin ermöglichte mir dieses Stipendium meinen Auslandsaufenthalt in Schottland und die Teilnahme an internationalen Konferenzen.

Ich danke allen Mitgliedern des Prüfungsausschusses für ihre Teilnahmebereitschaft, besonders auch Prof. Dr. Hendrik Zipse für die Übernahme des Zweitgutachtens, sowie für seine hilfreichen Anregungen auf dem Gebiet der Pyridinkatalyse.

Bei Dr. Armin Ofial möchte ich für die kritische Durchsicht meiner Publikationen und die hilfreichen Verbesserungsvorschläge bedanken.

Besonderer Dank gilt auch allen aktuellen und ehemaligen Mitgliedern des Arbeitskreises, vor allem den Kollegen aus meinem Labor, Johannes Ammer, Dominik Allgäuer, Dr. Wei Han, Dr. Jan Keller, Dr. Jörg Lippstreu, Dr. Dorothea Richter, Dr. Nicolas Streidl, Konstantin Troshin, Alexander Wagner und besonders meinem Mentor im Forschungspraktikum Dr. Martin Westermaier. Dank

der angenehmen Arbeitsatmosphäre und der zahlreichen gemeinsamen Aktivitäten innerhalb sowie außerhalb der Universität wird mir die gemeinsame Zeit in schöner Erinnerung bleiben. Mögen die entstanden Freundschaften noch lange fortbestehen.

Erik Breuer, Nathalie Hampel, Brigitte Janker und Hildegard Lüpfer danke ich für die übernommenen organisatorischen Angelegenheiten sowie für bedachte Ratschläge und Hilfestellungen bei so manchen nicht trivialen Synthesen.

Meinem Forschungspraktikant, Andreas Maier, danke ich für die überaus erfolgreiche Zusammenarbeit die seinem großen Engagement bei den durchgeführten Experimenten zu verdanken ist. Mögen sich viele deiner Schüler dich zum Vorbild nehmen.

Für die sorgfältige und zügige Durchsicht dieser Arbeit danke ich Johannes Ammer, Dr. Jörg Bartl, Dominik Allgäuer, Dr. Saloua Chelli, Francisco Corral, Hans Laub, Konstantin Troshin, Alexander Wagner und Elija Wiedemann.

Weiterhin möchte ich mich bei meinen Kooperationspartnern Johannes Ammer, Anna Antipova, Dr. Caroline Joannesse, Lydia Klier und ihrem Doktorvater Prof. Dr. Paul Knochel sowie Raman Tandon und seinem Doktorvater Prof. Dr. Hendrik Zipse erkenntlich zeigen für die Hilfsbereitschaft bei der Planung der Experimente und der Interpretation der Ergebnisse, ohne die ein großer Teil dieser Arbeit nicht zustande gekommen wäre.

Zuletzt möchte ich mich bei all meinen Freunden sowie bei meiner Familie bedanken, in erster Linie Michael und Iris, die mit mir nicht nur die schönen Augenblicke genießen konnten, sondern mich auch in so manchen schwierigen Zeiten ertragen mussten.

Der größte Dank gebührt sicherlich meinen Eltern. Ihre steten Ermutigungen, der grenzenlose Rückhalt, sowie ihre immerwährende Unterstützung haben mir das Studium und die Promotion erst ermöglicht.

Publikationsverzeichnis

- [1] **Spectroscopic and structural characterization of cationic *N*-(2-aminoethyl)-aziridine-*N,N'* chelate complexes of the d⁶-metals Rh(III) and Ir(III)**
R. Bobka, J. N. Roedel, B. Neumann, T. Nigst, I.-P. Lorenz, *Polyhedron* **2008**, *27*, 955–961
- [2] **Nucleophilic Reactivities of Pyrroles**
T. A. Nigst, M. Westermaier, A. R. Ofial, H. Mayr in *Eur. J. Org. Chem.* **2008**, 2369–2374 (Titelbild)
- [3] **Nucleophilic Reactivities of Primary and Secondary Amines in Acetonitrile**
T. Kanzian, T. A. Nigst, A. Maier, S. Pichl, H. Mayr, *Eur. J. Org. Chem.* **2009**, 6379–6385
- [4] **Nucleophilicities and Lewis Basicities of Isothiourea Derivatives**
B. Maji, C. Joannesse, T. A. Nigst, A. D. Smith, H. Mayr, *J. Org. Chem.* **2011**, *76*, 5104–5112
- [5] **Ambident Reactivities of Methylhydrazines** [Ambidente Reaktivität von Methylhydrazinen]
T. A. Nigst, J. Ammer, H. Mayr, *Angew. Chem.* **2012**, *124*, 1381–1385; *Angew. Chem. Int. Ed.* **2012**, *51*, 1353–1356 (VIP)
- [6] **Isothiourea-Mediated Asymmetric *O*- to *C*-Carboxyl Transfer of Oxazolyl Carbonates: Structure-Selectivity Profiles and Mechanistic Studies**
C. Joannesse, C. P. Johnston, L. C. Morrill, P. A. Woods, M. Kieffer, T. A. Nigst, H. Mayr, T. Lebl, D. Philp, R. A. Bragg, A. D. Smith, *Chem. Eur. J.* **2012**, *18*, 2398–2408
- [7] **Lewis Acid-Triggered Selective Zincation of Chromones, Quinolones, and Thiochromones: Application to the Preparation of Natural Flavones and Isoflavones**
L. Klier, T. Bresser, T. A. Nigst, K. Karaghiosoff, P. Knochel, *J. Am. Chem. Soc.* **2012**, *134*, 13584–13587

[8] **Photogeneration of Benzhydryl Cations by Near-UV Laser Flash Photolysis of Pyridinium Salts**

T. A. Nigst, J. Ammer, H. Mayr, *J. Phys. Chem. A* **2012**, *116*, 8494–8499

[9] **Nucleophilic Reactivities of Hydrazines and Amines: The Futile Search for the α -Effect in Hydrazine Reactivities**

T. A. Nigst, A. Antipova, H. Mayr, *J. Org. Chem.* **2012**, *77*, 8142–8155

Konferenzbeiträge

März 2008 SFB 749-Symposium, Wildbad Kreuth, Vortrag: “Ambident Reactivities of *N*-Acylpyridinium Ions”

Sept. 2008 2nd EUCHEMS CHEMISTRY CONGRESS, Turin, Italien, Posterpräsentation: “Observation of the Individual Steps in Pyridine-Catalyzed Acylation Reactions”

März 2009 SFB 749-Symposium, Wildbad Kreuth, Vortrag: “Electrophilic Reactivities of Acyl Compounds”

Apr. 2009 SymPOC 2009, Glasgow, Schottland, Posterpräsentation: “Observation of the Individual Steps in Pyridine-Catalyzed Acylation Reactions”

Table of Contents

| | | |
|----------|---|------------|
| 1 | SUMMARY | 1 |
| 2 | INTRODUCTION AND OBJECTIVES | 17 |
| 3 | NUCLEOPHILIC REACTIVITIES OF PRIMARY AND SECONDARY AMINES IN ACETONITRILE | 27 |
| | 3.1 INTRODUCTION | 27 |
| | 3.2 RESULTS AND DISCUSSION | 28 |
| | 3.2.1 Product Characterization | 28 |
| | 3.2.2 Kinetics of the Reactions of the Amines 2–15 with the Reference Electrophiles 1 | 30 |
| | 3.3 CONCLUSION | 41 |
| | 3.4 EXPERIMENTAL SECTION | 42 |
| | 3.4.1 General Comment | 42 |
| | 3.4.2 Kinetic Experiments | 43 |
| | 3.4.3 Product Characterization | 60 |
| | 3.5 REFERENCES | 65 |
| 4 | NUCLEOPHILIC REACTIVITIES OF HYDRAZINES AND AMINES: THE FUTILE SEARCH FOR THE α-EFFECT IN HYDRAZINE REACTIVITIES | 68 |
| | 4.1 INTRODUCTION | 68 |
| | 4.2 RESULTS AND DISCUSSION | 72 |
| | 4.2.1 Product Characterization | 72 |
| | 4.2.2 Kinetics of the Reactions of 1–15 with the Reference Electrophiles 16 | 77 |
| | 4.2.3 Ambident Reactivities of Asymmetrical Hydrazines | 86 |
| | 4.2.4 Structure Reactivity Relationship | 92 |
| | 4.2.5 Correlation of Kinetic with Thermodynamic Data | 97 |
| | 4.2.6 Computational Results | 106 |
| | 4.3 CONCLUSION | 108 |
| | 4.4 EXPERIMENTAL SECTION | 109 |
| | 4.4.1 General Comment | 109 |
| | 4.4.2 Kinetic Experiments | 113 |
| | 4.4.3 Determination of Equilibrium Constants | 157 |
| | 4.4.4 Product Characterization | 162 |
| | 4.4.4 Computational Details | 177 |
| | 4.5 REFERENCES | 184 |
| 5 | LIMITATIONS OF THE BENZHYDRILIUM-BASED NUCLEOPHILICITY SCALES FOR PREDICTING RATES OF ACYLATION REACTIONS | 192 |
| | 5.1 INTRODUCTION | 192 |
| | 5.2 RESULTS AND DISCUSSION | 196 |
| | 5.2.1 Reaction Products | 196 |

| | |
|--|------------|
| 5.2.2 Kinetic Investigations | 197 |
| 5.2.3 Correlation Analysis | 202 |
| 5.3 CONCLUSION | 210 |
| 5.4 EXPERIMENTAL SECTION | 211 |
| 5.4.1 General Comment | 211 |
| 5.4.2 Kinetic Experiments | 213 |
| 5.4.3 Product Characterization | 238 |
| 5.5 REFERENCES | 239 |
| 6 REACTIVITIES OF PYRIDINES AND <i>N</i>-ACYLPYRIDINIUM IONS: KINETICS OF MODEL REACTIONS OF AN ORGANOCATALYTIC CYCLE | 243 |
| 6.1 INTRODUCTION | 243 |
| 6.2 RESULTS AND DISCUSSION | 246 |
| 6.2.1 Synthesis of <i>N</i> -Acylpyridinium Ions | 246 |
| 6.2.2 Kinetics of the Reactions of the Benzoyl Chlorides 2a–n with the Pyridines 1a–q | 248 |
| 6.2.3 Kinetics of the Reactions of DMAP (2a) with Other Acyl Chlorides and Anhydrides | 256 |
| 6.2.4 Kinetics of the Reactions of <i>N</i> -Acylpyridinium ions with Benzylamine (9) | 261 |
| 6.3 CONCLUSION | 269 |
| 6.4 EXPERIMENTAL SECTION | 271 |
| 6.4.1 General Comment | 271 |
| 6.4.2 Kinetic Experiments | 275 |
| 6.4.3 Product Characterization | 311 |
| 6.5 REFERENCES | 315 |
| 7 INDUCTIVE EFFECTS THROUGH ALKYL GROUPS — HOW LONG IS LONG ENOUGH? | 317 |
| 7.1 INTRODUCTION | 317 |
| 7.2 RESULTS AND DISCUSSION | 318 |
| 7.3 CONCLUSION | 327 |
| 7.4 EXPERIMENTAL SECTION | 327 |
| 7.4.1 General Comment | 327 |
| 7.4.2 Kinetic Experiments | 328 |
| 7.5 REFERENCES | 332 |
| 8 PHOTOGENERATION OF BENZHYDRYL CATIONS BY NEAR-UV LASER FLASH PHOTOLYSIS OF PYRIDINIUM SALTS | 333 |
| 8.1 Introduction | 333 |
| 8.2 RESULTS AND DISCUSSION | 336 |
| 8.2.1 Photo-generation of Benzhydrylium Ions | 336 |
| 8.2.2 Kinetic Investigations | 341 |
| 8.3 CONCLUSION | 346 |
| 8.4 EXPERIMENTAL SECTION | 346 |
| 8.4.1 General Comment | 346 |
| 8.4.2 Kinetic Experiments | 348 |
| 8.4.3 Product Characterization | 363 |

| | |
|---|------------|
| 8.5 REFERENCES | 364 |
| 9 NUCLEOPHILICITIES AND LEWIS BASICITIES OF ISOTHIUREA | 367 |
| DERIVATIVES | |
| 9.1 INTRODUCTION | 367 |
| 9.2 RESULTS AND DISCUSSION | 370 |
| 9.2.1 Product Studies | 370 |
| 9.2.2 Kinetics | 371 |
| 9.2.3 Correlation Analysis | 374 |
| 9.2.4 Lewis Basicities and Intrinsic Reactivities of Isothioureas | 376 |
| 9.2.5 Structure Reactivity Relationships | 379 |
| 9.2.6 Nucleofugalities of Isothioureas | 381 |
| 9.3 CONCLUSION | 382 |
| 9.4 EXPERIMENTAL SECTION | 385 |
| 9.4.1 General Comment | 385 |
| 9.4.2 Kinetics of the reactions of isothioureas with benzhydrylium ions (Ar ₂ CH ⁺) | 386 |
| 9.4.3 Equilibrium constants (<i>K</i>) for the reactions of benzhydrylium ions (Ar ₂ CH ⁺) with isothioureas in CH ₂ Cl ₂ . | 396 |
| 9.5 REFERENCES | 400 |

Chapter 1

SUMMARY

1.1 General

Nitrogen nucleophiles, for example, primary, secondary and tertiary amines, pyridines, and isothiouras, have been successfully used as organocatalysts for diverse enantioselective functionalizations.

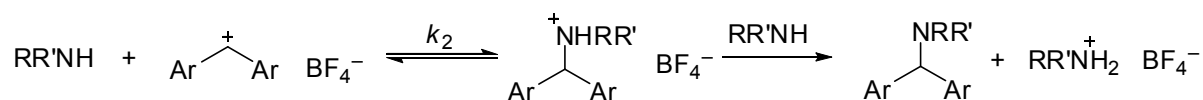
These reaction cascades often contain steps which are combinations of electrophiles and nucleophiles, the rates of which were shown to be accessible by the linear free energy relationship [Eq. (1.1)], where nucleophiles are characterized by the solvent-dependent nucleophilicity parameters N (nucleophilicity) and s_N (sensitivity), and electrophiles are characterized by the solvent-independent electrophilicity parameter E .

$$\log k_2(20\text{ }^\circ\text{C}) = s_N(N + E) \quad (1.1)$$

In this work we show the scope and limitations of Equation 1.1 to predict rates of the reactions of carbocations and acylation agents with various nitrogen nucleophiles, including α -effect amines.

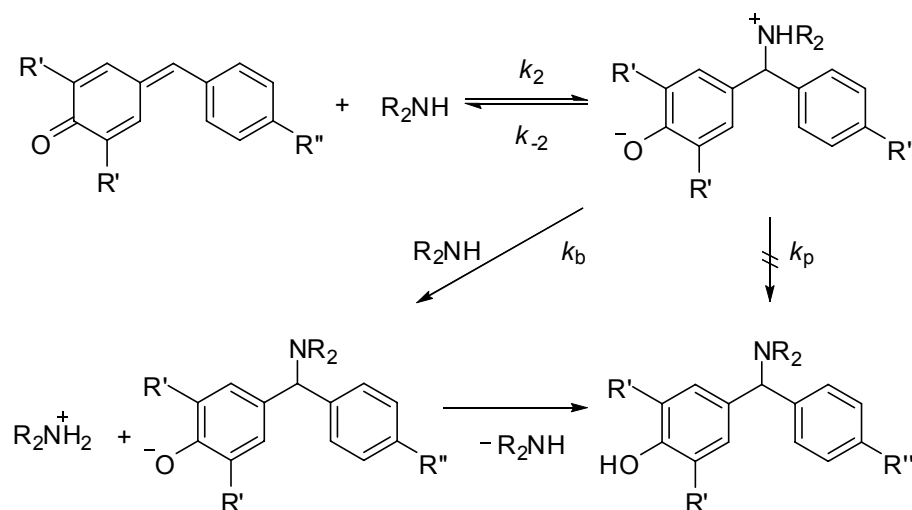
1.2 Nucleophilic Reactivities of Primary and Secondary Amines in Acetonitrile

The kinetics of the reactions of primary and secondary amines with benzhydrylium ions and quinone methides in acetonitrile were studied under first-order conditions (high excess of amines) by UV/Vis spectroscopy (Scheme 1.1). Generally the plots of k_{obs} versus the amine concentrations were linear, which is in line with a second-order rate law.



Scheme 1.1. Reactions of amines with benzhydrylium ions.

For some reactions of secondary amines with quinone methides, however, the plots of k_{obs} versus the amine concentration showed an upward curvature. In these cases, the formation of the zwitterionic intermediate is reversible and followed by subsequent rate limiting deprotonation by a second molecule of the amine (Scheme 1.2).



Scheme 1.2. Reactions of secondary amines with quinone methides.

The application of Equation (1.2), derived from the rate law of the reaction, allowed the determination of the second-order rate constants k_2 for the initial attack of the amines on the electrophilic double bond of the quinone methides.

$$k_{\text{obs}} = \frac{k_2 k_b [\text{Amine}]^2}{k_{-2} + k_b [\text{Amine}]} \quad (1.2)$$

When the logarithms of the second-order rate constants k_2 for the attack of the amines on the electrophiles were plotted against the electrophilicity parameters E of the benzhydrylium ions and quinone methides, linear correlations were obtained (Figure 1.1), from which the

nucleophile-specific parameters N and s_N were determined according to the linear free energy relationship [Eq. (1.1)].

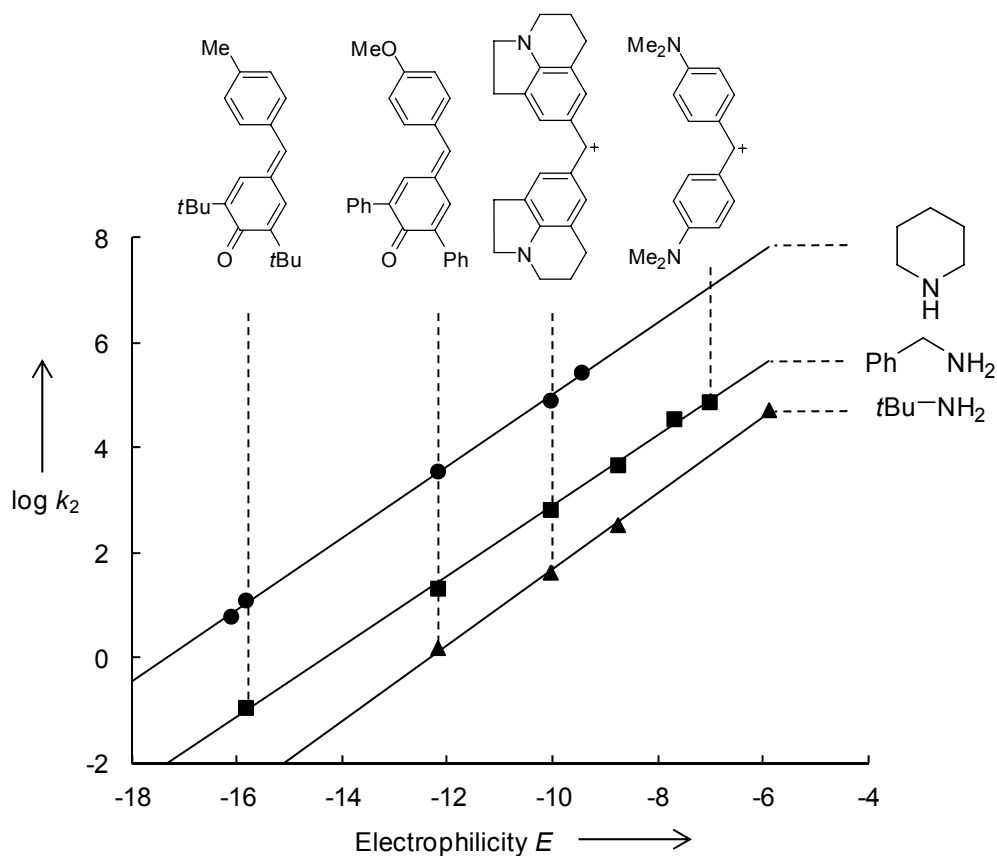


Figure 1.1. Plots of the second-order rate constants $\log k_2$ (20 °C) for the reactions of piperidine, benzylamine, and *tert*-butylamine with benzhydrylium ions and quinone methides in CH₃CN versus the E parameters of the reference electrophiles.

The reactivity range of the amines ($10 < N < 19$) demonstrates that benzhydrylium ions react with amines of low reactivity with similar rates as with silyl ketene acetals and trialkyl-substituted pyrroles, whereas the nucleophilicities N of highly reactive amines are similar to those of stabilized carbanions (Figure 1.2).

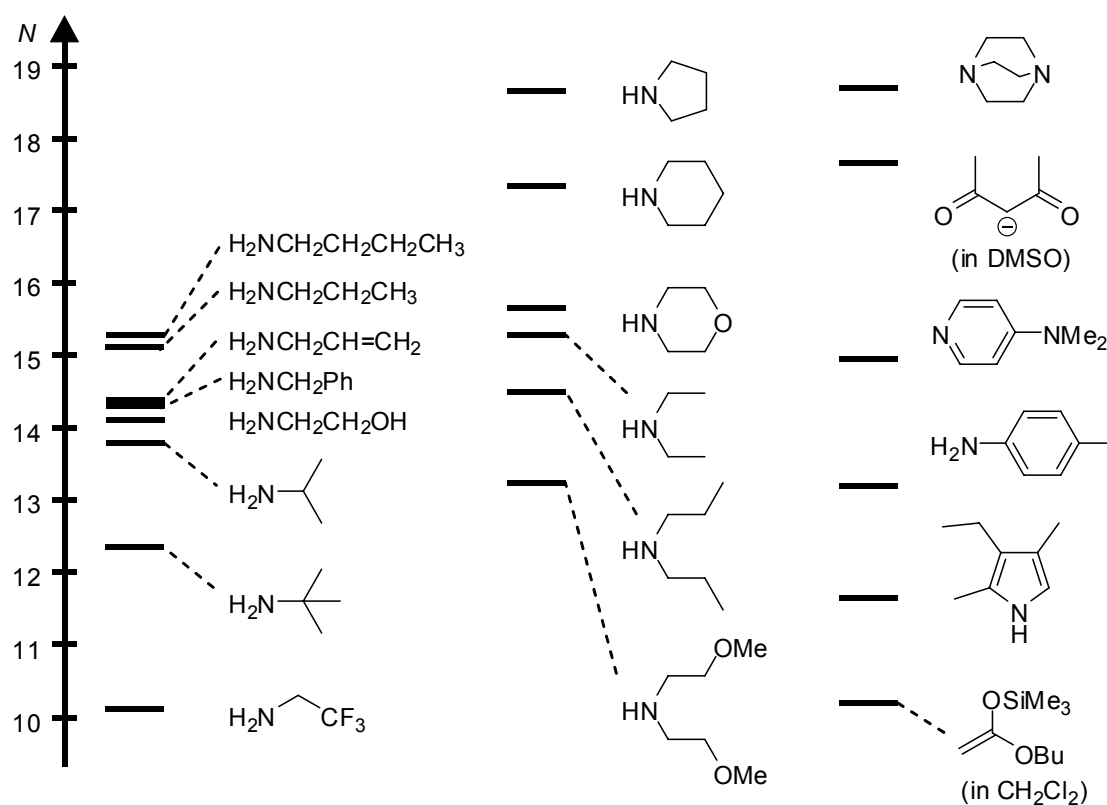


Figure 1.2. Comparison of the nucleophilic reactivities of amines in acetonitrile with other nucleophiles.

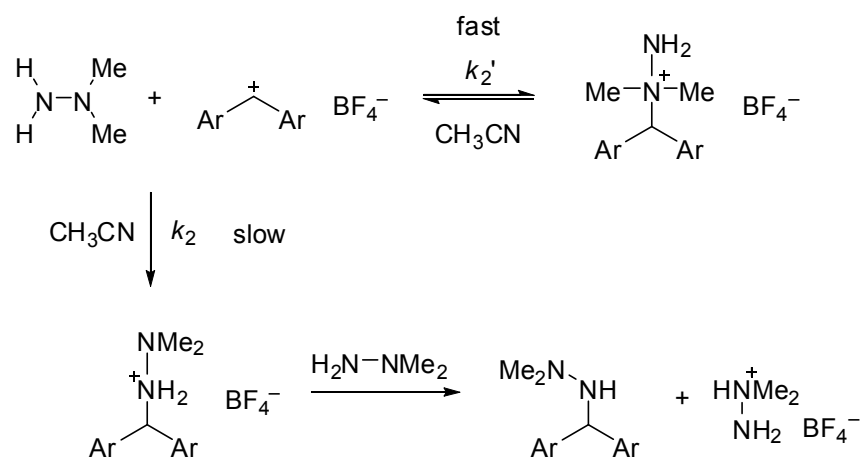
The poor correlation between the nucleophilicity N of the amines and the corresponding $\text{p}K_{\text{aH}}$ values shows that relative basicities cannot be used to predict relative nucleophilicities.

Solvent polarity affects the reactivities of alkylamines and anilines quite differently: Whereas anilines react approximately two times faster with benzhydrylium ions in water than in acetonitrile, primary alkylamines react approximately 10^2 times faster in acetonitrile than in water. The opposite solvent effect on these closely related reactions demonstrates the limitation of the Hughes–Ingold rules to predict solvent effects on polar organic reactions on the basis of the relative charge dispersal in the ground and transition states.

1.3 Nucleophilic Reactivities of Hydrazines and Amines: The Futile Search for the α -Effect in Hydrazine Reactivities

The kinetics of the reactions of amines, hydrazines, hydrazides, and hydroxylamines with benzhydrylium ions and quinone methides were studied in acetonitrile and water by UV/Vis spectroscopy, using conventional spectrometers, stopped-flow and laser-flash photolytic techniques. Plots of the logarithms of the second-order rate constants k_2 for these reactions versus the electrophilicity parameters E of the reference electrophiles were linear, from which the nucleophilicity parameters N and s_N were determined according to the linear free energy relationship [Eq. (1.1)].

For the asymmetric hydrazines 1,1-dimethylhydrazine and trimethylhydrazine different kinetic behavior was observed depending on the concentrations of the hydrazines and the nature of the electrophiles, which was explained by the mechanism depicted in Scheme 1.3. ^1H NMR spectroscopy proved that the reactions of the tertiary centers of the hydrazines are fast and reversible, whereas substitution of the primary or secondary center of the hydrazines is observed under conditions of thermodynamic control. For these nucleophiles, two separate correlation lines were observed in plots of the second-order rate constants versus the electrophilicities E of the reference electrophiles which correspond to the two modes of attack (Figure 1.3).



Scheme 1.3. Ambident reactivity of 1,1-dimethylhydrazine in reactions with benzhydrylium ions.

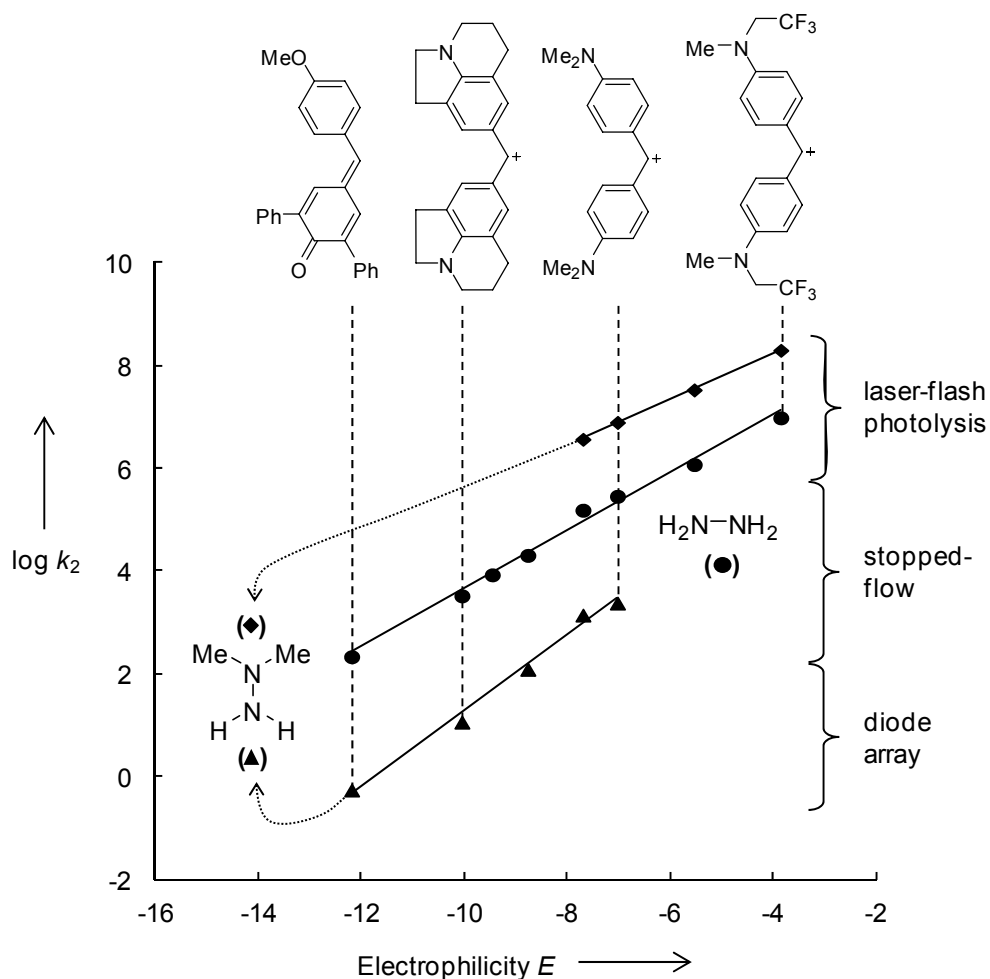


Figure 1.3. Plots of the second-order rate constants $\log k_2$ for the reactions of hydrazine and 1,1-dimethylhydrazine with benzhydrylium ions and quinone methides in CH_3CN at 20°C versus the electrophilicity parameters E of the reference electrophiles.

Remarkably, alkyl effects are almost identical in the amine and hydrazine series, that is, in both series methyl-substitution in α -position causes a significant increase of nucleophilicity while methyl-substitution in β -position causes a significant decrease of nucleophilicity. (Figure 1.4).

| | Amines | | | Hydrazines and Hydrazides | | | Hydroxylamines |
|-----------|-------------------|-------------------|-------------------|---------------------------|----------------------------------|------|-------------------|
| | | | | | | | |
| k_{rel} | 1.0 | 2.6×10^2 | 93 | 96 ^[a] | not accessible | 0.28 | 2.8 |
| | | | | | | | |
| k_{rel} | 2.6×10^2 | 5.1×10^3 | 5.2×10^2 | 1.1×10^3 | 5.3×10^2 ^[a] | | 1.2×10^2 |
| | | | | | | | |
| k_{rel} | 5.1×10^3 | 1.3×10^4 | 1.1×10^2 | 5.3×10^3 | 3.2×10^2 | 17 | |

Figure 1.4. Comparison of the relative second-order rate constants for the reactions of 4,4'-bis(dimethylamino)benzhydrylium tetrafluoroborate with ammonia, amines, hydrazines, hydrazides, and hydroxylamines in CH_3CN at 20 °C (the relative rate constants refer to the centers of attack marked with arrows).

[a] The rate constants for the reactions of 4,4'-bis(dimethylamino)benzhydrylium tetrafluoroborate with the symmetrical hydrazines were statistically corrected by a factor of 2.

Despite the 10^2 times lower reactivities of amines and hydrazines in water than in acetonitrile, the relative reactivities of differently substituted amines and hydrazines are almost identical in the two solvents. In both solvents, the parent hydrazine has a similar reactivity as methylamine. If one takes into account that hydrazine has two reactive centers, this observation implies that a methyl group activates amines twice as efficiently as an amino group.

The rate constants of the reactions of amines and hydrazines with 4,4'-bis(dimethylamino)-benzhydrylium tetrafluoroborate in water and acetonitrile are not correlated with their basicities. When the Brønsted-type correlation for the reactions in water is restricted to structurally related α -unbranched primary amines, a linear correlation with small slope is

obtained, from which hydrazine, hydroxylamine and semicarbazide do not deviate significantly (Figure 1.5). This demonstrates the absence of an α -effect for these nucleophiles. However, one might also argue that alkyl groups, like NH_2 and OH show an α -effect, because NH_3 is considerably below their common correlation line. Whatever definition is employed, as anilines are more reactive than ammonia and are considerably more nucleophilic than isobasic alkylamines, hydrazines and hydroxylamines, they should be considered as α -effect amines par excellence.

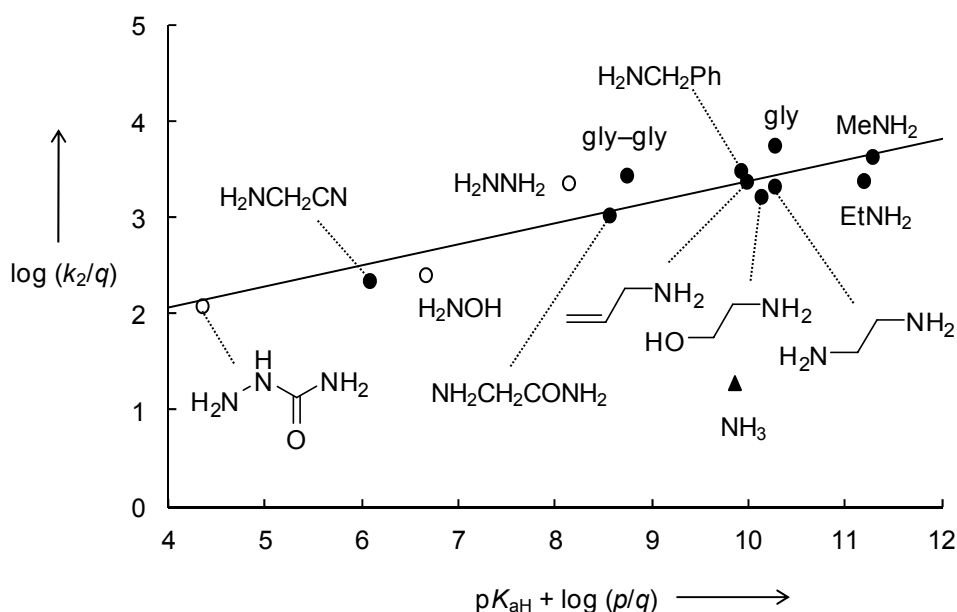


Figure 1.5. Brønsted plots of the statistically corrected second-order rate constants versus the statistically corrected basicities for the reactions of 4,4'-bis(dimethylamino)benzhydrylium tetrafluoroborate with unbranched primary amines in H_2O at 20°C (p = number of equivalent protons of the conjugated acids; q = number of equivalent nucleophilic centers).

Similar to the Brønsted correlation, a plot of $\log k_2$ versus the corresponding equilibrium constants ($\log K$) for the reactions of amines and 1,1-dimethylhydrazines with 4,4'-bis(*N*-pyrrolidino)benzhydrylium tetrafluoroborate does not show enhanced nucleophilicities (α -effect) for the hydrazines relative to alkylamines.

1.4 Limitations of the Benzhydrylium-Based Nucleophilicity Scales for Predicting Rates of Acylation Reactions

The kinetics of the reactions of carbanions, carboxylate anions, primary and secondary amines with acylating agents were studied in acetonitrile and DMSO under first-order conditions by UV/Vis spectrophotometry or conductivity measurements.

The relative reactivities of the different acyl compounds depend strongly on the nature of the nucleophilic reaction partner as exemplified in Figure 1.6 by the different relative reactivities of acid anhydrides, benzoyl chloride, and 1-benzoyl-4-(dimethylamino)pyridinium chloride towards *n*-propylamine (left) and diethylamine (right).

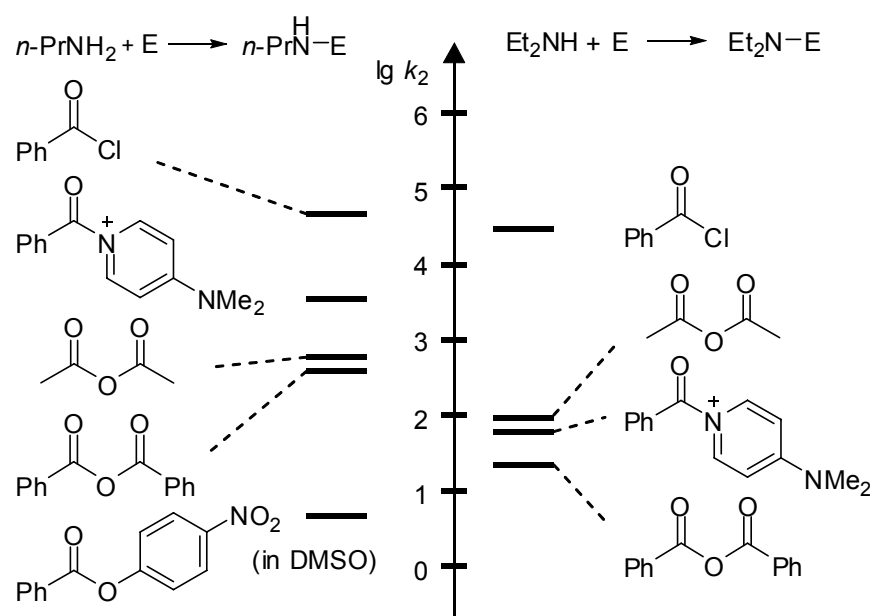


Figure 1.6. Comparison of the second-order rate constants k_2 for reactions of 4-nitrophenyl benzoate, benzoic anhydride, acetic anhydride, 1-benzoyl-4-(dimethylamino)pyridinium chloride, and benzoyl chloride with *n*-propylamine (left side) and diethylamine (right side).

The rate constants for the reactions of 4-nitrophenyl benzoate with carbanions can be described by the linear free energy relationship [Eq. (1.1)], using the benzhydrylium-derived nucleophile-specific parameters N and s_N for carbanions (Figure 1.7). Amines and alkoxide anions react considerably faster than expected from their reactivity parameters N and s_N ,

which can be explained by the anomeric stabilization of the tetrahedral intermediate that is already reflected in the transition state.

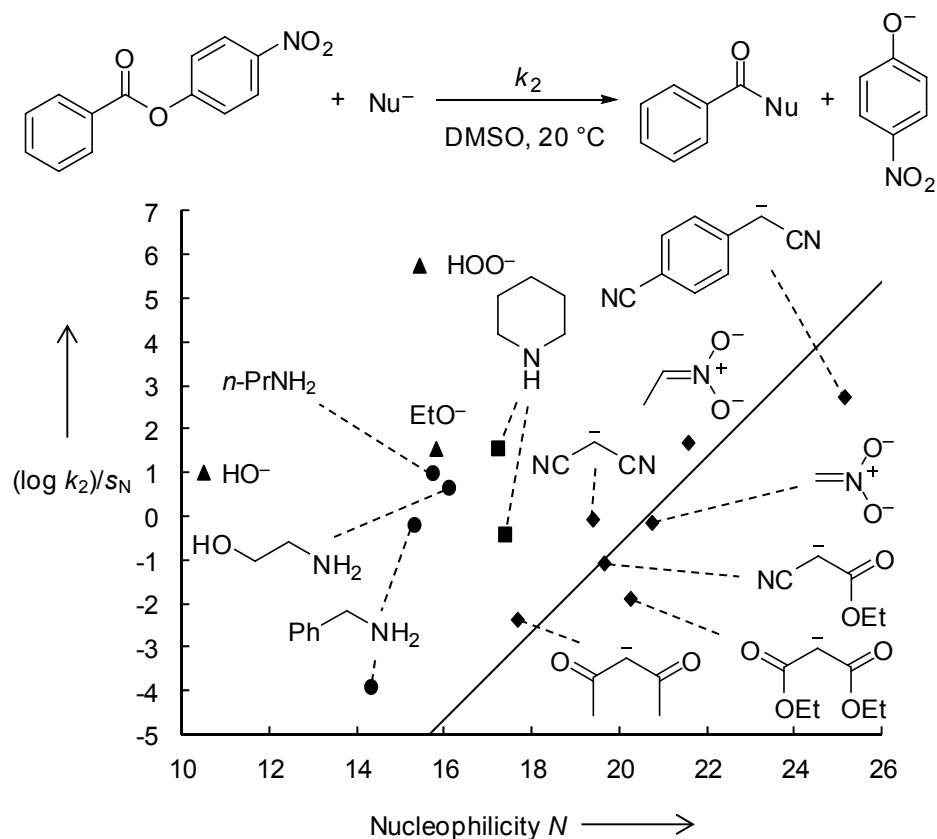


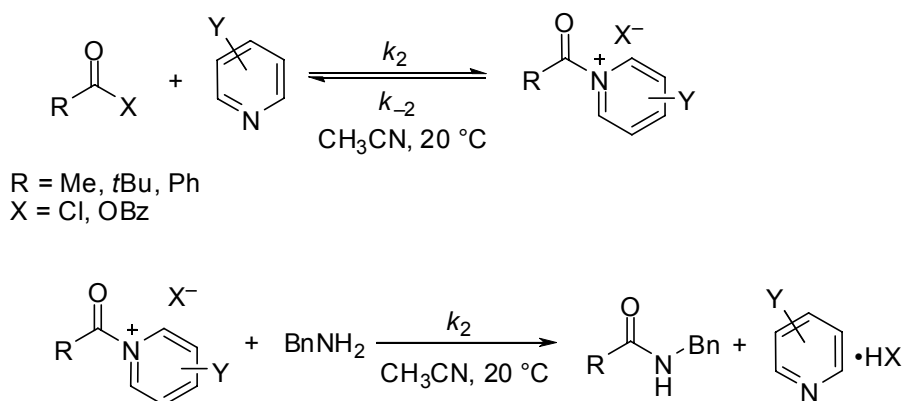
Figure 1.7. Plot of $(\log k_2)/s_N$ versus the corresponding nucleophilicity parameters N for the reactions of 4-nitrophenyl benzoate with carbanions (diamonds), alkoxide anions (triangle), primary (circles) and secondary amines (squares).

The second-order rate constants for the reactions of primary amines with the highly electrophilic acylating agents benzoic anhydride, acetic anhydride, benzoyl chloride, and 1-benzoyl-4-(dimethylamino)pyridinium chloride correlate well with the benzhydrylium-derived nucleophile-specific parameters N and s_N of the amines. The same is true for the corresponding reactions of secondary amines. Both series of amines follow separate correlations, however, that we have to conclude that a single set of reactivity parameters for nucleophiles and electrophiles is not sufficient to describe the rates of acylation reactions, even in cases where the nucleophilic attack is rate determining.

As the second-order rate constants for the reactions of benzoic anhydride and 1-benzoyl-4-(dimethylamino)pyridinium chloride with hydrazine, methylhydrazine and 1,2-dimethylhydrazine correlate well with those for the corresponding reactions with alkyl amines demonstrates that the α -effect is less important than the inductive electron donating effect of alkyl groups for their reactions with acylating agents bearing good leaving groups.

1.5 Reactivities of Pyridines and *N*-Acylpyridinium Ions: Kinetics of Model Reactions of an Organocatalytic Cycle

The kinetics of two model reactions, which are related to the catalytic cycle of pyridine-catalyzed acylation reactions, namely the formation of *N*-acylpyridinium ions by reactions of substituted pyridines with acylating agents, and their consumption by benzylamine as reference nucleophile were systematically investigated in acetonitrile at 20 °C (Scheme 1.4).



Scheme 1.4. Reactions of acylating agents with pyridines and reactions of *N*-acylpyridinium ions with benzylamine.

While most 4-alkylaminopyridines react with benzoyl chloride irreversibly according to a second-order rate law, a more complicated rate law was found for the reaction of benzoic anhydride with DMAP.

The amination reactions of the *N*-benzoylpyridinium chlorides and triflates in acetonitrile proceed either in a concerted way or by formation of tetrahedral intermediates, which are rapidly deprotonated in a subsequent reaction.

While electron-withdrawing groups in the benzoyl moiety increase the reactivities of benzoyl chlorides and that of the *N*-benzoylpyridinium ions, the electrophilicities of *N*-benzoylpyridinium ions decrease with increasing nucleophilicities of the pyridines. The rates of formation of the *N*-benzoylpyridinium ions from benzoyl chloride and substituted pyridines are more sensitive to the electron-donating ability of the substituents in the pyridine than the aminolysis reactions of the *N*-benzoylpyridinium ions (Figure 1.8).

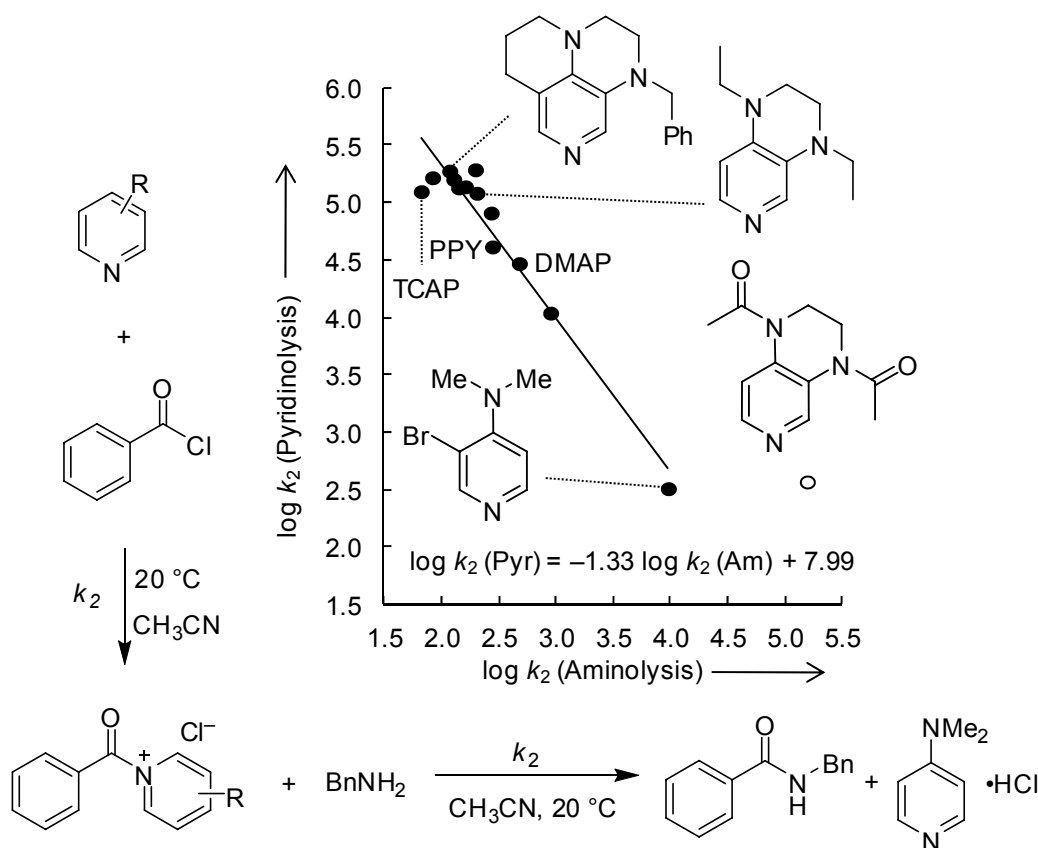


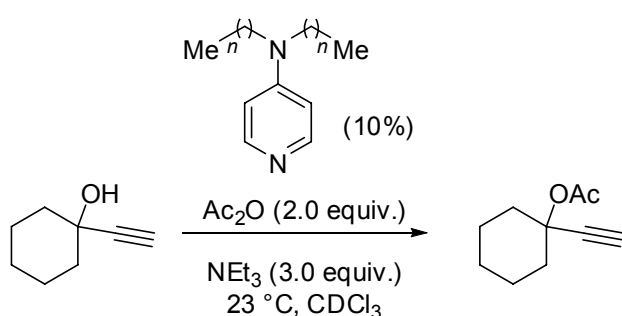
Figure 1.8. Correlation between the rate of the aminolysis reaction of 1-benzoylpyridinium chlorides with benzylamine (“Am”) and the corresponding rate of the pyridinolysis reaction of benzoyl chloride (“Pyr”).

The kinetic data allow the prediction which amination reactions can be catalyzed by pyridines. The following requirements have to be met: (1) The pyridines have to be more nucleophilic than the amines, and (2) the formed *N*-acylpyridinium ions have to be more electrophilic than the original acylating agents.

1.6 Inductive Effects Through Alkyl Groups — How Long is Long Enough?

The influence of alkyl groups of variable length on the catalytic activities of 4-dialkylaminopyridines was investigated.

In the pyridine-catalyzed acylation of 1-ethynylcyclohexanol with acetic anhydride, the catalytic activities increase with the chain length of the alkylamino groups of the pyridines by a factor of 2.6 until saturation of the inductive effects is observed for butyl groups (Scheme 1.5).



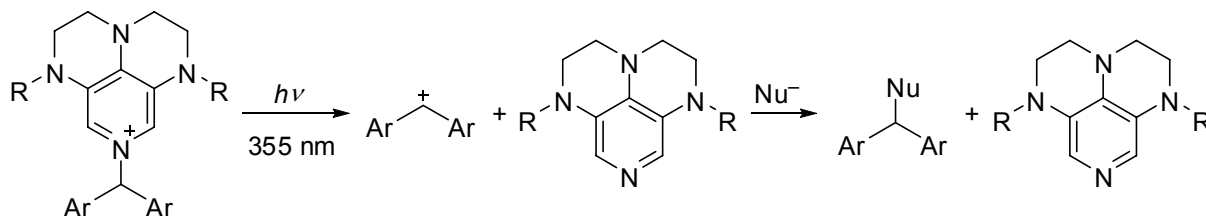
Scheme 1.5. 4-Dialkylaminopyridine-catalyzed acylation of 1-ethynylcyclohexanol with acetic anhydride.

Similarly the rates of the reactions of benzoyl chloride with 4-dialkylpyridines grew by a factor of 1.4 from NMe₂ to NBU₂ and the reactions of the formed *N*-benzoylpyridinium chlorides with benzylamine (compare Scheme 1.4) decreased by a factor of 1.3 from the DMAP- to the 4-dibutylaminopyridine-derived *N*-benzoylpyridinium ion.

1.7 Photogeneration of Benzhydryl Cations by Near-UV Laser Flash Photolysis of Pyridinium Salts

The reactions of benzhydrylium ions with pyridines cannot be studied by laser flash photolysis with established precursors such as benzhydryl triarylphosphonium ions because pyridines absorb at 266 nm, the wavelength used to cleave these phosphonium ions. Laser flash irradiation of substituted *N*-benzhydrylpyridinium salts yields benzhydryl cations (diarylcarbenium ions) and/or benzhydryl radicals (diarylmethyl radicals). The use of 3,4,5-

triamino-substituted pyridines as photo-leaving groups allowed us to employ the third harmonic of a Nd/YAG laser (355 nm) for the photogeneration of benzhydryl cations (Scheme 1.6).



R = H, Me, Et, Bn

Scheme 1.6. Generation of benzhydrylium ions by 355 nm laser flash photolysis of pyridinium ions with different substituents R on the pyridine moiety.

In this way benzhydryl cations covering more than 10 orders of reactivity can be photogenerated in the presence of aromatic compounds and in solvents which are opaque at the wavelength of the quadrupled Nd/YAG laser (266 nm). To demonstrate the scope and limitations of this method, the rate constants for the bimolecular reactions of benzhydryl cations with several substituted pyridines were determined in acetonitrile, DMSO, DMF, and acetone as well as with water in acetone. From the second-order rate constants, the nucleophilicity parameters N and s_N for the substituted pyridines were derived (Figure 1.10), as defined by the linear free energy relationship [Eq. (1.1)].

Laser flash photolysis of substituted pyridinium salts at 355 nm thus supplements the established kinetic methods and is particularly useful for characterizing nucleophiles which do not react with stabilized carbocations for thermodynamic reasons and which cannot be studied with 266 nm laser flash photolytically generated carbocations due to the absorbance of the sample solutions.

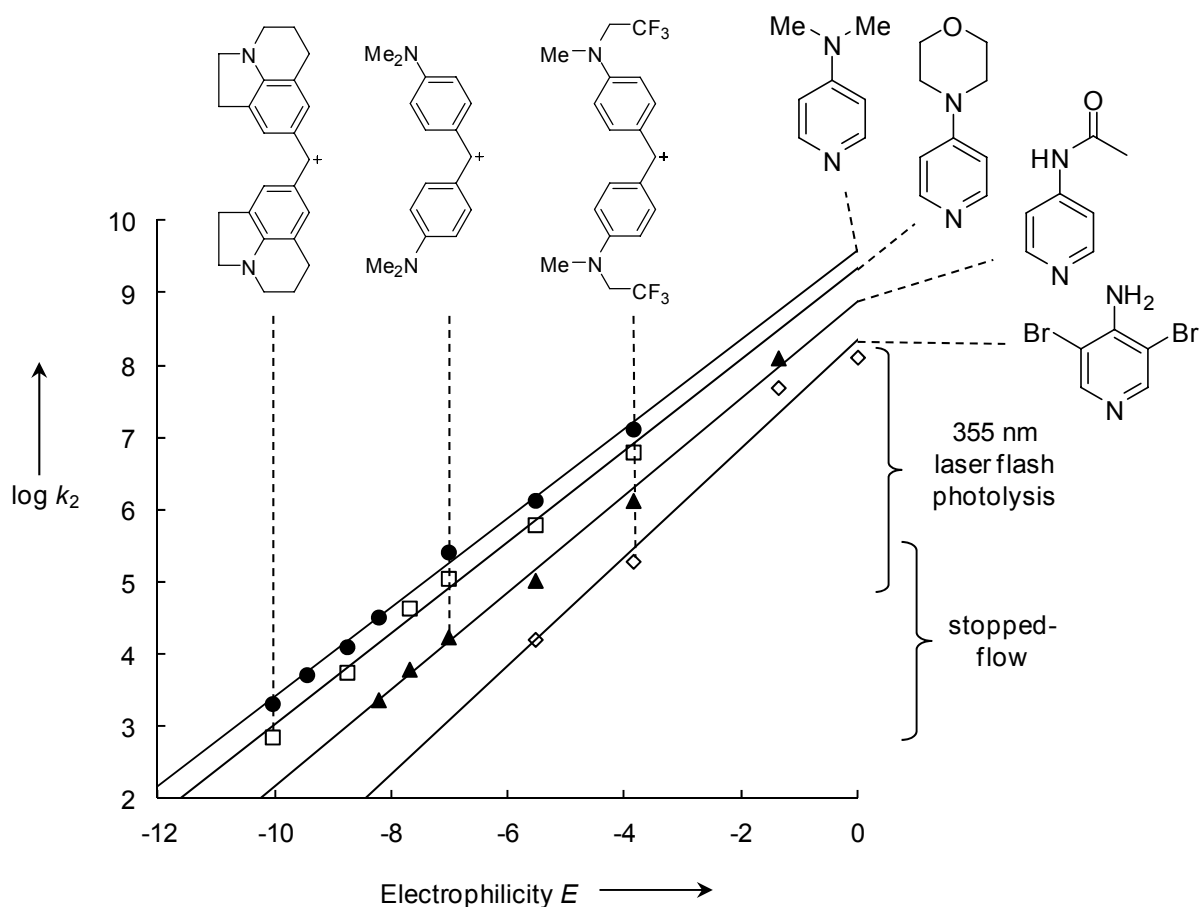
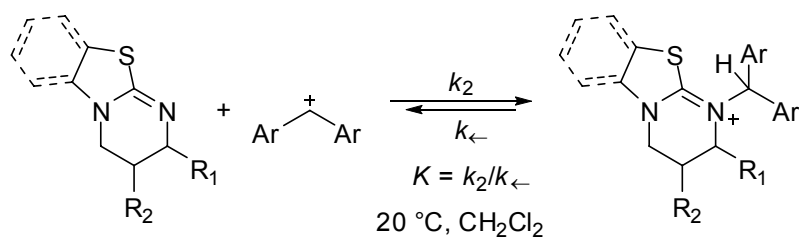


Figure 1.10. Plot of $\log k_2$ for the reactions of benzhydrylium ions with 3,5-dibromo-4-aminopyridine, 4-(acetylamino)pyridine, 4-(*N*-morpholino)pyridine, and 4-(dimethylamino)pyridine versus the electrophilicity parameters E of the reference electrophiles.

1.8 Nucleophilicities and Lewis Basicities of Isothiourea Derivatives

The second-order rate constants for the reactions of isothiureas with benzhydrylium ions were determined spectrophotometrically in dichloromethane at 20 °C (Scheme 1.7). As these reactions follow the linear free energy relationship [Eq. (1.1)], it was possible to determine the nucleophilicity parameters N and s_N for several isothiureas. The nucleophilicity parameters N of these acyl transfer catalysts are in between those of the classical organocatalysts 4-(dimethylamino)pyridine and 1-methylimidazole (Figure 1.11).



Scheme 1.7. Reactions of isothioureas with benzhydrylium ions.

The reactions of three achiral and of four C(2)-substituted chiral isothioureas with several amino-substituted benzhydrylium ions proceeded incompletely, which allowed the measurement of the equilibrium constants for these reactions by UV/Vis spectroscopy and the construction of quantitative energy profile diagrams.

Imidazoles are less nucleophilic as well as less Lewis basic than isothioureas. Although the kinetic and thermodynamic properties of most isothioureas investigated are comparable to those of DMAP, DABCO is a stronger nucleophile than all isothioureas investigated, while its Lewis basicity is comparable to those of the least basic isothioureas.

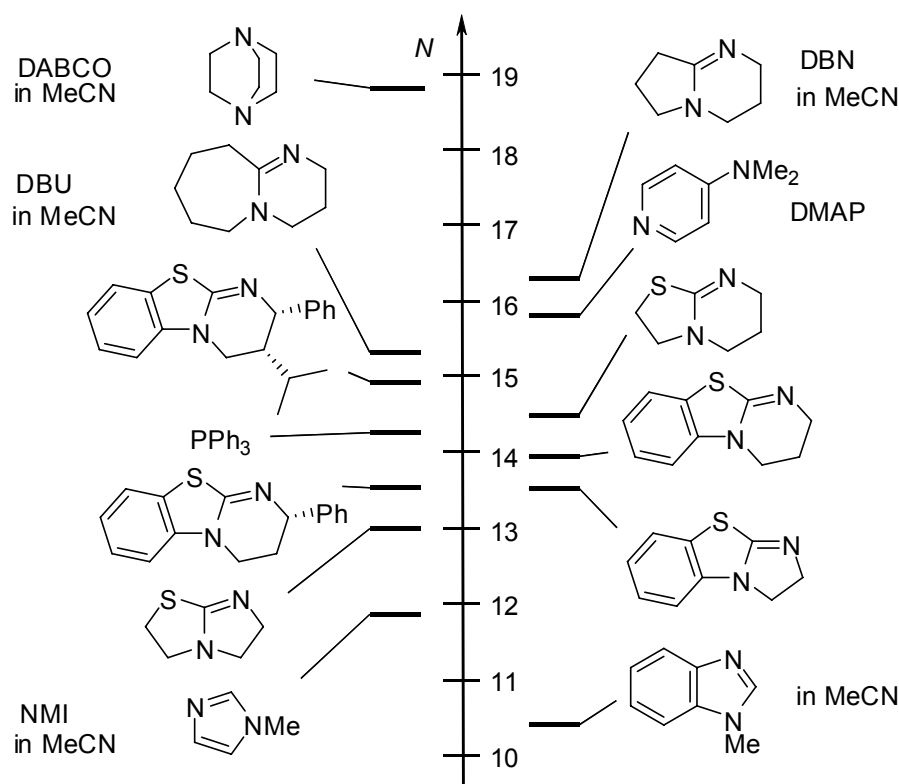


Figure 1.11. Comparison of the nucleophilicities N of isothioureas with those of other nucleophilic organocatalysts (solvent is CH₂Cl₂ unless stated otherwise).

Chapter 2

INTRODUCTION AND OBJECTIVES

Quantification of the reactivities of organic compounds has been a crucial aim in physical organic chemistry since the beginning of the last century, when the concept of nucleophilicity and electrophilicity to account for electron-rich and electron-deficient species was introduced by Ingold.^[1]

In 1953, the first quantitative approach to nucleophilic reactivity was reported by Swain and Scott, who investigated the rates of S_N2 reactions and postulated a constant order of nucleophilicity.^[2]

In 1972, Ritchie discovered that the relative reactivities of two nucleophiles do not depend on the electrophilic reaction partner in reactions of nucleophiles with carbocations and diazonium ions.^[3] Thereupon, he constructed a nucleophilicity scale based on the constant selectivity relationship [Eq. (2.1)], which describes a given nucleophile in a certain solvent with one electrophile-independent nucleophilicity parameter N_+ while the corresponding rate constant for the reaction of the electrophile with water (k_0) is used as reference.^[4] Later, the limitations of Equation (2.1) were demonstrated by showing that better correlations are obtained when different classes of electrophiles were treated separately.^[5]

$$\log (k/k_0) = N_+ \quad (2.1)$$

In 1994, Mayr and Patz reported the modified linear free energy relationship [Eq. (2.2)], where electrophiles are characterized by one solvent-independent parameter E and nucleophiles are characterized by two solvent-dependent parameters s_N (nucleophile-specific sensitivity) and N (nucleophilicity).^[6]

$$\log k_2 (20\text{ }^\circ\text{C}) = s_N(N + E) \quad (2.2)$$

Benzhydrylium ions and structurally related quinone methides were chosen as reference electrophiles as they exhibit similar steric surroundings at the reaction centers, while their reactivities can be varied widely by substituents at the aromatic rings.

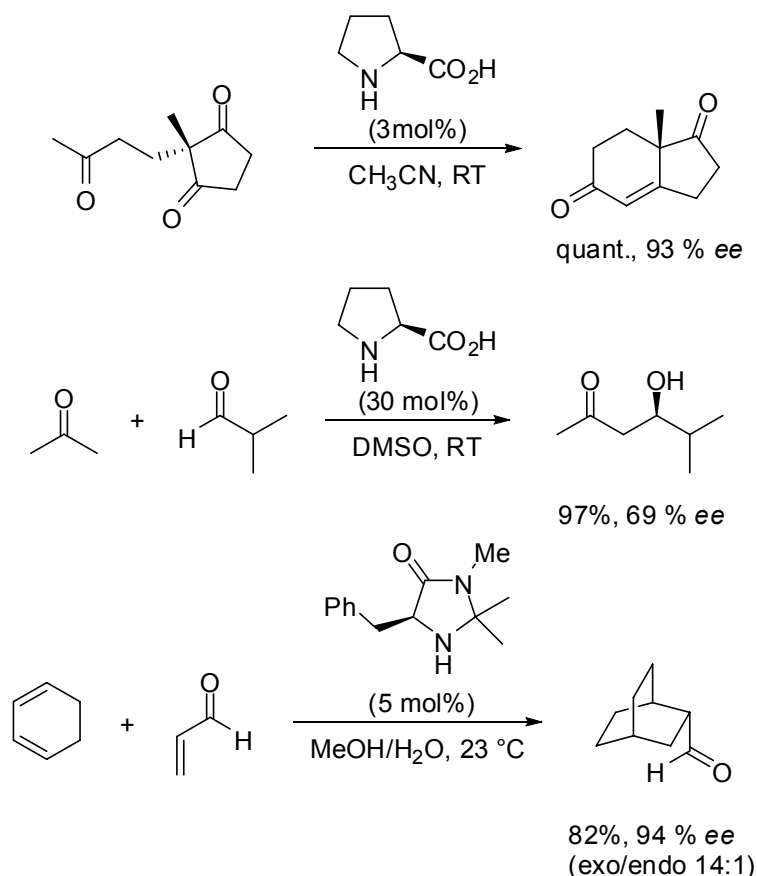
Over the past years, the reactivities of numerous classes of n -, π -, and σ -nucleophiles have been characterized by this approach.^[7] In contrast, electrophilic reactivities have only been determined for few classes of compounds, mainly for carbocations, cationic metal π -complexes, and electron-deficient Michael acceptors. Recently, it was shown that it is also possible to use Equation (2.2) for quantifying the electrophilicities of aldehydes, imines, and enones by studying their reactions with sulfur ylides.^[8]

While countless investigations were concerned with the detailed mechanisms of acylation reactions,^[9] a general reactivity scale for nucleophilic substitution reactions at acyl derivatives has not been acquired yet. It was a goal of this thesis to investigate the scope and limitations of Equation (2.2) for the prediction of rates of acylation reactions.

Organocatalysis is one of the fastest growing fields in organic chemistry.^[10] According to the definition by MacMillan in 2000, this term accounts for “the acceleration of a chemical reaction through addition of a sub-stoichiometric amount of an organic compound which does not contain a metal atom”.^[11]

In 1859, Liebig discovered the first organocatalytic reaction by converting dicyan into oxamide in the presence of an aqueous solution of acetaldehyde.^[12] In the following decades, fundamental progress in organic synthesis was achieved by discoveries such as piperidine-catalyzed Knoevenagel condensations,^[13] DMAP-catalyzed esterifications,^[14] and DABCO-catalyzed Baylis-Hillman reactions.^[15]

Despite the long history of achiral organocatalysis, the interest in this topic excessively grew with the discovery of its asymmetric modifications. Pioneering work in the 1970s established the first proline-catalyzed intramolecular enantioselective aldol reaction, known as the Hajos-Parrish-Sauer-Wiechert reaction.^[16] The great breakthrough was finally achieved by List and Barbas who investigated proline-catalyzed intermolecular aldol reactions,^[17] as well as MacMillan who showed that enantioselective Diels-Alder reactions can be catalyzed with chiral imidazolidinones (Scheme 2.1).^[11]



Scheme 2.1. Pioneering enantioselective organocatalytic aldol and Diels-Alder reactions.

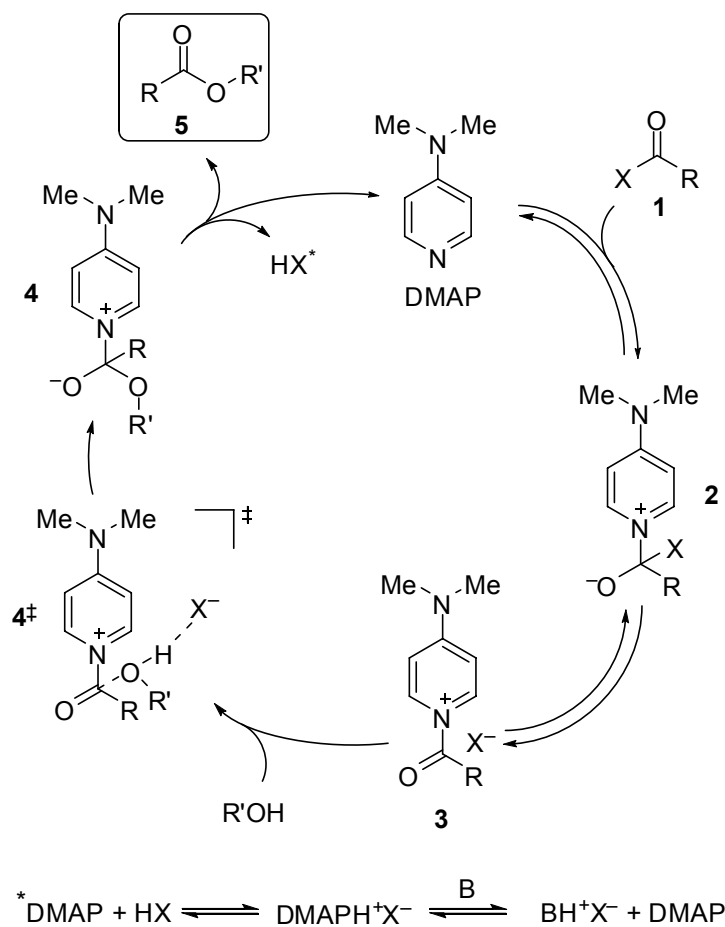
Development of modern chiral organocatalysts led to a huge variety of asymmetric reactions with high enantioselectivities such as Michael additions, Friedel-Crafts alkylations, epoxidation, aldol, Mannich, Diels-Alder, and hydrogen transfer reactions as well as functionalizations of carbonyl groups.^[10]

In the majority of these reactions, nitrogen nucleophiles are used as catalysts, which act as Lewis bases to activate one of the reactants.^[18]

As the key steps of most organocatalytic reaction cascades are combinations of electrophiles with nucleophiles, Equation (2.2) has been applied to demonstrate the scope of substrates which can be used in numerous organocatalytic reactions.^[19] Furthermore, Equation (2.2) was shown to be useful to unravel controversies in the literature concerning the mechanisms of iminium- and enamine-activated organocatalytic reactions by studying the reactivities of the isolated intermediates.^[19]

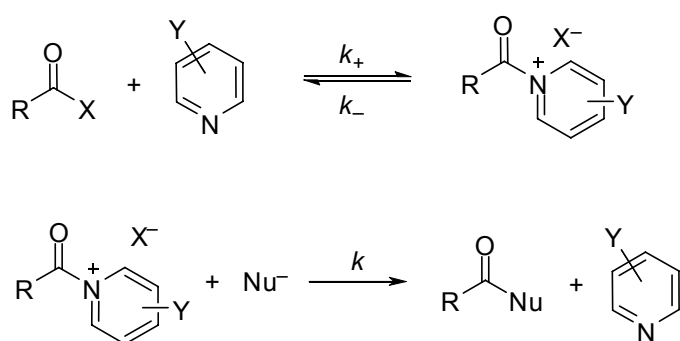
Litvinenko and Kirichenko as well as Steglich and Höfle demonstrated that catalytic amounts of 4-(dimethylamino)pyridine (DMAP) efficiently promoted acyl transfer reactions.^[14] Until today, DMAP is the catalyst of choice for acylations in terms of cost-benefit ratio.^[21]

In pyridine-catalyzed acylations, the *N*-acylpyridinium salt **3** is formed by the reversible reaction of DMAP with the acyl donor (**1**) either concertedly or via the tetrahedral intermediate **2** (Scheme 2.2).^[21] In the second step, which is rate-determining, the alcohol, R'OH reacts with the *N*-acylpyridinium ion **3** to yield the intermediate **4**. According to quantum chemical calculations, the nucleophilic attack of the alcohol is assisted by a proton transfer to the counterion X⁻ in the transition state **4**[‡] for the DMAP-catalyzed reaction of *tert*-butanol with acetic anhydride.^[22] The formation of the ester **5** by elimination of DMAP is accompanied by the generation of HX which has to be trapped by an auxiliary base of adequate basicity to avoid deactivation of the catalyst. A more detailed mechanism also includes dissociated *N*-acylpyridinium ions of lower reactivity, potential precipitation of the salts and alternative pathways via acylium ions or ketenes.^[21b]



Scheme 2.2. Simplified mechanism for the DMAP-catalyzed acylation of alcohols.

In previous attempts to improve the efficiency of the pyridine-based organocatalysts, structure-reactivity relationships have been investigated by studying the rates of the overall reaction.^[21–23] Investigations of the kinetics of the individual steps of the organocatalytic cycle of DMAP-catalyzed acylation reactions, namely the reactions of pyridines with acylating agents, and the subsequent reactions of the resulting *N*-acylpyridinium ions with reference nucleophiles seemed to be useful to obtain more insight into pyridine-catalyzed acylations and to acquire rules of the thumb which acylation reactions can be catalyzed by pyridines (Scheme 2.3).

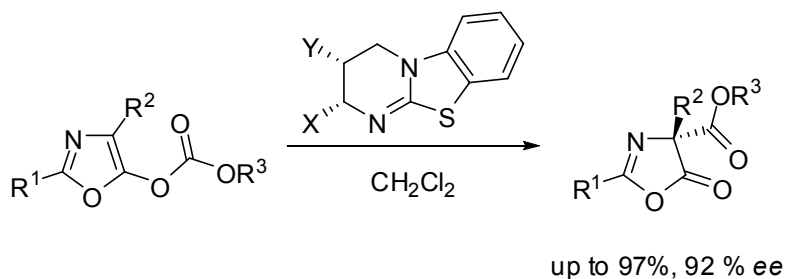


Scheme 2.3. Reactions of acylating agents with pyridines and reactions of *N*-acylpyridinium ions with nucleophiles.

The influence of alkyl groups of variable length on ground state properties of organic molecules and on their reactivities in unimolecular and bimolecular transformations has been discussed in terms of steric and electronic substituent effects.^[24] As the reactivities of 4-(dialkylamino)pyridines are only influenced by the inductive effects of the alkyl groups and not by the steric demand of the substituents, kinetic and thermodynamic properties of diverse reactions of those pyridines should apply as a general measure for the inductive effects of the alkyl groups.

Chiral derivatives of DMAP have successfully been used as catalysts for enantioselective acylations and kinetic resolutions of alcohols and amines.^[25] However, applications are rather limited because of the complicated syntheses of these catalysts along with frequently observed low enantioselectivities. Based on the pioneering work of Birman,^[26] isothiureas were shown to be highly efficient catalysts for various acyl transfer reactions,^[21a,27] such as the asymmetric *O*- to *C*-carboxyl transfer of oxazolyl carbonates (Scheme 2.4).^[28] Therefore,

reactivity parameters for these nucleophiles seemed to provide a quantitative basis for planning enantioselective acylation reactions.



Scheme 2.4. Asymmetric isothioureia-promoted *O*- to *C*-carboxyl transfer (Steglich rearrangement) of oxazolyl carbonates.

Allen *et al.* showed that transamination reactions of primary and secondary carboxamides with secondary amines can be catalyzed by hydroxylamine hydrochloride, a catalyst which is a prototype for an α -effect nucleophile.^[29] The α -effect, a phenomenon which was reported for the first time by Pearson and Edwards in 1962, accounts for the enhanced reactivity of nucleophiles, which bear an unshared pair of electrons at the atom adjacent to the nucleophilic center.^[30] Because of the difficulty to specify a reference nucleophile with which the α -effect nucleophile should be compared, Hoz' and Buncl's definition of the α -effect as the positive deviation from a Brønsted plot was adopted by the IUPAC Glossary of Terms used in Physical Organic Chemistry.^[31]

Although the α -effect was studied for various reactions, the controversial discussions reveal that it strongly depends on the system investigated.^[32] Several theories on the origin of the α -effect which have emerged, which include the destabilization of the ground state by electron repulsions, the stabilization of the transition state, thermodynamic stabilization of the products, and solvent effects, but obviously more than one of these factors seems to be operative in general.^[31b,32]

In view of the controversial discussions, the characterization of the nucleophilic reactivities of classical α -effect nucleophiles with reactive nitrogen centers, for example, hydrazines, hydrazides, and hydroxylamines, along with those of structurally related alkyl amines in reactions with carbocations and carbonyl compounds should provide a quantitative basis for the discussion of the α -effect.

Apart from the α -effect, investigations of the nucleophilic reactivities of hydrazines are also interesting with respect to their ambident reactivity, as they have two adjacent nucleophilic nitrogen centers. For unsymmetrically substituted hydrazines, reactions at both termini were observed.^[33] In analogy to previous investigations of the ambident reactivity of numerous nucleophiles,^[34] the benzhydrylium methodology should be used to quantify the reactivities of unsymmetrical hydrazines and to elucidate the factors which control their regioselectivities.

In summary, the investigations in this work should be devoted to the quantification of the nucleophilic reactivities of amines, hydrazines and pyridines, which shall subsequently be employed to characterize the electrophilic reactivities of acyl derivatives.

As most parts of this thesis that have already been published or accepted for publication, individual introductions will be given at the beginning of each chapter. In order to identify my contribution to multi-author publications, only the experiments, which were performed by me, are described within the corresponding Experimental Sections.

References

- [1] a) C. K. Ingold, *Recl. Trav. Chim. Pays-Bas* **1929**, *42*, 797–812; b) C. K. Ingold, *J. Chem. Soc.* **1933**, 1120–1127; c) C. K. Ingold, *Chem. Rev.* **1934**, *15*, 225–274.
- [2] C. G. Swain, C. B. Scott, *J. Am. Chem. Soc.* **1953**, *75*, 141–147.
- [3] C. D. Ritchie, *Acc. Chem. Res.* **1972**, *5*, 348–354.
- [4] a) C. D. Ritchie, *J. Am. Chem. Soc.* **1984**, *106*, 7187–7194; b) C. D. Ritchie, J. E. Van Verth, P. O. I. Virtanen, *J. Am. Chem. Soc.* **1982**, *104*, 3491–3497; c) C. D. Ritchie, *Pure Appl. Chem.* **1978**, *50*, 1281–1290; d) C. D. Ritchie, J. E. Van Verth, M. Sawada, *J. Am. Chem. Soc.* **1977**, *99*, 3754–3761.
- [5] C. D. Ritchie, *Can. J. Chem.* **1986**, *64*, 2239–2250.
- [6] H. Mayr, M. Patz, *Angew. Chem.* **1994**, *106*, 990–1010; *Angew. Chem. Int. Ed. Engl.* **1994**, *33*, 938–957.
- [7] a) H. Mayr, A. R. Ofial, *Pure Appl. Chem.* **2005**, *77*, 1807–1821; b) H. Mayr, B. Kempf, A. R. Ofial, *Acc. Chem. Res.* **2003**, *36*, 66–77; c) R. Lucius, R. Loos, H. Mayr, *Angew. Chem.* **2002**, *114*, 97–102; *Angew. Chem. Int. Ed.* **2002**, *41*, 91–95; d) H. Mayr, T. Bug, M. F. Gotta, N. Hering, B. Irrgang, B. Janker, B. Kempf, R. Loos, A. R. Ofial,

- G. Remennikov, H. Schimmel, *J. Am. Chem. Soc.* **2001**, *123*, 9500–9512; e) For a comprehensive listing of nucleophilicity parameters N , s_N and electrophilicity parameters E see <http://www.cup.uni-muenchen.de/oc/mayr/DBintro.html>.
- [8] R. Appel, H. Mayr, *J. Am. Chem. Soc.* **2011**, *133*, 8240–8251.
- [9] Selected examples: a) J. P. Guthrie in *Reviews of Reactive Intermediate Chemistry* (Eds.: M. S. Platz, R. A. Moss, M. Jones, Jr.), Wiley-Interscience, Hoboken, **2007**, pp. 3–45; b) D. P. N. Satchell, R. S. Satchell in *Supplement B: The Chemistry of Acid Derivatives, Vol. 2* (Ed.: S. Patai), John Wiley & Sons, New York, **1992**, pp. 748–802 and references cited therein.
- [10] Selected Examples: a) C. Grondal, M. Jeanty, D. Enders, *Nature Chem.* **2010**, *2*, 167–178; b) D. W. C. MacMillan, *Nature* **2008**, *455*, 304–308; c) J. Seayad, B. List, *Org. Biomol. Chem.* **2005**, *3*, 719–724; d) P. I. Dalko, L. Moisan, *Angew. Chem.* **2004**, *116*, 5248–5286; *Angew. Chem. Int. Ed.* **2004**, *43*, 5138–5175 and references cited therein.
- [11] K. A. Ahrendt, C. J. Borths, D. W. C. MacMillan, *J. Am. Chem. Soc.* **2000**, *122*, 4243–4244.
- [12] J. von Liebig, *Liebigs Ann. Chem.* **1860**, *113*, 246–247.
- [13] B. List, *Angew. Chem.* **2010**, *122*, 1774–1779; *Angew. Chem. Int. Ed.* **2010**, *49*, 1730–1734.
- [14] a) G. Höfle, W. Steglich, H. Vorbrüggen, *Angew. Chem.* **1969**, *81*, 1001; *Angew. Chem. Int. Ed. Engl.* **1969**, *8*, 981. b) L. M. Litvinenko, A. I. Kirichenko, *Dokl. Akad. Nauk SSSR, Ser. Khim.* **1967**, *176*, 97–100.
- [15] A. B. Baylis, M. E. D. Hillman, US Pat. 3,743,669, **1973**; *Chem. Abstr.* **1972**, *77*, 34174q.
- [16] a) Z. G. Hajos, D. R. J. Parrish, *J. Org. Chem.* **1974**, *39*, 1615–1621; b) U. Eder, G. Sauer, R. Wiechert, *Angew. Chem.* **1971**, *83*, 492–493; *Angew. Chem. Int. Ed. Engl.* **1971**, *10*, 496–497.
- [17] B. List, R. A. Lerner, C F. Barbas III, *J. Am. Chem. Soc.* **2000**, *122*, 2395–2396.
- [18] a) J. Seayad, B. List, *Org. Biomol. Chem.* **2005**, *3*, 719–724; b) S. E. Denmark, G. L. Beutner, *Angew. Chem.* **2008**, *120*, 1584–1663; *Angew. Chem. Int. Ed.* **2008**, *47*, 1560–1638.
- [19] H. Mayr, S. Lakhdar, B. Maji, A. R. Ofial, *Beilstein J. Org. Chem.* **2012**, accepted and references cited therein.

- [20] S. Lakhdar, R. Appel, H. Mayr, *Angew. Chem.* **2009**, *121*, 5134–5137; *Angew. Chem. Int. Ed.* **2009**, *48*, 5034–5037.
- [21] a) N. De Rycke, F. Couty, O. R. P. David, *Chem. Eur. J.* **2011**, *17*, 12852–12871; b) C. E. Müller, P. R. Schreiner, *Angew. Chem.* **2011**, *123*, 6136–6167; *Angew. Chem. Int. Ed.* **2011**, *50*, 6012–6042; c) A. C. Spivey, S. Arseniyadis, *Angew. Chem.* **2004**, *116*, 5552–5557; *Angew. Chem. Int. Ed.* **2004**, *43*, 5436–5441; d) R. Murugan, E. F. V. Scriven, *Aldrichimica Acta* **2003**, *36*, 21–27 and references cited therein.
- [22] a) S. Xu, I. Held, B. Kempf, H. Mayr, W. Steglich, H. Zipse, *Chem. Eur. J.* **2005**, *11*, 4751–4757.
- [23] Selected examples: a) I. Held, S. Xu, H. Zipse, *Synthesis* **2007**, *8*, 1185–1196; b) S. Singh, G. Das, O. V. Singh, H. Han, *Org. Lett.* **2007**, *9*, 401–404; c) M. R. Heinrich, H. S. Klisa, H. Mayr, W. Steglich, H. Zipse, *Angew. Chem.* **2003**, *115*, 4975–4977; *Angew. Chem. Int. Ed.* **2003**, *42*, 4826–4828; d) W. Steglich, G. Höfle, *Tetrahedron Lett.* **1970**, *11*, 4727–4730.
- [24] a) O. Exner, *J. Phys. Org. Chem.* **1999**, *12*, 265–274; b) M. Charton, *J. Phys. Org. Chem.* **1999**, *12*, 275–282; c) V. Galkin, *J. Phys. Org. Chem.* **1999**, *12*, 283–288; d) O. Exner, M. Charton, V. Galkin, *J. Phys. Org. Chem.* **1999**, *12*, 289.
- [25] G. C. Fu in *Asymmetric Synthesis* (Eds.: M. Christmann, S. Braese), *2nd ed.*, Wiley-VCH, Weinheim, **2008**, pp 195–199; b) G. C. Fu, *Acc. Chem. Res.* **2004**, *37*, 542–547 and references cited therein.
- [26] a) V. B. Birman, H. Jiang, X. Li, L. Guo, E. W. Uffman, *J. Am. Chem. Soc.* **2006**, *128*, 6536–6537; b) V. B. Birman, L. Guo, *Org. Lett.* **2006**, *8*, 4859–4861; c) V. B. Birman, X. Li, *Org. Lett.* **2006**, *8*, 1351–1354.
- [27] J. E. Taylor, S. D. Bull, J. M. J. Williams, *Chem. Soc. Rev.* **2012**, *41*, 2109–2121 and references cited therein.
- [28] C. Joannesse, C. P. Johnston, L. C. Morrill, P. A. Woods, M. Kieffer, T. A. Nigst, H. Mayr, T. Lebl, D. Philp, R. A. Bragg, A. D. Smith, *Chem. Eur. J.* **2012**, *18*, 2398–2408.
- [29] C. L. Allen, B. N. Atkinson, J. M. J. Williams, *Angew. Chem.* **2012**, *124*, 1412–1415; *Angew. Chem. Int. Ed.* **2012**, *51*, 1383–1386.
- [30] J. O. Edwards, R. G. Pearson, *J. Am. Chem. Soc.* **1962**, *84*, 16–24.
- [31] a) P. Muller, *Pure Appl. Chem.* **1994**, *66*, 1077–1184; b) S. Hoz, E. Buncl, E. *Isr. J. Chem.* **1985**, *26*, 313–319.

- [32] a) E. Buncl, I.-H. Um, *Tetrahedron* **2004**, *60*, 7801–7825; b) A. P. Grekov, V. Y. Veselov, *Russ. Chem. Rev.* **1978**, *47*, 631–648; c) N. J. Fina, J. O. Edwards, *Int. J. Chem. Kinet.* **1973**, *5*, 1–26; d) W. P. Jencks, *Catalysis in Chemistry and Enzymology*, McGraw-Hill, New York, **1969**, pp. 107–110 and references cited therein.
- [33] a) U. Ragnarsson, *Chem. Soc. Rev.* **2001**, *30*, 205–213; b) E. W. Schmidt, *Hydrazines and its Derivatives: Preparation, Properties, Applications, 2nd ed.*, VCH, Weinheim, **2001** and references therein.
- [34] H. Mayr, M. Breugst, A. R. Ofial, *Angew. Chem.* **2011**, *123*, 6598–6634; *Angew. Chem. Int. Ed.* **2011**, *50*, 6470–6505.

Chapter 3

NUCLEOPHILIC REACTIVITIES OF PRIMARY AND SECONDARY AMINES IN ACETONITRILE

Tanja Kanzian, Tobias A. Nigst, Andreas Maier, Stefan Pichl, and Herbert Mayr in *Eur. J. Org. Chem.* **2009**, 6379–6385.

The results obtained by T. Kanzian are not listed in the Experimental Section.

3.1 Introduction

Amines are amongst the most important reagents in organic synthesis, and numerous kinetic investigations have been performed to determine their nucleophilic reactivities in various types of reactions.^[1] They have been characterized on the Swain-Scott n scale as well as on the Ritchie N_+ scale.^[1d,2]

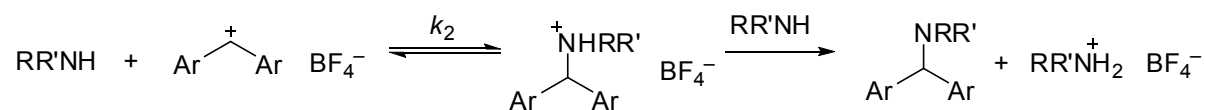
Recently, we employed Equation (3.1), which characterizes nucleophiles by the parameters N and s_N , and electrophiles by the parameter E ,^[3] for determining N and s_N for a variety of amines in aqueous solution.^[4] In this way it became possible to add amines to our comprehensive nucleophilicity scale, which includes n , π , and σ nucleophiles.^[5] Comparison with the few available data in DMSO^[4a,6] and methanol^[7] showed that amine nucleophilicities are strongly dependent on the solvent, in contrast to the nucleophilicities of most neutral π and σ nucleophiles.

$$\log k_2(20\text{ }^\circ\text{C}) = s_N(N + E) \quad (3.1)$$

Systematic investigations of the nucleophilic reactivities of amines in acetonitrile have so far not been reported. Such data are of eminent importance for two reasons. (a) Acetonitrile is an ideal solvent for exploring the combat zone of nucleophilic aliphatic substitutions, that is, the zone in which the change from the S_N1 to S_N2 mechanism occurs.^[6,8] (b) Acetonitrile is the solvent of choice for the photoheterolytic cleavage of carbocation precursors.^[9] By using nanosecond laser pulses it is possible to generate carbocations in acetonitrile in the presence

of various nucleophiles and to determine the rates of reactions along the borderline between activation and diffusion control, typically second-order rate constants from 10^8 to $10^{10} \text{ M}^{-1} \text{ s}^{-1}$.^[10]

Knowledge of rate constants along this borderline is crucial for the understanding of structure–reactivity relationships, for example, correlations between reactivity and selectivity as well as the breakdown of linear free energy relationships.^[11] Because many of these investigations involve reactions with amines in acetonitrile,^[9a,9b] we have now determined the N and s_N parameters of primary and secondary amines using benzhydryl cations (Table 3.1) as reference electrophiles as described previously (Scheme 3.1).^[5a]



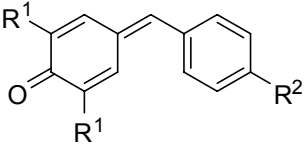
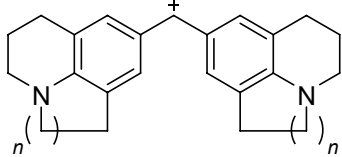
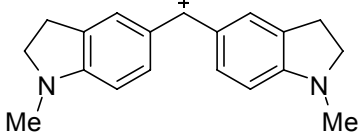
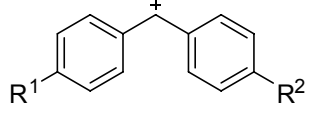
Scheme 3.1. Reactions of amines with benzhydrylium ions.

3.2 Results and Discussion

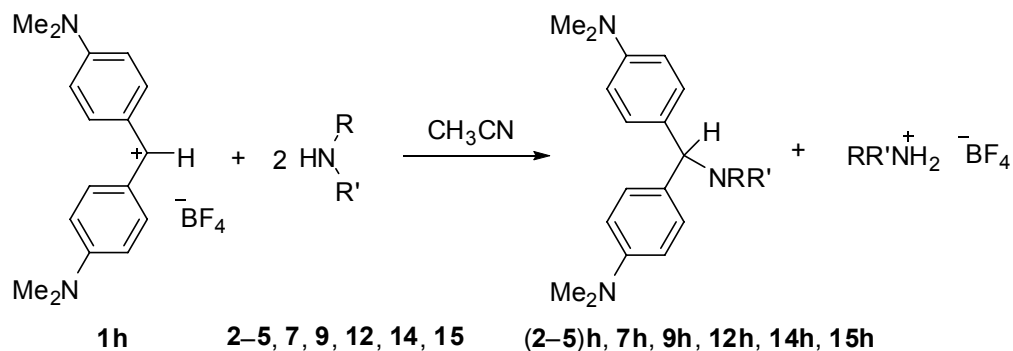
3.2.1 Product Characterization

A combination of the benzhydrylium salt **1h**BF₄ with 2–3 equiv. of the amines **2–5**, **7**, **9**, **12**, **14**, and **15** in acetonitrile gave the corresponding benzhydrylamines **2h–5h**, **7h**, **9h**, **12h**, **14h**, and **15h**, respectively (Scheme 3.2). The chemical shifts of the Ar₂CH-protons and the isolated yields are listed in Table 3.1.

Table 3.1. List of electrophiles used in this study.

| Reference Electrophile ^[a] | $E^{[b]}$ |
|--|---|
|  | $R^1 = tBu, R^2 = OMe$ ani(<i>t</i> Bu) ₂ QM (1a) -16.11 $R^1 = tBu, R^2 = Me$ tol(<i>t</i> Bu) ₂ QM (1b) -15.83 $R^1 = Ph, R^2 = OMe$ ani(Ph) ₂ QM (1c) -12.18 |
|  | $n = 1$ (lil) ₂ CH ⁺ (1d) -10.04 $n = 2$ (jul) ₂ CH ⁺ (1e) -9.45 |
|  | (ind) ₂ CH ⁺ (1f) -8.76 |
|  | $R^1 = R^2 = N$ -pyrrolidino (pyr) ₂ CH ⁺ (1g) -7.69 $R^1 = R^2 = NMe_2$ (dma) ₂ CH ⁺ (1h) -7.02 $R^1 = R^2 = N(Me)Ph$ (mpa) ₂ CH ⁺ (1i) -5.89 $R^1 = R^2 = N(Me)CH_2CF_3$ (mfa) ₂ CH ⁺ (1j) -3.85 $R^1 = R^2 = OMe$ (ani) ₂ CH ⁺ (1k) 0.00 $R^1 = OMe, R^2 = Me$ (ani)(tol)CH ⁺ (1l) 1.48 $R^1 = R^2 = Me$ (tol) ₂ CH ⁺ (1m) 3.63 $R^1 = Me, R^2 = H$ Ph(tol)CH ⁺ (1n) 4.59 $R^1 = R^2 = H$ Ph ₂ CH ⁺ (1o) 5.90 |

[a] Counterion of the benzhydryl cations: BF₄⁻. [b] Electrophilicity parameters E from Refs. [5a,b].



Scheme 3.2. Reactions of amines with 4,4'-bis(dimethylamino)benzhydrylium tetrafluoroborate **1h**BF₄.

Table 3.2. ^1H NMR chemical shifts of the Ar_2CH group of the products of the reactions of **1h** with **2–5**, **7**, **9**, **12**, **14**, and **15** and yields of the isolated products.

| Amine | Product | δ_{H} [ppm] | Yield [%] |
|--|------------|---------------------------|-----------|
| 2,2,2-Trifluoroethylamine (2) | 2h | 4.80 | 85 |
| <i>tert</i> -Butylamine (3) | 3h | 4.88 | 98 |
| Isopropylamine (4) | 4h | 4.81 | 90 |
| Ethanolamine (5) | 5h | 4.69 | 98 |
| Allylamine (7) | 7h | 4.70 | 97 |
| <i>n</i> -Butylamine (9) | 9h | 4.65 | 95 |
| Diethylamine (12) | 12h | 4.50 | 45 |
| Piperidine (14) | 14h | 3.99 | 71 |
| Pyrrolidine (15) | 15h | 3.97 | 67 |

3.2.2 Kinetics of the Reactions of the Amines **2–15** with the Reference Electrophiles **1**

The rates of the reactions of the amines with the reference electrophiles **1a–j** were determined spectrophotometrically in CH_3CN at 20 °C. For the kinetic studies, the amines **2–15** were used in large excess (over 10 equiv.) relative to the electrophiles **1** to ensure first-order conditions. Details are given in the Experimental Section. The first-order rate constants k_{obs} were obtained from the exponential decays of the absorbances of the electrophiles (Figure 3.1).

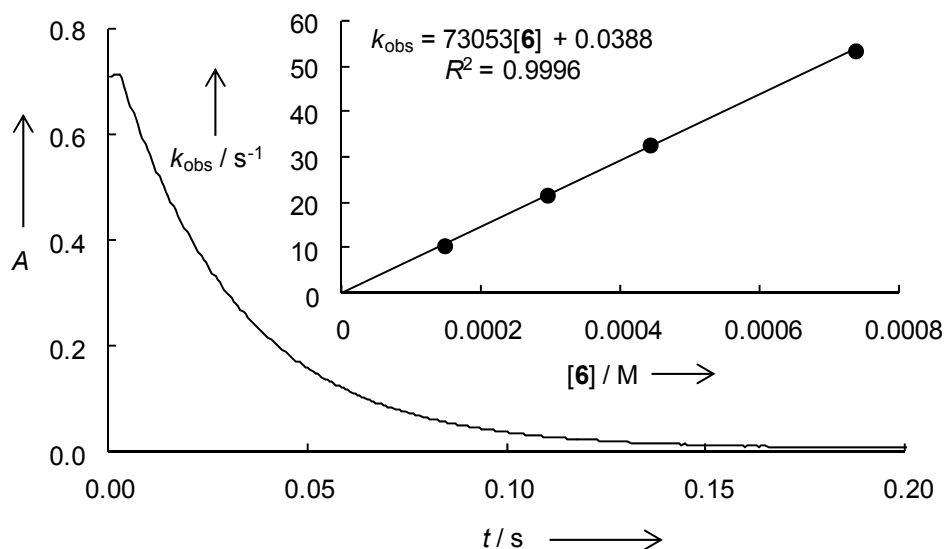


Figure 3.1. Exponential decay of the absorbance at 613 nm during the reaction of **1h** with benzylamine ($[\mathbf{6}] = 4.42 \times 10^{-4} \text{ M}$; $k_{\text{obs}} = 32.7 \text{ s}^{-1}$). Inset: Determination of the second-order rate constant k_2 ($7.31 \times 10^4 \text{ M}^{-1} \text{ s}^{-1}$) as the slope of the first-order rate constants k_{obs} versus the concentration of the amine **6**.

Plots of k_{obs} versus amine concentration were linear for the reactions of the primary and secondary amines **2–15** with the benzhydrylium ions **1d–o** (inset of Figure 3.1) and for the reactions of the primary amines **2–9** with the quinone methides **1a–c**. In these reactions the attack of the amines on the electrophiles is rate-limiting and the slopes of these plots give the second-order rate constants k_2 [Eq. (3.2)], which are listed in Table 3.3.

$$k_{\text{obs}} = k_2[\text{amine}] \quad (3.2)$$

Table 3.3. Second-order rate constants for the reactions of the reference electrophiles **1** with the amines **2–15** in acetonitrile at 20 °C.

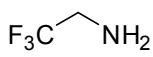
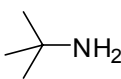
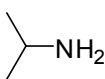
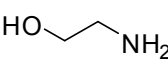
| Amine | N, s_N | Electrophile | k_2 [$M^{-1} s^{-1}$] |
|---|-------------|--------------|---------------------------|
|  2 | 10.13, 0.75 | 1h | 1.43×10^2 |
| | | 1i | 2.53×10^3 |
| | | 1j | 4.03×10^4 |
| | | 1k | 3.50×10^7 [a] |
| | | 1l | 1.50×10^8 [a,b] |
| | | 1m | 8.50×10^8 [a,b] |
| | | 1n | 1.70×10^9 [a,b] |
| | | 1o | 2.00×10^9 [a,b] |
|  3 | 12.35, 0.72 | 1c | 1.52 |
| | | 1d | 4.15×10^1 |
| | | 1f | 3.34×10^2 |
| | | 1i | 5.13×10^4 |
| | | 1j | 5.13×10^4 |
|  4 | 13.77, 0.70 | 1c | 1.56×10^1 |
| | | 1d | 2.97×10^2 |
| | | 1f | 2.43×10^3 |
| | | 1g | 2.13×10^4 |
| | | 1h | 5.24×10^4 |
| | | 1i | 5.24×10^4 |
|  5 | 14.11, 0.71 | 1c | 2.71×10^1 |
| | | 1d | 5.85×10^2 |
| | | 1f | 4.94×10^3 |
| | | 1g | 4.24×10^4 |
| | | 1h | 1.02×10^5 |

Table 3.3 (continued).

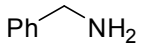
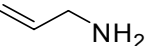
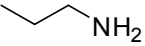
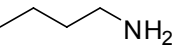
| Amine | N, s_N | Electrophile | k_2 [$M^{-1} s^{-1}$] |
|---|--------------------------|---|---------------------------|
|  6 | 14.29, 0.67 | 1b | 1.10×10^{-1} |
| | | 1c | 2.06×10^1 |
| | | 1d | 6.53×10^2 |
| | | 1f | 4.61×10^3 |
| | | 1g | 3.48×10^4 |
| | | 1h | 7.29×10^4 |
|  7 | 14.37, 0.66 | 1b | 1.25×10^{-1} |
| | | 1d | 5.09×10^2 |
| | | 1f | 4.32×10^3 |
| | | 1g | 3.64×10^4 |
| | | 1h | 8.61×10^4 |
| | |  8 | 15.11, 0.63 |
| 1b | 3.82×10^{-1} | | |
| 1c | 5.46×10^1 | | |
| 1d | 1.38×10^3 | | |
| 1e | 3.87×10^3 | | |
| 1f | 7.54×10^3 | | |
| 1g | 6.77×10^4 | | |
| 1h | 1.43×10^5 | | |
| 1k | 1.00×10^9 [a,b] | | |
| 1l | 2.30×10^9 [a,b] | | |
| 1m | 4.10×10^9 [a,b] | | |
| 1n | 4.40×10^9 [a,b] | | |
| 1o | 4.50×10^9 [a,b] | | |
|  9 | 15.27, 0.63 | 1a | 3.41×10^{-1} |
| | | 1c | 7.49×10^1 |
| | | 1f | 1.03×10^4 |
| | | 1h | 2.12×10^5 |

Table 3.3 (continued).

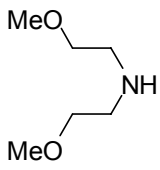
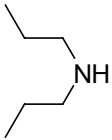
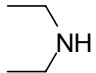
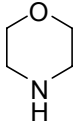
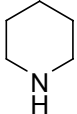
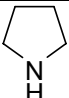
| Amine | N, s_N | Electrophile | k_2 [$M^{-1} s^{-1}$] |
|--|-------------|--------------|--|
|  10 | 13.24, 0.93 | 1c | 7.89 ^[b,c] |
| | | 1d | 1.12×10^3 |
| | | 1e | 4.47×10^3 |
| | | 1f | 1.25×10^4 |
| | | 1g | 1.17×10^5 |
|  11 | 14.51, 0.80 | 1c | 6.74×10^1 ^[c] |
| | | 1d | 3.95×10^3 |
| | | 1e | 1.38×10^4 |
| | | 1f | 3.17×10^4 |
| | | 1g | 2.77×10^5 |
|  12 | 15.10, 0.73 | 1c | 1.51×10^2 ^[c] |
| | | 1d | 4.62×10^3 |
| | | 1e | 1.29×10^4 |
| | | 1f | 3.49×10^4 |
| | | 1g | 3.24×10^5 |
|  13 | 15.65, 0.74 | 1b | 2.03×10^{-1} ^[b,c] |
| | | 1c | 3.85×10^2 ^[c] |
| | | 1d | 1.15×10^4 |
| | | 1e | 4.11×10^4 |
| | | 1f | 1.04×10^5 |
| | | 1g | 8.03×10^5 |
|  14 | 17.35, 0.68 | 1a | 6.04 ^[c] |
| | | 1b | 1.23×10^1 ^[c] |
| | | 1c | 3.52×10^3 |
| | | 1d | 7.85×10^4 |
| | | 1e | 2.69×10^5 |

Table 3.3 (continued).

| Amine | N, s_N | Electrophile | k_2 [$M^{-1} s^{-1}$] |
|--|-------------|--------------|---------------------------|
|  15 | 18.64, 0.60 | 1a | 3.25×10^1 |
| | | 1b | 4.82×10^1 |
| | | 1d | 1.18×10^5 |
| | | 1e | 3.50×10^5 |

[a] Second-order rate constants k_2 from Ref. [9b]. [b] Not included in the determination of the N and s_N parameters. [c] k_2 was derived from Equation (3.7) and is less precise.

In the case of trifluoroethylamine (**2**) and N,N -bis(2-methoxyethyl)amine (**10**) the reactions with benzhydrylium ions of low reactivity become reversible, which is reflected by the positive intercepts in the plots of k_{obs} versus amine concentration.

For the reactions of the secondary amines **10–12** with the quinone methide **1c** (**1a** and **1b** were not studied), of morpholine (**13**) with the quinone methides **1b** and **1c**, and of piperidine (**14**) with the quinone methides **1a** and **1b**, the plots of k_{obs} versus amine concentration are not linear (Figure 3.2).

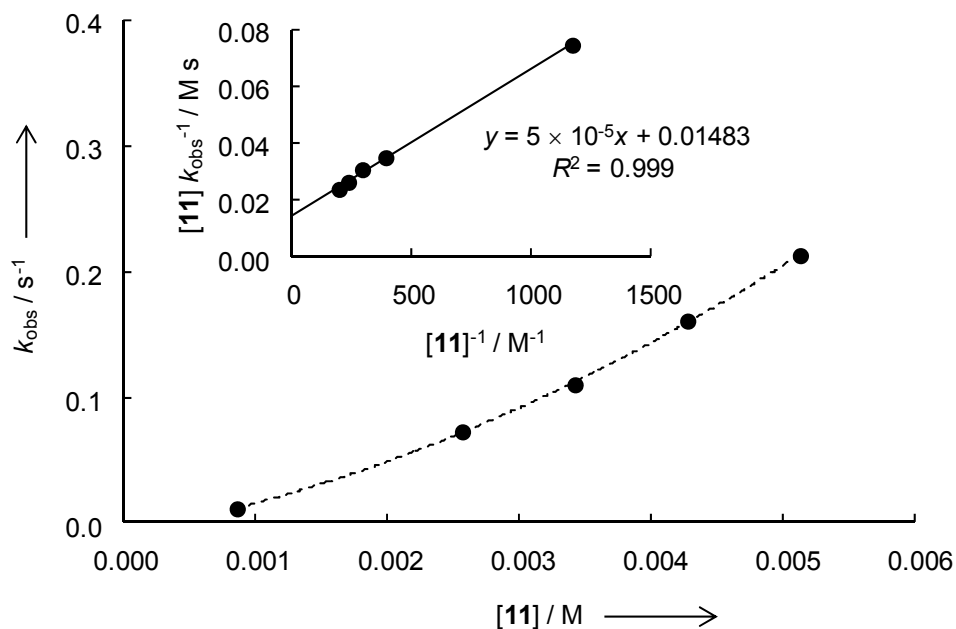
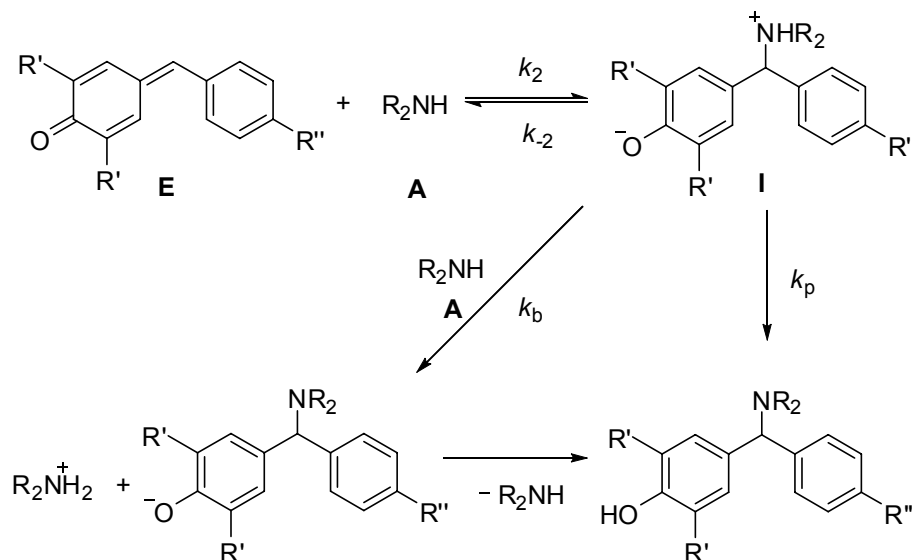


Figure 3.2. Plots of k_{obs} versus $[11]$ and $[11]/k_{\text{obs}}$ versus $1/[11]$ (inset) for the reaction of **11** with the quinone methide **1c**. The k_2 value for the reaction is $1/(0.0148 \text{ M s}) = 67.4 \text{ M}^{-1} \text{ s}^{-1}$.

The upward curvature in the plots of k_{obs} versus amine concentration indicate that a second molecule of the amine is involved in the reaction as a base catalyst (Scheme 3.3).



Scheme 3.3. Reactions of secondary amines with quinone methides.

Analogous behavior has been reported for the reactions of secondary amines with thiocarbonates,^[12] thionobenzoates,^[13] and activated esters of indole-3-acetic acid.^[14] The change in the concentration of the zwitterionic intermediate **I** can be expressed by Equation (3.3).

$$\frac{d[\mathbf{I}]}{dt} = k_2[\mathbf{E}][\mathbf{A}] - k_{-2}[\mathbf{I}] - k_b[\mathbf{I}][\mathbf{A}] - k_p[\mathbf{I}] \quad (3.3)$$

By assuming a steady-state concentration for the intermediate **I**, the rate law can be expressed by Equations (3.4) and (3.5).

$$-d[\mathbf{E}]/dt = k_2[\mathbf{E}][\mathbf{A}](k_a[\mathbf{A}] + k_p)/(k_{-2} + k_b[\mathbf{A}] + k_p) \quad (3.4)$$

$$k_{\text{obs}} = k_2[\mathbf{A}](k_a[\mathbf{A}] + k_p)/(k_{-2} + k_b[\mathbf{A}] + k_p) \quad (3.5)$$

Let us first neglect the direct proton-transfer from NH^+ to O^- in the zwitterionic intermediate **I**. Equation (3.5) is then reduced to Equation (3.6), which can be transformed into Equation (3.7).

$$k_{\text{obs}} = k_2[\mathbf{A}]^2 k_a / (k_{-2} + k_b[\mathbf{A}]) \quad (3.6)$$

$$[\mathbf{A}] / k_{\text{obs}} = 1/k_2 + k_{-2}/k_2[\mathbf{A}]k_b \quad (3.7)$$

The linear plot of $[\mathbf{A}] / k_{\text{obs}}$ against $1/[\mathbf{A}]$, as depicted in the inset of Figure 3.2, shows that this formalism holds for a wide range of concentrations. As shown in the Experimental Section, deviations from these linear plots occur only at very low amine concentrations and are explained by the operation of k_p . If the k_{obs} values at very low amine concentrations are neglected, the k_2 values can be obtained from the intercepts ($1/k_2$) of the linear correlations [see inset of Figure 3.2 and Eq. (3.7)]. If $k_{-2} \ll k_a[\mathbf{A}]$, Equation (3.6) is transformed into Equation (3.2), that is, a second-order reaction with rate-determining formation of the CN bond. Although this situation holds for all reactions with benzhydrylium ions, linearity between k_{obs} and [amine] was never reached for reactions of the quinone methide **1a** with **14**, **1b** with **13**, and **1c** with **10–14**, even when very high amine concentrations were used. The second-order rate constants k_2 are listed in Table 3.3.

When the logarithms of the second-order rate constants are plotted against the previously reported electrophilicity parameters E of the reference systems, linear correlations are obtained (Figure 3.3), which yield the nucleophile-specific parameters N and s that are listed in Table 3.3. The rate constants for the reactions of trifluoroethylamine (**2**) with **11–o** and for the reactions of *n*-propylamine (**8**) with **1k–o**^[9b] were not included in the determination of the nucleophilicity parameters, because these reactions are close to diffusion controlled. As the s_N parameters of the amines differ only slightly, their relative nucleophilicities are almost independent of the nature of the electrophiles, and the reactivities of the amines can be compared by only regarding their N parameters, which cover the reactivity range of $10 < N < 19$. The less reactive amines react with similar rates as silyl ketene acetals, trialkyl-substituted pyrroles, and pyridines, whereas the more reactive amines show a similar nucleophilicity to stabilized carbanions (Figure 3.4).

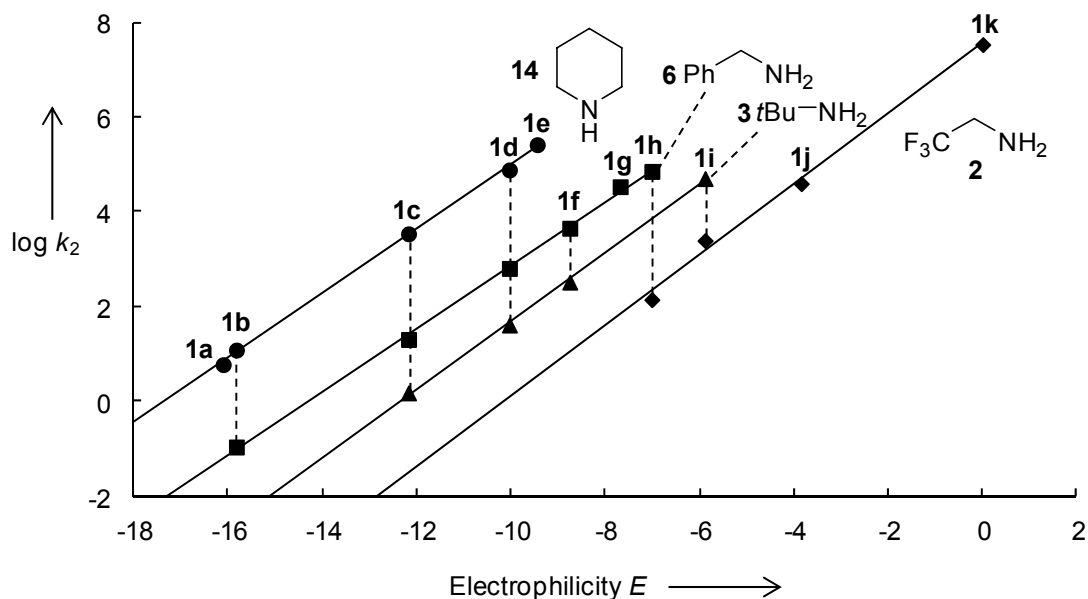


Figure 3.3. Plots of the second-order rate constants $\log k_2$ (20 °C) for the reactions of **2**, **3**, **6**, and **14** with benzhydrylium ions and quinone methides in CH_3CN versus the E parameters of the reference electrophiles

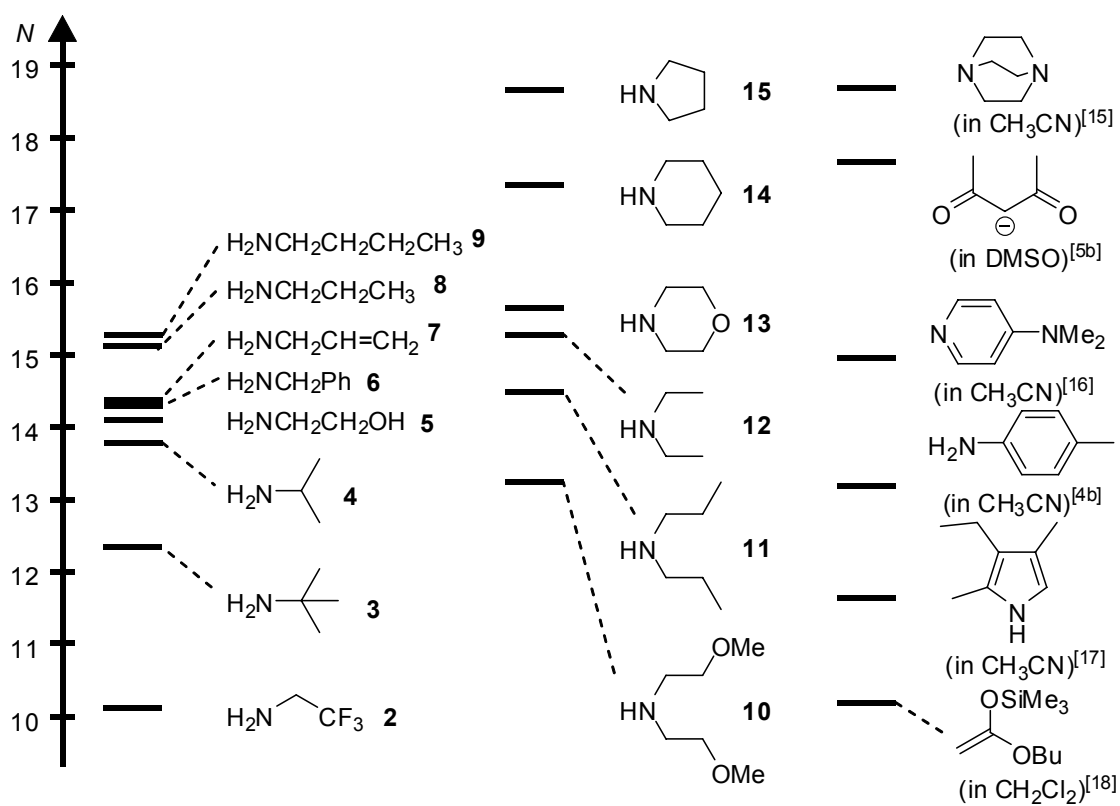


Figure 3.4. Comparison of the nucleophilic reactivities of amines in acetonitrile with other nucleophiles.

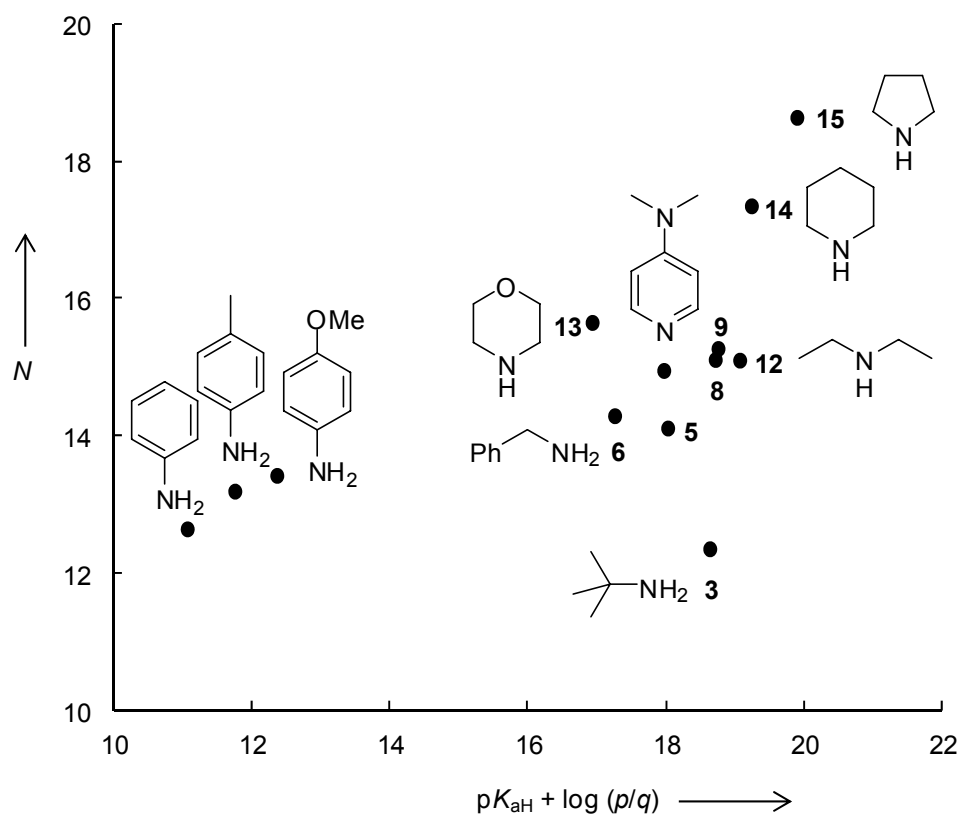


Figure 3.5. Plot of the N parameters of amines in acetonitrile versus the statistically corrected basicities in acetonitrile (p = numbers of protons of the conjugated acid).^[4b,19]

Figure 3.5 shows that the nucleophilic reactivities of the amines correlate only poorly with the corresponding pK_{aH} values in acetonitrile.^[19] As previously reported for the reactions of amines in water,^[4b] it is thus not possible to predict nucleophilic reactivities of amines in CH_3CN on the basis of their pK_{aH} values.

In previous work we have reported that aniline is approximately five times more nucleophilic in water than propylamine^[4b] despite the considerably higher basicity (pK_{aH}) of the aliphatic amine. We now find that in CH_3CN the reactivity order is reverse, and primary and secondary alkylamines are more nucleophilic than aniline^[4b] ($N = 12.64$, $s = 0.68$).

This reversal of the relative reactivities is due to the different effects of solvent on the reactivities of aromatic and aliphatic amines. Whereas aniline and *p*-toluidine have similar nucleophilicities in water and acetonitrile (for aniline + **1h**: $k_{CH_3CN}/k_{H_2O} = 0.42$), alkylamines are typically one to two orders of magnitude more reactive in acetonitrile than in water (for propylamine + **1h**: $k_{CH_3CN}/k_{H_2O} = 46$).

Thus, although the nucleophilicity order alkylamines > aniline in acetonitrile is the same as that of the relative basicities (pK_{aH}), the correlation in Figure 3.5 shows that anilines in acetonitrile are considerably more reactive than expected on the basis of their basicities. In other words, the previously reported surprisingly high nucleophilicities of anilines are not a water-specific phenomenon.

In previous work we mentioned that the reliability of Equation (3.1) to predict rate constants for the addition of amines to various Michael acceptors is limited because of variable stabilizing interactions between the NH protons and the different basic sites in the Michael acceptors.^[20] Although Figure 3.3 demonstrates that the reactivities of amines towards benzhydrylium ions and quinone methides correlate excellently with their electrophilicity parameters E , which have been derived from their reactivities towards C nucleophiles, significant deviations are found by applying Equation (3.1) to the addition of amines to other types of Michael acceptors in CH_3CN . Table 3.4 shows that in several cases the calculated rate constants deviate by more than a factor of 10^2 [the common confidence limit of Equation (3.1)] from the experimental values. It is presently not clear whether these unusually high deviations are due to variable interactions of the NH protons with the basic sites of the Michael acceptors or whether these reactions require a specific treatment of solvent effects.

Table 3.4. Comparison of calculated and experimental rate constants ($\text{M}^{-1} \text{s}^{-1}$) for the additions of amines to Michael acceptors in acetonitrile

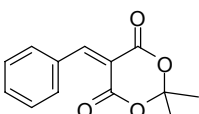
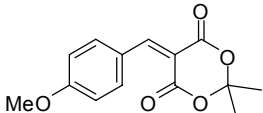
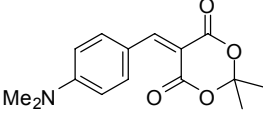
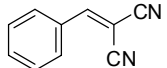
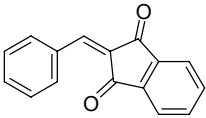
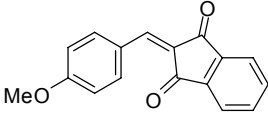
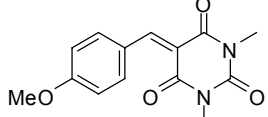
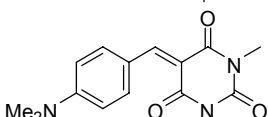
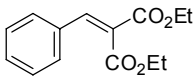
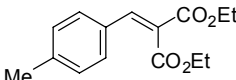
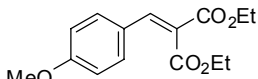
| Electrophile | E | Amine | N, s_N | $k_{\text{calc}} (20\text{ }^\circ\text{C})^{[a]}$ | k_{exp} |
|---|-----------------------|-----------|-------------|--|--|
|  | -9.15 ^[b] | 14 | 17.35, 0.68 | 3.8×10^5 | $2.3 \times 10^6 (25\text{ }^\circ\text{C})^{[c]}$ |
| | | 13 | 15.65, 0.74 | 6.5×10^4 | $4.0 \times 10^5 (25\text{ }^\circ\text{C})^{[c]}$ |
| | | 6 | 14.29, 0.67 | 2.8×10^3 | $8.7 \times 10^1 (20\text{ }^\circ\text{C})^{[d]}$ |
|  | -10.28 ^[b] | 14 | 17.35, 0.68 | 6.4×10^4 | $9.5 \times 10^5 (25\text{ }^\circ\text{C})^{[c]}$ |
| | | 6 | 14.29, 0.67 | 4.9×10^2 | $6.7 \times 10^1 (20\text{ }^\circ\text{C})^{[d]}$ |
|  | -12.76 ^[b] | 14 | 17.35, 0.68 | 1.3×10^3 | $1.1 \times 10^5 (25\text{ }^\circ\text{C})^{[c]}$ |
|  | -9.42 ^[e] | 6 | 14.29, 0.67 | 1.8×10^3 | $1.5 (20\text{ }^\circ\text{C})^{[f]}$ |

Table 3.4 (continued).

| Electrophile | E | Amine | N, s_N | $k_{\text{calc}} (20\text{ }^\circ\text{C})^{[a]}$ | k_{exp} |
|---|-----------------------|-----------|-------------|--|---|
|  | -10.11 ^[g] | 6 | 14.29, 0.67 | 6.3×10^2 | 1.5 (25 °C) ^[h] |
|  | -11.32 ^[g] | 6 | 14.29, 0.67 | 9.8×10^1 | 1.1 (25 °C) ^[h] |
|  | -10.37 ^[i] | 14 | 17.35, 0.68 | 5.6×10^4 | 3.2×10^5 (25 °C) ^[c] |
|  | -12.76 ^[i] | 14 | 17.35, 0.68 | 1.3×10^3 | 2.9×10^4 (25 °C) ^[c] |
|  | -20.55 ^[j] | 6 | 14.29, 0.67 | 6.4×10^{-5} | 2.5×10^{-2} (20 °C) ^[k] |
|  | -21.11 ^[j] | 6 | 14.29, 0.67 | 2.7×10^{-5} | 1.8×10^{-2} (20 °C) ^[k] |
|  | -21.47 ^[j] | 6 | 14.29, 0.67 | 1.5×10^{-5} | 1.3×10^{-2} (20 °C) ^[k] |

[a] Calculated on the basis of Equation (3.1). [b] From Ref. [20c]. [c] From Ref. [1b]. [d] From Ref. [1w]. [e] From Ref. [23]. [f] From Ref. [1m]. [g] From Ref. [20a]. [h] From Ref. [1q]. [i] From Ref. [20b]. [j] From Ref. [24]. [k] From Ref. [1y].

3.3 Conclusion

The reactions of primary and secondary amines with benzhydrylium ions **1d–o** and of primary amines with quinone methides **1a–c** in acetonitrile follow a second-order rate law, which indicates rate-determining attack of the amines on the electrophiles. In contrast, for most of the reactions of the secondary amines **10–15** with the quinone methides **1a–c** the initial electrophile–nucleophile combination step is reversible and the more complicated rate law Equation (3.6) has to be employed to derive the rate constants k_2 for the attack of the amines on the electrophiles. From the linear correlations of $\log k_2$ with the electrophilicity parameters E of the benzhydrylium ions, the nucleophile-specific parameters N and s_N for amines in CH_3CN have been derived. The poor correlation between N and $\text{p}K_{\text{aH}}$ shows that also in acetonitrile, relative basicities cannot be used to predict relative nucleophilicities. Solvent

polarity affects the reactivities of alkylamines and anilines quite differently: Whereas anilines react approximately two times faster with benzhydrylium ions in water than in acetonitrile, primary alkylamines react at least 10 times faster in acetonitrile than in water. The opposite solvent effect on these closely related reactions demonstrates the limitation of the Hughes–Ingold rules^[21] to predict solvent effects on polar organic reactions on the basis of the relative charge dispersal in the ground and transition states.

3.4 Experimental Section

3.4.1 General Comment

Materials. 2,2,2-Trifluoroethylamine (**2**), *tert*-butylamine (**3**), isopropylamine (**4**), ethanolamine (**5**), benzylamine (**6**), allylamine (**7**), *n*-butylamine (**9**), were purchased and purified by distillation prior to use.

Analytics. ¹H (300 or 400 MHz), ¹³C (75.5 or 100 MHz) and ¹⁹F NMR (282 MHz) spectra were recorded with a Bruker ARX 300 or Varian Inova 400 instrument. The chemical shifts in ppm refer to the solvent residual signal of CDCl₃ ($\delta_{\text{H}} = 7.26$, $\delta_{\text{C}} = 77.0$) as internal standard. The following abbreviations were used for signal multiplicities: s = singlet, d = doublet, t = triplet, q = quartet, m = multiplet, br = broad. NMR signal assignments were based on additional 2D-NMR experiments (COSY, HSQC, and HMBC). For reasons of simplicity, the ¹H NMR signals of AA'BB'-spin systems of *p*-substituted aromatic rings were treated as doublets.

Mass spectra were recorded with a MAT 95 Q instrument.

Kinetics. The kinetics of the reactions of the benzhydrylium ions with the amines were followed by UV/Vis spectrophotometry by using work-stations similar to those described previously.^[5a,22]

For slow reactions ($\tau_{1/2} > 10$ s) the UV/Vis spectra were collected at different times by using a J&M TIDAS diode array spectrophotometer connected to a Hellma 661.502-QX quartz Suprasil immersion probe (5 mm light path) by fiber optic cables with standard SMA connectors. All the kinetic measurements were carried out in Schlenk glassware with the

exclusion of moisture. The temperature of the solutions during the kinetic studies was maintained to 20 ± 0.1 °C by using circulating bath cryostats and monitored with thermocouple probes that were inserted into the reaction mixture.

Stopped-flow spectrophotometer systems (Applied Photophysics SX.18MV-R or Hi-Tech SF-61DX2) were used to investigate fast reactions of benzhydrylium ions with nucleophiles ($10 \text{ ms} < \tau_{1/2} < 10 \text{ s}$). The kinetic runs were initiated by mixing equal volumes of acetonitrile solutions of the amines and the benzhydrylium salts.

From the exponential decays of the absorbances at λ_{max} of the electrophiles **1**, the first-order rate constants k_{obs} (s^{-1}) were obtained.

3.4.2 Kinetic Experiments

Kinetics of the reactions of benzhydrylium ions (1) with trifluoroethylamine (2)

Table 3.5. Rate constants for the reactions of 2,2,2-trifluoroethylamine (**2**) with $(\text{dma})_2\text{CH}^+\text{BF}_4^-$ (**1h**) in CH_3CN (Stopped-flow, 20 °C, $\lambda = 613 \text{ nm}$).

| $[\mathbf{1h}]_0/\text{M}$ | $[\mathbf{2}]_0/\text{M}$ | $[\mathbf{2}]_0/[\mathbf{1h}]_0$ | $k_{\text{obs}}/\text{s}^{-1}$ |
|--|---------------------------|----------------------------------|--------------------------------|
| 2.00×10^{-5} | 4.03×10^{-4} | 20 | 7.17×10^{-1} |
| 2.00×10^{-5} | 8.07×10^{-4} | 40 | 7.59×10^{-1} |
| 2.00×10^{-5} | 1.21×10^{-3} | 61 | 8.30×10^{-1} |
| 2.00×10^{-5} | 1.61×10^{-3} | 81 | 8.87×10^{-1} |
| 2.00×10^{-5} | 2.02×10^{-3} | 101 | 9.40×10^{-1} |
| $k_2 = 1.43 \times 10^2 \text{ M}^{-1} \text{ s}^{-1}$ | | | |

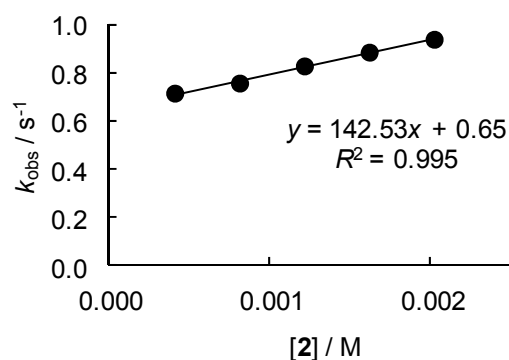
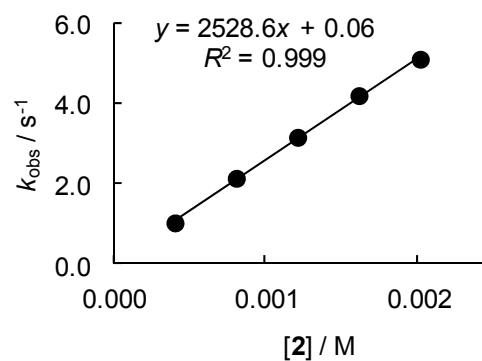
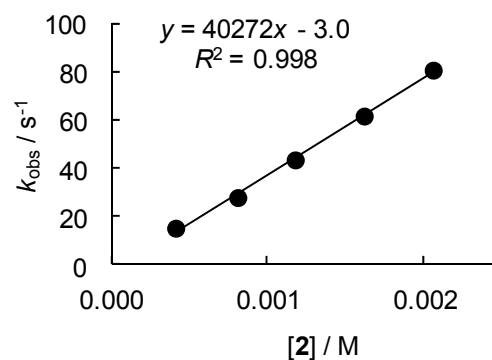


Table 3.6. Rate constants for the reactions of 2,2,2-trifluoroethylamine (**2**) with (mpa)₂CH⁺BF₄⁻ (**1i**) in CH₃CN (Stopped-flow, 20 °C, λ = 613 nm).

| [1i] ₀ /M | [2] ₀ /M | [2] ₀ /[1i] ₀ | <i>k</i> _{obs} /s ⁻¹ |
|--|------------------------------|---|--|
| 1.96 × 10 ⁻⁵ | 4.03 × 10 ⁻⁴ | 21 | 1.03 |
| 1.96 × 10 ⁻⁵ | 8.07 × 10 ⁻⁴ | 41 | 2.14 |
| 1.96 × 10 ⁻⁵ | 1.21 × 10 ⁻³ | 62 | 3.16 |
| 1.96 × 10 ⁻⁵ | 1.61 × 10 ⁻³ | 82 | 4.19 |
| 1.96 × 10 ⁻⁵ | 2.02 × 10 ⁻³ | 103 | 5.10 |
| <i>k</i> ₂ = 2.53 × 10 ³ M ⁻¹ s ⁻¹ | | | |

**Table 3.7.** Rate constants for the reactions of 2,2,2-trifluoroethylamine (**2**) with (mfa)₂CH⁺BF₄⁻ (**1j**) in CH₃CN (Stopped-flow, 20 °C, λ = 586 nm).

| [1j] ₀ /M | [2] ₀ /M | [2] ₀ /[1j] ₀ | <i>k</i> _{obs} /s ⁻¹ |
|--|------------------------------|---|--|
| 2.02 × 10 ⁻⁵ | 4.11 × 10 ⁻⁴ | 20 | 1.52 × 10 ¹ |
| 2.02 × 10 ⁻⁵ | 8.08 × 10 ⁻⁴ | 40 | 2.79 × 10 ¹ |
| 2.02 × 10 ⁻⁵ | 1.18 × 10 ⁻³ | 58 | 4.36 × 10 ¹ |
| 2.02 × 10 ⁻⁵ | 1.62 × 10 ⁻³ | 80 | 6.17 × 10 ¹ |
| 2.02 × 10 ⁻⁵ | 2.06 × 10 ⁻³ | 102 | 8.08 × 10 ¹ |
| <i>k</i> ₂ = 4.03 × 10 ⁴ M ⁻¹ s ⁻¹ | | | |



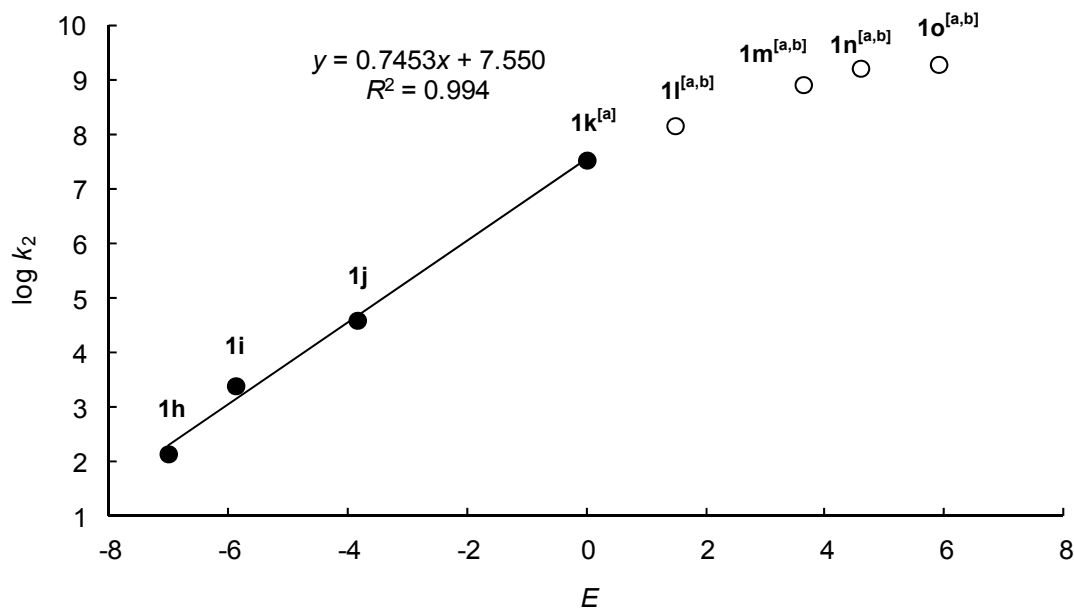


Figure 3.6. Plot of $\log k_2$ versus E for the reactions of 2,2,2-trifluoroethylamine (2).

[a] Rate constants were taken from Ref. [9b]. [b] Not included in the determination of N and s_N parameter due to diffusion control.

$$N = 10.13, s_N = 0.75$$

Kinetics of the reactions of benzhydrylium ions and quinone methides (1) with tert-butylamine (3)

Table 3.8. Rate constants for the reactions of *tert*-butylamine (3) with ani(Ph)₂QM (1c) in CH₃CN (diode array spectrophotometer, 20 °C, $\lambda = 415$ nm).

| [1c] ₀ /M | [3] ₀ /M | [3] ₀ /[1c] ₀ | $k_{\text{obs}}/\text{s}^{-1}$ |
|--|-----------------------|-------------------------------------|--------------------------------|
| 6.02×10^{-5} | 1.20×10^{-3} | 20 | 1.74×10^{-3} |
| 5.61×10^{-5} | 2.23×10^{-3} | 40 | 3.33×10^{-3} |
| 5.57×10^{-5} | 3.26×10^{-3} | 59 | 4.85×10^{-3} |
| 5.86×10^{-5} | 4.66×10^{-3} | 80 | 7.01×10^{-3} |
| 5.74×10^{-5} | 5.71×10^{-3} | 100 | 8.61×10^{-3} |
| $k_2 = 1.52 \text{ M}^{-1} \text{ s}^{-1}$ | | | |

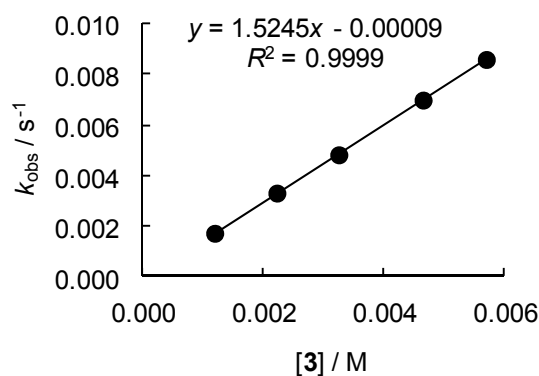
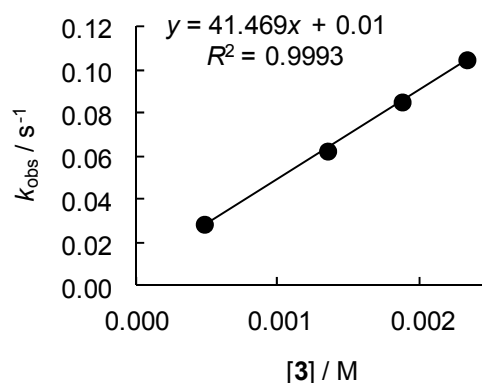
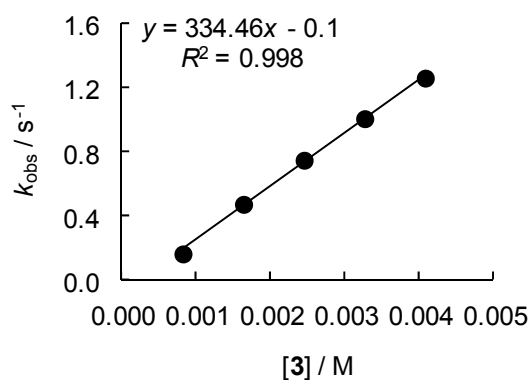


Table 3.9. Rate constants for the reactions of *tert*-butylamine (**3**) with (lil)₂CH⁺BF₄⁻ (**1d**) in CH₃CN (diode array spectrophotometer, 20 °C, λ = 639 nm).

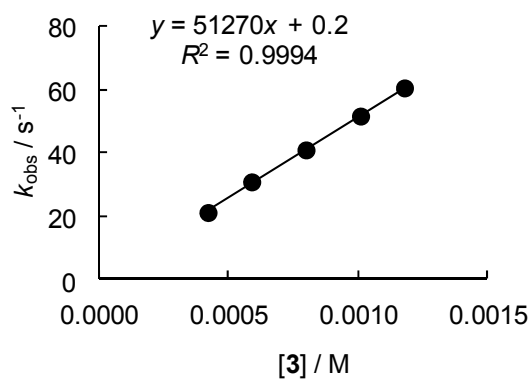
| [1d] ₀ /M | [3] ₀ /M | [3] ₀ /[1d] ₀ | <i>k</i> _{obs} /s ⁻¹ |
|--|------------------------------|---|--|
| 1.81 × 10 ⁻⁵ | 4.80 × 10 ⁻⁴ | 27 | 2.87 × 10 ⁻² |
| 1.69 × 10 ⁻⁵ | 1.35 × 10 ⁻³ | 80 | 6.27 × 10 ⁻² |
| 1.76 × 10 ⁻⁵ | 1.87 × 10 ⁻³ | 106 | 8.55 × 10 ⁻² |
| 1.75 × 10 ⁻⁵ | 2.32 × 10 ⁻³ | 133 | 1.05 × 10 ⁻¹ |
| <i>k</i> ₂ = 4.15 × 10 ¹ M ⁻¹ s ⁻¹ | | | |

**Table 3.10.** Rate constants for the reactions of *tert*-butylamine (**3**) with (ind)₂CH⁺BF₄⁻ (**1f**) in CH₃CN (Stopped-flow, 20 °C, λ = 625 nm).

| [1f] ₀ /M | [3] ₀ /M | [3] ₀ /[1f] ₀ | <i>k</i> _{obs} /s ⁻¹ |
|--|------------------------------|---|--|
| 2.02 × 10 ⁻⁵ | 8.17 × 10 ⁻⁴ | 40 | 1.67 × 10 ⁻¹ |
| 2.02 × 10 ⁻⁵ | 1.63 × 10 ⁻³ | 81 | 4.77 × 10 ⁻¹ |
| 2.02 × 10 ⁻⁵ | 2.45 × 10 ⁻³ | 121 | 7.52 × 10 ⁻¹ |
| 2.02 × 10 ⁻⁵ | 3.27 × 10 ⁻³ | 162 | 1.01 |
| 2.02 × 10 ⁻⁵ | 4.08 × 10 ⁻³ | 202 | 1.27 |
| <i>k</i> ₂ = 3.34 × 10 ² M ⁻¹ s ⁻¹ | | | |

**Table 3.11.** Rate constants for the reactions of *tert*-butylamine (**3**) with (mpa)₂CH⁺BF₄⁻ (**1i**) in CH₃CN (Stopped-flow, 20 °C, λ = 612 nm).

| [1h] ₀ /M | [3] ₀ /M | [3] ₀ /[1h] ₀ | <i>k</i> _{obs} /s ⁻¹ |
|--|------------------------------|---|--|
| 2.00 × 10 ⁻⁵ | 4.20 × 10 ⁻⁴ | 21 | 2.13 × 10 ¹ |
| 2.00 × 10 ⁻⁵ | 5.89 × 10 ⁻⁴ | 29 | 3.10 × 10 ¹ |
| 2.00 × 10 ⁻⁵ | 7.99 × 10 ⁻⁴ | 40 | 4.11 × 10 ¹ |
| 2.00 × 10 ⁻⁵ | 1.01 × 10 ⁻³ | 50 | 5.18 × 10 ¹ |
| 2.00 × 10 ⁻⁵ | 1.18 × 10 ⁻³ | 59 | 6.07 × 10 ¹ |
| <i>k</i> ₂ = 5.13 × 10 ⁴ M ⁻¹ s ⁻¹ | | | |



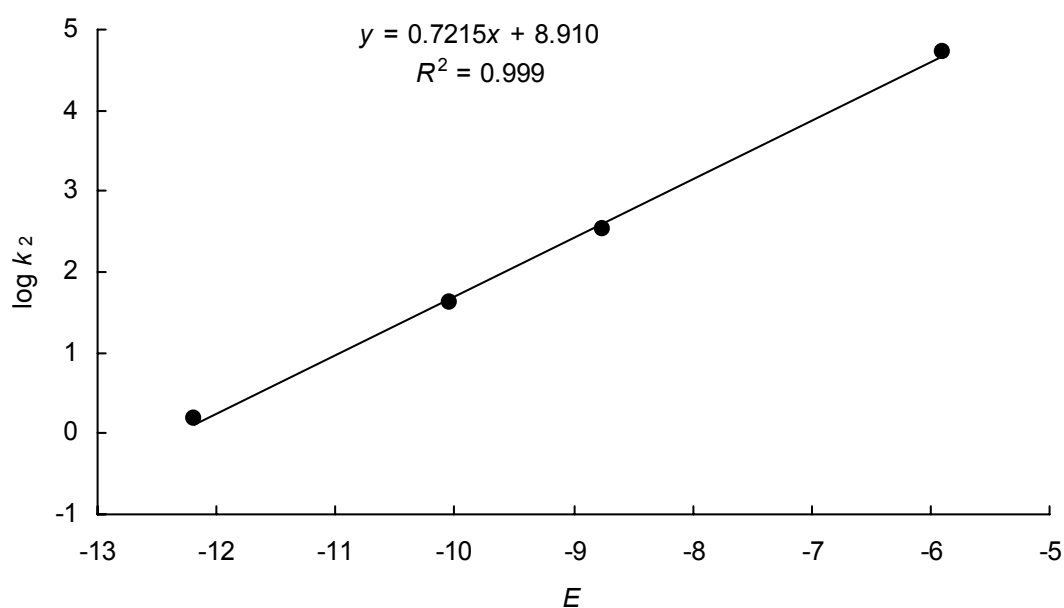


Figure 3.7. Plot of $\log k_2$ versus E for the reactions of *tert*-butylamine (**3**).

$$N = 12.35, s_N = 0.72$$

Kinetics of the reactions of benzhydrylium ions and quinone methides (1) with isopropylamine (4)

Table 3.12. Rate constants for the reactions of isopropylamine (**4**) with ani(Ph)₂QM (**1c**) in CH₃CN (diode array spectrophotometer, 20 °C, $\lambda = 414$ nm).

| [1c] ₀ /M | [4] ₀ /M | [4] ₀ /[1c] ₀ | $k_{\text{obs}}/\text{s}^{-1}$ |
|--|------------------------------|---|--------------------------------|
| 5.41×10^{-5} | 6.37×10^{-4} | 12 | 9.18×10^{-3} |
| 5.11×10^{-5} | 1.21×10^{-3} | 24 | 1.80×10^{-2} |
| 5.64×10^{-5} | 2.00×10^{-3} | 35 | 3.01×10^{-2} |
| 5.16×10^{-5} | 2.43×10^{-3} | 47 | 3.65×10^{-2} |
| 5.18×10^{-5} | 3.66×10^{-3} | 71 | 5.66×10^{-2} |
| $k_2 = 1.56 \times 10^1 \text{ M}^{-1} \text{ s}^{-1}$ | | | |

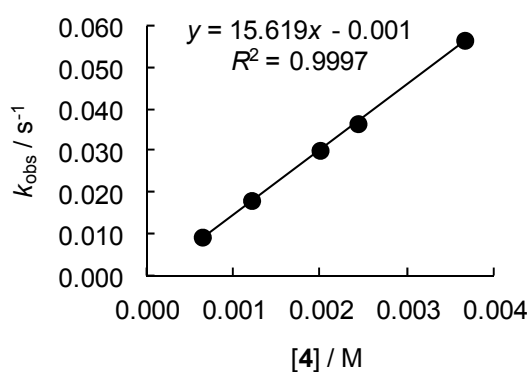
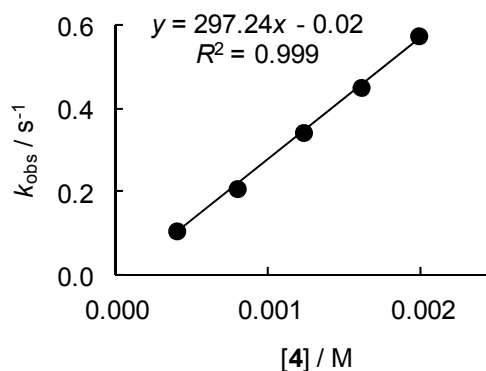
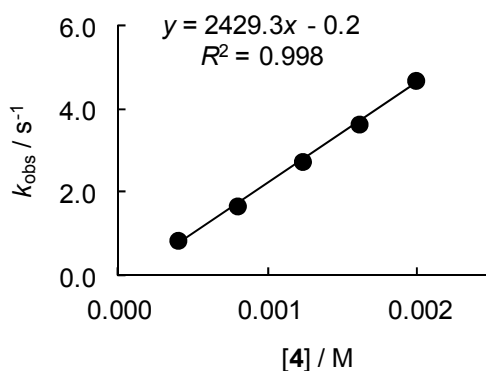


Table 3.13. Rate constants for the reactions of isopropylamine (**4**) with (lil)₂CH⁺BF₄⁻ (**1d**) in CH₃CN (Stopped-flow, 20 °C, λ = 631 nm).

| [1d] ₀ /M | [4] ₀ /M | [4] ₀ /[1d] ₀ | <i>k</i> _{obs} /s ⁻¹ |
|--|------------------------------|---|--|
| 1.60 × 10 ⁻⁵ | 3.96 × 10 ⁻⁴ | 25 | 1.05 × 10 ⁻¹ |
| 1.60 × 10 ⁻⁵ | 7.93 × 10 ⁻⁴ | 49 | 2.07 × 10 ⁻¹ |
| 1.60 × 10 ⁻⁵ | 1.23 × 10 ⁻³ | 77 | 3.42 × 10 ⁻¹ |
| 1.60 × 10 ⁻⁵ | 1.60 × 10 ⁻³ | 100 | 4.51 × 10 ⁻¹ |
| 1.60 × 10 ⁻⁵ | 1.98 × 10 ⁻³ | 124 | 5.75 × 10 ⁻¹ |
| <i>k</i> ₂ = 2.97 × 10 ² M ⁻¹ s ⁻¹ | | | |

**Table 3.14.** Rate constants for the reactions of isopropylamine (**4**) with (ind)₂CH⁺BF₄⁻ (**1f**) in CH₃CN (Stopped-flow, 20 °C, λ = 616 nm).

| [1f] ₀ /M | [4] ₀ /M | [4] ₀ /[1f] ₀ | <i>k</i> _{obs} /s ⁻¹ |
|--|------------------------------|---|--|
| 1.98 × 10 ⁻⁵ | 3.96 × 10 ⁻⁴ | 20 | 8.34 × 10 ⁻¹ |
| 1.98 × 10 ⁻⁵ | 7.93 × 10 ⁻⁴ | 40 | 1.66 |
| 1.98 × 10 ⁻⁵ | 1.23 × 10 ⁻³ | 62 | 2.74 |
| 1.98 × 10 ⁻⁵ | 1.60 × 10 ⁻³ | 81 | 3.64 |
| 1.98 × 10 ⁻⁵ | 1.98 × 10 ⁻³ | 100 | 4.69 |
| <i>k</i> ₂ = 2.43 × 10 ³ M ⁻¹ s ⁻¹ | | | |

**Table 3.15.** Rate constants for the reactions of isopropylamine (**4**) with (pyr)₂CH⁺BF₄⁻ (**1g**) in CH₃CN (Stopped-flow, 20 °C, λ = 611 nm).

| [1g] ₀ /M | [4] ₀ /M | [4] ₀ /[1g] ₀ | <i>k</i> _{obs} /s ⁻¹ |
|--|------------------------------|---|--|
| 1.99 × 10 ⁻⁵ | 3.68 × 10 ⁻⁴ | 19 | 6.54 |
| 1.99 × 10 ⁻⁵ | 7.83 × 10 ⁻⁴ | 39 | 1.53 × 10 ¹ |
| 1.99 × 10 ⁻⁵ | 1.20 × 10 ⁻³ | 60 | 2.46 × 10 ¹ |
| 1.99 × 10 ⁻⁵ | 1.57 × 10 ⁻³ | 79 | 3.23 × 10 ¹ |
| 1.99 × 10 ⁻⁵ | 2.03 × 10 ⁻³ | 102 | 4.17 × 10 ¹ |
| <i>k</i> ₂ = 2.13 × 10 ⁴ M ⁻¹ s ⁻¹ | | | |

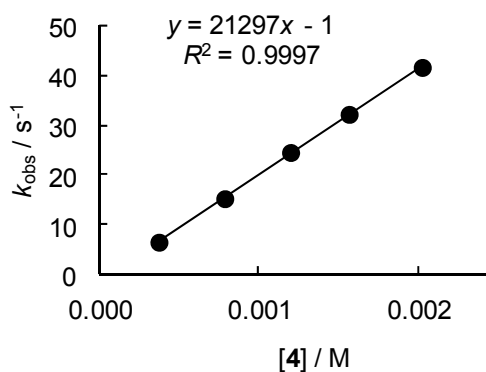


Table 3.16. Rate constants for the reactions of isopropylamine (**4**) with $(\text{dma})_2\text{CH}^+\text{BF}_4^-$ (**1h**) in CH_3CN (Stopped-flow, 20 °C, $\lambda = 611 \text{ nm}$).

| $[\mathbf{1h}]_0/\text{M}$ | $[\mathbf{4}]_0/\text{M}$ | $[\mathbf{4}]_0/[\mathbf{1h}]_0$ | $k_{\text{obs}}/\text{s}^{-1}$ |
|----------------------------|---------------------------|----------------------------------|--------------------------------|
| 2.00×10^{-5} | 3.96×10^{-4} | 20 | 1.77×10^1 |
| 2.00×10^{-5} | 7.93×10^{-4} | 40 | 4.16×10^1 |
| 2.00×10^{-5} | 1.22×10^{-3} | 61 | 5.85×10^1 |
| 2.00×10^{-5} | 1.60×10^{-3} | 80 | 8.17×10^1 |
| 2.00×10^{-5} | 1.98×10^{-3} | 99 | 1.02×10^2 |

$k_2 = 5.24 \times 10^4 \text{ M}^{-1} \text{ s}^{-1}$

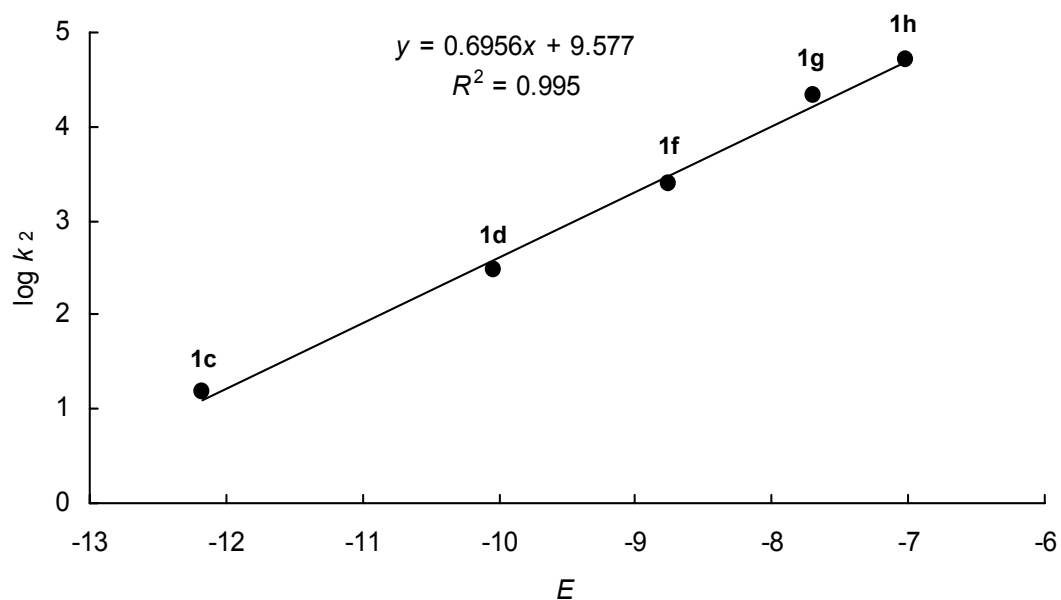
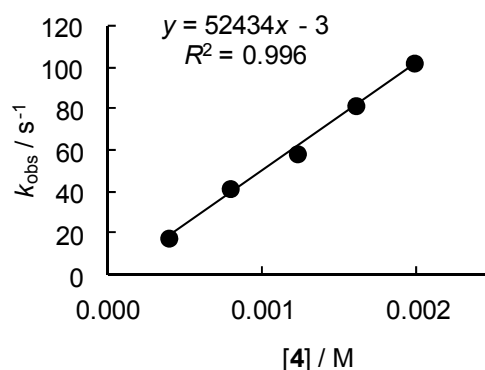


Figure 3.8. Plot of $\log k_2$ versus E for the reactions of isopropylamine (**4**).

$$N = 13.77, s_N = 0.70$$

Kinetics of the reactions of benzhydrylium ions and quinone methides (1) with ethanolamine (5)

Table 3.17. Rate constants for the reactions of ethanolamine (5) with ani(Ph)₂QM (1c) in CH₃CN (diode array spectrophotometer, 20 °C, λ = 414 nm).

| [1c] ₀ /M | [5] ₀ /M | [5] ₀ /[1c] ₀ | k _{obs} /s ⁻¹ |
|--|-------------------------|-------------------------------------|-----------------------------------|
| 5.44 × 10 ⁻⁵ | 6.44 × 10 ⁻⁴ | 12 | 1.82 × 10 ⁻² |
| 5.43 × 10 ⁻⁵ | 9.65 × 10 ⁻⁴ | 18 | 2.93 × 10 ⁻² |
| 5.29 × 10 ⁻⁵ | 1.88 × 10 ⁻³ | 36 | 5.25 × 10 ⁻² |
| 5.29 × 10 ⁻⁵ | 2.50 × 10 ⁻³ | 47 | 6.95 × 10 ⁻² |
| $k_2 = 2.71 \times 10^1 \text{ M}^{-1} \text{ s}^{-1}$ | | | |

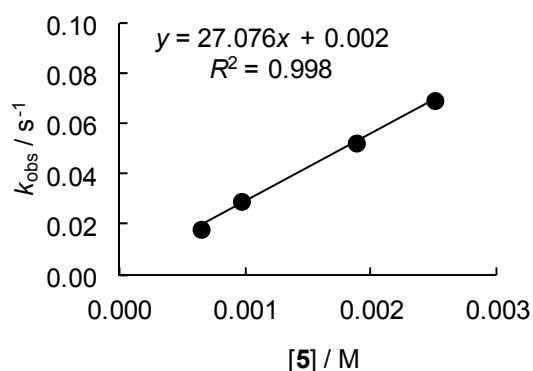


Table 3.18. Rate constants for the reactions of ethanolamine (5) with (lil)₂CH⁺BF₄⁻ (1d) in CH₃CN (Stopped-flow, 20 °C, λ = 639 nm).

| [1d] ₀ /M | [5] ₀ /M | [5] ₀ /[1d] ₀ | k _{obs} /s ⁻¹ |
|--|-------------------------|-------------------------------------|-----------------------------------|
| 2.02 × 10 ⁻⁵ | 3.97 × 10 ⁻⁴ | 20 | 2.31 × 10 ⁻¹ |
| 2.02 × 10 ⁻⁵ | 7.94 × 10 ⁻⁴ | 39 | 4.68 × 10 ⁻¹ |
| 2.02 × 10 ⁻⁵ | 1.25 × 10 ⁻³ | 62 | 7.33 × 10 ⁻¹ |
| 2.02 × 10 ⁻⁵ | 1.59 × 10 ⁻³ | 79 | 9.23 × 10 ⁻¹ |
| 2.02 × 10 ⁻⁵ | 2.04 × 10 ⁻³ | 101 | 1.20 |
| $k_2 = 5.85 \times 10^2 \text{ M}^{-1} \text{ s}^{-1}$ | | | |

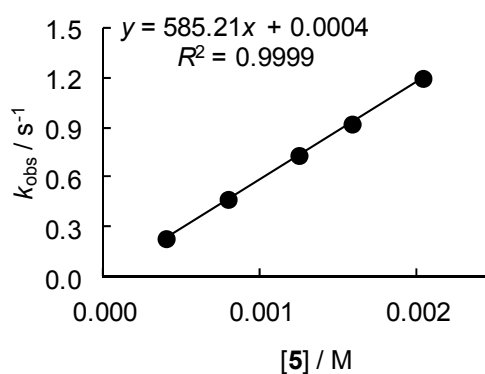
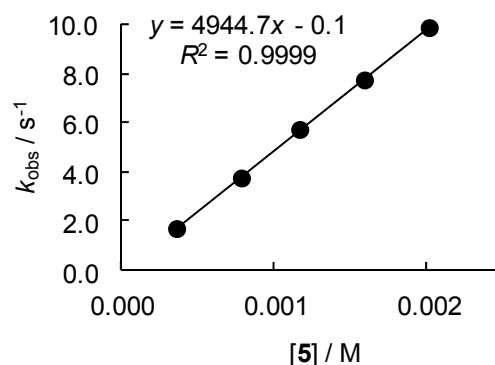
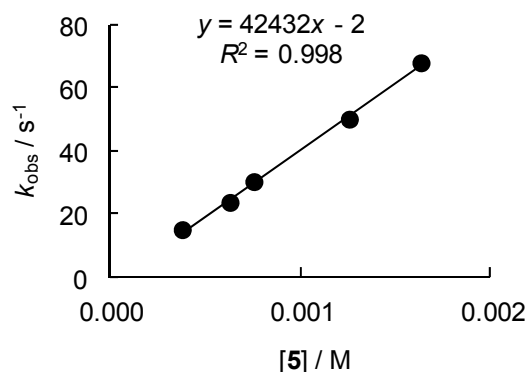


Table 3.19. Rate constants for the reactions of ethanolamine (**5**) with (ind)₂CH⁺BF₄⁻ (**1f**) in CH₃CN (Stopped-flow, 20 °C, λ = 616 nm).

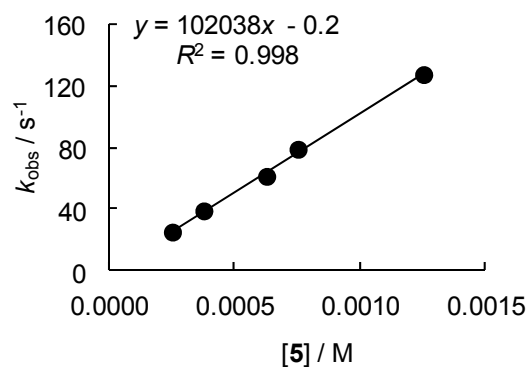
| [1f] ₀ /M | [5] ₀ /M | [5] ₀ /[1f] ₀ | <i>k</i> _{obs} /s ⁻¹ |
|--|------------------------------|---|--|
| 1.98 × 10 ⁻⁵ | 3.60 × 10 ⁻⁴ | 18 | 1.71 |
| 1.98 × 10 ⁻⁵ | 7.83 × 10 ⁻⁴ | 40 | 3.77 |
| 1.98 × 10 ⁻⁵ | 1.16 × 10 ⁻³ | 59 | 5.74 |
| 1.98 × 10 ⁻⁵ | 1.59 × 10 ⁻³ | 80 | 7.75 |
| 1.98 × 10 ⁻⁵ | 2.01 × 10 ⁻³ | 101 | 9.88 |
| <i>k</i> ₂ = 4.94 × 10 ³ M ⁻¹ s ⁻¹ | | | |

**Table 3.20.** Rate constants for the reactions of ethanolamine (**5**) with (pyr)₂CH⁺BF₄⁻ (**1g**) in CH₃CN (Stopped-flow, 20 °C, λ = 611 nm).

| [1g] ₀ /M | [5] ₀ /M | [5] ₀ /[1g] ₀ | <i>k</i> _{obs} /s ⁻¹ |
|--|------------------------------|---|--|
| 2.01 × 10 ⁻⁵ | 3.76 × 10 ⁻⁴ | 19 | 1.50 × 10 ¹ |
| 2.01 × 10 ⁻⁵ | 6.27 × 10 ⁻⁴ | 31 | 2.37 × 10 ¹ |
| 2.01 × 10 ⁻⁵ | 7.53 × 10 ⁻⁴ | 38 | 3.03 × 10 ¹ |
| 2.01 × 10 ⁻⁵ | 1.25 × 10 ⁻³ | 63 | 5.02 × 10 ¹ |
| 2.01 × 10 ⁻⁵ | 1.63 × 10 ⁻³ | 81 | 6.82 × 10 ¹ |
| <i>k</i> ₂ = 4.24 × 10 ⁴ M ⁻¹ s ⁻¹ | | | |

**Table 3.21.** Rate constants for the reactions of ethanolamine (**5**) with (dma)₂CH⁺BF₄⁻ (**1h**) in CH₃CN (Stopped-flow, 20 °C, λ = 605 nm).

| [1h] ₀ /M | [5] ₀ /M | [5] ₀ /[1h] ₀ | <i>k</i> _{obs} /s ⁻¹ |
|--|------------------------------|---|--|
| 2.01 × 10 ⁻⁵ | 2.51 × 10 ⁻⁴ | 12 | 2.51 × 10 ¹ |
| 2.01 × 10 ⁻⁵ | 3.76 × 10 ⁻⁴ | 19 | 3.89 × 10 ¹ |
| 2.01 × 10 ⁻⁵ | 6.27 × 10 ⁻⁴ | 31 | 6.14 × 10 ¹ |
| 2.01 × 10 ⁻⁵ | 7.53 × 10 ⁻⁴ | 37 | 7.90 × 10 ¹ |
| 2.01 × 10 ⁻⁵ | 1.25 × 10 ⁻³ | 62 | 1.27 × 10 ² |
| <i>k</i> ₂ = 1.02 × 10 ⁵ M ⁻¹ s ⁻¹ | | | |



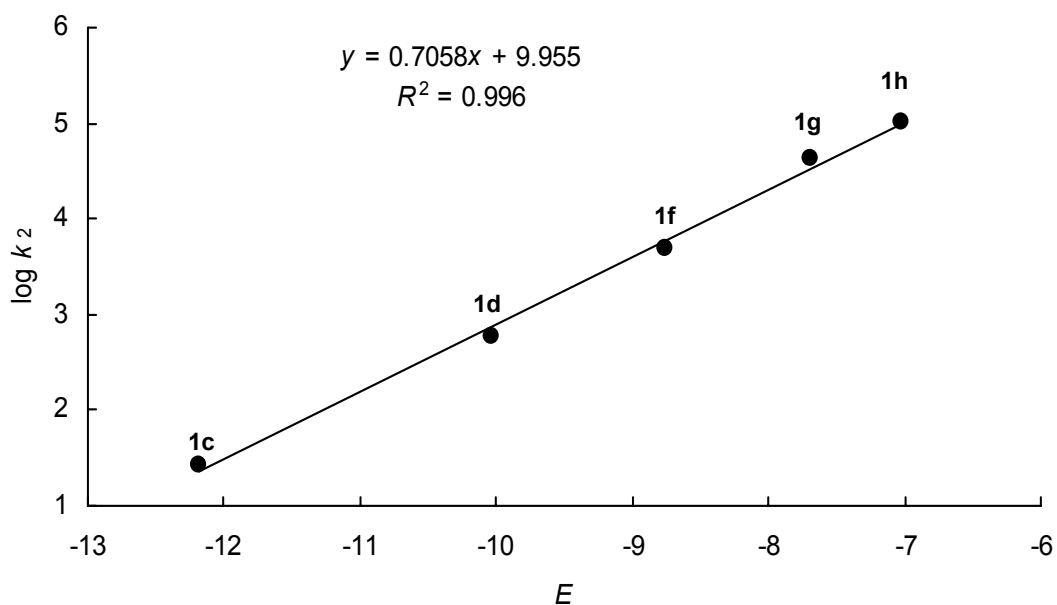


Figure 3.9. Plot of $\log k_2$ versus E for the reactions of ethanolamine (5).

$$N = 14.11, s_N = 0.71$$

Kinetics of the reactions of benzhydrylium ions and quinone methides (1) with benzylamine (6)

Table 3.22. Rate constants for the reactions of benzylamine (6) with tol(*t*Bu)₂QM (1b) in CH₃CN (diode array spectrophotometer, 20 °C, $\lambda = 364$ nm).

| [1b] ₀ /M | [6] ₀ /M | [6] ₀ /[1b] ₀ | $k_{\text{obs}}/\text{s}^{-1}$ |
|---|-----------------------|-------------------------------------|--------------------------------|
| 5.12×10^{-5} | 1.04×10^{-3} | 20 | 8.77×10^{-5} |
| 5.13×10^{-5} | 2.08×10^{-3} | 40 | 2.04×10^{-4} |
| 5.24×10^{-5} | 3.18×10^{-3} | 61 | 3.28×10^{-4} |
| 5.15×10^{-5} | 4.10×10^{-3} | 80 | 4.37×10^{-4} |
| 4.95×10^{-5} | 4.94×10^{-3} | 100 | 5.12×10^{-4} |
| $k_2 = 1.10 \times 10^{-1} \text{ M}^{-1} \text{ s}^{-1}$ | | | |

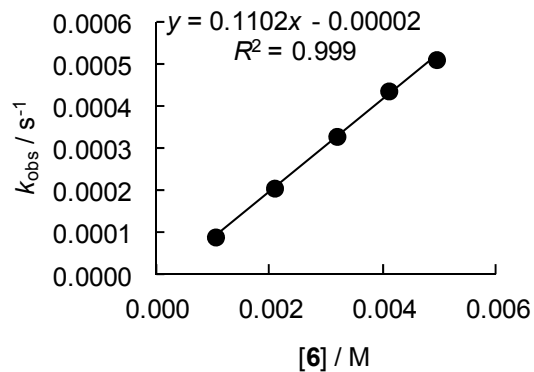
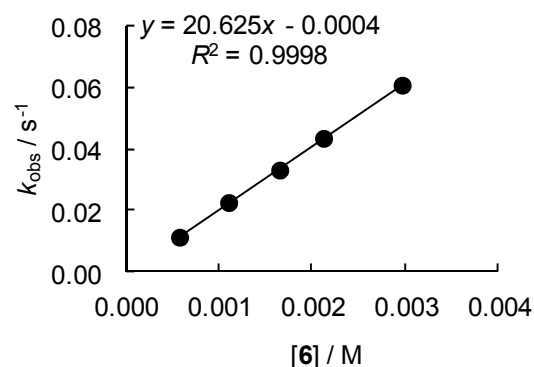
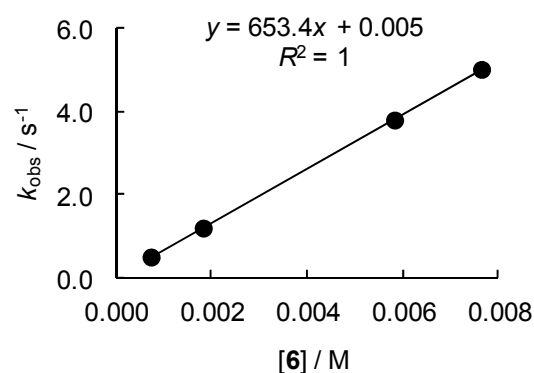


Table 3.23. Rate constants for the reactions of benzylamine (**6**) with ani(Ph)₂QM (**1c**) in CH₃CN (diode array spectrophotometer, 20 °C, λ = 414 nm).

| [1c] ₀ /M | [6] ₀ /M | [6] ₀ /[1c] ₀ | <i>k</i> _{obs} /s ⁻¹ |
|--|------------------------------|---|--|
| 5.55 × 10 ⁻⁵ | 5.73 × 10 ⁻⁴ | 10 | 1.14 × 10 ⁻² |
| 5.64 × 10 ⁻⁵ | 1.10 × 10 ⁻³ | 19 | 2.26 × 10 ⁻² |
| 5.53 × 10 ⁻⁵ | 1.65 × 10 ⁻³ | 30 | 3.32 × 10 ⁻² |
| 5.28 × 10 ⁻⁵ | 2.12 × 10 ⁻³ | 40 | 4.35 × 10 ⁻² |
| 5.87 × 10 ⁻⁵ | 2.96 × 10 ⁻³ | 50 | 6.08 × 10 ⁻² |
| <i>k</i> ₂ = 2.06 × 10 ¹ M ⁻¹ s ⁻¹ | | | |

**Table 3.24.** Rate constants for the reactions of benzylamine (**6**) with (lil)₂CH⁺BF₄⁻ (**1d**) in CH₃CN (Stopped-flow, 20 °C, λ = 632 nm).

| [1d] ₀ /M | [6] ₀ /M | [6] ₀ /[1d] ₀ | <i>k</i> _{obs} /s ⁻¹ |
|--|------------------------------|---|--|
| 7.81 × 10 ⁻⁶ | 7.28 × 10 ⁻⁴ | 94 | 4.90 × 10 ⁻¹ |
| 7.81 × 10 ⁻⁶ | 1.82 × 10 ⁻³ | 236 | 1.19 |
| 7.81 × 10 ⁻⁶ | 5.82 × 10 ⁻³ | 755 | 3.79 |
| 7.81 × 10 ⁻⁶ | 7.64 × 10 ⁻³ | 991 | 5.01 |
| <i>k</i> ₂ = 6.53 × 10 ² M ⁻¹ s ⁻¹ | | | |

**Table 3.25.** Rate constants for the reactions of benzylamine (**6**) with (ind)₂CH⁺BF₄⁻ (**1f**) in CH₃CN (Stopped-flow, 20 °C, λ = 616 nm).

| [1f] ₀ /M | [6] ₀ /M | [6] ₀ /[1f] ₀ | <i>k</i> _{obs} /s ⁻¹ |
|--|------------------------------|---|--|
| 7.41 × 10 ⁻⁶ | 1.60 × 10 ⁻⁴ | 22 | 7.20 × 10 ⁻¹ |
| 7.41 × 10 ⁻⁶ | 2.66 × 10 ⁻⁴ | 36 | 1.17 |
| 7.41 × 10 ⁻⁶ | 4.26 × 10 ⁻⁴ | 57 | 1.89 |
| 7.41 × 10 ⁻⁶ | 5.86 × 10 ⁻⁴ | 79 | 2.68 |
| <i>k</i> ₂ = 4.61 × 10 ³ M ⁻¹ s ⁻¹ | | | |

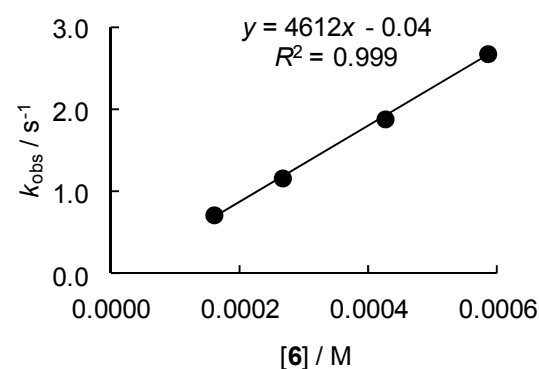
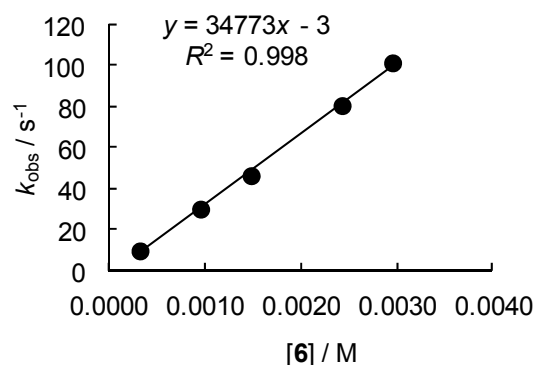
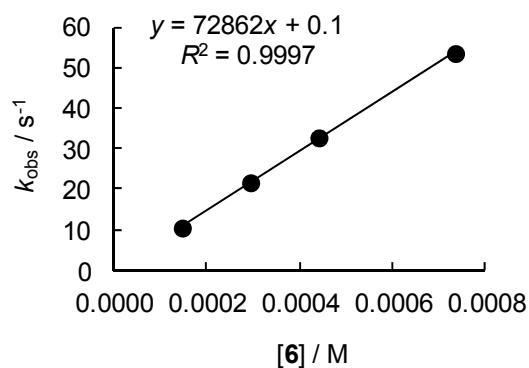


Table 3.26. Rate constants for the reactions of benzylamine (**6**) with $(\text{pyr})_2\text{CH}^+\text{BF}_4^-$ (**1g**) in CH_3CN (Stopped-flow, 20 °C, $\lambda = 612$ nm).

| $[\mathbf{1g}]_0/\text{M}$ | $[\mathbf{6}]_0/\text{M}$ | $[\mathbf{6}]_0/[\mathbf{1g}]_0$ | $k_{\text{obs}}/\text{s}^{-1}$ |
|--|---------------------------|----------------------------------|--------------------------------|
| 1.52×10^{-5} | 3.16×10^{-4} | 21 | 9.66 |
| 1.52×10^{-5} | 9.48×10^{-4} | 63 | 3.01×10^1 |
| 1.52×10^{-5} | 1.48×10^{-3} | 97 | 4.64×10^1 |
| 1.52×10^{-5} | 2.42×10^{-3} | 160 | 8.06×10^1 |
| 1.52×10^{-5} | 2.95×10^{-3} | 194 | 1.01×10^2 |
| $k_2 = 3.48 \times 10^4 \text{ M}^{-1} \text{ s}^{-1}$ | | | |

**Table 3.27.** Rate constants for the reactions of benzylamine (**6**) with $(\text{dma})_2\text{CH}^+\text{BF}_4^-$ (**1h**) in CH_3CN (Stopped-flow, 20 °C, $\lambda = 613$ nm).

| $[\mathbf{1h}]_0/\text{M}$ | $[\mathbf{6}]_0/\text{M}$ | $[\mathbf{6}]_0/[\mathbf{1h}]_0$ | $k_{\text{obs}}/\text{s}^{-1}$ |
|--|---------------------------|----------------------------------|--------------------------------|
| 7.68×10^{-6} | 1.47×10^{-4} | 19 | 1.05×10^1 |
| 7.68×10^{-6} | 2.94×10^{-4} | 38 | 2.17×10^1 |
| 7.68×10^{-6} | 4.42×10^{-4} | 57 | 3.27×10^1 |
| 7.68×10^{-6} | 7.36×10^{-4} | 96 | 5.35×10^1 |
| $k_2 = 7.29 \times 10^4 \text{ M}^{-1} \text{ s}^{-1}$ | | | |



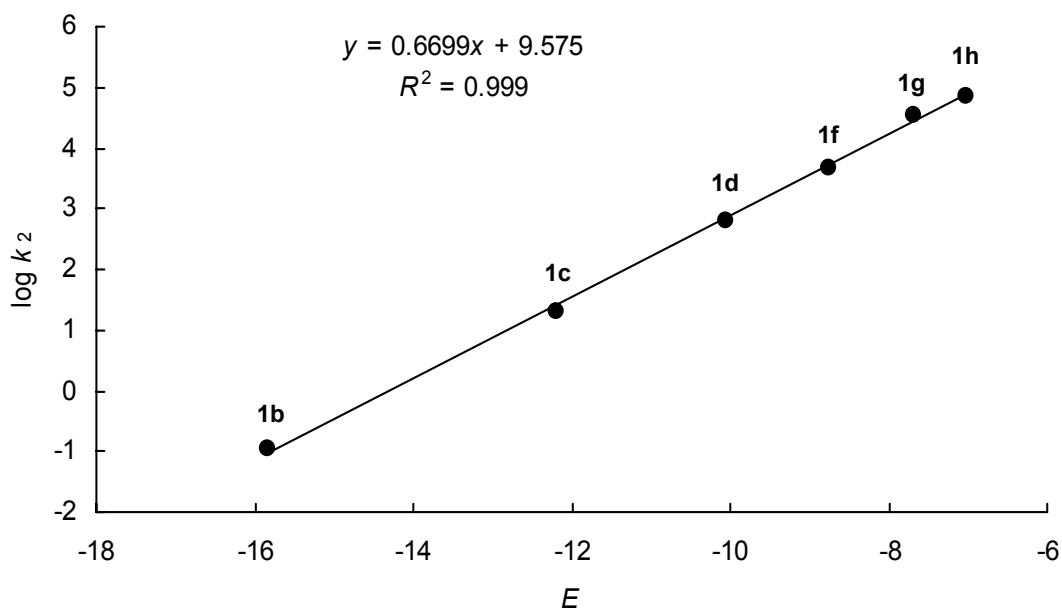


Figure 3.10. Plot of $\log k_2$ versus E for the reactions of benzylamine (6).

$$N = 14.29, s_N = 0.67$$

Kinetics of the reactions of benzhydrylium ions and quinone methides (1) with allylamine (7)

Table 3.28. Rate constants for the reactions of allylamine (7) with tol(*t*Bu)₂QM (1b) in CH₃CN (diode array spectrophotometer, 20 °C, $\lambda = 371$ nm).

| [1b] ₀ /M | [7] ₀ /M | [7] ₀ /[1b] ₀ | $k_{\text{obs}}/\text{s}^{-1}$ |
|---|-----------------------|-------------------------------------|--------------------------------|
| 5.78×10^{-5} | 1.16×10^{-3} | 20 | 1.39×10^{-4} |
| 5.97×10^{-5} | 2.39×10^{-3} | 40 | 3.00×10^{-4} |
| 5.55×10^{-5} | 3.25×10^{-3} | 59 | 3.95×10^{-4} |
| 5.41×10^{-5} | 4.17×10^{-3} | 77 | 5.14×10^{-4} |
| 5.55×10^{-5} | 5.57×10^{-3} | 100 | 6.93×10^{-4} |
| $k_2 = 1.25 \times 10^{-1} \text{ M}^{-1} \text{ s}^{-1}$ | | | |

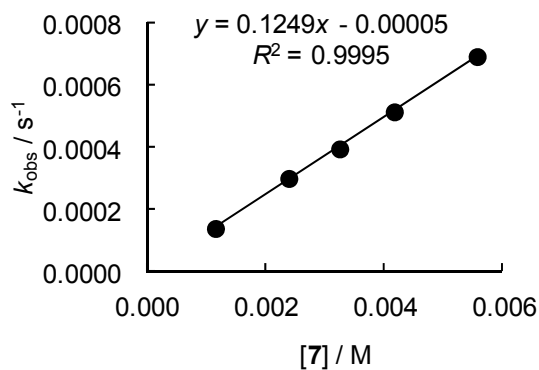
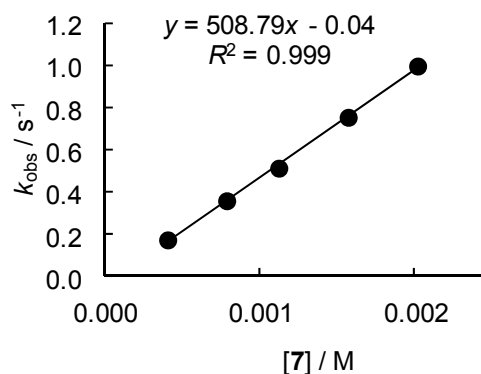
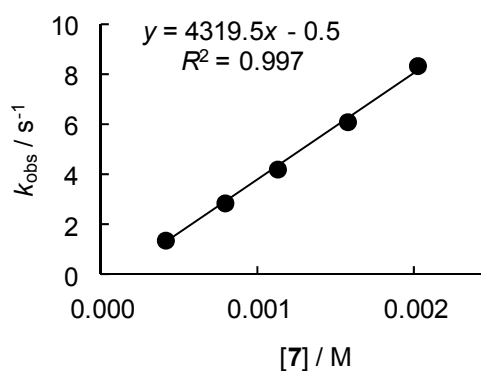


Table 3.29. Rate constants for the reactions of allylamine (**7**) with (lil)₂CH⁺BF₄⁻ (**1d**) in CH₃CN (Stopped-flow, 20 °C, λ = 631 nm).

| [1d] ₀ /M | [7] ₀ /M | [7] ₀ /[1d] ₀ | <i>k</i> _{obs} /s ⁻¹ |
|--|------------------------------|---|--|
| 2.00 × 10 ⁻⁵ | 4.04 × 10 ⁻⁴ | 20 | 1.78 × 10 ⁻¹ |
| 2.00 × 10 ⁻⁵ | 7.85 × 10 ⁻⁴ | 39 | 3.63 × 10 ⁻¹ |
| 2.00 × 10 ⁻⁵ | 1.12 × 10 ⁻³ | 56 | 5.18 × 10 ⁻¹ |
| 2.00 × 10 ⁻⁵ | 1.57 × 10 ⁻³ | 79 | 7.59 × 10 ⁻¹ |
| 2.00 × 10 ⁻⁵ | 2.02 × 10 ⁻³ | 101 | 1.00 |
| <i>k</i> ₂ = 5.09 × 10 ² M ⁻¹ s ⁻¹ | | | |

**Table 3.30.** Rate constants for the reactions of allylamine (**7**) with (ind)₂CH⁺BF₄⁻ (**1f**) in CH₃CN (Stopped-flow, 20 °C, λ = 631 nm).

| [1f] ₀ /M | [7] ₀ /M | [7] ₀ /[1f] ₀ | <i>k</i> _{obs} /s ⁻¹ |
|--|------------------------------|---|--|
| 1.99 × 10 ⁻⁵ | 4.04 × 10 ⁻⁴ | 20 | 1.35 |
| 1.99 × 10 ⁻⁵ | 7.85 × 10 ⁻⁴ | 39 | 2.85 |
| 1.99 × 10 ⁻⁵ | 1.12 × 10 ⁻³ | 56 | 4.21 |
| 1.99 × 10 ⁻⁵ | 1.57 × 10 ⁻³ | 79 | 6.11 |
| 1.99 × 10 ⁻⁵ | 2.02 × 10 ⁻³ | 101 | 8.37 |
| <i>k</i> ₂ = 4.32 × 10 ³ M ⁻¹ s ⁻¹ | | | |

**Table 3.31.** Rate constants for the reactions of allylamine (**7**) with (pyr)₂CH⁺BF₄⁻ (**1g**) in CH₃CN (Stopped-flow, 20 °C, λ = 611 nm).

| [1g] ₀ /M | [7] ₀ /M | [7] ₀ /[1g] ₀ | <i>k</i> _{obs} /s ⁻¹ |
|--|------------------------------|---|--|
| 1.99 × 10 ⁻⁵ | 4.07 × 10 ⁻⁴ | 20 | 1.22 × 10 ¹ |
| 1.99 × 10 ⁻⁵ | 7.94 × 10 ⁻⁴ | 40 | 2.54 × 10 ¹ |
| 1.99 × 10 ⁻⁵ | 1.02 × 10 ⁻³ | 51 | 3.33 × 10 ¹ |
| 1.99 × 10 ⁻⁵ | 1.53 × 10 ⁻³ | 77 | 5.18 × 10 ¹ |
| 1.99 × 10 ⁻⁵ | 2.04 × 10 ⁻³ | 102 | 7.15 × 10 ¹ |
| <i>k</i> ₂ = 3.64 × 10 ⁴ M ⁻¹ s ⁻¹ | | | |

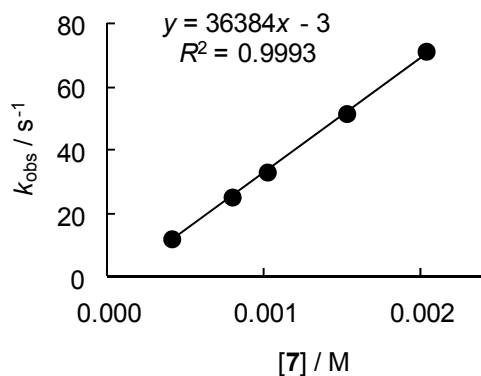
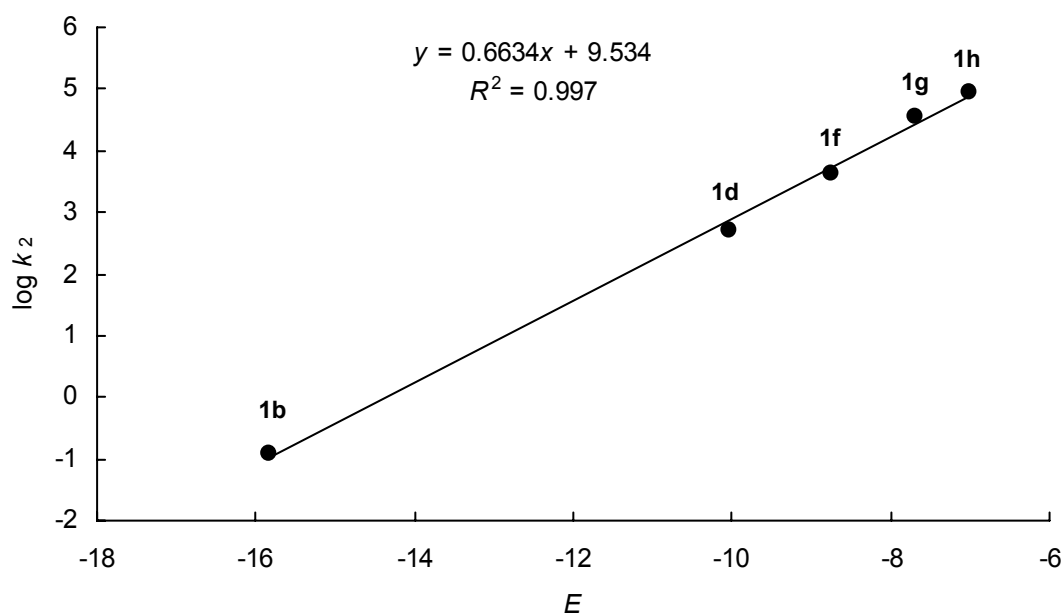
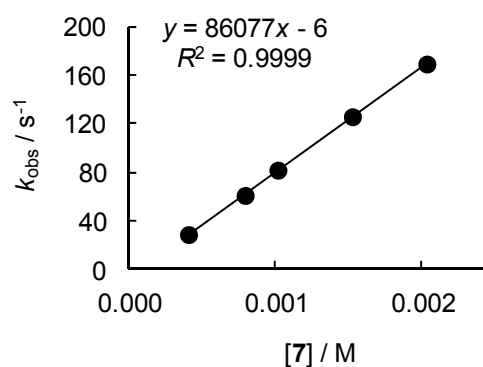


Table 3.32. Rate constants for the reactions of allylamine (**7**) with $(\text{dma})_2\text{CH}^+\text{BF}_4^-$ (**1h**) in CH_3CN (Stopped-flow, 20 °C, $\lambda = 605 \text{ nm}$).

| $[\mathbf{1h}]_0/\text{M}$ | $[\mathbf{7}]_0/\text{M}$ | $[\mathbf{7}]_0/[\mathbf{1h}]_0$ | $k_{\text{obs}}/\text{s}^{-1}$ |
|----------------------------|---------------------------|----------------------------------|--------------------------------|
| 2.01×10^{-5} | 4.07×10^{-4} | 20 | 2.90×10^1 |
| 2.01×10^{-5} | 7.94×10^{-4} | 40 | 6.12×10^1 |
| 2.01×10^{-5} | 1.02×10^{-3} | 51 | 8.20×10^1 |
| 2.01×10^{-5} | 1.53×10^{-3} | 76 | 1.26×10^1 |
| 2.01×10^{-5} | 2.04×10^{-3} | 101 | 1.69×10^2 |

$k_2 = 8.61 \times 10^4 \text{ M}^{-1} \text{ s}^{-1}$

**Figure 3.11.** Plot of $\log k_2$ versus E for the reactions of allylamine (**7**).

$$N = 14.37, s_N = 0.66$$

*Kinetics of the reactions of benzhydrylium ions and quinone methides (1) with *n*-butylamine (9)*

Table 3.33. Rate constants for the reactions of *n*-butylamine (9) with ani(*t*Bu)₂QM (1a) in CH₃CN (diode array spectrophotometer, 20 °C, λ = 384 nm).

| [1a] ₀ /M | [9] ₀ /M | [9] ₀ /[1a] ₀ | <i>k</i> _{obs} /s ⁻¹ |
|---|-------------------------|-------------------------------------|--|
| 6.13 × 10 ⁻⁵ | 1.22 × 10 ⁻³ | 20 | 4.25 × 10 ⁻⁴ |
| 6.44 × 10 ⁻⁵ | 2.57 × 10 ⁻³ | 40 | 8.75 × 10 ⁻⁴ |
| 5.92 × 10 ⁻⁵ | 3.54 × 10 ⁻³ | 60 | 1.24 × 10 ⁻³ |
| 5.71 × 10 ⁻⁵ | 4.56 × 10 ⁻³ | 80 | 1.59 × 10 ⁻³ |
| 6.40 × 10 ⁻⁵ | 6.38 × 10 ⁻³ | 100 | 2.18 × 10 ⁻³ |
| <i>k</i> ₂ = 3.41 × 10 ⁻¹ M ⁻¹ s ⁻¹ | | | |

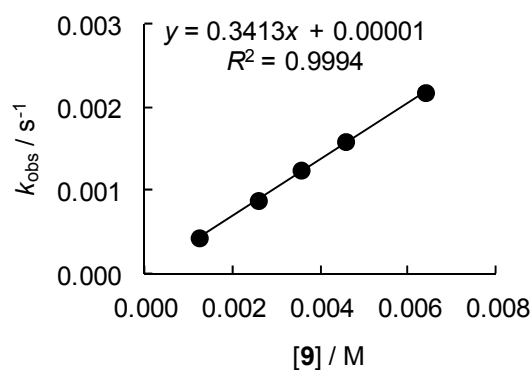


Table 3.34. Rate constants for the reactions of *n*-butylamine (9) with ani(Ph)₂QM (1c) in CH₃CN (Stopped-flow, 20 °C, λ = 415 nm).

| [1d] ₀ /M | [9] ₀ /M | [9] ₀ /[1d] ₀ | <i>k</i> _{obs} /s ⁻¹ |
|--|-------------------------|-------------------------------------|--|
| 5.99 × 10 ⁻⁵ | 1.18 × 10 ⁻³ | 20 | 7.64 × 10 ⁻² |
| 5.99 × 10 ⁻⁵ | 2.43 × 10 ⁻³ | 40 | 1.69 × 10 ⁻¹ |
| 5.99 × 10 ⁻⁵ | 3.60 × 10 ⁻³ | 60 | 2.58 × 10 ⁻¹ |
| 5.99 × 10 ⁻⁵ | 4.85 × 10 ⁻³ | 81 | 3.53 × 10 ⁻¹ |
| 5.99 × 10 ⁻⁵ | 5.96 × 10 ⁻³ | 99 | 4.34 × 10 ⁻¹ |
| <i>k</i> ₂ = 7.49 × 10 ¹ M ⁻¹ s ⁻¹ | | | |

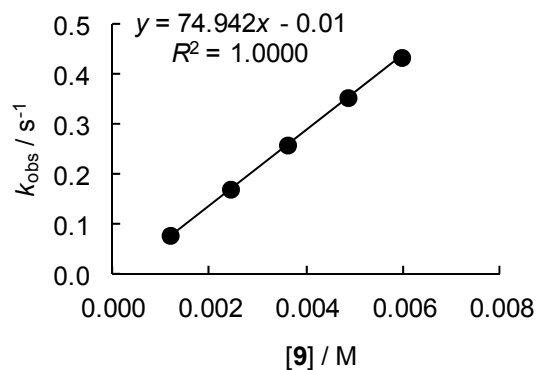
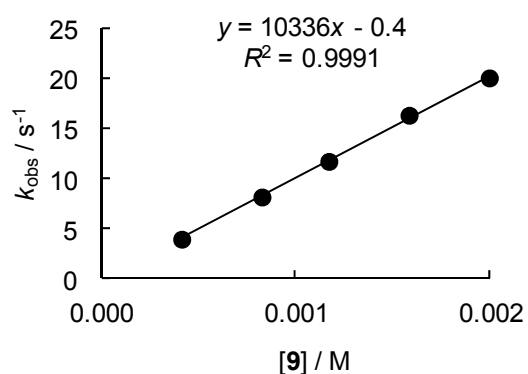
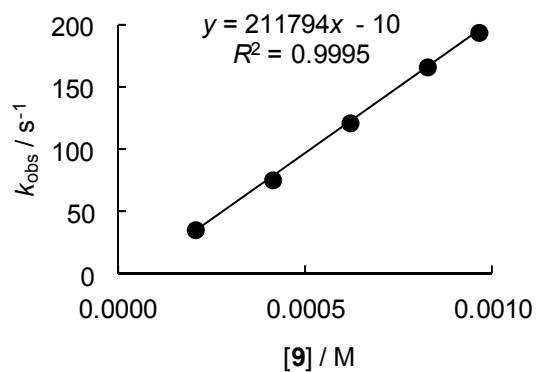


Table 3.35. Rate constants for the reactions of *n*-butylamine (**9**) with (ind)₂CH⁺BF₄⁻ (**1f**) in CH₃CN (Stopped-flow, 20 °C, λ = 625 nm).

| [1f] ₀ /M | [9] ₀ /M | [9] ₀ /[1f] ₀ | <i>k</i> _{obs} /s ⁻¹ |
|--|------------------------------|---|--|
| 1.99 × 10 ⁻⁵ | 4.13 × 10 ⁻⁴ | 21 | 3.88 |
| 1.99 × 10 ⁻⁵ | 8.27 × 10 ⁻⁴ | 41 | 8.11 |
| 1.99 × 10 ⁻⁵ | 1.17 × 10 ⁻³ | 59 | 1.17 × 10 ¹ |
| 1.99 × 10 ⁻⁵ | 1.58 × 10 ⁻³ | 80 | 1.63 × 10 ¹ |
| 1.99 × 10 ⁻⁵ | 2.00 × 10 ⁻³ | 100 | 2.01 × 10 ¹ |
| <i>k</i> ₂ = 1.03 × 10 ⁴ M ⁻¹ s ⁻¹ | | | |

**Table 3.36.** Rate constants for the reactions of *n*-butylamine (**9**) with (dma)₂CH⁺BF₄⁻ (**1h**) in CH₃CN (Stopped-flow, 20 °C, λ = 613 nm).

| [1h] ₀ /M | [9] ₀ /M | [9] ₀ /[1h] ₀ | <i>k</i> _{obs} /s ⁻¹ |
|--|------------------------------|---|--|
| 2.02 × 10 ⁻⁵ | 2.07 × 10 ⁻⁴ | 10 | 3.56 × 10 ¹ |
| 2.02 × 10 ⁻⁵ | 4.13 × 10 ⁻⁴ | 21 | 7.57 × 10 ¹ |
| 2.02 × 10 ⁻⁵ | 6.20 × 10 ⁻⁴ | 31 | 1.22 × 10 ² |
| 2.02 × 10 ⁻⁵ | 8.27 × 10 ⁻⁴ | 41 | 1.67 × 10 ² |
| 2.02 × 10 ⁻⁵ | 9.65 × 10 ⁻⁴ | 48 | 1.94 × 10 ² |
| <i>k</i> ₂ = 2.12 × 10 ⁵ M ⁻¹ s ⁻¹ | | | |



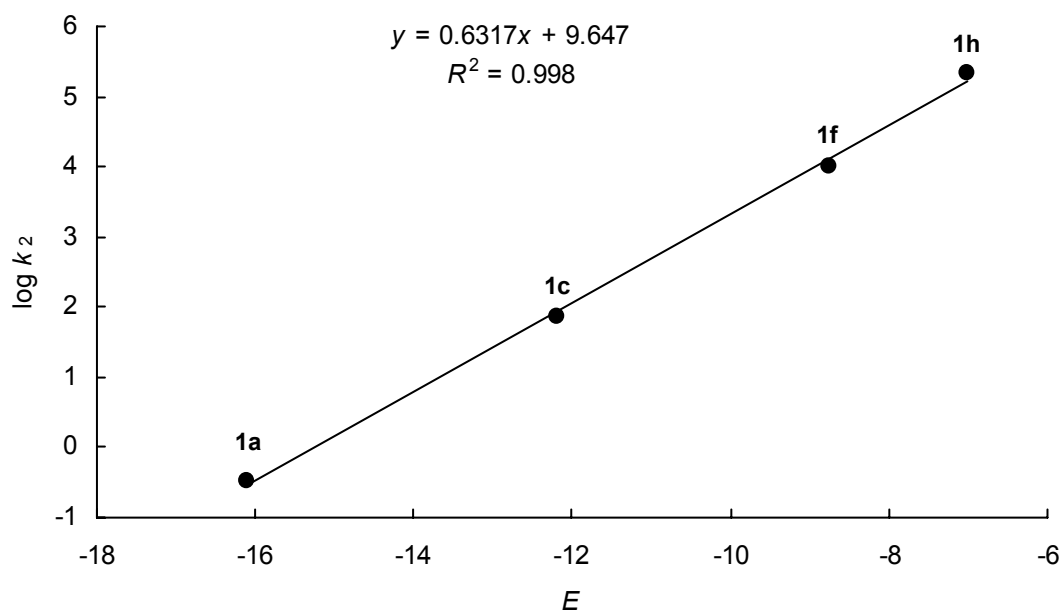
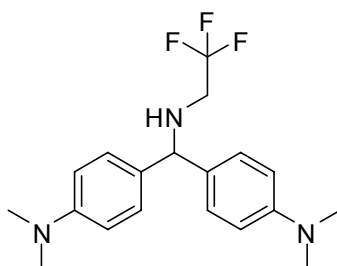


Figure 3.12. Plot of $\log k_2$ versus E for the reactions of *n*-butylamine (**9**).

$$N = 15.27, s = 0.63$$

3.4.3 Product Characterization

[Bis-(4-dimethylaminophenyl)methyl]-(2,2,2-trifluoroethyl)amine (**2h**)



2h

2,2,2-Trifluoroethylamine (**2**, 70 μ L, 0.88 mmol) was added to a mixture of $(\text{dma})_2\text{CH}^+\text{BF}_4^-$ (**1h**, 149 mg, 0.438 mmol) and K_2CO_3 (0.6 g, 4 mmol) in acetonitrile (8 mL) over 5 min. at 20 °C. After adding diethyl ether (20 mL), the solution was washed with 2M NaOH (25 mL),

dried (MgSO₄), filtered, and the solvent was removed under reduced pressure: **2h** (131 mg, 0.373 mmol, 85%), pale blue oil.

¹H NMR (300 MHz, CDCl₃): δ = 1.79 (br s, 1 H, NH), 2.89 (s, 12 H, 2 × NMe₂), 3.12 (q, ³J_{H,F} = 9.6 Hz, 2 H, CH₂), 4.80 (s, 1 H, Ar₂CH), 6.67 (d, 4 H, H_{ar}, *J* = 8.9 Hz), 7.23 (d, 4 H, H_{ar}, *J* = 8.8 Hz).

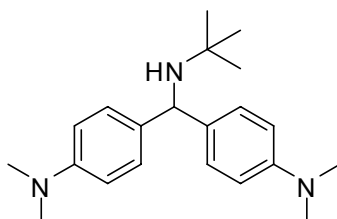
¹³C-NMR (75.5 MHz, CDCl₃): δ = 40.7 (q), 48.3 (tq, ²J_{C,F} = 31 Hz), 64.9 (d, Ar₂CH), 112.7 (d), 124.1 (s), 125.9 (sq, ¹J_{C,F} = 279 Hz, CF₃), 127.9 (d), 131.5 (s), 149.9 (s).

¹⁹F-NMR (282 MHz, CDCl₃): δ = -71.2 (t, CF₃, ³J_{F,H} = 9.6 Hz).

MS (EI, 70 eV) *m/z* (%) = 351 (13) [M⁺], 254 (25), 253 (100), 237 (12), 126 (10).

HR-MS (EI, 70 eV) calcd. for C₁₉H₂₄F₃N₃: 351.1922, found 351.1912.

[Bis-(4-dimethylaminophenyl)methyl]-*t*-butylamine (**3h**)



3h

tert-Butylamine (**3**, 0.40 mL, 3.8 mmol) was added to a solution of (dma)₂CH⁺BF₄⁻ (**1h**, 100 mg, 0.294 mmol) in acetonitrile (25 mL) over 5 min. at 20 °C. After adding diethyl ether (20 mL), the solution was washed with 2M NaOH (25 mL), dried (MgSO₄), filtered, and the solvent was removed under reduced pressure: **3h** (94 mg, 0.29 mmol, 98%), pale yellow crystals.

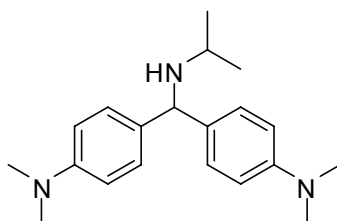
¹H NMR (300 MHz, CDCl₃): δ = 1.06 (s, 9 H, C(CH₃)₃), 1.42 (br s, 1 H, NH), 2.87 (s, 12 H, 2 × NMe₂), 4.88 (s, 1 H, Ar₂CH), 6.65 (d, *J* = 8.8 Hz, 4 H, H_{ar}), 7.24 (d, *J* = 8.8 Hz, 4 H, H_{ar}).

^{13}C -NMR (75.5 MHz, CDCl_3): δ = 30.2 (q), 40.8 (q), 51.6 (s), 60.2 (d, Ar_2CH), 112.6 (d), 128.0 (d), 135.6 (s), 149.2 (s).

MS (EI, 70 eV): m/z (%) = 325 (10) [M^+], 254 (41), 253 (100), 237 (14), 126 (15).

HR-MS (EI, 70 eV): calcd. for $\text{C}_{21}\text{H}_{31}\text{N}_3$: 325.2518, found 325.2508.

[Bis-(4-dimethylaminophenyl)methyl]-2-propylamine (**4h**)



4h

Isopropylamine (**4**, 58 μL , 0.68 mmol) was added to a solution of $(\text{dma})_2\text{CH}^+\text{BF}_4^-$ (**1h**, 114 mg, 0.335 mmol) in acetonitrile (8 mL) over 5 min. at 20 $^\circ\text{C}$. After adding diethyl ether (20 mL), the solution was washed with 2M NaOH (25 mL), dried (MgSO_4), filtered, and the solvent was removed under reduced pressure: **4h** (94 mg, 0.30 mmol, 90 %), pale blue oil.

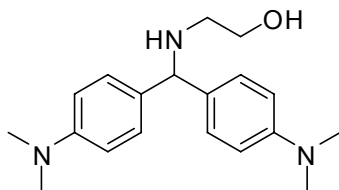
^1H NMR (300 MHz, CDCl_3): δ = 1.06 (d, J = 6.3 Hz, 6 H, $\text{CH}(\text{CH}_3)_2$), 1.53 (br s, 1 H, NH), 2.74 (sept, J = 6.3 Hz, 1 H, $\text{CH}(\text{CH}_3)_2$), 2.88 (s, 12 H, $2 \times \text{NMe}_2$), 4.81 (s, 1 H, Ar_2CH), 6.67 (d, J = 8.8 Hz, 4 H, H_{ar}), 7.21 (d, J = 8.8 Hz, 4 H, H_{ar}).

^{13}C -NMR (75.5 MHz, CDCl_3): δ = 23.2 (q), 40.8 (q), 45.9 (d), 62.9 (d, Ar_2CH), 112.7 (d), 128.0 (d), 133.4 (s), 149.5 (s).

MS (EI, 70 eV): m/z (%) = 311 (25) [M^+], 255 (11), 254 (90), 253 (100), 253 (55), 237 (35), 210 (12), 191 (32), 147 (18), 134 (10), 126 (15), 126 (38), 118 (19).

HR-MS (EI, 70 eV): calcd. for $\text{C}_{20}\text{H}_{29}\text{N}_3$: 311.2361, found 311.2359.

[Bis-(4-dimethylaminophenyl)methyl]-2-hydroxyethylamine (**5h**)



5h

Ethanolamine (**5**, 36 μ L, 0.60 mmol) was added to a solution of $(\text{dma})_2\text{CH}^+\text{BF}_4^-$ (**1h**, 103 mg, 0.303 mmol) in acetonitrile (8 mL) over 5 min. at 20 °C. After adding diethyl ether (20 mL), the solution was washed with 2M NaOH (25 mL), dried (MgSO_4), filtered, and the solvent was removed under reduced pressure: **5h** (93 mg, 0.30 mmol, 98%), pale blue oil.

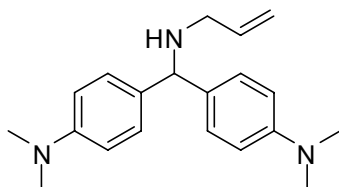
^1H NMR: (300 MHz, CDCl_3) δ = 2.26 (br s, 2 H, OH and NH), 2.74 (t, J = 5.2 Hz, 2 H, CH_2OH), 2.90 (s, 12 H, $2 \times \text{NMe}_2$), 3.61 (t, J = 5.2 Hz, 2 H, NHCH_2), 4.69 (s, 1 H, Ar_2CH), 6.67 (d, J = 8.8 Hz, 4 H, H_{ar}), 7.21 (d, J = 8.8 Hz, 4 H, H_{ar}).

^{13}C -NMR: (75.5 MHz, CDCl_3) δ = 40.7 (q), 49.4 (t), 61.4 (t), 65.8 (d, Ar_2CH), 112.7 (d), 127.9 (d), 132.2 (s), 149.7 (s).

MS (EI, 70 eV): m/z (%) = 313 (7) [M^+], 269 (13), 255 (15), 254 (100), 253 (31), 253 (70), 253 (45), 237 (27), 210 (20), 134 (28), 126 (25), 118 (16).

HR-MS (EI, 70 eV): calcd. for $\text{C}_{19}\text{H}_{27}\text{N}_3\text{O}$: 313.2154, found 313.2156.

[Bis-(4-dimethylaminophenyl)methyl]-allylamine (**7h**)



7h

Allylamine (**7**, 54 μ L, 0.70 mmol) was added to a solution of $(\text{dma})_2\text{CH}^+\text{BF}_4^-$ (**1h**, 120 mg, 0.353 mmol) in acetonitrile (8 mL) over 5 min. at 20 °C. After adding diethyl ether (20 mL),

the solution was washed with 2M NaOH (25 mL), dried (MgSO₄), filtered, and the solvent was removed under reduced pressure: **7h** (106 mg, 0.343 mmol, 97%), pale blue crystals.

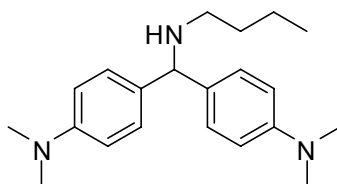
¹H NMR (300 MHz, CDCl₃): δ = 2.89 (s, 12 H, 2 × NMe₂), 3.18 (d, *J* = 5.9 Hz, 2 H, NHCH₂), 4.70 (s, 1 H, Ar₂CH), 5.04–5.20 (m, 2 H, -CH=CH₂), 5.87–6.01 (m, 1 H, -CH=CH₂), 6.67 (d, *J* = 8.8 Hz, 4 H, H_{ar}), 7.23 (d, *J* = 9.0 Hz, 4 H, H_{ar}).

¹³C-NMR (75.5 MHz, CDCl₃): δ = 40.8 (q), 50.4 (t), 65.2 (d, Ar₂CH), 112.7 (d), 115.4 (t), 127.9 (d), 132.9 (s), 137.2 (d), 149.6 (s).

MS (EI, 70 eV): *m/z* (%) = 309 (3) [M⁺], 254 (56), 253 (100), 237 (21), 210 (16), 200 (28), 134 (14), 126 (15), 123 (13), 118 (11), 105 (39), 95 (10), 84 (14), 82 (20), 77 (16), 44 (16).

HR-MS (EI, 70 eV): calcd. for C₂₀H₂₇N₃: 309.2205, found 309.2208.

[Bis-(4-dimethylaminophenyl)methyl]-*n*-butylamine (**9h**)



9h

n-Butylamine (**9**, 80 μL, 0.80 mmol) was added to a solution of (dma)₂CH⁺BF₄⁻ (**1h**, 136 mg, 0.400 mmol) in acetonitrile (8 mL) over 5 min. at 20 °C. After adding diethyl ether (20 mL), the solution was washed with 2M NaOH (25 mL), dried (MgSO₄), filtered, and the solvent was removed under reduced pressure: **9h** (124 mg, 0.381 mmol, 95%), colorless oil.

¹H NMR (300 MHz, CDCl₃): δ = 0.88 (t, *J* = 7.3 Hz, 3 H, CH₃), 1.33 (sext, *J* = 7.2 Hz, 2 H, CH₃CH₂), 1.48 (quint, *J* = 7.2 Hz, 2 H, CH₃CH₂CH₂), 2.55 (t, *J* = 7.1 Hz, 2 H, NHCH₂), 2.88 (s, 12 H, 2 × NMe₂), 4.65 (s, 1 H, Ar₂CH), 6.66 (d, *J* = 8.8 Hz, 4 H, H_{ar}), 7.23 (d, *J* = 8.7 Hz, 4 H, H_{ar}).

¹³C-NMR (75.5 MHz, CDCl₃): δ = 14.1 (q), 20.5 (t), 32.4 (t), 40.8 (q), 47.9 (t), 66.2 (d, Ar₂CH), 112.7 (d), 127.9 (d), 133.3 (s), 149.5 (s).

MS (EI, 70 eV): m/z (%) = 326 (11), 325 (52) [M^+], 324 (20), 255 (10), 254 (100), 253 (76), 253 (31), 238 (13), 237 (46), 206 (10), 205 (69), 162 (15), 161 (10), 147 (12), 134 (12), 126 (32), 126 (71), 118 (27).

HR-MS (EI, 70 eV): calcd. for $C_{21}H_{31}N_3$: 325.2518, found 325.2502.

3.5 References

- [1] a) W. P. Jencks, M. Gilchrist, *J. Am. Chem. Soc.* **1968**, *90*, 2622–2637; b) B. Schreiber, H. Martinek, P. Wolschann, P. Schuster, *J. Am. Chem. Soc.* **1979**, *101*, 4708–4713; c) L. A. P. Kane-Maguire, E. D. Honig, D. A. Sweigart, *Chem. Rev.* **1984**, *84*, 525–543; d) C. D. Ritchie, *Can. J. Chem.* **1986**, *64*, 2239–2250; e) C. F. Bernasconi, M. Panda, *J. Org. Chem.* **1987**, *52*, 3042–3050; f) Z. Rappoport, A. Topol, *J. Org. Chem.* **1989**, *54*, 5967–5977; g) N. S. Nudelman, *J. Phys. Org. Chem.* **1989**, *2*, 1–14; h) C. F. Bernasconi, M. W. Stronach, *J. Am. Chem. Soc.* **1991**, *113*, 2222–2227; i) J. P. Richard, T. L. Amyes, T. Vontor, *J. Am. Chem. Soc.* **1992**, *114*, 5626–5634; j) C. F. Bernasconi, A. E. Leyes, *J. Am. Chem. Soc.* **1993**, *115*, 7513–7514; k) L. García-Río, E. Iglesias, J. R. Leis, M. E. Peña, A. Ríos, *J. Chem. Soc. Perkin Trans. 2* **1993**, 29–37; l) C. K. M. Heo, J. W. Bunting, *J. Chem. Soc. Perkin Trans. 2* **1994**, 2279–2290; m) B. Varghese, S. Kothari, K. K. Banerji, *Int. J. Chem. Kinet.* **1999**, *31*, 245–252; n) A. D. Allen, T. T. Tidwell, *J. Org. Chem.* **1999**, *64*, 266–271; o) M. R. Crampton, J. Delaney, L. C. Rabbitt, *J. Chem. Soc. Perkin Trans. 2* **1999**, 2473–2480; p) J. P. Richard, M. M. Toteva, J. Crugeiras, *J. Am. Chem. Soc.* **2000**, *122*, 1664–1674; q) H. K. Oh, J. H. Yang, H. W. Lee, *J. Org. Chem.* **2000**, *65*, 5391–5395; r) I.-H. Um, J.-S. Min, J.-A. Ahn, H.-J. Hahn, *J. Org. Chem.* **2000**, *65*, 5659–5663; s) C. F. Bernasconi, C. Whitesell, R. A. Johnson, *Tetrahedron* **2000**, *56*, 4917–4924; t) E. A. Castro, M. G. Ruiz, J. G. Santos, *Int. J. Chem. Kinet.* **2001**, *33*, 281–287; u) N. C. de Lucas, J. C. Netto-Ferreira, J. Andraos, J. C. Scaiano, *J. Org. Chem.* **2001**, *66*, 5016–5021; v) D. Rajarathnam, T. Jeyakumar, P. A. Nadar, *Int. J. Chem. Kinet.* **2002**, *34*, 366–373; w) H. K. Oh, T. S. Kim, H. W. Lee, I. Lee, *Bull. Korean Chem. Soc.* **2003**, *24*, 193–196; x) P. M. Mancini, G. G. Fortunato, L. R. Vottero, *J. Phys. Org. Chem.* **2004**, *17*, 138–147; y) H. K. Oh, I. K. Kim, H. W. Lee, I. Lee, *J. Org. Chem.* **2004**, *69*, 3806–3810; z) M. R. Crampton, T. A. Emokpae, C. Isanbor, *J. Phys. Org. Chem.* **2006**, *19*, 75–80.

- [2] a) C. G. Swain, C. B. Scott, *J. Am. Chem. Soc.* **1953**, *75*, 141–147; b) C. D. Ritchie, *Acc. Chem. Res.* **1972**, *5*, 348–354; c) C. D. Ritchie, R. J. Minasz, A. A. Kamego, M. Sawada, *J. Am. Chem. Soc.* **1977**, *99*, 3747–3753; d) C. D. Ritchie, C. Kubisty, G. Y. Ting, *J. Am. Chem. Soc.* **1983**, *105*, 279–284.
- [3] H. Mayr, M. Patz, *Angew. Chem.* **1994**, *106*, 990–1010; *Angew. Chem. Int. Ed. Engl.* **1994**, *33*, 938–957.
- [4] a) S. Minegishi, H. Mayr, *J. Am. Chem. Soc.* **2003**, *125*, 286–295; b) F. Brotzel, Y. C. Chu, H. Mayr, *J. Org. Chem.* **2007**, *72*, 3679–3688.
- [5] a) H. Mayr, T. Bug, M. F. Gotta, N. Hering, B. Irrgang, B. Janker, B. Kempf, R. Loos, A. R. Ofial, G. Remennikov, H. Schimmel, *J. Am. Chem. Soc.* **2001**, *123*, 9500–9512; b) R. Lucius, R. Loos, H. Mayr, *Angew. Chem.* **2002**, *114*, 97–102; *Angew. Chem. Int. Ed.* **2002**, *41*, 91–95; c) H. Mayr, B. Kempf, A. R. Ofial, *Acc. Chem. Res.* **2003**, *36*, 66–77; d) H. Mayr, A. R. Ofial, *Pure Appl. Chem.* **2005**, *77*, 1807–1821; e) H. Mayr, A. R. Ofial, *J. Phys. Org. Chem.* **2008**, *21*, 584–595.
- [6] T. B. Phan, C. Nolte, S. Kobayashi, A. R. Ofial, H. Mayr, *J. Am. Chem. Soc.* **2009**, *131*, 11392–11401.
- [7] T. B. Phan, M. Breugst, H. Mayr, *Angew. Chem.* **2006**, *118*, 3954–3959; *Angew. Chem. Int. Ed.* **2006**, *45*, 3869–3874.
- [8] a) W. P. Jencks, *Chem. Soc. Rev.* **1981**, *10*, 345–375; b) J. P. Richards in *Advances in Carbocation Chemistry* (Ed.: X. Creary), JAI Press, Greenwich, London, **1989**, vol. 1, pp 121–169; c) T. L. Amyes, M. M. Toteva, J. P. Richard, in: *Reactive Intermediate Chemistry* (Eds.: R. A. Moss, M. S. Platz, M. Jones Jr.), Wiley-Interscience, Hoboken, NJ, **2004**, pp. 41–68; d) J. P. Richard, T. L. Amyes, M. M. Toteva, Y. Tsuji, *Adv. Phys. Org. Chem.* **2004**, *39*, 1–26.
- [9] a) R. A. McClelland, N. Banait, S. Steenken, *J. Am. Chem. Soc.* **1989**, *111*, 2929–2935; b) R. A. McClelland, V. M. Kanagasabapathy, N. S. Banait, S. Steenken, *J. Am. Chem. Soc.* **1992**, *114*, 1816–1823; c) R. A. McClelland, in: *Reactive Intermediate Chemistry* (Eds.: R. A. Moss, M. S. Platz, M. Jones Jr.), Wiley-Interscience, Hoboken, NJ, **2004**, pp. 3–40.
- [10] a) J. Bartl, S. Steenken, H. Mayr, R. A. McClelland, *J. Am. Chem. Soc.* **1990**, *112*, 6918–6928; b) J. Bartl, S. Steenken, H. Mayr, *J. Am. Chem. Soc.* **1991**, *113*, 7710–7716; c) S. Minegishi, R. Loos, S. Kobayashi, H. Mayr, *J. Am. Chem. Soc.* **2005**, *127*, 2641–2649.

- [11] H. Mayr, A. R. Ofial, *Angew. Chem.* **2006**, *118*, 1876–1886; *Angew. Chem. Int. Ed.* **2006**, *45*, 1844–1854.
- [12] a) I.-H. Um, S. Yoon, H.-R. Park, H.-J. Han, *Org. Biomol. Chem.* **2008**, *6*, 1618–1624; b) E. A. Castro, *Pure Appl. Chem.* **2009**, *81*, 685–696.
- [13] I.-H. Um, J.-A. Seok, H.-T. Kim, S.-K. Bae, *J. Org. Chem.* **2003**, *68*, 7742–7746.
- [14] M. J. Pfeiffer, S. B. Hanna, *J. Org. Chem.* **1993**, *58*, 735–740.
- [15] M. Baidya, S. Kobayashi, F. Brotzel, U. Schmidhammer, E. Riedle, H. Mayr, *Angew. Chem.* **2007**, *119*, 6288–6292; *Angew. Chem. Int. Ed.* **2007**, *46*, 6176–6179.
- [16] F. Brotzel, B. Kempf, T. Singer, H. Zipse, H. Mayr, *Chem. Eur. J.* **2007**, *13*, 336–345.
- [17] T. A. Nigst, M. Westermaier, A. R. Ofial, H. Mayr, *Eur. J. Org. Chem.* **2008**, 2369–2374.
- [18] T. Tokuyasu, H. Mayr, *Eur. J. Org. Chem.* **2004**, 2791–2796.
- [19] a) R. P. Bell, *The Proton in Chemistry*, Methuen, London, **1959**, p. 159; b) J. F. Coetzee, G. R. Padmanabhan, *J. Am. Chem. Soc.* **1965**, *87*, 5005–5010; c) I. Kaljurand, T. Rodima, I. Leito, I. A. Koppel, R. Schwesinger, *J. Org. Chem.* **2000**, *65*, 6202–6208; d) I. Kaljurand, A. Kütt, L. Sooväli, T. Rodima, V. Mäemets, I. Leito, I. A. Koppel, *J. Org. Chem.* **2005**, *70*, 1019–1028.
- [20] a) S. T. A. Berger, F. H. Seeliger, F. Hofbauer, H. Mayr, *Org. Biomol. Chem.* **2007**, *5*, 3020–3026; b) F. Seeliger, S. T. A. Berger, G. Y. Remennikov, K. Polborn, H. Mayr, *J. Org. Chem.* **2007**, *72*, 9170–9180; c) O. Kaumanns, H. Mayr, *J. Org. Chem.* **2008**, *73*, 2738–2745; see also: d) C. F. Bernasconi, *Tetrahedron* **1989**, *45*, 4017–4090.
- [21] For a discussion of the Hughes–Ingold rules and their limitations see: C. Reichardt, *Solvents and Solvent Effects in Organic Chemistry*, 3rd ed., Wiley-VCH, Weinheim, **2003**, pp. 163, 215.
- [22] H. Mayr, R. Schneider, C. Schade, J. Bartl, R. Bederke, *J. Am. Chem. Soc.* **1990**, *112*, 4446–4454.
- [23] T. Lemek, H. Mayr, *J. Org. Chem.* **2003**, *68*, 6880–6886.
- [24] O. Kaumanns, R. Lucius, H. Mayr, *Chem. Eur. J.* **2008**, *14*, 9675–9682.

Chapter 4

NUCLEOPHILIC REACTIVITIES OF HYDRAZINES AND AMINES: THE FUTILE SEARCH FOR THE α -EFFECT IN HYDRAZINE REACTIVITIES

Tobias A. Nigst, Johannes Ammer, and Herbert Mayr in *Angew. Chem.* **2012**, *124*, 1381–1385; *Angew. Chem. Int. Ed.* **2012**, *51*, 1353–1356 and Tobias A. Nigst, Anna Antipova, and Herbert Mayr, *J. Org. Chem.*, **2012**, *77*, 8142–8155.

The results obtained by J. Ammer and A. Antipova are not listed in the Experimental Section.

4.1 Introduction

In 1962, Pearson and Edwards created the term α -effect to account for the enhanced reactivity of nucleophiles, which bear an unshared pair of electrons at the atom adjacent to the nucleophilic center.^[1] This definition was adopted by the 1979 version of the IUPAC Glossary of Terms used in Physical Organic Chemistry and exemplified by the higher nucleophilicity of HOO^- compared to HO^- .^[2a] Because of the problem to specify a reference nucleophile with which the α -effect nucleophile should be compared, Hoz and Buncl defined the α -effect as the positive deviation from a Brønsted plot.^[3] This definition has been accepted by the 1994 version of the IUPAC glossary.^[2b] Um, Im, and Buncl have later introduced the additional criterion that the α -effect nucleophiles and the reference nucleophiles should react by the same mechanisms.^[4] They pointed out, that the classical assessment of the α -effect fails for reactions of HOO^- with substituted phenyl methanesulfonates, because the mechanisms differ from those of the corresponding reactions with HO^- .

The α -effect, which has been investigated for various reactions of nucleophiles including acylations, Michael additions, $\text{S}_{\text{N}}2$ reactions, and nucleophilic aromatic substitutions, has been the topic of several reviews,^[3,5] but its origin and extent are still discussed controversially.^[5,6] Over the years, several factors have been specified, which are supposed to

contribute to the magnitude of the α -effect. The α -effect was claimed to depend on the hybridization of the reaction center of the electrophilic reaction partner and to increase in the order $sp^3 < sp^2 < sp$.^[5] Large slopes β_{nuc} in Brønsted correlations, which are attributed to a large extent of bond formation in the transition state, have been claimed to be associated with large α -effects.^[5] Fina and Edwards emphasized, however, that the magnitude of β_{nuc} can only be related to the α -effect when similar substrates are compared.^[5c] Bunce, Um and co-workers have concluded that the magnitude of the α -effect strongly depends on the nature of the solvent system.^[5a,6e,i]

Several theories on the origin of the α -effect have emerged, which include the destabilization of the ground state by electron repulsions, the stabilization of the transition state, thermodynamic stabilization of the products, and solvent effects.^[5] In order to properly elucidate the influence of the product stabilities, Ren and Yamataka proposed to compare the reaction rates with the equilibrium constants for the reactions under consideration rather than with the corresponding Brønsted basicities.^[7]

In recent years, a renewed interest in the topic arose with the newly established mass-spectrometric techniques^[8] and the progress in quantum chemical methods,^[7,9] which reveal the intrinsic reactivities of the unsolvated α -effect nucleophiles. However, experimental studies in the gas-phase showed that the α -effect depends on the system investigated. For example, an α -effect was found for the nucleophilic substitution reactions of the hydroperoxide anion with methyl fluoride, anisoles and dimethyl methylphosphonate,^[8a,c] but not for its reactions with methyl formate and alkyl chlorides.^[8b,d]

Ren and Yamataka investigated the activation energies of S_N2 reactions of alkyl halides and of E2 reactions of ethyl chloride with a series of anionic bases in the gas phase using the G2(+) level of theory.^[7,9c,d,f] They found that α -effect nucleophiles deviated significantly from plots of the activation barriers of both reactions versus the proton affinities and claimed that α -effect nucleophiles react with lower deformation energies. However, the hydrazide anion H_2NNH^- has been calculated to react more slowly with methyl chloride than expected from the correlation with the proton affinities though it has been calculated to react faster than the more basic amide anion NH_2^- .^[9f]

Hydrazines are an important class of compounds which find considerable technical and commercial applications.^[10] Furthermore, numerous biological activities of hydrazine

derivatives have been discovered which make them potent drugs, peptidomimetics, and pesticides.^[10,11]

Besides their synthetic relevance, hydrazines are also interesting from a mechanistic point of view, as they have two adjacent nucleophilic nitrogen centers. Unsymmetrically substituted hydrazines are, therefore, ambident nucleophiles, and the factors that determine the regioselectivities of their reactions have been studied intensively.^[10] Typically, protonations as well as alkylations of alkyl-substituted hydrazines take place at the more-substituted nitrogen atom.^[10,12] Thus, in the case of 1,1-dialkyl hydrazines, quaternary ammonium salts are formed. Kinetic investigations often focused on the parent hydrazine^[6f,k,l,m,o,p,u,13] as α -effect nucleophiles and little is known about the nucleophilic reactivities of substituted hydrazines^[6r,s,w,x,z] though this information is crucial for predicting the regioselectivities in a variety of heterocyclic syntheses.

The relative reactivities of hydrazines and hydroxylamines depend strongly on the electrophilic reaction partners and the reaction conditions, and the magnitude of the α -effect is much smaller than for other typical α -effect nucleophiles, like oximates and hydroperoxide anions.^[5] Bernasconi and Murray found that the rates of nucleophilic attack of hydrazine, hydroxylamine and semicarbazide at benzylidene Meldrum's acid correlated well with those of normal primary amines in the Brønsted plot.^[6l] On the other hand, the equilibrium constants for the formation of the zwitterionic adducts from benzylidene Meldrum's acid with hydrazine, semicarbazide and methoxyamine were significantly larger than those with isobasic amines.^[6l] Dixon and Bruice reported that hydrazines add to malachite green faster and with greater equilibrium constants than primary amines of the same Brønsted basicities.^[6s] The linear correlation between the rate and equilibrium constants with a slope of 1.0 shows that the different product stabilities are fully reflected by the transition states.

To clarify the influence of substituents on the nucleophilic reactivities of potential α -effect nucleophiles and the factors which control the relative reactivities of the different sites of unsymmetrical hydrazines, we have now studied the kinetics of the reactions of the hydrazines **1–5**, hydrazides **6–9**, hydroxylamines **10–11**, ammonia (**12**), and methylamines **13–15** (Figure 4.1) with quinone methides **16a–c** and benzhydrylium ions **16d–n** as reference electrophiles (Table 4.1) in acetonitrile and water and evaluated their N and s_N parameters according to the linear free energy relationship [Eq. (4.1)].^[14]

In Equation (4.1), electrophiles are characterized by one solvent-independent parameter (E), and nucleophiles are characterized by two solvent-dependent parameters, N and s_N .^[15]

$$\log k_2(20\text{ }^\circ\text{C}) = s_N(N + E) \quad (4.1)$$

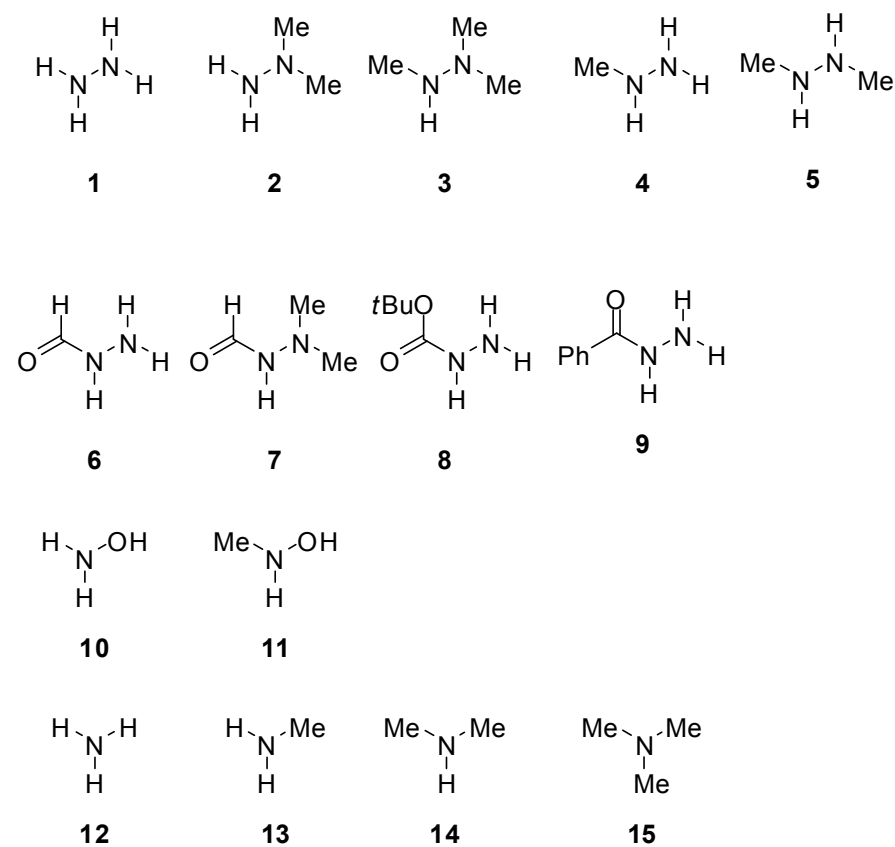


Figure 4.1. Structures of the nucleophiles 1–15.

Table 4.1. List of the reference electrophiles **16** used in this study.

| Reference Electrophile ^[a] | | $E^{[b]}$ | |
|---------------------------------------|---|---|----------------------|
| | $R^1 = t\text{Bu}, R^2 = \text{OMe}$ | ani(<i>t</i> Bu) ₂ QM (16a) | -16.11 |
| | $R^1 = t\text{Bu}, R^2 = \text{Me}$ | tol(<i>t</i> Bu) ₂ QM (16b) | -15.83 |
| | $R^1 = \text{Ph}, R^2 = \text{OMe}$ | ani(Ph) ₂ QM (16c) | -12.18 |
| | $n = 1$ | (lil) ₂ CH ⁺ (16d) | -10.04 |
| | $n = 2$ | (jul) ₂ CH ⁺ (16e) | -9.45 |
| | $n = 1$ | (ind) ₂ CH ⁺ (16f) | -8.76 |
| | $n = 2$ | (thq) ₂ CH ⁺ (16g) | -8.22 |
| | $R = N\text{-pyrrolidino}$ | (pyr) ₂ CH ⁺ (16h) | -7.69 |
| | $R = \text{NMe}_2$ | (dma) ₂ CH ⁺ (16i) | -7.02 |
| | $R = N\text{-morpholino}$ | (mor) ₂ CH ⁺ (16j) | -5.53 |
| | $R = \text{N}(\text{Me})\text{CH}_2\text{CF}_3$ | (mfa) ₂ CH ⁺ (16k) | -3.85 |
| | | (fur) ₂ CH ⁺ (16l) | -1.36 |
| | | (ani)(fur)CH ⁺ (16m) | -0.81 ^[c] |
| | | (ani) ₂ CH ⁺ (16n) | 0.00 |

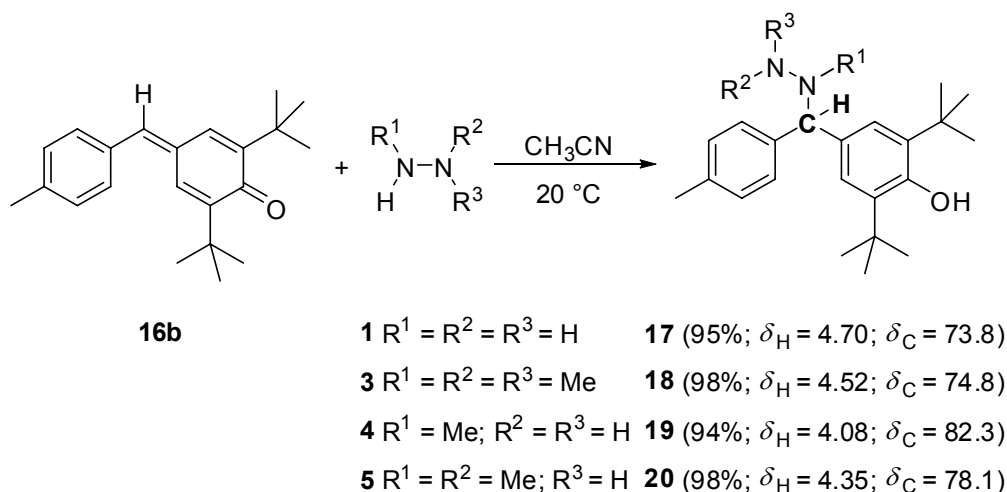
[a] Counterion of the benzhydryl cations: BF_4^- . [b] Electrophilicity parameters E from Refs. [15c,d,f]. [c] Revised electrophilicity parameter from Ref. [16].

4.2 Results and Discussion

4.2.1 Product Characterization

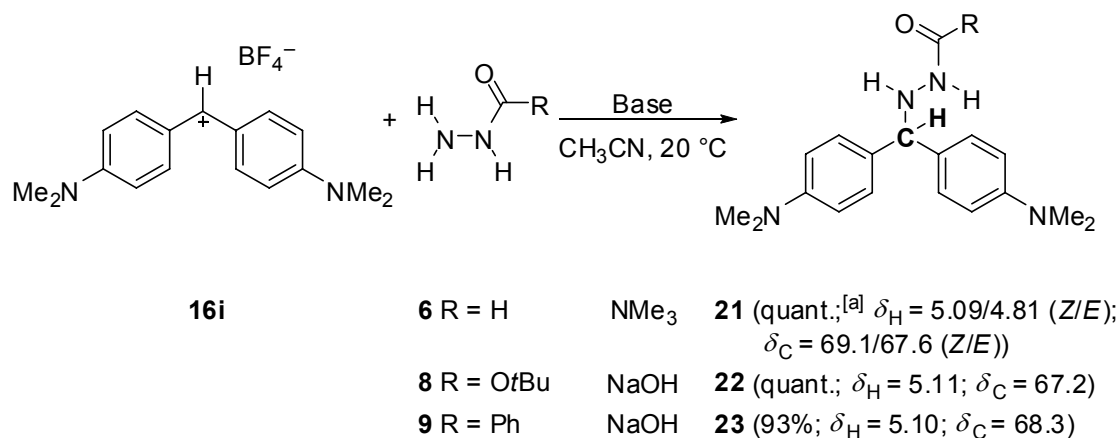
The parent hydrazine (**1**), trimethylhydrazine (**3**), methylhydrazine (**4**), and 1,2-dimethylhydrazine (**5**) reacted smoothly with the quinone methide tol(*t*Bu)₂QM (**16b**) in

acetonitrile at 20 °C to form the 1:1-addition products **17–20**, respectively, (Scheme 4.1). While **1** and **5** have two equivalent nucleophilic centers, **3** could, in principle, attack the quinone methide with either the secondary or the tertiary amino function, and **4** with the primary or the secondary amino function, respectively. We obtained only the products from regioselective reaction at the NHMe groups in 94–98% yield.^[17,18]



Scheme 4.1. Products of the reactions of the hydrazines **1–5** with **16b** and 1H and ^{13}C NMR chemical shifts (ppm) of the Ar_2CH group.

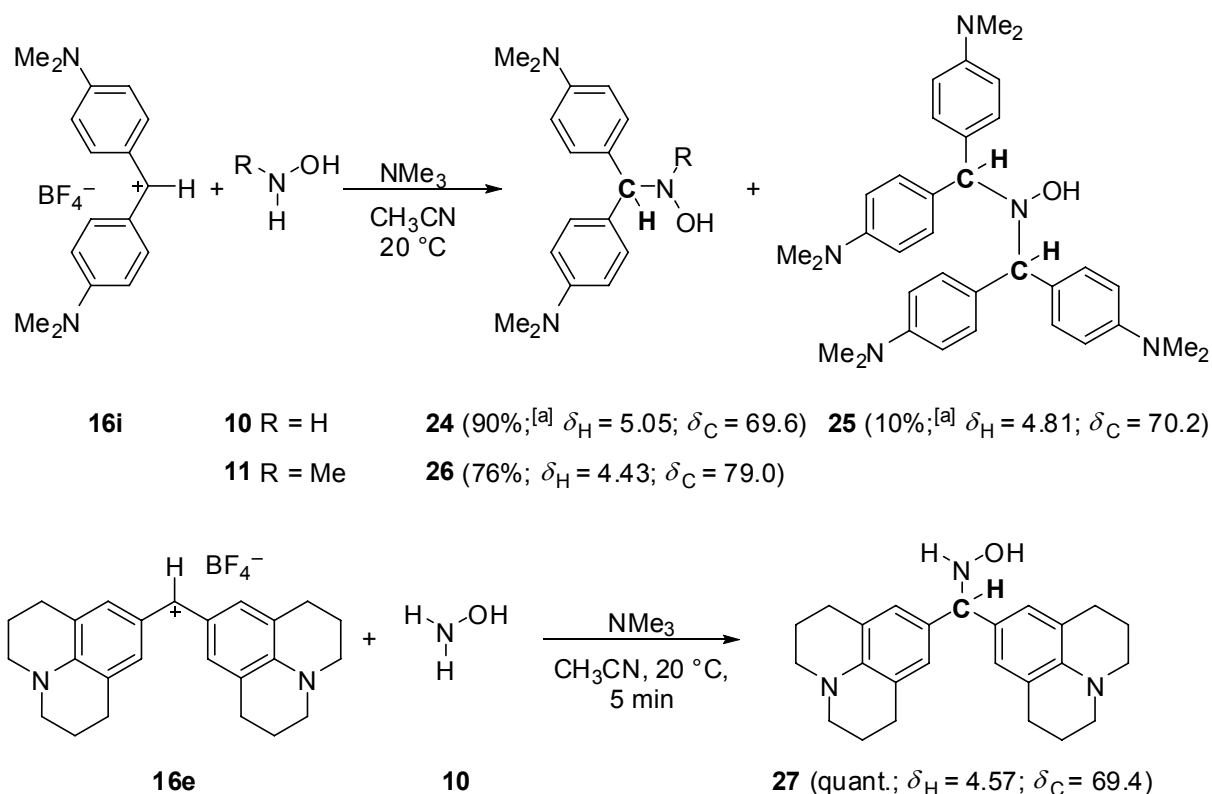
Regioselective reactions at the NH_2 groups were found for the reactions of the benzhydrylium salt $(dma)_2CH^+ BF_4^-$ (**16i**) with formohydrazide (**6**), *tert*-butyl hydrazinecarboxylate (**8**), and benzohydrazide (**9**). After alkaline work-up, the products **21–23** were obtained (Scheme 4.2). Like formohydrazide (**6**), the product **21** exists as a mixture of (*Z*)- and (*E*)-isomers (2:1 in $CDCl_3$). These results are in agreement with those of other researchers who showed a large preference for attack at the NH_2 group of hydrazides under various reaction conditions.^[10,19] The regioselectivity can only be reversed when the more acidic acylated NH group is deprotonated.^[20] No reaction was observed when *N,N*-dimethylformohydrazide (**7**) was combined with equimolar amounts of 4,4'-dimethoxybenzhydryl chloride (**16n-Cl**) at 20 °C, which can be explained by the low equilibrium constant for attack of **16n** at the NMe_2 group of **7** (see below).



Scheme 4.2. Products of the reaction of **6**, **8**, and **9** with **16i** and ^1H and ^{13}C NMR chemical shifts (ppm) of the Ar_2CH group.

[a] ^1H NMR spectroscopic analysis of the crude product showed the exclusive formation of **21** as a 2:1 mixture of (*Z*)- and (*E*)-isomers.

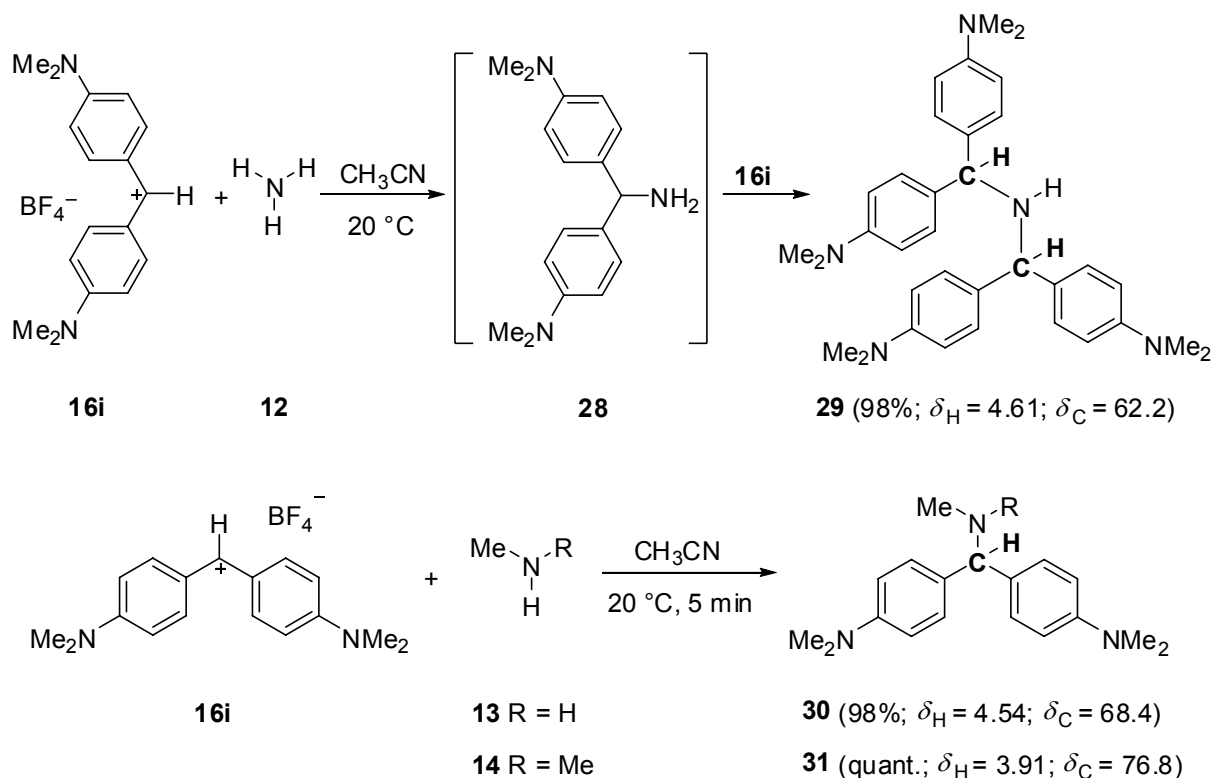
Combination of **16i** with 5.5 equivalents of hydroxylamine (**10**), which was generated by treatment of its hydrochloride with 1.7 equivalents of trimethylamine (**15**), yielded a 9:1 mixture of the mono- and double-alkylation products **24** and **25** (Scheme 4.3). On the other hand, the combination of **10** with an equimolar amount of **16e** yielded the mono-alkylated hydroxylamine **27** selectively. Regioselective mono-alkylation of the nitrogen to give **26** was also found for the combination of **16i** with 2.4 equivalents of *N*-methylhydroxylamine (**11**), which was generated from the corresponding hydrochloride with one equivalent of trimethylamine (Scheme 4.3). In line with these results, *N*-alkylation of hydroxylamine has previously been observed.^[6z,21] Only derivatives of hydroxamic acid, that is, hydroxylamines carrying electron-withdrawing groups at nitrogen, were found to react at oxygen in transition-metal catalyzed allylic substitution reactions^[22] and in $\text{S}_{\text{N}}2$ reactions when the hydroxyl group was deprotonated with NaH.^[23]



Scheme 4.3. Products of the reactions of **10** and **11** with **16i** or **16e** and ^1H and ^{13}C NMR chemical shifts (ppm) of the Ar_2CH group.

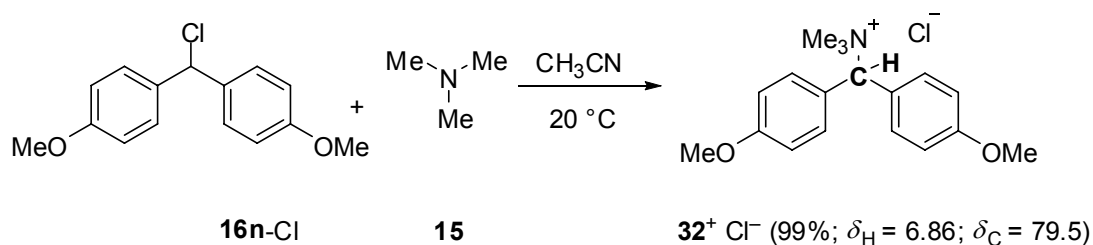
[a] The ratio **24/25** was determined by ^1H NMR spectroscopic analysis of the crude product.

When **16i** was added to 18 equivalents of ammonia (**12**) in acetonitrile at 20 °C, we observed the exclusive formation of the secondary amine **29** (Scheme 4.4). Unlike ammonia (**12**), methylamine (**13**) and dimethylamine (**14**) reacted with **16i** to yield the 1:1 products **30** and **31** exclusively.



Scheme 4.4. Products of the reactions of **12–14** with **16i** and ^1H and ^{13}C NMR chemical shifts (ppm) of the Ar_2CH group.

Treatment of $(\text{ani})_2\text{CHCl}$ (**16n-Cl**) with an ethanolic solution of 5 equivalents of trimethylamine (**15**) in acetonitrile at $20\text{ }^\circ\text{C}$ resulted in the formation of the quaternary ammonium salt $\text{32}^+ \text{Cl}^-$ (Scheme 4.5). Less reactive carbocations, like **16i**, reacted reversibly with trimethylamine (**15**), and products could not be isolated (detailed discussion below).



Scheme 4.5. Formation of the quaternary ammonium salt $\text{32}^+ \text{Cl}^-$ by treatment of **16n-Cl** with trimethylamine (**15**) and ^1H and ^{13}C NMR chemical shifts (ppm) of the Ar_2CH group.

4.2.2 Kinetics of the Reactions of 1–15 with the Reference Electrophiles 16

The rates of the reactions of the amines, hydrazines, hydrazides, and hydroxylamines **1–15** with the reference electrophiles **16** were determined spectrophotometrically in acetonitrile or water at 20 °C using conventional and stopped-flow methods as described elsewhere.^[15] The nucleophiles **1–15** were used in large excess (over 8 equivalents) relative to the electrophiles **16** to ensure first-order conditions. For the fast reactions ($k_2 > 10^6 \text{ M}^{-1} \text{ s}^{-1}$), benzhydrylium ions **16h–n** were generated by laser-flash photolysis (7 ns pulse, 266 nm) of substituted benzhydryl triphenyl or tributyl phosphonium tetrafluoroborates in acetonitrile in the presence of excess nucleophile.^[14a]

Monoexponential decays of the absorbances of the electrophiles were observed for all reactions, and the first-order rate constants k_{obs} (s^{-1}) were obtained by least-squares fitting of the exponential function $A = A_0 e^{-k_{\text{obs}} t} + C$ to the decays of the absorbances; a typical example is shown in Figure 4.2. Plots of k_{obs} versus the nucleophile concentrations were linear for all reactions of **1–3** and **6–15** with the reference electrophiles **16**. According to Equation (4.2), the second-order rate constants k_2 ($\text{M}^{-1} \text{ s}^{-1}$) were obtained as the slopes of these plots (Table 4.2). Theoretically, k_0 corresponds to the sum of all first-order side reactions of the benzhydrylium ions and the reverse reaction. As it is usually very small compared with $k_2[\text{Nu}]$, it is dominated by inaccuracies in k_{obs} and will, therefore, not be discussed in the following.

$$k_{\text{obs}} = k_2[\text{Nu}] + k_0 \quad (4.2)$$

We will first discuss the reactions of the nucleophiles **1** and **4–15** with the reference electrophiles **16** because these show the more simple kinetics.

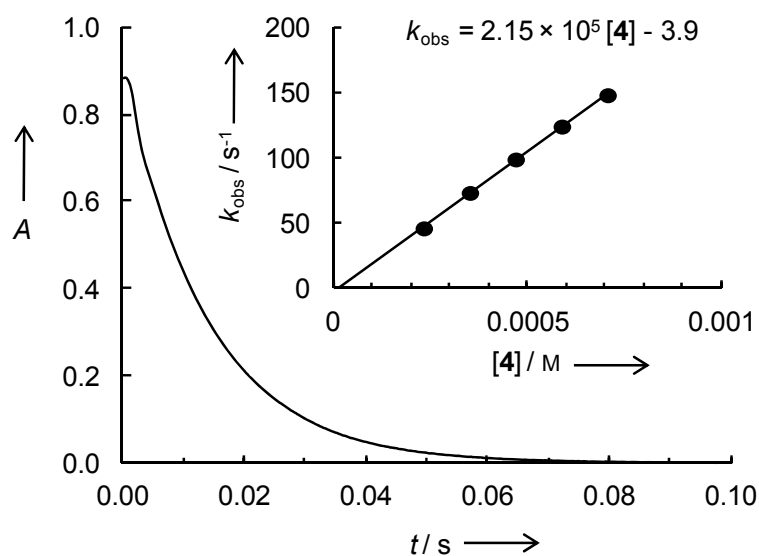


Figure 4.2. Exponential decay of the absorbance at 616 nm during the reaction of **16f** (1.74×10^{-5} M) with methylhydrazine ($[4] = 3.56 \times 10^{-4}$ M; $k_{\text{obs}} = 73.2 \text{ s}^{-1}$) in acetonitrile at 20 °C. Inset: The plot of k_{obs} versus $[4]$ yielded the second-order rate constant $k_2 = 2.15 \times 10^5 \text{ M}^{-1} \text{ s}^{-1}$.

Due to the explosive nature of neat anhydrous hydrazine (**1**), the kinetic measurements were either performed using hydrazine monohydrate or hydrazinium dihydrochloride [$\text{p}K_{\text{aH}}(\text{N}_2\text{H}_4 \text{ in } \text{CH}_3\text{CN}) = 16.61$]^[24] which was deprotonated with 2.00 equivalents of 1,8-diazabicyclo[5.4.0]undec-7-ene (DBU; $\text{p}K_{\text{aH}}(\text{DBU in } \text{CH}_3\text{CN}) = 24.34$).^[25] The complete deprotonation of the hydrazinium dihydrochloride by DBU was confirmed by the fact that the rate constants for the reaction of **1** with **16f** determined with both methods differed by less than 5 %. Similarly, hydroxylamine (**10**), *N*-methylhydroxylamine (**11**), methylamine (**13**), and dimethylamine (**14**) were generated by partial deprotonation of the corresponding hydrochlorides with 0.50–0.95 equivalents of DBU. For the reaction of methylamine (**13**) with **16h**, $\text{KO}t\text{Bu}$ was used as an alternative deprotonation agent. The similar rate constants obtained with both bases confirmed the complete deprotonation of methylamine hydrochloride by DBU and proved that the reactivities of the amines were not affected by hydrogen bonding of the amines to the protonated amines or the protonated DBU. Stock solutions of ammonia (**12**) were prepared by gas injection in acetonitrile, and trimethylamine

was used as a 33% solution in ethanol. In both cases, the concentrations of the stock solutions were determined by titration with hydrochloric acid.

Tetramethylhydrazine was not used in our kinetic studies, because we could not obtain this compound in sufficient purity, and even small contaminations by trimethylhydrazine (**3**) are problematic since we consider trimethylhydrazine (**3**) to be more nucleophilic than tetramethylhydrazine (see below).

While linear k_{obs} versus [nucleophile] plots were also obtained for the reactions of methylhydrazine (**4**) and 1,2-dimethylhydrazine (**5**) with most electrophiles, the correlations between k_{obs} and the hydrazine concentrations showed upward curvatures for the reactions of **4** with **16b** and **5** with **16c** in acetonitrile (Figure 4.3).

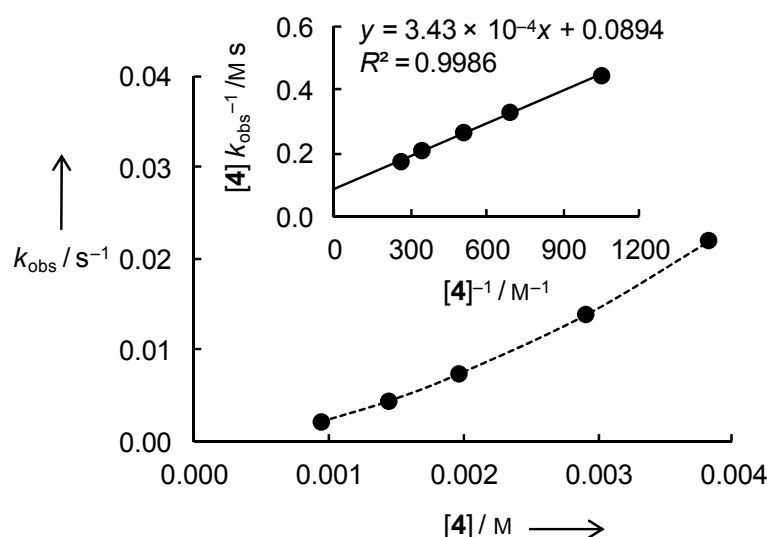
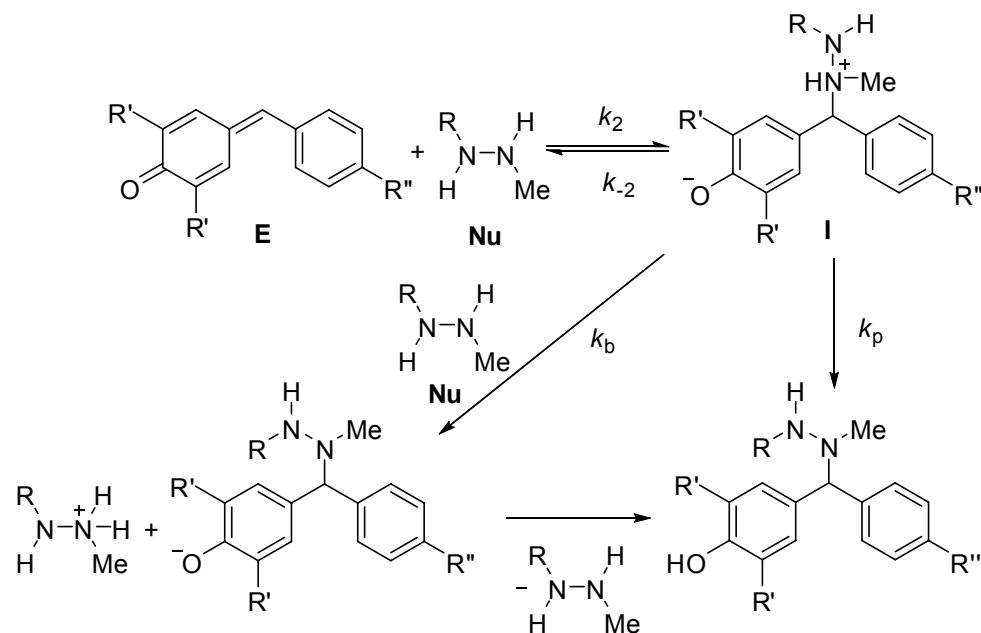


Figure 4.3. Plot of k_{obs} versus $[4]$ for the reaction of methylhydrazine (**4**) with **16b** in CH_3CN at 20°C . Inset: Plot of $[4]/k_{\text{obs}}$ versus $1/[4]$ from which the second-order rate constant k_2 ($1/0.0894 \text{ M s} = 11.2 \text{ M}^{-1} \text{ s}^{-1}$) was obtained as the reciprocal intercept.

In these cases, the attack of the hydrazines is followed by a rate determining proton transfer step, in which a second hydrazine molecule acts as general base catalyst (Scheme 4.6). An analogous behavior was previously observed for the reactions of secondary amines with quinone methides,^[14d] as well as with thiocarbonates, thionobenzoates, and activated esters of indole-3-acetic acid.^[26]



Scheme 4.6. Reactions of the quinone methides **16b** and **16c** (**E**) with the mono- and 1,2-dimethylhydrazines **4** and **5** (**Nu**).

The kinetics of the reactions in Scheme 4.6 follow the rate law of Equation (4.3) which is derived in the Experimental Section; it can be rewritten as Equation (4.4).

$$k_{\text{obs}} = \frac{k_2 k_b [\text{Nu}]^2}{k_{-2} + k_b [\text{Nu}]} \quad (4.3)$$

$$\frac{[\text{Nu}]}{k_{\text{obs}}} = \frac{1}{k_2} + \frac{k_{-2}}{k_2 k_b [\text{Nu}]} \quad (4.4)$$

In line with Equations (4.3) and (4.4), plots of $[\text{Nu}]/k_{\text{obs}}$ against $1/[\text{Nu}]$ were linear for a wide range of concentrations, as illustrated in the inset of Figure 4.3 for the reaction of **4** with **16b**. The second-order rate constants k_2 marked with footnote [h] in Table 4.2 were obtained from the intercepts ($1/k_2$) of these linear correlations.

Since in all other reactions, including those of dimethylamine (**14**) and methylhydrazine (**4**) with quinone methides in acetonitrile, linear correlations of the observed rate constants with the concentrations of the nucleophiles were obtained (see Experimental Section), one can conclude that the initial attack of the nucleophiles is generally irreversible, that is, $k_{-2} \ll k_b [\text{Nu}]$.

The reactions of hydrazine (**1**) and methylhydrazine (**4**) with the benzhydrylium ions **16** have also been studied in water, where competing reactions with either water or hydroxide ions have to be considered. The observed first-order rate constants k_{obs} are the sum of the rate constants for the reactions of the benzhydrylium ions **16** with the hydrazines (k_2), with hydroxide ($k_{2,\text{OH}}$) and with water (k_w) as described previously [Eq. (4.5)].^[14h,i]

$$k_{\text{obs}} = k_2[\text{hydrazine}] + k_{2,\text{OH}}[\text{OH}^-] + k_w \quad (4.5)$$

The concentrations of the hydrazines and of hydroxide were calculated from the $\text{p}K_{\text{aH}}$ values. With these concentrations and the previously published values for $k_{2,\text{OH}}$ ^[14k] one can calculate $k_{1,\text{eff}}$ as defined by Equation (4.6).

$$k_{1,\text{eff}} = k_{\text{obs}} - k_{2,\text{OH}}[\text{OH}^-] = k_2[\text{hydrazine}] + k_w \quad (4.6)$$

As a consequence, the second-order rate constants k_2 for the reactions of hydrazines **1** and **4** with **16** in water were obtained from the slopes of the correlations of $k_{1,\text{eff}}$ with the hydrazine concentrations. It is observed that neither the reactions with hydroxide nor with water contribute more than 1% to the overall observed rate constants. As described above for the reactions in acetonitrile, the linearity of the $k_{1,\text{eff}}$ versus [hydrazine] plots indicates a rate law which is first order in hydrazine, implying that the C-N-bond formation and not the subsequent deprotonation is the rate determining step.

Table 4.3. Second-order rate constants k_2 for the reactions of the reference electrophiles **16** with the amines **1–15** and **28** at 20 °C and resulting N and s_N parameters.

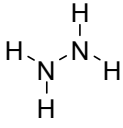
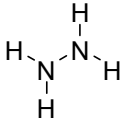
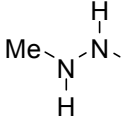
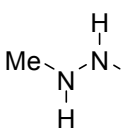
| Nucleophile | N | s_N | Ar_2CH^+ [a] | $k_2/\text{M}^{-1} \text{s}^{-1}$ |
|--|----------------------|---------------------|------------------------------|-----------------------------------|
| 1  in H_2O | 13.46 ^[b] | 0.57 ^[b] | 16e | 1.97×10^2 |
| | | | 16f | 4.31×10^2 |
| | | | 16g | 9.25×10^2 [c] |
| | | | 16h | 1.89×10^3 |
| | | | 16i | 4.52×10^3 [d] |
| 1  in CH_3CN | 16.45 ^[e] | 0.56 ^[e] | 16c | 2.23×10^2 [f] |
| | | | 16d | 3.41×10^3 [g] |
| | | | 16e | 8.74×10^3 [f] |
| | | | 16f | 2.04×10^4 [f] |
| | | | 16f | 2.14×10^4 [g] |
| | | | 16h | 1.58×10^5 [f] |
| | | | 16i | 2.95×10^5 [g] |
| | | | 16j | 1.22×10^6 [g] |
| | | | 16k | 9.90×10^6 [g] |
| 4  in H_2O | 17.23 | 0.45 | 16d | 1.59×10^3 |
| | | | 16e | 3.75×10^3 |
| | | | 16f | 5.83×10^3 |
| | | | 16g | 1.16×10^4 |
| 4  in CH_3CN | 17.73 | 0.58 | 16b | 1.12×10^1 [h] |
| | | | 16c | 1.46×10^3 |
| | | | 16d | 3.32×10^4 |
| | | | 16f | 2.15×10^5 |
| | | | 16j | 1.22×10^7 |
| | | | 16k | 8.65×10^7 |

Table 4.2 (continued).

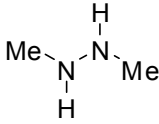
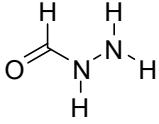
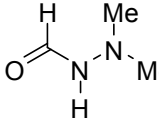
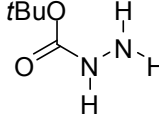
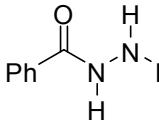
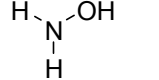
| Nucleophile | N | s_N | Ar_2CH^+ [a] | $k_2/\text{M}^{-1} \text{s}^{-1}$ |
|---|-------|-------|------------------------------|-----------------------------------|
| 5  in CH_3CN | 16.15 | 0.68 | 16c | 4.44×10^2 [h] |
| | | | 16d | 1.64×10^4 |
| | | | 16e | 4.46×10^4 |
| | | | 16f | 9.24×10^4 |
| | | | 16h | 5.24×10^5 |
| 6  in CH_3CN | 10.35 | 0.76 | 16i | 4.24×10^2 |
| | | | 16j | 4.33×10^3 |
| | | | 16k | 6.53×10^4 |
| | | | 16l | 1.26×10^7 |
| | | | 16n | 6.50×10^7 |
| 7  in CH_3CN | 15.69 | 0.51 | 16l | 2.18×10^7 |
| | | | 16m | 4.08×10^7 |
| | | | 16n | 1.08×10^8 |
| 8  in CH_3CN | 11.40 | 0.70 | 16i | 1.31×10^3 |
| | | | 16j | 1.06×10^4 |
| | | | 16k | 1.37×10^5 |
| | | | 16l | 1.42×10^7 |
| | | | 16n | 7.12×10^7 |
| 9  in CH_3CN | 12.49 | 0.66 | 16i | 4.06×10^3 |
| | | | 16j | 3.66×10^4 |
| | | | 16k | 4.92×10^5 |
| 10  in CH_3CN | 12.80 | 0.63 | 16c | 2.44 [f] |
| | | | 16d | 5.80×10^1 [f] |
| | | | 16f | 3.01×10^2 [f] |
| | | | 16i | 4.33×10^3 [f] |

Table 4.2 (continued).

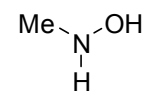
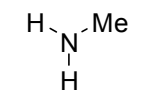
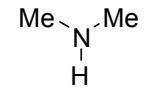
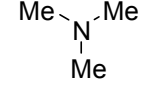
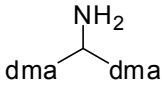
| Nucleophile | N | s_N | Ar_2CH^+ [a] | $k_2/\text{M}^{-1} \text{s}^{-1}$ |
|--|----------------------|---------------------|------------------------------|-----------------------------------|
| 11  in CH_3CN | 14.10 | 0.76 | 16d | 1.09×10^3 [f] |
| | | | 16f | 1.09×10^4 [f] |
| | | | 16h | 9.20×10^4 [f] |
| | | | 16i | 1.78×10^5 [f] |
| 12  in CH_3CN | 11.39 | 0.69 | 16c | 2.88×10^{-1} |
| | | | 16f | 4.76×10^1 |
| | | | 16h | 4.54×10^2 |
| | | | 16i | 1.53×10^3 |
| | | | 16j | 9.05×10^3 |
| 13  in CH_3CN | 15.19 ^[e] | 0.68 ^[e] | 16c | 1.37×10^2 [f] |
| | | | 16d | 2.65×10^3 [f] |
| | | | 16f | 2.03×10^4 [f] |
| | | | 16h | 1.68×10^5 [f] |
| | | | 16h | 1.71×10^5 [i] |
| | | | 16i | 4.00×10^5 [i] |
| 14  in CH_3CN | 17.96 | 0.63 | 16a | 1.50×10^1 [f] |
| | | | 16c | 4.63×10^3 [f] |
| | | | 16d | 9.77×10^4 [i] |
| | | | 16e | 2.65×10^5 [f] |
| 15  in CH_3CN | 23.05 | 0.45 | 16h | 6.54×10^6 |
| | | | 16i | 2.00×10^7 |
| | | | 16j | 7.27×10^7 |
| | | | 16k | 4.05×10^8 |

Table 4.2 (continued).

| Nucleophile | N | s_N | Ar_2CH^+ [a] | $k_2/\text{M}^{-1} \text{s}^{-1}$ |
|---|-----|-------|------------------------------|-----------------------------------|
| 28  in CH_3CN | | | 16i | 4.20×10^3 |

[a] Counterion of the benzhydryl cations: BF_4^- . [b] Nucleophilicity parameters in methanol/acetonitrile (91:9 v/v): $N = 13.47$; $s_N = 0.70$ from Ref. [27]. [c] Cosolvent: 0.75 vol-% CH_3CN . [d] Cosolvent: 1.0 vol-% CH_3CN . [e] For the determination of the nucleophilicity parameters N and s_N , the average of the second-order rate constants obtained from reactions of **16f** with $\text{N}_2\text{H}_4 \cdot \text{H}_2\text{O}$ or using a 1:2 mixture of $\text{N}_2\text{H}_4 \cdot 2 \text{HCl}$ and for the reaction of **16h** with **13** generated from methylamine hydrochloride (**13**·HCl) with $\text{KO}t\text{Bu}$ or DBU was used. [f] The nucleophiles were generated by deprotonation of the corresponding hydrochloride salts with DBU. [g] Determined using $\text{N}_2\text{H}_4 \cdot \text{H}_2\text{O}$. [h] Second-order rate constants k_2 were derived from Equation (4.4) and are less precise. [i] The nucleophiles were generated by deprotonation of the corresponding hydrochloride salts with $\text{KO}t\text{Bu}$.

As ammonia (**12**) yielded the secondary amine **29** in the reaction with **16i** (Scheme 4.4) we also determined the kinetics of the reaction of **16i** with the intermediate primary amine **28**, which was synthesized by treatment of $(\text{dma})_2\text{CHOH}$ with phthalimide and subsequent hydrolysis with hydrochloric acid according to the literature.^[28] As shown in Table 4.2, **28** reacts 2.7 times faster with **16i** than ammonia (**12**). As more than 70 equivalents of ammonia were used for the determination of its nucleophilic reactivity towards **16i**, the measured rate constants refer to the formation of the mono-substituted product **28**, which did not react with further **16i** under the conditions of the kinetic experiments. This interpretation is confirmed by the linear dependence of the observed rate constants on the concentration of NH_3 in the investigated concentration range, which would not be obtained if the subsequent reaction of **28** with **16i** would contribute to the observed rate constant. The formation of the secondary amine **29** under synthetic conditions must, therefore, be the result of thermodynamic control. Traces of protons may regenerate **16i** from **28** and thus lead to the thermodynamically more favored product **29**. This interpretation is in line with the results by Villiger and Kopetschni who showed that **28** disproportionates to ammonia (**12**) and **29** under proton catalysis.^[29]

When the logarithms of the second-order rate constants k_2 were plotted against the previously reported electrophilicity parameters E of the benzhydrylium ions and quinone methides **16**, linear correlations were obtained (Figure 4.4), from which the nucleophile-specific parameters N and s_N (Table 4.2) were determined according to Equation (4.1).

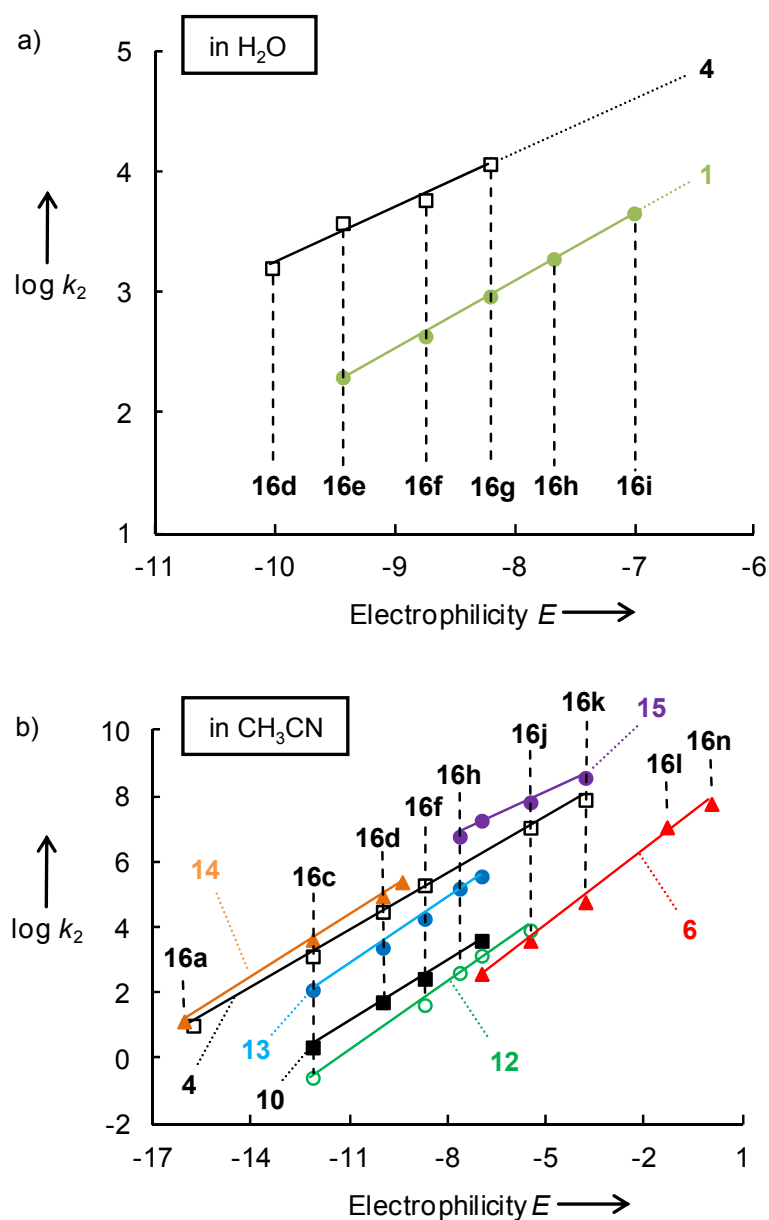


Figure 4.4. Correlations of the second-order rate constants $\log k_2$ with the E parameters of the reference electrophiles for the reactions of selected representative nucleophiles with benzhydrylium ions and quinone methides **16** at 20 °C in (a) H₂O and (b) acetonitrile.

4.2.3 Ambident Reactivities of Asymmetrical Hydrazines

The situation is more complicated for 1,1-dimethylhydrazine (**2**) and trimethylhydrazine (**3**) which contain tertiary amine groups. With these systems, we observed different kinetic behavior depending on the concentration of the hydrazines and the nature of the electrophile. For the reactions of **2** with **16h** and **16i** we could even observe two separate exponential

decays on different time scales when different concentrations of **2** were employed. Figure 4.5a shows the decay of the absorbance of **16h** which was generated by laser-flash photolysis of the phosphonium salt **16h**-PBU₃ in the presence of **2** (8.43×10^{-2} M) in acetonitrile at 20 °C. A monoexponential decay of the absorbance of the carbocation was observed within 15 μ s (approximately 80% conversion), while the remaining absorbance disappeared within around 100 ms. With increasing hydrazine concentrations, the conversion arising from the fast reaction increased, and eventually the fast decay was observed almost exclusively. From the linear increase of k_{obs} with the concentration of **2**, we obtained the second-order rate constant $k_2' = 3.78 \times 10^6 \text{ M}^{-1} \text{ s}^{-1}$ (Table 4.3).

At lower concentrations of the hydrazine, the slower decay became more dominant, and for $[\mathbf{2}] < 3 \times 10^{-4}$ M, the initial fast decay of the absorbance was almost absent and a monoexponential decay on a longer timescale was observed. Figure 4.5b shows the decay of **16h** in the presence of 1.45×10^{-4} M **2** determined with the stopped-flow technique. Again, a monoexponential decay of the absorbance of the carbocation was observed and a linear correlation of k_{obs} with the hydrazine concentration was obtained, the slope of which yielded another significantly lower second-order rate constant of $k_2 = 1.44 \times 10^3 \text{ M}^{-1} \text{ s}^{-1}$ (Table 4.3).

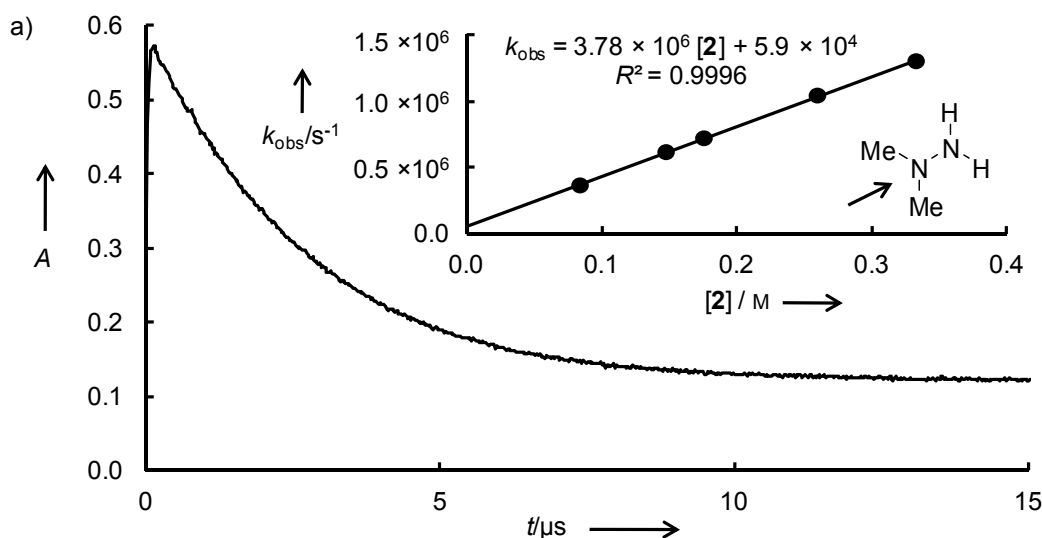


Figure 4.5. a) Fast exponential decay of the absorbance at 611 nm during the reaction of **16h** (generated from $[\mathbf{16h}\text{-PBU}_3] = 1.47 \times 10^{-5}$ M) with 1,1-dimethylhydrazine ($[\mathbf{2}] = 8.43 \times 10^{-2}$ M; $k_{\text{obs}} = 3.71 \times 10^5 \text{ s}^{-1}$). b) Slow exponential decay of the absorbance at 611 nm during the reaction of **16h** ($[\mathbf{16h}] = 1.80 \times 10^{-5}$ M) with 1,1-dimethylhydrazine ($[\mathbf{2}] = 1.45 \times 10^{-4}$ M; $k_{\text{obs}} = 1.78 \times 10^{-1} \text{ s}^{-1}$). Insets: Plots of k_{obs} versus $[\mathbf{2}]$ yielded the second-order rate constants $k_2' = 3.78 \times 10^6 \text{ M}^{-1} \text{ s}^{-1}$ and $k_2 = 1.44 \times 10^3 \text{ M}^{-1} \text{ s}^{-1}$.

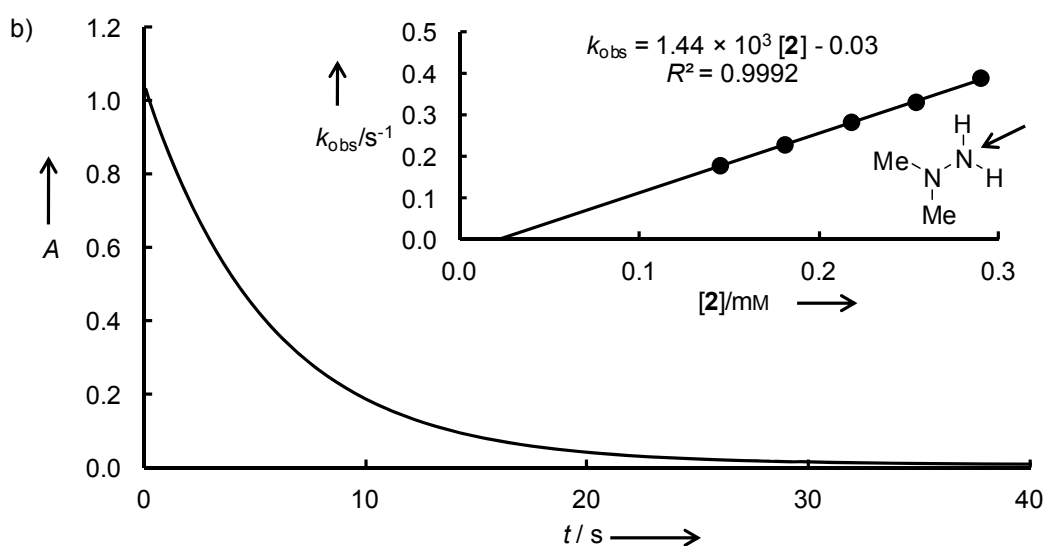
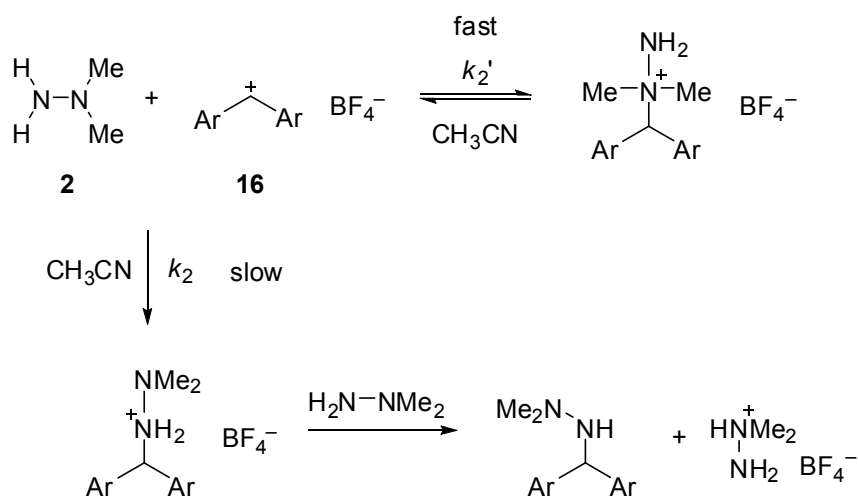


Figure 4.5 (continued).

Table 4.3. Second-order rate constants k_2 and k_2' for the reactions of the reference electrophiles **16** with the primary, secondary, and tertiary amine functions of the unsymmetrical hydrazines **2** and **3** in CH_3CN at 20 °C.

| Nucleophile | Ar_2CH^+ | $k_2/\text{M}^{-1}\text{s}^{-1}$ | $k_2'/\text{M}^{-1}\text{s}^{-1}$ |
|--------------|--------------------------|----------------------------------|-----------------------------------|
| 2 | 16c | 5.69×10^{-1} | |
| | 16d | 1.18×10^1 | |
| | 16f | 1.27×10^2 | |
| | 16h | 1.44×10^3 | 3.78×10^6 |
| | 16i | 2.46×10^3 | 8.06×10^6 |
| | 16j | | 3.46×10^7 |
| | 16k | | 2.04×10^8 |
| 3 | 16f | 6.15×10^2 | |
| | 16g | 1.26×10^3 | |
| | 16h | 3.74×10^3 | |
| | 16i | 1.17×10^4 | |
| | 16j | | 3.01×10^6 |
| | 16k | | 1.81×10^7 |
| | 16l | | 4.58×10^8 |

This behavior can be explained by the mechanism depicted in Scheme 4.7. The fast and reversible reaction corresponds to the attack at the tertiary nitrogen while the slower reaction, which becomes irreversible by deprotonation with a second molecule of the hydrazine, corresponds to the attack at the NH_2 group of **2**. At low concentrations of 1,1-dimethylhydrazine (**2**), the equilibrium for the fast reaction, which leads to the kinetically controlled product, is almost completely on the side of the starting material, and the slow process (reaction at the NH_2 group) is observed exclusively.



Scheme 4.7. Ambident reactivity of 1,1-dimethylhydrazine (**2**) in reactions with **16**.

When we investigated the reactions of **2** with other reference electrophiles, one of the two modes of attack was always predominant, so that we obtained only one second-order rate constant for each reaction: For the weak electrophiles **16c–f**, the equilibrium of the fast reaction is on the side of the reactants and we observed only the slow decay. For the stronger electrophiles **16j,k**, we observed exclusively the fast reaction because the formation of the quaternary hydrazinium ions is almost quantitative even at low hydrazine concentrations (Table 4.3).^[30]

While for the parent hydrazine (**1**) and methylhydrazine (**4**) the rate constants measured with the three different methods all correlated linearly with the electrophilicity parameter E as required by Equation (4.1), two correlation lines were found for 1,1-dimethylhydrazine (**2**) which are assigned to the two sites of attack (Figure 4.6). It can be seen that the methyl substituents increase the nucleophilicity of the substituted nitrogen by more than one order of

magnitude and decrease the reactivity of the neighboring site by more than two orders of magnitude.

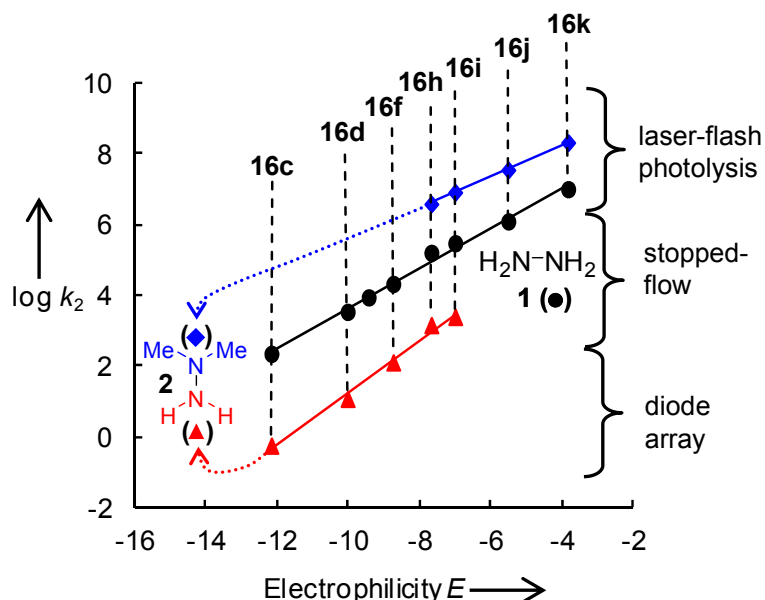
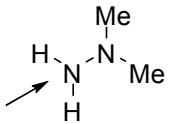
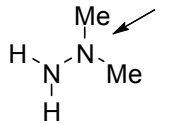
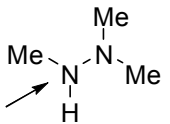
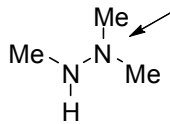


Figure 4.6. Plots of the second-order rate constants $\log k_2$ or $\log k_2'$ for the reactions of hydrazine (**1**) and 1,1-dimethylhydrazine (**2**) with benzhydrylium ions and quinone methides in CH_3CN at 20 °C versus the E parameters of **16**.

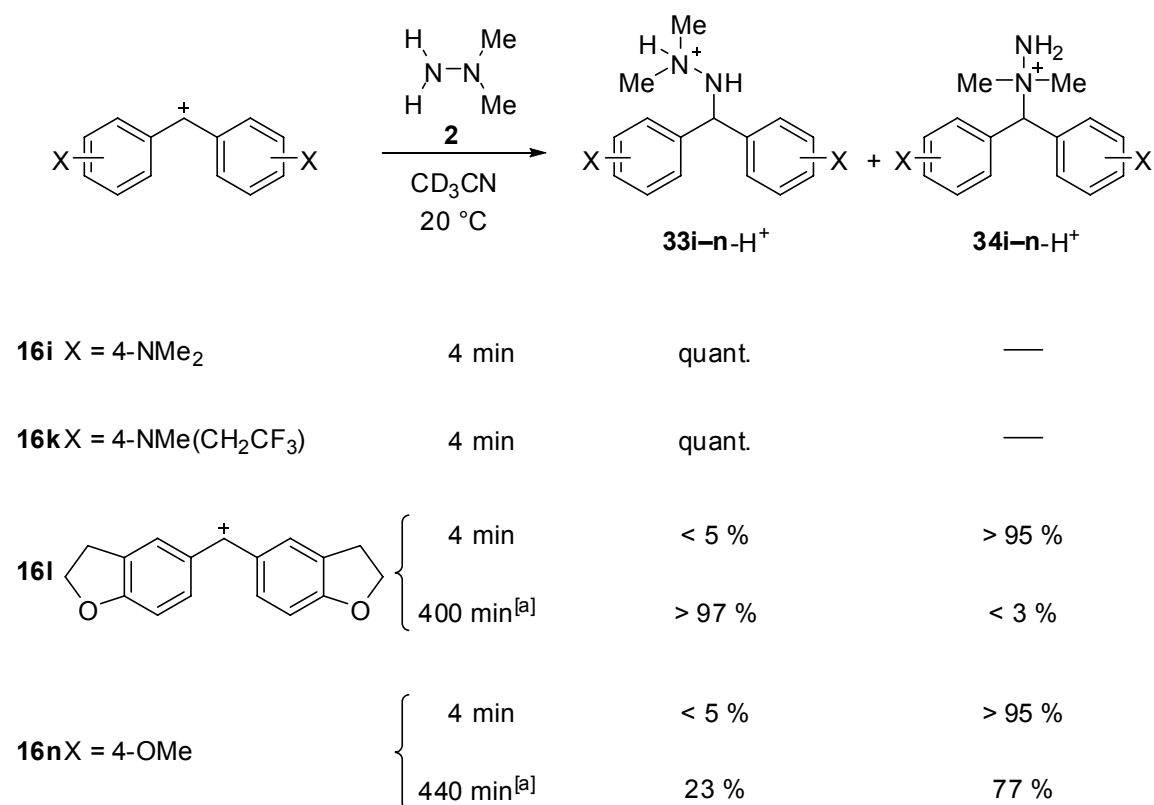
An analogous behavior was found for the reactions of trimethylhydrazine (**3**; Tables 4.3 and 4.4). Though we did not find systems where the two competing reactions could be observed separately, Figure 4.14 in the Experimental Section clearly shows two correlation lines, the higher one for the reaction at the tertiary nitrogen and the lower one for the reaction at the NHMe position. Again, methyl substitution increases the nucleophilicity of the substituted center while it reduces that of the adjacent nitrogen.

This information is also given by the nucleophilicity parameters N and s_N in Table 4.4, which have been derived from the correlations in Figure 4.6 and 4.14 (Experimental Section). The different values of s_N for the two sites in **2** and **3** imply, however, that the positional selectivities decrease with increasing reactivity of the electrophiles (Table 4.4).

Table 4.4. N and s_N parameters of **2** and **3** in CH_3CN .

| Hydrazine | N | s_N | | N | s_N |
|---|-------|-------|---|-------|-------|
| 2  | 11.72 | 0.73 |  | 22.41 | 0.45 |
| 3  | 12.43 | 0.75 |  | 17.75 | 0.53 |

The reaction mechanism, derived from the kinetic experiments (Scheme 4.7) is in line with structural investigations by NMR-spectroscopy.^[17] NMR spectroscopic analysis of the product obtained from **16i** and **2** showed the exclusive formation of **33i**- $\text{H}^+ \text{BF}_4^-$, which arises from electrophilic attack at the NH_2 group of **2** (Scheme 4.8).^[31] In contrast to the interpretation of the kinetic data, NMR analysis of the product obtained from **16k** and **2** also showed exclusive attack at the NH_2 group of **2** (\rightarrow **33k**- $\text{H}^+ \text{BF}_4^-$).^[32] We, therefore, assumed that the initial formation of the quaternary hydrazinium ion **34k**- $\text{H}^+ \text{BF}_4^-$ is followed by re-ionization and eventual formation of the thermodynamically favored product **33k**- $\text{H}^+ \text{BF}_4^-$. To confirm this hypothesis, we have also studied the reactions of the more electrophilic benzhydrylium ions **16l** and **16n** with **2**. At short reaction times we observed the predominant formation of the quaternary hydrazinium ions **34l**- $\text{H}^+ \text{Cl}^-$ and **34n**- $\text{H}^+ \text{Br}^-$, which subsequently rearranged to **33l**- $\text{H}^+ \text{Cl}^-$ and **33n**- $\text{H}^+ \text{Br}^-$, respectively (Scheme 4.8).



Scheme 4.8. Reactions of 1,1-dimethylhydrazine (**2**) with **16i–n** in CD₃CN.

[a] Formation of **33i**-H⁺ Cl⁻ and **33n**-H⁺ Br⁻ is accompanied by some decomposition.

4.2.4 Structure Reactivity Relationship

We can now compare the nucleophilic reactivities of the amines and hydrazines **1–15**, which cover the reactivity range from $10 < N < 24$, with each other and with those of other amines. The s_N parameters of the nucleophiles studied in this work vary from 0.45 to 0.76, that is, the relative reactivities of these amines will depend on the reactivities of the reference electrophiles. In order to avoid ambiguity, the following discussion will focus on the rates of the reactions with (dma)₂CH⁺ (**16i**) (Figures 4.7 and 4.8). Whereas the nucleophilicity parameters N in Tables 4.2 and 4.4 refer to the gross reactivities of the molecules, the rate constants for the symmetrical nucleophiles hydrazine (**1**) and 1,2-dimethylhydrazine (**5**) in Figures 4.7 and 4.8 were corrected by the statistical factor of 2 to reflect the relative reactivities of the individual nucleophilic centers. Figure 4.7 shows a comparison of the second-order rate constants for the reactions of **16i** with differently substituted amines, hydrazines, hydrazides, and hydroxylamines in acetonitrile. The rows illustrate the influence

of α -substitution as well as branching (β -substitution), while the columns reflect the effect of methylation of the reactive center, that is, the change from primary over secondary to tertiary centers.

Replacement of the hydrogen atoms in ammonia (**12**) by alkyl groups significantly increases the nucleophilicity. While substitution of one hydrogen by a methyl group results in a 2.6×10^2 times higher reactivity, the second and third methyl groups increase the reactivity by factors of 20 (**14/13**) and 2.6 (**15/14**). The activation by long-chained alkyl groups is considerably smaller: One propyl group activates by a factor of 93 (**36/12**). In comparison, diethylamine (**39**) is 5.5 times more reactive than **36** and the third ethyl group even lowers the reactivity by a factor of 4.5 (**40/39**). We thus arrive at the noticeable conclusion that trimethylamine (**15**) is 1.1×10^2 times more nucleophilic than triethylamine (**39**).

As shown in the first line of Figure 4.7, branching of the alkyl groups in primary amines leads to a steady reduction of reactivity, and *tert*-butylamine (**38**) is 58 times less nucleophilic than methylamine (**13**).

The vertical comparison of hydrazine (**1**), methylhydrazine (**4**), and 1,1-dimethylhydrazine (**2**) shows that the methyl groups in hydrazine activate the substituted nitrogen by factors of 11 (**4/1**) and 4.9 (**2/4**), respectively, that is, the trend is similar to that in the series methylamine (**13**), dimethylamine (**14**), trimethylamine (**15**).

The retarding effect of methyl groups on the reactivity of the adjacent nitrogen corresponds to the branching effect in the series of the primary amines. This effect is more pronounced in the series of hydrazines, however. While isopropylamine (**37**) is 7.6 times less reactive than methylamine (**13**), the NH_2 group in 1,1-dimethylhydrazine (**2**) is 60 times less reactive than one NH_2 group in the parent hydrazine (**1**). Similar retarding effects of methyl groups at the adjacent nitrogen center can be observed in the series of hydrazines with secondary and tertiary nitrogen reaction centers: the NHMe group of trimethylhydrazine (**3**) is 69 times less reactive than one position in 1,2-dimethylhydrazine (**5**), which in turn reacts 2.0 times slower than the NHMe group of methylhydrazine (**4**); analogously the NMe_2 group of trimethylhydrazine (**3**) is 17 times less reactive than the corresponding group in 1,1-dimethylhydrazine (**2**).

1,1-Dimethylation of formohydrazide (**6**→**7**) increases the reactivity by a similar amount (factor 62) as 1,1-dimethylation of hydrazine (**1**→**2**, factor 54).

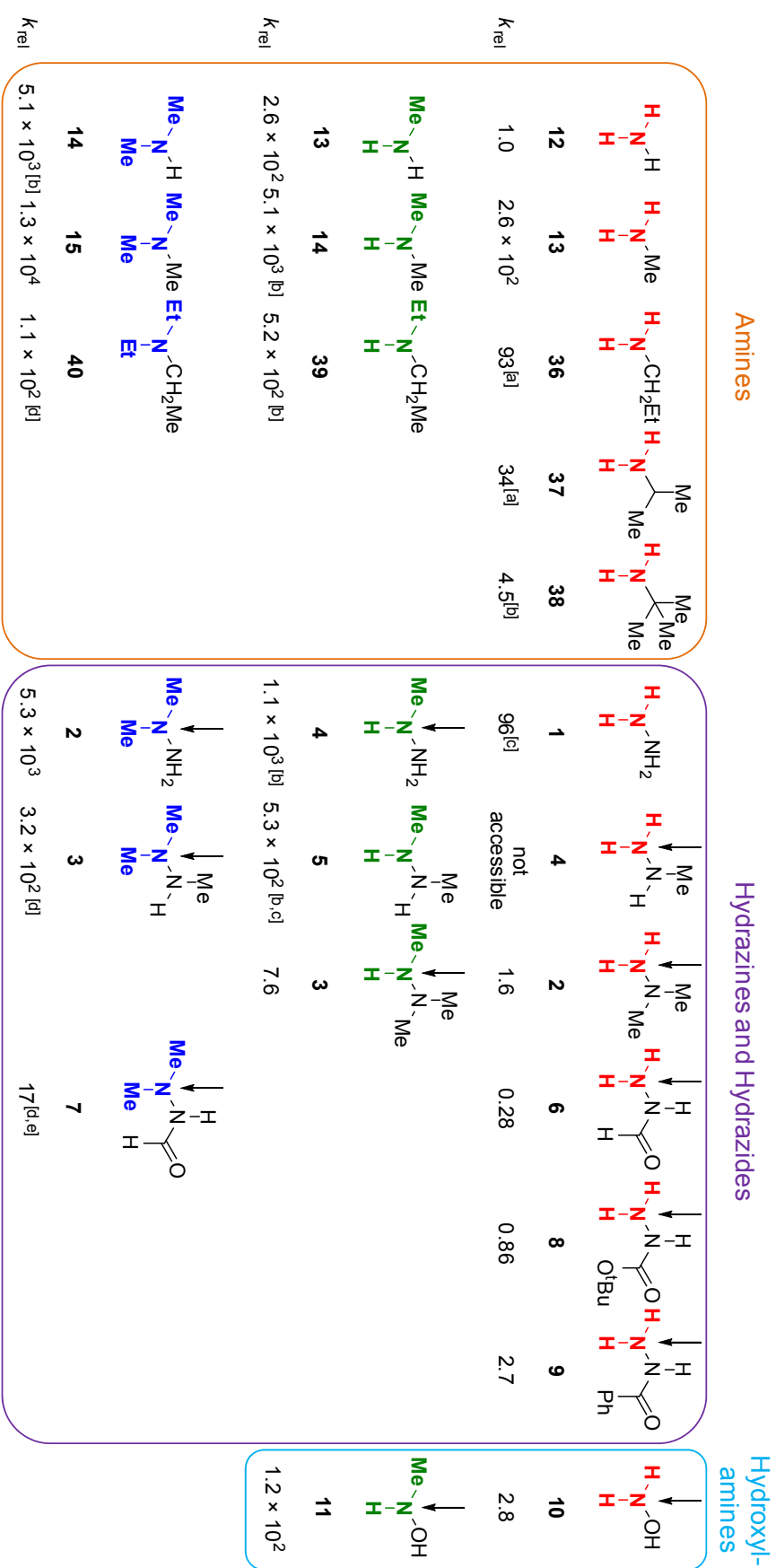


Figure 4.7. Comparison of relative second-order rate constants for the reactions of $(dma)_2CH^+$ (**16i**) with ammonia, amines, hydrazines, hydrazides, and hydroxylamines in CH_3CN at $20\text{ }^\circ C$ (the relative rate constants refer to the centers of attack marked with arrows).

[a] Rate constants for the reactions of **16i** with and **36** and **37** from Ref. [14d]. [b] The rate constants were calculated by Equation (4.1) using the E , N and S_N parameters from this work and Refs. [14a,d]. [c] The rate constants for the reactions of **16i** with the symmetrical hydrazines **1** and **5** were statistically corrected by a factor of 2. [d] Nucleophiles **7**, **40**, and the NMe_2 group of **3** do not react with $(dma)_2CH^+$ (**16i**), and rate constants for these reactions were calculated by Equation (4.1) using the E , N and S_N parameters from this work or Ref. [14a]. [e] The rate constant for the reaction of **7** with **16i** was obtained by extrapolation over a wide range and has to be considered approximate.

An increase of reactivity by *N*-methylation was also observed in the series of hydroxylamines. With a factor of 41 (**11/10**) the effect is somewhat larger than in the series of amines (**14/13** factor of 20) and hydrazines (**4/1** factor of 11).

We will now compare the effects of heteroatom substitution. While replacement of one hydrogen in NH₃ (**12**) by methyl increases the reactivity 2.6×10^2 fold (**13/12**), the NH₂ group activates by a factor of 96 (**1/12**) and OH by a factor of 2.8 (**10/12**). Slight retarding effects are observed for the formamido group (**6/12**, factor 0.28) and the *tert*-butoxycarbonylamido group (**8/12**, factor 0.86), whereas the benzamido group in **9** induces a 2.7-fold higher reactivity.

A similar trend can be observed in the series of the secondary reaction centers (second row of Figure 4.7). While methylation of methylamine activates by a factor of 20 (**14/13**), amination activates less (**4/13** = 4.1) and hydroxylation even deactivates slightly (**11/13** = 0.45).

The third row of Figure 4.7 shows, that replacement of H in dimethylamine by methyl activates only 2.6 fold (**15/14**) and that replacement of H by NH₂ does not affect the nucleophilicity (**2** \approx **14**), while the formamido group deactivates significantly (**7/14** = $1/3.0 \times 10^2$).

In summary, in all three rows discussed, hydrazines R₂N–NH₂ are generally less nucleophilic than the corresponding amines R₂N–Me, independent of the nature of R.

We have thus shown that the tertiary nitrogen in 1,1-dimethylhydrazine (**2**) is approximately 3000 times (!) more reactive than the NH₂ group and that methyl groups generally activate the substituted and deactivate the adjacent nitrogen center. In line with these conclusions, methylhydrazine (**4**) reacts smoothly at the higher substituted nucleophilic center of **4** with most electrophiles.^[18] Analogously, the unsymmetrical hydrazine **2** has been reported to yield quaternary hydrazinium salts in alkylations which proceed by irreversible S_N2 reactions.^[33] In reversible reactions, for example, acylations, the thermodynamically more-favored product is formed, however, which results from attack at the NH₂ group and subsequent deprotonation.^[34] As shown for many other ambident nucleophiles, the observed regioselectivity does not depend on the hardness of the reaction partner, whereas the reversibility of the electrophilic attack plays a decisive role.^[35]

These results are in contrast to theoretical predictions (DFT) by Hocquet and co-workers based on the principle of maximum hardness.^[36] While the nucleophilic Fukui function $f^-(r)$ predicted similar reactivities of the two centers, the “dual descriptor” (second-order Fukui

function) $\Delta f(r)^{[37]}$ and the calculated charge densities indicated a higher nucleophilicity for the NH_2 terminus in 1,1-dimethylhydrazine (**2**) and methylhydrazine (**4**), respectively.

Though the absolute rate constants for the reactions of amines and hydrazines are approximately 10^2 times smaller in water than in acetonitrile, the relative reactivities of ammonia (**12**), primary and secondary amines, as well as hydrazines are almost identical in the two solvents (Figure 4.8). One, therefore, has to conclude that the differences in reactivities of the amines and hydrazines derived from these kinetic data reflect intrinsic properties of these nucleophiles, which are only slightly affected by solvation. Only hydroxylamine (**10**) deviates somewhat, as it reacts 13 times faster than ammonia (**12**) in water, while the reactivity ratio is only 2.8 in acetonitrile. Possibly, in water the electrophilic attack at nitrogen is accompanied by simultaneous deprotonation of the amino group.

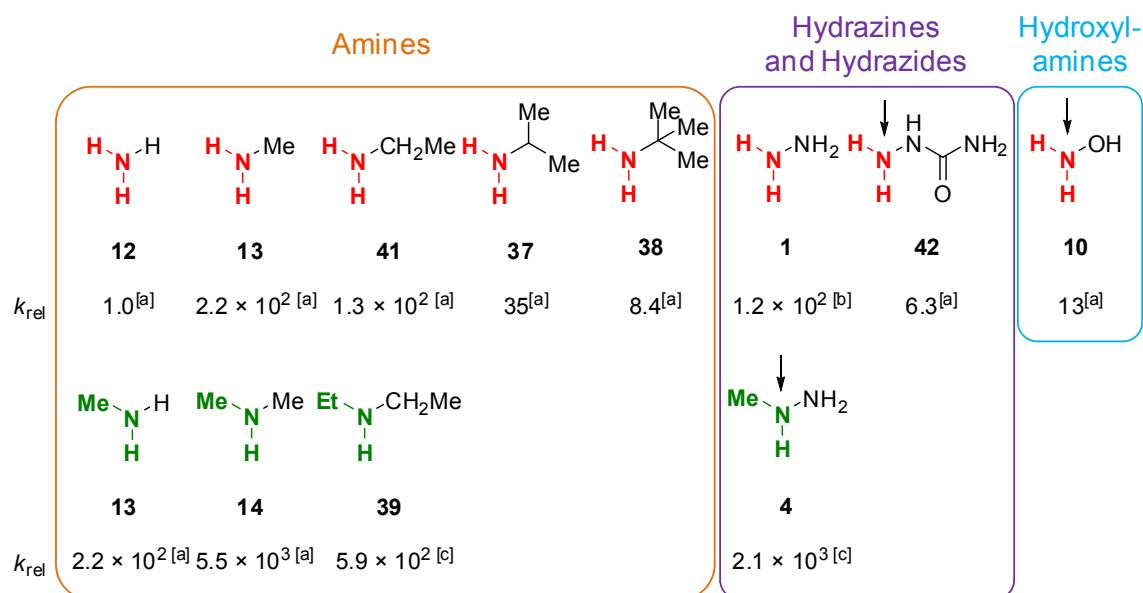


Figure 4.8. Comparison of relative second-order rate constants for reactions of $(\text{dma})_2\text{CH}^+$ (**16i**) with amines, hydrazines, semicarbazide (**42**), and hydroxylamine (**10**) in H_2O at 20 °C (the relative rate constants refer to the centers of attack marked with arrows).

[a] Rate constants for the reactions of **16i** with **10**, **12–14**, **37–39**, **41**, and **42** from Refs. [14h,k]. [b] The rate constant for the reaction of **16i** with hydrazine (**1**) was statistically corrected by a factor of 2. [c] The rate constants were calculated by Equation (4.1) using the E , N and s_N parameters from this work or Ref. [14h].

4.2.5 Correlation of Kinetic with Thermodynamic Data

As shown in Figure 4.9, the rate constants of the reactions of amines and hydrazines with $(\text{dma})_2\text{CH}^+$ (**16i**) in water (Figure 4.9a) and acetonitrile (Figure 4.9b) are not correlated with their basicities, in agreement with earlier reports.^[14d,h,38] One can see some general trends, however, which were previously reported for reactions with other electrophiles:^[6j,o,v,w] Secondary amines (open circles in Figure 4.9) generally react faster than primary amines (filled circles in Figure 4.9) of the same basicities, which are again more reactive than ammonia (**12**). Among the primary amines, anilines have the lowest basicities but nevertheless are among the strongest nucleophiles in water and react with similar rates as other primary amines in acetonitrile.^[14d,h] Increasing size of the alkyl groups reduces the nucleophilic reactivities but not the Brønsted basicities as shown by the low reactivities of isopropylamine (**37**) and *tert*-butylamine (**38**) compared to other primary amines or by the greatly reduced reactivity of triethylamine (**40**) in comparison with the slightly less basic trimethylamine (**15**).

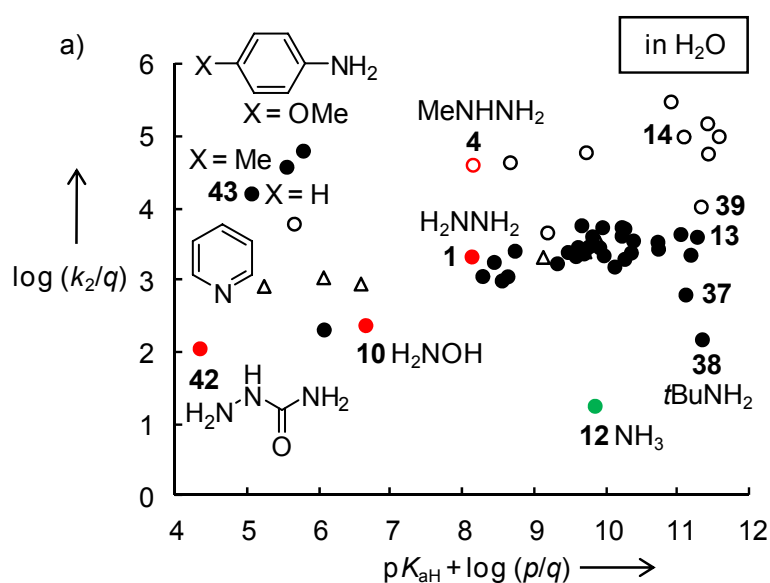


Figure 4.9. Brønsted plots of the statistically corrected second-order rate constants versus the statistically corrected basicities^[14,24,25,39] for the reactions of $(\text{dma})_2\text{CH}^+$ (**16i**) with amines at 20 °C (a) in H₂O and (b) acetonitrile (p = number of equivalent protons of the conjugated acids,^[38c,40] q = number of equivalent nucleophilic centers,^[38c,40] filled circles: primary amines, open circles: secondary amines, filled triangles: tertiary amines; open triangles: pyridines).^[14]

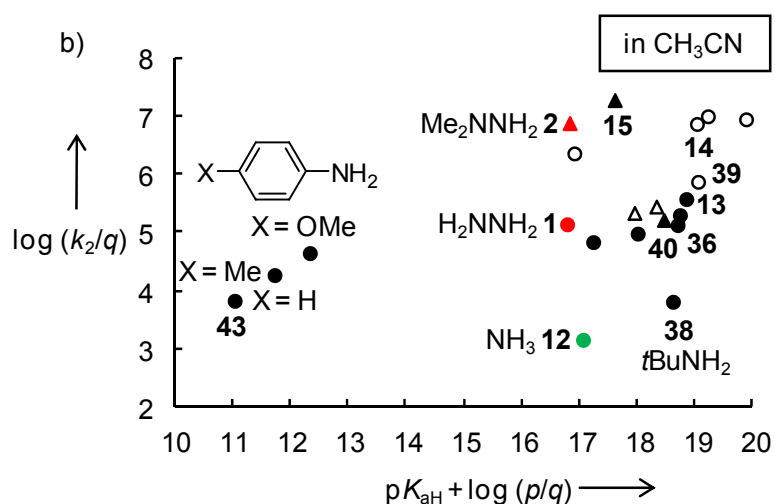


Figure 4.9 (continued).

When the Brønsted-type correlation for the reactions in water is restricted to structurally related α -unbranched primary amines, a linear correlation with $\beta_{\text{Nu}} = 0.22$ is obtained, from which hydrazine (**1**), hydroxylamine (**10**), and semicarbazide (**42**) do not deviate significantly (Figure 4.10a). The Brønsted correlation for the reactions of secondary amines with the benzhydrylium ion **16i** shows more scatter (Figure 4.10b) than that of the primary unbranched amines (Figure 4.10a). Again, no significant deviation for the α -nucleophile methylhydrazine (**4**) is observed.

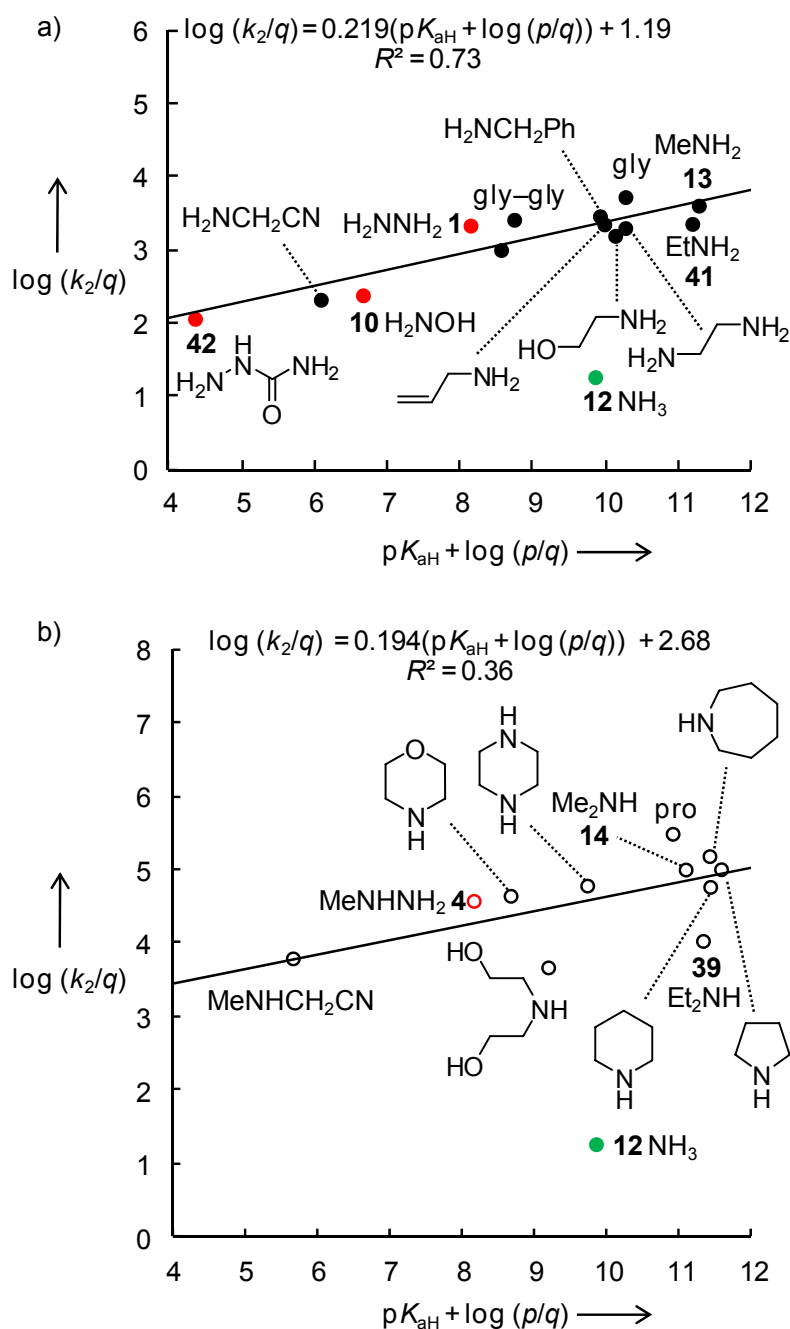


Figure 4.10. Brønsted plots of the statistically corrected second-order rate constants versus the statistically corrected basicities^[14] for the reactions of $(dma)_2CH^+$ (**16i**) with (a) unbranched primary and (b) secondary amines in H_2O at 20 °C (p = number of equivalent protons of the conjugated acids,^[38c,40] q = number of equivalent nucleophilic centers^[38c,40]).^[14]

This observation contrasts an earlier report that α -nucleophiles, including hydrazine (**1**), methylhydrazine (**4**) and semicarbazide (**42**), showed an upward deviation of 1.5 orders of

magnitude in an analogous Brønsted correlation for the reactions of malachite green with primary amines ($\beta_{\text{Nu}} = 0.42$).^[6s] Though previous analyses indicated that the magnitude of the α -effect increases with β_{nuc} ,^[5] the large difference in reactions with benzhydrylium ions and malachite green is surprising. Figure 4.11 shows a plot of the second-order rate constants for the reactions of amines and hydrazines with malachite green^[6s] versus the corresponding reactions with $(\text{dma})_2\text{CH}^+$ (**16i**). While the reactivity of hydrazine (**1**) towards **16i** is quite similar to that of the other primary amines, large differences are found in the reactivities towards malachite green, for example malachite green reacts 28 times faster with hydrazine (**1**) than with glycylglycine. However, conclusions are yet problematic as there are only very limited data available for a comparison and further experiments would be needed. As previously noted, the reactivities of tritylium ions correlate with those of benzhydrylium ions only when nucleophiles with negligible steric requirements are considered.^[41] Accordingly, the reversal of the relative reactivities of hydrazine (**1**) and methylhydrazine (**4**) towards **16i** in comparison to malachite green is most likely caused by steric reasons.

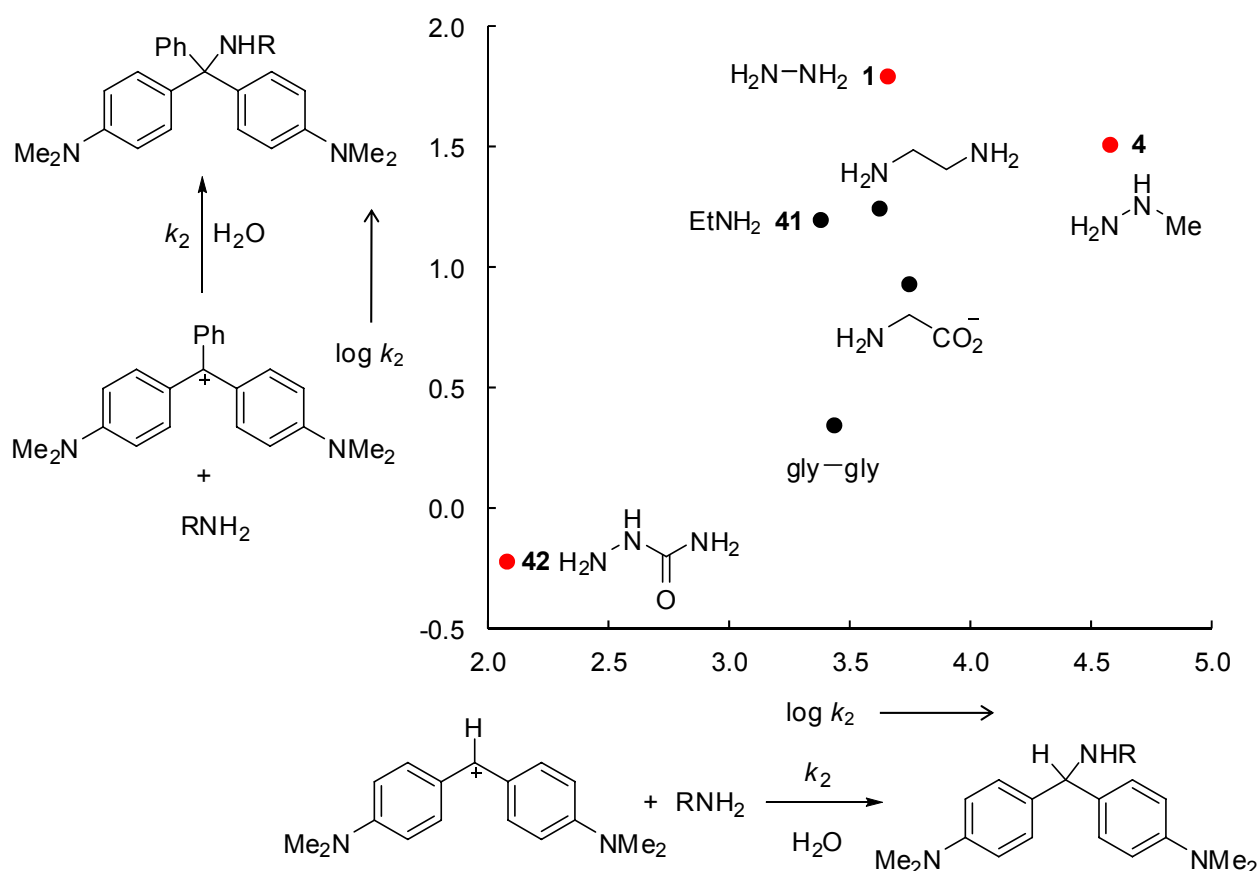


Figure 4.11. Plot of the second-order rate constants for the reactions of amines with malachite green versus the corresponding reactions with $(\text{dma})_2\text{CH}^+$ (**16i**).^[6s]

As previously reported, the reactions of stabilized benzhydrylium ions with tertiary amines proceed incompletely,^[14a,f] in contrast to the analogous reactions with primary or secondary amines, where the initially formed ammonium ions are subsequently deprotonated. We were, therefore, able to determine equilibrium constants for the reactions of benzhydrylium ions with DABCO (**44**) and quinuclidine (**45**) in acetonitrile.^[14f]

An analogous determination of equilibrium constants for the attack of benzhydrylium ions at the NMe₂ groups of the hydrazines **2** and **3** was not possible, because the initial formations of the quaternary hydrazinium ions were reversible and the benzhydrylium ions were consumed completely by the subsequent slower reactions with the adjacent NH₂ or NHMe group (Scheme 4.7). However, when the reactions of the carbocations **16h,i** with high concentrations of **2** were monitored on the μ s time scale using the laser-flash photolysis setup, monoexponential decays of the absorbances of **16h,i** were found (Figures 4.5 and 4.12). After these decays, which correspond to the fast attack at the NMe₂ group ($k_2' = 3.78 \times 10^6 \text{ M}^{-1} \text{ s}^{-1}$ for **16h** and $8.05 \times 10^6 \text{ M}^{-1} \text{ s}^{-1}$ for **16i** [Table 4.3]), the benzhydrylium absorbances reached plateaus because the subsequent reactions at the NH₂ group ($k_2 = 1.44 \times 10^3 \text{ M}^{-1} \text{ s}^{-1}$ for **16h** and $2.46 \times 10^3 \text{ M}^{-1} \text{ s}^{-1}$ for **16i** [Table 4.3]) occurred on the seconds time scale.

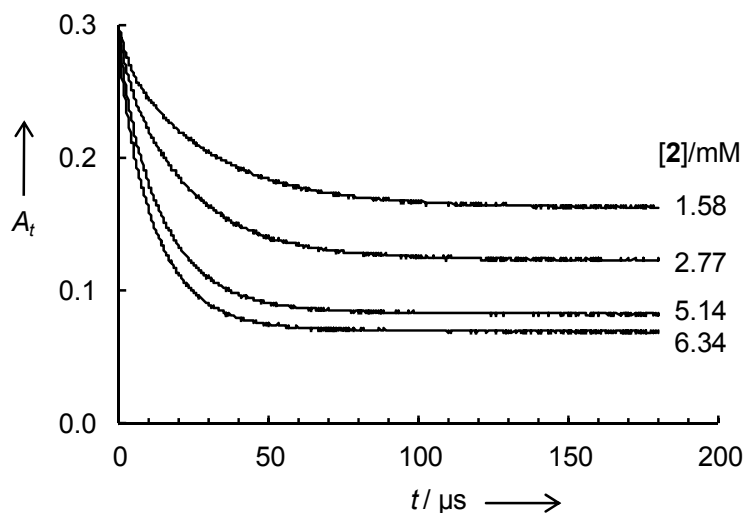


Figure 4.12. Exponential decays of the absorbance at $\lambda = 605 \text{ nm}$ on the μ s time scale during the reaction of **16i** generated from **16i**-PBU₃ ($[\text{16i-PBU}_3] = 1.41 \times 10^{-5} \text{ M}$) with different concentrations of 1,1-dimethylhydrazine (**2**) in acetonitrile at 20 °C.

From the initial absorbances (A_0) of the benzhydrylium ions generated by the 7 ns laser pulse and the absorbances at the plateaus on the μs time scale (A_{eq}), the equilibrium constants (K) as defined by Equation (4.7), were determined as the slopes of the linear correlations of $(A_0 - A_{\text{eq}})/A_{\text{eq}}$ with $[\text{Nu}]$ (Table 4.5).

$$K = \frac{[\text{Ar}_2\text{CHNu}^+]}{[\text{Ar}_2\text{CH}^+][\text{Nu}]} = \frac{A_0 - A_{\text{eq}}}{A_{\text{eq}}[\text{Nu}]} \quad (4.7)$$

We were not able to determine the equilibrium constants for the reactions of other benzhydrylium ions with **2**. The less stabilized carbocations (**16d–f**) gave so low concentrations of quaternary hydrazinium ions by attack at the NMe_2 group that only the slower reactions at the NH_2 group were observable. With more reactive carbocations (**16j,k**), on the other hand, the formation of the quaternary hydrazinium ions was almost quantitative, even when low concentrations of the hydrazine **2** were used, that the determination of K was again impossible.

For the same reasons, the reaction of the benzhydrylium ion **16j** with trimethylhydrazine (**3**) was the only one, for which the equilibrium constant for the attack at the NMe_2 group of **3** could be determined.

Equilibrium constants for the reactions of **16l–n** with the NMe_2 group of N',N' -dimethylformohydrazide (**7**) were similarly determined on the μs time scale, because the fast initial reactions were followed by unknown subsequent reactions on a slower time-scale. As the subsequent reactions were not considerably slower than the initial ones, the equilibrium constants K were determined from the initial absorbances A_0 and the constant C obtained by fitting the monoexponential function $A = A_0 e^{-k_{\text{obs}} t} + C$ to the time-dependent absorbances.

Due to unknown subsequent reactions it was also impossible to determine the equilibrium constants for the formation of quaternary ammonium ions from the benzhydrylium ions **16g–n** with N -methylpiperidine (**46**) and N -methylpyrrolidine (**47**) using conventional UV/Vis spectrometers.^[14a] Therefore, the corresponding equilibrium constants were determined by the same procedure described above for the 1,1-dimethylhydrazines.

Table 4.5. Equilibrium constants K for the reactions of benzhydrylium ions Ar_2CH^+ (**16**) with the hydrazines containing tertiary nitrogen centers **2**, **3**, **7** and the tertiary amines **15**, **44–47** in acetonitrile at 20 °C.

| | Amine | Ar_2CH^+ | $K [\text{M}^{-1}]$ | $k_2 [\text{M}^{-1} \text{s}^{-1}]$ |
|--------------------------|-------|--------------------------|-----------------------------------|-------------------------------------|
| 2 | | 16h | 3.3×10^1 | 3.78×10^6 |
| | | 16i | 4.7×10^2 | 8.06×10^6 |
| 3 | | 16j | 1.0×10^3 | 3.00×10^6 |
| | | | | |
| 7 | | 16l | 1.9×10^1 | 2.18×10^7 |
| | | 16m | 1.1×10^2 | 4.08×10^7 |
| | | 16n | 1.2×10^3 | 1.08×10^8 |
| 15 ^[a] | | 16h | 1.3×10^2 | 6.54×10^6 |
| | | 16i | 1.2×10^3 | 2.00×10^7 |
| 44 | | 16h | 4.89×10^3 ^[b] | 6.95×10^7 ^[b] |
| 45 | | 16h | 4.49×10^4 ^[b] | 5.22×10^7 ^[b] |
| 46 | | 16h | 5.9 | 5.44×10^5 ^[c] |
| 47 | | 16h | 3.5×10^2 | 7.19×10^6 ^[d] |

[a] Since trimethylamine (**15**) was used as a 33% ethanolic solution, K was determined from measurements on the μs time scale, where the reaction with ethanol did not occur. [b] From Ref. [14f]. [c] The rate constant for the reactions of **46** with **16h** was calculated by Equation (4.1) using the published E , N and s_N parameters from Ref. [14a]. [d] From Ref. [14a].

The exchange of a methyl group in trimethylamine (**15**) by the electronegative NH_2 group (\rightarrow **2**) reduces the equilibrium constants for the reactions with benzhydrylium ions approximately by factors of 3 to 4. The strong electron-withdrawing formamide group

adjacent to the dimethylamino group (**7**) has a large reducing effect on the Lewis basicities of the hydrazines as it reacts only with the most reactive carbocations in the series.

A correlation of the rate constants for the reactions of the tertiary amines and hydrazines with $(\text{pyr})_2\text{CH}^+ \text{BF}_4^-$ (**16h**) with the corresponding equilibrium constants is linear with a slope of 0.52 (Figure 4.12) from which 1,1-dimethylhydrazine (**2**) and trimethylhydrazine (**3**)^[42] do not deviate. A linear correlation with a slope of approximately unity was reported for the reactions of primary amines with malachite green.^[6s] In comparison, the smaller slope for the corresponding reactions with the benzhydrylium ion indicates an earlier transition state, where only half of the thermodynamic product stabilization is present. Similar linear correlations of the rate constants versus the equilibrium constants were also observed for the reactions of other classes of nucleophiles like pyridines and aromatic phosphanes with benzhydrylium ions.^[14g,43]

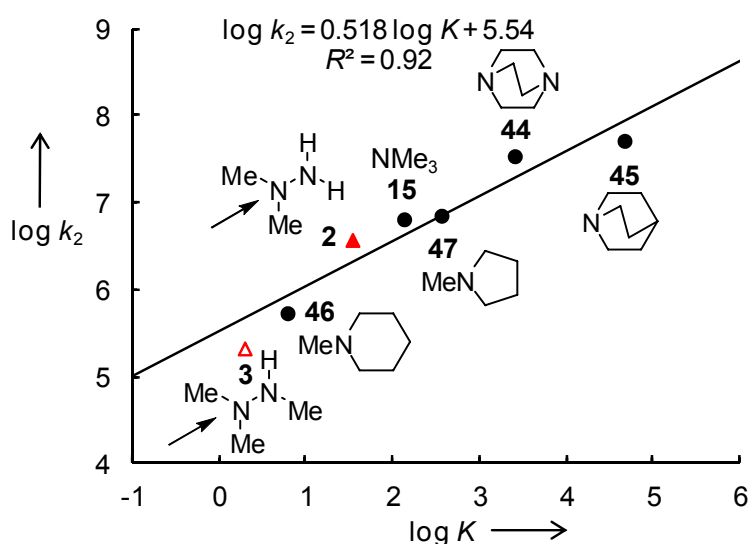


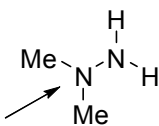
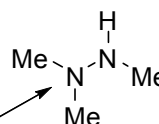
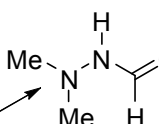
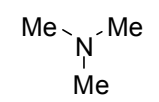
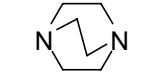
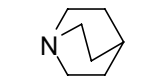
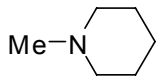
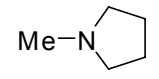
Figure 4.12. Plot of the rate constants for reactions of tertiary amines (circles) and 1,1-dimethylhydrazines (triangles) with $(\text{pyr})_2\text{CH}^+ \text{BF}_4^-$ (**16h**) in acetonitrile at 20 °C versus the corresponding equilibrium constants.^[a,b,c]

[a] Data points for **2** and **3** were not included for the determination of the slope. [b] The rate constant for the reactions of **3** with **16h** were calculated with the E , N and s_N -parameters. [c] The rate and equilibrium constants for the reactions of **16h** with DABCO (**43**) were statistically corrected by a factor of 2.

Substitution of the activation free energies (ΔG^\ddagger) and Gibbs free energies (ΔG^0) into the Marcus equation [Eq. (4.8)]^[44] yields the intrinsic barriers ΔG_0^\ddagger (that is, the barriers of the corresponding reactions with $\Delta G^0 = 0$), which are listed in Table 4.6.

$$\Delta G^\ddagger = \Delta G_0^\ddagger + 0.5\Delta G^0 + ((\Delta G_0)^2/16\Delta G_0^\ddagger) \quad (4.8)$$

Table 4.6. Activation free energies ΔG^\ddagger , reaction free energies ΔG^0 , and intrinsic barriers ΔG_0^\ddagger for the reactions of benzhydrylium ions Ar_2CH^+ (**16**) with **2**, **3**, **7**, **15**, **44–47**, as well as rate constants k_ζ and nucleofugality parameters N_f for the reverse reactions.

| Amine | Ar_2CH^+ | ΔG^\ddagger [a] | ΔG^0 [b] | ΔG_0^\ddagger [c] | k_ζ [d] | N_f [e] |
|--|--------------------------|-------------------------|-------------------------|---------------------------|--------------------|----------------------|
| | | [kJ mol ⁻¹] | [kJ mol ⁻¹] | [kJ mol ⁻¹] | [s ⁻¹] | |
| 2  | 16h | 34.8 | -8.5 | 39 | 1.1×10^5 | -0.46 |
| | 16i | 33.0 | -15 | 40 | 1.7×10^4 | |
| 3  | 16j | 35.4 | -17 | 43 | 3.0×10^3 | 0.45 |
| 7  | 16l | 30.6 | -7.2 | 34 | 1.1×10^6 | 4.96 |
| | 16m | 29.0 | -11 | 34 | 3.7×10^5 | |
| | 16n | 26.7 | -17 | 35 | 9.0×10^4 | |
| 15  | 16h | 33.5 | -12 | 39 | 5.0×10^4 | -0.63 |
| | 16i | 30.8 | -17 | 39 | 1.7×10^4 | |
| 44  | 16h | 27.7 | -20.7 | 37.3 | 1.42×10^4 | -1.00 ^[f] |
| 45  | 16h | 28.4 | -26.1 | 40.4 | 1.16×10^3 | -2.18 ^[g] |
| 46  | 16h | 39.6 | -4.3 | 42 | 9.2×10^4 | -0.38 |
| 47  | 16h | 33.3 | -14 | 40 | 2.1×10^4 | -1.03 |

[a] Calculated from rate constants in Table 4.5 using the Eyring equation. [b] Calculated from the equilibrium constants K in Table 4.5. [c] Calculated from Equation (4.8). [d] $k_\zeta = k_2 K^{-1}$. [e] Calculated from Equation (4.9) with the assumption of $s_f = 1$. [f] From Ref. [45]. [g] Calculated using additional data from Ref. [14f].

The rate constants for the heterolyses of the adducts of benzhydrylium ions and amines or hydrazines (k_ζ) can be calculated from the second-order rate constants k_2 and the equilibrium

constants K for the combination reactions. The leaving group ability decreases in the order **7** \gg **3** $>$ **15** $>$ **2** \approx **46** $>$ **44** \approx **47** $>$ **45**.

In analogy to Equation (4.1), the rate constants for heterolysis reactions can be predicted using Equation (4.9), where nucleofuges are characterized with two parameters (nucleofugality N_f and nucleofuge-specific sensitivity parameters s_f) and electrofuges are characterized by their electrofugality E_f .^[45]

$$\log k_{\leftarrow}(25\text{ }^{\circ}\text{C}) = s_f(N_f + E_f) \quad (4.9)$$

In general, N_f and s_f parameters are obtained from the linear correlations of solvolyses rate constants with the previously published E_f -parameters of benzhydrylium ions. However, the k_{\leftarrow} values given in Table 4.6 were only determined indirectly and refer to benzhydrylium ions of similar electrofugality. Therefore we followed the previous suggestion to assume $s_f = 1$ and derive the N_f -parameters of **2**, **3**, **7**, **15**, **44–47** (listed in Table 4.6) from Equation (4.9).^[45]

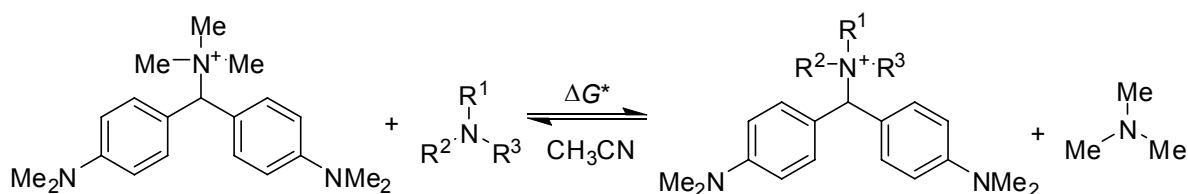
The nucleofugality parameters N_f obtained in this study allow a direct comparison of the leaving group abilities of the amines and hydrazines with other classes of nucleofuges, indicating that their nucleofugalities are in between that of methyl carbonate in 10% aqueous ethanol ($N_f = -2.20$) and the bromide ion in 40% aqueous acetonitrile ($N_f = 5.23$), and more than five orders of magnitude higher than that of DMAP ($N_f = -6.29$).^[45]

4.2.6 Computational Results

As the equilibrium constants for the reactions of primary and secondary amine groups with benzhydrylium ions are not accessible experimentally, we have calculated those for the reactions of $(\text{dma})_2\text{CH}^+ \text{BF}_4^-$ (**16i**) with ammonia (**12**), methylamine (**13**), dimethylamine (**14**), *tert*-butylamine (**38**), aniline (**43**), 2,2,2-trifluoroethylamine (**48**), hydrazine (**1**), the primary center of 1,1-dimethylhydrazine (**2**), hydroxylamine (**10**), and *N*-methylhydroxylamine (**11**) to expand the investigation of Figure 4.12 to other types of amines. In order to safely estimate the benzhydrylium ion affinities of the amines, a homodesmotic reaction was constructed (Scheme 4.9) and the Gibbs energies were calculated at the IEF-PCM-MP2/6-311+G(2d,p)//IEF-PCM-B3LYP/6-31+G(d,p) level of theory in acetonitrile (radii = Bondi).

In Scheme 4.9, ΔG^* is the Gibbs energy change of the homodesmotic reaction, which is equal to the difference in **16i**-affinities between the amine and trimethylamine (**15**). The **16i**-

affinities (ΔG^0_{298} , Table 4.7) were calculated as the sum of the Gibbs energy change of the homodesmotic reaction and the experimental value calculated from the equilibrium constant for the reaction of **16i** with trimethylamine (**15**).



Scheme 4.9. Homodesmotic reaction used for the calculation of the Gibbs energies for the reactions of **16i** with amines, hydrazines and hydroxylamines in acetonitrile.

Table 4.7. Reaction enthalpies ΔH^* and Gibbs energies ΔG^* for the homodesmotic reaction and Gibbs energies ΔG^0_{298} for the reactions of amines with **16i**.

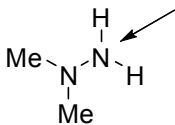
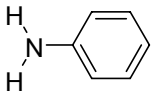
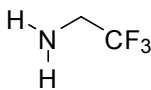
| Nucleophile | ΔH^* [kJ mol ⁻¹] | ΔG^* [kJ mol ⁻¹] | ΔG^0_{298} [kJ mol ⁻¹] |
|---|--------------------------------------|--------------------------------------|--|
| 1 N ₂ H ₄ | 34.8 | 20.9 | 3.9 |
| 2  | 41.1 | 35.6 | 18.6 |
| 10 NH ₂ OH | 60.1 | 51.6 | 34.6 |
| 11 MeNHOH | 39.5 | 33.5 | 16.5 |
| 12 NH ₃ | 54.6 | 41.8 | 24.8 |
| 13 MeNH ₂ | 23.0 | 14.7 | -2.3 |
| 14 Me ₂ NH | 5.2 | 3.1 | -13.9 |
| 38 <i>t</i> BuNH ₂ | 28.0 | 20.3 | 3.3 |
| 43  | 56.3 | 51.0 | 34.0 |
| 48  | 60.8 | 53.1 | 36.1 |

Figure 4.13 shows that the second-order rate constants for the reactions of amines, hydrazines and hydroxylamines correlate moderately with the calculated Gibbs energies for the corresponding reactions. If the linear correlation of Figure 4.13 is converted to a correlation of

$\log k_2$ versus $\log K$, a slope of 0.41 is obtained. The slope of Figure 4.13 is in good agreement with the slope of Figure 4.12, which plots the experimental rate constants versus the experimental equilibrium constants for the reactions of tertiary amines with **16h**.

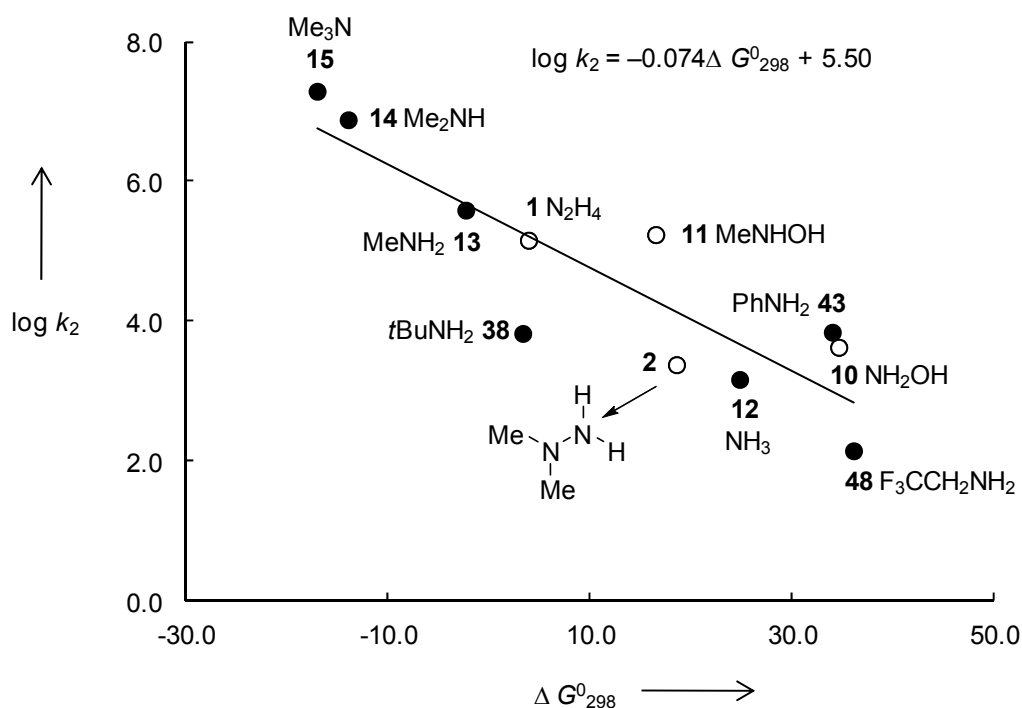


Figure 4.13. Plot of the rate constants of reactions of amines, hydrazines and hydroxylamine with $(\text{dma})_2\text{CH}^+\text{BF}_4^-$ (**16i**) versus the calculated Gibbs free energies of the corresponding reactions (filled circles: amines; open circles: α -nucleophiles).^[a,b,c]

[a] The rate constants for the reaction of **13** and **38** with **16i** were calculated from the nucleophilicity parameters N and s_N and the electrophilicity parameter E from this work or Ref. [14d]. [b] Rate constants for the reactions of **42** and **48** with **16i** from Refs. [14d,f]. [c] The rate constant for the reactions of **16h** with hydrazine (**1**) was statistically corrected by a factor of 2.

4.3 Conclusion

As previously described for numerous classes of nucleophiles,^[15] including amines,^[14] the reactions of hydrazines and hydroxylamines with benzhydrylium ions follow the linear free energy relationship [Eq. (4.1)], which provides a quantitative comparison of their nucleophilicities and allows us to include them into our comprehensive nucleophilicity scale.^[15] Remarkably, alkyl effects are almost identical in the amine and hydrazine series, that is, in both series methyl-substitution in α -position causes a significant increase of

nucleophilicity while methyl-substitution in β -position causes a significant decrease of nucleophilicity.

If the enhanced nucleophilicity of hydrazine (factor 10^2) and hydroxylamine (factor 3) relative to ammonia is assigned to an α -effect one has to realize that this α -effect is smaller than the activating effect of the α -methyl group in methylamine, whatever its origin is. The problem of the reference system remains, when we follow the current, more generally accepted definition for the α -effect, that α -nucleophiles show positive deviations in Brønsted plots.

Though we feel unable to interpret the contrasting results obtained with malachite green, our investigations clearly show that neither hydrazines nor hydroxylamine deviate from $\log k_2$ versus pK_{aH} correlations for the reactions of primary alkylamines with benzhydrylium ions. If alkylamines are considered as references, the common $\log k_2$ vs pK_{aH} correlation implies that neither hydrazines nor hydroxylamines show an α -effect. However, one might also argue that alkyl groups, like NH_2 and OH show an α -effect, because NH_3 is considerably below their common correlation line. Whatever definition is employed, as anilines are more reactive than ammonia and are considerably more nucleophilic than isobasic hydrazines and hydroxylamines, they should be considered as α -effect amines par excellence.

In order to elucidate the significance of the α -effect in reactions with other electrophiles we are presently investigating the kinetics of the reactions of amines, hydrazines, and hydroxylamines with acyl derivatives and alkyl halides.

4.4 Experimental Section

4.4.1 General Comment

Materials. Hydrazine monohydrate ($1 \cdot H_2O$), hydroxylamine hydrochloride ($10 \cdot HCl$), *N*-methylhydroxylamine hydrochloride ($11 \cdot HCl$), methylamine hydrochloride ($13 \cdot HCl$), dimethylamine hydrochloride ($14 \cdot HCl$), and trimethylamine (**15**, 33% ethanolic solution) were purchased and used without further purification. Methylhydrazine (**4**), benzohydrazide (**9**) and 1,8-diazabicyclo[5.4.0]undec-7-ene (DBU) were purchased and purified by distillation or recrystallization prior to use. *N*-Methylpyrrolidine (**46**) and *N*-methylpiperidine (**47**) were distilled over $LiAlH_4$ prior to use. Commercially available 1,2-dimethylhydrazine

hydrochloride (**5**·HCl) was deprotonated with NaOH in analogy to a literature procedure.^[46] Solutions of ammonia (**12**) in acetonitrile were prepared by gas injection.

Formohydrazide (**6**),^[47] *N,N'*-dimethylformohydrazide (**7**),^[46] *tert*-butyl hydrazinecarboxylate (**8**),^[48] and (dma)₂CHNH₂ (**28**)^[28] were synthesized according to literature procedures. Trimethylhydrazine (**3**) was generated by treating *tert*-butyl trimethylhydrazinecarboxylate^[49] with HBF₄ in methanol,^[50] followed by deprotonation with NaOH,^[46] and purified by distillation through a Vigreux column.

The phosphonium tetrafluoroborates (**16h–k**)-PR₃ were prepared by adding equimolar amounts of PR₃ to solutions of the benzhydrylium tetrafluoroborates **16h–k** which gave completely or almost colorless solutions.^[43] The phosphonium tetrafluoroborates **16l–n**-PPh₃ were obtained by reactions of the benzhydrols **16l–n**-OH with HPPh₃⁺ BF₄⁻.^[51]

Acetonitrile (> 99.9%, extra dry) was purchased and used without further purification.

Analytics. In the ¹H and ¹³C NMR spectra the chemical shifts in ppm refer to tetramethylsilane ($\delta_{\text{H}} = 0.00$) or the solvent residual signals as internal standard: CDCl₃ ($\delta_{\text{H}} = 7.26$, $\delta_{\text{C}} = 77.0$), CD₃CN ($\delta_{\text{H}} = 1.94$, $\delta_{\text{C}} = 1.32$) or *d*₆-DMSO ($\delta_{\text{H}} = 2.50$, $\delta_{\text{C}} = 39.5$). The following abbreviations were used for signal multiplicities: s = singlet, d = doublet, t = triplet, q = quartet, m = multiplet, br = broad. NMR signal assignments were based on additional 2D-NMR experiments (COSY, HSQC, and HMBC). For reasons of simplicity, the ¹H NMR signals of AA'BB'-spin systems of *p*-substituted aromatic rings were treated as doublets.

HRMS in EI mode (70 eV) were determined on a Thermo Finnigan MAT 95 or a Jeol MStation with sector field detectors. HRMS-ESI spectra were obtained with a Thermo Finnigan LTQ FT Ultra (IonMax ion source, 4 kV).

Kinetic Experiments. The kinetics of the reactions of **1–15** and **28** with the benzhydrylium ions and quinone methides **16** were monitored by UV/Vis spectroscopy in acetonitrile at 20 °C.

For slow reactions ($\tau_{1/2} > 10$ s), the spectra were collected at different times by using a J&M TIDAS diodearray spectrophotometer that was connected to a Hellma 661.502-QX quartz Suprasil immersion probe (5 mm light path) by fiber optic cables with standard SMA connectors. All kinetic measurements in CH₃CN were carried out in Schlenk glassware under exclusion of moisture. The temperature of the solutions during the kinetic studies was

maintained at $20\text{ }^{\circ}\text{C} \pm 0.1\text{ }^{\circ}\text{C}$ and monitored with a thermo-couple probe that was inserted into the reaction mixture.

Stopped-flow spectrophotometer systems (Applied Photophysics SX.18MV-R or Hi-Tech SF-61DX2) were used for the investigation of faster reactions ($10\text{ ms} < \tau_{1/2} < 10\text{ s}$). The kinetic runs were initiated by mixing equal volumes of the solutions of the amines and the electrophiles **16**.

Reactions with $\tau_{1/2} < 10\text{ ms}$ were analyzed by laser-flash photolytic generation of **16h–n** from phosphonium ions in presence of excess nucleophile. Solutions of the carbocation precursors were irradiated with a 7 ns pulse from a quadrupled Nd:YAG laser (266 nm, 40–60 mJ/pulse), and a xenon lamp was used as probe light for UV/Vis detection. The system is equipped with a fluorescence flow cell and a synchronized pump system which allows to completely exchange the sample volume between subsequent laser pulses. For each concentration, ≥ 50 individual measurements were averaged.^[52]

The nucleophiles **1–15** and **28** were used in large excess (over 8 equivalents) relative to the electrophiles **16** to ensure first-order conditions with $k_{\text{obs}} = k_2[\text{Nu}]_0 + k_0$. The first-order rate constants k_{obs} (s^{-1}) were obtained by least-squares fitting of the single-exponential curve $A_t = A_0e^{-k_{\text{obs}}t} + C$ to the decays of the absorbance of **16** at λ_{max} . The slopes of the plots of k_{obs} versus the concentrations of the nucleophiles yielded the second-order rate constants k_2 in ($\text{M}^{-1}\text{ s}^{-1}$).

The measurements of the rate constants for the reactions of **16** with hydrazine (**1**) were either performed using hydrazine monohydrate or hydrazinium dihydrochloride which was deprotonated with 2.00 equivalents of 1,8-diazabicyclo[5.4.0]undec-7-ene (DBU). Stock solutions of hydroxylamine (**10**), *N*-methylhydroxylamine (**11**), methylamine (**13**) and dimethylamine (**14**) were generated for the kinetic measurements by partial deprotonation of the corresponding hydrochloride salts with 0.50–0.95 equivalents of DBU. For the reactions of **13** with **16h,i** and of **14** with **16d**, $\text{KO}t\text{Bu}$ was used as alternative deprotonation agent. Stock solutions of ammonia (**12**) were prepared by gas injection in acetonitrile, and trimethylamine was used as a 33% solution in ethanol. In both cases, the concentrations of the stock solutions were determined by titration with hydrochloric acid.

For hydrazines bearing secondary amine groups (**4** and **5**) some correlations between k_{obs} and the hydrazine concentrations showed an upward curvature. In these cases, the rate determining step of the reaction changes from the attack of the hydrazine to the proton transfer, in which a second hydrazine molecule acts as general base catalyst (Scheme 4.6).

The change of the concentration of the zwitterionic intermediate **I** can be expressed by Equation (4.10).

$$\frac{d[\mathbf{I}]}{dt} = k_2[\mathbf{E}][\mathbf{Nu}] - k_{-2}[\mathbf{I}] - k_b[\mathbf{I}][\mathbf{Nu}] - k_p[\mathbf{I}] \quad (4.10)$$

The rate law can be expressed by Equations (4.11) and (4.12) if we assume a steady-state concentration for the intermediate **I**.

$$-\frac{d[\mathbf{E}]}{dt} = \frac{k_2[\mathbf{E}][\mathbf{Nu}](k_b[\mathbf{Nu}] + k_p)}{k_{-2} + k_b[\mathbf{Nu}] + k_p} \quad (4.11)$$

$$k_{\text{obs}} = \frac{k_2[\mathbf{Nu}](k_b[\mathbf{Nu}] + k_p)}{k_{-2} + k_b[\mathbf{Nu}] + k_p} \quad (4.12)$$

At high hydrazine concentrations, the direct proton-transfer (k_p) can be neglected, and Equation (4.12) is reduced to Equation (4.3) which can be rewritten as Equation (4.4).

Second-order rate constants for the C-N-bond formation (k_2) were obtained as the reciprocal intercepts of plots of $[\mathbf{Nu}]/k_{\text{obs}}$ versus $1/[\mathbf{Nu}]$.

At very high nucleophile concentrations where $k_{-2} \ll k_b[\mathbf{Nu}]$, Equation (4.3) is reduced to Equation (4.13) resulting in a linear dependence between rate and nucleophile concentration.

$$k_{\text{obs}} = k_2[\mathbf{Nu}] \quad (4.13)$$

Thermodynamic Investigations. Equilibrium constants for the reactions of tertiary amines and hydrazines with benzhydrylium ions were determined by UV/Vis spectrophotometry. The benzhydrylium ions **16** were generated by photolytic cleavage of phosphonium ions in presence of variable concentrations of the nucleophiles. From the initial absorbances (A_0) of the benzhydrylium ions generated by the 7 ns laser pulse and the absorbances at the plateau on the μs -time scale (A_{eq}), the equilibrium constants (K) as defined by Equation (4.7), were determined as the slopes of the linear correlations of $(A_0 - A_{\text{eq}})/A_{\text{eq}}$ with $[\mathbf{Nu}]$ assuming a proportional relationship between the absorbances and the concentrations of the electrophiles.

In some cases, the absorbances did not stay constant on the μs time scale due to unknown subsequent reactions and we determined the equilibrium constants K from the initial absorbances A_0 and the constant C obtained by fitting the monoexponential function $A = A_0e^{-k_{\text{obs}}t} + C$ to the time-dependent absorbances.

4.4.2 Kinetic Experiments

Kinetics of the reactions of hydrazine (1) with benzhydrylium ions and quinone methides (16)

Table 4.8. Rate constants for the reactions of ani(Ph)₂QM (**16c**) with hydrazine (**1**) generated from hydrazine dihydrochloride (**1**·2 HCl) with DBU (2.00 equiv.) in CH₃CN (stopped-flow technique, 20 °C, $\lambda = 415$ nm).

| [16c] ₀ /M | [1] ₀ /M | [1] ₀ /[16c] ₀ | $k_{\text{obs}}/\text{s}^{-1}$ |
|--|------------------------------|--|--------------------------------|
| 6.85×10^{-5} | 1.17×10^{-3} | 20 | 2.17×10^{-1} |
| 6.85×10^{-5} | 2.41×10^{-3} | 40 | 4.86×10^{-1} |
| 6.85×10^{-5} | 3.54×10^{-3} | 60 | 7.24×10^{-1} |
| 6.85×10^{-5} | 4.82×10^{-3} | 80 | 1.02 |
| 6.85×10^{-5} | 6.02×10^{-3} | 100 | 1.30 |
| $k_2 = 2.23 \times 10^2 \text{ M}^{-1} \text{ s}^{-1}$ | | | |

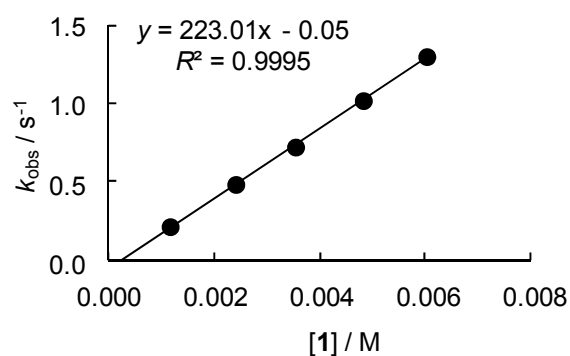


Table 4.9. Rate constants for the reactions of hydrazine monohydrate (**1**·H₂O) with (iil)₂CH⁺BF₄⁻ (**16d**) in CH₃CN (Stopped-flow technique, 20 °C, $\lambda = 631$ nm).

| [16d] ₀ /M | [1] ₀ /M | [1] ₀ /[16d] ₀ | $k_{\text{obs}}/\text{s}^{-1}$ |
|--|------------------------------|--|--------------------------------|
| 1.24×10^{-5} | 2.43×10^{-4} | 20 | 7.55×10^{-1} |
| 1.24×10^{-5} | 4.85×10^{-4} | 39 | 1.62 |
| 1.24×10^{-5} | 7.28×10^{-4} | 59 | 2.41 |
| 1.24×10^{-5} | 1.01×10^{-3} | 82 | 3.38 |
| 1.24×10^{-5} | 1.21×10^{-3} | 98 | 4.07 |
| $k_2 = 3.41 \times 10^3 \text{ M}^{-1} \text{ s}^{-1}$ | | | |

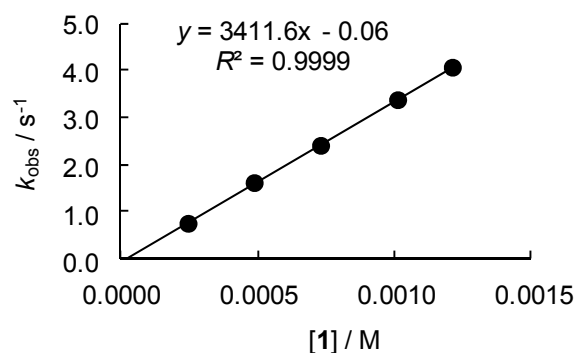


Table 4.10. Rate constants for the reactions of $(\text{jul})_2\text{CH}^+ \text{BF}_4^-$ (**16e**) with hydrazine (**1**) generated from hydrazine dihydrochloride (1:2 HCl) with DBU (2.00 equiv.) in CH_3CN (stopped-flow technique, 20 °C, $\lambda = 630 \text{ nm}$).

| $[\mathbf{16e}]_0/\text{M}$ | $[\mathbf{1}]_0/\text{M}$ | $[\mathbf{1}]_0/[\mathbf{16e}]_0$ | $k_{\text{obs}}/\text{s}^{-1}$ |
|--|---------------------------|-----------------------------------|--------------------------------|
| 1.82×10^{-5} | 3.90×10^{-4} | 21 | 2.57 |
| 1.82×10^{-5} | 7.80×10^{-4} | 43 | 5.96 |
| 1.82×10^{-5} | 1.17×10^{-3} | 64 | 9.24 |
| 1.82×10^{-5} | 1.56×10^{-3} | 86 | 1.28×10^1 |
| 1.82×10^{-5} | 1.95×10^{-3} | 107 | 1.62×10^1 |
| $k_2 = 8.74 \times 10^3 \text{ M}^{-1} \text{ s}^{-1}$ | | | |

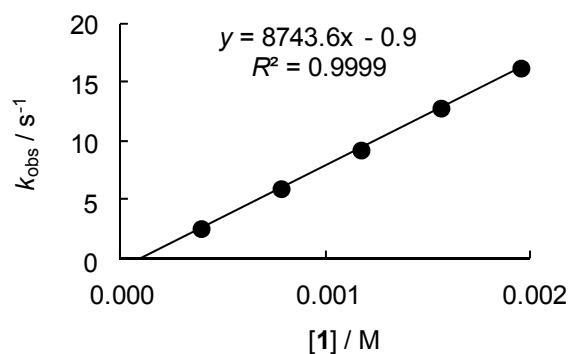


Table 4.11. Rate constants for the reactions of $(\text{ind})_2\text{CH}^+ \text{BF}_4^-$ (**16f**) with hydrazine (**1**) generated from hydrazine dihydrochloride (1:2 HCl) with DBU (2.00 equiv.) in CH_3CN (stopped-flow technique, 20 °C, $\lambda = 625 \text{ nm}$).

| $[\mathbf{16f}]_0/\text{M}$ | $[\mathbf{1}]_0/\text{M}$ | $[\mathbf{1}]_0/[\mathbf{16f}]_0$ | $k_{\text{obs}}/\text{s}^{-1}$ |
|--|---------------------------|-----------------------------------|--------------------------------|
| 1.99×10^{-5} | 3.90×10^{-4} | 20 | 6.93 |
| 1.99×10^{-5} | 6.02×10^{-4} | 30 | 1.12×10^1 |
| 1.99×10^{-5} | 7.80×10^{-4} | 39 | 1.49×10^1 |
| 1.99×10^{-5} | 9.92×10^{-4} | 50 | 1.93×10^1 |
| 1.99×10^{-5} | 1.20×10^{-3} | 60 | 2.34×10^1 |
| $k_2 = 2.04 \times 10^4 \text{ M}^{-1} \text{ s}^{-1}$ | | | |

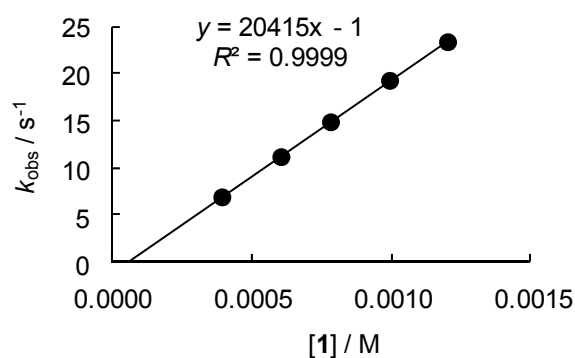


Table 4.12. Rate constants for the reactions of hydrazine monohydrate ($1 \cdot \text{H}_2\text{O}$) with $(\text{ind})_2\text{CH}^+ \text{BF}_4^-$ (**16f**) in CH_3CN (stopped-flow technique, 20°C , $\lambda = 616 \text{ nm}$).

| $[\mathbf{16f}]_0/\text{M}$ | $[\mathbf{1}]_0/\text{M}$ | $[\mathbf{1}]_0/[\mathbf{16f}]_0$ | $k_{\text{obs}}/\text{s}^{-1}$ |
|--|---------------------------|-----------------------------------|--------------------------------|
| 1.17×10^{-5} | 2.43×10^{-4} | 21 | 4.43 |
| 1.17×10^{-5} | 4.85×10^{-4} | 41 | 9.99 |
| 1.17×10^{-5} | 7.28×10^{-4} | 62 | 1.50×10^1 |
| 1.17×10^{-5} | 1.01×10^{-3} | 86 | 2.08×10^1 |
| 1.17×10^{-5} | 1.21×10^{-3} | 104 | 2.54×10^1 |
| $k_2 = 2.14 \times 10^4 \text{ M}^{-1} \text{ s}^{-1}$ | | | |

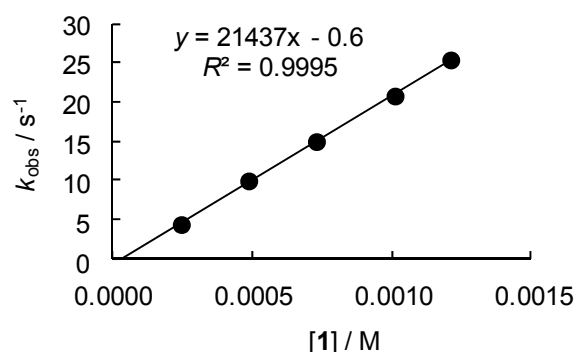


Table 4.13. Rate constants for the reactions of $(\text{pyr})_2\text{CH}^+ \text{BF}_4^-$ (**16h**) with hydrazine (**1**) generated from hydrazine dihydrochloride ($1 \cdot 2 \text{ HCl}$) with DBU (2.00 equiv.) in CH_3CN (stopped-flow technique, 20°C , $\lambda = 611 \text{ nm}$).

| $[\mathbf{16h}]_0/\text{M}$ | $[\mathbf{1}]_0/\text{M}$ | $[\mathbf{1}]_0/[\mathbf{16h}]_0$ | $k_{\text{obs}}/\text{s}^{-1}$ |
|--|---------------------------|-----------------------------------|--------------------------------|
| 1.98×10^{-5} | 3.90×10^{-4} | 20 | 5.06×10^1 |
| 1.98×10^{-5} | 6.02×10^{-4} | 30 | 8.23×10^1 |
| 1.98×10^{-5} | 7.80×10^{-4} | 39 | 1.10×10^2 |
| 1.98×10^{-5} | 9.92×10^{-4} | 50 | 1.45×10^2 |
| 1.98×10^{-5} | 1.20×10^{-3} | 61 | 1.78×10^2 |
| $k_2 = 1.58 \times 10^5 \text{ M}^{-1} \text{ s}^{-1}$ | | | |

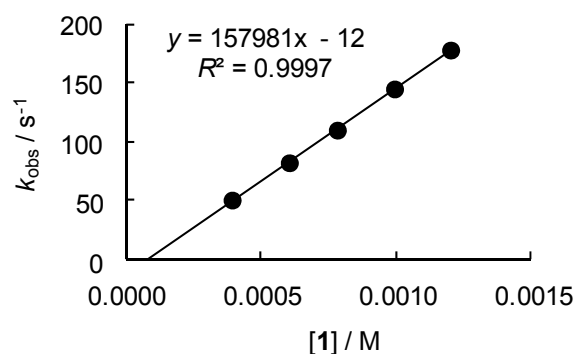


Table 4.14. Rate constants for the reactions of hydrazine monohydrate ($1 \cdot \text{H}_2\text{O}$) with $(\text{dma})_2\text{CH}^+ \text{BF}_4^-$ (**16i**) in CH_3CN (stopped-flow technique, 20°C , $\lambda = 605 \text{ nm}$).

| $[\mathbf{16i}]_0/\text{M}$ | $[\mathbf{1}]_0/\text{M}$ | $[\mathbf{1}]_0/[\mathbf{16i}]_0$ | $k_{\text{obs}}/\text{s}^{-1}$ |
|--|---------------------------|-----------------------------------|--------------------------------|
| 9.85×10^{-6} | 1.01×10^{-4} | 10 | 2.61×10^1 |
| 9.85×10^{-6} | 1.21×10^{-4} | 12 | 3.22×10^1 |
| 9.85×10^{-6} | 2.02×10^{-4} | 21 | 5.75×10^1 |
| 9.85×10^{-6} | 2.43×10^{-4} | 25 | 6.81×10^1 |
| 9.85×10^{-6} | 2.83×10^{-4} | 29 | 7.97×10^1 |
| $k_2 = 2.95 \times 10^5 \text{ M}^{-1} \text{ s}^{-1}$ | | | |

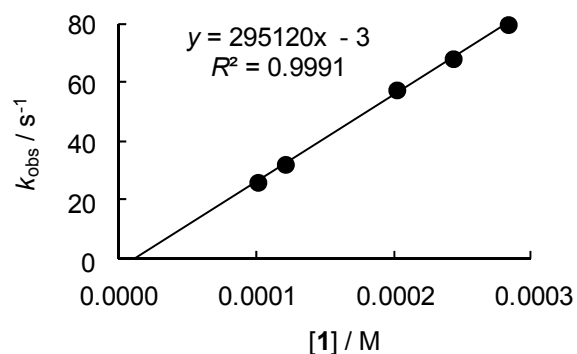


Table 4.15. Rate constants for the reactions of hydrazine monohydrate ($\mathbf{1}\cdot\text{H}_2\text{O}$) with $(\text{mor})_2\text{CH}^+ \text{BF}_4^-$ ($\mathbf{16j}$) generated from $(\text{mor})_2\text{CHPBu}_3^+ \text{BF}_4^-$ ($\mathbf{16j}\text{-PBu}_3$) in CH_3CN (laser-flash photolysis, 20 °C, $\lambda = 611 \text{ nm}$).

| $[\mathbf{16j}\text{-PBu}_3]_0/\text{M}$ | $[\mathbf{1}]_0/\text{M}$ | $k_{\text{obs}}/\text{s}^{-1}$ |
|--|---------------------------|--------------------------------|
| 1.13×10^{-5} | 5.56×10^{-2} | 8.04×10^4 |
| 1.13×10^{-5} | 9.67×10^{-2} | 1.34×10^5 |
| 1.13×10^{-5} | 1.06×10^{-1} | 1.47×10^5 |
| 1.13×10^{-5} | 1.44×10^{-1} | 1.82×10^5 |
| 1.13×10^{-5} | 2.12×10^{-1} | 2.57×10^5 |
| 1.13×10^{-5} | 2.78×10^{-1} | 3.70×10^5 |
| 1.13×10^{-5} | 3.46×10^{-1} | 4.30×10^5 |
| $k_2 = 1.22 \times 10^6 \text{ M}^{-1} \text{ s}^{-1}$ | | |

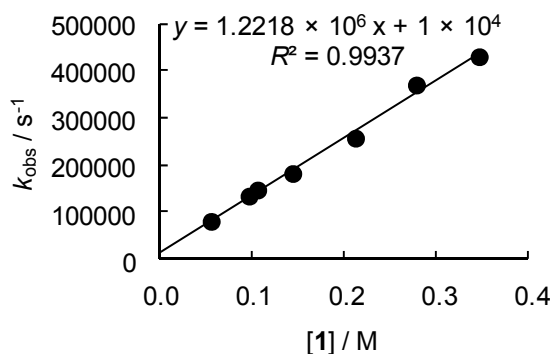


Table 4.16. Rate constants for the reactions of hydrazine monohydrate ($\mathbf{1}\cdot\text{H}_2\text{O}$) with $(\text{mfa})_2\text{CH}^+ \text{BF}_4^-$ ($\mathbf{16k}$) generated from $(\text{mfa})_2\text{CHPBu}_3^+ \text{BF}_4^-$ ($\mathbf{16k}\text{-PBu}_3$) in CH_3CN (laser-flash photolysis, 20 °C, $\lambda = 586 \text{ nm}$).

| $[\mathbf{16k}\text{-PBu}_3]_0/\text{M}$ | $[\mathbf{1}]_0/\text{M}$ | $k_{\text{obs}}/\text{s}^{-1}$ |
|--|---------------------------|--------------------------------|
| 7.48×10^{-6} | 1.09×10^{-1} | 1.46×10^6 |
| 7.48×10^{-6} | 1.94×10^{-1} | 2.40×10^6 |
| 7.48×10^{-6} | 2.66×10^{-1} | 3.01×10^6 |
| 7.48×10^{-6} | 3.22×10^{-1} | 3.60×10^6 |
| $k_2 = 9.90 \times 10^6 \text{ M}^{-1} \text{ s}^{-1}$ | | |

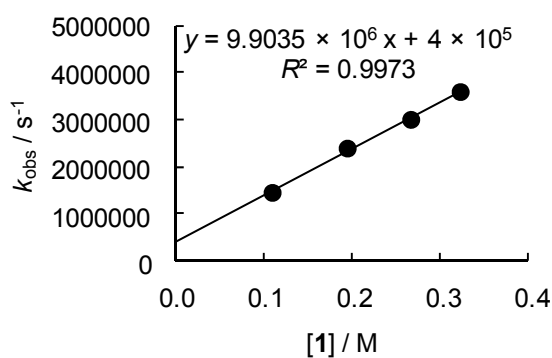
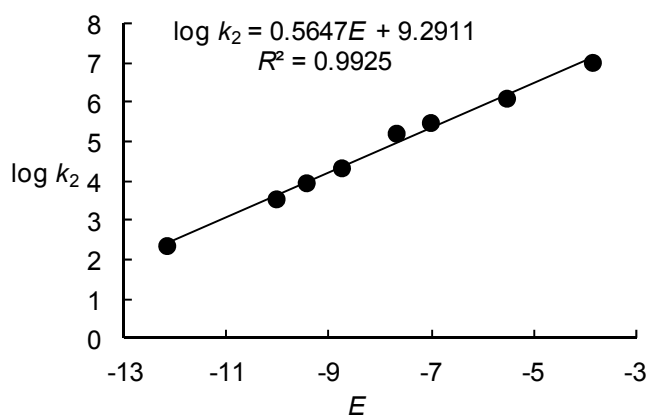


Table 4.17. Determination of the nucleophilicity parameters N and s_N for hydrazine (**1**) in CH_3CN .

| Electrophile (E) | $k_2/\text{M}^{-1} \text{s}^{-1}$ | $\log k_2$ |
|----------------------|-----------------------------------|------------|
| 16c (-12.18) | 2.23×10^2 | 2.35 |
| 16d (-10.04) | 3.41×10^3 | 3.53 |
| 16e (-9.45) | 8.74×10^3 | 3.94 |
| 16f (-8.76) | 2.09×10^4 [a] | 4.32 |
| 16g (-7.69) | 1.58×10^5 | 5.20 |
| 16i (-7.02) | 2.95×10^5 | 5.47 |
| 16j (-5.53) | 1.22×10^6 | 6.09 |
| 16k (-3.85) | 9.90×10^6 | 7.00 |

$$N = 16.45, s_N = 0.56$$



[a] Average of the independently determined second-order rate constants obtained from reactions of **16f** with **1**· H_2O and **1**· 2HCl .

Kinetics of the reactions of 1,1-dimethylhydrazine (2) with benzhydrylium ions and quinone methides (16)

Table 4.18. Rate constants for the reactions of the NH_2 group of 1,1-dimethylhydrazine (**2**) with $\text{ani}(\text{Ph})_2\text{QM}$ (**16c**) in CH_3CN (diodearray spectrophotometer, 20°C , $\lambda = 414 \text{ nm}$).

| $[\mathbf{16c}]_0/\text{M}$ | $[\mathbf{2}]_0/\text{M}$ | $[\mathbf{2}]_0/[\mathbf{16c}]_0$ | $k_{\text{obs}}/\text{s}^{-1}$ |
|-----------------------------|---------------------------|-----------------------------------|--------------------------------|
| 5.87×10^{-5} | 4.77×10^{-4} | 8 | 2.55×10^{-4} |
| 5.84×10^{-5} | 6.32×10^{-4} | 11 | 3.44×10^{-4} |
| 5.86×10^{-5} | 7.93×10^{-4} | 14 | 4.51×10^{-4} |
| 5.75×10^{-5} | 1.01×10^{-3} | 18 | 5.42×10^{-4} |
| 5.80×10^{-5} | 1.26×10^{-3} | 22 | 7.46×10^{-4} |
| 5.47×10^{-5} | 1.93×10^{-3} | 35 | 1.08×10^{-3} |
| 5.76×10^{-5} | 2.50×10^{-3} | 43 | 1.41×10^{-3} |

$$k_2 = 5.69 \times 10^{-1} \text{ M}^{-1} \text{ s}^{-1}$$

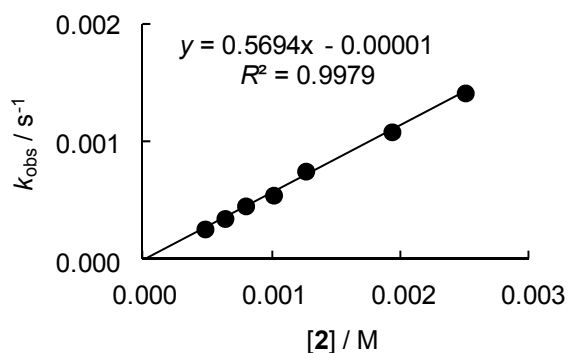


Table 4.19. Rate constants for the reactions of the NH₂ group of 1,1-dimethylhydrazine (**2**) with (lil)₂CH⁺ BF₄⁻ (**16d**) in CH₃CN (diodearray spectrophotometer, 20 °C, λ = 631 nm).

| [16d] ₀ /M | [2] ₀ /M | [2] ₀ /[16d] ₀ | $k_{\text{obs}}/\text{s}^{-1}$ |
|--|------------------------------|--|--------------------------------|
| 1.35×10^{-5} | 1.43×10^{-4} | 11 | 3.43×10^{-3} |
| 1.34×10^{-5} | 1.71×10^{-4} | 13 | 3.71×10^{-3} |
| 1.33×10^{-5} | 1.97×10^{-4} | 15 | 3.94×10^{-3} |
| 1.32×10^{-5} | 2.24×10^{-4} | 17 | 4.23×10^{-3} |
| 1.35×10^{-5} | 2.57×10^{-4} | 19 | 4.77×10^{-3} |
| 1.29×10^{-5} | 2.73×10^{-4} | 21 | 4.95×10^{-3} |
| $k_2 = 1.18 \times 10^1 \text{ M}^{-1} \text{ s}^{-1}$ | | | |

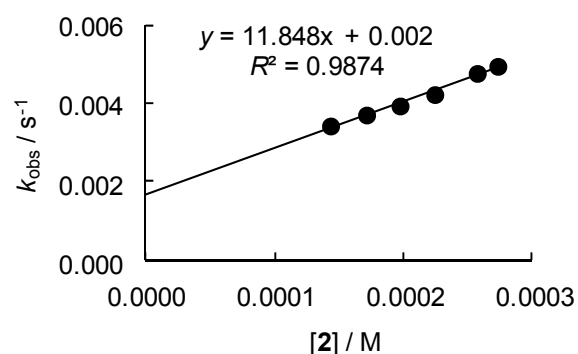


Table 4.20. Rate constants for the reactions of the NH₂ group of 1,1-dimethylhydrazine (**2**) with (ind)₂CH⁺ BF₄⁻ (**16f**) in CH₃CN (diodearray spectrophotometer, 20 °C, λ = 616 nm).

| [16f] ₀ /M | [2] ₀ /M | [2] ₀ /[16f] ₀ | $k_{\text{obs}}/\text{s}^{-1}$ |
|--|------------------------------|--|--------------------------------|
| 1.35×10^{-5} | 1.42×10^{-4} | 11 | 2.02×10^{-2} |
| 1.27×10^{-5} | 1.59×10^{-4} | 13 | 2.26×10^{-2} |
| 1.36×10^{-5} | 1.98×10^{-4} | 15 | 2.76×10^{-2} |
| 1.35×10^{-5} | 2.25×10^{-4} | 17 | 3.08×10^{-2} |
| 1.36×10^{-5} | 2.55×10^{-4} | 19 | 3.46×10^{-2} |
| 1.35×10^{-5} | 2.80×10^{-4} | 21 | 3.79×10^{-2} |
| $k_2 = 1.27 \times 10^2 \text{ M}^{-1} \text{ s}^{-1}$ | | | |

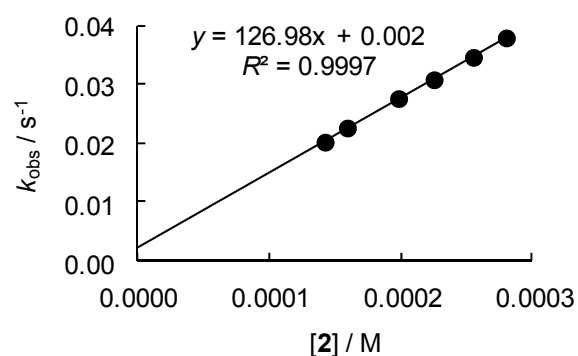


Table 4.21. Rate constants for the reactions of the NH₂ group of 1,1-dimethylhydrazine (**2**) with (pyr)₂CH⁺ BF₄⁻ (**16h**) in CH₃CN (stopped-flow technique, 20 °C, λ = 611 nm).

| [16h] ₀ /M | [2] ₀ /M | [2] ₀ /[16h] ₀ | $k_{\text{obs}}/\text{s}^{-1}$ |
|--------------------------------|------------------------------|--|--------------------------------|
| 1.80×10^{-5} | 1.45×10^{-4} | 8 | 1.78×10^{-1} |
| 1.80×10^{-5} | 1.81×10^{-4} | 10 | 2.28×10^{-1} |
| 1.80×10^{-5} | 2.18×10^{-4} | 12 | 2.82×10^{-1} |
| 1.80×10^{-5} | 2.54×10^{-4} | 14 | 3.30×10^{-1} |
| 1.80×10^{-5} | 2.90×10^{-4} | 16 | 3.88×10^{-1} |

$k_2 = 1.44 \times 10^3 \text{ M}^{-1} \text{ s}^{-1}$

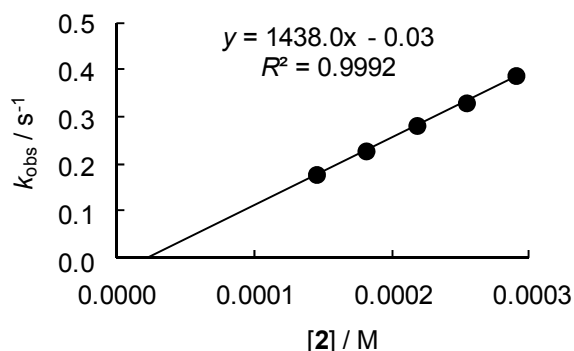


Table 4.22. Rate constants for the reactions of the NH₂ group of 1,1-dimethylhydrazine (**2**) with (dma)₂CH⁺ BF₄⁻ (**16i**) in CH₃CN (stopped-flow technique, 20 °C, λ = 605 nm).

| [16i] ₀ /M | [2] ₀ /M | [2] ₀ /[16i] ₀ | $k_{\text{obs}}/\text{s}^{-1}$ |
|--------------------------------|------------------------------|--|--------------------------------|
| 1.99×10^{-5} | 1.52×10^{-4} | 8 | 3.95×10^{-1} |
| 1.99×10^{-5} | 2.03×10^{-4} | 10 | 4.91×10^{-1} |
| 1.99×10^{-5} | 2.54×10^{-4} | 13 | 6.29×10^{-1} |
| 1.99×10^{-5} | 3.05×10^{-4} | 15 | 7.78×10^{-1} |
| 1.99×10^{-5} | 3.56×10^{-4} | 18 | 8.79×10^{-1} |

$k_2 = 2.46 \times 10^3 \text{ M}^{-1} \text{ s}^{-1}$

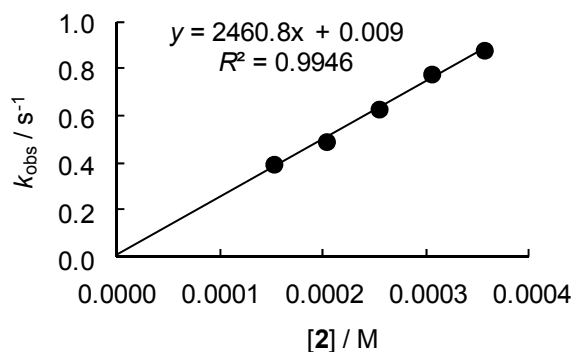


Table 4.23. Determination of the nucleophilicity parameters N and s_N for the NH₂ group of 1,1-dimethylhydrazine (**2**) in CH₃CN.

| Electrophile (E) | $k_2/\text{M}^{-1} \text{ s}^{-1}$ | $\log k_2$ |
|----------------------|------------------------------------|------------|
| 16c (-12.18) | 5.69×10^{-1} | -0.24 |
| 16d (-10.04) | 1.19×10^1 | 1.08 |
| 16f (-8.76) | 1.27×10^2 | 2.10 |
| 16h (-7.69) | 1.44×10^3 | 3.16 |
| 16i (-7.02) | 2.46×10^3 | 3.39 |

$N = 11.72, s_N = 0.73$

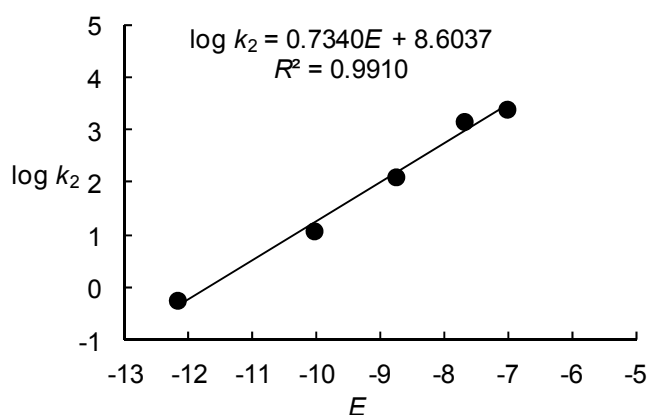


Table 4.24. Rate constants for the reactions of the NMe₂ group of 1,1-dimethylhydrazine (**2**) with (pyr)₂CH⁺ BF₄⁻ (**16h**) generated from (pyr)₂CHPBu₃⁺ BF₄⁻ (**16h**-PBu₃) in CH₃CN (laser-flash photolysis, 20 °C, λ = 611 nm).

| [16h -PBu ₃] ₀ /M | [2] ₀ /M | $k_{\text{obs}}/\text{s}^{-1}$ |
|---|------------------------------|--------------------------------|
| 1.47×10^{-5} | 8.43×10^{-2} | 3.71×10^5 |
| 1.47×10^{-5} | 1.48×10^{-1} | 6.22×10^5 |
| 1.47×10^{-5} | 1.76×10^{-1} | 7.27×10^5 |
| 1.47×10^{-5} | 2.60×10^{-1} | 1.05×10^6 |
| 1.47×10^{-5} | 3.33×10^{-1} | 1.31×10^6 |
| $k_2' = 3.78 \times 10^6 \text{ M}^{-1} \text{ s}^{-1}$ | | |

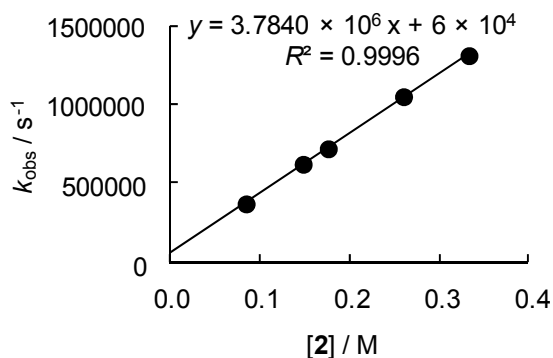


Table 4.25. Rate constants for the reactions of the NMe₂ group of 1,1-dimethylhydrazine (**2**) with (dma)₂CH⁺ BF₄⁻ (**16i**) generated from (dma)₂CHPBu₃⁺ BF₄⁻ (**16i**-PBu₃) in CH₃CN (laser-flash photolysis, 20 °C, λ = 605 nm).

| [16i -PBu ₃] ₀ /M | [2] ₀ /M | $k_{\text{obs}}/\text{s}^{-1}$ |
|---|------------------------------|--------------------------------|
| 3.46×10^{-6} | 7.96×10^{-2} | 6.68×10^5 |
| 3.46×10^{-6} | 1.23×10^{-1} | 1.01×10^6 |
| 3.46×10^{-6} | 1.64×10^{-1} | 1.35×10^6 |
| 3.46×10^{-6} | 1.94×10^{-1} | 1.59×10^6 |
| 3.46×10^{-6} | 2.75×10^{-1} | 2.24×10^6 |
| $k_2' = 8.06 \times 10^6 \text{ M}^{-1} \text{ s}^{-1}$ | | |

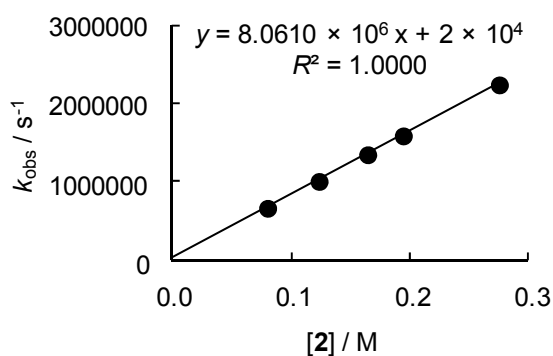


Table 4.26. Rate constants for the reactions of the NMe₂ group of 1,1-dimethylhydrazine (**2**) with (mor)₂CH⁺ BF₄⁻ (**16j**) generated from (mor)₂CHP(tol)₃⁺ BF₄⁻ (**16j**-P(tol)₃) in CH₃CN (laser-flash photolysis, 20 °C, λ = 611 nm).

| [16j -P(tol) ₃] ₀ /M | [2] ₀ /M | $k_{\text{obs}}/\text{s}^{-1}$ |
|---|------------------------------|--------------------------------|
| 1.90×10^{-5} | 1.73×10^{-2} | 6.23×10^5 |
| 1.90×10^{-5} | 3.77×10^{-2} | 1.35×10^6 |
| 1.90×10^{-5} | 4.65×10^{-2} | 1.61×10^6 |
| 1.90×10^{-5} | 5.39×10^{-2} | 1.93×10^6 |
| 1.90×10^{-5} | 8.55×10^{-2} | 2.98×10^6 |
| $k_2' = 3.46 \times 10^7 \text{ M}^{-1} \text{ s}^{-1}$ | | |

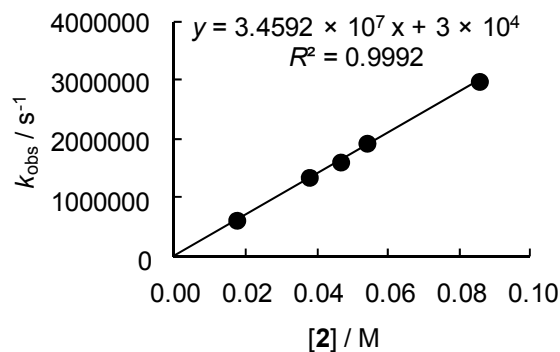
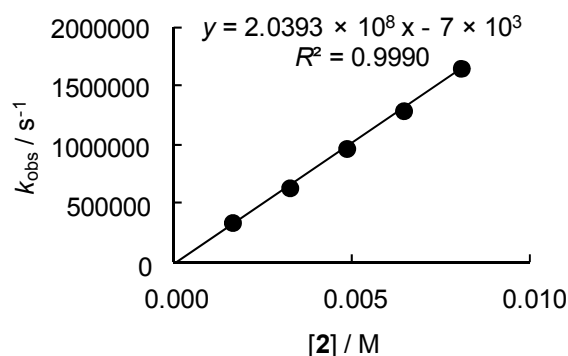


Table 4.27. Rate constants for the reactions of the NMe₂ group of 1,1-dimethylhydrazine (**2**) with (mfa)₂CH⁺ BF₄⁻ (**16k**) generated from (mfa)₂CHPBu₃⁺ BF₄⁻ (**16k**-PBu₃) in CH₃CN (laser-flash photolysis, 20 °C, λ = 586 nm).

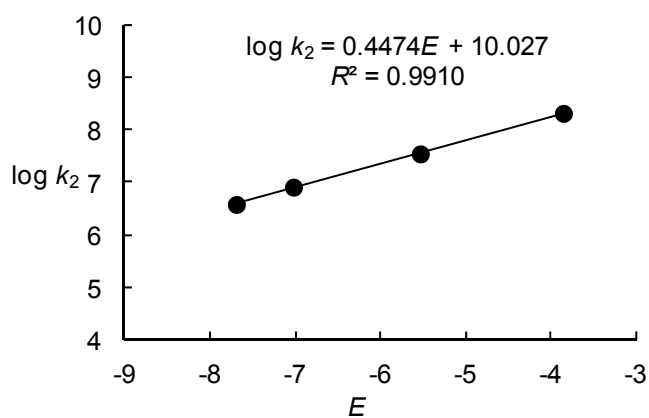
| [16k -PBu ₃] ₀ /M | [2] ₀ /M | $k_{\text{obs}}/\text{s}^{-1}$ |
|---|------------------------------|-------------------------------------|
| 7.49×10^{-6} ^[a] | 1.58×10^{-5} | (4.18×10^3) ^[b] |
| 7.51×10^{-6} | 1.61×10^{-3} | 3.40×10^5 |
| 7.51×10^{-6} | 3.22×10^{-3} | 6.35×10^5 |
| 7.51×10^{-6} | 4.82×10^{-3} | 9.69×10^5 |
| 7.51×10^{-6} | 6.43×10^{-3} | 1.29×10^6 |
| 7.51×10^{-6} | 8.04×10^{-3} | 1.65×10^6 |
| $k_2' = 2.04 \times 10^8 \text{ M}^{-1} \text{ s}^{-1}$ | | |



[a] From the initial absorbance of $A_{586 \text{ nm}} = 0.40$ and the absorption coefficient ($\epsilon = 159200 \text{ M}^{-1} \text{ cm}^{-1}$), an initial concentration of $2.5 \times 10^{-6} \text{ M}$ is estimated for **16k**. [b] At these conditions, pseudo-first order kinetics are not observed.

Table 4.28. Determination of the nucleophilicity parameters N and s_N for the NMe_2 group of 1,1-dimethylhydrazine (**2**) in CH_3CN .

| Electrophile (E) | $k_2'/\text{M}^{-1} \text{s}^{-1}$ | $\log k_2'$ |
|-------------------------|------------------------------------|-------------|
| 16h (-7.69) | 3.78×10^6 | 6.58 |
| 16i (-7.02) | 8.05×10^6 | 6.91 |
| 16j (-5.53) | 3.46×10^7 | 7.54 |
| 16k (-3.85) | 2.04×10^8 | 8.31 |
| $N = 22.41, s_N = 0.45$ | | |



Kinetics of the reactions of trimethylhydrazine (3) with benzhydrylium ions and quinone methides (4)

Table 4.29. Rate constants for the reactions of the NHMe group of trimethylhydrazine (**3**) with $(\text{ind})_2\text{CH}^+ \text{BF}_4^-$ (**16f**) in CH_3CN (stopped-flow technique, 20°C , $\lambda = 616 \text{ nm}$).

| $[\mathbf{16f}]_0/\text{M}$ | $[\mathbf{3}]_0/\text{M}$ | $[\mathbf{3}]_0/[\mathbf{16f}]_0$ | $k_{\text{obs}}/\text{s}^{-1}$ |
|--|---------------------------|-----------------------------------|--------------------------------|
| 1.46×10^{-5} | 1.19×10^{-3} | 81 | 5.96×10^{-1} |
| 1.46×10^{-5} | 1.78×10^{-3} | 122 | 9.28×10^{-1} |
| 1.46×10^{-5} | 2.38×10^{-3} | 163 | 1.26 |
| 1.46×10^{-5} | 3.57×10^{-3} | 244 | 2.02 |
| 1.46×10^{-5} | 4.76×10^{-3} | 352 | 2.78 |
| $k_2 = 6.15 \times 10^2 \text{ M}^{-1} \text{ s}^{-1}$ | | | |

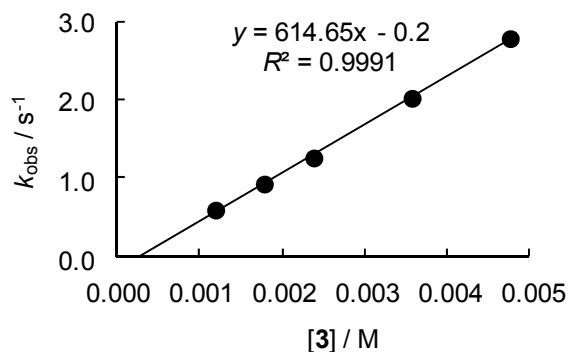


Table 4.30. Rate constants for the reactions of the NHMe group of trimethylhydrazine (**3**) with (thq)₂CH⁺ BF₄⁻ (**16g**) in CH₃CN (stopped-flow technique, 20 °C, λ = 619 nm).

| [16g] ₀ /M | [3] ₀ /M | [3] ₀ /[16g] ₀ | $k_{\text{obs}}/\text{s}^{-1}$ |
|--|------------------------------|--|--------------------------------|
| 1.78×10^{-5} | 2.38×10^{-4} | 13 | 4.09×10^{-1} |
| 1.78×10^{-5} | 2.97×10^{-4} | 17 | 4.60×10^{-1} |
| 1.78×10^{-5} | 3.57×10^{-4} | 20 | 5.35×10^{-1} |
| 1.78×10^{-5} | 4.16×10^{-4} | 23 | 6.06×10^{-1} |
| 1.78×10^{-5} | 8.92×10^{-4} | 50 | 1.22 |
| $k_2 = 1.26 \times 10^3 \text{ M}^{-1} \text{ s}^{-1}$ | | | |

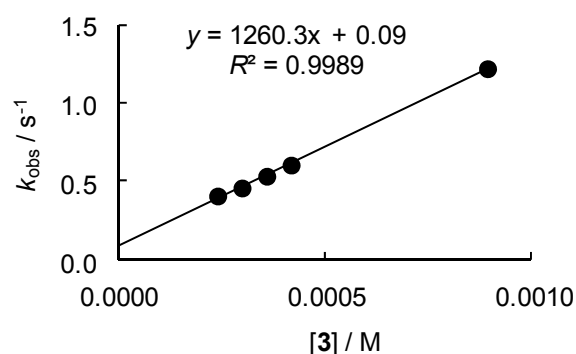


Table 4.31. Rate constants for the reactions of the NHMe group of trimethylhydrazine (**3**) with (pyr)₂CH⁺ BF₄⁻ (**16h**) in CH₃CN (stopped-flow technique, 20 °C, λ = 611 nm).

| [16h] ₀ /M | [3] ₀ /M | [3] ₀ /[16h] ₀ | $k_{\text{obs}}/\text{s}^{-1}$ |
|--|------------------------------|--|--------------------------------|
| 1.82×10^{-5} | 2.38×10^{-4} | 16 | 1.05 |
| 1.82×10^{-5} | 2.97×10^{-4} | 20 | 1.24 |
| 1.82×10^{-5} | 3.57×10^{-4} | 23 | 1.48 |
| 1.82×10^{-5} | 4.16×10^{-4} | 49 | 1.71 |
| $k_2 = 3.74 \times 10^3 \text{ M}^{-1} \text{ s}^{-1}$ | | | |

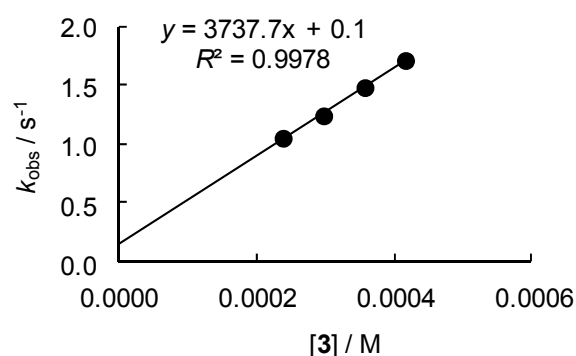


Table 4.32. Rate constants for the reactions of the NHMe group of trimethylhydrazine (**3**) with (dma)₂CH⁺ BF₄⁻ (**16i**) in CH₃CN (stopped-flow technique, 20 °C, λ = 605 nm).

| [16i] ₀ /M | [3] ₀ /M | [3] ₀ /[16i] ₀ | $k_{\text{obs}}/\text{s}^{-1}$ |
|--|------------------------------|--|--------------------------------|
| 1.79×10^{-5} | 1.64×10^{-4} | 9 | 1.87 |
| 1.79×10^{-5} | 1.91×10^{-4} | 11 | 2.20 |
| 1.79×10^{-5} | 2.18×10^{-4} | 12 | 2.51 |
| 1.79×10^{-5} | 2.73×10^{-4} | 15 | 3.12 |
| 1.79×10^{-5} | 3.00×10^{-4} | 17 | 3.48 |
| $k_2 = 1.17 \times 10^4 \text{ M}^{-1} \text{ s}^{-1}$ | | | |

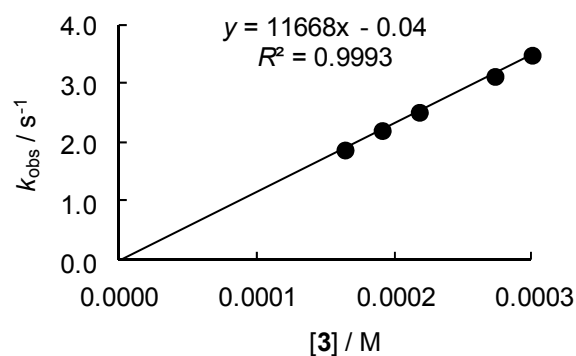


Table 4.33. Determination of the nucleophilicity parameters N and s_N for the NHMe group of trimethylhydrazine (**3**) in CH_3CN .

| Electrophile (E) | $k_2/\text{M}^{-1} \text{s}^{-1}$ | $\log k_2$ |
|-------------------------|-----------------------------------|------------|
| 16f (-8.76) | 6.15×10^2 | 2.79 |
| 16g (-8.22) | 1.26×10^3 | 3.10 |
| 16h (-7.69) | 3.74×10^3 | 3.57 |
| 16i (-7.02) | 1.17×10^4 | 4.07 |
| $N = 12.43, s_N = 0.75$ | | |

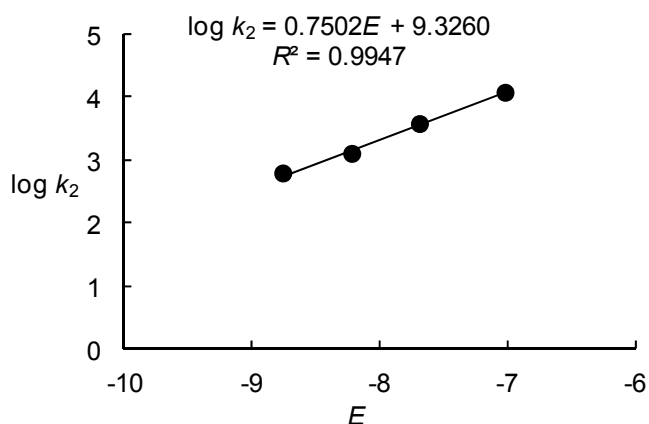


Table 4.34. Rate constants for the reactions of the NMe_2 group of trimethylhydrazine (**3**) with $(\text{mor})_2\text{CH}^+ \text{BF}_4^-$ (**16j**) generated from $(\text{mor})_2\text{CHPBu}_3^+ \text{BF}_4^-$ (**16j-PBu}_3**) in CH_3CN (laser-flash photolysis, 20°C , $\lambda = 611 \text{ nm}$).

| $[\mathbf{16j-PBu}_3]_0/\text{M}$ | $[\mathbf{3}]_0/\text{M}$ | $k_{\text{obs}}/\text{s}^{-1}$ |
|---|---------------------------|--------------------------------|
| 1.02×10^{-5} | 2.10×10^{-3} | 1.02×10^4 |
| 1.02×10^{-5} | 4.21×10^{-3} | 1.63×10^4 |
| 1.02×10^{-5} | 6.31×10^{-3} | 2.27×10^4 |
| 1.02×10^{-5} | 1.05×10^{-2} | 3.54×10^4 |
| $k_2' = 3.01 \times 10^6 \text{ M}^{-1} \text{ s}^{-1}$ | | |

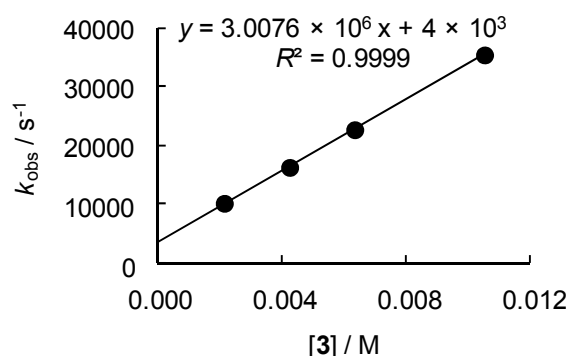


Table 4.35. Rate constants for the reactions of the NMe_2 group of trimethylhydrazine (**3**) with $(\text{mfa})_2\text{CH}^+ \text{BF}_4^-$ (**16k**) generated from $(\text{mfa})_2\text{CHPBu}_3^+ \text{BF}_4^-$ (**16k-PBu}_3**) in CH_3CN (laser-flash photolysis, 20°C , $\lambda = 586 \text{ nm}$).

| $[\mathbf{16k-PBu}_3]_0/\text{M}$ | $[\mathbf{3}]_0/\text{M}$ | $k_{\text{obs}}/\text{s}^{-1}$ |
|---|---------------------------|--------------------------------|
| 7.86×10^{-6} | 1.96×10^{-3} | 6.02×10^4 |
| 7.86×10^{-6} | 2.61×10^{-3} | 7.40×10^4 |
| 7.86×10^{-6} | 3.27×10^{-3} | 8.46×10^4 |
| 7.86×10^{-6} | 4.24×10^{-3} | 1.02×10^5 |
| $k_2' = 1.81 \times 10^7 \text{ M}^{-1} \text{ s}^{-1}$ | | |

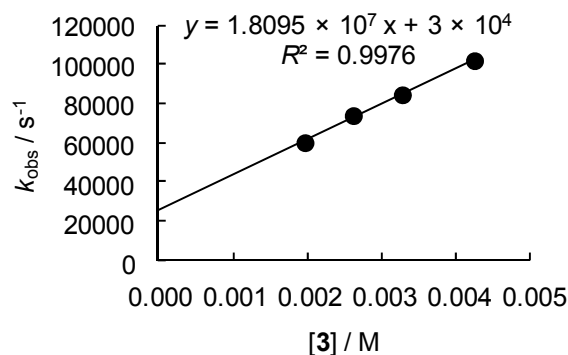


Table 4.36. Rate constants for the reactions of the NMe₂ group of trimethylhydrazine (**3**) with (fur)₂CH⁺ BF₄⁻ (**16l**) generated from (fur)₂CHPPh₃⁺ BF₄⁻ (**16l**-PPh₃) in CH₃CN (laser-flash photolysis, 20 °C, $\lambda = 520$ nm).

| [16l -PPh ₃] ₀ /M | [3] ₀ /M | $k_{\text{obs}}/\text{s}^{-1}$ |
|---|------------------------------|--------------------------------|
| 1.10×10^{-5} | 6.53×10^{-4} | 3.48×10^5 |
| 1.10×10^{-5} | 9.79×10^{-4} | 5.09×10^5 |
| 1.10×10^{-5} | 1.31×10^{-3} | 6.55×10^5 |
| 1.10×10^{-5} | 1.63×10^{-3} | 7.97×10^5 |
| $k_2' = 4.58 \times 10^8 \text{ M}^{-1} \text{ s}^{-1}$ | | |

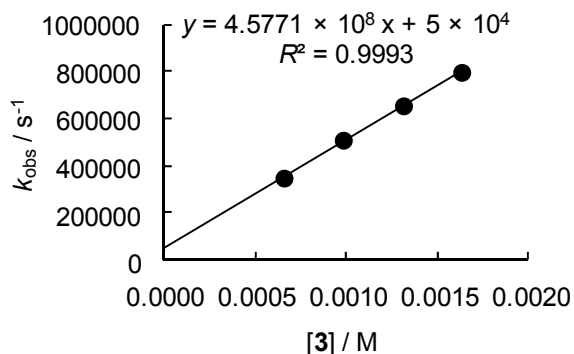
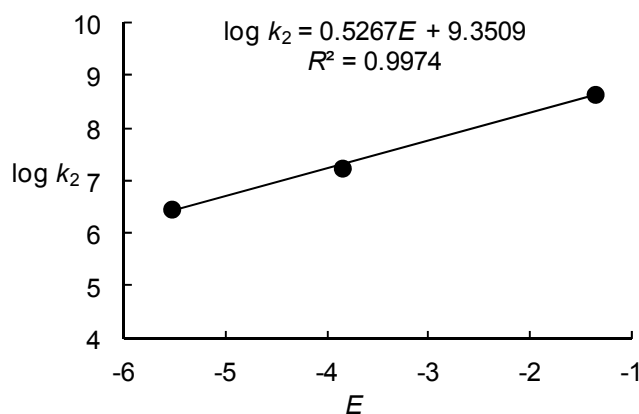


Table 4.37. Determination of the nucleophilicity parameters N and s_N for the NMe₂ group of trimethylhydrazine (**3**) in CH₃CN.

| Electrophile (E) | $k_2'/\text{M}^{-1} \text{ s}^{-1}$ | $\log k_2'$ |
|-------------------------|-------------------------------------|-------------|
| 16j (-5.53) | 3.00×10^6 | 6.48 |
| 16k (-3.85) | 1.81×10^7 | 7.26 |
| 16l (-1.36) | 4.58×10^8 | 8.66 |
| $N = 17.75, s_N = 0.53$ | | |



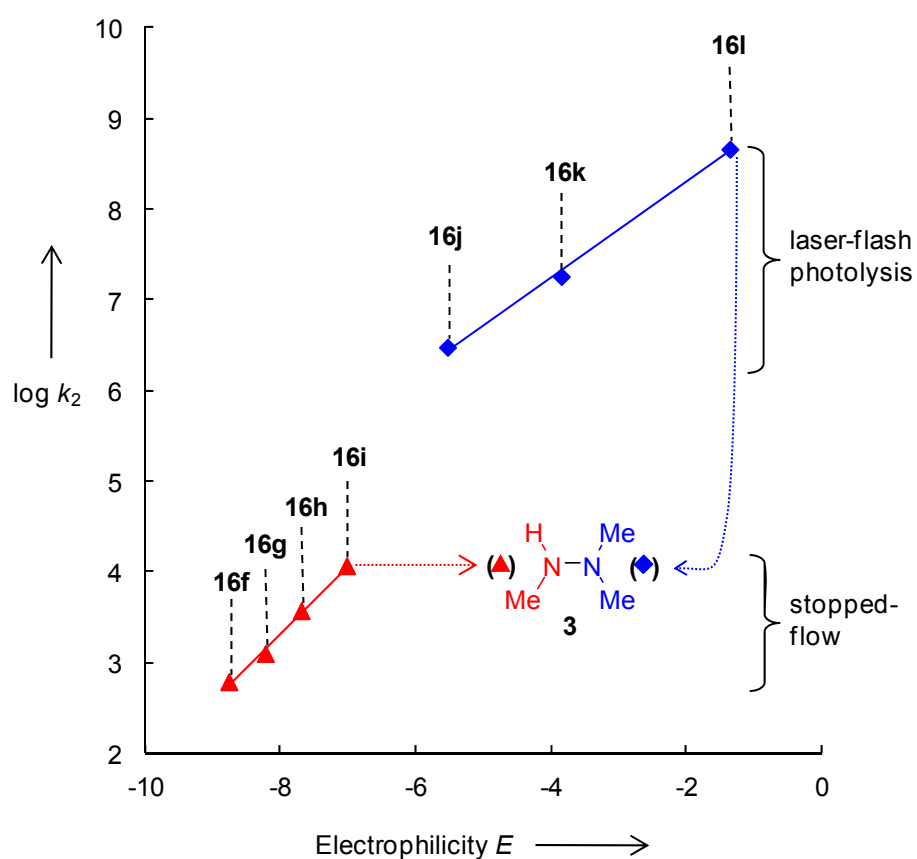


Figure 4.14. Plots of the second-order rate constants $\log k_2$ or $\log k_2'$ for the reactions of trimethylhydrazine (**3**) with benzhydrylium ions and quinone methides in CH_3CN at 20°C versus the E parameters of **16**.

Kinetics of the reactions of methylhydrazine (4) with benzhydrylium ions and quinone methides (16)

Table 4.38. Rate constants for the reactions of methylhydrazine (4) with tol(*t*Bu)₂QM (16b) in CH₃CN (diodearray spectrophotometer, 20 °C, λ = 364 nm).

| [16b] ₀ /M | [4] ₀ /M | [4] ₀ ⁻¹ /M ⁻¹ | [4] ₀ /[16b] ₀ | <i>k</i> _{obs} /s ⁻¹ | [4] ₀ × <i>k</i> _{obs} ⁻¹ /M s |
|-------------------------|-------------------------|---|--------------------------------------|--|---|
| 4.94 × 10 ⁻⁵ | 9.51 × 10 ⁻⁴ | 1.05 × 10 ³ | 19 | 2.13 × 10 ⁻³ | 4.46 × 10 ⁻¹ |
| 4.92 × 10 ⁻⁵ | 1.45 × 10 ⁻³ | 6.90 × 10 ² | 30 | 4.40 × 10 ⁻³ | 3.30 × 10 ⁻¹ |
| 4.95 × 10 ⁻⁵ | 1.97 × 10 ⁻³ | 5.08 × 10 ² | 40 | 7.40 × 10 ⁻³ | 2.66 × 10 ⁻¹ |
| 4.82 × 10 ⁻⁵ | 2.91 × 10 ⁻³ | 3.44 × 10 ² | 60 | 1.39 × 10 ⁻² | 2.09 × 10 ⁻¹ |
| 4.80 × 10 ⁻⁵ | 3.82 × 10 ⁻³ | 2.62 × 10 ² | 80 | 2.20 × 10 ⁻² | 1.74 × 10 ⁻¹ |

$$k_2 = 1.12 \times 10^1 \text{ M}^{-1} \text{ s}^{-1}$$

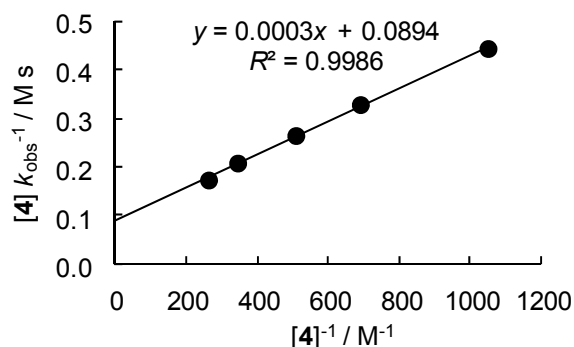
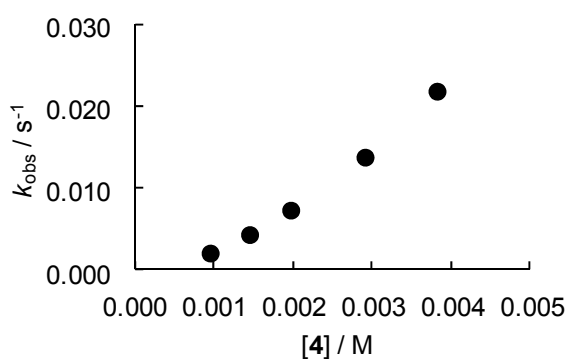


Table 4.39. Rate constants for the reactions of methylhydrazine (4) with ani(Ph)₂QM (16c) in CH₃CN (stopped-flow technique, 20 °C, λ = 415 nm).

| [16c] ₀ /M | [4] ₀ /M | [4] ₀ /[16c] ₀ | <i>k</i> _{obs} /s ⁻¹ |
|-------------------------|-------------------------|--------------------------------------|--|
| 6.82 × 10 ⁻⁵ | 1.07 × 10 ⁻³ | 16 | 1.46 |
| 6.82 × 10 ⁻⁵ | 2.37 × 10 ⁻³ | 35 | 3.42 |
| 6.82 × 10 ⁻⁵ | 3.56 × 10 ⁻³ | 52 | 5.11 |
| 6.82 × 10 ⁻⁵ | 4.74 × 10 ⁻³ | 70 | 6.86 |
| 6.82 × 10 ⁻⁵ | 5.93 × 10 ⁻³ | 87 | 8.58 |

$$k_2 = 1.46 \times 10^3 \text{ M}^{-1} \text{ s}^{-1}$$

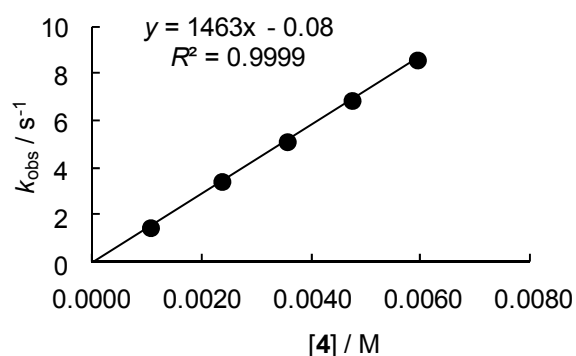


Table 4.40. Rate constants for the reactions of methylhydrazine (**4**) with $(\text{lil})_2\text{CH}^+ \text{BF}_4^-$ (**16d**) in CH_3CN (stopped-flow technique, 20 °C, $\lambda = 631 \text{ nm}$).

| $[\mathbf{16d}]_0/\text{M}$ | $[\mathbf{4}]_0/\text{M}$ | $[\mathbf{4}]_0/[\mathbf{16d}]_0$ | $k_{\text{obs}}/\text{s}^{-1}$ |
|--|---------------------------|-----------------------------------|--------------------------------|
| 1.73×10^{-5} | 3.56×10^{-4} | 20 | 1.02×10^1 |
| 1.73×10^{-5} | 7.11×10^{-4} | 41 | 2.14×10^1 |
| 1.73×10^{-5} | 1.07×10^{-3} | 61 | 3.37×10^1 |
| 1.73×10^{-5} | 1.42×10^{-3} | 82 | 4.54×10^1 |
| $k_2 = 3.32 \times 10^4 \text{ M}^{-1} \text{ s}^{-1}$ | | | |

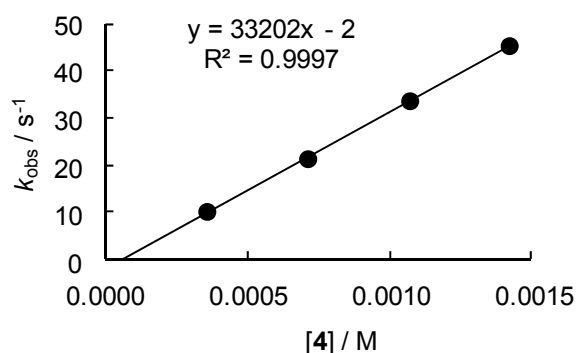


Table 4.41. Rate constants for the reactions of methylhydrazine (**4**) with $(\text{ind})_2\text{CH}^+ \text{BF}_4^-$ (**16f**) in CH_3CN (stopped-flow technique, 20 °C, $\lambda = 616 \text{ nm}$).

| $[\mathbf{16f}]_0/\text{M}$ | $[\mathbf{4}]_0/\text{M}$ | $[\mathbf{4}]_0/[\mathbf{16f}]_0$ | $k_{\text{obs}}/\text{s}^{-1}$ |
|--|---------------------------|-----------------------------------|--------------------------------|
| 1.74×10^{-5} | 2.37×10^{-4} | 14 | 4.61×10^1 |
| 1.74×10^{-5} | 3.56×10^{-4} | 20 | 7.32×10^1 |
| 1.74×10^{-5} | 4.74×10^{-4} | 27 | 9.88×10^1 |
| 1.74×10^{-5} | 5.93×10^{-4} | 34 | 1.24×10^2 |
| 1.74×10^{-5} | 7.11×10^{-4} | 41 | 1.48×10^2 |
| $k_2 = 2.15 \times 10^5 \text{ M}^{-1} \text{ s}^{-1}$ | | | |

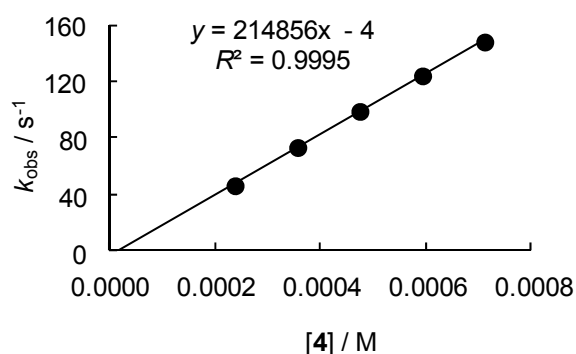


Table 4.42. Rate constants for the reactions of methylhydrazine (**4**) with $(\text{mor})_2\text{CH}^+ \text{BF}_4^-$ (**16j**) generated from $(\text{mor})_2\text{CHPBu}_3^+ \text{BF}_4^-$ (**16j-PBu₃**) in CH_3CN (laser-flash photolysis, 20 °C, $\lambda = 611 \text{ nm}$).

| $[\mathbf{16j-PBu}_3]_0/\text{M}$ | $[\mathbf{4}]_0/\text{M}$ | $k_{\text{obs}}/\text{s}^{-1}$ |
|--|---------------------------|--------------------------------|
| 9.96×10^{-6} | 1.17×10^{-1} | 1.41×10^6 |
| 9.96×10^{-6} | 1.24×10^{-1} | 1.47×10^6 |
| 9.96×10^{-6} | 1.60×10^{-1} | 1.91×10^6 |
| 9.96×10^{-6} | 2.09×10^{-1} | 2.46×10^6 |
| 9.96×10^{-6} | 2.41×10^{-1} | 2.95×10^6 |
| $k_2 = 1.22 \times 10^7 \text{ M}^{-1} \text{ s}^{-1}$ | | |

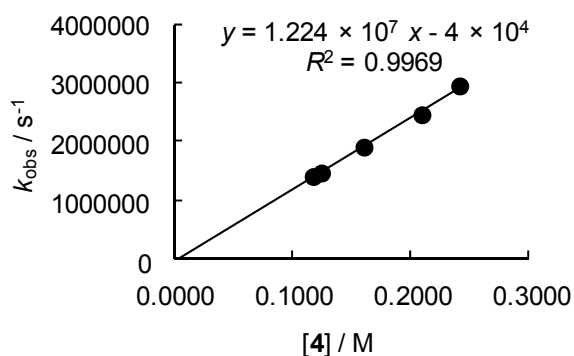


Table 4.43. Rate constants for the reactions of methylhydrazine (**4**) with $(\text{mfa})_2\text{CH}^+ \text{BF}_4^-$ (**16k**) generated from $(\text{mfa})_2\text{CHPBu}_3^+ \text{BF}_4^-$ (**16k-PBu₃**) in CH_3CN (laser-flash photolysis, 20 °C, $\lambda = 586 \text{ nm}$).

| $[\mathbf{16k-PBu}_3]_0/\text{M}$ | $[\mathbf{4}]_0/\text{M}$ | $k_{\text{obs}}/\text{s}^{-1}$ |
|-----------------------------------|---------------------------|--------------------------------|
| 7.76×10^{-6} | 1.56×10^{-2} | 1.34×10^6 |
| 7.76×10^{-6} | 3.05×10^{-2} | 2.59×10^6 |
| 7.76×10^{-6} | 4.65×10^{-2} | 4.06×10^6 |
| 7.76×10^{-6} | 6.14×10^{-2} | 5.27×10^6 |

$k_2 = 8.65 \times 10^7 \text{ M}^{-1} \text{ s}^{-1}$

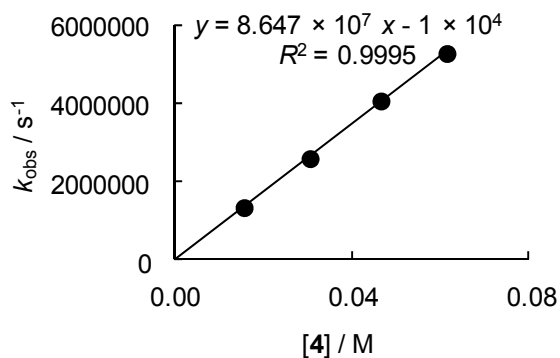
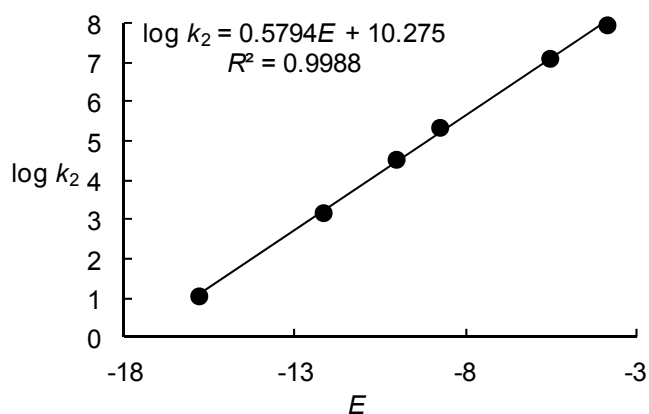


Table 4.44. Determination of the nucleophilicity parameters N and s_N for methylhydrazine (**4**) in CH_3CN .

| Electrophile (E) | $k_2/\text{M}^{-1} \text{ s}^{-1}$ | $\log k_2$ |
|----------------------|------------------------------------|------------|
| 16b (-15.83) | 1.12×10^1 | 1.05 |
| 16c (-12.18) | 1.46×10^3 | 3.16 |
| 16d (-10.04) | 3.32×10^4 | 4.52 |
| 16f (-8.76) | 2.15×10^5 | 5.33 |
| 16j (-5.53) | 1.22×10^7 | 7.09 |
| 16k (-3.85) | 8.65×10^7 | 7.94 |

$N = 17.73, s_N = 0.58$



Kinetics of the reactions of 1,2-dimethylhydrazine (5) with benzhydrylium ions and quinone methides (16)

Table 4.45. Rate constants for the reactions of 1,2-dimethylhydrazine (5) with ani(Ph)₂QM (16c) in CH₃CN (stopped-flow technique, 20 °C, λ = 415 nm).

| [16c] ₀ /M | [5] ₀ /M | [5] ₀ ⁻¹ /M ⁻¹ | [5] ₀ /[16c] ₀ | $k_{\text{obs}}/\text{s}^{-1}$ | [5] ₀ × $k_{\text{obs}}^{-1}/\text{M s}$ |
|-----------------------|-----------------------|---|--------------------------------------|--------------------------------|---|
| 3.16×10^{-5} | 6.35×10^{-4} | 1.57×10^3 | 20 | 1.49×10^{-1} | 4.26×10^{-3} |
| 3.16×10^{-5} | 1.27×10^{-3} | 7.87×10^2 | 40 | 3.80×10^{-1} | 3.34×10^{-3} |
| 3.16×10^{-5} | 1.91×10^{-3} | 5.24×10^2 | 60 | 6.31×10^{-1} | 3.03×10^{-3} |
| 3.16×10^{-5} | 2.54×10^{-3} | 3.94×10^2 | 80 | 9.13×10^{-1} | 2.78×10^{-3} |
| 3.16×10^{-5} | 3.18×10^{-3} | 3.14×10^2 | 100 | 1.23 | 2.59×10^{-3} |

$$k_2 = 4.44 \times 10^2 \text{ M}^{-1} \text{ s}^{-1}$$

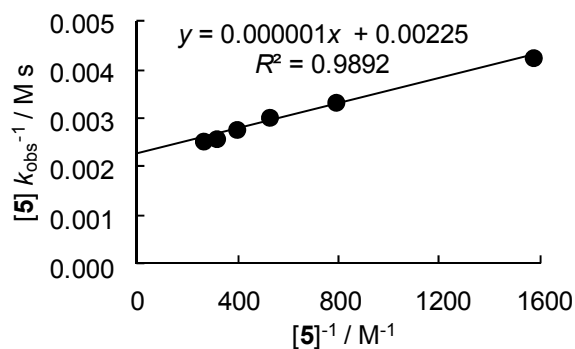
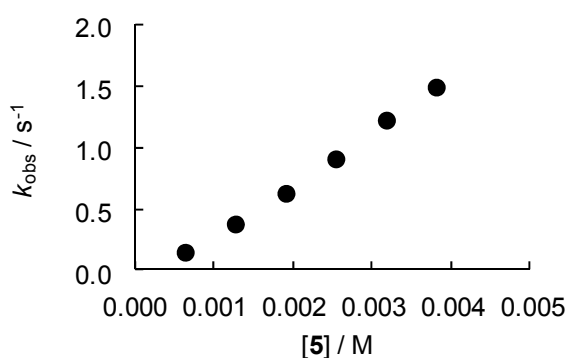


Table 4.46. Rate constants for the reactions of 1,2-dimethylhydrazine (5) with (lil)₂CH⁺ BF₄⁻ (16d) in CH₃CN (stopped-flow technique, 20 °C, λ = 631 nm).

| [16d] ₀ /M | [5] ₀ /M | [5] ₀ /[16d] ₀ | $k_{\text{obs}}/\text{s}^{-1}$ |
|-----------------------|-----------------------|--------------------------------------|--------------------------------|
| 7.40×10^{-6} | 1.58×10^{-4} | 21 | 1.67 |
| 7.40×10^{-6} | 3.16×10^{-4} | 43 | 3.81 |
| 7.40×10^{-6} | 4.43×10^{-4} | 60 | 5.69 |
| 7.40×10^{-6} | 6.01×10^{-4} | 81 | 8.17 |
| 7.40×10^{-6} | 7.27×10^{-4} | 98 | 1.16×10^1 |
| 7.40×10^{-6} | 1.14×10^{-3} | 154 | 1.76×10^1 |
| 7.40×10^{-6} | 1.58×10^{-3} | 154 | 2.46×10^1 |

$$k_2 = 1.64 \times 10^4 \text{ M}^{-1} \text{ s}^{-1}$$

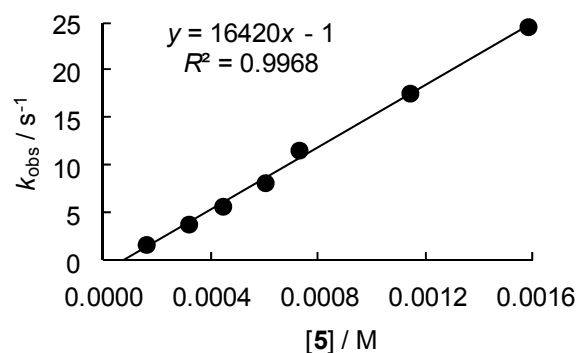


Table 4.47. Rate constants for the reactions of 1,2-dimethylhydrazine (**5**) with (jul)₂CH⁺ BF₄⁻ (**16e**) in CH₃CN (stopped-flow technique, 20 °C, λ = 635 nm).

| [16e] ₀ /M | [5] ₀ /M | [5] ₀ /[16e] ₀ | $k_{\text{obs}}/\text{s}^{-1}$ |
|--|------------------------------|--|--------------------------------|
| 7.55×10^{-6} | 1.46×10^{-4} | 19 | 6.82 |
| 7.55×10^{-6} | 2.92×10^{-4} | 39 | 1.39×10^1 |
| 7.55×10^{-6} | 3.64×10^{-4} | 48 | 1.65×10^1 |
| 7.55×10^{-6} | 4.37×10^{-4} | 58 | 2.01×10^1 |
| 7.55×10^{-6} | 5.10×10^{-4} | 68 | 2.31×10^1 |
| $k_2 = 4.46 \times 10^4 \text{ M}^{-1} \text{ s}^{-1}$ | | | |

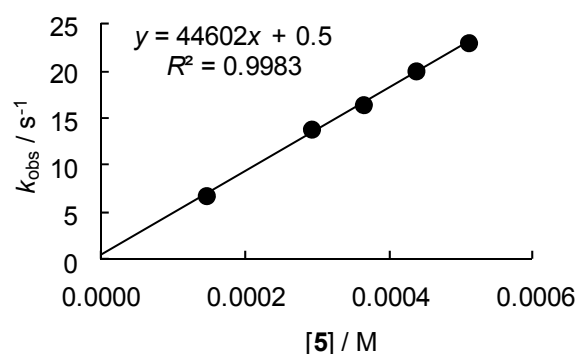


Table 4.48. Rate constants for the reactions of 1,2-dimethylhydrazine (**5**) with (ind)₂CH⁺ BF₄⁻ (**16f**) in CH₃CN (stopped-flow technique, 20 °C, λ = 616 nm).

| [16f] ₀ /M | [5] ₀ /M | [5] ₀ /[16f] ₀ | $k_{\text{obs}}/\text{s}^{-1}$ |
|--|------------------------------|--|--------------------------------|
| 7.33×10^{-6} | 1.58×10^{-4} | 22 | 6.50 |
| 7.33×10^{-6} | 3.16×10^{-4} | 43 | 2.03×10^1 |
| 7.33×10^{-6} | 7.27×10^{-4} | 99 | 6.04×10^1 |
| 7.33×10^{-6} | 1.14×10^{-3} | 155 | 1.00×10^2 |
| 7.33×10^{-6} | 1.58×10^{-3} | 216 | 1.36×10^2 |
| $k_2 = 9.24 \times 10^4 \text{ M}^{-1} \text{ s}^{-1}$ | | | |

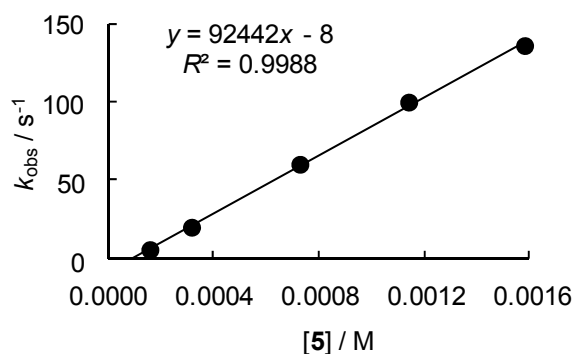


Table 4.49. Rate constants for the reactions of 1,2-dimethylhydrazine (**5**) with (pyr)₂CH⁺ BF₄⁻ (**16h**) in CH₃CN (stopped-flow technique, 20 °C, λ = 616 nm).

| [16h] ₀ /M | [5] ₀ /M | [5] ₀ /[16h] ₀ | $k_{\text{obs}}/\text{s}^{-1}$ |
|--|------------------------------|--|--------------------------------|
| 7.55×10^{-6} | 1.46×10^{-4} | 19 | 1.03×10^2 |
| 7.55×10^{-6} | 2.19×10^{-4} | 29 | 1.49×10^2 |
| 7.55×10^{-6} | 2.92×10^{-4} | 39 | 1.96×10^2 |
| 7.55×10^{-6} | 3.64×10^{-4} | 48 | 2.12×10^2 |
| 7.55×10^{-6} | 4.37×10^{-4} | 58 | 2.57×10^2 |
| 7.55×10^{-6} | 5.10×10^{-4} | 68 | 3.02×10^2 |
| $k_2 = 5.24 \times 10^5 \text{ M}^{-1} \text{ s}^{-1}$ | | | |

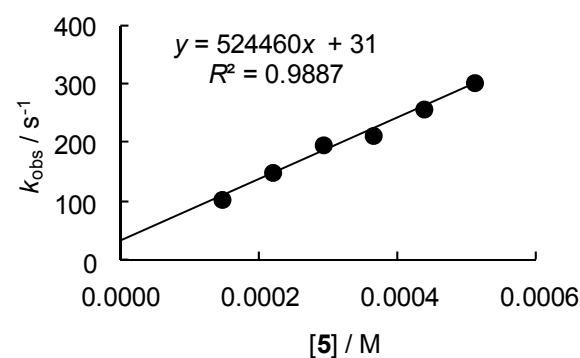
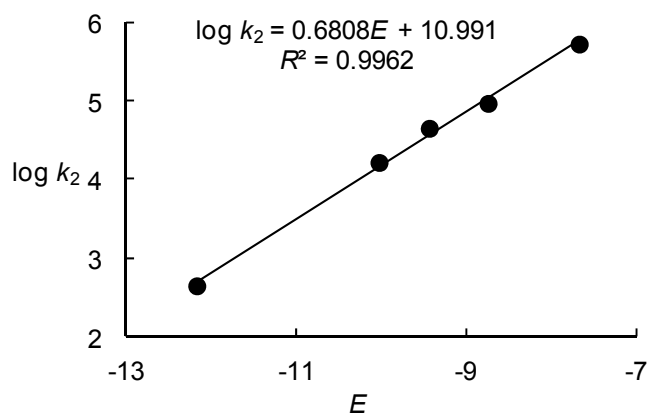


Table 4.50. Determination of the nucleophilicity parameters N and s_N for 1,2-dimethylhydrazine (**5**) in CH_3CN .

| Electrophile (E) | $k_2/\text{M}^{-1} \text{s}^{-1}$ | $\log k_2$ |
|----------------------|-----------------------------------|------------|
| 16c (-12.18) | 4.44×10^2 | 2.65 |
| 16d (-10.04) | 1.64×10^4 | 4.21 |
| 16e (-9.45) | 4.46×10^4 | 4.65 |
| 16f (-8.76) | 9.24×10^4 | 4.97 |
| 16h (-7.69) | 5.24×10^5 | 5.72 |

$N = 16.15, s_N = 0.68$



Kinetics of the reactions of formohydrazide (6) with benzhydrylium ions (16)

Table 4.51. Rate constants for the reactions of formohydrazide (**6**) with $(\text{dma})_2\text{CH}^+ \text{BF}_4^-$ (**16i**) in CH_3CN (stopped-flow technique, 20°C , $\lambda = 605 \text{ nm}$).

| $[\mathbf{16i}]_0/\text{M}$ | $[\mathbf{5}]_0/\text{M}$ | $[\mathbf{5}]_0/[\mathbf{16i}]_0$ | $k_{\text{obs}}/\text{s}^{-1}$ |
|-----------------------------|---------------------------|-----------------------------------|--------------------------------|
| 1.49×10^{-5} | 6.26×10^{-4} | 42 | 1.76 |
| 1.49×10^{-5} | 1.17×10^{-3} | 79 | 2.02 |
| 1.49×10^{-5} | 1.80×10^{-3} | 121 | 2.30 |
| 1.49×10^{-5} | 2.35×10^{-3} | 157 | 2.49 |
| 1.49×10^{-5} | 2.97×10^{-3} | 200 | 2.77 |

$k_2 = 4.24 \times 10^2 \text{ M}^{-1} \text{ s}^{-1}$

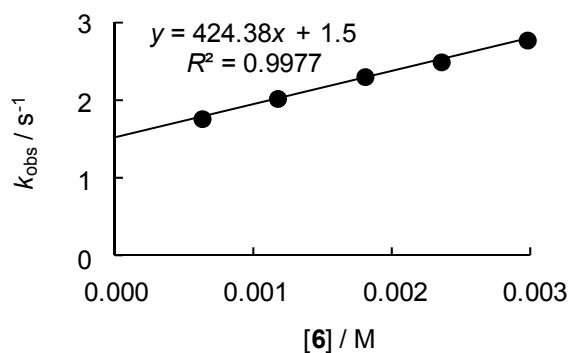


Table 4.52. Rate constants for the reactions of formohydrazide (**6**) with (mor)₂CH⁺ BF₄⁻ (**16j**) in CH₃CN (stopped-flow technique, 20 °C, λ = 611 nm).

| [16j] ₀ /M | [6] ₀ /M | [6] ₀ /[16j] ₀ | $k_{\text{obs}}/\text{s}^{-1}$ |
|--|------------------------------|--|--------------------------------|
| 1.49×10^{-5} | 6.26×10^{-4} | 42 | 2.71 |
| 1.49×10^{-5} | 1.17×10^{-3} | 79 | 5.10 |
| 1.49×10^{-5} | 1.80×10^{-3} | 121 | 7.78 |
| 1.49×10^{-5} | 2.35×10^{-3} | 157 | 1.01×10^1 |
| 1.49×10^{-5} | 2.97×10^{-3} | 200 | 1.29×10^1 |
| $k_2 = 4.33 \times 10^3 \text{ M}^{-1} \text{ s}^{-1}$ | | | |

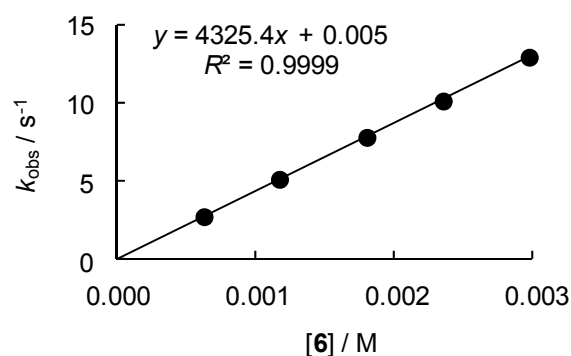


Table 4.53. Rate constants for the reactions of formohydrazide (**6**) with (mfa)₂CH⁺ BF₄⁻ (**16k**) in CH₃CN (stopped-flow technique, 20 °C, λ = 586 nm).

| [16j] ₀ /M | [6] ₀ /M | [6] ₀ /[16j] ₀ | $k_{\text{obs}}/\text{s}^{-1}$ |
|--|------------------------------|--|--------------------------------|
| 7.72×10^{-6} | 2.98×10^{-4} | 40 | 1.57×10^1 |
| 7.72×10^{-6} | 8.95×10^{-4} | 116 | 5.56×10^1 |
| 7.72×10^{-6} | 1.19×10^{-3} | 155 | 7.40×10^1 |
| 7.72×10^{-6} | 1.49×10^{-3} | 193 | 9.37×10^1 |
| $k_2 = 6.53 \times 10^4 \text{ M}^{-1} \text{ s}^{-1}$ | | | |

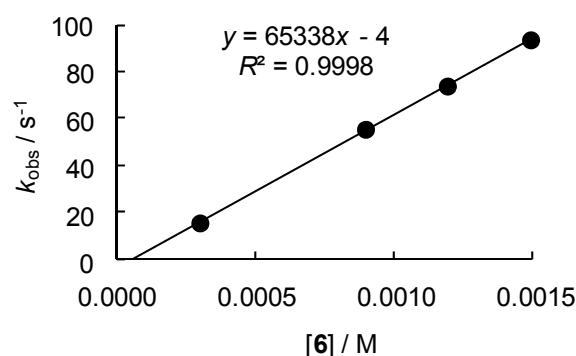


Table 4.54. Rate constants for the reactions of formohydrazide (**6**) with (fur)₂CH⁺ BF₄⁻ (**16l**) generated from (fur)₂CHPPh₃⁺ BF₄⁻ (**16l-PPh₃**) in CH₃CN (laser-flash photolysis, 20 °C, λ = 530 nm).

| [16l-PPh₃] ₀ /M | [6] ₀ /M | $k_{\text{obs}}/\text{s}^{-1}$ |
|--|------------------------------|--------------------------------|
| 1.08×10^{-5} | 6.04×10^{-2} | 8.13×10^5 |
| 1.08×10^{-5} | 8.16×10^{-2} | 1.24×10^6 |
| 1.08×10^{-5} | 1.04×10^{-1} | 1.34×10^6 |
| 1.08×10^{-5} | 1.22×10^{-1} | 1.65×10^6 |
| $k_2 = 1.26 \times 10^7 \text{ M}^{-1} \text{ s}^{-1}$ | | |

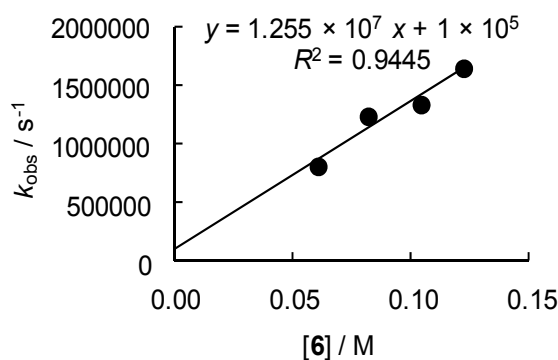


Table 4.55. Rate constants for the reactions of formohydrazide (**6**) with $(\text{ani})_2\text{CH}^+ \text{BF}_4^-$ (**16n**) generated from $(\text{ani})_2\text{CHPPH}_3^+ \text{BF}_4^-$ (**16n-PPh₃**) in CH_3CN (laser-flash photolysis, 20 °C, $\lambda = 513 \text{ nm}$).

| $[\mathbf{16n-PPh}_3]_0/\text{M}$ | $[\mathbf{6}]_0/\text{M}$ | $k_{\text{obs}}/\text{s}^{-1}$ |
|-----------------------------------|---------------------------|--------------------------------|
| 1.11×10^{-5} | 4.25×10^{-3} | 3.39×10^5 |
| 1.11×10^{-5} | 8.50×10^{-3} | 5.92×10^5 |
| 1.11×10^{-5} | 1.28×10^{-2} | 8.73×10^5 |
| 1.11×10^{-5} | 1.70×10^{-2} | 1.16×10^6 |
| 1.11×10^{-5} | 2.13×10^{-2} | 1.44×10^6 |

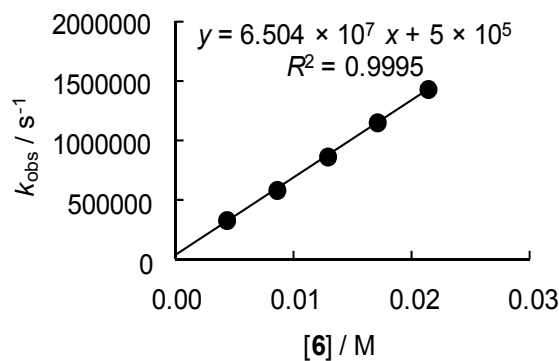
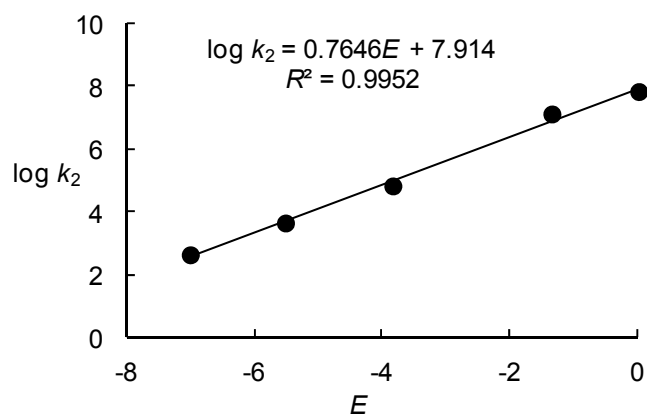
$$k_2 = 6.50 \times 10^7 \text{ M}^{-1} \text{ s}^{-1}$$


Table 4.56. Determination of the nucleophilicity parameters N and s_N for formohydrazide (**6**) in CH_3CN .

| Electrophile (E) | $k_2 / \text{M}^{-1} \text{ s}^{-1}$ | $\log k_2$ |
|----------------------|--------------------------------------|------------|
| 16i (-7.02) | 4.24×10^2 | 2.63 |
| 16j (-5.53) | 4.33×10^3 | 3.64 |
| 16k (-3.85) | 6.53×10^4 | 4.81 |
| 16l (-1.36) | 1.26×10^7 | 7.10 |
| 16n (0.00) | 6.50×10^7 | 7.81 |

$$N = 10.35, s_N = 0.76$$


Kinetics of the reactions of N,N' -dimethylformohydrazide (7) with benzhydrylium ions (16)

Table 4.57. Rate constants for the reactions of N,N' -dimethylformohydrazide (7) with $(\text{fur})_2\text{CH}^+ \text{BF}_4^-$ (**16l**) generated from $(\text{fur})_2\text{CHPPh}_3^+ \text{BF}_4^-$ (**16l-PPh₃**) in CH_3CN (laser-flash photolysis, 20 °C, $\lambda = 535$ nm).

| $[\mathbf{16l-PPh}_3]_0/\text{M}$ | $[\mathbf{7}]_0/\text{M}$ | $k_{\text{obs}}/\text{s}^{-1}$ |
|--|---------------------------|--------------------------------|
| 1.05×10^{-5} | 3.83×10^{-2} | 1.30×10^6 |
| 1.05×10^{-5} | 5.71×10^{-2} | 1.76×10^6 |
| 1.05×10^{-5} | 7.16×10^{-2} | 2.11×10^6 |
| 1.05×10^{-5} | 9.24×10^{-2} | 2.50×10^6 |
| 1.05×10^{-5} | 1.17×10^{-1} | 3.04×10^6 |
| $k_2 = 2.18 \times 10^7 \text{ M}^{-1} \text{ s}^{-1}$ | | |

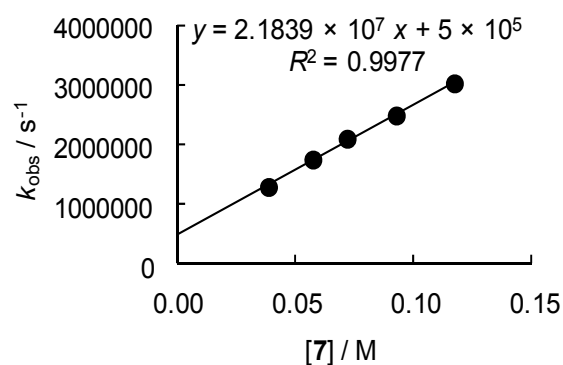


Table 4.58. Rate constants for the reactions of N,N' -dimethylformohydrazide (7) with $(\text{ani})(\text{fur})\text{CH}^+ \text{BF}_4^-$ (**16m**) generated from $(\text{ani})(\text{fur})\text{CHPPh}_3^+ \text{BF}_4^-$ (**16m-PPh₃**) in CH_3CN (laser-flash photolysis, 20 °C, $\lambda = 513$ nm).

| $[\mathbf{16m-PPh}_3]_0/\text{M}$ | $[\mathbf{7}]_0/\text{M}$ | $k_{\text{obs}}/\text{s}^{-1}$ |
|--|---------------------------|--------------------------------|
| 1.06×10^{-5} | 4.66×10^{-3} | 5.51×10^5 |
| 1.06×10^{-5} | 9.32×10^{-3} | 7.50×10^5 |
| 1.06×10^{-5} | 1.40×10^{-2} | 9.41×10^5 |
| 1.06×10^{-5} | 1.86×10^{-2} | 1.13×10^6 |
| 1.06×10^{-5} | 2.33×10^{-2} | 1.31×10^6 |
| $k_2 = 4.08 \times 10^7 \text{ M}^{-1} \text{ s}^{-1}$ | | |

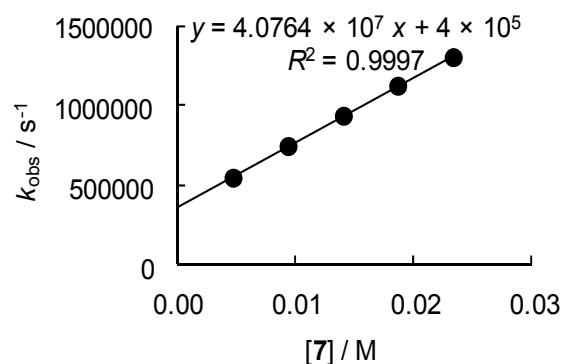


Table 4.59. Rate constants for the reactions of N',N' -dimethylformohydrazide (**7**) with $(\text{ani})\text{CH}^+ \text{BF}_4^-$ (**16n**) generated from $(\text{ani})_2\text{CHPPH}_3^+ \text{BF}_4^-$ (**16n-PPh}_3**) in CH_3CN (laser-flash photolysis, 20 °C, $\lambda = 513 \text{ nm}$).

| $[\mathbf{16n-PPh}_3]_0/\text{M}$ | $[\mathbf{7}]_0/\text{M}$ | $k_{\text{obs}}/\text{s}^{-1}$ |
|--|---------------------------|--------------------------------|
| 1.11×10^{-5} | 1.08×10^{-3} | 2.61×10^5 |
| 1.11×10^{-5} | 1.44×10^{-3} | 3.00×10^5 |
| 1.11×10^{-5} | 1.80×10^{-3} | 3.46×10^5 |
| 1.11×10^{-5} | 2.16×10^{-3} | 3.76×10^5 |
| 1.11×10^{-5} | 2.52×10^{-3} | 4.19×10^5 |
| $k_2 = 1.08 \times 10^8 \text{ M}^{-1} \text{ s}^{-1}$ | | |

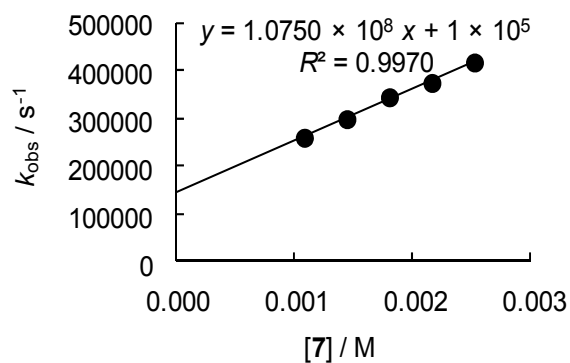
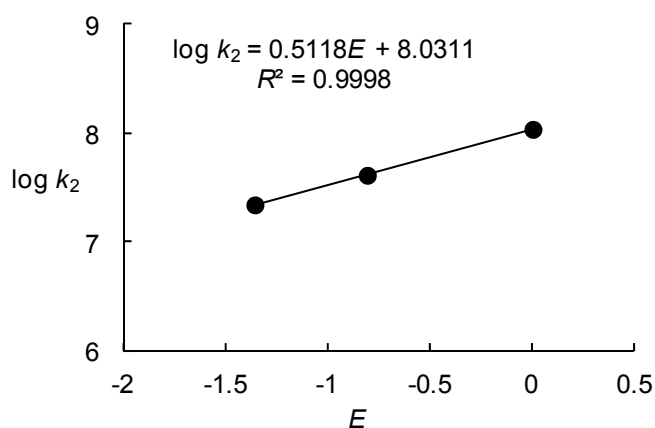


Table 4.60. Determination of the nucleophilicity parameters N and s_N for N',N' -dimethylformohydrazide (**7**) in CH_3CN .

| Electrophile (E) | $k_2/\text{M}^{-1} \text{ s}^{-1}$ | $\log k_2$ |
|-------------------------|------------------------------------|------------|
| 16l (-1.36) | 2.18×10^7 | 7.34 |
| 16m (-0.81) | 4.08×10^7 | 7.61 |
| 16n (0.00) | 1.08×10^8 | 8.03 |
| $N = 15.69, s_N = 0.51$ | | |



Kinetics of the reactions of tert-butyl hydrazinecarboxylate (8) with benzhydrylium ions (16)

Table 4.61. Rate constants for the reactions of *tert*-butyl hydrazinecarboxylate (**8**) with (dma)₂CH⁺ BF₄⁻ (**16i**) in CH₃CN (stopped-flow technique, 20 °C, λ = 605 nm).

| [16i] ₀ /M | [8] ₀ /M | [8] ₀ /[16i] ₀ | $k_{\text{obs}}/\text{s}^{-1}$ |
|--|------------------------------|--|--------------------------------|
| 1.49×10^{-5} | 1.18×10^{-3} | 79 | 2.10 |
| 1.49×10^{-5} | 1.81×10^{-3} | 121 | 2.89 |
| 1.49×10^{-5} | 2.40×10^{-3} | 161 | 3.69 |
| 1.49×10^{-5} | 2.99×10^{-3} | 200 | 4.47 |
| $k_2 = 1.31 \times 10^3 \text{ M}^{-1} \text{ s}^{-1}$ | | | |

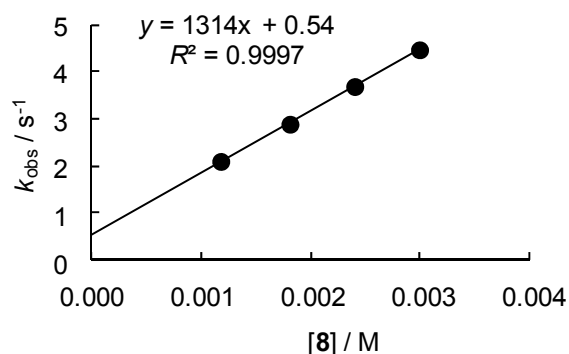


Table 4.62. Rate constants for the reactions of *tert*-butyl hydrazinecarboxylate (**8**) with (mor)₂CH⁺ BF₄⁻ (**16j**) in CH₃CN (stopped-flow technique, 20 °C, λ = 612 nm).

| [16j] ₀ /M | [8] ₀ /M | [8] ₀ /[16j] ₀ | $k_{\text{obs}}/\text{s}^{-1}$ |
|--|------------------------------|--|--------------------------------|
| 1.48×10^{-5} | 3.15×10^{-4} | 21 | 3.38 |
| 1.48×10^{-5} | 4.72×10^{-4} | 32 | 5.18 |
| 1.48×10^{-5} | 5.90×10^{-4} | 40 | 6.39 |
| 1.48×10^{-5} | 7.48×10^{-4} | 50 | 8.02 |
| 1.48×10^{-5} | 9.05×10^{-4} | 61 | 9.65 |
| $k_2 = 1.06 \times 10^4 \text{ M}^{-1} \text{ s}^{-1}$ | | | |

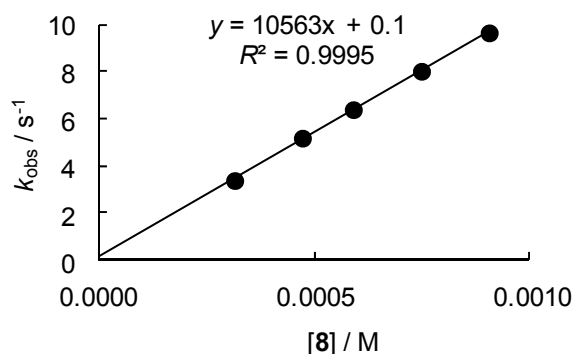


Table 4.63. Rate constants for the reactions of *tert*-butyl hydrazinecarboxylate (**8**) with (mfa)₂CH⁺ BF₄⁻ (**16k**) in CH₃CN (stopped-flow technique, 20 °C, λ = 586 nm).

| [16k] ₀ /M | [8] ₀ /M | [8] ₀ /[16k] ₀ | $k_{\text{obs}}/\text{s}^{-1}$ |
|--|------------------------------|--|--------------------------------|
| 1.50×10^{-5} | 3.15×10^{-4} | 21 | 4.35×10^1 |
| 1.50×10^{-5} | 4.72×10^{-4} | 32 | 6.60×10^1 |
| 1.50×10^{-5} | 5.90×10^{-4} | 40 | 8.17×10^1 |
| 1.50×10^{-5} | 7.48×10^{-4} | 50 | 1.04×10^2 |
| 1.50×10^{-5} | 9.05×10^{-4} | 61 | 1.24×10^2 |
| $k_2 = 1.37 \times 10^5 \text{ M}^{-1} \text{ s}^{-1}$ | | | |

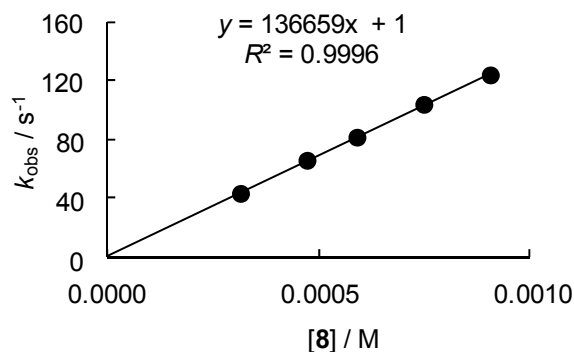


Table 4.64. Rate constants for the reactions of *tert*-butyl hydrazinecarboxylate (**8**) with (fur)₂CH⁺ BF₄⁻ (**16l**) generated from (fur)₂CHPPh₃⁺ BF₄⁻ (**16l**-PPh₃) in CH₃CN (laser-flash photolysis, 20 °C, $\lambda = 535$ nm).

| [16l -PPh ₃] ₀ /M | [8] ₀ /M | $k_{\text{obs}}/\text{s}^{-1}$ |
|--|------------------------------|--------------------------------|
| 1.05×10^{-5} | 2.14×10^{-2} | 3.64×10^5 |
| 1.05×10^{-5} | 5.33×10^{-2} | 8.38×10^5 |
| 1.05×10^{-5} | 7.36×10^{-2} | 1.11×10^6 |
| 1.05×10^{-5} | 9.18×10^{-2} | 1.37×10^6 |
| $k_2 = 1.42 \times 10^7 \text{ M}^{-1} \text{ s}^{-1}$ | | |

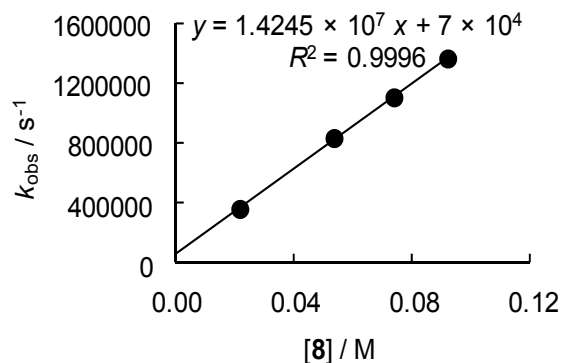


Table 4.65. Rate constants for the reactions of *tert*-butyl hydrazinecarboxylate (**8**) with (ani)₂CH⁺ BF₄⁻ (**16n**) generated from (ani)₂CHPPh₃⁺ BF₄⁻ (**16n**-PPh₃) in CH₃CN (laser-flash photolysis, 20 °C, $\lambda = 513$ nm).

| [16n -PPh ₃] ₀ /M | [8] ₀ /M | $k_{\text{obs}}/\text{s}^{-1}$ |
|--|------------------------------|--------------------------------|
| 1.11×10^{-5} | 3.09×10^{-3} | 2.61×10^5 |
| 1.11×10^{-5} | 4.64×10^{-3} | 3.74×10^5 |
| 1.11×10^{-5} | 6.18×10^{-3} | 4.87×10^5 |
| 1.11×10^{-5} | 7.73×10^{-3} | 5.90×10^5 |
| $k_2 = 7.12 \times 10^7 \text{ M}^{-1} \text{ s}^{-1}$ | | |

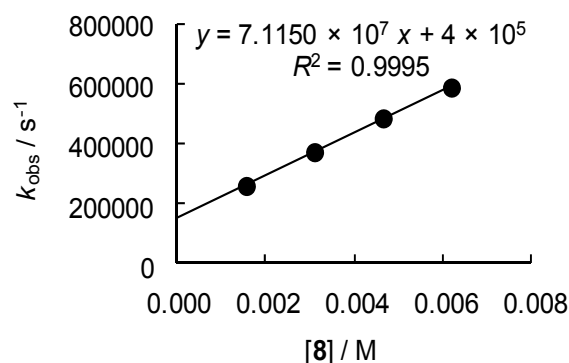
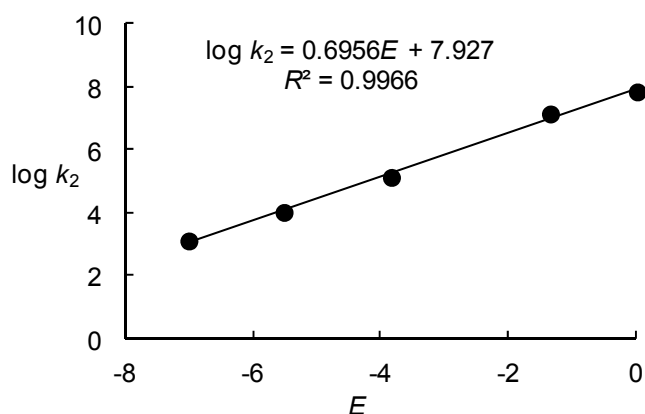


Table 4.66. Determination of the nucleophilicity parameters N and s_N for *tert*-butyl hydrazinecarboxylate (**8**) in CH₃CN.

| Electrophile (E) | $k_2/\text{M}^{-1} \text{ s}^{-1}$ | $\log k_2$ |
|-------------------------|------------------------------------|------------|
| 16i (-7.02) | 1.31×10^3 | 3.12 |
| 16j (-5.53) | 1.06×10^4 | 4.03 |
| 16k (-3.85) | 1.37×10^5 | 5.14 |
| 16l (-1.36) | 1.42×10^7 | 7.15 |
| 16n (0.00) | 7.12×10^7 | 7.85 |
| $N = 11.40, s_N = 0.70$ | | |



Kinetics of the reactions of benzohydrazide (9) with benzhydrylium ions (16)

Table 4.67. Rate constants for the reactions of benzohydrazide (9) with (dma)₂CH⁺ BF₄⁻ (16i) in CH₃CN (stopped-flow technique, 20 °C, λ = 605 nm).

| [16i] ₀ /M | [9] ₀ /M | [9] ₀ /[16i] ₀ | $k_{\text{obs}}/\text{s}^{-1}$ |
|-----------------------|-----------------------|--------------------------------------|--------------------------------|
| 1.78×10^{-5} | 1.07×10^{-3} | 60 | 8.48 |
| 1.78×10^{-5} | 1.45×10^{-3} | 81 | 1.02×10^1 |
| 1.78×10^{-5} | 1.80×10^{-3} | 101 | 1.15×10^1 |
| 1.78×10^{-5} | 2.14×10^{-3} | 121 | 1.29×10^1 |
| 1.78×10^{-5} | 2.49×10^{-3} | 140 | 1.43×10^1 |

$$k_2 = 4.06 \times 10^3 \text{ M}^{-1} \text{ s}^{-1}$$

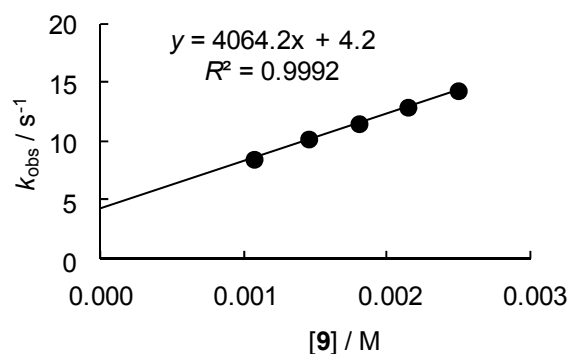


Table 4.68. Rate constants for the reactions of benzohydrazide (9) with (mor)₂CH⁺ BF₄⁻ (16j) in CH₃CN (stopped-flow technique, 20 °C, λ = 611 nm).

| [16j] ₀ /M | [9] ₀ /M | [9] ₀ /[16j] ₀ | $k_{\text{obs}}/\text{s}^{-1}$ |
|-----------------------|-----------------------|--------------------------------------|--------------------------------|
| 1.80×10^{-5} | 3.59×10^{-4} | 20 | 1.32×10^1 |
| 1.80×10^{-5} | 7.19×10^{-4} | 40 | 2.63×10^1 |
| 1.80×10^{-5} | 1.08×10^{-3} | 60 | 3.91×10^1 |
| 1.80×10^{-5} | 1.44×10^{-3} | 80 | 5.24×10^1 |
| 1.80×10^{-5} | 1.80×10^{-3} | 100 | 6.61×10^1 |

$$k_2 = 3.66 \times 10^4 \text{ M}^{-1} \text{ s}^{-1}$$

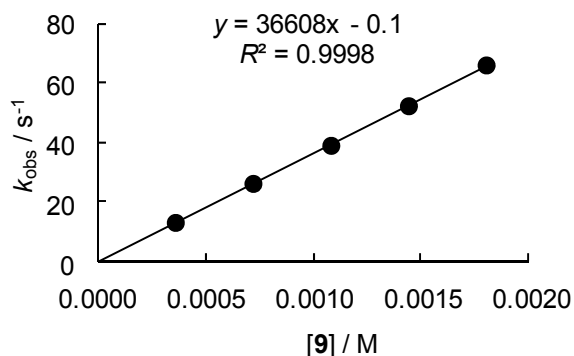


Table 4.69. Rate constants for the reactions of benzohydrazide (**9**) with $(\text{mfa})_2\text{CH}^+ \text{BF}_4^-$ (**16k**) in CH_3CN (stopped-flow technique, 20°C , $\lambda = 586 \text{ nm}$).

| $[\mathbf{16k}]_0/\text{M}$ | $[\mathbf{9}]_0/\text{M}$ | $[\mathbf{9}]_0/[\mathbf{16k}]_0$ | $k_{\text{obs}}/\text{s}^{-1}$ |
|-----------------------------|---------------------------|-----------------------------------|--------------------------------|
| 1.80×10^{-5} | 1.38×10^{-4} | 8 | 6.69×10^1 |
| 1.80×10^{-5} | 1.94×10^{-4} | 11 | 9.37×10^1 |
| 1.80×10^{-5} | 2.49×10^{-4} | 14 | 1.21×10^2 |
| 1.80×10^{-5} | 3.04×10^{-4} | 17 | 1.49×10^2 |
| 1.80×10^{-5} | 3.59×10^{-4} | 20 | 1.75×10^2 |

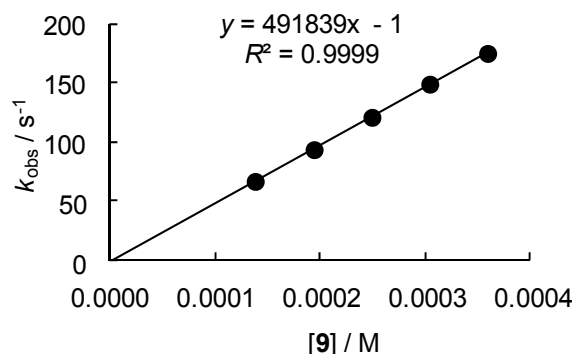
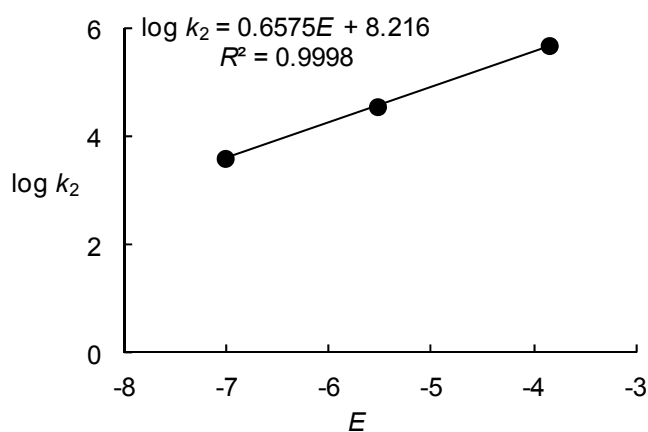
$$k_2 = 4.92 \times 10^5 \text{ M}^{-1} \text{ s}^{-1}$$


Table 4.70. Determination of the nucleophilicity parameters N and s_N for benzohydrazide (**9**) in CH_3CN .

| Electrophile (E) | $k_2/\text{M}^{-1} \text{ s}^{-1}$ | $\log k_2$ |
|----------------------|------------------------------------|------------|
| 16i (-7.02) | 4.06×10^3 | 3.61 |
| 16j (-5.53) | 3.66×10^4 | 4.56 |
| 16k (-3.85) | 4.92×10^5 | 5.69 |

$$N = 12.49, s_N = 0.66$$


Kinetics of the reactions of hydroxylamine (10) with benzhydrylium ions and quinone methides (16)

Table 4.71. Rate constants for the reactions of ani(Ph)₂QM (**16c**) with hydroxylamine (**10**) generated from hydroxylamine hydrochloride (**10**·HCl) with DBU (0.70–0.95 equiv.) in CH₃CN (diodearray spectrophotometer, 20 °C, λ = 412 nm).

| [16c] ₀ /M | [10] ₀ /M | [10] ₀ /[16c] ₀ | $k_{\text{obs}}/\text{s}^{-1}$ |
|--------------------------------|-------------------------------|---|--------------------------------|
| 5.65×10^{-5} | 3.18×10^{-3} | 56 | 5.45×10^{-3} |
| 5.69×10^{-5} | 3.71×10^{-3} | 65 | 6.64×10^{-3} |
| 5.53×10^{-5} | 4.16×10^{-3} | 75 | 7.82×10^{-3} |
| 5.69×10^{-5} | 4.64×10^{-3} | 82 | 8.83×10^{-3} |
| 5.51×10^{-5} | 5.18×10^{-3} | 94 | 1.03×10^{-2} |
| 5.56×10^{-5} | 5.74×10^{-3} | 103 | 1.13×10^{-2} |
| 5.48×10^{-5} | 6.85×10^{-3} | 125 | 1.45×10^{-2} |

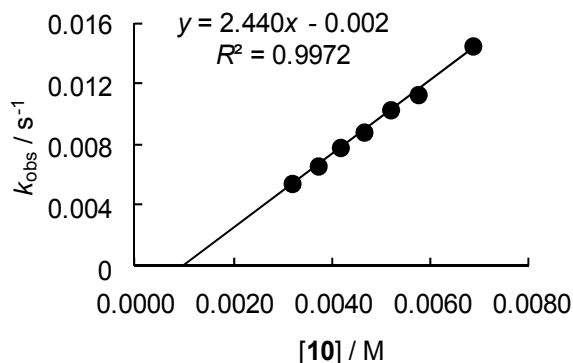
$$k_2 = 2.44 \text{ M}^{-1} \text{ s}^{-1}$$


Table 4.72. Rate constants for the reactions of (lil)₂CH⁺ BF₄⁻ (**16d**) with hydroxylamine (**10**) generated from hydroxylamine hydrochloride (**10**·HCl) with DBU (0.75 equiv.) in CH₃CN (diodearray spectrophotometer, 20 °C, λ = 631 nm).

| [16d] ₀ /M | [10] ₀ /M | [10] ₀ /[16d] ₀ | $k_{\text{obs}}/\text{s}^{-1}$ |
|--------------------------------|-------------------------------|---|--------------------------------|
| 1.58×10^{-5} | 4.84×10^{-4} | 18 | 2.13×10^{-2} |
| 1.58×10^{-5} | 8.48×10^{-4} | 54 | 3.94×10^{-2} |
| 1.57×10^{-5} | 1.50×10^{-3} | 96 | 7.64×10^{-2} |
| 1.63×10^{-5} | 1.94×10^{-3} | 119 | 1.06×10^{-1} |

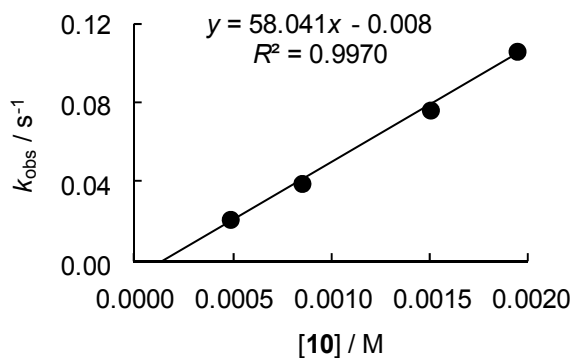
$$k_2 = 5.80 \times 10^1 \text{ M}^{-1} \text{ s}^{-1}$$


Table 4.73. Rate constants for the reactions of $(\text{ind})_2\text{CH}^+ \text{BF}_4^-$ (**16f**) with hydroxylamine (**10**) generated from hydroxylamine hydrochloride (**10**·HCl) with DBU (0.50 equiv.) in CH_3CN (stopped-flow technique, 20 °C, $\lambda = 616 \text{ nm}$).

| $[\mathbf{16f}]_0/\text{M}$ | $[\mathbf{10}]_0/\text{M}$ | $[\mathbf{10}]_0/[\mathbf{16f}]_0$ | $k_{\text{obs}}/\text{s}^{-1}$ |
|--|----------------------------|------------------------------------|--------------------------------|
| 1.70×10^{-5} | 1.33×10^{-4} | 8 | 3.27×10^{-2} |
| 1.70×10^{-5} | 2.08×10^{-4} | 12 | 5.11×10^{-2} |
| 1.70×10^{-5} | 2.67×10^{-4} | 17 | 6.98×10^{-2} |
| 1.70×10^{-5} | 3.41×10^{-4} | 20 | 9.01×10^{-2} |
| 1.70×10^{-5} | 4.15×10^{-4} | 24 | 1.18×10^{-1} |
| $k_2 = 3.01 \times 10^2 \text{ M}^{-1} \text{ s}^{-1}$ | | | |

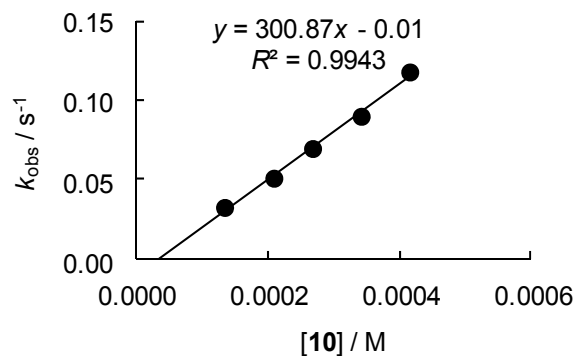


Table 4.74. Rate constants for the reactions of $(\text{dma})_2\text{CH}^+ \text{BF}_4^-$ (**16i**) with hydroxylamine (**10**) generated from hydroxylamine hydrochloride (**10**·HCl) with DBU (0.51 equiv.) in CH_3CN (stopped-flow technique, 20 °C, $\lambda = 605 \text{ nm}$).

| $[\mathbf{16i}]_0/\text{M}$ | $[\mathbf{10}]_0/\text{M}$ | $[\mathbf{10}]_0/[\mathbf{16i}]_0$ | $k_{\text{obs}}/\text{s}^{-1}$ |
|--|----------------------------|------------------------------------|--------------------------------|
| 1.70×10^{-5} | 1.67×10^{-4} | 10 | 5.72×10^{-1} |
| 1.70×10^{-5} | 2.60×10^{-4} | 15 | 9.28×10^{-1} |
| 1.70×10^{-5} | 3.52×10^{-4} | 21 | 1.29 |
| 1.70×10^{-5} | 4.26×10^{-4} | 25 | 1.60 |
| 1.70×10^{-5} | 5.19×10^{-4} | 31 | 2.12 |
| $k_2 = 4.33 \times 10^3 \text{ M}^{-1} \text{ s}^{-1}$ | | | |

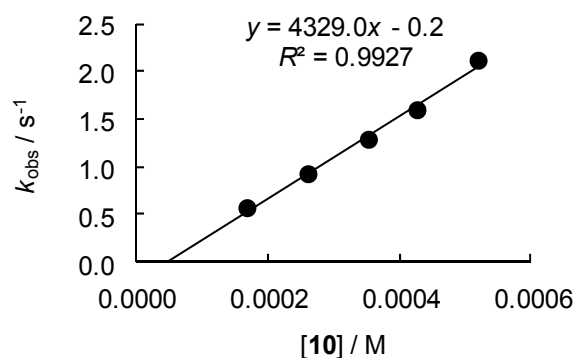
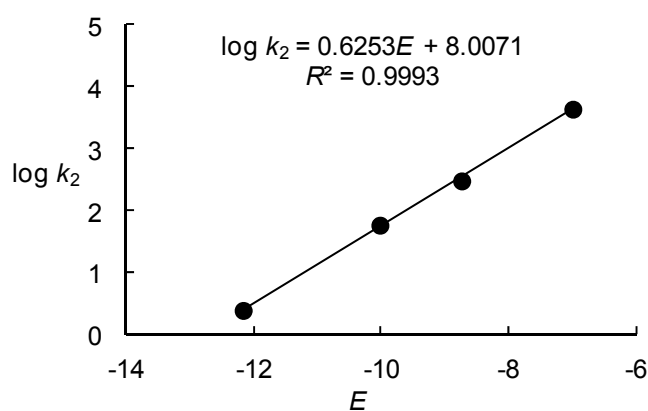


Table 4.75. Determination of the nucleophilicity parameters N and s_N for hydroxylamine (**10**) in CH_3CN .

| Electrophile (E) | $k_2/\text{M}^{-1} \text{s}^{-1}$ | $\log k_2$ |
|-------------------------|-----------------------------------|------------|
| 16c (-12.18) | 2.44 | 0.39 |
| 16h (-10.04) | 5.80×10^1 | 1.76 |
| 16f (-8.76) | 3.01×10^2 | 2.48 |
| 16i (-7.02) | 4.33×10^3 | 3.64 |
| $N = 12.80, s_N = 0.63$ | | |



Kinetics of the reactions of N-methylhydroxylamine (11) with benzhydrylium ions (16)

Table 4.76. Rate constants for the reactions of $(\text{lil})_2\text{CH}^+ \text{BF}_4^-$ (**16d**) with *N*-methylhydroxylamine (**11**) generated from *N*-methylhydroxylamine hydrochloride (**11**·HCl) with DBU (0.60 equiv.) in CH_3CN (stopped-flow technique, 20 °C, $\lambda = 631 \text{ nm}$).

| $[\mathbf{16d}]_0/\text{M}$ | $[\mathbf{11}]_0/\text{M}$ | $[\mathbf{11}]_0/[\mathbf{16d}]_0$ | $k_{\text{obs}}/\text{s}^{-1}$ |
|--|----------------------------|------------------------------------|--------------------------------|
| 7.65×10^{-6} | 2.57×10^{-4} | 34 | 5.71×10^{-1} |
| 7.65×10^{-6} | 3.59×10^{-4} | 47 | 6.79×10^{-1} |
| 7.65×10^{-6} | 4.36×10^{-4} | 57 | 7.67×10^{-1} |
| 7.65×10^{-6} | 5.65×10^{-4} | 74 | 9.07×10^{-1} |
| $k_2 = 1.09 \times 10^3 \text{ M}^{-1} \text{ s}^{-1}$ | | | |

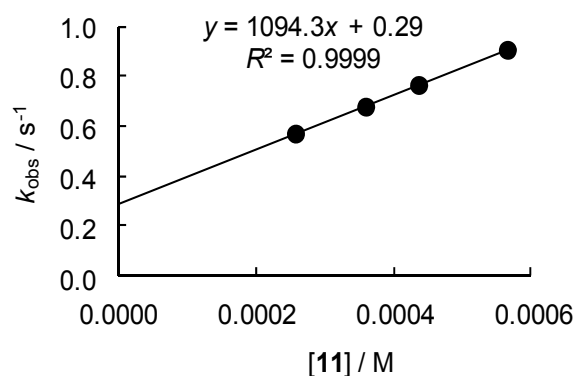


Table 4.77. Rate constants for the reactions of $(\text{ind})_2\text{CH}^+ \text{BF}_4^-$ (**16f**) with *N*-methylhydroxylamine (**10**) generated from *N*-methylhydroxylamine hydrochloride (**11**·HCl) with DBU (0.60 equiv.) in CH_3CN (stopped-flow technique, 20 °C, $\lambda = 616$ nm).

| $[\mathbf{16f}]_0/\text{M}$ | $[\mathbf{11}]_0/\text{M}$ | $[\mathbf{11}]_0/[\mathbf{16f}]_0$ | $k_{\text{obs}}/\text{s}^{-1}$ |
|--|----------------------------|------------------------------------|--------------------------------|
| 7.28×10^{-6} | 2.57×10^{-4} | 35 | 2.39 |
| 7.28×10^{-6} | 3.59×10^{-4} | 49 | 3.49 |
| 7.28×10^{-6} | 4.36×10^{-4} | 60 | 4.29 |
| 7.28×10^{-6} | 5.39×10^{-4} | 74 | 5.47 |
| $k_2 = 1.09 \times 10^4 \text{ M}^{-1} \text{ s}^{-1}$ | | | |

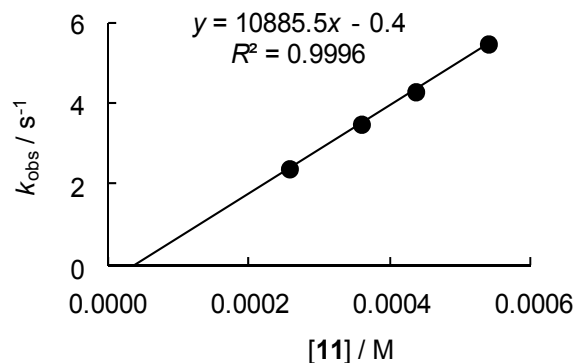


Table 4.78. Rate constants for the reactions of $(\text{pyr})_2\text{CH}^+ \text{BF}_4^-$ (**16h**) with *N*-methylhydroxylamine (**11**) generated from *N*-methylhydroxylamine hydrochloride (**11**·HCl) with DBU (0.75 equiv.) in CH_3CN (stopped-flow technique, 20 °C, $\lambda = 611$ nm).

| $[\mathbf{16h}]_0/\text{M}$ | $[\mathbf{11}]_0/\text{M}$ | $[\mathbf{11}]_0/[\mathbf{16h}]_0$ | $k_{\text{obs}}/\text{s}^{-1}$ |
|--|----------------------------|------------------------------------|--------------------------------|
| 7.11×10^{-6} | 2.01×10^{-4} | 28 | 1.40×10^1 |
| 7.11×10^{-6} | 3.35×10^{-4} | 47 | 2.58×10^1 |
| 7.11×10^{-6} | 4.36×10^{-4} | 61 | 3.53×10^1 |
| 7.11×10^{-6} | 5.37×10^{-4} | 76 | 4.49×10^1 |
| $k_2 = 9.20 \times 10^4 \text{ M}^{-1} \text{ s}^{-1}$ | | | |

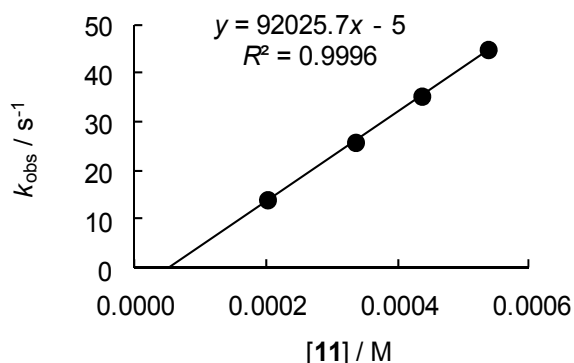


Table 4.79. Rate constants for the reactions of $(\text{dma})_2\text{CH}^+ \text{BF}_4^-$ (**16i**) with *N*-methylhydroxylamine (**11**) generated from *N*-methylhydroxylamine hydrochloride (**11**·HCl) with DBU (0.75 equiv.) in CH_3CN (stopped-flow technique, 20 °C, $\lambda = 605$ nm).

| $[\mathbf{16i}]_0/\text{M}$ | $[\mathbf{11}]_0/\text{M}$ | $[\mathbf{11}]_0/[\mathbf{16i}]_0$ | $k_{\text{obs}}/\text{s}^{-1}$ |
|--|----------------------------|------------------------------------|--------------------------------|
| 7.41×10^{-6} | 2.01×10^{-4} | 27 | 2.92×10^1 |
| 7.41×10^{-6} | 3.35×10^{-4} | 45 | 5.33×10^1 |
| 7.41×10^{-6} | 4.36×10^{-4} | 59 | 7.15×10^1 |
| 7.41×10^{-6} | 5.37×10^{-4} | 72 | 8.88×10^1 |
| $k_2 = 1.78 \times 10^5 \text{ M}^{-1} \text{ s}^{-1}$ | | | |

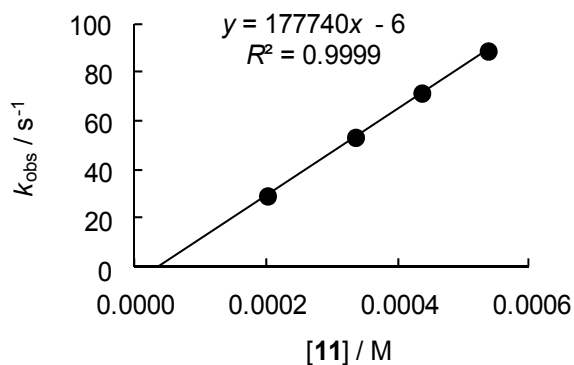
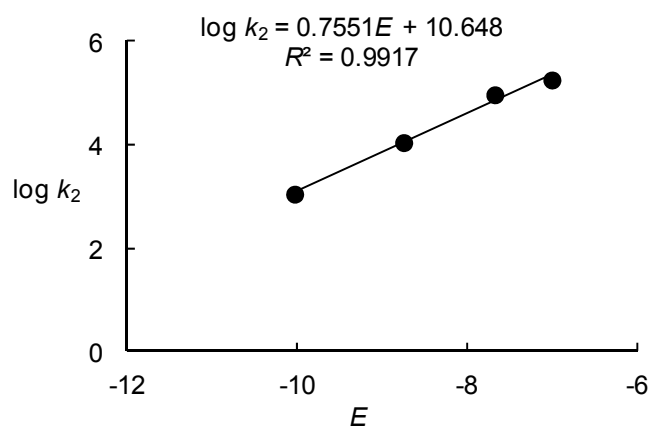


Table 4.80. Determination of the nucleophilicity parameters N and s_N for N -methylhydroxylamine (**11**) in CH_3CN .

| Electrophile (E) | $k_2/\text{M}^{-1} \text{s}^{-1}$ | $\log k_2$ |
|-------------------------|-----------------------------------|------------|
| 16d (-10.04) | 1.09×10^3 | 3.04 |
| 16f (-8.76) | 1.09×10^4 | 4.04 |
| 16h (-7.69) | 9.20×10^4 | 4.96 |
| 16i (-7.02) | 1.78×10^5 | 5.25 |
| $N = 14.10, s_N = 0.76$ | | |



Kinetics of the reactions of ammonia (12) with benzhydrylium ions and quinone methides (16)

Table 4.81. Rate constants for the reactions of ammonia (**12**) with ani(Ph)₂QM (**16c**) in CH_3CN (diodearray spectrophotometer, 20 °C, $\lambda = 412 \text{ nm}$).

| [16c] ₀ /M | [12] ₀ /M | [12] ₀ /[16c] ₀ | $k_{\text{obs}}/\text{s}^{-1}$ |
|---|-------------------------------|---|--------------------------------|
| 9.46×10^{-5} | 6.35×10^{-3} | 67 | 1.49×10^{-3} |
| 9.91×10^{-5} | 8.87×10^{-3} | 90 | 2.22×10^{-3} |
| 9.69×10^{-5} | 1.30×10^{-2} | 134 | 3.40×10^{-3} |
| 9.57×10^{-5} | 1.71×10^{-2} | 179 | 4.53×10^{-3} |
| 9.67×10^{-5} | 2.16×10^{-2} | 224 | 5.89×10^{-3} |
| $k_2 = 2.88 \times 10^{-1} \text{ M}^{-1} \text{ s}^{-1}$ | | | |

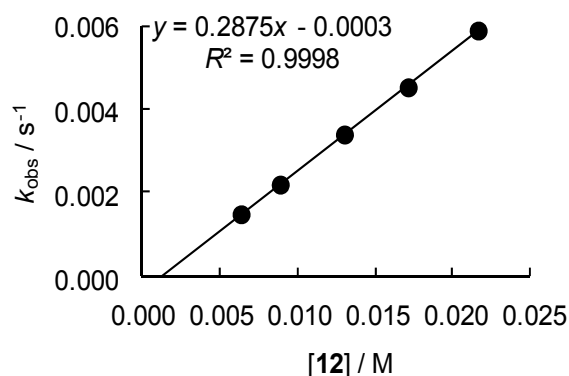


Table 4.82. Rate constants for the reactions of ammonia (**12**) with (ind)₂CH⁺ BF₄⁻ (**16f**) in CH₃CN (stopped-flow technique, 20 °C, λ = 616 nm).

| [16f] ₀ /M | [12] ₀ /M | [12] ₀ /[16f] ₀ | $k_{\text{obs}}/\text{s}^{-1}$ |
|--|-------------------------------|---|--------------------------------|
| 1.81×10^{-5} | 1.03×10^{-3} | 57 | 6.72×10^{-2} |
| 1.81×10^{-5} | 2.06×10^{-3} | 114 | 1.11×10^{-1} |
| 1.81×10^{-5} | 3.09×10^{-3} | 171 | 1.66×10^{-1} |
| 1.81×10^{-5} | 4.12×10^{-3} | 227 | 2.04×10^{-1} |
| 1.81×10^{-5} | 5.15×10^{-3} | 284 | 2.66×10^{-1} |
| $k_2 = 4.76 \times 10^1 \text{ M}^{-1} \text{ s}^{-1}$ | | | |

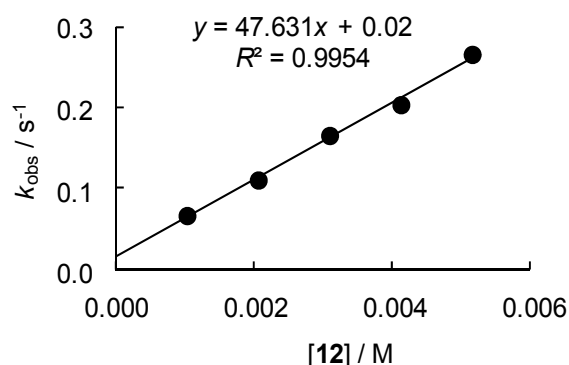


Table 4.83. Rate constants for the reactions of ammonia (**12**) with (pyr)₂CH⁺ BF₄⁻ (**16h**) in CH₃CN (stopped-flow technique, 20 °C, λ = 611 nm).

| [16h] ₀ /M | [12] ₀ /M | [12] ₀ /[16h] ₀ | $k_{\text{obs}}/\text{s}^{-1}$ |
|--|-------------------------------|---|--------------------------------|
| 1.80×10^{-5} | 1.03×10^{-3} | 57 | 5.05×10^{-1} |
| 1.80×10^{-5} | 2.06×10^{-3} | 115 | 9.30×10^{-1} |
| 1.80×10^{-5} | 3.09×10^{-3} | 172 | 1.42 |
| 1.80×10^{-5} | 4.12×10^{-3} | 227 | 1.90 |
| $k_2 = 4.54 \times 10^2 \text{ M}^{-1} \text{ s}^{-1}$ | | | |

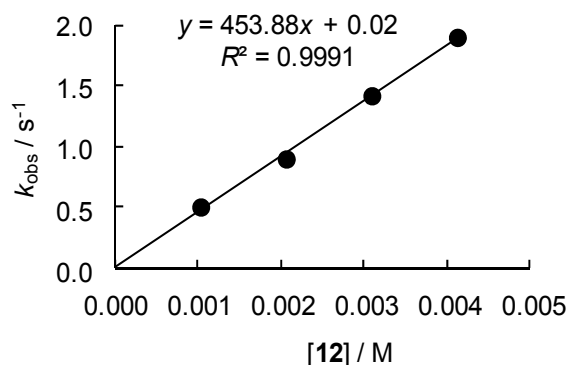


Table 4.84. Rate constants for the reactions of ammonia (**12**) with (dma)₂CH⁺ BF₄⁻ (**16i**) in CH₃CN (stopped-flow technique, 20 °C, λ = 605 nm).

| [16i] ₀ /M | [12] ₀ /M | [12] ₀ /[16i] ₀ | $k_{\text{obs}}/\text{s}^{-1}$ |
|--|-------------------------------|---|--------------------------------|
| 1.48×10^{-5} | 1.03×10^{-3} | 70 | 2.03 |
| 1.48×10^{-5} | 2.06×10^{-3} | 139 | 3.61 |
| 1.48×10^{-5} | 3.09×10^{-3} | 209 | 5.03 |
| 1.48×10^{-5} | 4.12×10^{-3} | 278 | 6.69 |
| 1.48×10^{-5} | 5.15×10^{-3} | 348 | 8.35 |
| $k_2 = 1.53 \times 10^3 \text{ M}^{-1} \text{ s}^{-1}$ | | | |

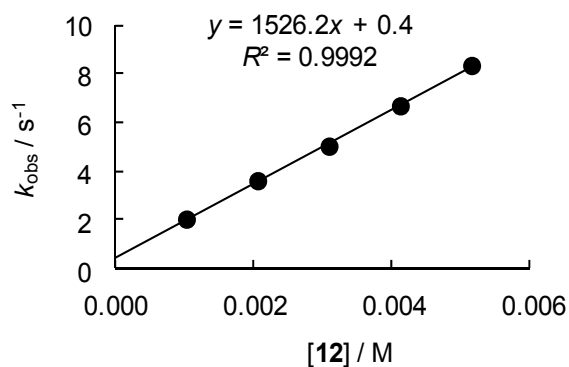


Table 4.85. Rate constants for the reactions of ammonia (**12**) with (mor)₂CH⁺ BF₄⁻ (**16j**) in CH₃CN (stopped-flow technique, 20 °C, $\lambda = 611$ nm).

| [16j] ₀ /M | [12] ₀ /M | [12] ₀ /[16j] ₀ | $k_{\text{obs}}/\text{s}^{-1}$ |
|--|-------------------------------|---|--------------------------------|
| 1.82×10^{-5} | 1.03×10^{-3} | 57 | 1.09×10^1 |
| 1.82×10^{-5} | 3.09×10^{-3} | 170 | 2.90×10^1 |
| 1.82×10^{-5} | 4.12×10^{-3} | 227 | 3.98×10^1 |
| 1.82×10^{-5} | 5.15×10^{-3} | 284 | 4.77×10^1 |
| $k_2 = 9.05 \times 10^3 \text{ M}^{-1} \text{ s}^{-1}$ | | | |

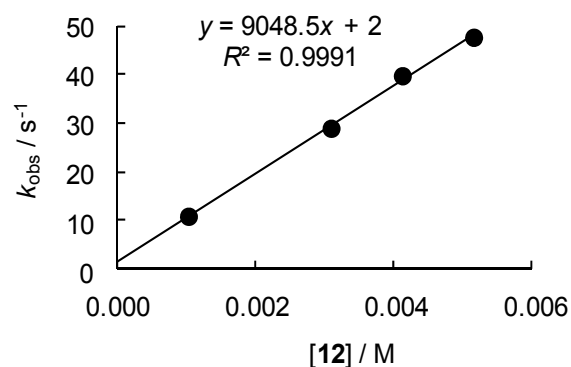
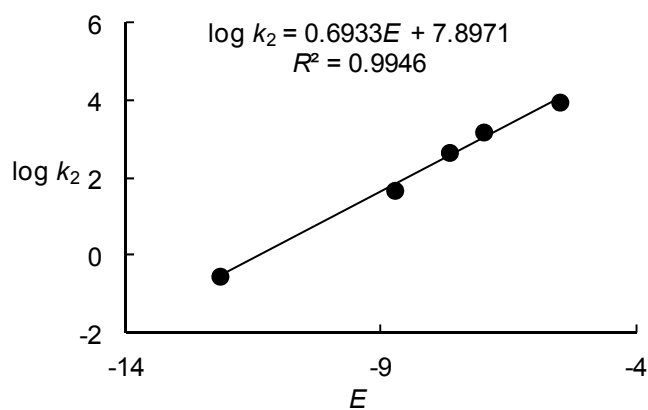


Table 4.86. Determination of the nucleophilicity parameters N and s_N for ammonia (**12**) in CH₃CN.

| Electrophile (E) | $k_2/\text{M}^{-1} \text{ s}^{-1}$ | $\log k_2$ |
|-------------------------|------------------------------------|------------|
| 16c (-12.18) | 2.88×10^{-1} | -0.54 |
| 16f (-8.76) | 4.76×10^1 | 1.68 |
| 16h (-7.69) | 4.54×10^2 | 2.66 |
| 16i (-7.02) | 1.53×10^3 | 3.18 |
| 16g (-5.53) | 9.05×10^3 | 3.96 |
| $N = 11.39, s_N = 0.69$ | | |



Kinetics of the reactions of methylamine (13) with benzhydrylium ions and quinone methides (16)

Table 4.87. Rate constants for the reactions of ani(Ph)₂QM (**16c**) with methylamine (**13**) generated from methylamine hydrochloride (**13**·HCl) with DBU (0.78 equiv.) in CH₃CN (stopped-flow technique, 20 °C, λ = 412 nm).

| [16c] ₀ /M | [13] ₀ /M | [13] ₀ /[16c] ₀ | $k_{\text{obs}}/\text{s}^{-1}$ |
|--|-------------------------------|---|--------------------------------|
| 6.75×10^{-5} | 5.20×10^{-4} | 8 | 7.46×10^{-2} |
| 6.75×10^{-5} | 1.04×10^{-3} | 90 | 1.49×10^{-1} |
| 6.75×10^{-5} | 1.56×10^{-3} | 134 | 2.22×10^{-1} |
| 6.75×10^{-5} | 2.08×10^{-3} | 179 | 2.87×10^{-1} |
| 6.75×10^{-5} | 2.60×10^{-3} | 224 | 3.62×10^{-1} |
| $k_2 = 1.37 \times 10^2 \text{ M}^{-1} \text{ s}^{-1}$ | | | |

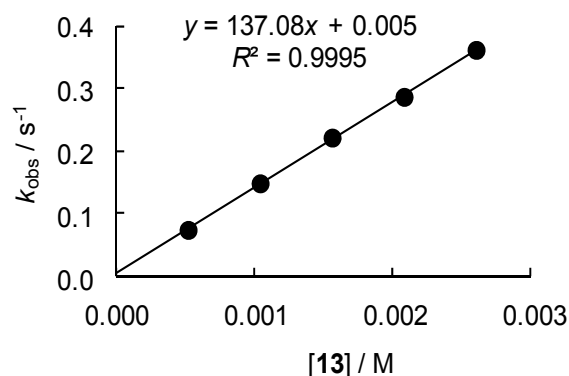


Table 4.88. Rate constants for the reactions of (lil)₂CH⁺ BF₄⁻ (**16d**) with methylamine (**13**) generated from methylamine hydrochloride (**13**·HCl) with DBU (0.78 equiv.) in CH₃CN (stopped-flow technique, 20 °C, λ = 631 nm).

| [16d] ₀ /M | [13] ₀ /M | [13] ₀ /[16d] ₀ | $k_{\text{obs}}/\text{s}^{-1}$ |
|--|-------------------------------|---|--------------------------------|
| 1.73×10^{-5} | 5.20×10^{-4} | 30 | 1.41 |
| 1.73×10^{-5} | 1.04×10^{-3} | 60 | 2.79 |
| 1.73×10^{-5} | 1.56×10^{-3} | 90 | 4.17 |
| 1.73×10^{-5} | 2.08×10^{-3} | 120 | 5.45 |
| 1.73×10^{-5} | 2.60×10^{-3} | 150 | 6.98 |
| $k_2 = 2.65 \times 10^3 \text{ M}^{-1} \text{ s}^{-1}$ | | | |

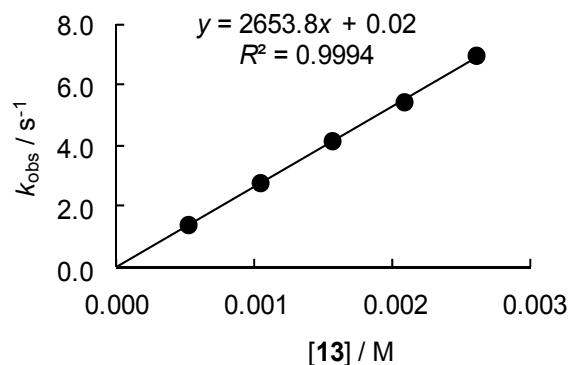


Table 4.89. Rate constants for the reactions of (ind)₂CH⁺ BF₄⁻ (**16f**) with methylamine (**13**) generated from methylamine hydrochloride (**13**·HCl) with DBU (0.50 equiv.) in CH₃CN (stopped-flow technique, 20 °C, λ = 616 nm).

| [16f] ₀ /M | [13] ₀ /M | [13] ₀ /[16f] ₀ | $k_{\text{obs}}/\text{s}^{-1}$ |
|--|-------------------------------|---|--------------------------------|
| 1.81×10^{-5} | 1.94×10^{-4} | 11 | 3.56 |
| 1.81×10^{-5} | 3.88×10^{-4} | 21 | 7.40 |
| 1.81×10^{-5} | 5.82×10^{-4} | 32 | 1.14×10^1 |
| 1.81×10^{-5} | 7.54×10^{-4} | 42 | 1.50×10^1 |
| 1.81×10^{-5} | 9.70×10^{-4} | 54 | 1.92×10^1 |
| $k_2 = 2.03 \times 10^4 \text{ M}^{-1} \text{ s}^{-1}$ | | | |

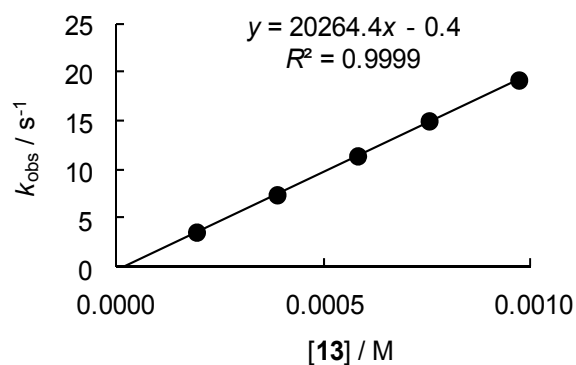


Table 4.90. Rate constants for the reactions of (pyr)₂CH⁺ BF₄⁻ (**16h**) with methylamine (**13**) generated from methylamine hydrochloride (**13**·HCl) with DBU (0.50 equiv.) in CH₃CN (stopped-flow technique, 20 °C, λ = 611 nm).

| [16h] ₀ /M | [13] ₀ /M | [13] ₀ /[16h] ₀ | $k_{\text{obs}}/\text{s}^{-1}$ |
|--|-------------------------------|---|--------------------------------|
| 1.80×10^{-5} | 1.94×10^{-4} | 11 | 2.64×10^1 |
| 1.80×10^{-5} | 3.88×10^{-4} | 22 | 5.43×10^1 |
| 1.80×10^{-5} | 5.82×10^{-4} | 32 | 9.05×10^1 |
| 1.80×10^{-5} | 7.54×10^{-4} | 42 | 1.20×10^2 |
| 1.80×10^{-5} | 9.70×10^{-4} | 54 | 1.55×10^2 |
| $k_2 = 1.68 \times 10^5 \text{ M}^{-1} \text{ s}^{-1}$ | | | |

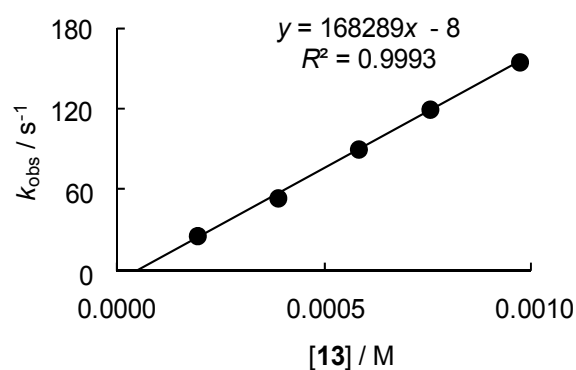


Table 4.91. Rate constants for the reactions of $(\text{pyr})_2\text{CH}^+ \text{BF}_4^-$ (**16h**) with methylamine (**13**) generated from methylamine hydrochloride (**13**·HCl) with KO t Bu (0.75 equiv.) in CH₃CN (stopped-flow technique, 20 °C, λ = 611 nm).

| [16h] ₀ /M | [13] ₀ /M | [13] ₀ /[16h] ₀ | $k_{\text{obs}}/\text{s}^{-1}$ |
|--|-------------------------------|---|--------------------------------|
| 1.80×10^{-5} | 2.36×10^{-4} | 13 | 2.97×10^1 |
| 1.80×10^{-5} | 3.15×10^{-4} | 18 | 4.35×10^1 |
| 1.80×10^{-5} | 3.93×10^{-4} | 22 | 5.57×10^1 |
| 1.80×10^{-5} | 4.46×10^{-4} | 25 | 6.61×10^1 |
| $k_2 = 1.71 \times 10^5 \text{ M}^{-1} \text{ s}^{-1}$ | | | |

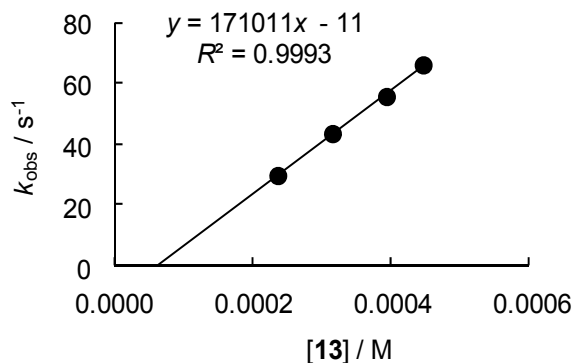


Table 4.92. Rate constants for the reactions of $(\text{dma})_2\text{CH}^+ \text{BF}_4^-$ (**16i**) with methylamine (**13**) generated from methylamine hydrochloride (**13**·HCl) with KO t Bu (0.75 equiv.) in CH₃CN (stopped-flow technique, 20 °C, λ = 605 nm).

| [16i] ₀ /M | [13] ₀ /M | [13] ₀ /[16i] ₀ | $k_{\text{obs}}/\text{s}^{-1}$ |
|--|-------------------------------|---|--------------------------------|
| 2.03×10^{-5} | 2.36×10^{-4} | 12 | 6.57×10^1 |
| 2.03×10^{-5} | 3.15×10^{-4} | 16 | 9.87×10^1 |
| 2.03×10^{-5} | 3.93×10^{-4} | 19 | 1.29×10^2 |
| 2.03×10^{-5} | 4.46×10^{-4} | 22 | 1.50×10^2 |
| $k_2 = 4.00 \times 10^5 \text{ M}^{-1} \text{ s}^{-1}$ | | | |

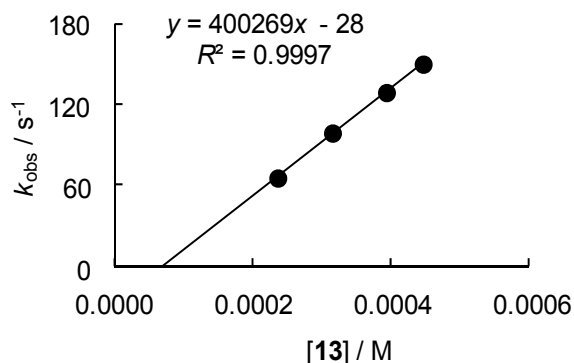
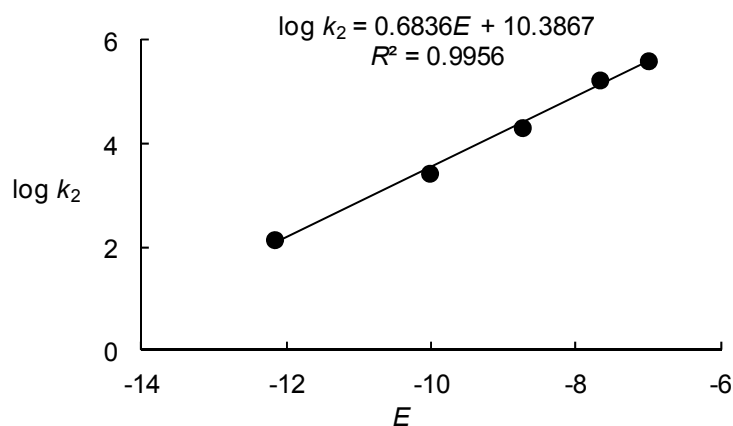


Table 4.93. Determination of the nucleophilicity parameters N and s_N for methylamine (**13**) in CH_3CN .

| Electrophile (E) | $k_2/\text{M}^{-1} \text{s}^{-1}$ | $\log k_2$ |
|----------------------|-----------------------------------|------------|
| 16c (-12.18) | 1.37×10^2 | 2.14 |
| 16e (-10.04) | 2.65×10^3 | 3.42 |
| 16f (-8.76) | 2.03×10^4 | 4.31 |
| 16h (-7.69) | 1.70×10^5 [a] | 5.23 |
| 16i (-7.02) | 4.00×10^5 | 5.60 |

$N = 15.19, s_N = 0.68$



[a] Average of the independently determined second-order rate constants obtained from reactions of **16h** with **13** generated from methylamine hydrochloride (**13**·HCl) with KO t Bu or DBU.

Kinetics of the reactions of dimethylamine (14) with benzhydrylium ions and quinone methides (16)

Table 4.94. Rate constants for the reactions of ani(t Bu) $_2$ QM (**16a**) with dimethylamine (**14**) generated from dimethylamine hydrochloride (**14**·HCl) with DBU (0.50 equiv.) in CH_3CN (diodearray spectrophotometer, 20 °C, $\lambda = 383 \text{ nm}$).

| $[\mathbf{16a}]_0/\text{M}$ | $[\mathbf{14}]_0/\text{M}$ | $[\mathbf{14}]_0/[\mathbf{16a}]_0$ | $k_{\text{obs}}/\text{s}^{-1}$ |
|-----------------------------|----------------------------|------------------------------------|--------------------------------|
| 6.21×10^{-5} | 7.12×10^{-4} | 11 | 8.57×10^{-3} |
| 6.22×10^{-5} | 1.43×10^{-3} | 23 | 1.84×10^{-2} |
| 6.10×10^{-5} | 2.10×10^{-3} | 34 | 2.89×10^{-2} |
| 6.05×10^{-5} | 2.78×10^{-3} | 46 | 3.98×10^{-2} |
| 5.98×10^{-5} | 3.43×10^{-3} | 57 | 4.88×10^{-2} |

$k_2 = 1.50 \times 10^1 \text{ M}^{-1} \text{ s}^{-1}$

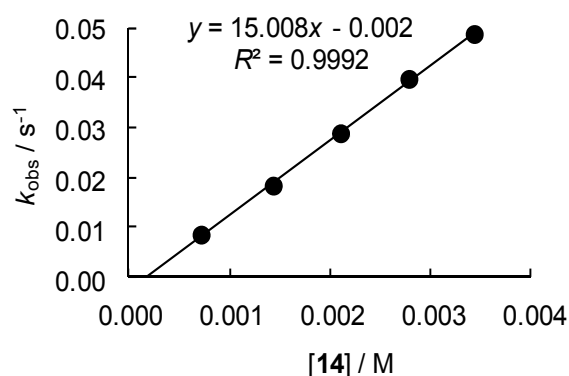


Table 4.95. Rate constants for the reactions of $\text{ani(Ph)}_2\text{QM}$ (**16c**) with dimethylamine (**14**) generated from dimethylamine hydrochloride (**14**·HCl) with DBU (0.75 equiv.) in CH_3CN (stopped-flow technique, 20 °C, $\lambda = 412$ nm).

| $[\mathbf{16c}]_0/\text{M}$ | $[\mathbf{14}]_0/\text{M}$ | $[\mathbf{14}]_0/[\mathbf{16c}]_0$ | $k_{\text{obs}}/\text{s}^{-1}$ |
|--|----------------------------|------------------------------------|--------------------------------|
| 6.75×10^{-5} | 7.10×10^{-4} | 11 | 2.67 |
| 6.75×10^{-5} | 1.18×10^{-3} | 17 | 5.00 |
| 6.75×10^{-5} | 1.66×10^{-3} | 25 | 6.76 |
| 6.75×10^{-5} | 2.13×10^{-3} | 32 | 9.34 |
| 6.75×10^{-5} | 2.37×10^{-3} | 35 | 1.04×10^1 |
| $k_2 = 4.63 \times 10^3 \text{ M}^{-1} \text{ s}^{-1}$ | | | |

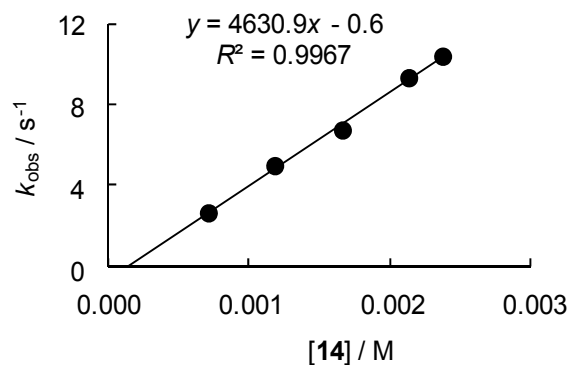


Table 4.96. Rate constants for the reactions of $(\text{lil})_2\text{CH}^+ \text{BF}_4^-$ (**16d**) with dimethylamine (**14**) generated from dimethylamine hydrochloride (**14**·HCl) with $\text{KO}t\text{Bu}$ (0.50 equiv.) in CH_3CN (stopped-flow technique, 20 °C, $\lambda = 632$ nm).

| $[\mathbf{16d}]_0/\text{M}$ | $[\mathbf{14}]_0/\text{M}$ | $[\mathbf{14}]_0/[\mathbf{16d}]_0$ | $k_{\text{obs}}/\text{s}^{-1}$ |
|--|----------------------------|------------------------------------|--------------------------------|
| 1.82×10^{-5} | 3.68×10^{-4} | 20 | 2.94×10^1 |
| 1.82×10^{-5} | 5.52×10^{-4} | 30 | 4.59×10^1 |
| 1.82×10^{-5} | 7.36×10^{-4} | 40 | 6.36×10^1 |
| 1.82×10^{-5} | 9.21×10^{-4} | 51 | 8.35×10^1 |
| $k_2 = 9.77 \times 10^4 \text{ M}^{-1} \text{ s}^{-1}$ | | | |

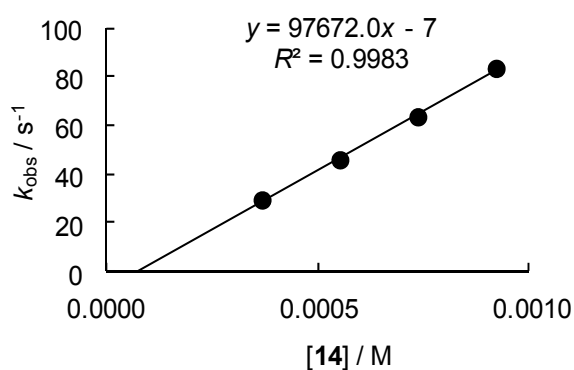


Table 4.97. Rate constants for the reactions of $(\text{jul})_2\text{CH}^+ \text{BF}_4^-$ (**16e**) with dimethylamine (**14**) generated from dimethylamine hydrochloride (**14**·HCl) with DBU (0.50 equiv.) in CH_3CN (stopped-flow technique, 20 °C, $\lambda = 635 \text{ nm}$).

| $[\mathbf{16e}]_0/\text{M}$ | $[\mathbf{14}]_0/\text{M}$ | $[\mathbf{14}]_0/[\mathbf{16e}]_0$ | $k_{\text{obs}}/\text{s}^{-1}$ |
|--|----------------------------|------------------------------------|--------------------------------|
| 1.79×10^{-5} | 1.72×10^{-4} | 10 | 3.59×10^1 |
| 1.79×10^{-5} | 2.73×10^{-4} | 15 | 6.18×10^1 |
| 1.79×10^{-5} | 3.59×10^{-4} | 20 | 8.47×10^1 |
| 1.79×10^{-5} | 4.45×10^{-4} | 25 | 1.10×10^2 |
| 1.79×10^{-5} | 5.32×10^{-4} | 30 | 1.30×10^2 |
| $k_2 = 2.65 \times 10^5 \text{ M}^{-1} \text{ s}^{-1}$ | | | |

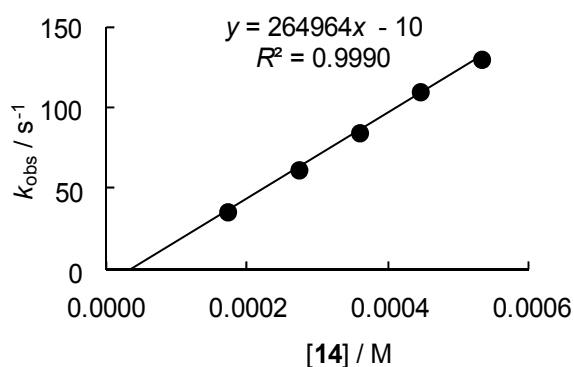
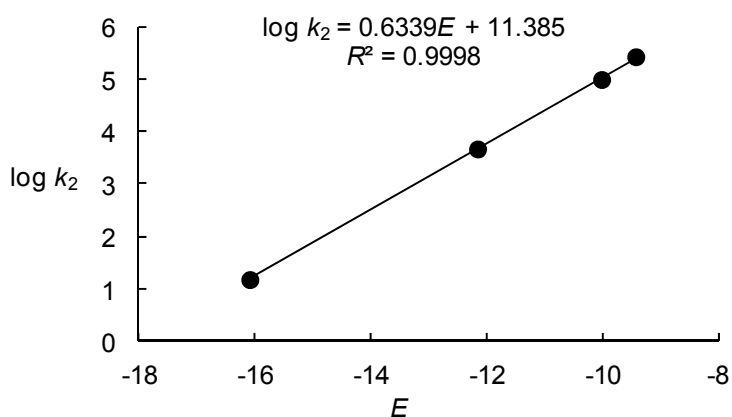


Table 4.98. Determination of the nucleophilicity parameters N and s_N for dimethylamine (**14**) in CH_3CN .

| Electrophile (E) | $k_2/\text{M}^{-1} \text{ s}^{-1}$ | $\log k_2$ |
|-------------------------|------------------------------------|------------|
| 16a (-16.11) | 1.50×10^1 | 1.18 |
| 16c (-12.18) | 4.63×10^3 | 3.67 |
| 16d (-10.04) | 9.77×10^4 | 4.99 |
| 16e (-9.45) | 2.65×10^5 | 5.42 |
| $N = 17.96, s_N = 0.63$ | | |



Kinetics of the reactions of trimethylamine (15) with benzhydrylium ions (16)

Table 4.99. Rate constants for the reactions of trimethylamine (**15**) with (pyr)₂CH⁺ BF₄⁻ (**16h**) generated from (pyr)₂CHP Bu₃⁺ BF₄⁻ (**16h-PBu₃**) in CH₃CN (laser-flash photolysis, 20 °C, λ = 611 nm).

| [16h-PBu₃] ₀ /M | [15] ₀ /M | $k_{\text{obs}}/\text{s}^{-1}$ |
|--|-------------------------------|--------------------------------|
| 1.01×10^{-5} | 1.58×10^{-3} | 1.18×10^5 |
| 1.01×10^{-5} | 3.16×10^{-3} | 1.18×10^5 |
| 1.01×10^{-5} | 4.74×10^{-3} | 1.34×10^5 |
| 1.01×10^{-5} | 6.32×10^{-3} | 1.44×10^5 |
| 1.01×10^{-5} | 7.90×10^{-3} | 1.57×10^5 |
| 1.01×10^{-5} | 9.48×10^{-3} | 1.66×10^5 |
| 1.01×10^{-5} | 1.11×10^{-2} | 1.75×10^5 |
| $k_2 = 6.54 \times 10^6 \text{ M}^{-1} \text{ s}^{-1}$ | | |

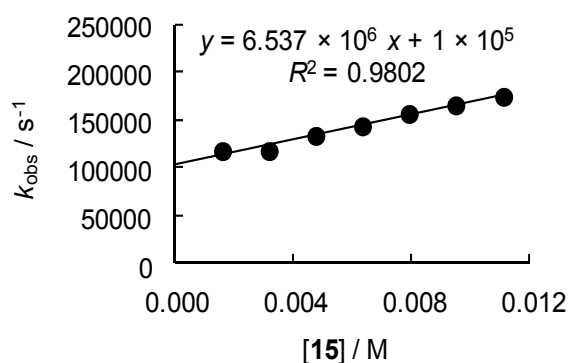


Table 4.100. Rate constants for the reactions of trimethylamine (**15**) with (dma)₂CH⁺ BF₄⁻ (**16i**) generated from (dma)₂CHP Bu₃⁺ BF₄⁻ (**16i-PBu₃**) in CH₃CN (laser-flash photolysis, 20 °C, λ = 605 nm).

| [16i-PPh₃] ₀ /M | [15] ₀ /M | $k_{\text{obs}}/\text{s}^{-1}$ |
|--|-------------------------------|--------------------------------|
| 6.70×10^{-6} | 7.90×10^{-4} | 4.21×10^4 |
| 6.70×10^{-6} | 1.58×10^{-3} | 5.80×10^4 |
| 6.70×10^{-6} | 3.16×10^{-3} | 9.72×10^4 |
| 6.70×10^{-6} | 6.32×10^{-3} | 1.80×10^5 |
| 6.70×10^{-6} | 9.48×10^{-3} | 2.11×10^5 |
| 6.70×10^{-6} | 1.26×10^{-2} | 2.80×10^5 |
| 6.70×10^{-6} | 1.58×10^{-2} | 3.49×10^5 |
| $k_2 = 2.00 \times 10^7 \text{ M}^{-1} \text{ s}^{-1}$ | | |

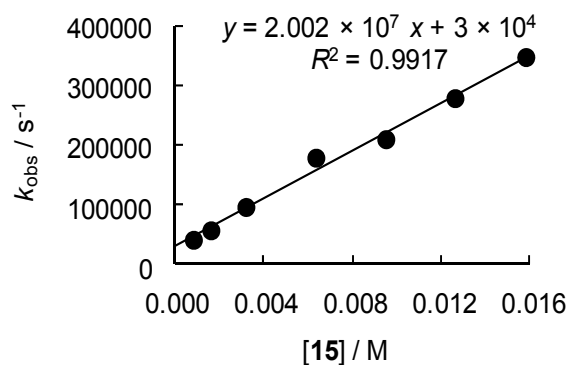


Table 4.101. Rate constants for the reactions of trimethylamine (**15**) with $(\text{mor})_2\text{CH}^+ \text{BF}_4^-$ (**16j**) generated from $(\text{mor})_2\text{CHPBu}_3^+ \text{BF}_4^-$ (**16j-PBu₃**) in CH_3CN (laser-flash photolysis, 20 °C, $\lambda = 611 \text{ nm}$).

| $[\mathbf{16j-PPh}_3]_0/\text{M}$ | $[\mathbf{15}]_0/\text{M}$ | $k_{\text{obs}}/\text{s}^{-1}$ |
|--|----------------------------|--------------------------------|
| 9.99×10^{-6} | 3.16×10^{-4} | 2.55×10^5 |
| 9.99×10^{-6} | 6.32×10^{-3} | 5.03×10^5 |
| 9.99×10^{-6} | 9.48×10^{-3} | 7.21×10^5 |
| 9.99×10^{-6} | 1.26×10^{-2} | 9.88×10^5 |
| 9.99×10^{-6} | 1.58×10^{-2} | 1.16×10^6 |
| $k_2 = 7.27 \times 10^7 \text{ M}^{-1} \text{ s}^{-1}$ | | |

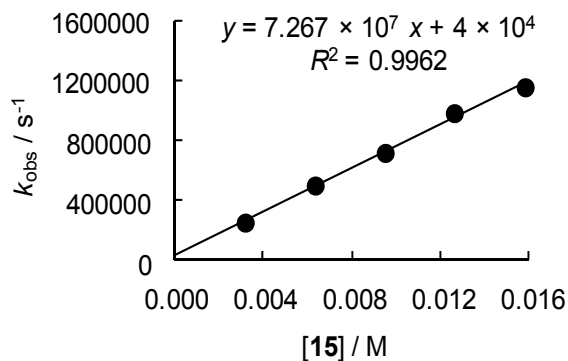


Table 4.102. Rate constants for the reactions of trimethylamine (**15**) with $(\text{mfa})_2\text{CH}^+ \text{BF}_4^-$ (**16k**) generated from $(\text{mfa})_2\text{CHPBu}_3^+ \text{BF}_4^-$ (**16k-PBu₃**) in CH_3CN (laser-flash photolysis, 20 °C, $\lambda = 586 \text{ nm}$).

| $[\mathbf{16k-PPh}_3]_0/\text{M}$ | $[\mathbf{15}]_0/\text{M}$ | $k_{\text{obs}}/\text{s}^{-1}$ |
|--|----------------------------|--------------------------------|
| 7.86×10^{-6} | 1.58×10^{-3} | 8.08×10^5 |
| 7.86×10^{-6} | 3.16×10^{-3} | 1.50×10^6 |
| 7.86×10^{-6} | 4.74×10^{-3} | 2.12×10^6 |
| 7.86×10^{-6} | 6.32×10^{-3} | 2.94×10^6 |
| 7.86×10^{-6} | 7.90×10^{-3} | 3.29×10^6 |
| $k_2 = 4.05 \times 10^8 \text{ M}^{-1} \text{ s}^{-1}$ | | |

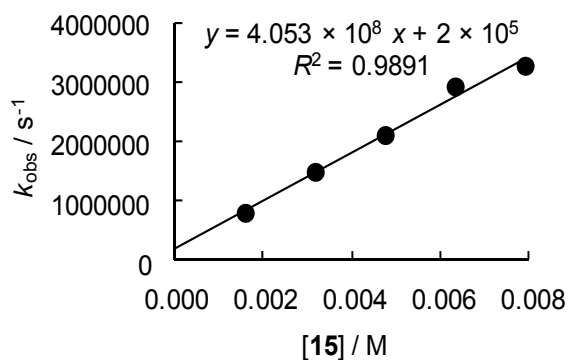
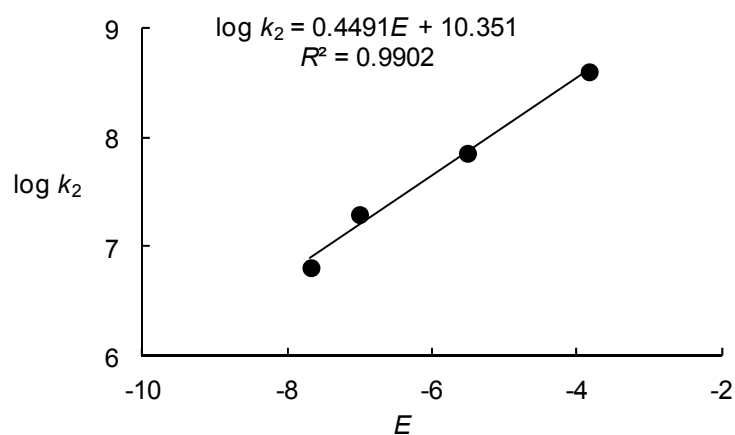


Table 4.103. Determination of the nucleophilicity parameters N and s_N for trimethylamine (**15**) in CH_3CN .

| Electrophile (E) | $k_2/\text{M}^{-1} \text{s}^{-1}$ | $\log k_2$ |
|----------------------|-----------------------------------|------------|
| 16h (-7.69) | 6.54×10^6 | 6.82 |
| 16i (-7.02) | 2.00×10^7 | 7.30 |
| 16j (-5.53) | 7.27×10^7 | 7.86 |
| 16k (-3.85) | 4.05×10^8 | 8.61 |

$N = 23.05 \quad s_N = 0.45$

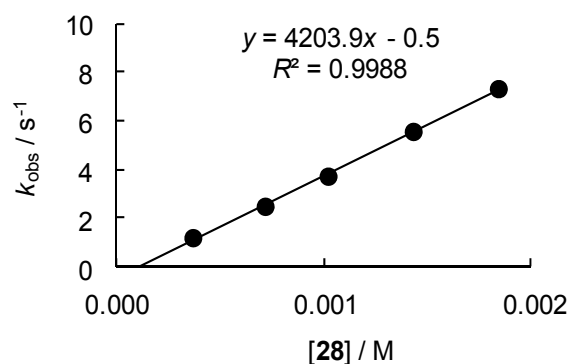


*Kinetics of the reactions of $(\text{dma})_2\text{CHNH}_2$ (**28**) with benzhydrylium ions (**16**)*

Table 4.104. Rate constants for the reactions of $(\text{dma})_2\text{CHNH}_2$ (**28**) with $(\text{dma})_2\text{CH}^+ \text{BF}_4^-$ (**16i**) in CH_3CN (stopped-flow technique, 20°C , $\lambda = 605 \text{ nm}$).

| $[\mathbf{16i}]_0/\text{M}$ | $[\mathbf{28}]_0/\text{M}$ | $[\mathbf{28}]_0/[\mathbf{16i}]_0$ | $k_{\text{obs}}/\text{s}^{-1}$ |
|-----------------------------|----------------------------|------------------------------------|--------------------------------|
| 1.79×10^{-5} | 3.69×10^{-4} | 11 | 1.20 |
| 1.79×10^{-5} | 7.17×10^{-4} | 22 | 2.49 |
| 1.79×10^{-5} | 1.02×10^{-3} | 32 | 3.73 |
| 1.79×10^{-5} | 1.43×10^{-3} | 42 | 5.56 |
| 1.79×10^{-5} | 1.84×10^{-3} | 54 | 7.33 |

$k_2 = 4.20 \times 10^3 \text{ M}^{-1} \text{ s}^{-1}$



4.4.3 Determination of Equilibrium Constants

Determination of the equilibrium constants for the reactions of 1,1-dimethylhydrazine (**2**) with benzhydrylium ions (**16**).

Table 4.105. Determination of the equilibrium constant for the reactions of 1,1-dimethylhydrazine (**2**) with $(\text{pyr})_2\text{CH}^+ \text{BF}_4^-$ (**16h**) generated from $(\text{pyr})_2\text{CHPBu}_3^+ \text{BF}_4^-$ (**16h-PBu₃**) in CH_3CN (laser-flash photolysis, 20 °C, $\lambda = 611 \text{ nm}$).

| [16h-PBu₃]/M | [2] ₀ /M | A_0 | A_{eq} |
|--------------------------------------|------------------------------|-----------------------|-----------------------|
| 1.47×10^{-5} | 8.43×10^{-2} | 5.71×10^{-1} | 1.22×10^{-1} |
| 1.47×10^{-5} | 1.48×10^{-1} | 5.45×10^{-1} | 7.78×10^{-2} |
| 1.47×10^{-5} | 1.76×10^{-1} | 5.38×10^{-1} | 6.50×10^{-2} |
| 1.47×10^{-5} | 2.60×10^{-1} | 6.02×10^{-1} | 5.63×10^{-2} |
| 1.47×10^{-5} | 3.33×10^{-1} | 5.67×10^{-1} | 4.33×10^{-2} |
| $K = 3.3 \times 10^1 \text{ M}^{-1}$ | | | |

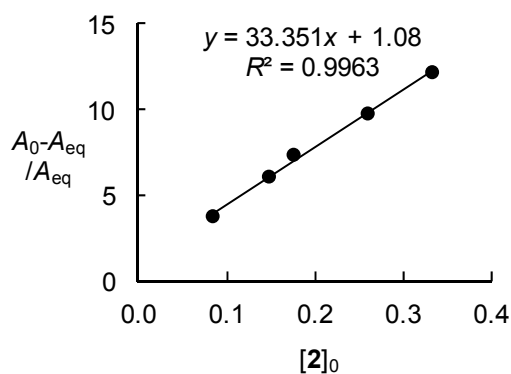
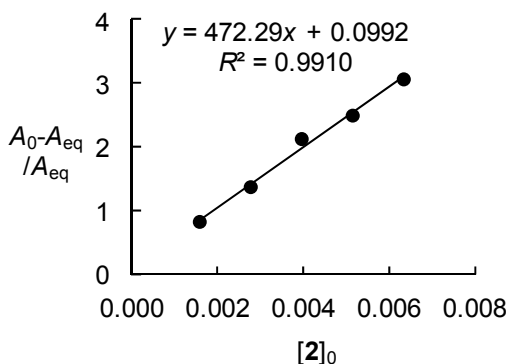


Table 4.106. Determination of the equilibrium constant for the reactions of 1,1-dimethylhydrazine (**2**) with $(\text{dma})_2\text{CH}^+ \text{BF}_4^-$ (**16i**) generated from $(\text{dma})_2\text{CHPBu}_3^+ \text{BF}_4^-$ (**16i-PBu₃**) in CH_3CN (laser-flash photolysis, 20 °C, $\lambda = 605 \text{ nm}$).

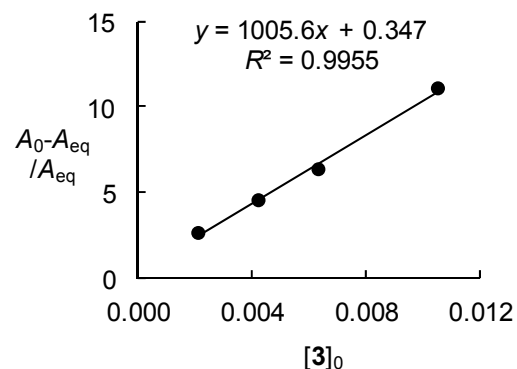
| [16i-PBu₃]/M | [2] ₀ /M | A_0 | A_{eq} |
|--------------------------------------|------------------------------|-----------------------|-----------------------|
| 1.41×10^{-5} | 1.58×10^{-3} | 2.95×10^{-1} | 1.63×10^{-1} |
| 1.41×10^{-5} | 2.77×10^{-3} | 2.90×10^{-1} | 1.23×10^{-1} |
| 7.06×10^{-6} | 3.96×10^{-3} | 1.69×10^{-1} | 5.41×10^{-2} |
| 1.41×10^{-5} | 5.15×10^{-3} | 2.87×10^{-1} | 8.22×10^{-2} |
| 1.41×10^{-5} | 6.34×10^{-3} | 2.79×10^{-1} | 6.88×10^{-2} |
| $K = 4.7 \times 10^2 \text{ M}^{-1}$ | | | |



Determination of the equilibrium constants for the reactions of trimethylhydrazine (3) with benzhydrylium ions (16).

Table 4.107. Determination of the equilibrium constant for the reactions of trimethylhydrazine (3) with $(\text{mor})_2\text{CH}^+ \text{BF}_4^-$ (16j) generated from $(\text{mor})_2\text{CHPBu}_3^+ \text{BF}_4^-$ (16j-PBu₃) in CH₃CN (laser-flash photolysis, 20 °C, $\lambda = 611$ nm).

| [16j-PBu ₃]/M | [3] ₀ /M | A_0 | A_{eq} |
|--------------------------------------|-----------------------|-----------------------|---------------------------|
| 1.02×10^{-5} | 2.10×10^{-3} | 1.35×10^{-1} | 3.71×10^{-2} |
| 1.02×10^{-5} | 4.21×10^{-3} | 1.35×10^{-1} | 2.43×10^{-2} |
| 1.02×10^{-5} | 6.31×10^{-3} | 1.43×10^{-1} | 1.94×10^{-2} [a] |
| 1.02×10^{-5} | 1.05×10^{-2} | 1.44×10^{-1} | 1.19×10^{-2} |
| $K = 1.0 \times 10^3 \text{ M}^{-1}$ | | | |

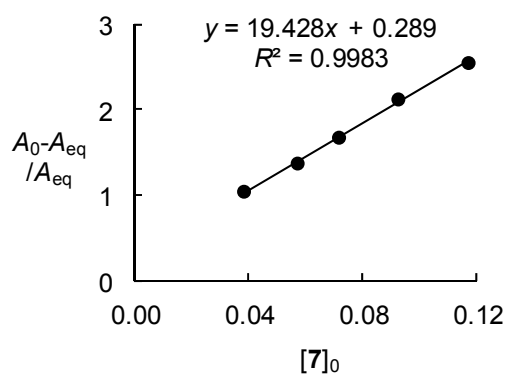


[a] The equilibrium absorbance has been determined from the constant C obtained by fitting the monoexponential function $A = A_0 e^{-k_{\text{obs}} t} + C$ to the time-dependent absorbance.

Determination of the equilibrium constants for the reactions of N,N' -dimethylformohydrazide (7) with benzhydrylium ions (16)

Table 4.108. Determination of the equilibrium constant for the reaction of N,N' -dimethylformohydrazide (7) with $(\text{fur})_2\text{CH}^+ \text{BF}_4^-$ (16l) generated from $(\text{fur})_2\text{CHPPH}_3^+ \text{BF}_4^-$ (16l-PPh₃) in CH₃CN (laser-flash photolysis, 20 °C, $\lambda = 535$ nm).

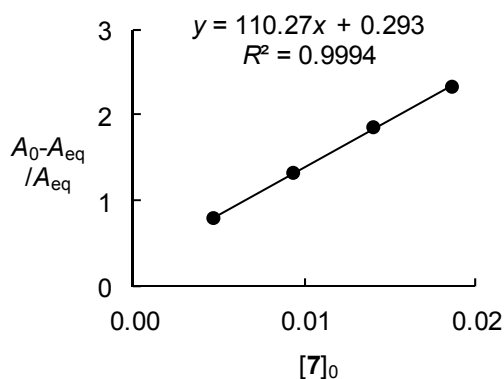
| [16l-PPh ₃]/M | [7] ₀ /M | A_0 | A_{eq} [a] |
|--------------------------------------|-----------------------|-----------------------|-----------------------|
| 1.05×10^{-5} | 3.83×10^{-2} | 2.04×10^{-1} | 9.98×10^{-2} |
| 1.05×10^{-5} | 5.71×10^{-2} | 2.06×10^{-1} | 8.68×10^{-2} |
| 1.05×10^{-5} | 7.16×10^{-2} | 2.14×10^{-1} | 8.00×10^{-2} |
| 1.05×10^{-5} | 9.24×10^{-2} | 2.05×10^{-1} | 6.57×10^{-2} |
| 1.05×10^{-5} | 1.17×10^{-1} | 2.06×10^{-1} | 5.81×10^{-2} |
| $K = 1.9 \times 10^1 \text{ M}^{-1}$ | | | |



[a] The equilibrium absorbances have been determined from the constant C obtained by fitting the monoexponential function $A = A_0 e^{-k_{\text{obs}} t} + C$ to the time-dependent absorbances.

Table 4.109. Determination of the equilibrium constant for the reactions of *N,N'*-dimethylformohydrazide (**7**) with (ani)(fur)CH⁺ BF₄⁻ (**16m**) generated from (ani)(fur)CHPPh₃⁺ BF₄⁻ (**16m**-PPh₃) in CH₃CN (laser-flash photolysis, 20 °C, $\lambda = 513$ nm).

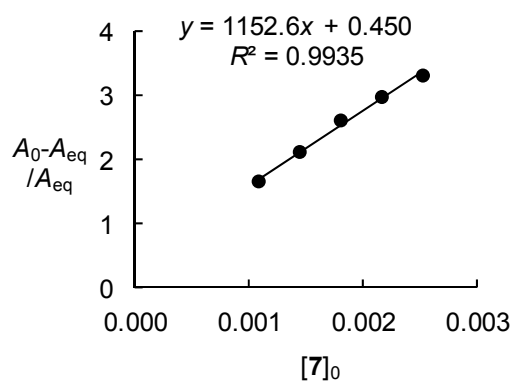
| [16m -PPh ₃]/M | [7] ₀ /M | <i>A</i> ₀ | <i>A</i> _{eq} ^[a] |
|--------------------------------------|------------------------------|-----------------------|---------------------------------------|
| 1.06×10^{-5} | 4.66×10^{-3} | 3.02×10^{-1} | 1.68×10^{-1} |
| 1.06×10^{-5} | 9.32×10^{-3} | 3.00×10^{-1} | 1.29×10^{-1} |
| 1.06×10^{-5} | 1.40×10^{-2} | 3.00×10^{-1} | 1.05×10^{-1} |
| 1.06×10^{-5} | 1.86×10^{-2} | 2.91×10^{-1} | 8.74×10^{-2} |
| $K = 1.1 \times 10^2 \text{ M}^{-1}$ | | | |



[a] The equilibrium absorbances have been determined from the constant *C* obtained by fitting the monoexponential function $A = A_0 e^{-k_{obs}t} + C$ to the time-dependent absorbances.

Table 4.110. Determination of the equilibrium constant for the reactions of *N,N'*-dimethylformohydrazide (**7**) with (ani)₂CH⁺ BF₄⁻ (**16n**) generated from (ani)₂CHPPh₃⁺ BF₄⁻ (**16n**-PPh₃) in CH₃CN (laser-flash photolysis, 20 °C, $\lambda = 513$ nm).

| [16n -PPh ₃]/M | [7] ₀ /M | <i>A</i> ₀ | <i>A</i> _{eq} ^[a] |
|--------------------------------------|------------------------------|-----------------------|---------------------------------------|
| 1.11×10^{-5} | 1.08×10^{-3} | 2.41×10^{-1} | 9.09×10^{-2} |
| 1.11×10^{-5} | 1.44×10^{-3} | 2.36×10^{-1} | 7.59×10^{-2} |
| 1.11×10^{-5} | 1.80×10^{-3} | 2.43×10^{-1} | 6.75×10^{-2} |
| 1.11×10^{-5} | 2.16×10^{-3} | 2.41×10^{-1} | 6.08×10^{-2} |
| 1.11×10^{-5} | 2.52×10^{-3} | 2.36×10^{-1} | 5.49×10^{-2} |
| $K = 1.2 \times 10^3 \text{ M}^{-1}$ | | | |



[a] The equilibrium absorbances have been determined from the constant *C* obtained by fitting the monoexponential function $A = A_0 e^{-k_{obs}t} + C$ to the time-dependent absorbances.

Determination of the equilibrium constants for the reactions of trimethylamine (**15**) with benzhydrylium ions (**16**)

Table 4.111. Determination of the equilibrium constant for the reactions of trimethylamine (**15**) with $(\text{pyr})_2\text{CH}^+ \text{BF}_4^-$ (**16h**) generated from $(\text{pyr})_2\text{CHPBu}_3^+ \text{BF}_4^-$ (**16h-PBu₃**) in CH_3CN (laser-flash photolysis, 20 °C, $\lambda = 611 \text{ nm}$).

| [16h -PBu ₃]/M | [15] ₀ /M | A_0 | A_{eq} |
|--------------------------------------|-------------------------------|-----------------------|-----------------------|
| 1.01×10^{-5} | 1.58×10^{-3} | 3.19×10^{-1} | 2.49×10^{-1} |
| 1.01×10^{-5} | 3.16×10^{-3} | 3.12×10^{-1} | 2.09×10^{-1} |
| 1.01×10^{-5} | 4.74×10^{-3} | 2.99×10^{-1} | 1.70×10^{-1} |
| 1.01×10^{-5} | 6.32×10^{-3} | 2.80×10^{-1} | 1.41×10^{-1} |
| 1.01×10^{-5} | 7.90×10^{-3} | 2.84×10^{-1} | 1.31×10^{-1} |
| 1.01×10^{-5} | 9.48×10^{-3} | 3.12×10^{-1} | 1.36×10^{-1} |
| 1.01×10^{-5} | 1.11×10^{-2} | 2.93×10^{-1} | 1.18×10^{-1} |
| $K = 1.3 \times 10^2 \text{ M}^{-1}$ | | | |

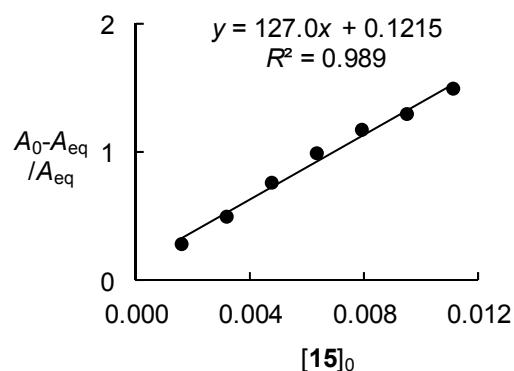
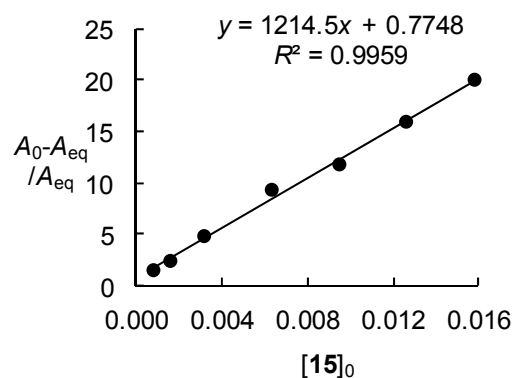


Table 4.112. Determination of the equilibrium constant for the reactions of trimethylamine (**15**) with $(\text{dma})_2\text{CH}^+ \text{BF}_4^-$ (**16i**) generated from $(\text{dma})_2\text{CHPBu}_3^+ \text{BF}_4^-$ (**16i-PBu₃**) in CH_3CN (laser-flash photolysis, 20 °C, $\lambda = 605 \text{ nm}$).

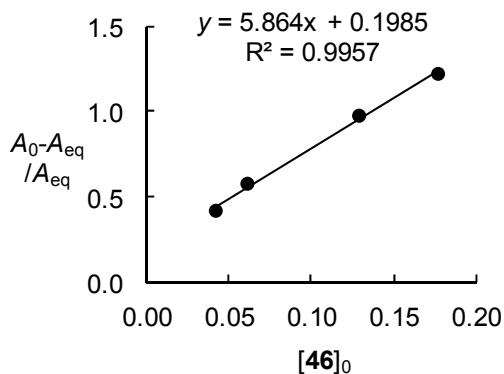
| [16i -PBu ₃]/M | [15] ₀ /M | A_0 | A_{eq} |
|--------------------------------------|-------------------------------|-----------------------|-----------------------|
| 6.70×10^{-6} | 7.90×10^{-4} | 3.31×10^{-1} | 1.32×10^{-1} |
| 6.70×10^{-6} | 1.58×10^{-3} | 3.31×10^{-1} | 9.70×10^{-2} |
| 6.70×10^{-6} | 3.16×10^{-3} | 2.99×10^{-1} | 5.13×10^{-2} |
| 6.70×10^{-6} | 6.32×10^{-3} | 3.82×10^{-1} | 3.70×10^{-2} |
| 6.70×10^{-6} | 9.48×10^{-3} | 2.81×10^{-1} | 2.19×10^{-2} |
| 6.70×10^{-6} | 1.26×10^{-2} | 2.82×10^{-1} | 1.66×10^{-2} |
| 6.70×10^{-6} | 1.58×10^{-2} | 2.59×10^{-1} | 1.23×10^{-2} |
| $K = 1.2 \times 10^3 \text{ M}^{-1}$ | | | |



Determination of the equilibrium constants for the reactions of N-methylpiperidine (46) with benzhydrylium ions (16)

Table 4.113. Determination of the equilibrium constant for the reactions of N-methylpiperidine (46) with (pyr)₂CH⁺ BF₄⁻ (16h) generated from (pyr)₂CHPBu₃⁺ BF₄⁻ (16h-PBu₃) in CH₃CN (laser-flash photolysis, 20 °C, λ = 611 nm).

| [16h-PBu ₃]/M | [46] ₀ /M | A ₀ | A _{eq} ^[a] |
|---------------------------|-------------------------|-------------------------|--------------------------------|
| 1.01 × 10 ⁻⁵ | 4.20 × 10 ⁻² | 5.04 × 10 ⁻¹ | 3.55 × 10 ⁻¹ |
| 1.01 × 10 ⁻⁵ | 6.12 × 10 ⁻² | 4.86 × 10 ⁻¹ | 3.09 × 10 ⁻¹ |
| 1.01 × 10 ⁻⁵ | 1.29 × 10 ⁻¹ | 4.34 × 10 ⁻¹ | 2.45 × 10 ⁻¹ |
| 1.01 × 10 ⁻⁵ | 1.77 × 10 ⁻¹ | 4.64 × 10 ⁻¹ | 2.10 × 10 ⁻¹ |
| $K = 5.9 \text{ M}^{-1}$ | | | |

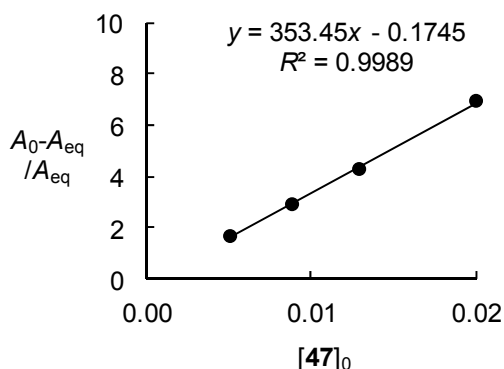


[a] The equilibrium absorbances have been determined from the constant C obtained by fitting the monoexponential function $A = A_0 e^{-k_{\text{obs}} t} + C$ to the time-dependent absorbances.

Determination of the equilibrium constants for the reactions of N-methylpyrrolidine (47) with benzhydrylium ions (16)

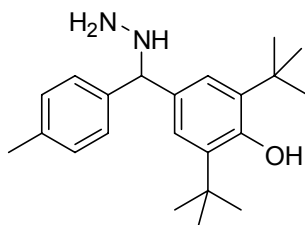
Table 4.114. Determination of the equilibrium constant for the reactions of N-methylpyrrolidine (47) with (pyr)₂CH⁺ BF₄⁻ (16h) generated from (pyr)₂CHPBu₃⁺ BF₄⁻ (16h-PBu₃) in CH₃CN (laser-flash photolysis, 20 °C, λ = 611 nm).

| [16h-PBu ₃]/M | [47] ₀ /M | A ₀ | A _{eq} |
|--------------------------------------|-------------------------|-------------------------|-------------------------|
| 1.01 × 10 ⁻⁵ | 5.07 × 10 ⁻³ | 6.22 × 10 ⁻¹ | 2.32 × 10 ⁻¹ |
| 1.01 × 10 ⁻⁵ | 8.83 × 10 ⁻³ | 6.19 × 10 ⁻¹ | 1.58 × 10 ⁻¹ |
| 1.01 × 10 ⁻⁵ | 1.29 × 10 ⁻² | 6.13 × 10 ⁻¹ | 1.16 × 10 ⁻¹ |
| 1.01 × 10 ⁻⁵ | 2.00 × 10 ⁻² | 6.13 × 10 ⁻¹ | 7.71 × 10 ⁻² |
| $K = 3.5 \times 10^2 \text{ M}^{-1}$ | | | |



4.4.4 Product Characterization

2,6-Di-*tert*-butyl-4-(hydrazinyl(*p*-tolyl)methyl)phenol (**17**)



17

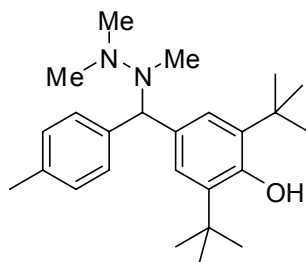
A solution of $\text{tol}(t\text{Bu})_2\text{QM}$ (**16b**, 50.0 mg, 0.162 mmol) in acetonitrile (2 mL) was added to a solution of hydrazine monohydrate (**1**, 0.10 mL, 2.1 mmol) in acetonitrile (8 mL) over 5 min at RT. The solvent was removed under reduced pressure: **17** (52.5 mg, 0.154 mmol, 95%), colorless oil.

^1H NMR (400 MHz, CD_3CN): δ = 1.38 (s, 18 H, $2 \times \text{C}(\text{CH}_3)_3$), 2.28 (s, 3 H, CH_3), 2.90–2.34 (brs, 3 H, NH, NH_2), 4.70 (s, 1 H, Ar_2CH), 5.34 (brs, 1 H, OH) 7.12 (d, H_{ar} , $J = 7.9$ Hz, 2 H), 7.19 (s, 2 H, H_{ar}), 7.28 (d, $J = 8.1$ Hz, 2 H, H_{ar}).

^{13}C NMR (100 MHz, CD_3CN): δ = 21.1 (q), 30.6 (q), 35.2 (s), 73.8 (d, Ar_2CH), 124.9 (d), 128.2 (d), 130.0 (d), 135.2 (s), 137.4 (s), 138.2 (s), 141.7 (s), 153.6 (s).

HR-MS (ESI, negative): m/z calcd. for $\text{C}_{22}\text{H}_{31}\text{N}_2\text{O}^-$ $[\text{M}-\text{H}]^-$: 339.2442, found 339.2441.

2,6-Di-*tert*-butyl-4-(*p*-tolyl-(1,2,2-trimethylhydrazinyl)methyl)phenol (**18**)



18

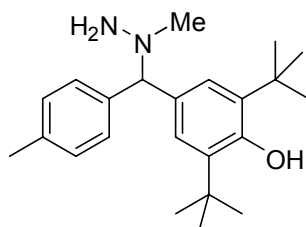
Trimethylhydrazine (**3**, 0.20 mL, 2.1 mmol) was added to a solution of $\text{tol}(t\text{-Bu})_2\text{QM}$ (**16b**, 100 mg, 0.324 mmol) in acetonitrile (10 mL) and stirred over night at RT. The solvent was removed under reduced pressure: **20** (122 mg, 0.319 mmol, 98%), colorless oil.

^1H NMR (400 MHz, CD_3CN): δ = 1.39 (s, 18 H, $2 \times \text{C}(\text{CH}_3)_3$), 2.09 (s, 3 H, NCH_3), 2.26 (s, 3 H, CH_3), 2.28 (s, 6 H, $\text{N}(\text{CH}_3)_2$), 4.52 (s, 1 H, Ar_2CH), 5.25 (brs, 1 H, OH) 7.06 (d, H_{ar} , J = 7.8 Hz, 2 H), 7.25 (s, 2 H, H_{ar}), 7.31 (d, J = 8.0 Hz, 2 H, H_{ar}).

^{13}C NMR (100 MHz, CD_3CN): δ = 21.1 (q), 30.65 (q), 30.74 (q), 35.2 (s), 39.0 (q), 74.8 (d, Ar_2CH), 124.7 (d), 128.2 (d), 129.8 (d), 136.8 (s), 137.1 (s), 137.9 (s), 143.5 (s), 153.0 (s).

HR-MS (EI, positive) : m/z calcd. for $\text{C}_{25}\text{H}_{38}\text{N}_2\text{O}^+$: 382.2979, found 382.2979.

2,6-Di-*tert*-butyl-4-((1-methylhydrazinyl)(*p*-tolyl)methyl)-phenol (**19**)



19

Methylhydrazine (**4**, 25 μL , 0.48 mmol) was added to a solution of $\text{tol}(t\text{-Bu})_2\text{QM}$ (**16b**, 50 mg, 0.16 mmol) in acetonitrile (10 mL) over 5 min at RT. After 30 min of stirring, the

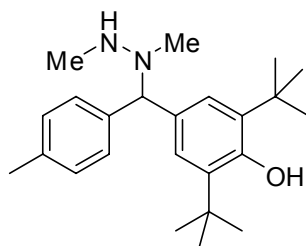
volatile compounds were evaporated under reduced pressure: **19** (54 mg, 0.15 mmol, 94%), colorless crystals; mp 94–96 °C (hexane).

^1H NMR (400 MHz, CD_3CN): δ = 1.38 (s, 18 H, $\text{C}(\text{CH}_3)_3$), 2.27 (s, 3 H, CH_3), 2.31 (s, 3 H, NCH_3), 4.08 (s, 1 H, Ar_2CH), 5.34 (br s, 1 H, OH), 7.10 (d, J = 7.8 Hz, 2 H, H_{ar}), 7.24 (s, 2 H, H_{ar}), 7.32 (d, J = 8.1 Hz, 2 H, H_{ar}).

^{13}C NMR (100 MHz, CD_3CN): δ = 21.1 (q), 30.6 (q), 35.2 (s), 47.1 (q), 82.3 (d, Ar_2CH), 124.9 (d), 128.3 (d), 130.1 (d), 135.7 (s), 137.3 (s), 138.3 (s), 142.4 (s), 153.5 (s).

HRMS (ESI, positive): m/z calcd. for $\text{C}_{23}\text{H}_{35}\text{N}_2\text{O}^+$ $[\text{M}+\text{H}]^+$: 355.2744, found: 355.2744.

2,6-Di-*tert*-butyl-4-((1,2-dimethylhydrazinyl)(*p*-tolyl)methyl)phenol (**20**)



20

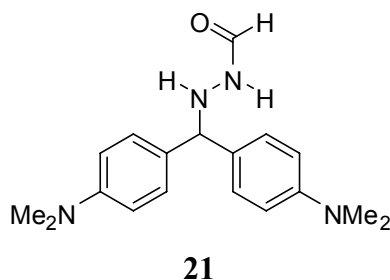
1,2-Dimethylhydrazine (**5**, 60 μL , 0.83 mmol) was added to a solution of $\text{tol}(t\text{-Bu})_2\text{QM}$ (**16b**, 100 mg, 0.324 mmol) in acetonitrile (15 mL) over 15 min at RT. After 30 min of stirring, the volatile compounds were evaporated under reduced pressure: **20** (117 mg, 0.317 mmol, 98%), colorless oil.

^1H NMR (400 MHz, CD_3CN): δ = 1.40 (s, 18 H, $\text{C}(\text{CH}_3)_3$), 2.23 (s br, 1 H, NH), 2.27 (s, 3 H, CH_3), 2.30 (s, 3 H, NCH_3), 2.45 (s, 3 H, NHCH_3), 4.35 (s, 1 H, Ar_2CH), 5.29 (br s, 1 H, OH), 7.08 (d, J = 8.2 Hz, 2 H, H_{ar}), 7.24 (s, 2 H, H_{ar}), 7.30 (d, J = 8.1 Hz, 2 H, H_{ar}).

^{13}C NMR (100 MHz, CD_3CN): δ = 21.1 (q), 30.7 (q), 35.2 (q), 35.5 (s), 42.3 (q), 78.1 (d, Ar_2CH), 124.9 (d), 128.4 (d), 129.8 (d), 136.4 (s), 136.9 (s), 137.9 (s), 142.7 (s), 153.2 (s).

HRMS (ESI, positive): m/z calcd. for $\text{C}_{24}\text{H}_{37}\text{N}_2\text{O}^+$ $[\text{M}+\text{H}]^+$: 369.2900, found: 369.2898.

N'-(Bis(4-(dimethylamino)phenyl)methyl)-formohydrazide (**21**)



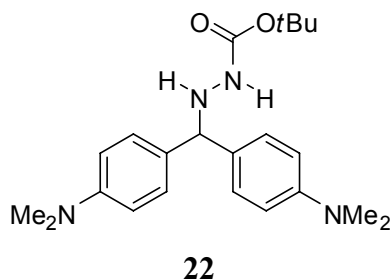
A solution of $(\text{dma})_2\text{CH}^+ \text{BF}_4^-$ (**16i**, 50 mg, 0.15 mmol) in acetonitrile (5 mL) was added to a solution of formohydrazide (**6**, 9.0 mg, 0.15 mmol) in acetonitrile (5 mL) at RT. Then trimethylamine (0.1 mL, 33% in ethanol) was added and volatile compounds were evaporated under reduced pressure after 5 min stirring at RT. The residue was dissolved in CDCl_3 and filtered. According to the ^1H NMR, the product **21** was formed exclusively as a 2:1 mixture of the (*Z*)- and (*E*)- isomers.^[53]

^1H NMR (400 MHz, CDCl_3): δ = 2.91 (s, 12 H, CH_3 *Z*), 2.92 (s, 12 H, CH_3 *E*), 4.14 (d, J = 5.6 Hz, 1 H, NHCH *E*), 4.81 (d, J = 5.0 Hz, 1 H, Ar_2CH *E*), 5.09 (s, 1 H, Ar_2CH *Z*), 6.67-6.69 (m, 9 H, $4 \times \text{H}_{\text{ar}}$ *Z*, $4 \times \text{H}_{\text{ar}}$ *E*, NHCHO *E* superimposed), 6.97 (s, 1 H, NHCHO *Z*), 7.17 (d, J = 8.8 Hz, 4 H, H_{ar} *E*), 7.28 (d, J = 8.6 Hz, 4 H, H_{ar} *Z*), 8.00 (s, 1 H, CHO *Z*), 8.26 (d, J = 10.9 Hz, 1 H, CHO *E*).

^{13}C NMR (100 MHz, CDCl_3): δ = 40.7 (q, $\text{N}(\text{CH}_3)_2$ *E*), 40.8 (q, $\text{N}(\text{CH}_3)_2$ *Z*), 67.6 (d, Ar_2CH *E*), 69.1 (d, Ar_2CH *Z*), 112.8 (d, ArH *Z* and *E* superimposed), 128.1 (s, q_{Ar} *E*), 128.5 (d, ArH *Z*), 128.5 (d, ArH *Z*), 129.5 (s, q_{Ar} *E*), 150.1 (s, q_{Ar} *Z*), 150.2 (s, q_{Ar} *E*), 160.0 (d, CHO *Z*), 166.9 (d, CHO *E*).

HR-MS (ESI, negative) : m/z calcd. for $\text{C}_{18}\text{H}_{23}\text{N}_4\text{O}^-$ [$\text{M}-\text{H}$] $^-$: 311.1877, found: 311.1881.

tert-Butyl 2-(bis(4-(dimethylamino)phenyl)methyl)-hydrazinecarboxylate (**22**)



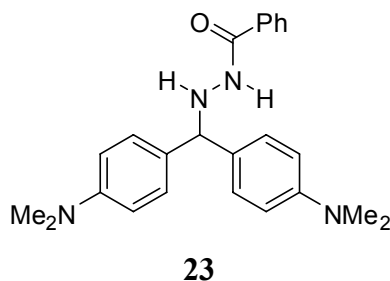
tert-Butyl hydrazinecarboxylate (**8**, 39 mg, 0.30 mmol) was added to a solution of $(\text{dma})_2\text{CH}^+ \text{BF}_4^-$ (**16i**, 100 mg, 0.294 mmol) in acetonitrile (5 mL) and stirred for 5 min at RT. Then 2 M NaOH (10 mL) was added and the solution was extracted with diethyl ether (15 mL). The ethereal phase was dried (Na_2SO_4), filtered and the volatile compounds were evaporated under reduced pressure: **22** (113 mg, 0.294 mmol, quantitative), colorless oil.

^1H NMR (400 MHz, CDCl_3): δ = 1.42 (s, 9 H, $\text{C}(\text{CH}_3)_3$), 2.88 (s, 12 H, $\text{N}(\text{CH}_3)_2$), 4.30 (s br, 1 H, NH), 5.11 (s, 1 H, Ar_2CH), 6.09 (s br, 1 H, NH), 6.66 (d, J = 8.9 Hz, 4 H, H_{ar}), 7.25 (d, J = 8.7 Hz, 4 H, H_{ar}).

^{13}C NMR (100 MHz, CDCl_3): δ = 28.5 (q), 40.8 (q), 67.2 (d, Ar_2CH), 80.2 (s), 112.7 (d), 128.6 (d), 130.2 (s), 149.9 (s), 156.7 (s).

HR-MS (EI, positive) : m/z calcd. for $\text{C}_{22}\text{H}_{32}\text{N}_4\text{O}_2^+$: 384.2520, found: 384.2512.

N'-(Bis(4-(dimethylamino)phenyl)methyl)-benzohydrazide (**23**)



Benzohydrazide (**9**, 60 mg, 0.44 mmol) was added to a solution of $(\text{dma})_2\text{CH}^+ \text{BF}_4^-$ (**16i**, 150 mg, 0.441 mmol) in acetonitrile (5 mL) over 5 min at RT. Then 2 M NaOH (5 mL) was added, and the solution was extracted with diethyl ether (15 mL) and the ethereal phase was

dried (Na_2SO_4) and filtered. The solvent was partially evaporated under reduced pressure and the residue was cooled to $-60\text{ }^\circ\text{C}$ to crystallize the product: **23** (161 mg, 0.41 mmol, 93%), colorless crystals.

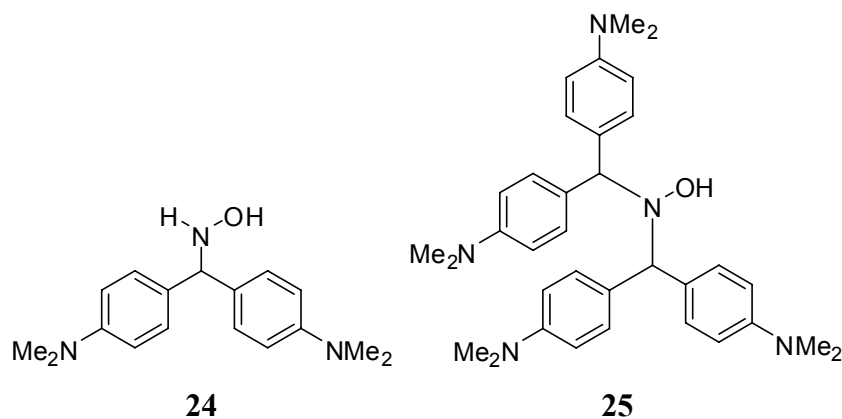
Mp: 143–144 $^\circ\text{C}$ (Et_2O).

^1H NMR (300 MHz, CD_3CN): δ = 2.88 (s, 12 H, CH_3), 5.10 (s br, 2 H, Ar_2CH , NH), 6.71 (d, J = 8.9 Hz, 4 H, H_{ar}), 7.28 (d, J = 8.8 Hz, 4 H, H_{ar}), 7.38–7.42 (m, 2 H, H_{ar}), 7.46–7.53 (m, 1 H, H_{ar}), 7.61–7.66 (m, 2 H, H_{ar}), 8.36 (d br, J = 6.4 Hz, 1 H, NH).

^{13}C NMR (75 MHz, CD_3CN): δ = 40.9 (q), 68.3 (d, Ar_2CH), 113.5 (d), 128.0 (d), 129.3 (d), 129.5 (d), 131.6 (s), 132.5 (d), 134.5 (s), 151.2 (s), 167.9 (s).

HR-MS (ESI, negative) : m/z calcd. for $\text{C}_{24}\text{H}_{27}\text{N}_4\text{O}^-$ [$\text{M}-\text{H}$] $^-$: 387.2190, found: 387.2190.

N'-(Bis(4-(dimethylamino)phenyl)methyl)-hydroxylamine (**24**) and *N,N*-(Bis(bis(4-(dimethylamino)phenyl)methyl))-hydroxylamine (**25**)



Trimethylamine (**15**, 0.5 mL 33% in ethanol, 0.1 mg, 2 mmol) was added to hydroxylamine hydrochloride (**10**·HCl, 85 mg, 1.2 mmol) at RT and acetonitrile (10 mL) was added. A solution of $(\text{dma})_2\text{CH}^+ \text{BF}_4^-$ (**16i**, 75 mg, 0.22 mmol) in acetonitrile (10 mL) was added dropwise at RT. The solution was concentrated under reduced pressure, diethyl ether (5 mL) was added, the precipitate was filtered off and volatile compounds were evaporated under reduced pressure. According to the ^1H NMR spectrum of the crude product, a 9:1 mixture of **24** and **25** was obtained.

24:

^1H NMR (300 MHz, CDCl_3): δ = 2.89 (s, 12 H, CH_3), 5.05 (s, 1 H, Ar_2CH), 5.53 (br s, 2 H, NH and OH superimposed), 6.68 (d, J = 8.7 Hz, 4 H, H_{ar}), 7.22 (d, J = 8.8 Hz, 4 H, H_{ar}).

^{13}C NMR (75 MHz, CDCl_3): δ = 40.8 (q), 69.6 (d, Ar_2CH), 112.8 (d), 128.6 (d), 129.1 (s), 150.0 (s).

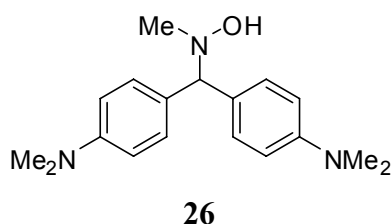
HR-MS (EI, positive) : m/z calcd. for $\text{C}_{17}\text{H}_{24}\text{N}_3\text{O}^+$ $[\text{M}+\text{H}]^+$: 286.1914, found 286.1914

25:

^1H NMR (300 MHz, CDCl_3): δ = 2.89 (s, 24 H, CH_3), 4.81 (s, 2 H, Ar_2CH), 5.53 (br s, 1 H, OH superimposed by **22**), 6.68 (d, 8.7, 8 H, H_{ar}), 7.29 (d, J = 8.7 Hz, 8 H, H_{ar}).

^{13}C NMR (75 MHz, CDCl_3): δ = 40.9 (q), 70.2 (d, Ar_2CH), 112.6 (d), 129.6 (d), 130.6 (s), 149.6 (s).

N-(Bis(4-(dimethylamino)phenyl)methyl)-*N*-methylhydroxylamine (**26**)



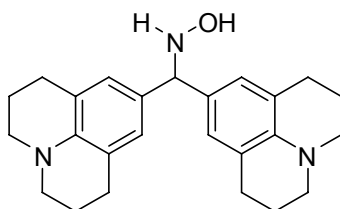
Trimethylamine (**15**, 0.3 mL 33% in ethanol, 0.08 g, 1 mmol) was added to *N*-methylhydroxylamine hydrochloride (**11**·HCl, 60 mg, 0.72 mmol) at RT. A solution of $(\text{dma})_2\text{CH}^+ \text{BF}_4^-$ (**16i**, 100 mg, 0.294 mmol) in acetonitrile (5 mL) was added dropwise over 5 min. 2 M NaOH (10 mL) was added and the solution was extracted with diethyl ether (15 mL). The ethereal phase was dried (Na_2SO_4), filtered and the volatile compounds were evaporated under reduced pressure: **26** (67 mg, 0.22 mmol, 76 %), colorless oil.

^1H NMR (400 MHz, CDCl_3): δ = 2.56 (s, 3 H, $\text{N}(\text{OH})(\text{CH}_3)$), 2.87 (s, 12 H, $\text{N}(\text{CH}_3)_2$), 4.43 (s, 1 H, Ar_2CH), 5.16 (s br, 1 H, OH), 6.65 (d, J = 8.8 Hz, 4 H, H_{ar}), 7.28 (d, J = 8.7 Hz, 4 H, H_{ar}).

^{13}C NMR (100 MHz, CDCl_3): δ = 40.8 (q), 46.2 (q), 79.0 (d, Ar_2CH), 112.8 (d), 128.5 (d), 130.8 (s), 149.8 (s).

HR-MS (EI, positive) : m/z calcd. for $C_{18}H_{25}N_3O^+$: 299.1998, found: 299.2006.

N-(Bis(1,2,3,5,6,7-hexahydropyrido(3,2,1-*ij*)quinolin-9-yl)methyl)-hydroxylamine (**27**)



27

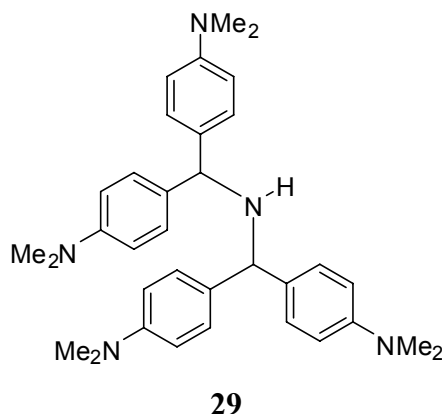
Trimethylamine (**15**, 0.5 mL 33% in ethanol, 0.1 mg, 2 mmol) was added to hydroxylamine hydrochloride (**10**·HCl, 7.8 mg, 0.11 mmol) at RT. A solution of $(jul)_2CH^+ BF_4^-$ (**16e**, 50 mg, 0.11 mmol) in acetonitrile (5 mL) was added dropwise at RT. The solution was concentrated under reduced pressure, diethyl ether (5 mL) was added, the precipitate was filtered off, and volatile compounds were evaporated under reduced pressure: **27** (41 mg, 0.11 mmol, quant.), colorless oil.

1H NMR (400 MHz, d_6 -DMSO): δ = 1.24 (s br, 1 H, NH), 1.80–1.86 (m, 8 H, $CH_2CH_2CH_2$), 2.61 (t, J = 6.5 Hz, 8 H, $CH_2CH_2CH_2N$), 3.02 (t, J = 5.5 Hz, 8 H, $CH_2CH_2CH_2N$), 4.57 (s, 1 H, Ar_2CH), 6.64 (s, 4 H, H_{Ar}), 7.15 (s br, OH).

^{13}C NMR (100 MHz, d_6 -DMSO): δ = 21.8 (t), 27.2 (t), 49.4 (t), 69.4 (d, Ar_2CH), 120.4 (s), 125.8 (d), 130.0 (s), 141.4 (s).

HR-MS (ESI, positive): m/z calcd. for $C_{25}H_{29}N_2^+ [M-NHOH]^+$: 357.2325, found: 357.2325.

Bis-(bis(4-(dimethylamino)phenyl)methyl)-amine (**29**)



A solution of $(\text{dma})_2\text{CH}^+ \text{BF}_4^-$ (**16i**, 100 mg, 0.294 mmol) in acetonitrile (10 mL) was added to a solution of ammonia (**12**, 10 mL, 0.54 M, 5.4 mmol) in acetonitrile over 30 min at RT. After adding diethyl ether (20 mL), the solution was washed with 2 M NaOH (25 mL), dried (Na_2SO_4), filtered, and the solvent was evaporated under reduced pressure: **29** (75 mg, 0.14 mmol, 98%), colorless crystals.

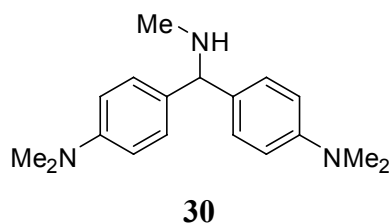
Mp: 191–192 °C (pentane). Ref. [29]: mp 188 °C (benzene, ethanol).

^1H NMR (300 MHz, CDCl_3): δ = 1.62 (s br, 1 H, NH), 2.91 (s, 24 H, $\text{N}(\text{CH}_3)_2$), 4.61 (s, 2 H, Ar_2CH), 6.68 (d, J = 8.8 Hz, 8 H, H_{ar}), 7.22 (d, J = 8.7 Hz, 8 H, H_{ar}).

^{13}C NMR (75 MHz, CDCl_3): δ = 41.0 (q), 62.2 (d, Ar_2CH), 112.8 (d), 128.4 (d), 133.5 (s), 149.6 (s).

HR-MS (EI, positive) : m/z calcd. for $\text{C}_{34}\text{H}_{43}\text{N}_5^+$: 521.3518, found: 521.3513.

(Bis(4-(dimethylamino)phenyl)methyl)-methylamine (**30**)



Methylamine (**13**, 1 mL, 33% in ethanol, 0.2 g, 8 mmol) was added to a solution of $(\text{dma})_2\text{CH}^+ \text{BF}_4^-$ (**16i**, 100 mg, 0.294 mmol) in acetonitrile (10 mL) and stirred for 5 min at

RT. Then 2 M NaOH (10 mL) was added, and the solution was extracted with diethyl ether (15 mL). The ethereal phase was dried (MgSO_4), filtered and the volatile compounds were evaporated under reduced pressure: **30** (82 mg, 0.29 mmol, 98 %), colorless crystals.

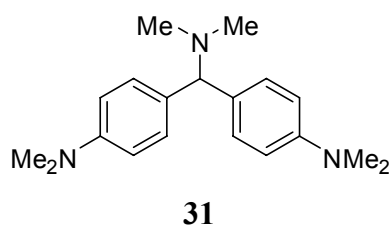
Mp: 125–126 °C (pentane).

^1H NMR (300 MHz, CDCl_3): δ = 2.39 (s, 3 H, $\text{NH}(\text{CH}_3)$), 2.90 (s, 12 H, $\text{N}(\text{CH}_3)_2$), 4.54 (s, 1 H, Ar_2CH), 6.68 (d, J = 8.8 Hz, 4 H, H_{ar}), 7.23 (d, J = 8.7 Hz, 4 H, H_{ar}).

^{13}C NMR (75 MHz, CDCl_3): δ = 35.2 (q), 40.9 (q), 68.4 (d, Ar_2CH), 112.9 (d), 128.0 (d), 132.9 (s), 149.7 (s).

HR-MS (EI, positive) : m/z calcd. for $\text{C}_{18}\text{H}_{25}\text{N}_3^+$: 283.2048, found: 283.2038.

(Bis(4-(dimethylamino)phenyl)methyl)-dimethylamine (**31**)



Dimethylamine (**14**, 0.5 mL 40% in water, 0.2 g, 4 mmol) was added to a solution of $(\text{dma})_2\text{CH}^+ \text{BF}_4^-$ (**16i**, 100 mg, 0.294 mmol) in acetonitrile (10 mL) and stirred for 5 min at RT. Then 2 M NaOH (10 mL) was added and the solution was extracted with diethyl ether (15 mL). The ethereal phase was dried (Na_2SO_4), filtered and the volatile compounds were evaporated under reduced pressure: **31** (89 mg, 0.30 mmol, quantitative), pale yellow crystals.

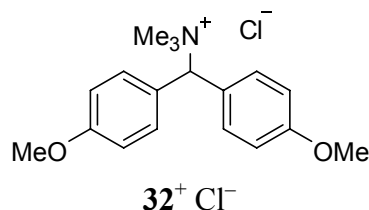
Mp: 92–93 °C (hexane). Ref. [54]: mp 94 °C.

^1H NMR (300 MHz, CDCl_3): δ = 2.19 (s, 6 H, $\text{Ar}_2\text{CHN}(\text{CH}_3)_2$), 2.88 (s, 12 H, $\text{N}(\text{CH}_3)_2$), 3.91 (s, 1 H, Ar_2CH), 6.65 (d, J = 8.8 Hz, 4 H, H_{ar}), 7.25 (d, J = 8.9 Hz, 4 H, H_{ar}).

^{13}C NMR (75 MHz, CDCl_3): δ = 40.9 (q), 44.9 (q), 76.8 (d, Ar_2CH), 112.8 (d); 128.5 (d), 132.2 (s), 149.6 (s).

HR-MS (EI, positive) : m/z calcd. for $C_{19}H_{27}N_3^+$: 297.2205, found: 297.2201.

(Bis(4-(methoxy)phenyl)methyl)-trimethylammonium chloride (**32**⁺ Cl⁻)



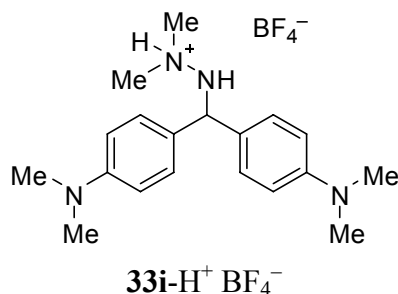
A solution of (ani)₂CHCl (**16n**-Cl, 50 mg, 0.19 mmol) in acetonitrile (5 mL) was added to trimethylamine (**15**, 0.2 mL 33% in ethanol, 0.05 g, 0.8 mmol) at RT. Volatile compounds were evaporated under reduced pressure: **32**⁺ Cl⁻ (60.5 mg, 0.188 mmol, 99%) colorless oil.

¹H NMR (400 MHz, CD₃CN): δ = 3.16 (s, 9 H, N(CH₃)₃), 3.77 (s, 6 H, OCH₃), 6.86 (s, 1 H, Ar₂CH), 6.98 (d, J = 9.0 Hz, 4 H, H_{ar}), 7.91 (d, J = 8.9 Hz, 4 H, H_{ar}).

¹³C NMR (100 MHz, CD₃CN): δ = 52.2 (q), 56.2 (q), 79.5 (d, Ar₂CH), 115.5 (d), 126.3 (s), 133.8 (d), 161.7 (s).

HR-MS (ESI, negative) : m/z calcd. for $C_{18}H_{24}Cl_2NO_2^-$: 356.1190, found: 356.1196.

2-(Bis(4-(dimethylamino)phenyl)methyl)-1,1-dimethylhydrazinium tetrafluoroborate (**33i**-H⁺ BF₄⁻)



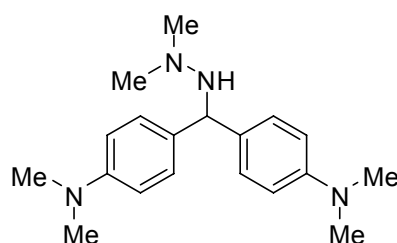
In an NMR tube, 1,1-dimethylhydrazine (**2**, 5.3 mg, 0.11 mmol) and (dma)₂CH⁺BF₄⁻ (**16i**, 30 mg, 0.088 mmol) were mixed in CD₃CN (1 mL) and analyzed immediately by NMR spectroscopy.

^1H NMR (400 MHz, CD_3CN): $\delta = 2.90$ (s, 12 H, $2 \times \text{N}(\text{CH}_3)_2$), 2.99 (s, 6 H, $^+\text{N}(\text{CH}_3)_2$), 3.26 (brs, 1 H, NH), 5.18 (s, 1 H, Ar_2CH), 6.73 (d, $J = 8.9$ Hz, 4 H, H_{ar}), 7.27 (d, $J = 8.9$ Hz, 4 H, H_{ar}).

^{13}C NMR (100 MHz, CD_3CN): $\delta = 40.7$ (q), 46.2 (q), 63.9 (d, Ar_2CH), 113.7 (d), 127.3 (s), 129.1 (d), 151.8 (s).

HR-MS (ESI, positive) : m/z calcd. for $\text{C}_{19}\text{H}_{27}\text{N}_4^+$ $[\text{M}-2\text{H}]^+$: 311.2230, found 311.2231.

2-(Bis(4-(dimethylamino)phenyl)methyl)-1,1-dimethylhydrazine (**33i**)



33i

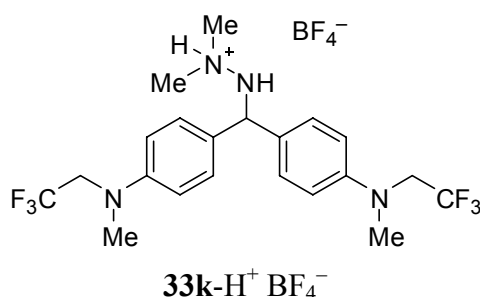
A solution of $(\text{dma})_2\text{CH}^+ \text{BF}_4^-$ (**16i**, 100 mg, 0.294 mmol) in acetonitrile (2 mL) was added to a solution of 1,1-dimethylhydrazine (**2**, 0.10 mL, 1.3 mmol) in acetonitrile (8 mL) over 5 min at RT. The solvent was removed under reduced pressure, the remaining solid was extracted with diethyl ether. Evaporation of the solvent gave **33i** (61.0 mg, 0.195 mmol, 66%) as colorless solid that turned blue under reduced pressure.

^1H NMR (400 MHz, CD_3CN): $\delta = 2.42$ (s, 6 H, $\text{NH}-\text{N}(\text{CH}_3)_2$), 2.85 (s, 12 H, $2 \times \text{N}(\text{CH}_3)_2$), 4.89 (s, 1 H, Ar_2CH), 6.67 (d, $J = 8.9$ Hz, 4 H, H_{ar}), 7.20 (d, $J = 8.9$ Hz, 4 H, H_{ar}).

^{13}C NMR (100 MHz, CD_3CN): $\delta = 41.0$ (q), 47.6 (q), 65.5 (d, Ar_2CH), 113.6 (d), 128.9 (d), 133.8 (s), 150.9 (s).

HR-MS (ESI, positive) : m/z calcd. for $\text{C}_{19}\text{H}_{27}\text{N}_4^+$ $[\text{M}-\text{H}]^+$: 311.2230, found 311.2231.

2-(Bis(4-(methyl(2,2,2-trifluoroethyl)amino)phenyl)methyl)-1,1-dimethylhydrazinium tetrafluoroborate (**33k-H⁺ BF₄⁻**)



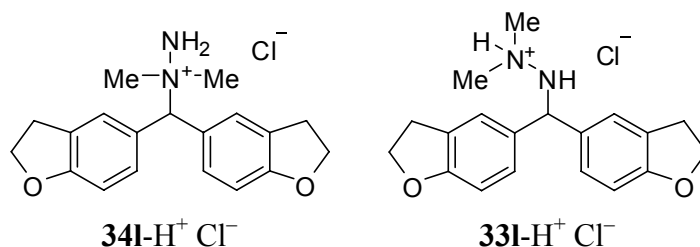
In an NMR tube, 1,1-dimethylhydrazine (**2**, 6.3 mg, 0.11 mmol) and (mfa)₂CH⁺BF₄⁻ (**16k**, 50 mg, 0.11 mmol) were mixed in CD₃CN (2 mL) and analyzed immediately by NMR spectroscopy.

¹H NMR (400 MHz, CD₃CN): δ = 2.98 (s, 6 H, ⁺N(CH₃)₂), 3.02 (s, 6 H, 2 × NCH₃), 4.00 (q, ³J_{H,F} = 9.3 Hz, 4 H, 2 × CH₂), 5.22 (s, 1 H, Ar₂CH), 6.84 (d, *J* = 8.9 Hz, 4 H, H_{ar}), 7.32 (d, *J* = 8.9 Hz, 4 H, H_{ar}).

¹³C NMR (100 MHz, CD₃CN): δ = 39.7 (q), 46.3 (q), 53.8 (qt, ²J_{C,F} = 32 Hz), 63.7 (d, Ar₂CH), 114.0 (d), 127.1 (q, ¹J_{C,F} = 281 Hz), 129.2 (d), 129.2 (s), 149.7 (s).

HR-MS (ESI, positive) : *m/z* calcd. for C₂₁H₂₅F₆N₂⁺ [M-2H]⁺: 447.1978, found 447.1977.

1-(Bis(2,3-dihydroxybenzofuran-5-yl)methyl)-1,1-dimethylhydrazinium chloride (**34I-H⁺ Cl⁻**) and 2-(bis(2,3-dihydroxybenzofuran-5-yl)methyl)-1,1-dimethylhydrazinium chloride (**33I-H⁺ Cl⁻**)



In an NMR tube, 1,1-dimethylhydrazine (**2**, 8.4 mg, 0.14 mmol) and (fur)₂CHCl (**16I-Cl**, 41 mg, 0.14 mmol) were mixed in CD₃CN (1.5 mL) at RT. Immediately after mixing, the solution was cooled down to -30 °C to obtain the NMR spectra of **34I-H⁺ Cl⁻** (containing < 5% **33I-H⁺ Cl⁻**).

34I-H⁺ Cl⁻:

¹H NMR (400 MHz, CD₃CN): δ = 3.17 (t, J = 8.8 Hz, 4 H, 2 \times CH₂CH₂O), 3.31 (s, 6 H, ⁺N(CH₃)₂), 4.54 (t, J = 9.4 Hz, 4 H, 2 \times CH₂CH₂O), 5.97 (brs, 2 H, NH₂), 6.26 (s, 1 H, Ar₂CH), 6.76 (d, J = 8.3 Hz, 2 H, H_{ar}), 7.57 (d, J = 8.3 Hz, 1.4 Hz, 2 H, H_{ar}), 7.76 (brs, 2 H, H_{ar}).

¹³C NMR (100 MHz, CD₃CN): δ = 29.6 (t), 55.1 (q), 72.5 (t), 82.0 (d, Ar₂CH), 109.8 (d), 125.8 (s), 128.2 (d), 129.6 (s), 132.1 (d), 161.7 (s).

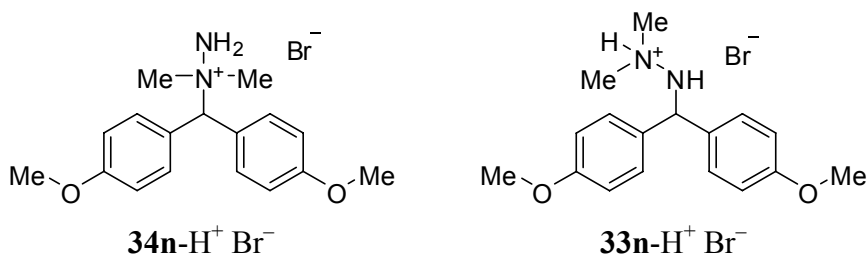
Repeating the reaction under analogous conditions but recording the ¹H NMR spectra 400 min after mixing **2** and **16I-Cl** at RT resulted in the observation of **33I-H⁺ Cl⁻**.

33I-H⁺ Cl⁻:

¹H NMR (400 MHz, CD₃CN): δ = 2.78 (s, 6 H, ⁺N(CH₃)₂), 3.16 (t, J = 8.8 Hz, 4 H, CH₂CH₂O), 4.51 (t, J = 8.7 Hz, 4 H, CH₂CH₂O), 5.59 (s, 1 H, Ar₂CH), 6.69 (d, J = 8.3 Hz, 2 H, H_{ar}), 7.20 (d, J = 8.3 Hz, 2 H, H_{ar}), 7.32 (s, 2 H, H_{ar}).

HR-MS (ESI, positive) : m/z calcd. for C₁₉H₂₃N₂O₂⁺: 311.1754, found 311.1758.

1-(Bis(4-methoxyphenyl)methyl)-1,1-dimethylhydrazinium bromide (**34n-H⁺ Br⁻**) and 2-(bis(4-methoxyphenyl)methyl)-1,1-dimethylhydrazinium bromide (**33n-H⁺ Br⁻**)



In an NMR tube, 1,1-dimethylhydrazine (**2**, 5.3 mg, 0.088 mmol) and (ani)₂CHBr (**16n-Br**, 27 mg, 0.088 mmol) were mixed in CD₃CN (1.5 mL). The NMR spectra of **34n-H⁺ Br⁻** (containing 5% **33n-H⁺ Br⁻**) were recorded shortly after mixing.

34n-H⁺ Br⁻:

¹H NMR (400 MHz, CD₃CN): δ = 3.36 (s, 6 H, ⁺N(CH₃)₂), 3.79 (s, 6 H, 2 \times OCH₃), 5.63 (brs, 2 H, NH₂), 6.40 (s, 1 H, Ar₂CH), 7.00 (d, J = 8.9 Hz, 4 H, H_{ar}), 7.85 (d, J = 8.9 Hz, 4 H, H_{ar}).

¹³C NMR (100 MHz, CD₃CN): δ = 55.9 (q), 56.1 (q), 82.5 (d, Ar₂CH), 115.4 (d), 126.0 (s), 133.5 (d), 161.7 (s).

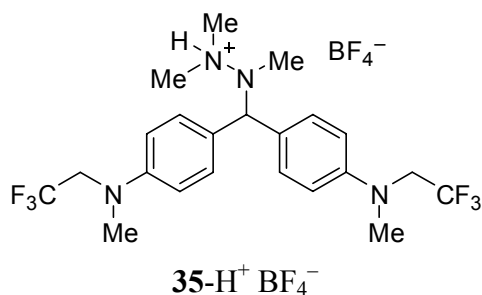
Repeating the reaction under analogous conditions but recording the ¹H NMR spectra 440 min after mixing **2** and **16n-Br** at RT resulted in a solution that contained **34n-H⁺ Br⁻** and **33n-H⁺ Br⁻** in a 77:23 ratio.

33n-H⁺ Br⁻:

¹H NMR (200 MHz, CD₃CN): δ = 2.41 (s, 6 H, ⁺N(CH₃)₂), 3.73 (s, 6 H, 2 \times OCH₃), 5.00 (s, 1 H, Ar₂CH), 7.00 (d, J = 9.0 Hz, 4 H, H_{ar}), 7.82 (d, J = 9.0 Hz, 4 H, H_{ar}).

HR-MS (ESI, positive) : m/z calcd. for C₁₇H₂₃N₂O₂⁺: 287.1754, found 287.1755.

2-(Bis(4-(methyl(2,2,2-trifluoroethyl)amino)phenyl)methyl)-1,1,2-trimethylhydrazinium tetrafluoroborate (**35-BF₄**)



In an NMR tube, trimethylhydrazine (**3**, 8.2 mg, 0.11 mmol) and (mfa)₂CH⁺BF₄⁻ (**16k**, 52 mg, 0.11 mmol) were mixed in CD₃CN (1.5 mL) and analyzed immediately by NMR spectroscopy.

^1H NMR (200 MHz, CD_3CN): δ = 2.40 (s, 3 H, NCH_3), 2.76 (s, 6 H, $^+\text{N}(\text{CH}_3)_2$), 3.00 (s, 6 H, $2 \times \text{N}(\text{CH}_3)\text{CH}_2\text{CF}_3$), 3.98 (q, $^3J_{\text{H,F}} = 9.3$ Hz, 4 H, CH_2), 4.71 (s, 1 H, Ar_2CH), 6.82 (d, $J = 8.9$ Hz, 4 H, H_{ar}), 7.34 (d, $J = 9.0$ Hz, 4 H, H_{ar}).

HR-MS (ESI, positive) : m/z calcd. for $\text{C}_{22}\text{H}_{29}\text{F}_6\text{N}_4^+$: 463.2291, found 463.2294.

4.4.4 Computational Details

The quantum-chemical computations reported in this work were carried out using the Gaussian 09 series of programs.^[55] Full geometry optimizations and vibrational analyses were performed at the IEF-PCM-B3LYP/6-31+G(d,p) level of theory in acetonitrile. The unscaled harmonic vibrational frequencies were used to calculate the thermal corrections to 298.15 K, which were applied to single point energies from IEF-PCM-MP2/6-311+G(2d,p) level calculations in acetonitrile (Radii = Bondi) to give H_{298} and G_{298} . The Boltzmann distribution was used to calculate the statistical weights of the single conformers and averaged energies were used for the calculations of the **16i**-affinities.

The archive entries of all stationary points are listed in the Appendix of this work.

Calculated Energies

Table 4.115. Single-point energies, enthalpies and free energies of the conformers of **1**, **2**, **10–15**, **38**, **43**, **48** and their adducts with **16i** at the IEF-PCM-MP2/6-311++G(2d,p)// IEF-PCM-B3LYP/6-31+G(d,p) level and their statistical weights according to the Boltzmann distribution (in Hartree).

| molecule (conformer) | E_{tot} | H_{298} | w_{Hi} | G_{298} | w_{Gi} |
|---|------------------|-------------|-----------------|-------------|-----------------|
| 1 (1) | -111.629164 | -111.571516 | 0.4911 | -111.597753 | 0.4827 |
| 1 (2) | -111.629164 | -111.571516 | 0.4911 | -111.597753 | 0.4827 |
| 1 (3) | -111.625027 | -111.568388 | 0.0179 | -111.595262 | 0.0345 |
| $\langle H_{298} \rangle = -111.571460$; $\langle G_{298} \rangle = -111.597667$ | | | | | |
| 16i-1 (1) | -879.462800 | -879.035539 | 0.1022 | -879.112335 | 0.2974 |
| 16i-1 (2) | -879.462271 | -879.035091 | 0.0635 | -879.111442 | 0.1154 |
| 16i-1 (3) | -879.462271 | -879.035090 | 0.0635 | -879.111426 | 0.1135 |
| 16i-1 (4) | -879.462355 | -879.035023 | 0.0591 | -879.110786 | 0.0576 |

Table 4.115 (continued).

| molecule (conformer) | E_{tot} | H_{298} | W_{H_i} | G_{298} | W_{G_i} |
|---|------------------|-------------|-----------|-------------|-----------|
| 16i-1 (5) | -879.462354 | -879.035022 | 0.0591 | -879.110783 | 0.0575 |
| 16i-1 (6) | -879.462293 | -879.034796 | 0.0465 | -879.110724 | 0.0540 |
| 16i-1 (7) | -879.462053 | -879.034782 | 0.0458 | -879.110720 | 0.0537 |
| 16i-1 (8) | -879.462053 | -879.034782 | 0.0458 | -879.110718 | 0.0536 |
| 16i-1 (9) | -879.462440 | -879.034917 | 0.0528 | -879.110597 | 0.0472 |
| 16i-1 (10) | -879.462059 | -879.034764 | 0.0449 | -879.110226 | 0.0318 |
| 16i-1 (11) | -879.462823 | -879.035302 | 0.0795 | -879.110089 | 0.0276 |
| 16i-1 (12) | -879.462589 | -879.035091 | 0.0635 | -879.109615 | 0.0167 |
| 16i-1 (13) | -879.462762 | -879.035164 | 0.0686 | -879.109591 | 0.0163 |
| 16i-1 (14) | -879.462451 | -879.034750 | 0.0443 | -879.109394 | 0.0132 |
| 16i-1 (15) | -879.461125 | -879.033710 | 0.0147 | -879.109204 | 0.0108 |
| 16i-1 (16) | -879.462492 | -879.034675 | 0.0409 | -879.109076 | 0.0094 |
| 16i-1 (17) | -879.461156 | -879.033610 | 0.0132 | -879.108366 | 0.0044 |
| 16i-1 (18) | -879.461863 | -879.034023 | 0.0205 | -879.108273 | 0.0040 |
| 16i-1 (19) | -879.461301 | -879.033519 | 0.0120 | -879.107764 | 0.0023 |
| 16i-1 (20) | -879.460914 | -879.033060 | 0.0074 | -879.107542 | 0.0019 |
| 16i-1 (21) | -879.460938 | -879.033225 | 0.0088 | -879.107509 | 0.0018 |
| 16i-1 (22) | -879.460924 | -879.033106 | 0.0078 | -879.107492 | 0.0018 |
| 16i-1 (23) | -879.461135 | -879.033399 | 0.0106 | -879.107486 | 0.0017 |
| 16i-1 (24) | -879.458987 | -879.031721 | 0.0018 | -879.107217 | 0.0013 |
| 16i-1 (25) | -879.460843 | -879.033073 | 0.0075 | -879.107205 | 0.0013 |
| 16i-1 (26) | -879.459150 | -879.031735 | 0.0018 | -879.106722 | 0.0008 |
| 16i-1 (27) | -879.459328 | -879.031940 | 0.0023 | -879.106407 | 0.0006 |
| 16i-1 (28) | -879.459328 | -879.031940 | 0.0023 | -879.106406 | 0.0006 |
| 16i-1 (29) | -879.459400 | -879.031909 | 0.0022 | -879.106183 | 0.0004 |
| 16i-1 (30) | -879.459399 | -879.031908 | 0.0022 | -879.106182 | 0.0004 |
| 16i-1 (31) | -879.459000 | -879.031384 | 0.0013 | -879.105738 | 0.0003 |
| 16i-1 (32) | -879.458707 | -879.031225 | 0.0011 | -879.105727 | 0.0003 |
| 16i-1 (33) | -879.458702 | -879.031187 | 0.0010 | -879.105308 | 0.0002 |
| 16i-1 (34) | -879.459221 | -879.031323 | 0.0012 | -879.105020 | 0.0001 |
| 16i-1 (35) | -879.456938 | -879.029323 | 0.0001 | -879.104713 | 0.0001 |
| 16i-1 (36) | -879.456961 | -879.029427 | 0.0002 | -879.104526 | 0.0001 |
| $\langle H_{298} \rangle = -879.034832$; $\langle G_{298} \rangle = -879.111169$ | | | | | |
| 2 (1) | -190.019486 | -189.904081 | 0.4880 | -189.937383 | 0.4812 |
| 2 (2) | -190.019486 | -189.904081 | 0.4880 | -189.937383 | 0.4812 |
| 2 (3) | -190.016614 | -189.901237 | 0.0240 | -189.934977 | 0.0376 |
| $\langle H_{298} \rangle = -189.904013$; $\langle G_{298} \rangle = -189.937292$ | | | | | |
| 16i-2 (1) | -957.8509208 | -957.365506 | 0.1640 | -957.446342 | 0.2770 |
| 16i-2 (2) | -957.8509123 | -957.365275 | 0.1285 | -957.445603 | 0.1267 |
| 16i-2 (3) | -957.8508426 | -957.365325 | 0.1354 | -957.445512 | 0.1150 |

Table 4.115 (continued).

| molecule (conformer) | E_{tot} | H_{298} | W_{H_i} | G_{298} | W_{G_i} |
|---|------------------|-------------|-----------|-------------|-----------|
| 16i-2 (4) | -957.8499770 | -957.364349 | 0.0482 | -957.445511 | 0.1149 |
| 16i-2 (5) | -957.8510673 | -957.365371 | 0.1423 | -957.445031 | 0.0691 |
| 16i-2 (6) | -957.8500882 | -957.364552 | 0.0598 | -957.444906 | 0.0605 |
| 16i-2 (7) | -957.8499795 | -957.364097 | 0.0369 | -957.444397 | 0.0353 |
| 16i-2 (8) | -957.8500801 | -957.364207 | 0.0415 | -957.444207 | 0.0289 |
| 16i-2 (9) | -957.8499124 | -957.364165 | 0.0397 | -957.444113 | 0.0261 |
| 16i-2 (10) | -957.8500019 | -957.364217 | 0.0419 | -957.443836 | 0.0195 |
| 16i-2 (11) | -957.8475693 | -957.362597 | 0.0075 | -957.443817 | 0.0191 |
| 16i-2 (12) | -957.8475693 | -957.362597 | 0.0075 | -957.443817 | 0.0191 |
| 16i-2 (13) | -957.8476350 | -957.362571 | 0.0073 | -957.443185 | 0.0098 |
| 16i-2 (14) | -957.8476347 | -957.362571 | 0.0073 | -957.443185 | 0.0098 |
| 16i-2 (15) | -957.8498318 | -957.363862 | 0.0288 | -957.442957 | 0.0077 |
| 16i-2 (16) | -957.8499403 | -957.363925 | 0.0308 | -957.442888 | 0.0071 |
| 16i-2 (17) | -957.8478230 | -957.362382 | 0.0060 | -957.442823 | 0.0067 |
| 16i-2 (18) | -957.8475856 | -957.362530 | 0.0070 | -957.442683 | 0.0057 |
| 16i-2 (19) | -957.8475856 | -957.362530 | 0.0070 | -957.442682 | 0.0057 |
| 16i-2 (20) | -957.8478855 | -957.362498 | 0.0068 | -957.442675 | 0.0057 |
| 16i-2 (21) | -957.8476226 | -957.362491 | 0.0067 | -957.442578 | 0.0051 |
| 16i-2 (22) | -957.8476226 | -957.362491 | 0.0067 | -957.442578 | 0.0051 |
| 16i-2 (23) | -957.8478278 | -957.362272 | 0.0053 | -957.442575 | 0.0051 |
| 16i-2 (24) | -957.8479426 | -957.362362 | 0.0059 | -957.441894 | 0.0025 |
| 16i-2 (25) | -957.8472081 | -957.361566 | 0.0025 | -957.441610 | 0.0018 |
| 16i-2 (26) | -957.8472081 | -957.361566 | 0.0025 | -957.441610 | 0.0018 |
| 16i-2 (27) | -957.8471381 | -957.361584 | 0.0026 | -957.441563 | 0.0018 |
| 16i-2 (28) | -957.8471381 | -957.361584 | 0.0026 | -957.441562 | 0.0018 |
| 16i-2 (29) | -957.8473126 | -957.361698 | 0.0029 | -957.441512 | 0.0017 |
| 16i-2 (30) | -957.8473126 | -957.361698 | 0.0029 | -957.441512 | 0.0017 |
| 16i-2 (31) | -957.8473655 | -957.361591 | 0.0026 | -957.441105 | 0.0011 |
| 16i-2 (32) | -957.8473655 | -957.361591 | 0.0026 | -957.441105 | 0.0011 |
| 16i-2 (33) | -957.8370146 | -957.351349 | 0.0000 | -957.431326 | 0.0000 |
| 16i-2 (34) | -957.8367081 | -957.351100 | 0.0000 | -957.431273 | 0.0000 |
| 16i-2 (35) | -957.8367805 | -957.351127 | 0.0000 | -957.430632 | 0.0000 |
| 16i-2 (36) | -957.8369151 | -957.350994 | 0.0000 | -957.430454 | 0.0000 |
| $\langle H_{298} \rangle = -957.364684$; $\langle G_{298} \rangle = -957.445216$ | | | | | |
| 10 (1) | -131.468674 | -131.424414 | 0.9048 | -131.451296 | 0.9274 |
| 10 (2) | -131.466535 | -131.422289 | 0.0952 | -131.448891 | 0.0726 |
| $\langle H_{298} \rangle = -131.424212$; $\langle G_{298} \rangle = -131.451122$ | | | | | |
| 16i-10 (1) | -899.290983 | -898.877424 | 0.0250 | -898.953698 | 0.1029 |
| 16i-10 (2) | -899.291147 | -898.877461 | 0.0260 | -898.953401 | 0.0751 |
| 16i-10 (3) | -899.292356 | -898.878417 | 0.0715 | -898.953330 | 0.0697 |

Table 4.115 (continued).

| molecule (conformer) | E_{tot} | H_{298} | W_{H_i} | G_{298} | W_{G_i} |
|---|------------------|-------------|-----------|-------------|-----------|
| 16i-10 (4) | -899.292625 | -898.878729 | 0.0995 | -898.953292 | 0.0670 |
| 16i-10 (5) | -899.292625 | -898.878729 | 0.0995 | -898.953288 | 0.0667 |
| 16i-10 (6) | -899.291456 | -898.877671 | 0.0324 | -898.953275 | 0.0657 |
| 16i-10 (7) | -899.292572 | -898.878504 | 0.0784 | -898.953271 | 0.0654 |
| 16i-10 (8) | -899.291923 | -898.878199 | 0.0567 | -898.953246 | 0.0637 |
| 16i-10 (9) | -899.291887 | -898.878218 | 0.0579 | -898.953203 | 0.0609 |
| 16i-10 (10) | -899.292426 | -898.878410 | 0.0710 | -898.952734 | 0.0371 |
| 16i-10 (11) | -899.292426 | -898.878410 | 0.0710 | -898.952734 | 0.0371 |
| 16i-10 (12) | -899.291354 | -898.877421 | 0.0249 | -898.952729 | 0.0369 |
| 16i-10 (13) | -899.291312 | -898.877469 | 0.0262 | -898.952701 | 0.0358 |
| 16i-10 (14) | -899.291275 | -898.877468 | 0.0262 | -898.952682 | 0.0351 |
| 16i-10 (15) | -899.291500 | -898.877468 | 0.0262 | -898.952001 | 0.0170 |
| 16i-10 (16) | -899.291500 | -898.877468 | 0.0262 | -898.952000 | 0.0170 |
| 16i-10 (17) | -899.290887 | -898.877231 | 0.0204 | -898.951998 | 0.0170 |
| 16i-10 (18) | -899.290715 | -898.877072 | 0.0172 | -898.951960 | 0.0163 |
| 16i-10 (19) | -899.290715 | -898.877072 | 0.0172 | -898.951960 | 0.0163 |
| 16i-10 (20) | -899.291383 | -898.877444 | 0.0255 | -898.951959 | 0.0163 |
| 16i-10 (21) | -899.290779 | -898.877025 | 0.0164 | -898.951761 | 0.0132 |
| 16i-10 (22) | -899.290779 | -898.877025 | 0.0164 | -898.951760 | 0.0132 |
| 16i-10 (23) | -899.290404 | -898.876286 | 0.0075 | -898.951713 | 0.0126 |
| 16i-10 (24) | -899.290556 | -898.876560 | 0.0100 | -898.951371 | 0.0088 |
| 16i-10 (25) | -899.290500 | -898.876342 | 0.0079 | -898.950930 | 0.0055 |
| 16i-10 (26) | -899.288954 | -898.875260 | 0.0025 | -898.950787 | 0.0047 |
| 16i-10 (27) | -899.290539 | -898.876498 | 0.0094 | -898.950692 | 0.0043 |
| 16i-10 (28) | -899.290668 | -898.876527 | 0.0097 | -898.950578 | 0.0038 |
| 16i-10 (29) | -899.290291 | -898.876060 | 0.0059 | -898.950545 | 0.0037 |
| 16i-10 (30) | -899.290284 | -898.876172 | 0.0066 | -898.950520 | 0.0036 |
| 16i-10 (31) | -899.289015 | -898.875133 | 0.0022 | -898.950305 | 0.0028 |
| 16i-10 (32) | -899.289235 | -898.875408 | 0.0030 | -898.950121 | 0.0023 |
| 16i-10 (33) | -899.289208 | -898.875519 | 0.0033 | -898.950024 | 0.0021 |
| 16i-10 (34) | -899.288097 | -898.873995 | 0.0007 | -898.948368 | 0.0004 |
| $\langle H_{298} \rangle = -898.877970$; $\langle G_{298} \rangle = -898.952930$ | | | | | |
| 11 (1) | -170.6634816 | -170.590090 | 0.8415 | -170.620655 | 0.8925 |
| 11 (2) | -170.6618875 | -170.588514 | 0.1585 | -170.618657 | 0.1075 |
| $\langle H_{298} \rangle = -170.589840$; $\langle G_{298} \rangle = -170.620440$ | | | | | |
| 16i-11 (1) | -938.494727 | -938.052070 | 0.1733 | -938.129916 | 0.2480 |
| 16i-11 (2) | -938.494689 | -938.051966 | 0.1552 | -938.129652 | 0.1875 |
| 16i-11 (3) | -938.494836 | -938.052133 | 0.1851 | -938.129559 | 0.1698 |
| 16i-11 (4) | -938.494804 | -938.052040 | 0.1677 | -938.129432 | 0.1485 |
| 16i-11 (5) | -938.493628 | -938.050657 | 0.0388 | -938.128352 | 0.0473 |

Table 4.115 (continued).

| molecule (conformer) | E_{tot} | H_{298} | W_{H_i} | G_{298} | W_{G_i} |
|---|------------------|-------------|-----------|-------------|-----------|
| 16i-11 (6) | -938.493541 | -938.050637 | 0.0380 | -938.128102 | 0.0363 |
| 16i-11 (7) | -938.493666 | -938.050869 | 0.0486 | -938.128029 | 0.0336 |
| 16i-11 (8) | -938.493738 | -938.050888 | 0.0495 | -938.127999 | 0.0325 |
| 16i-11 (9) | -938.492565 | -938.049802 | 0.0157 | -938.127689 | 0.0234 |
| 16i-11 (10) | -938.492128 | -938.049675 | 0.0137 | -938.127059 | 0.0120 |
| 16i-11 (11) | -938.492442 | -938.049436 | 0.0106 | -938.126945 | 0.0107 |
| 16i-11 (12) | -938.491891 | -938.049353 | 0.0097 | -938.126473 | 0.0065 |
| 16i-11 (13) | -938.492647 | -938.049771 | 0.0152 | -938.126373 | 0.0058 |
| 16i-11 (14) | -938.492458 | -938.049272 | 0.0089 | -938.126281 | 0.0053 |
| 16i-11 (15) | -938.491879 | -938.049301 | 0.0092 | -938.126153 | 0.0046 |
| 16i-11 (16) | -938.492640 | -938.049550 | 0.0120 | -938.126077 | 0.0043 |
| 16i-11 (17) | -938.491224 | -938.048234 | 0.0030 | -938.125913 | 0.0036 |
| 16i-11 (18) | -938.491229 | -938.048303 | 0.0032 | -938.125796 | 0.0032 |
| 16i-11 (19) | -938.492623 | -938.049306 | 0.0093 | -938.125731 | 0.0029 |
| 16i-11 (20) | -938.491333 | -938.048387 | 0.0035 | -938.125690 | 0.0028 |
| 16i-11 (21) | -938.492584 | -938.049239 | 0.0086 | -938.125641 | 0.0027 |
| 16i-11 (22) | -938.491371 | -938.048358 | 0.0034 | -938.125472 | 0.0022 |
| 16i-11 (23) | -938.492708 | -938.049420 | 0.0105 | -938.125433 | 0.0021 |
| 16i-11 (24) | -938.490096 | -938.047157 | 0.0010 | -938.124621 | 0.0009 |
| 16i-11 (25) | -938.490451 | -938.047178 | 0.0010 | -938.124257 | 0.0006 |
| 16i-11 (26) | -938.488336 | -938.045614 | 0.0002 | -938.124208 | 0.0006 |
| 16i-11 (27) | -938.490595 | -938.047332 | 0.0011 | -938.124051 | 0.0005 |
| 16i-11 (28) | -938.490651 | -938.047396 | 0.0012 | -938.124000 | 0.0005 |
| 16i-11 (29) | -938.490773 | -938.047487 | 0.0014 | -938.123731 | 0.0004 |
| 16i-11 (30) | -938.489750 | -938.046730 | 0.0006 | -938.123474 | 0.0003 |
| 16i-11 (31) | -938.488262 | -938.045588 | 0.0002 | -938.123415 | 0.0003 |
| 16i-11 (32) | -938.488937 | -938.046007 | 0.0003 | -938.122370 | 0.0001 |
| 16i-11 (33) | -938.487637 | -938.044751 | 0.0001 | -938.121955 | 0.0001 |
| 16i-11 (34) | -938.487849 | -938.044924 | 0.0001 | -938.121716 | 0.0000 |
| 16i-11 (35) | -938.487362 | -938.044535 | 0.0001 | -938.121566 | 0.0000 |
| 16i-11 (36) | -938.488488 | -938.045468 | 0.0002 | -938.121501 | 0.0000 |
| $\langle H_{298} \rangle = -938.051432$; $\langle G_{298} \rangle = -938.129147$ | | | | | |
| 12 | -56.436087 | -56.398037 | | -56.419885 | |
| 16i-12 (1) | -824.263035 | -823.853891 | 0.2575 | -823.925708 | 0.3444 |
| 16i-12 (2) | -824.263070 | -823.853752 | 0.2224 | -823.925352 | 0.2364 |
| 16i-12 (3) | -824.263014 | -823.853912 | 0.2633 | -823.925329 | 0.2305 |
| 16i-12 (4) | -824.263141 | -823.853888 | 0.2568 | -823.925139 | 0.1886 |
| $\langle H_{298} \rangle = -823.853865$; $\langle G_{298} \rangle = -823.925429$ | | | | | |

Table 4.115 (continued).

| molecule (conformer) | E_{tot} | H_{298} | W_{Hi} | G_{298} | W_{Gi} |
|---|------------------|-------------|----------|-------------|----------|
| 13 | -95.619892 | -95.551595 | | -95.578895 | |
| 16i-13 (1) | -863.458117 | -863.019553 | 0.1343 | -863.095437 | 0.3038 |
| 16i-13 (2) | -863.458397 | -863.019760 | 0.1673 | -863.095053 | 0.2023 |
| 16i-13 (3) | -863.458181 | -863.019300 | 0.1028 | -863.094560 | 0.1200 |
| 16i-13 (4) | -863.458361 | -863.019522 | 0.1301 | -863.094504 | 0.1132 |
| 16i-13 (5) | -863.458237 | -863.019246 | 0.0971 | -863.094093 | 0.0732 |
| 16i-13 (6) | -863.458498 | -863.019639 | 0.1472 | -863.094022 | 0.0679 |
| 16i-13 (7) | -863.458360 | -863.019392 | 0.1133 | -863.093905 | 0.0600 |
| 16i-13 (8) | -863.458337 | -863.019322 | 0.1052 | -863.093874 | 0.0580 |
| 16i-13 (9) | -863.453329 | -863.014390 | 0.0006 | -863.089406 | 0.0005 |
| 16i-13 (10) | -863.453434 | -863.014480 | 0.0006 | -863.089210 | 0.0004 |
| 16i-13 (11) | -863.453678 | -863.014692 | 0.0008 | -863.089009 | 0.0003 |
| 16i-13 (12) | -863.453667 | -863.014631 | 0.0007 | -863.088952 | 0.0003 |
| $\langle H_{298} \rangle = -863.019484$; $\langle G_{298} \rangle = -863.094761$ | | | | | |
| 14 | -134.810515 | -134.712946 | | -134.743742 | |
| 16i-14 (1) | -902.656027 | -902.187855 | 0.2715 | -902.264660 | 0.3772 |
| 16i-14 (2) | -902.655929 | -902.187714 | 0.2340 | -902.264248 | 0.2440 |
| 16i-14 (3) | -902.656050 | -902.187728 | 0.2373 | -902.263833 | 0.1571 |
| 16i-14 (4) | -902.655982 | -902.187637 | 0.2156 | -902.263758 | 0.1451 |
| 16i-14 (5) | -902.652134 | -902.184083 | 0.0050 | -902.261569 | 0.0143 |
| 16i-14 (6) | -902.652133 | -902.184082 | 0.0050 | -902.261568 | 0.0143 |
| 16i-14 (7) | -902.652203 | -902.184091 | 0.0050 | -902.261563 | 0.0142 |
| 16i-14 (8) | -902.652203 | -902.184091 | 0.0050 | -902.261562 | 0.0142 |
| 16i-14 (9) | -902.652368 | -902.184188 | 0.0056 | -902.260588 | 0.0051 |
| 16i-14 (10) | -902.652368 | -902.184188 | 0.0056 | -902.260588 | 0.0051 |
| 16i-14 (11) | -902.652337 | -902.184118 | 0.0052 | -902.260535 | 0.0048 |
| 16i-14 (12) | -902.652336 | -902.184117 | 0.0052 | -902.260534 | 0.0048 |
| $\langle H_{298} \rangle = -902.187590$; $\langle G_{298} \rangle = -902.264042$ | | | | | |
| 15 | -174.001616 | -173.875272 | | -173.908905 | |
| 16i-15 (1) | -941.848989 | -941.351917 | 0.2543 | -941.430584 | 0.3174 |
| 16i-15 (2) | -941.849150 | -941.352015 | 0.2823 | -941.430415 | 0.2655 |
| 16i-15 (3) | -941.848987 | -941.351777 | 0.2193 | -941.430283 | 0.2308 |
| 16i-15 (4) | -941.849169 | -941.351878 | 0.2440 | -941.430081 | 0.1863 |
| $\langle H_{298} \rangle = -941.351904$; $\langle G_{298} \rangle = -941.430376$ | | | | | |

Table 4.115 (continued).

| molecule (conformer) | E_{tot} | H_{298} | W_{Hi} | G_{298} | W_{Gi} |
|---|------------------|--------------|----------|--------------|----------|
| 38 | -213.241999 | -213.086307 | | -213.122951 | |
| 16i-38 (1) | -981.078843 | -980.552675 | 0.2063 | -980.637475 | 0.5904 |
| 16i-38 (2) | -981.078814 | -980.552435 | 0.1598 | -980.636032 | 0.1279 |
| 16i-38 (3) | -981.078411 | -980.552018 | 0.1028 | -980.635741 | 0.0941 |
| 16i-38 (4) | -981.078859 | -980.552387 | 0.1521 | -980.635496 | 0.0726 |
| 16i-38 (5) | -981.078862 | -980.552322 | 0.1419 | -980.635274 | 0.0574 |
| 16i-38 (6) | -981.078519 | -980.551957 | 0.0964 | -980.634387 | 0.0224 |
| 16i-38 (7) | -981.078364 | -980.551659 | 0.0703 | -980.634159 | 0.0176 |
| 16i-38 (8) | -981.078364 | -980.551659 | 0.0703 | -980.634159 | 0.0176 |
| 16i-38 (9) | -981.067669 | -980.541199 | 0.0000 | -980.623484 | 0.0000 |
| 16i-38 (10) | -981.067575 | -980.540993 | 0.0000 | -980.623403 | 0.0000 |
| 16i-38 (11) | -981.067755 | -980.541234 | 0.0000 | -980.623330 | 0.0000 |
| 16i-38 (12) | -981.067651 | -980.541079 | 0.0000 | -980.623206 | 0.0000 |
| $\langle H_{298} \rangle = -980.552263$; $\langle G_{298} \rangle = -980.636672$ | | | | | |
| 43 | -286.882284 | -286.758709 | | -286.794594 | |
| 16i-43 (1) | -1054.708123 | -1054.214154 | 0.1341 | -1054.297298 | 0.2179 |
| 16i-43 (2) | -1054.708158 | -1054.214306 | 0.1576 | -1054.297069 | 0.1711 |
| 16i-43 (3) | -1054.708057 | -1054.214067 | 0.1223 | -1054.296883 | 0.1404 |
| 16i-43 (4) | -1054.708071 | -1054.214010 | 0.1152 | -1054.296730 | 0.1195 |
| 16i-43 (5) | -1054.707979 | -1054.213812 | 0.0934 | -1054.296417 | 0.0858 |
| 16i-43 (6) | -1054.708056 | -1054.213827 | 0.0949 | -1054.296057 | 0.0585 |
| 16i-43 (7) | -1054.708084 | -1054.213926 | 0.1053 | -1054.296024 | 0.0565 |
| 16i-43 (8) | -1054.708048 | -1054.213824 | 0.0946 | -1054.295828 | 0.0459 |
| 16i-43 (9) | -1054.705866 | -1054.212441 | 0.0219 | -1054.295661 | 0.0385 |
| 16i-43 (10) | -1054.706028 | -1054.212605 | 0.0260 | -1054.295403 | 0.0293 |
| 16i-43 (11) | -1054.705886 | -1054.212259 | 0.0180 | -1054.294993 | 0.0190 |
| 16i-43 (12) | -1054.705952 | -1054.212186 | 0.0167 | -1054.294923 | 0.0176 |
| $\langle H_{298} \rangle = -1054.213888$; $\langle G_{298} \rangle = -1054.296641$ | | | | | |
| 48 | -432.163745 | -432.086991 | 0.6457 | -432.123778 | 0.5956 |
| | -432.162470 | -432.085769 | 0.1772 | -432.122757 | 0.2022 |
| | -432.162470 | -432.085769 | 0.1772 | -432.122757 | 0.2022 |
| $\langle H_{298} \rangle = -432.086558$; $\langle G_{298} \rangle = -432.123365$ | | | | | |
| 16i-48 (1) | -1199.987531 | -1199.540428 | 0.1155 | -1199.625729 | 0.3941 |
| 16i-48 (2) | -1199.987543 | -1199.540501 | 0.1247 | -1199.624649 | 0.1255 |
| 16i-48 (3) | -1199.987283 | -1199.540428 | 0.1155 | -1199.624324 | 0.0890 |
| 16i-48 (4) | -1199.987249 | -1199.540382 | 0.1100 | -1199.624287 | 0.0856 |

Table 4.115 (continued).

| molecule (conformer) | E_{tot} | H_{298} | W_{H_i} | G_{298} | W_{G_i} |
|-------------------------|------------------|--------------|-----------|--------------|-----------|
| 16i-48 (5) | -1199.987341 | -1199.540450 | 0.1182 | -1199.624285 | 0.0854 |
| 16i-48 (6) | -1199.987311 | -1199.540413 | 0.1136 | -1199.624031 | 0.0652 |
| 16i-48 (7) | -1199.986939 | -1199.539813 | 0.0602 | -1199.623112 | 0.0247 |
| 16i-48 (8) | -1199.986879 | -1199.539666 | 0.0515 | -1199.622912 | 0.0199 |
| 16i-48 (9) | -1199.985603 | -1199.538638 | 0.0173 | -1199.622759 | 0.0170 |
| 16i-48 (10) | -1199.985603 | -1199.538638 | 0.0173 | -1199.622759 | 0.0170 |
| 16i-48 (11) | -1199.986152 | -1199.539376 | 0.0379 | -1199.622652 | 0.0151 |
| 16i-48 (12) | -1199.986152 | -1199.539376 | 0.0379 | -1199.622652 | 0.0151 |
| 16i-48 (13) | -1199.985717 | -1199.538645 | 0.0175 | -1199.622287 | 0.0103 |
| 16i-48 (14) | -1199.985717 | -1199.538645 | 0.0175 | -1199.622287 | 0.0103 |
| 16i-48 (15) | -1199.985574 | -1199.538556 | 0.0159 | -1199.622175 | 0.0091 |
| 16i-48 (16) | -1199.985574 | -1199.538556 | 0.0159 | -1199.622175 | 0.0091 |
| 16i-48 (17) | -1199.982839 | -1199.535950 | 0.0010 | -1199.619988 | 0.0009 |
| 16i-48 (18) | -1199.982738 | -1199.536035 | 0.0011 | -1199.619817 | 0.0008 |
| 16i-48 (19) | -1199.982738 | -1199.536035 | 0.0011 | -1199.619815 | 0.0008 |
| 16i-48 (20) | -1199.982957 | -1199.536096 | 0.0012 | -1199.619803 | 0.0007 |
| 16i-48 (21) | -1199.982860 | -1199.536127 | 0.0012 | -1199.619581 | 0.0006 |
| 16i-48 (22) | -1199.982860 | -1199.536127 | 0.0012 | -1199.619580 | 0.0006 |
| 16i-48 (23) | -1199.982875 | -1199.536129 | 0.0012 | -1199.619564 | 0.0006 |
| 16i-48 (24) | -1199.982875 | -1199.536129 | 0.0012 | -1199.619564 | 0.0006 |
| 16i-48 (25) | -1199.982787 | -1199.535829 | 0.0009 | -1199.619559 | 0.0006 |
| 16i-48 (26) | -1199.982963 | -1199.536212 | 0.0013 | -1199.619515 | 0.0005 |
| 16i-48 (27) | -1199.982963 | -1199.536212 | 0.0013 | -1199.619515 | 0.0005 |
| 16i-48 (28) | -1199.982950 | -1199.535923 | 0.0010 | -1199.619348 | 0.0005 |
| 16i-48 (29) | -1199.978876 | -1199.532262 | 0.0000 | -1199.616029 | 0.0000 |
| 16i-48 (30) | -1199.978876 | -1199.532262 | 0.0000 | -1199.616029 | 0.0000 |
| 16i-48 (31) | -1199.978637 | -1199.531907 | 0.0000 | -1199.615768 | 0.0000 |
| 16i-48 (32) | -1199.978637 | -1199.531907 | 0.0000 | -1199.615767 | 0.0000 |
| 16i-48 (33) | -1199.978630 | -1199.531879 | 0.0000 | -1199.615630 | 0.0000 |
| 16i-48 (34) | -1199.978630 | -1199.531879 | 0.0000 | -1199.615630 | 0.0000 |
| 16i-48 (35) | -1199.978860 | -1199.532155 | 0.0000 | -1199.615578 | 0.0000 |
| 16i-48 (36) | -1199.978860 | -1199.532155 | 0.0000 | -1199.615577 | 0.0000 |

$\langle H_{298} \rangle = -1199.540032$; $\langle G_{298} \rangle = -1199.624614$

4.5 References

- [1] J. O. Edwards, R. G. Pearson, *J. Am. Chem. Soc.* **1962**, *84*, 16–24.
 [2] a) V. Gold, *Pure Appl. Chem.* **1979**, *51*, 1725–1801; b) P. Muller, *Pure Appl. Chem.* **1994**, *66*, 1077–1184.

- [3] S. Hoz, E. Buncel, E. *Isr. J. Chem.* **1985**, *26*, 313–319.
- [4] I.-H Um, L.-R. Im, E. Buncel, *J. Org. Chem.* **2010**, *75*, 8571–8577.
- [5] a) E. Buncel, I.-H. Um, *Tetrahedron* **2004**, *60*, 7801–7825; b) A. P. Grekov, V. Y. Veselov, *Russ. Chem. Rev.* **1978**, *47*, 631–648; c) N. J. Fina, J. O. Edwards, *Int. J. Chem. Kinet.* **1973**, *5*, 1–26; d) W. P. Jencks, *Catalysis in Chemistry and Enzymology*, McGraw-Hill, New York, **1969**, pp. 107–110.
- [6] Selected examples: (a) A. J. Kirby, A. M. Manfredi, B. S. Souza, M. Medeiros, J. P. Priebe, T. A. S. Brandão, F. Nome, *ARKIVOC* **2009**, *iii*, 28–38; b) X. Han, V. K. Balakrishnan, G. W. vanLoon, E. Buncel, *Langmuir* **2006**, *22*, 9009–9017; c) F. Terrier, P. Rodriguez-Dafonte, E. Le Guével, G. Moutiers, *Org. Biomol. Chem.* **2006**, *4*, 4352–4363; d) N. I. Yanchuk, *Russ. J. Gen. Chem.* **2006**, 1240–1242; e) I.-H. Um, S.-J. Hwang, E. Buncel, *J. Org. Chem.* **2006**, *71*, 915–920; f) I.-H. Um, E.-J. Lee, J.-A. Seok, K.-H. Kim, *J. Org. Chem.* **2005**, *70*, 7530–7536; g) G. Moutiers, E. Le Guével, C. Cannes, F. Terrier, E. Buncel, *Eur. J. Org. Chem.* **2001**, 3279–3284; h) I.-H. Um, E. Buncel, *J. Org. Chem.* **2000**, *65*, 577–582; i) I.-H. Um, J.-Y. Hong, E. Buncel, *Chem. Commun.* **2001**, 27–28; j) S. Oae, Y. Kadoma, *Phosphorus, Sulfur Silicon* **1997**, *123*, 293–300; k) S. Oae, Y. Kadoma, *Can. J. Chem.* **1986**, *64*, 1184–1188; l) C. F. Bernasconi, C. J. Murray, *J. Am. Chem. Soc.* **1986**, *108*, 5251–5257; m) D. J. Palling, W. P. Jencks, *J. Am. Chem. Soc.* **1984**, *106*, 4869–4876; n) J. J. Morris, M. I. Page, *J. Chem. Soc. Perkin Trans. 2* **1980**, 220–224; o) C. D. Ritchie, R. J. Minasz, A. A. Kamego, M. Sawada, *J. Am. Chem. Soc.* **1977**, *99*, 3747–3753; p) C. D. Ritchie, P. O. I. Virtanen, *J. Am. Chem. Soc.* **1973**, *95*, 1882–1889; q) J. E. Dixon, T. C. Bruice, *J. Am. Chem. Soc.* **1972**, *94*, 2052–2056; r) J. E. Dixon, T. C. Bruice, *J. Am. Chem. Soc.* **1971**, *93*, 6592–6597; s) J. E. Dixon, T. C. Bruice, *J. Am. Chem. Soc.* **1971**, *93*, 3248–3254; t) G. Klopman, K. Tsuda, J. B. Louis, R. E. Davis, *Tetrahedron* **1970**, *26*, 4549–4554; u) G. M. Blackburn, W. P. Jencks, *J. Am. Chem. Soc.* **1968**, *90*, 2638–2645; v) M. J. Gregory, T. C. Bruice, *J. Am. Chem. Soc.* **1967**, *89*, 4400–4402; w) M. J. Gregory, T. C. Bruice, *J. Am. Chem. Soc.* **1967**, *89*, 2327–2330; x) T. C. Bruice, A. Donzel, R. W. Huffman, A. R. Butler, *J. Am. Chem. Soc.* **1967**, *89*, 2106–2121; y) W. P. Jencks, J. Carriuolo, *J. Am. Chem. Soc.* **1960**, *82*, 675–681; z) W. P. Jencks, J. Carriuolo, *J. Am. Chem. Soc.* **1960**, *82*, 1778–1786.
- [7] Y. Ren, H. Yamataka, *J. Org. Chem.* **2007**, *72*, 5660–5667.

- [8] a) J. M. Garver, S. Gronert, V. M. Bierbaum, *J. Am. Chem. Soc.* **2011**, *133*, 13894–13897; b) S. M. Villano, N. Eyet, W. C. Lineberger, V. M. Bierbaum, *J. Am. Chem. Soc.* **2009**, *131*, 8227–8233; c) A. M. McAnoy, M. R. L. Paine, S. J. Blanksby, *Org. Biomol. Chem.* **2008**, *6*, 2316–2326; d) C. H. DePuy, E. W. Della, J. Filley, J. J. Grabowski, V. M. Bierbaum, *J. Am. Chem. Soc.* **1983**, *105*, 2481–2482.
- [9] a) D. J. Mazera, J. R. Pliego, Jr., G. I. Almerindo, J. C. Gesser, *J. Braz. Chem. Soc.* **2011**, *22*, 2165–2170; b) X.-G. Wei, X.-M. Sun, X.-P. Wu, Y. Ren, N.-B. Wong, W.-K. Li, *J. Org. Chem.* **2010**, *75*, 4212–4217; c) Y. Ren, H. Yamataka, *J. Comput. Chem.* **2008**, *30*, 358–365; d) Y. Ren, H. Yamataka, *Chem. Eur. J.* **2007**, *13*, 677–682; e) E. V. Patterson, K. R. Fountain, *J. Org. Chem.* **2006**, *71*, 8121–8125; f) Y. Ren, H. Yamataka, *Org. Lett.* **2006**, *8*, 119–121; g) R. F. Hudson, D. P. Hansell, S. Wolfe, D. J. Mitchell, *J. Chem. Soc. Chem. Commun.* **1985**, 1406–1407; h) S. Wolfe, D. J. Mitchell, H. B. Schlegel, C. Minot, O. Eisenstein, *Tetrahedron Lett.* **1982**, *23*, 615–618.
- [10] a) U. Ragnarsson, *Chem. Soc. Rev.* **2001**, *30*, 205–213 and references therein; b) E. W. Schmidt, *Hydrazines and its Derivatives: Preparation, Properties, Applications 2nd ed.*, VCH, Weinheim, **2001**.
- [11] Selected examples: a) E. M. Nurminen, M. Pihlavisto, L. Lázár, U. Pentikäinen, F. Fülöp, O. T. Pentikäinen, *J. Med. Chem.* **2011**, *54*, 2143–2154; b) J. H. Ahn, M. S. Shin, M. A. Jun, S. H. Jung, S. K. Kang, K. R. Kim, S. D. Rhee, N. S. Kang, S. Y. Kim, S.-K. Sohn, S. G. Kim, M. S. Jin, J. O. Lee, H. G. Cheon, S. S. Kim, *Bioorg. Med. Chem. Lett.* **2007**, *17*, 2622–2628; c) C. Ramesh, B. Bryant, T. Nayak, C. M. Revankar, T. Anderson, K. E. Carlson, J. A. Katzenellenbogen, L. A. Sklar, J. P. Norenberg, E. R. Prossnitz, J. B. Arterburn, *J. Am. Chem. Soc.* **2006**, *128*, 14476–14477; d) A. Raja, J. Lebbos, P. Kirkpatrick, *Nat. Rev. Drug Discovery* **2003**, *2*, 857–858; e) G. Campiani, F. Aiello, M. Fabbrini, E. Morelli, A. Ramunno, S. Armaroli, V. Nacci, A. Garofalo, G. Greco, E. Novellino, G. Maga, S. Spadari, A. Bergamini, L. Ventura, B. Bongiovanni, M. Capozzi, F. Bolacchi, S. Marini, M. Coletta, G. Guiso, S. Caccia, *J. Med. Chem.* **2001**, *44*, 305–315; f) L. Ling, L. J. Urichuk, B. D. Sloley, R. T. Coutts, G. B. Baker, J. J. Shan, P. K. T. Pang, *Bioorg. Med. Chem. Lett.* **2001**, *11*, 2715–2717; g) E. S. Lightcap, R. S. Silverman, *J. Med. Chem.* **1996**, *39*, 686–694; h) J. Gante, *Synthesis* **1989**, 405–413; i) T. Singh, J. F. Hoops, J. H. Biel, W. K. Hoya, R. G. Stein, D. R. Cruz, *J. Med. Chem.* **1971**, *14*, 532–535.

- [12] a) A. Bagno, E. Menna, E. Mezzina, G. Scorrano, D. Spinelli, *J. Phys. Chem. A* **1998**, *102*, 2888–2892; b) H. H. Sisler, G. M. Omietanski, B. Rudner, *Chem. Rev.* **1957**, *57*, 1021–1047; c) O. Westphal, *Ber. Dtsch. Chem. Ges.* **1941**, *74*, 759–776; d) C. Harries, T. Haga, *Ber. Dtsch. Chem. Ges.* **1898**, *31*, 56–64.
- [13] Selected examples: a) J. R. Leis, M. E. Peña, A. M. Rios, *J. Chem. Soc. Perkin Trans. 2* **1995**, 587–593; b) C. D. Ritchie, *J. Am. Chem. Soc.* **1975**, *97*, 1170–1179; c) R. N. Washburne, J. G. Miller, A. R. Day, *J. Am. Chem. Soc.* **1958**, *80*, 5963–5965; d) J. F. Bunnett, G. T. Davis, *J. Am. Chem. Soc.* **1958**, *80*, 4337–4339.
- [14] Earlier investigations of amine reactivities towards benzhydrylium ions: (a) J. Ammer, M. Baidya, S. Kobayashi, H. Mayr, *J. Phys. Org. Chem.* **2010**, *23*, 1029–1035; b) M. Baidya, F. Brotzel, H. Mayr, *Org. Biomol. Chem.* **2010**, *8*, 1929–1935; c) T. B. Phan, C. Nolte, S. Kobayashi, A. R. Ofial, H. Mayr, *J. Am. Chem. Soc.* **2009**, *131*, 11392–11401; d) T. Kanzian, T. A. Nigst, A. Maier, S. Pichl, H. Mayr, *Eur. J. Org. Chem.* **2009**, 6379–6385; e) M. Baidya, H. Mayr, *Chem. Commun.* **2008**, 1792–1794; f) M. Baidya, S. Kobayashi, F. Brotzel, U. Schmidhammer, E. Riedle, H. Mayr, *Angew. Chem.* **2007**, *119*, 6288–6292; *Angew. Chem. Int. Ed.* **2007**, *46*, 6176–6179; g) F. Brotzel, B. Kempf, T. Singer, H. Zipse, H. Mayr, *Chem. Eur. J.* **2007**, *13*, 336–345; h) F. Brotzel, Y. C. Chu, H. Mayr, *J. Org. Chem.* **2007**, *72*, 3679–3688; i) F. Brotzel, H. Mayr, *Org. Biomol. Chem.* **2007**, *5*, 3814–3820; j) T. B. Phan, M. Breugst, H. Mayr, *Angew. Chem.* **2006**, *118*, 3954–3959; *Angew. Chem. Int. Ed.* **2006**, *45*, 3869–3874; k) S. Minegishi, H. Mayr, *J. Am. Chem. Soc.* **2003**, *125*, 286–295.
- [15] a) H. Mayr, A. R. Ofial, *Pure Appl. Chem.* **2005**, *77*, 1807–1821; b) H. Mayr, B. Kempf, A. R. Ofial, *Acc. Chem. Res.* **2003**, *36*, 66–77; c) R. Lucius, R. Loos, H. Mayr, *Angew. Chem.* **2002**, *114*, 97–102; *Angew. Chem. Int. Ed.* **2002**, *41*, 91–95; d) H. Mayr, T. Bug, M. F. Gotta, N. Hering, B. Irrgang, B. Janker, B. Kempf, R. Loos, A. R. Ofial, G. Remennikov, H. Schimmel, *J. Am. Chem. Soc.* **2001**, *123*, 9500–9512; e) H. Mayr, M. Patz, *Angew. Chem.* **1994**, *106*, 990–1010; *Angew. Chem. Int. Ed. Engl.* **1994**, *33*, 938–957; f) For a comprehensive listing of nucleophilicity parameters N , s_N and electrophilicity parameters E see <http://www.cup.uni-muenchen.de/oc/mayr/DBintro.html>.
- [16] J. Ammer, C. Nolte, H. Mayr, *J. Am. Chem. Soc.* **2012**, *134*, 13902–13911.

- [17] The regioselectivities of the reactions of **2–4** with the reference electrophiles were determined from the 3J couplings of the methyl groups with the Ar_2CH group in HMBC NMR spectra.
- [18] Preferred attack at the methylated nitrogen of methylhydrazine (**4**) has previously been reported: (a) K. Too, D. M. Brown, E. Bongard, V. Yarley, L. Vivas, D. Loakes, *Bioorg. Med. Chem.* **2007**, *15*, 5551–5562; b) K. Banert, M. Hagedorn, J. Schlott, *Chem. Lett.* **2003**, *32*, 360–361; c) C. Gibson, S. L. Goodman, D. Hahn, G. Hölzemann, H. Kessler, *J. Org. Chem.* **1999**, *64*, 7388–7394; d) T. Ryckmans, H.-G. Viehe, J. Feneau-Dupont, B. Tinant, J.-P. Declercq, *Tetrahedron* **1997**, *53*, 1729–1734; e) C. L. Branch, A. W.; Guest, Finch (Beecham Group p.l.c.) US5275816, **1994**; f) A. W. Guest, R. G. Adams, M. J. Basker, E. G. Brain, C. L. Branch, F. P. Harrington, J. E. Neale, M. J. Pearson, I. I. Zomaya, *J. Antibiot.* **1993**, *46*, 1279–1288; g) H. Hilpert, A. S. Dreiding, *Helv. Chim. Acta* **1984**, *67*, 1547–1561; h) D. L. Trepanier, K. L. Shriver, J. N. Eble, *J. Med. Chem.* **1969**, *12*, 257–260; i) M. Busch, E. Opfermann, H. H. Walther, *Ber. Dtsch. Chem. Ges.* **1904**, *37*, 2318–2333.
- [19] a) C. P. Bergstrom, J. A. Bender, R. G. Gentles, P. Hewawasam, T. W. Hudyma, J. F. Kadow, S. W. Martin, A. Regueiro-Ren, K.-S. Yeung, Y. Tu, K. A. Grant-Young, X. Zheng, (Bristol-Myers Squibb Company) US2007/78122, **2007**; b) O. Tsubrik, U. Mäeorg, R. Sillard, U. Ragnarsson, *Tetrahedron* **2004**, *60*, 8363–8373; c) A. A. Yavolovskii, E. I. Ivanov, R. Y. Ianova, *Russ. J. Gen. Chem.* **2003**, *73*, 1326–1327; *Zh. Obshch. Khim.* **2003**, *73*, 1402–1403; d) K. Chantrapromma, W. D. Ollis, I. O. Sutherland, *J. Chem. Soc. Perkin Trans. 1* **1983**, 1029–1039; e) S. Wawzonek, E. Yeakey, *J. Am. Chem. Soc.* **1960**, *82*, 5718–5721.
- [20] a) K. Hisler, A. G. J. Commeureuc, S.-z. Zhou, J. A. Murphy, *Tetrahedron Lett.* **2009**, *50*, 3290–3293; b) S. Turner, (Reckitt and Colman Products Ltd) US4147794, **1979**.
- [21] Selected examples: a) M. Zh. Ovakimyan, S. K. Barsegyan, N. M. Kikoyan, M. G. Indzhikyan, *Russ. J. Gen. Chem.* **2005**, *75*, 1069–1073; *Zh. Obshch. Khim.* **2005**, *75*, 1132–1136; b) W. R. F. Goundry, J. E. Baldwin, V. Lee, *Tetrahedron* **2003**, *59*, 1719–1729; c) M. Zh. Ovakimyan, S. K. Barsegyan, A. A. Karapetyan, G. A. Panosyan, M. G. Indzhikyan, *Russ. Chem. Bull.* **2002**, *51*, 1744–1747; d) I. A. O’Neil, J. M. Southern, *Tetrahedron Lett.* **1998**, *39*, 9089–9092; e) M. Strasser, P. Cooper, B. Dewald, T. Payne, *Helv. Chim. Acta* **1988**, *71*, 1156–1176; f) A. O. Miller, G. G. Furin, *J. Fluorine Chem.* **1987**, *36*, 247–272; g) W. Kliegel, *Chem. Ber.* **1969**, *102*, 1776–1777.

- [22] H. Miyabe, K. Yoshida, M. Yamauchi, Y. Takemoto, *J. Org. Chem.* **2005**, *70*, 2148–2153.
- [23] D. E. Olberg, O. K. Hjelstuen, M. Solbakken, J. Arukwe, H. Karlsen, A. Cuthbertson, *Bioconjugate Chem.* **2008**, *19*, 1301–1308.
- [24] J. F. Coetzee, G. R. Padmanabhan, *J. Am. Chem. Soc.* **1965**, *87*, 5005–5010.
- [25] I. Kaljurand, A. Kütt, L. Sooväli, T. Rodima, V. Mäemets, I. Leito, I. A. Koppel, *J. Org. Chem.* **2005**, *70*, 1019–1028.
- [26] a) E. A. Castro, *Pure Appl. Chem.* **2009**, *81*, 685–696; b) I.-H.; Um, S. Yoon, H.-R. Park, H.-J. Han, *Org. Biomol. Chem.* **2008**, *6*, 1618–1624; c) I.-H. Um, J.-A. Seok, H.-T. Kim, S.-K. Bae, *J. Org. Chem.* **2003**, *68*, 7742–7746; d) M. J. Pfeiffer, S. B. Hanna, *J. Org. Chem.* **1993**, *58*, 735–740.
- [27] T. B. Phan, M. Breugst, H. Mayr, *Angew. Chem.* **2006**, *118*, 3954–3959; *Angew. Chem. Int. Ed.* **2006**, *45*, 3869–3874.
- [28] M. T. Bogert, A. Ruderman, *J. Am. Chem. Soc.* **1922**, *44*, 2612–2621.
- [29] V. Villiger, E. Kopetschni, *Ber. Dtsch. Chem. Ges.* **1912**, *45*, 2910–2922.
- [30] For the reaction of **2** with **16k**, we only observed the fast decay ($k_2' = 2.04 \times 10^8 \text{ M}^{-1} \text{ s}^{-1}$) even at concentrations as low as $[\mathbf{2}] = 1.58 \times 10^{-5} \text{ M}$. That we observed > 90 % conversion even at such low concentrations (only ~sixfold excess over **16k**) proves that the large rate constants measured for **16h–k** at high concentrations of **2** do not result from impurities in the hydrazine but reflect the nucleophilic reactivity of **2**.
- [31] Deprotonated **33i** was isolated in 66% yield after treatment of **16i** with an excess of **2** (see Experimental Section).
- [32] Reaction of the less-substituted nitrogen center was also detected in the reaction of **16k** with **3** ($\rightarrow\mathbf{35-H}^+ \text{BF}_4^-$, see Experimental Section).
- [33] a) S. A. Malin, B. M. Laskin, A. S. Malin, *Russ. J. Appl. Chem.* **2007**, *80*, 2165–2168; b) L. K. Dalton, S. Demerac, B. C. Elmes, *Aust. J. Chem.* **1980**, *33*, 1365–1372; c) E. Renouf, *Ber. Dtsch. Chem. Ges.* **1880**, *13*, 2169–2174; d) K.-H. König, B. Zeeh, *Chem. Ber.* **1970**, *103*, 2052–2061; e) G. Pollak, H. Yellin, A. Carmi, *J. Med. Chem.* **1964**, *7*, 220–224.
- [34] a) G. Zinner, T. Krause, *Arch. Pharm.* **1977**, *310*, 704–714; b) R. Ohme, H. Preuschhof, *J. Prakt. Chem.* **1971**, *313*, 626–635; c) W. Walter, K.-J. Reubke, *Chem. Ber.* **1970**, *103*, 2197–2207; d) R. C. Slagel, A. E. Bloomquist, *Can. J. Chem.* **1967**, *45*, 2625–

- 2628; e) W. G. Finnegan, R. A. Henry, *J. Org. Chem.* **1965**, *30*, 567–575; f) R. F. Meyer, *J. Org. Chem.* **1965**, *30*, 3451–3454.
- [35] Review: H. Mayr, M. Breugst, A. R. Ofial, *Angew. Chem.* **2011**, *123*, 6598–6634; *Angew. Chem. Int. Ed.* **2011**, *50*, 6470–6505.
- [36] C. Morell, A. Hocquet, A. Grand, B. Jamart-Grégoire, *J. Mol. Struct. THEOCHEM* **2008**, *849*, 46–51.
- [37] P. W. Ayers, C. Morell, F. De Pofst, P. Gerlings, *Chem. Eur. J.* **2007**, *13*, 8240–8247.
- [38] Selected examples: a) H. K. Hall, Jr., R. B. Bates, *Tetrahedron Lett.* **2012**, *53*, 1830–1832; b) P. Jaramillo, P. Perez, P. Fuentealba, *J. Phys. Org. Chem.* **2007**, *20*, 1050–1057; c) C. K. M. Heo, J. W. Bunting, *J. Chem. Soc. Perkin Trans. 2* **1994**, 2279–2290.
- [39] a) Y. V. Kolodyazhnyi, N. E. Drapkina, N. L. Chikina, L. S. Baturina, G. S. Gol'din, O. A. Osipov, *Russ. J. Gen. Chem.* **1980**, *50*, 845–850; b) F. E. Condon, R. T. Reece, D. G. Shapiro, D. C. Thakkar, T. B. Goldstein, *J. Chem. Soc. Perkin Trans. 2* **1974**, 1112–1121.
- [40] a) J. W. Bunting, J. M. Mason, C. K. M. Heo, *J. Chem. Soc. Perkin Trans 2* **1994**, 2291–2300; b) Bell, R. P. *The Proton in Chemistry*, Methuen, London, **1959**, p. 159.
- [41] M. Horn, H. Mayr, *Chem. Eur. J.* **2010**, *16*, 7478–7487.
- [42] Since the equilibrium constant for the reaction of **16h** with the dimethylamino group of trimethylhydrazine (**3**) could not be measured, we divided the equilibrium constant for the reaction of **3** (NMe₂ group) with **16j** by 3600, the ratio of equilibrium constants [$K(\mathbf{16j})/K(\mathbf{16h})$] for the reactions of these two benzhydrylium ions with several pyridines and phosphines: B. Maji, *Dissertation*, Ludwig-Maximilians-Universität München, **2012**.
- [43] B. Kempf, H. Mayr, *Chem. Eur. J.* **2005**, *11*, 917–927.
- [44] a) W. J. Albery, *Annu. Rev. Phys. Chem.* **1980**, *31*, 227–263; b) R. A. Marcus, *J. Phys. Chem.* **1968**, *72*, 891–899.
- [45] N. Streidl, B. Denegri, O. Kronja, H. Mayr, *Acc. Chem. Res.* **2010**, *43*, 1537–1549.
- [46] R. T. Beltrami, E. R. Bissell, *J. Am. Chem. Soc.* **1956**, *78*, 2467–2468.
- [47] Y. Boland, P. Hertsens, J. Marchand-Brynaert, Y. Garcia, *Synthesis* **2006**, 1504–1512.
- [48] A. Bredihhin, U. Mäeorg, *Tetrahedron* **2008**, *64*, 6788–6793.
- [49] A. Bredihhin, U. Mäorg, *Org. Lett.* **2007**, *9*, 4975–4977.
- [50] E. E. Boros, F. Bouvier, S. Randhawa, M. H. Rabinowitz, *J. Heterocycl. Chem.* **2001**, *38*, 613–616.

- [51] J. Ammer, C. Nolte, K. Karaghiosoff, H. Mayr, manuscript in preparation.
- [52] J. Ammer, C. F. Sailer, E. Riedle, H. Mayr, *J. Am. Chem. Soc.* **2012**, *134*, 11481–11494.
- [53] Assignment of the *E*- and *Z*-isomers has been based on the magnitude of the coupling constants according to Ref. [34c].
- [54] F. H. Kranz, (Allied Chemical Corporation) US2983756, **1958**.
- [55] M. J. Frisch, G. W. Trucks, H. B. Schlegel, G. E. Scuseria, M. A. Robb, J. R. Cheeseman, G. Scalmani, V. Barone, B. Mennucci, G. A. Petersson, H. Nakatsuji, M. Caricato, X. Li, H. P. Hratchian, A. F. Izmaylov, J. Bloino, G. Zheng, J. L. Sonnenberg, M. Hada, M. Ehara, K. Toyota, R. Fukuda, J. Hasegawa, M. Ishida, T. Nakajima, Y. Honda, O. Kitao, H. Nakai, T. Vreven, J. A. Montgomery, Jr., J. E. Peralta, F. Ogliaro, M. Bearpark, J. J. Heyd, E. Brothers, K. N. Kudin, V. N. Staroverov, R. Kobayashi, J. Normand, K. Raghavachari, A. Rendell, J. C. Burant, S. S. Iyengar, J. Tomasi, M. Cossi, N. Rega, J. M. Millam, M. Klene, J. E. Knox, J. B. Cross, V. Bakken, C. Adamo, J. Jaramillo, R. Gomperts, R. E. Stratmann, O. Yazyev, A. J. Austin, R. Cammi, C. Pomelli, J. W. Ochterski, R. L. Martin, K. Morokuma, V. G. Zakrzewski, G. A. Voth, P. Salvador, J. J. Dannenberg, S. Dapprich, A. D. Daniels, O. Farkas, J. B. Foresman, J. V. Ortiz, J. Cioslowski, D. J. Fox, *Gaussian 09*, Revision A.02, Inc., Wallingford CT, **2009**.

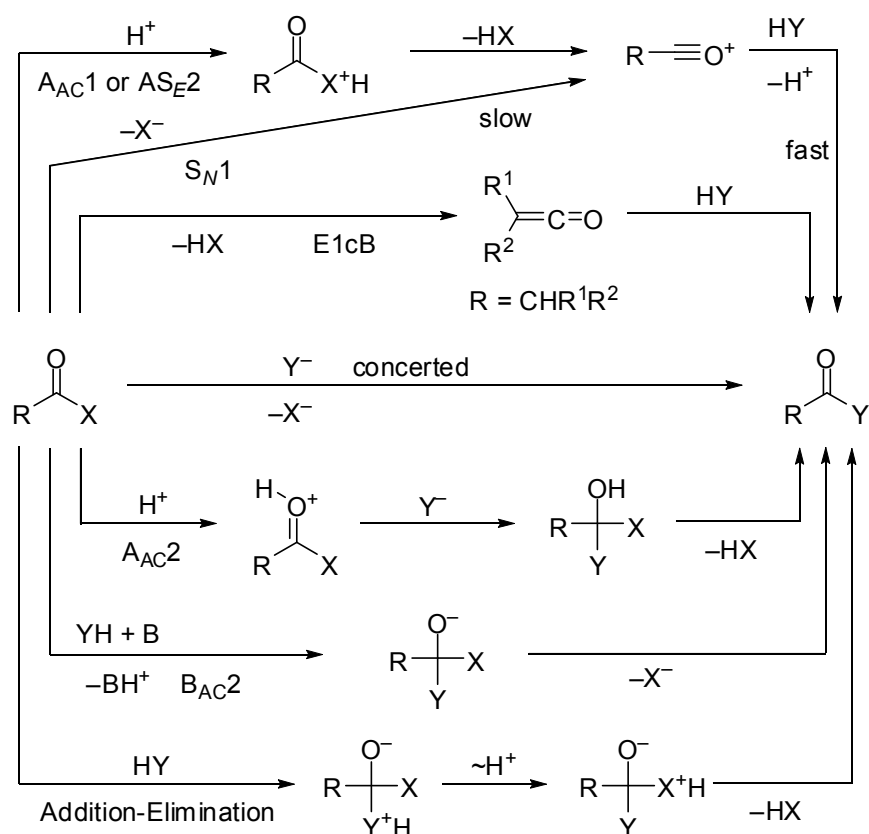
Chapter 5

LIMITATIONS OF THE BENZHYDRILIUM-BASED NUCLEOPHILICITY SCALES FOR PREDICTING RATES OF ACYLATION REACTIONS

Tobias A. Nigst and Herbert Mayr, manuscript in preparation.

5.1 Introduction

Nucleophilic substitution reactions at acyl derivatives are of eminent importance in chemistry and biology. Many investigations have dealt with the corresponding reaction mechanisms, which are summarized in Scheme 5.1.^[1] Usually acylations are multistep reactions, certain steps of which may be catalyzed by acids or bases. Several mechanistic scenarios have been discovered, and their occurrence was found to depend on the substrates and the reaction conditions. As shown on top of Scheme 5.1, acylium ions can be formed in different ways before they undergo fast subsequent reactions with the nucleophiles. When the substrates possess α -acidic protons, ketenes may be generated in the presence of bases. There has been much debate whether the attack of nucleophiles at the carbonyl group displaces X⁻ in a concerted manner or whether tetrahedral intermediates are involved.^[1,2]



Scheme 5.1. Mechanisms for acylation reactions.

In 1972, Ritchie discovered that the relative reactivities of various anionic nucleophiles towards triarylmethyl cations, aryl tropylium ions and aryldiazonium ions do not depend on the electrophile, and can be described by Equation (5.1), where $\lg k_0$ is an electrophile-specific parameter, and N_+ is a nucleophile-specific parameter.^[3]

$$\lg k = \lg k_0 + N_+ \quad (5.1)$$

As the rate constants for the reactions of aryl acetates showed a different reactivity pattern, Ritchie concluded that the reactivities of esters cannot be described by Equation (5.1).^[4]

We have previously reported that the reactions of carbocations and quinone methides with different classes of σ -, π -, and n-nucleophiles follow the linear free energy relationship [Eq. (5.2)], where electrophiles are characterized by one parameter (E) and nucleophiles are characterized by two solvent-dependent parameters (N and s_N).^[5]

$$\lg k_2(20\text{ }^\circ\text{C}) = s_N(N + E) \quad (5.2)$$

Recently, we studied the rates of the addition reactions of carbon nucleophiles to nonactivated carbonyl groups in aprotic solvents.^[6] For these investigations, acceptor-stabilized carbanions, like malonate or the highly nucleophilic phenylacetonitrile anions, could not be used as reference nucleophiles because of the high reversibility of these reactions. On the other hand, the reactions of sulfur ylides with aldehydes, imines, and enones yielded the corresponding epoxides, aziridines, and cyclopropanes quantitatively. Since in many of these reactions the initial C-C bond formation, which leads to betains, was found to be rate-determining, it became possible to quantify the electrophilicities of aldehydes, imines, and enones by Equation (5.2).

We now report on the electrophilic reactivities of the acyl compounds **1–5** (Figure 5.1) which undergo substitution reactions with the carbanions **6–12**, the amines and hydrazines **13–28**, and the carboxylate anions **29–30** (Figure 5.2). These data are used to examine the applicability of the linear free energy relationship [Eq. (5.2)] for the quantitative characterization of acyl electrophilicities.

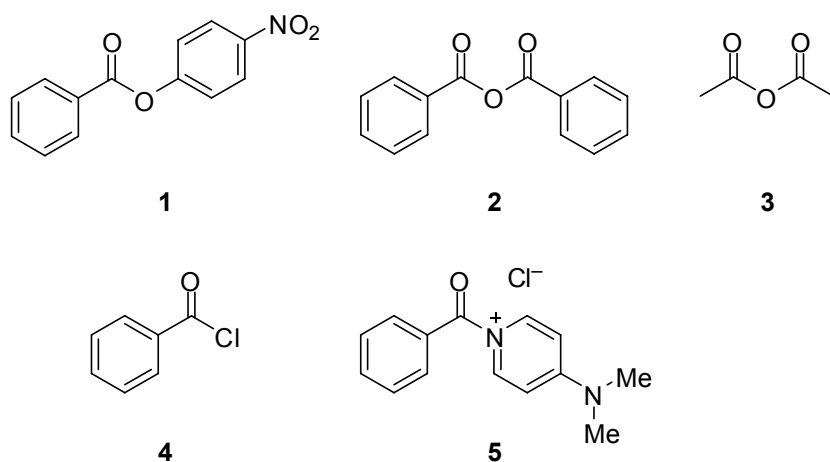


Figure 5.1. Electrophiles used in this study.

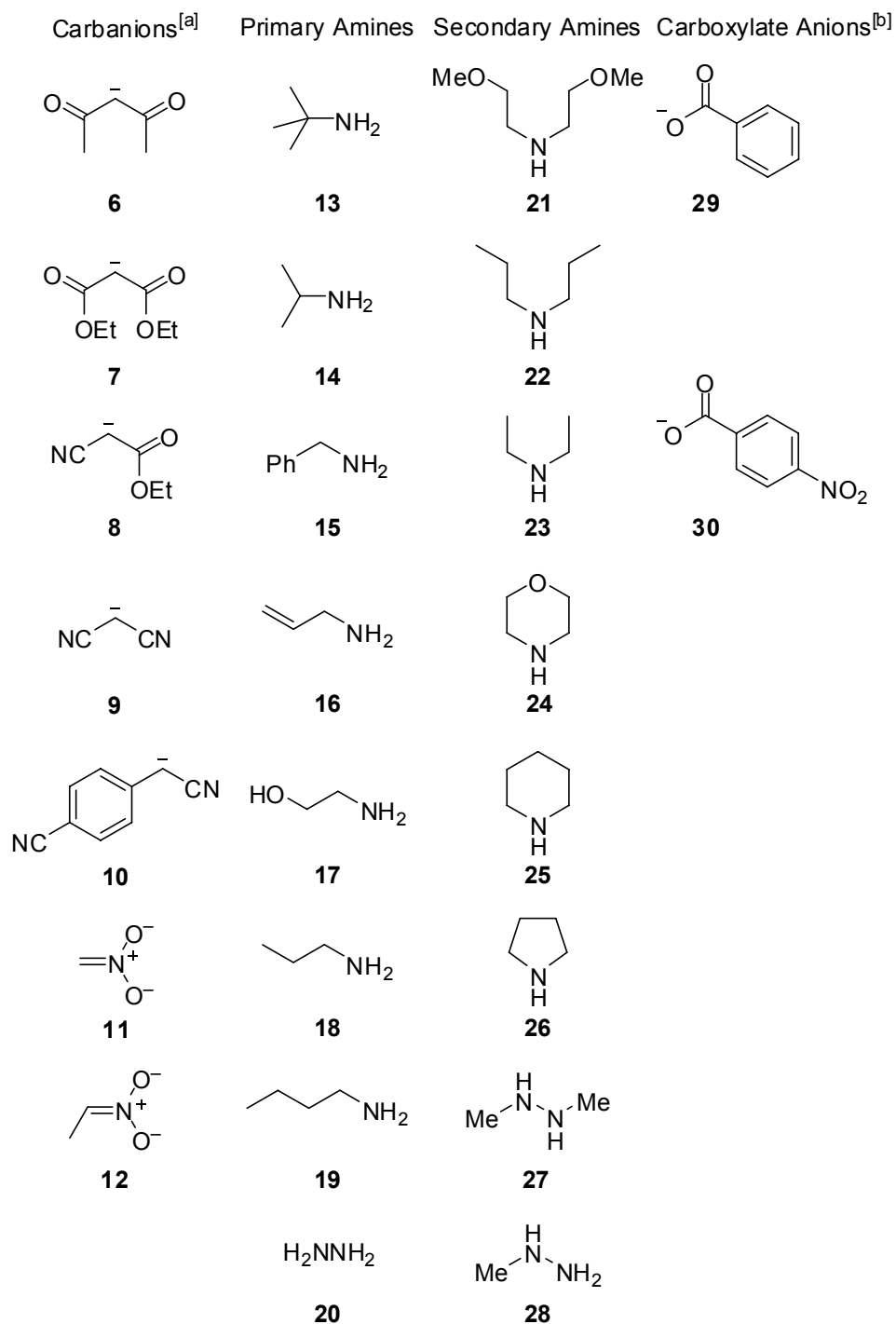


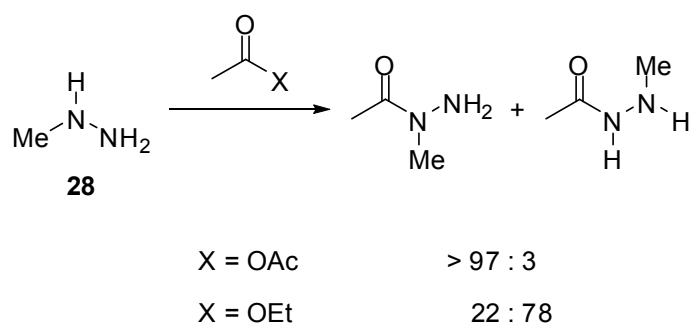
Figure 5.2. Nucleophiles used in this study.

^[a] Counterion of the carbanions: K^+ . ^[b] Counterion of the carboxylate anions: $n\text{-Bu}_4\text{N}^+$.

5.2 Results and Discussion

5.2.1 Reaction Products

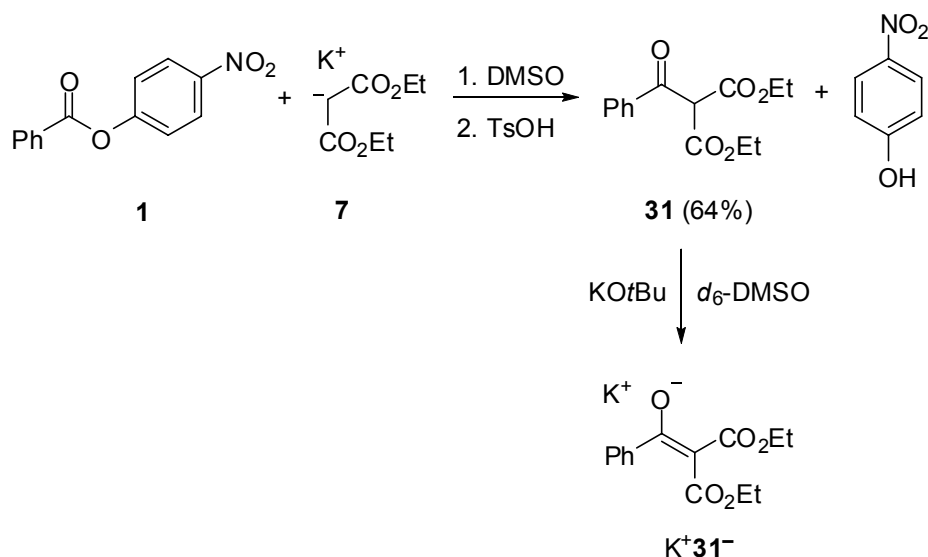
The products obtained by reactions of amines and hydrazines with carboxylic acid chlorides, anhydrides and esters have previously been reported.^[2b,7-9] Methylhydrazine (**28**) reacts smoothly at the methyl-substituted nucleophilic center of **28** with most electrophiles^[10] including benzhydrylium ions and quinone methides.^[11] However, the situation is more complicated in acylation reactions. While several anhydrides, including benzoic anhydride (**2**) and acetic anhydride (**3**), were found to react with methylhydrazine (**28**) selectively at the NHMe group, the corresponding reactions with ethyl acetate occurred at the NH₂ group predominately (Scheme 5.2).^[8,9] Nucleophilic displacement of the B_{Ac}2 type with rate-determining addition was claimed for the reaction of **28** with acetic anhydride, while the corresponding reaction with ethyl acetate was claimed to proceed via addition-elimination with rate-limiting proton transfer.^[8] Hinman and Fulton furthermore observed that the selectivity for NH₂ attack of methylhydrazine (**28**) in reactions with esters increased with increasing size of the acyl group, that is the percentage of 1-acyl-1-methylhydrazine decreased in the order methyl acetate > methyl propionate > methyl isobutyrate.^[9]



Scheme 5.2. Relative ratios of NH₂ and NHMe acylation of methylhydrazine (**28**) with different acylating agents.^[8]

The combination of 4-nitrophenyl benzoate (**1**) with two equivalents of potassium diethyl malonate (**7**) in DMSO at 20 °C yielded **31** after workup with 4-toluenesulfonic acid, that is, **1** reacted with nucleophilic replacement of 4-nitrophenolate by the carbanion (Scheme 5.3). Treatment of **31** with one equivalent of KO^tBu in DMSO yielded the corresponding enolate

$\text{K}^+\mathbf{31}^-$ quantitatively. Similar substitutions by carbon nucleophiles have previously been reported for the reactions of benzoic anhydride (**2**) with the anion of malononitrile (**9**),^[12] benzoyl chloride (**4**) with the anions of acetylacetone (**6**),^[13] ethyl cyanoacetate (**8**),^[14] and malononitrile (**9**),^[15] as well as for the reaction of phenyl benzoate with the anion of nitromethane (**11**).^[16]



Scheme 5.3. Reaction of potassium diethyl malonate (**7**) with 4-nitrophenyl benzoate (**1**) and subsequent deprotonation of **31** with KOtBu.

5.2.2 Kinetic Investigations

4-Nitrophenyl benzoate (**1**) is the least reactive acylating agent in the series **1–5**. The rates of its reactions with carbanions and amines were determined spectrophotometrically in DMSO solution at 20 °C by monitoring the appearance of the 4-nitrophenolate anion with conventional or stopped-flow UV/Vis spectrophotometry.

Stock solutions of the carbanions were prepared by partial deprotonation of the CH acids (**6–12-H**) with 0.5 equivalents of KOtBu in DMSO. Ethyl cyanoacetate (**8**) was used as the isolated potassium salt. The kinetics were performed under first-order conditions by using a high excess of the nucleophiles (over 10 equiv. relative to the electrophile). The first-order rate constants k_{obs} were obtained by least-squares fitting of the monoexponential function $A = A_0(1 - e^{-k_{\text{obs}}t}) + C$ to the increases of the UV/Vis absorbance of the 4-nitrophenolate; a typical example is shown in Figure 5.3. Plots of k_{obs} versus the nucleophile concentrations were linear

for all reactions and the second-order rate constants k_2 (Table 5.1) were obtained as the slopes of these plots according to Equation (5.3).

$$k_{\text{obs}} = k_2[\text{Nu}] + k_0 \quad (5.3)$$

It was not possible to employ the ester **1** as excess compound for these kinetic investigation, because the resulting products contain CH groups which are more acidic than the original CH acids, and protonate the carbanions **6–12**.

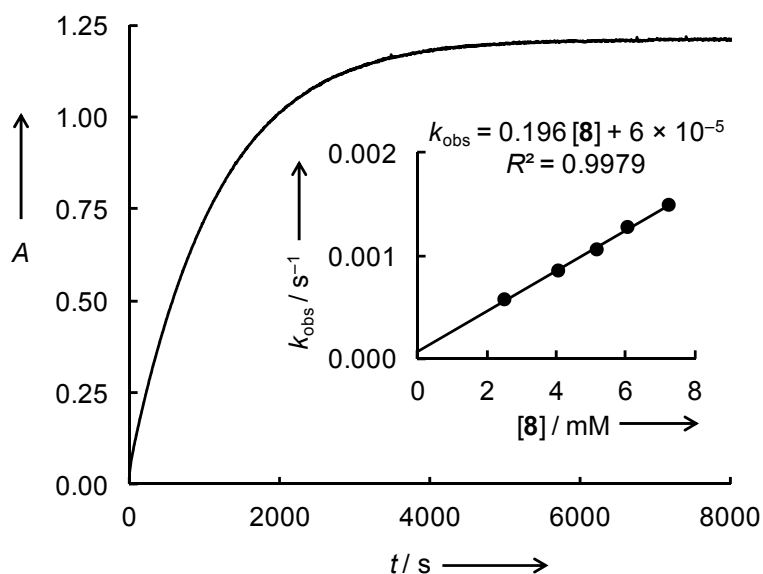


Figure 5.3. Exponential increase of the absorbance at $\lambda = 435$ nm during the reaction of 4-nitrophenyl benzoate ($[\mathbf{1}] = 6.79 \times 10^{-5}$ M) with potassium ethyl cyanoacetate ($[\mathbf{8}] = 4.08 \times 10^{-3}$ M; $k_{\text{obs}} = 8.51 \times 10^{-4}$ s^{-1}) in DMSO at 20 °C. Inset: A plot of k_{obs} versus $[\mathbf{8}]$ yields the second-order rate constant $k_2 = 1.96 \times 10^{-1}$ $\text{M}^{-1}\text{s}^{-1}$.

Table 5.1. Second-order rate constants k_2 for the reactions of 4-nitrophenyl benzoate (**1**) with carbanions, amines, and alkoxide anions at 20 °C — for an explanation of k_2^{calc} see chapter 5.2.3.

| Nu | Solvent | N, s_N | $k_2^{\text{exp}}/\text{M}^{-1} \text{ s}^{-1}$ | $k_2^{\text{calc}}/\text{M}^{-1} \text{ s}^{-1}$ | $k_2^{\text{exp}}/k_2^{\text{calc}}$ |
|------------------|--------------------|----------------------------|---|--|--------------------------------------|
| Carbanions | | | | | |
| 6 | DMSO | 17.64, 0.73 ^[a] | 1.93×10^{-2} | 6.46×10^{-3} | 2.99 |
| 7 | DMSO | 20.22, 0.65 ^[a] | 6.10×10^{-2} | 5.33×10^{-1} | 1.14×10^{-1} |
| 8 | DMSO | 19.62, 0.67 ^[a] | 1.96×10^{-1} | 2.07×10^{-1} | 9.45×10^{-1} |
| 9 | DMSO | 19.36, 0.67 ^[a] | 9.22×10^{-1} | 1.39×10^{-1} | 6.64 |
| 10 | DMSO | 25.11, 0.54 ^[b] | 3.06×10^1 | 2.59×10^2 | 1.18×10^{-1} |
| 11 | DMSO | 20.71, 0.60 ^[c] | 8.37×10^{-1} | 1.10 | 7.60×10^{-1} |
| 12 | DMSO | 21.54, 0.62 ^[d] | 1.14×10^1 | 3.61 | 3.15 |
| Amines | | | | | |
| 15 | DMSO | 15.28, 0.65 ^[e] | 7.70×10^{-1} | 3.28×10^{-4} | 2.35×10^3 |
| 15 | CH ₃ CN | 14.29, 0.67 ^[f] | 2.49×10^{-3} ^[g] | 5.57×10^{-5} | 4.47×10^1 |
| 17 | DMSO | 16.07, 0.61 ^[e] | 2.59 | 1.63×10^{-3} | 1.59×10^3 |
| 18 | DMSO | 15.70, 0.64 ^[h] | 4.45 | 6.89×10^{-4} | 6.46×10^3 |
| 25 | DMSO | 17.19, 0.71 ^[h] | 1.32×10^1 | 3.55×10^{-3} | 3.72×10^3 |
| 25 | CH ₃ CN | 17.35, 0.68 ^[f] | 5.39×10^{-1} ^[i] | 5.79×10^{-3} | 9.31×10^1 |
| Alkoxide Anions | | | | | |
| EtO ⁻ | EtOH | 15.78, 0.65 ^[j] | 1.05×10^1 ^[k] | 6.93×10^{-4} | 1.51×10^4 |
| HO ⁻ | H ₂ O | 10.47, 0.61 ^[h] | 4.20 ^[l] | 6.26×10^{-7} | 6.71×10^6 |
| HOO ⁻ | H ₂ O | 15.40, 0.55 ^[h] | 1.48×10^3 ^[l] | 1.31×10^{-3} | 1.13×10^6 |

[a] From Ref. [5c]. [b] From Ref. [17]. [c] From Ref. [18]. [d] From Ref. [19]. [e] From Ref. [20]. [f] From Ref. [21]. [g] Second-order rate constant extrapolated from the Eyring plot from Ref. [7c]. [h] From Ref. [22]. [i] Second-order rate constant at 25 °C from Ref. [23]. [j] From Ref. [24]. [k] Second-order rate constants at 25 °C from Ref. [25]. [l] Second-order rate constants at 25 °C from ref. [26].

As the reactions of the highly reactive acylating agents **2–5** with carbanions were too rapid for the stopped-flow method, and reactions with other carbon nucleophiles like enamines gave complicated kinetics, we limited our investigations to the kinetics of the reactions of **2–5** with amines and carboxylates in acetonitrile at 20 °C.

As benzoic anhydride (**2**) and 1-benzoyl-4-(dimethylamino)pyridinium chloride (**5**) have absorption maxima at higher wavelengths than the reaction products, their reactions with amines and carboxylates were monitored spectrophotometrically under first-order conditions with the nucleophiles in excess. The *N*-acylpyridinium chloride **5** was synthesized by treatment of benzoyl chloride (**4**) with equimolar amounts of DMAP in acetonitrile followed by subsequent precipitation (Et₂O) and isolation of the product.^[27] Alternatively, stock solutions of **5** were generated by mixing solutions of equal amounts of DMAP and benzoyl chloride (**4**). As demonstrated for the reaction of **5** with benzylamine (**15**), both methods gave rate constants which differed by less than 3%. For all reactions of **2** and **5** with amines and carboxylates, monoexponential decays of the absorbances at $\lambda = 280$ or 317 nm, respectively, were observed. Again, correlations of the first-order rate constants k_{obs} with the concentrations of the nucleophiles were linear, and the second-order rate constants k_2 were derived from the slopes of these correlations (Table 5.2).

The kinetics of the reactions of acetic anhydride (**3**) and benzoyl chloride (**4**) with primary and secondary amines were evaluated from measurements of the relative conductivities (κ_{rel}) under first-order conditions as we did not calibrate the conductivity cell to obtain absolute values of κ , but we have previously demonstrated the proportionality between concentration and conductivity of the ammonium salts under these conditions. For all reactions of **3** and **4**, monoexponential increases of the conductivity were observed due to the formed ammonium ions. The second-order rate constants k_2 were obtained from the linear correlations of the first-order rate constants with the concentrations of the nucleophiles (Table 5.2).

Table 5.2. Second-order rate constants k_2 [$M^{-1} s^{-1}$] for the reactions of **2–5** with amines, hydrazines and carboxylates in acetonitrile at 20 °C.

| Nu | N, s_N | 2 | 3 | 4 | 5 |
|--------------|----------------------------|-------------------------|--------------------|--------------------|-------------------------------------|
| Amines | | | | | |
| 13 | 12.35, 0.72 ^[a] | – | – | 6.28×10^2 | $1.64^{[b]}$ |
| 14 | 13.77, 0.70 ^[a] | 5.43×10^1 | 1.06×10^2 | 1.00×10^4 | 2.78×10^2 |
| 15 | 14.29, 0.67 ^[a] | 7.45×10^1 | 1.43×10^2 | 1.14×10^4 | 4.78×10^2 ^[c,d] |
| 16 | 14.37, 0.66 ^[a] | 7.55×10^1 | 1.76×10^2 | 1.63×10^4 | 6.56×10^2 |
| 17 | 14.11, 0.71 ^[a] | 1.80×10^2 | 4.49×10^2 | – | 1.53×10^3 |
| 18 | 15.11, 0.63 ^[a] | $3.82 \times 10^{2[b]}$ | 5.77×10^2 | 4.53×10^4 | $3.52 \times 10^{3[b]}$ |
| 19 | 15.27, 0.63 ^[a] | 4.54×10^2 | 7.35×10^2 | – | 4.27×10^3 |
| 20 | 16.45, 0.56 ^[e] | 2.01×10^3 | – | – | 1.81×10^4 |
| 21 | 13.24, 0.93 ^[a] | 4.05×10^{-1} | 7.88 | 4.14×10^3 | 2.13 |
| 22 | 14.51, 0.80 ^[a] | – | 6.54×10^1 | 2.86×10^4 | 2.68×10^1 |
| 23 | 15.10, 0.73 ^[a] | 2.23×10^1 | 9.15×10^1 | 2.96×10^4 | 6.14×10^1 ^[c] |
| 24 | 15.65, 0.74 ^[a] | 8.30×10^1 | 5.57×10^2 | 3.45×10^5 | 5.70×10^2 ^[c] |
| 25 | 17.35, 0.68 ^[a] | 3.16×10^3 | – | – | 1.43×10^4 |
| 26 | 18.64, 0.60 ^[a] | 2.07×10^4 | – | – | 1.80×10^5 |
| 27 | 16.15, 0.68 ^[f] | 5.81×10^1 | – | – | 2.87×10^2 |
| 28 | 17.73, 0.58 ^[f] | 1.36×10^3 | – | – | 6.10×10^3 |
| Carboxylates | | | | | |
| 29 | 16.82, 0.70 ^[g] | – | – | – | 1.19×10^6 |
| 30 | 15.30, 0.76 ^[g] | – | – | – | 4.93×10^4 |

[a] From Ref. [21]. [b] From Ref. [28]. [c] Re-evaluated from Ref. [28]. [d] The average of the second-order rate constants from the reaction of **15** with the isolated 1-benzoyl-(4-dimethylamino)pyridinium chloride **5** ($k_2 = 4.73 \times 10^2 M^{-1} s^{-1}$) and by mixing solutions of **4** with equimolar amounts of DMAP ($k_2 = 4.84 \times 10^2 M^{-1} s^{-1}$) was used. [e] From Ref. [29]. [f] From Ref. [11]. [g] Nucleophilicity parameters at 25 °C from Ref. [30].

5.2.3 Correlation Analysis

Figure 5.4 shows a plot of the second-order rate constants for the reactions of primary (closed circles) and secondary amines (open circles) with 1-benzoyl-4-(dimethylamino)pyridinium chloride (**5**) versus the corresponding rate constants for the reactions of these nucleophiles with benzoic anhydride (**2**). A linear correlation comprising both primary and secondary amines is found.

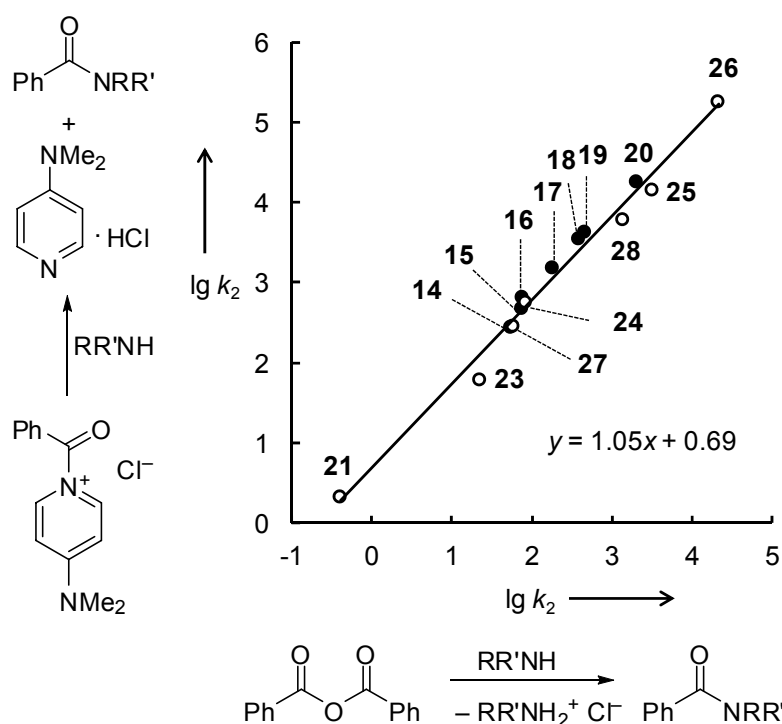


Figure 5.4. Correlation of the second-order rate constants k_2 for the reactions of 1-benzoyl-4-(dimethylamino)pyridinium chloride (**5**) with primary (filled circles) and secondary amines (open circles) versus the second-order rate constants for the corresponding reactions with benzoic anhydride (**2**).

However, when the second-order rate constants for the reactions of primary (closed symbols) and secondary amines (open symbols) with acetic anhydride (**3**, diamonds in Figure 5.5), benzoyl chloride (**4**, triangles in Figure 5.5) and 4-nitrophenyl benzoate (**1**, squares in Figure 5.5) are plotted versus the corresponding rate constants for the reactions of these nucleophiles with benzoic anhydride (**2**), the relative reactivities of primary amines differ from those of the secondary amines. While the correlation lines for secondary amines are above those of the

primary amines for benzoyl chloride (**4**) and acetic anhydride (**3**), the only secondary amine studied with 4-nitrophenyl benzoate (**1**) is located below the correlation line for the primary amines.

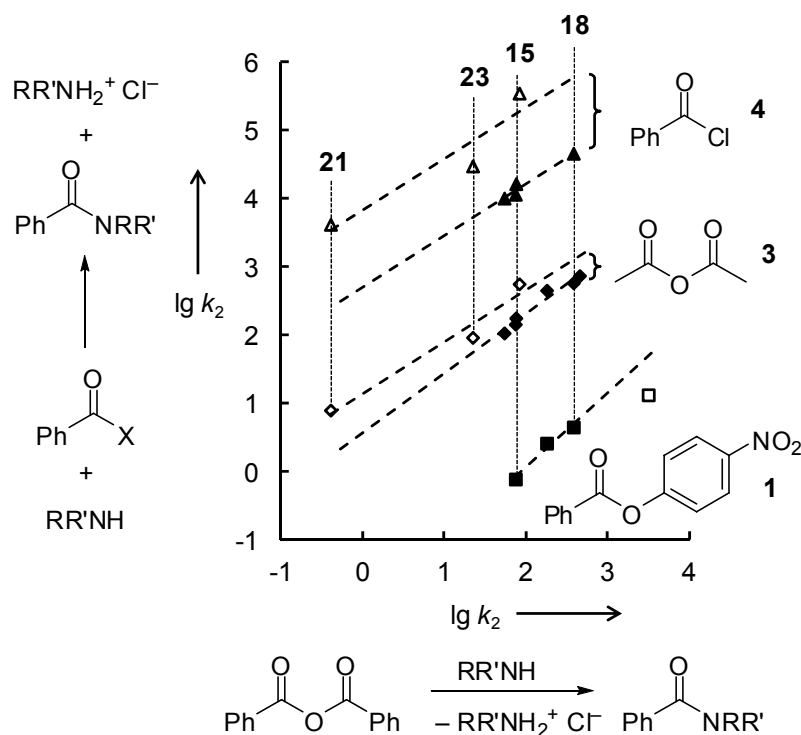


Figure 5.5. Correlation of the second-order rate constants k_2 for the reactions of the acylating agents **1** (squares), **3** (diamonds) and **4** (triangles) with primary (filled symbols) and secondary amines (open symbols) versus the second-order rate constants for the corresponding reactions with benzoic anhydride (**2**).

One, therefore, has to conclude that the relative reactivities of primary and secondary amines depend on the nature of the acylating agent. *Vice versa*, the relative reactivities of the different acyl compounds also depend on the nature of the nucleophilic reaction partner. For primary amines, the relative reactivities of the acylating agents **1–5** decrease in the order benzoyl chloride (**4**) \gg 1-benzoyl-4-(dimethylamino)pyridinium chloride (**5**) $>$ acetic anhydride (**3**) $>$ benzoic anhydride (**2**) \gg 4-nitrophenyl benzoate (**1**). In contrast, the acyclic secondary amines **21–23** react 1.5 to 3.7 times faster with acetic anhydride (**3**) than with 1-benzoyl-4-(dimethylamino)pyridinium chloride (**5**), while the reactivity order is reversed for the cyclic morpholine (**24**). A comparison of the reactivities of the acylating agents **1–5** towards *n*-propylamine (**18**, left side of Figure 5.6) and diethylamine (**23**, right side of Figure 5.6) shows

that the reactivities of these electrophiles are comparable to those of quinone methides and amino-substituted benzhydrylium ions.

In order to test the applicability of Equation (5.2) for predicting the rate constants for the aminations of **2–5**, we plotted $(\lg k_2)/s_N$ versus the nucleophilicity parameters N of the amines (Figure 5.7). For all of these highly reactive acyl compounds, where a concerted mechanism can be assumed or where the initial attack of the nucleophile is rate limiting,^[1,2b] separate linear correlation lines are found for primary (circles) and secondary amines (squares), showing that primary amines react up to 50 times faster than secondary amines of comparable nucleophilicity N towards benzhydrylium ions. In general, the gap between the reactivities of primary and secondary amines is smaller for better leaving groups and lower steric demand of the electrophile, that is, the gap decreases in the order 1-benzoyl-4-(dimethylamino)pyridinium chloride (**5**) > benzoic anhydride (**2**) > acetic anhydride (**3**) > benzoyl chloride (**4**). Furthermore, it can be noted, that the slopes of the correlation lines are significantly greater than unity, which implies that the acylation reactions are more sensitive towards changes of the nucleophiles than the corresponding reactions with benzhydrylium ions. The statistically corrected Brønsted correlation for the reaction of amines with **5** shows that primary amines have similar reactivities as isobasic secondary amines (Figure 5.8). This observation contrasts the relative reactivities towards benzhydrylium ions, where the secondary amines were found to be considerably more nucleophilic than isobasic primary amines.^[11,21] Obviously, the influence of steric effects is more pronounced for acylation reactions; the large negative deviation of *tert*-butylamine (**13**) is in line with this interpretation.

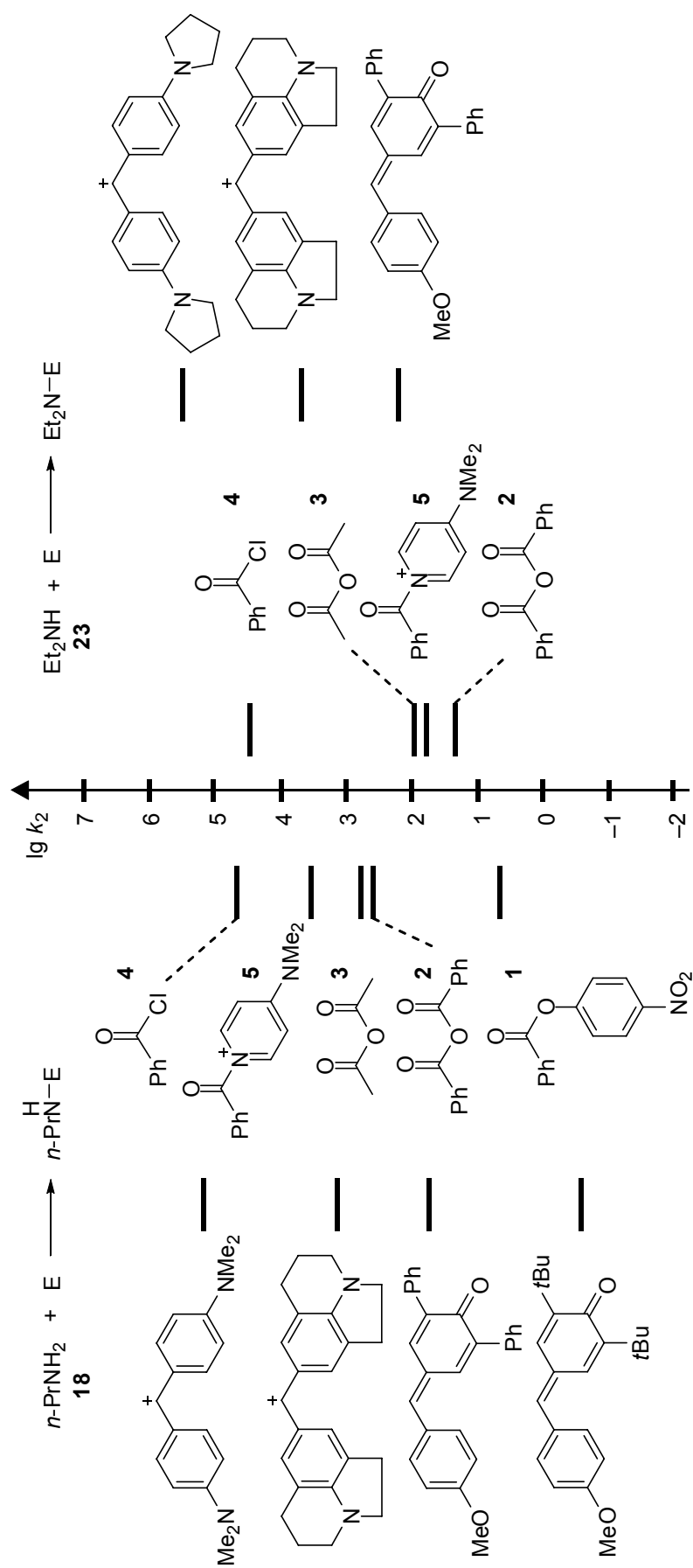


Figure 5.6. Comparison of the second-order rate constants k_2 for reactions of acylating agents **1-5**, benzhydrylium ions, and quinone methides^[21] with *n*-propylamine (**18**, left side) and diethylamine (**23**, right side).

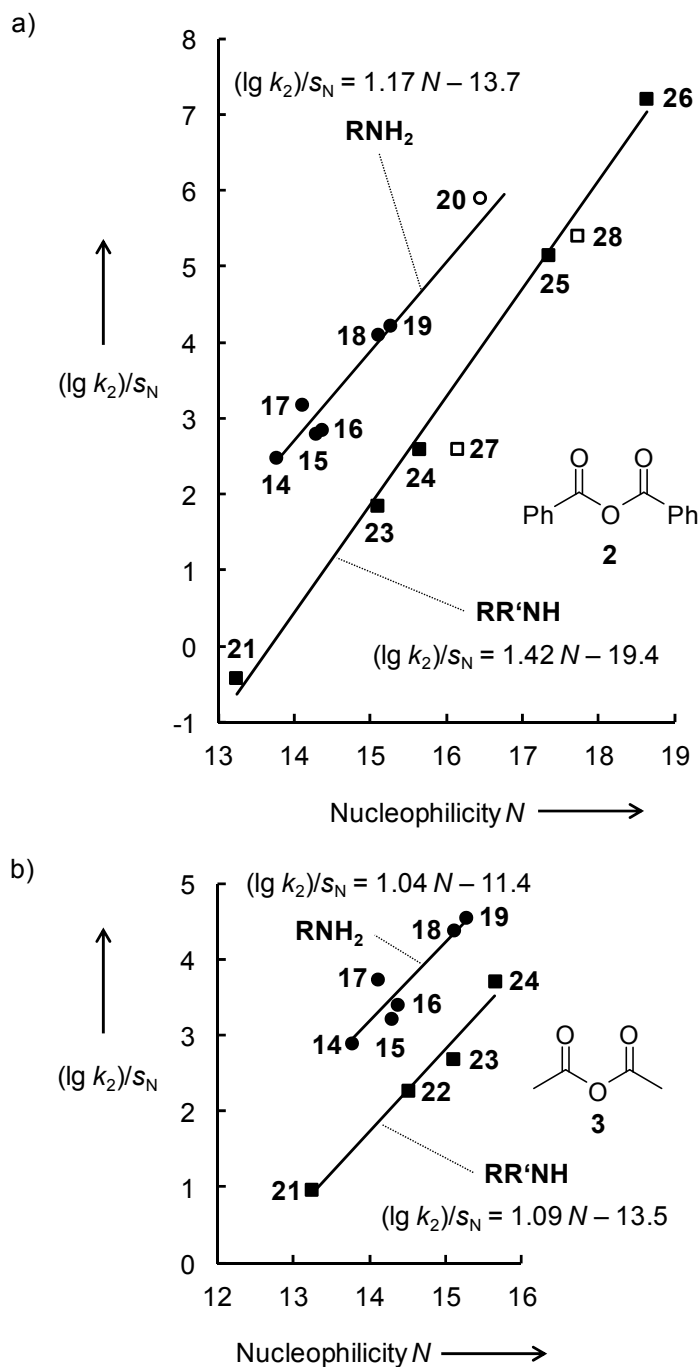


Figure 5.7. Plot of $(\lg k_2)/s_N$ versus N for the reactions of (a) benzoic anhydride (**2**), (b) acetic anhydride (**3**), (c) benzoyl chloride (**4**), and (d) 1-benzoyl-4-(dimethylamino)pyridinium chloride (**5**) with carboxylates (triangles), primary (circles) and secondary amines (squares) in acetonitrile at 20 °C.^[a]

[a] The second-order rate constants for the acylation reactions of hydrazines (open symbols) were not used for the calculation of the linear regressions for primary or secondary amines.

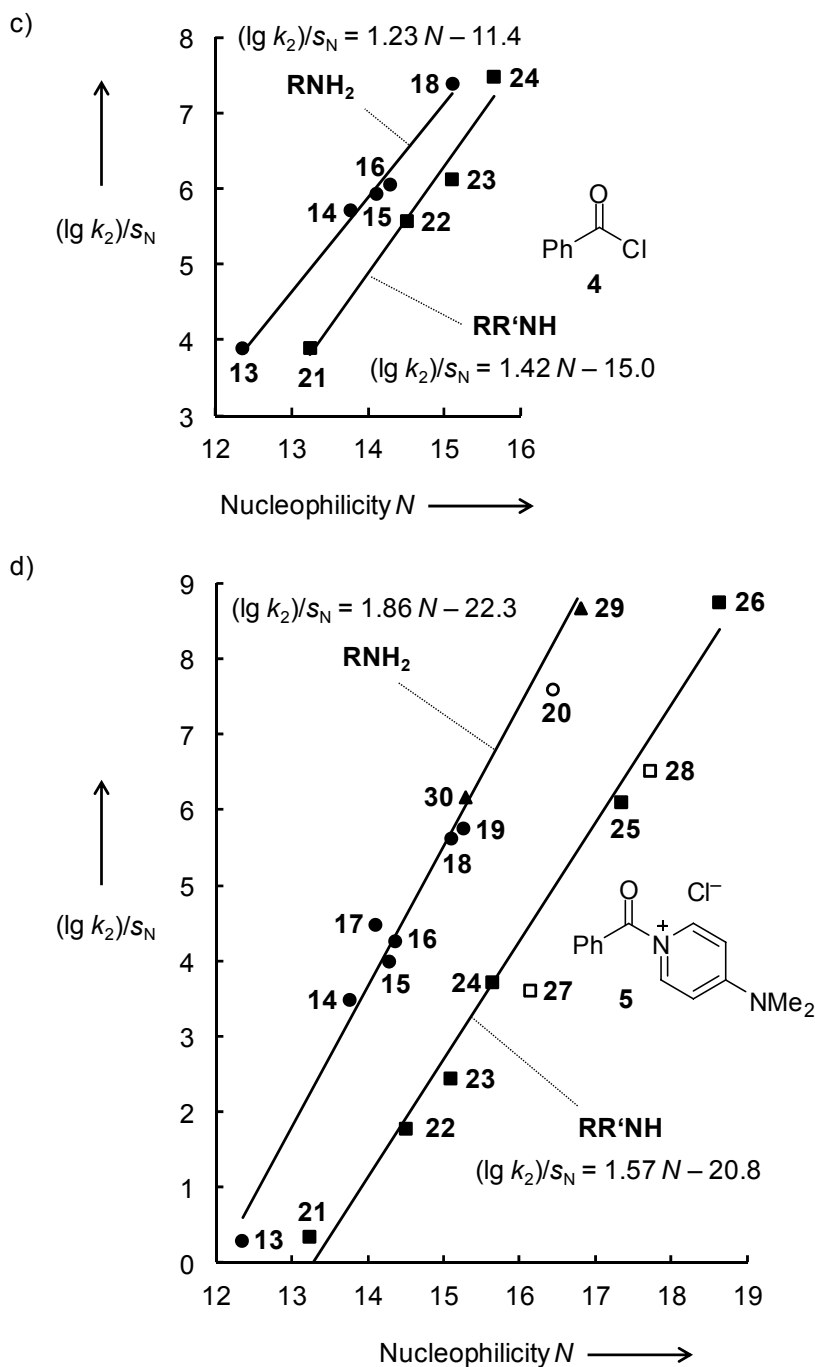


Figure 5.7 (continued).

Figure 5.7d also shows that the carboxylate anions **29** and **30** (triangles) exhibit similar reactivities towards 1-benzoyl-4-(dimethylamino)pyridinium chloride (**5**) as primary amines of the same nucleophilicity N .

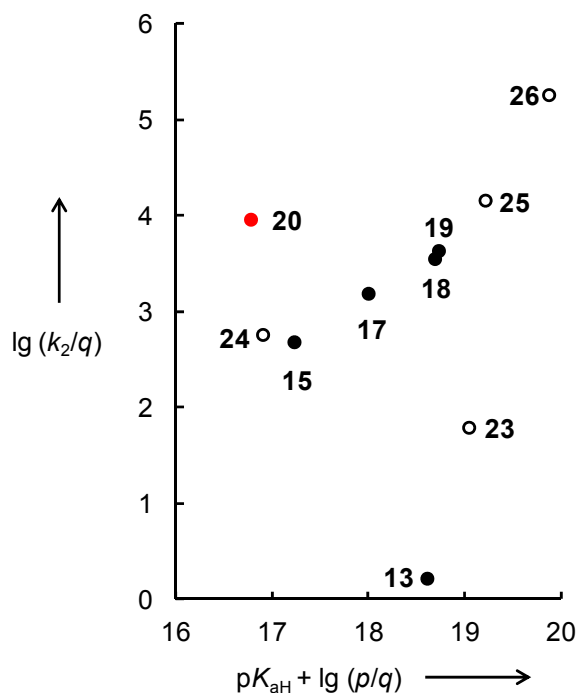


Figure 5.8. Brønsted plot of the statistically corrected second-order rate constants versus the statistically corrected basicities^[31] for the reactions of **5** with amines at 20 °C in acetonitrile (p = number of equivalent protons of the conjugated acids;^[32] q = number of equivalent nucleophilic centers;^[32] filled circles: primary amines, open circles: secondary amines).

In our recent investigations of the reactivities of hydrazines towards benzhydrylium ions, we did not find enhanced nucleophilicities of hydrazines compared with isobasic primary amines, that is, we did not find evidence for the α -effect.^[11] Figure 5.7 shows that the parent hydrazine (**20**) has a similar reactivity as ordinary primary amines in reactions with benzoic anhydride (**2**) and the 1-benzoyl-4-(dimethylamino)pyridinium chloride (**5**), while methylhydrazine (**28**) and 1,2-dimethylhydrazine (**27**) lie on or slightly below the correlation lines for secondary amines. However, hydrazine (**20**) deviates by two orders of magnitude from the linear Brønsted correlation for the α -unbranched primary amines (Figure 5.8). These contrasting results can be rationalized by the higher sensitivity of the acylation reactions towards the variation of the nucleophile compared to the addition reactions with carbocations, which is in line with the previous statement that the magnitude of the α -effect depends on the extent of bond formation in the transition state.^[33]

Bruice *et al.*^[34] reported that methylhydrazine (**28**) reacted more slowly with phenyl acetate than the parent hydrazine (**20**), in contrast to their relative reactivities towards benzhydrylium ions where **28** reacted 8 times faster than **20**.^[11] In line with Bruice, we now find

methylhydrazine (**28**) to react 1.5 to 3 times more slowly than hydrazine (**20**) with benzoic anhydride (**2**) and 1-benzoyl-4-(dimethylamino)pyridinium chloride (**5**). Even when we consider a statistical correction of the reactivity of hydrazine (**20**) due to the presence of two nucleophilic centers, its reactivity towards **5** still exceeds that of the HNMe terminus of methylhydrazine (**28**). This behavior is in line with the up to 50 times higher reactivity of primary amines compared to secondary amines of the same nucleophilicity N , which overcompensates the 8 times higher reactivity of **28** compared to **20** in reactions with benzhydrylium ions (Figure 5.7). Depending on the size of the gap between the correlations, the reactivity of the NHMe terminus of **28** can be below or above that of **20**, and methylhydrazine (**28**) may alternatively react with the methylated or nonmethylated terminus (Scheme 5.2).

Ritchie reported that rate constants for the reactions of esters with a variety of nucleophiles could not be described by the N_+ parameters defined by Equation (5.1).^[4] If both, the nucleophilic attack and the subsequent expulsion of the leaving group contribute to the second-order rate constants, as in the reactions of less reactive acylating agents, for example esters, good correlations of the second-order rate constants with the nucleophilicity parameters N according to Equation (5.2) cannot be expected.

A linear correlation of moderate quality is obtained when $(\lg k_2)/s_N$ for the reactions of carbanions with 4-nitrophenyl benzoate (**1**) is plotted versus the nucleophilicity parameters N of the carbanions (diamonds in Figure 5.9). According to Equation (5.2), the electrophilicity parameter E of **1** ($E = -20.64$) was determined by a least squares fit, that is, by minimization of $\Delta^2 = \sum(\lg k_2 - s_N(N + E))^2$. The last column of Table 5.1 shows that the experimental rate constants for the carbanions with **1**, where the CC-bond forming step is rate determining, agree within a factor of 9 with those calculated by Equation (5.2), which is within the error limit of the equation. The reactivity of **1** is one order of magnitude lower than that of benzaldehyde ($E = -19.52$),^[6] which can be rationalized by ground-state stabilization due to the mesomeric interaction of the oxygen lone pair with the carbonyl group.

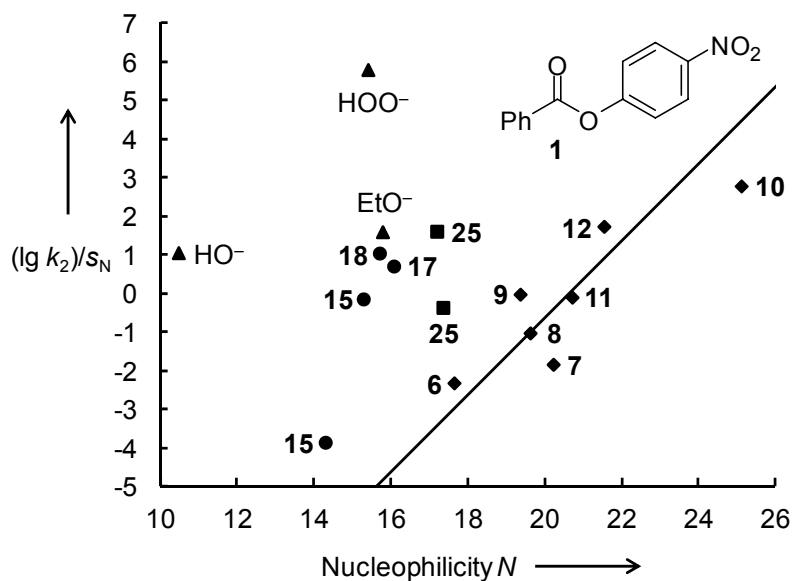


Figure 5.9. Plot of $(\lg k_2)/s_N$ versus the corresponding nucleophilicity parameters N for the reactions of 4-nitrophenyl benzoate (**1**) with carbanions (diamonds), alkoxide anions (triangle), primary (circles) and secondary amines (squares). When the slope is set to unity as required by Equation (5.2), $E = -20.64$ is obtained.^[a]

[a] The second-order rate constants for the acylation reactions of the amines and alkoxide anions were not used for the linear regression.

A remarkable deviation from the correlation line for the carbanions is found for the reactions of **1** with primary and secondary amines, which are 1.5 to 4 orders of magnitude faster than predicted by their benzhydrylium-based nucleophilicity parameters (circles and squares in Figure 5.9). An even greater deviation of 4 to 7 orders of magnitude is observed for alkoxide anions (triangles in Figure 5.9) showing that in reactions with *O*- and *N*-nucleophiles the anomeric stabilization^[35] of the tetrahedral intermediates is already affecting the transition states.

5.3 Conclusion

We have shown that the rate constants for the reactions of the ester **1** with carbanions can be described by the linear free energy relationship [Eq. (5.2)], using the benzhydrylium-derived nucleophilicity parameters N and s_N for carbanions. Amines and alkoxide anions react considerably faster than expected from their reactivity parameters N and s_N , which can be

explained by the anomeric stabilization of the tetrahedral intermediate. The second-order rate constants for the reactions of primary amines with the highly electrophilic acylating agents **2–5** correlate well with the benzhydrylium-derived nucleophile-specific parameters N and s_N of the amines. The same is true for the corresponding reactions of secondary amines. Both series of amines follow separate correlations, however, which implies that a single set of reactivity parameters for nucleophiles and electrophiles is not sufficient to describe the rates of acylation reactions, even in cases where the nucleophilic attack at the carbonyl-group is rate-determining.

5.4 Experimental Section

5.4.1 General Comment

Materials. Acetylacetone, (**6-H**), diethyl malonate (**7-H**), ethyl cyanoacetate (**8-H**), malononitrile (**9-H**), nitromethane (**11-H**), nitroethane (**12-H**), *tert*-butylamine (**13**), isopropylamine (**14**), benzylamine (**15**), allylamine (**16**), ethanolamine (**17**), *n*-propylamine (**18**), *n*-butylamine (**19**), *N,N*-bis(2-methoxyethyl)amine (**21**), di-*n*-propylamine (**22**), diethylamine (**23**), morpholine (**24**), piperidine (**25**), pyrrolidine (**26**), and methylhydrazine (**28**) were purchased and purified by distillation prior to use. 4-Nitrophenyl benzoate (**1**), benzoic anhydride (**2**), acetic anhydride (**3**), benzoyl chloride (**4**), 4-cyanophenylacetonitrile (**10-H**), hydrazine monohydrate (**20**·H₂O), tetra-*n*-butylammonium benzoate (**29**), tetra-*n*-butylammonium 4-nitrobenzoate (**30**), potassium *tert*-butoxide, toluenesulfonic acid monohydrate, and 4-(dimethylamino)pyridine were purchased and used without further purification.

Acetonitrile (> 99.9%, extra dry) and DMSO (> 99.9%, extra dry) were purchased and used without further purification.

1-Benzoyl 4-(dimethylamino)pyridinium chloride (**5**),^[27] potassium diethyl malonate (**7**),^[36] potassium ethyl cyanoacetate (**8**)^[36] and 1,2-dimethylhydrazine (**27**)^[11] were synthesized as described previously.

Analytics. ¹H (400 or 600 MHz) and ¹³C NMR (100 or 150 MHz) spectra were measured on a Varian Inova 400 or Varian 600 instrument. The chemical shifts refer to the solvent residual

signals as internal standard: CDCl_3 ($\delta_{\text{H}} = 7.26$, $\delta_{\text{C}} = 77.2$), or d_6 -DMSO ($\delta_{\text{H}} = 2.50$, $\delta_{\text{C}} = 39.5$). The following abbreviations were used for signal multiplicities: s = singlet, d = doublet, t = triplet, q = quartet, m = multiplet, br = broad. NMR signal assignments were based on additional 2D-NMR experiments (COSY, HSQC, and HMBC).

Mass spectra were recorded with a MAT 95 Q instrument.

Kinetics. The kinetics of the reactions of 4-nitrophenyl benzoate (**1**), benzoic anhydride (**2**), and 1-benzoyl-4-(dimethylamino)pyridinium chloride (**5**) with carbanions **6–12**, amines **13–28** and carboxylates **29** and **30** were followed by UV/Vis spectroscopy in acetonitrile or DMSO at 20 °C. The kinetics of the reactions of acetic anhydride (**3**) and benzoyl chloride (**4**) with the amines **13–28** were followed by conductimetry in acetonitrile at 20 °C.

For slow reactions ($\tau_{1/2} > 10$ s), the spectra were collected at different times by using a J&M TIDAS diode array spectrophotometer that was connected to a Hellma 661.502-QX quartz Suprasil immersion probe (5 mm light path) by fiber optic cables with standard SMA connectors. All kinetic measurements were carried out in Schlenk glassware under exclusion of moisture. The temperature of the solutions during the kinetic studies was maintained at 20 °C \pm 0.1 °C by circulating bath thermostats and monitored with thermo-couple probes that were inserted into the reaction mixture.

A stopped-flow system (Hi-Tech SF-61DX2, Pt electrodes) was used for the conductometric investigation. The kinetic runs were initiated by mixing equal volumes solutions of the nucleophiles and the electrophiles.

5.4.2 Kinetic Experiments

Kinetics of the reactions of 4-nitrophenyl benzoate (1) with carbanions in DMSO

Table 5.3. Rate constants for the reactions of 4-nitrophenyl benzoate (**1**) with potassium acetylacetonate (**6**) generated from acetylacetone with 0.50 equiv. KO*t*Bu in DMSO (diode array spectrophotometer, 20 °C, $\lambda = 435$ nm).

| [1] ₀ /M | [6] ₀ /M | [6] ₀ /[1] ₀ | $k_{\text{obs}}/\text{s}^{-1}$ |
|---|------------------------------|--|--------------------------------|
| 6.42×10^{-5} | 2.69×10^{-3} | 42 | 6.39×10^{-5} |
| 6.12×10^{-5} | 4.95×10^{-3} | 81 | 1.09×10^{-4} |
| 5.82×10^{-5} | 6.99×10^{-3} | 120 | 1.51×10^{-4} |
| 5.97×10^{-5} | 9.50×10^{-3} | 159 | 1.98×10^{-4} |
| 5.86×10^{-5} | 1.18×10^{-2} | 201 | 2.39×10^{-4} |
| $k_2 = 1.93 \times 10^{-2} \text{ M}^{-1} \text{ s}^{-1}$ | | | |

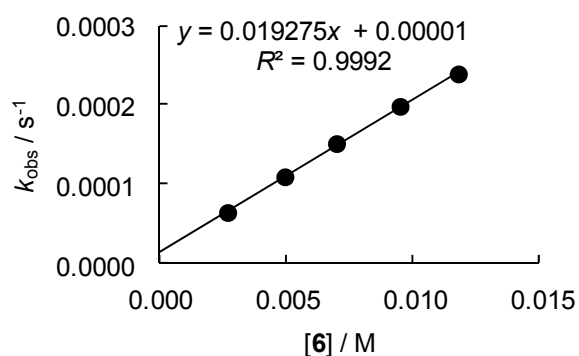


Table 5.4. Rate constants for the reactions of 4-nitrophenyl benzoate (**1**) with potassium diethyl malonate (**7**) generated from diethyl malonate with 0.50 equiv. KO*t*Bu in DMSO (diode array spectrophotometer, 20 °C, $\lambda = 435$ nm).

| [1] ₀ /M | [7] ₀ /M | [7] ₀ /[1] ₀ | $k_{\text{obs}}/\text{s}^{-1}$ |
|---|------------------------------|--|--------------------------------|
| 5.08×10^{-5} | 2.55×10^{-3} | 50 | 1.80×10^{-4} |
| 4.87×10^{-5} | 4.89×10^{-3} | 100 | 3.51×10^{-4} |
| 4.82×10^{-5} | 7.25×10^{-3} | 151 | 4.69×10^{-4} |
| 4.63×10^{-5} | 9.30×10^{-3} | 201 | 6.14×10^{-4} |
| 4.59×10^{-5} | 1.15×10^{-2} | 251 | 7.29×10^{-4} |
| $k_2 = 6.10 \times 10^{-2} \text{ M}^{-1} \text{ s}^{-1}$ | | | |

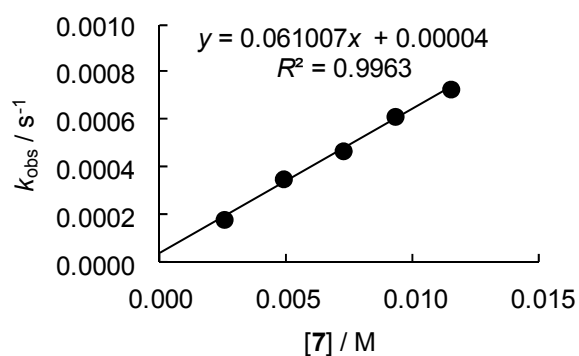


Table 5.5. Rate constants for the reactions of 4-nitrophenyl benzoate (**1**) with potassium ethyl cyanoacetate (**8**) in DMSO (diode array spectrophotometer, 20 °C, $\lambda = 435$ nm).

| [1] ₀ /M | [8] ₀ /M | [8] ₀ /[1] ₀ | $k_{\text{obs}}/\text{s}^{-1}$ |
|---|------------------------------|--|--------------------------------|
| 6.42×10^{-5} | 2.52×10^{-3} | 39 | 5.71×10^{-4} |
| 6.79×10^{-5} | 4.08×10^{-3} | 60 | 8.51×10^{-4} |
| 6.41×10^{-5} | 5.19×10^{-3} | 81 | 1.06×10^{-3} |
| 6.11×10^{-5} | 6.07×10^{-3} | 99 | 1.27×10^{-3} |
| 1.26×10^{-4} | 7.26×10^{-3} | 58 | 1.49×10^{-3} |
| $k_2 = 1.96 \times 10^{-1} \text{ M}^{-1} \text{ s}^{-1}$ | | | |

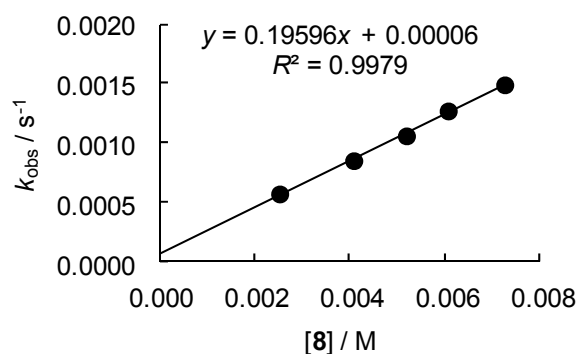


Table 5.6. Rate constants for the reactions of 4-nitrophenyl benzoate (**1**) with potassium malononitrile (**9**) generated from malononitrile with 0.50 equiv. KOtBu in DMSO (diode array spectrophotometer, 20 °C, $\lambda = 435$ nm).

| [1] ₀ /M | [9] ₀ /M | [9] ₀ /[1] ₀ | $k_{\text{obs}}/\text{s}^{-1}$ |
|---|------------------------------|--|--------------------------------|
| 5.05×10^{-5} | 2.03×10^{-3} | 40 | 1.98×10^{-3} |
| 5.03×10^{-5} | 4.04×10^{-3} | 80 | 3.99×10^{-3} |
| 5.30×10^{-5} | 6.38×10^{-3} | 121 | 5.98×10^{-3} |
| 4.78×10^{-5} | 7.68×10^{-3} | 161 | 7.12×10^{-3} |
| 4.79×10^{-5} | 9.62×10^{-3} | 201 | 9.09×10^{-3} |
| $k_2 = 9.22 \times 10^{-1} \text{ M}^{-1} \text{ s}^{-1}$ | | | |

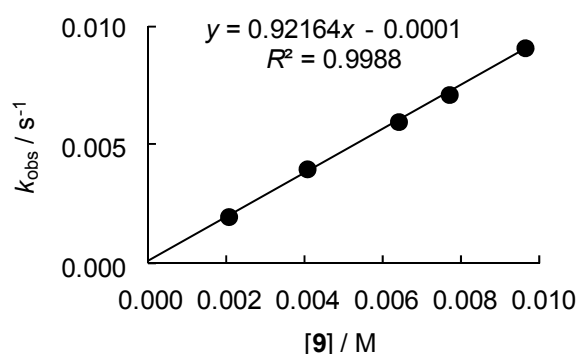


Table 5.7. Rate constants for the reactions of 4-nitrophenyl benzoate (**1**) with potassium 4-cyanophenylacetonitrile (**10**) generated from 4-cyanophenylacetonitrile with 0.50 equiv. KO t Bu in DMSO (stopped-flow technique, 20 °C, $\lambda = 435$ nm).

| [1] ₀ /M | [10] ₀ /M | [10] ₀ /[1] ₀ | $k_{\text{obs}}/\text{s}^{-1}$ |
|--|-------------------------------|---|--------------------------------|
| 2.91×10^{-5} | 1.17×10^{-3} | 40 | 3.86×10^{-2} |
| 2.91×10^{-5} | 1.76×10^{-3} | 61 | 5.94×10^{-2} |
| 2.91×10^{-5} | 2.31×10^{-3} | 79 | 7.23×10^{-2} |
| 2.91×10^{-5} | 2.90×10^{-3} | 100 | 9.30×10^{-2} |
| 2.91×10^{-5} | 3.48×10^{-3} | 120 | 1.10×10^{-1} |
| $k_2 = 3.06 \times 10^1 \text{ M}^{-1} \text{ s}^{-1}$ | | | |

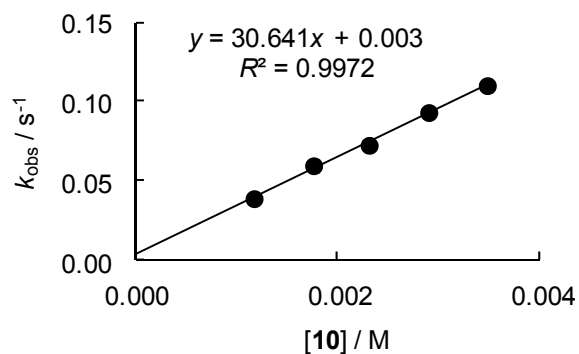


Table 5.8. Rate constants for the reactions of 4-nitrophenyl benzoate (**1**) with potassium nitromethanide (**11**) generated from nitromethane with 0.49 equiv. KO t Bu in DMSO (diode array spectrophotometer, 20 °C, $\lambda = 435$ nm).

| [1] ₀ /M | [11] ₀ /M | [11] ₀ /[1] ₀ | $k_{\text{obs}}/\text{s}^{-1}$ |
|---|-------------------------------|---|--------------------------------|
| 6.00×10^{-5} | 6.27×10^{-4} | 11 | 6.34×10^{-4} |
| 6.10×10^{-5} | 2.45×10^{-3} | 40 | 2.49×10^{-3} |
| 5.92×10^{-5} | 5.06×10^{-3} | 86 | 4.84×10^{-3} |
| 6.40×10^{-5} | 7.70×10^{-3} | 120 | 6.85×10^{-3} |
| 5.72×10^{-5} | 9.18×10^{-3} | 161 | 8.03×10^{-3} |
| 5.57×10^{-5} | 1.12×10^{-2} | 201 | 9.56×10^{-3} |
| $k_2 = 8.37 \times 10^{-1} \text{ M}^{-1} \text{ s}^{-1}$ | | | |

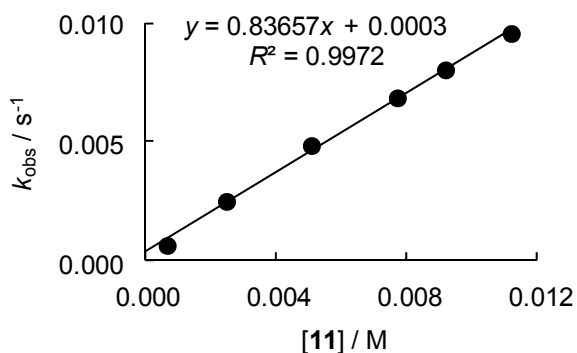
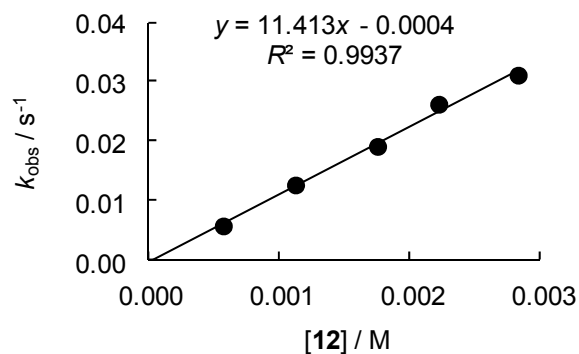


Table 5.9. Rate constants for the reactions of 4-nitrophenyl benzoate (**1**) with potassium nitroethanide (**12**) generated from nitroethane with 0.50 equiv. KOtBu in DMSO (diode array spectrophotometer, 20 °C, $\lambda = 435$ nm).

| $[1]_0/\text{M}$ | $[12]_0/\text{M}$ | $[12]_0/[1]_0$ | $k_{\text{obs}}/\text{s}^{-1}$ |
|--|-----------------------|----------------|--------------------------------|
| 5.57×10^{-5} | 5.65×10^{-4} | 10 | 5.70×10^{-3} |
| 5.54×10^{-5} | 1.12×10^{-3} | 20 | 1.26×10^{-2} |
| 5.87×10^{-5} | 1.75×10^{-3} | 30 | 1.91×10^{-2} |
| 5.46×10^{-5} | 2.22×10^{-3} | 41 | 2.62×10^{-2} |
| 5.57×10^{-5} | 2.83×10^{-3} | 51 | 3.11×10^{-2} |
| $k_2 = 1.14 \times 10^1 \text{ M}^{-1} \text{ s}^{-1}$ | | | |



Kinetics of the reactions of 4-nitrophenyl benzoate (1) with amines in DMSO

Table 5.10. Rate constants for the reactions of 4-nitrophenyl benzoate (**1**) with benzylamine (**15**) in DMSO (diode array spectrophotometer, 20 °C, $\lambda = 435$ nm).

| $[1]_0/\text{M}$ | $[15]_0/\text{M}$ | $[15]_0/[1]_0$ | $k_{\text{obs}}/\text{s}^{-1}$ |
|---|-----------------------|----------------|--------------------------------|
| 6.04×10^{-5} | 1.24×10^{-3} | 21 | 1.28×10^{-3} |
| 5.86×10^{-5} | 2.40×10^{-3} | 41 | 2.21×10^{-3} |
| 5.68×10^{-5} | 3.49×10^{-3} | 61 | 3.08×10^{-3} |
| 5.62×10^{-5} | 4.60×10^{-3} | 82 | 3.91×10^{-3} |
| 5.47×10^{-5} | 5.60×10^{-3} | 102 | 4.63×10^{-3} |
| $k_2 = 7.70 \times 10^{-1} \text{ M}^{-1} \text{ s}^{-1}$ | | | |

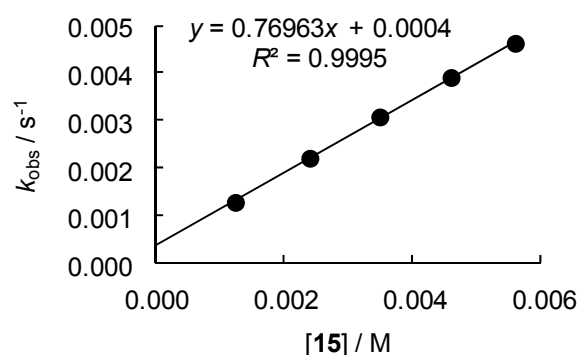


Table 5.11. Rate constants for the reactions of 4-nitrophenyl benzoate (**1**) with ethanolamine (**17**) in DMSO (diode array spectrophotometer, 20 °C, $\lambda = 435$ nm).

| [1] ₀ /M | [17] ₀ /M | [17] ₀ /[1] ₀ | $k_{\text{obs}}/\text{s}^{-1}$ |
|--|-------------------------------|---|--------------------------------|
| 6.40×10^{-5} | 1.29×10^{-3} | 20 | 3.45×10^{-3} |
| 6.20×10^{-5} | 2.49×10^{-3} | 40 | 6.69×10^{-3} |
| 6.08×10^{-5} | 3.67×10^{-3} | 60 | 9.43×10^{-3} |
| 6.11×10^{-5} | 4.92×10^{-3} | 80 | 1.25×10^{-2} |
| 6.29×10^{-5} | 6.32×10^{-3} | 100 | 1.67×10^{-2} |
| $k_2 = 2.59 \text{ M}^{-1} \text{ s}^{-1}$ | | | |

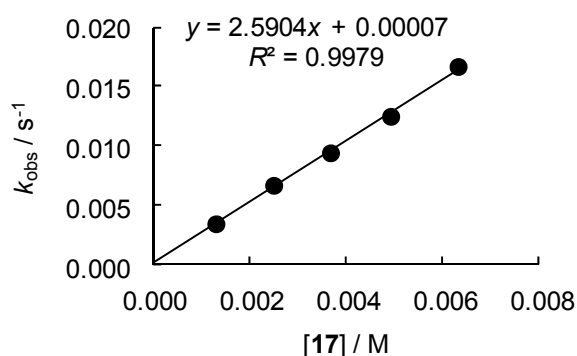


Table 5.12. Rate constants for the reactions of 4-nitrophenyl benzoate (**1**) with *n*-propylamine (**18**) in DMSO (diode array spectrophotometer, 20 °C, $\lambda = 435$ nm).

| [1] ₀ /M | [18] ₀ /M | [18] ₀ /[1] ₀ | $k_{\text{obs}}/\text{s}^{-1}$ |
|--|-------------------------------|---|--------------------------------|
| 6.26×10^{-5} | 1.25×10^{-3} | 20 | 5.94×10^{-3} |
| 6.00×10^{-5} | 2.39×10^{-3} | 40 | 1.12×10^{-2} |
| 6.10×10^{-5} | 3.64×10^{-3} | 60 | 1.66×10^{-2} |
| 5.84×10^{-5} | 4.65×10^{-3} | 80 | 2.08×10^{-2} |
| 5.76×10^{-5} | 5.73×10^{-3} | 99 | 2.61×10^{-2} |
| $k_2 = 4.45 \text{ M}^{-1} \text{ s}^{-1}$ | | | |

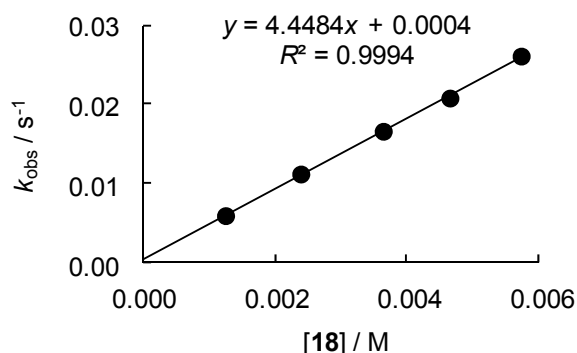
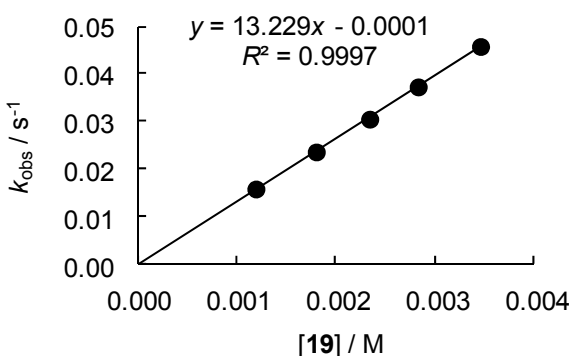


Table 5.13. Rate constants for the reactions of 4-nitrophenyl benzoate (**1**) with piperidine (**25**) in DMSO (diode array spectrophotometer, 20 °C, $\lambda = 436$ nm).

| [1] ₀ /M | [25] ₀ /M | [25] ₀ /[1] ₀ | $k_{\text{obs}}/\text{s}^{-1}$ |
|--|-------------------------------|---|--------------------------------|
| 5.84×10^{-5} | 1.19×10^{-3} | 20 | 1.58×10^{-2} |
| 5.92×10^{-5} | 1.80×10^{-3} | 30 | 2.36×10^{-2} |
| 5.76×10^{-5} | 2.34×10^{-3} | 41 | 3.05×10^{-2} |
| 5.73×10^{-5} | 2.83×10^{-3} | 49 | 3.73×10^{-2} |
| 5.82×10^{-5} | 3.46×10^{-3} | 59 | 4.58×10^{-2} |
| $k_2 = 1.32 \times 10^1 \text{ M}^{-1} \text{ s}^{-1}$ | | | |



Kinetics of the reactions of benzoic anhydride (2) with amines in CH₃CN

Table 5.14. Rate constants for the reactions of benzoic anhydride (2) with isopropylamine (14) in CH₃CN (stopped-flow technique, 20 °C, λ = 280 nm).

| [2] ₀ /M | [14] ₀ /M | [14] ₀ /[2] ₀ | k _{obs} /s ⁻¹ |
|-------------------------|-------------------------|-------------------------------------|-----------------------------------|
| 3.42 × 10 ⁻⁴ | 6.93 × 10 ⁻³ | 20 | 3.36 × 10 ⁻¹ |
| 3.42 × 10 ⁻⁴ | 1.39 × 10 ⁻² | 41 | 7.05 × 10 ⁻¹ |
| 3.42 × 10 ⁻⁴ | 2.08 × 10 ⁻² | 61 | 1.09 |
| 3.42 × 10 ⁻⁴ | 2.60 × 10 ⁻² | 76 | 1.37 |
| 3.42 × 10 ⁻⁴ | 3.47 × 10 ⁻² | 101 | 1.84 |

$k_2 = 5.43 \times 10^1 \text{ M}^{-1} \text{ s}^{-1}$

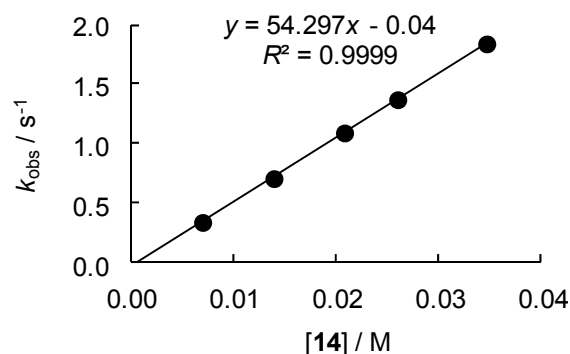


Table 5.15. Rate constants for the reactions of benzoic anhydride (2) with benzylamine (15) in CH₃CN (stopped-flow technique, 20 °C, λ = 280 nm).

| [2] ₀ /M | [15] ₀ /M | [15] ₀ /[2] ₀ | k _{obs} /s ⁻¹ |
|-------------------------|-------------------------|-------------------------------------|-----------------------------------|
| 3.59 × 10 ⁻⁴ | 7.30 × 10 ⁻³ | 20 | 4.85 × 10 ⁻¹ |
| 3.59 × 10 ⁻⁴ | 1.43 × 10 ⁻² | 40 | 9.75 × 10 ⁻¹ |
| 3.59 × 10 ⁻⁴ | 2.12 × 10 ⁻² | 59 | 1.52 |
| 3.59 × 10 ⁻⁴ | 2.85 × 10 ⁻² | 79 | 2.06 |
| 3.59 × 10 ⁻⁴ | 3.32 × 10 ⁻² | 92 | 2.40 |

$k_2 = 7.45 \times 10^1 \text{ M}^{-1} \text{ s}^{-1}$

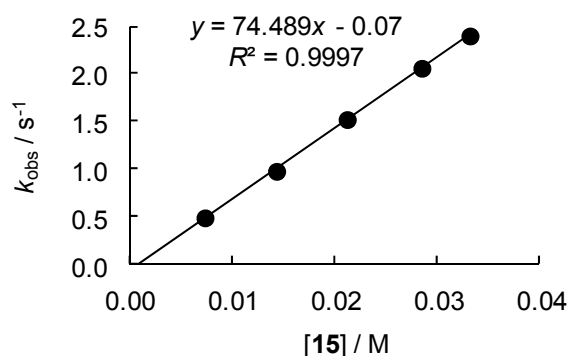


Table 5.16. Rate constants for the reactions of benzoic anhydride (**2**) with allylamine (**16**) in CH₃CN (stopped-flow technique, 20 °C, λ = 280 nm).

| [2] ₀ /M | [16] ₀ /M | [16] ₀ /[2] ₀ | <i>k</i> _{obs} /s ⁻¹ |
|------------------------------|-------------------------------|---|--|
| 3.59 × 10 ⁻⁴ | 6.73 × 10 ⁻³ | 19 | 4.63 × 10 ⁻¹ |
| 3.59 × 10 ⁻⁴ | 1.35 × 10 ⁻² | 38 | 9.47 × 10 ⁻¹ |
| 3.59 × 10 ⁻⁴ | 2.15 × 10 ⁻² | 60 | 1.56 |
| 3.59 × 10 ⁻⁴ | 2.83 × 10 ⁻² | 79 | 2.08 |
| 3.59 × 10 ⁻⁴ | 3.37 × 10 ⁻² | 94 | 2.49 |

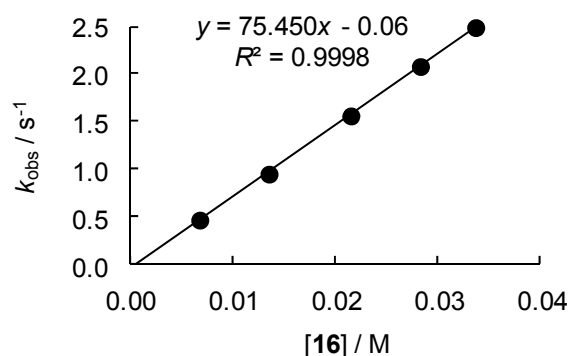
$$k_2 = 7.55 \times 10^1 \text{ M}^{-1} \text{ s}^{-1}$$


Table 5.17. Rate constants for the reactions of benzoic anhydride (**2**) with ethanolamine (**17**) in CH₃CN (stopped-flow technique, 20 °C, λ = 280 nm).

| [2] ₀ /M | [17] ₀ /M | [17] ₀ /[2] ₀ | <i>k</i> _{obs} /s ⁻¹ |
|------------------------------|-------------------------------|---|--|
| 3.54 × 10 ⁻⁴ | 6.92 × 10 ⁻³ | 20 | 1.10 |
| 3.54 × 10 ⁻⁴ | 1.43 × 10 ⁻² | 40 | 2.40 |
| 3.54 × 10 ⁻⁴ | 2.12 × 10 ⁻² | 60 | 3.62 |
| 3.54 × 10 ⁻⁴ | 2.87 × 10 ⁻² | 81 | 4.96 |
| 3.54 × 10 ⁻⁴ | 3.56 × 10 ⁻² | 100 | 6.28 |

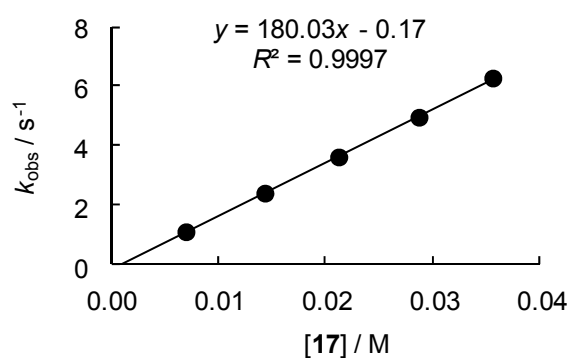
$$k_2 = 1.80 \times 10^2 \text{ M}^{-1} \text{ s}^{-1}$$


Table 5.18. Rate constants for the reactions of benzoic anhydride (**2**) with *n*-butylamine (**19**) in CH₃CN (stopped-flow technique, 20 °C, λ = 280 nm).

| [2] ₀ /M | [19] ₀ /M | [19] ₀ /[2] ₀ | <i>k</i> _{obs} /s ⁻¹ |
|------------------------------|-------------------------------|---|--|
| 3.42 × 10 ⁻⁴ | 7.14 × 10 ⁻³ | 21 | 3.21 |
| 3.42 × 10 ⁻⁴ | 1.36 × 10 ⁻² | 40 | 6.09 |
| 3.42 × 10 ⁻⁴ | 2.08 × 10 ⁻² | 61 | 9.40 |
| 3.42 × 10 ⁻⁴ | 2.72 × 10 ⁻² | 80 | 1.24 × 10 ¹ |
| 3.42 × 10 ⁻⁴ | 3.24 × 10 ⁻² | 95 | 1.46 × 10 ¹ |

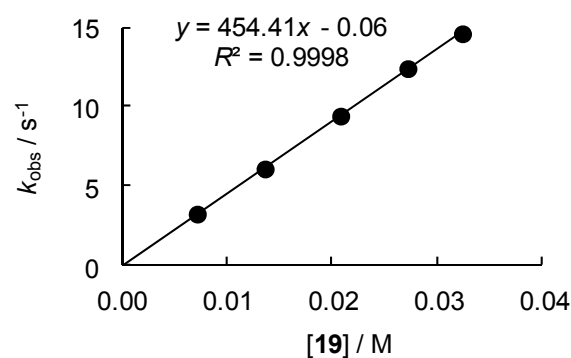
$$k_2 = 4.54 \times 10^2 \text{ M}^{-1} \text{ s}^{-1}$$


Table 5.19. Rate constants for the reactions of benzoic anhydride (**2**) with hydrazine (**20**) in CH₃CN (stopped-flow technique, 20 °C, λ = 280 nm).

| [2] ₀ /M | [20] ₀ /M | [20] ₀ /[2] ₀ | <i>k</i> _{obs} /s ⁻¹ |
|--|-------------------------------|---|--|
| 3.54 × 10 ⁻⁴ | 3.54 × 10 ⁻³ | 10 | 7.66 |
| 3.54 × 10 ⁻⁴ | 7.08 × 10 ⁻³ | 20 | 1.50 × 10 ¹ |
| 3.54 × 10 ⁻⁴ | 1.07 × 10 ⁻² | 30 | 2.19 × 10 ¹ |
| 3.54 × 10 ⁻⁴ | 1.41 × 10 ⁻² | 40 | 2.86 × 10 ¹ |
| 3.54 × 10 ⁻⁴ | 1.78 × 10 ⁻² | 50 | 3.65 × 10 ¹ |
| <i>k</i> ₂ = 2.01 × 10 ³ M ⁻¹ s ⁻¹ | | | |

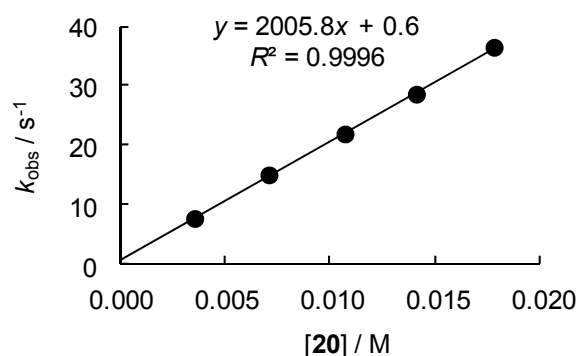


Table 5.20. Rate constants for the reactions of benzoic anhydride (**2**) with *N,N*-bis-(2-methoxyethyl)amine (**21**) in CH₃CN (diode array spectrophotometer, 20 °C, λ = 280 nm).

| [2] ₀ /M | [21] ₀ /M | [21] ₀ /[2] ₀ | <i>k</i> _{obs} /s ⁻¹ |
|---|-------------------------------|---|--|
| 8.20 × 10 ⁻⁴ | 1.61 × 10 ⁻² | 20 | 5.56 × 10 ⁻³ |
| 8.21 × 10 ⁻⁴ | 3.32 × 10 ⁻² | 40 | 1.22 × 10 ⁻² |
| 8.33 × 10 ⁻⁴ | 5.09 × 10 ⁻² | 61 | 1.95 × 10 ⁻² |
| 8.09 × 10 ⁻⁴ | 6.53 × 10 ⁻² | 81 | 2.52 × 10 ⁻² |
| 8.02 × 10 ⁻⁴ | 7.87 × 10 ⁻² | 98 | 3.09 × 10 ⁻² |
| <i>k</i> ₂ = 4.05 × 10 ⁻¹ M ⁻¹ s ⁻¹ | | | |

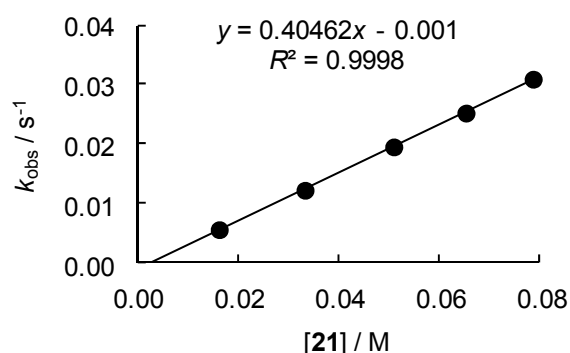


Table 5.21. Rate constants for the reactions of benzoic anhydride (**2**) with diethylamine (**23**) in CH₃CN (stopped-flow technique, 20 °C, λ = 280 nm).

| [2] ₀ /M | [23] ₀ /M | [23] ₀ /[2] ₀ | <i>k</i> _{obs} /s ⁻¹ |
|--|-------------------------------|---|--|
| 3.42 × 10 ⁻⁴ | 6.94 × 10 ⁻³ | 20 | 1.58 × 10 ⁻¹ |
| 3.42 × 10 ⁻⁴ | 1.39 × 10 ⁻² | 41 | 3.13 × 10 ⁻¹ |
| 3.42 × 10 ⁻⁴ | 2.08 × 10 ⁻² | 61 | 4.63 × 10 ⁻¹ |
| 3.42 × 10 ⁻⁴ | 2.78 × 10 ⁻² | 81 | 6.22 × 10 ⁻¹ |
| 3.42 × 10 ⁻⁴ | 3.47 × 10 ⁻² | 102 | 7.79 × 10 ⁻¹ |
| <i>k</i> ₂ = 2.23 × 10 ¹ M ⁻¹ s ⁻¹ | | | |

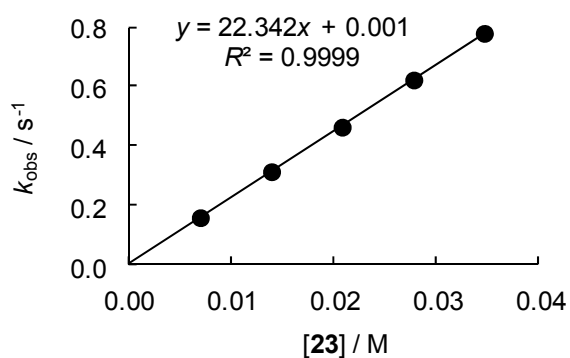


Table 5.22. Rate constants for the reactions of benzoic anhydride (**2**) with morpholine (**24**) in CH₃CN (stopped-flow technique, 20 °C, λ = 280 nm).

| [2] ₀ /M | [24] ₀ /M | [24] ₀ /[2] ₀ | <i>k</i> _{obs} /s ⁻¹ |
|------------------------------|-------------------------------|---|--|
| 3.42 × 10 ⁻⁴ | 6.87 × 10 ⁻³ | 20 | 5.34 × 10 ⁻¹ |
| 3.42 × 10 ⁻⁴ | 1.37 × 10 ⁻² | 40 | 1.10 |
| 3.42 × 10 ⁻⁴ | 2.06 × 10 ⁻² | 60 | 2.02 |
| 3.42 × 10 ⁻⁴ | 2.75 × 10 ⁻² | 80 | 2.24 |
| 3.42 × 10 ⁻⁴ | 3.44 × 10 ⁻² | 101 | 2.82 |

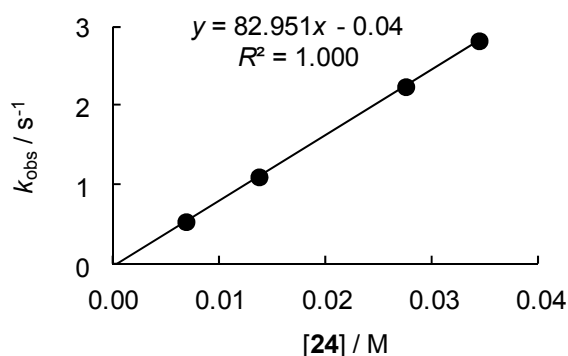
$$k_2 = 8.30 \times 10^1 \text{ M}^{-1} \text{ s}^{-1}$$


Table 5.23. Rate constants for the reactions of benzoic anhydride (**2**) with piperidine (**25**) in CH₃CN (stopped-flow technique, 20 °C, λ = 280 nm).

| [2] ₀ /M | [25] ₀ /M | [25] ₀ /[2] ₀ | <i>k</i> _{obs} /s ⁻¹ |
|------------------------------|-------------------------------|---|--|
| 3.77 × 10 ⁻⁴ | 7.35 × 10 ⁻³ | 19 | 2.42 × 10 ¹ |
| 3.77 × 10 ⁻⁴ | 1.54 × 10 ⁻² | 41 | 4.89 × 10 ¹ |
| 3.77 × 10 ⁻⁴ | 2.27 × 10 ⁻² | 60 | 7.22 × 10 ¹ |
| 3.77 × 10 ⁻⁴ | 3.01 × 10 ⁻² | 99 | 9.56 × 10 ¹ |
| 3.77 × 10 ⁻⁴ | 3.74 × 10 ⁻² | 101 | 1.19 × 10 ² |

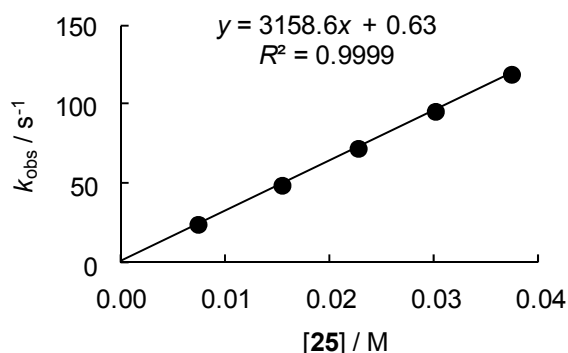
$$k_2 = 3.16 \times 10^3 \text{ M}^{-1} \text{ s}^{-1}$$


Table 5.24. Rate constants for the reactions of benzoic anhydride (**2**) with pyrrolidine (**26**) in CH₃CN (stopped-flow technique, 20 °C, λ = 280 nm).

| [2] ₀ /M | [26] ₀ /M | [26] ₀ /[2] ₀ | <i>k</i> _{obs} /s ⁻¹ |
|------------------------------|-------------------------------|---|--|
| 3.77 × 10 ⁻⁴ | 5.77 × 10 ⁻³ | 15 | 1.12 × 10 ² |
| 3.77 × 10 ⁻⁴ | 7.59 × 10 ⁻³ | 20 | 1.45 × 10 ² |
| 3.77 × 10 ⁻⁴ | 9.41 × 10 ⁻³ | 25 | 1.87 × 10 ² |
| 3.77 × 10 ⁻⁴ | 1.12 × 10 ⁻² | 30 | 2.26 × 10 ² |
| 3.77 × 10 ⁻⁴ | 1.31 × 10 ⁻² | 35 | 2.61 × 10 ² |

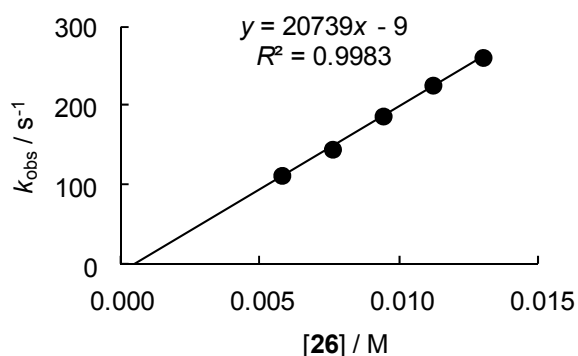
$$k_2 = 2.07 \times 10^4 \text{ M}^{-1} \text{ s}^{-1}$$


Table 5.25. Rate constants for the reactions of benzoic anhydride (**2**) with 1,2-dimethylhydrazine (**27**) in CH₃CN (stopped-flow technique, 20 °C, λ = 280 nm).

| [2] ₀ /M | [27] ₀ /M | [27] ₀ /[2] ₀ | <i>k</i> _{obs} /s ⁻¹ |
|------------------------------|-------------------------------|---|--|
| 3.27 × 10 ⁻⁴ | 6.48 × 10 ⁻³ | 20 | 3.49 × 10 ⁻¹ |
| 3.27 × 10 ⁻⁴ | 9.72 × 10 ⁻³ | 30 | 5.37 × 10 ⁻¹ |
| 3.27 × 10 ⁻⁴ | 1.30 × 10 ⁻² | 40 | 7.21 × 10 ⁻¹ |
| 3.27 × 10 ⁻⁴ | 1.62 × 10 ⁻² | 50 | 9.02 × 10 ⁻¹ |
| 3.27 × 10 ⁻⁴ | 1.91 × 10 ⁻² | 59 | 1.08 |
| 3.27 × 10 ⁻⁴ | 2.21 × 10 ⁻² | 68 | 1.26 |

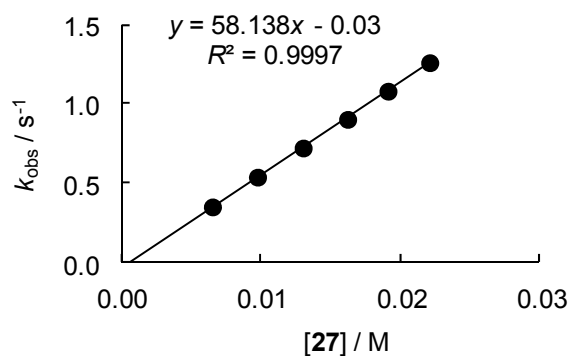
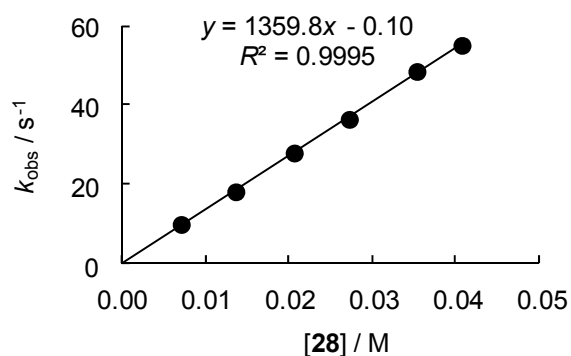
$$k_2 = 5.81 \times 10^1 \text{ M}^{-1} \text{ s}^{-1}$$


Table 5.26. Rate constants for the reactions of benzoic anhydride (**2**) with methylhydrazine (**28**) in CH₃CN (stopped-flow technique, 20 °C, λ = 280 nm).

| [2] ₀ /M | [28] ₀ /M | [28] ₀ /[2] ₀ | <i>k</i> _{obs} /s ⁻¹ |
|------------------------------|-------------------------------|---|--|
| 3.47 × 10 ⁻⁴ | 7.06 × 10 ⁻³ | 20 | 9.85 |
| 3.47 × 10 ⁻⁴ | 1.36 × 10 ⁻² | 39 | 1.81 × 10 ¹ |
| 3.47 × 10 ⁻⁴ | 2.06 × 10 ⁻² | 59 | 2.79 × 10 ¹ |
| 3.47 × 10 ⁻⁴ | 2.72 × 10 ⁻² | 78 | 3.64 × 10 ¹ |
| 3.47 × 10 ⁻⁴ | 3.53 × 10 ⁻² | 102 | 4.85 × 10 ¹ |
| 3.47 × 10 ⁻⁴ | 4.07 × 10 ⁻² | 117 | 5.51 × 10 ¹ |

$$k_2 = 1.36 \times 10^3 \text{ M}^{-1} \text{ s}^{-1}$$


Kinetics of the reactions of acetic anhydride (3) with amines in CH₃CN

Table 5.27. Rate constants for the reactions of acetic anhydride (3) with isopropylamine (14) in CH₃CN (stopped-flow technique, 20 °C, conductimetry).

| [3] ₀ /M | [14] ₀ /M | [14] ₀ /[3] ₀ | <i>k</i> _{obs} /s ⁻¹ |
|--|-------------------------|-------------------------------------|--|
| 4.44 × 10 ⁻³ | 4.41 × 10 ⁻² | 10 | 4.16 |
| 4.44 × 10 ⁻³ | 8.48 × 10 ⁻² | 19 | 8.99 |
| 4.44 × 10 ⁻³ | 1.36 × 10 ⁻¹ | 31 | 1.45 × 10 ¹ |
| 4.44 × 10 ⁻³ | 1.70 × 10 ⁻¹ | 38 | 1.77 × 10 ¹ |
| 4.44 × 10 ⁻³ | 2.21 × 10 ⁻¹ | 50 | 2.30 × 10 ¹ |
| <i>k</i> ₂ = 1.06 × 10 ² M ⁻¹ s ⁻¹ | | | |

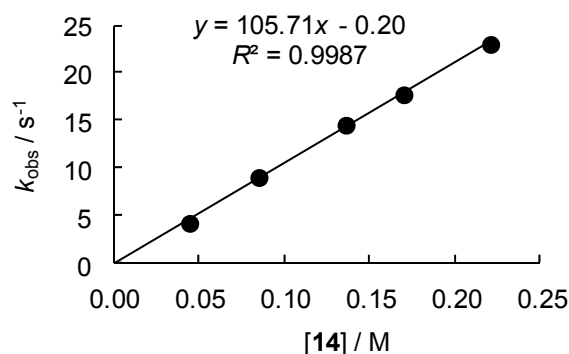


Table 5.28. Rate constants for the reactions of acetic anhydride (3) with benzylamine (15) in CH₃CN (stopped-flow technique, 20 °C, conductimetry)

| [3] ₀ /M | [15] ₀ /M | [15] ₀ /[3] ₀ | <i>k</i> _{obs} /s ⁻¹ |
|--|-------------------------|-------------------------------------|--|
| 5.33 × 10 ⁻³ | 5.32 × 10 ⁻² | 10 | 7.40 |
| 5.33 × 10 ⁻³ | 1.08 × 10 ⁻¹ | 20 | 1.51 × 10 ¹ |
| 5.33 × 10 ⁻³ | 1.66 × 10 ⁻¹ | 31 | 2.51 × 10 ¹ |
| 5.33 × 10 ⁻³ | 2.16 × 10 ⁻¹ | 41 | 2.98 × 10 ¹ |
| 5.33 × 10 ⁻³ | 2.66 × 10 ⁻¹ | 50 | 3.81 × 10 ¹ |
| <i>k</i> ₂ = 1.43 × 10 ² M ⁻¹ s ⁻¹ | | | |

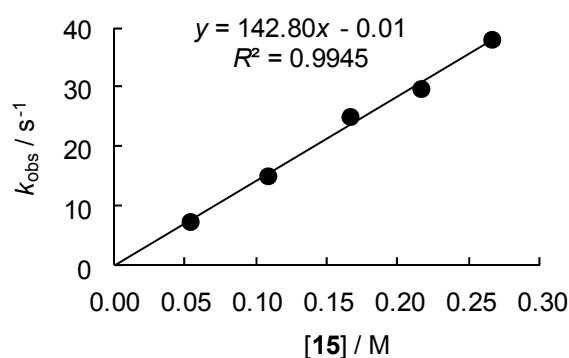


Table 5.29. Rate constants for the reactions of acetic anhydride (**3**) with allylamine (**16**) in CH₃CN (stopped-flow technique, 20 °C, conductimetry).

| [3] ₀ /M | [16] ₀ /M | [16] ₀ /[3] ₀ | <i>k</i> _{obs} /s ⁻¹ |
|------------------------------|-------------------------------|---|--|
| 1.83 × 10 ⁻³ | 1.86 × 10 ⁻² | 10 | 2.96 |
| 1.83 × 10 ⁻³ | 3.71 × 10 ⁻² | 20 | 6.25 |
| 1.83 × 10 ⁻³ | 5.57 × 10 ⁻² | 30 | 9.45 |
| 1.83 × 10 ⁻³ | 7.42 × 10 ⁻² | 41 | 1.28 × 10 ¹ |
| 1.83 × 10 ⁻³ | 9.28 × 10 ⁻² | 51 | 1.60 × 10 ¹ |

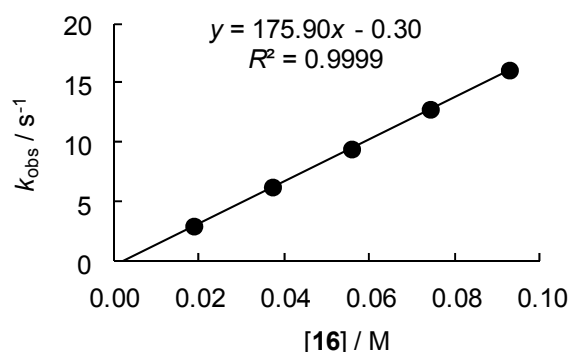
$$k_2 = 1.76 \times 10^2 \text{ M}^{-1} \text{ s}^{-1}$$


Table 5.30. Rate constants for the reactions of acetic anhydride (**3**) with ethanolamine (**17**) in CH₃CN (stopped-flow technique, 20 °C, conductimetry).

| [3] ₀ /M | [17] ₀ /M | [17] ₀ /[3] ₀ | <i>k</i> _{obs} /s ⁻¹ |
|------------------------------|-------------------------------|---|--|
| 4.55 × 10 ⁻³ | 9.60 × 10 ⁻² | 21 | 3.26 × 10 ¹ |
| 4.55 × 10 ⁻³ | 1.12 × 10 ⁻¹ | 26 | 4.20 × 10 ¹ |
| 4.55 × 10 ⁻³ | 1.80 × 10 ⁻¹ | 40 | 6.75 × 10 ¹ |
| 4.55 × 10 ⁻³ | 2.40 × 10 ⁻¹ | 53 | 9.60 × 10 ¹ |
| 4.55 × 10 ⁻³ | 2.88 × 10 ⁻¹ | 63 | 1.21 × 10 ² |

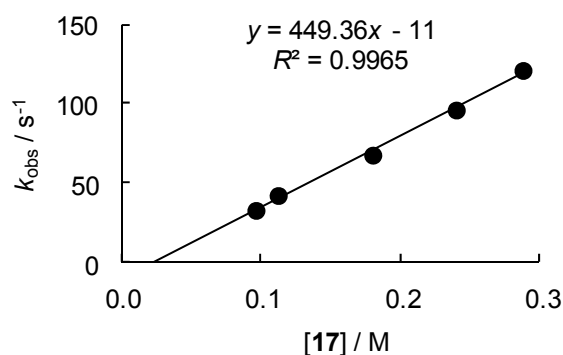
$$k_2 = 4.49 \times 10^2 \text{ M}^{-1} \text{ s}^{-1}$$


Table 5.31. Rate constants for the reactions of acetic anhydride (**3**) with *n*-propylamine (**18**) in CH₃CN (stopped-flow technique, 20 °C, conductimetry).

| [3] ₀ /M | [18] ₀ /M | [18] ₀ /[3] ₀ | <i>k</i> _{obs} /s ⁻¹ |
|------------------------------|-------------------------------|---|--|
| 1.36 × 10 ⁻³ | 1.37 × 10 ⁻² | 10 | 7.36 |
| 1.36 × 10 ⁻³ | 2.73 × 10 ⁻² | 20 | 1.61 × 10 ¹ |
| 1.36 × 10 ⁻³ | 4.10 × 10 ⁻² | 30 | 2.38 × 10 ¹ |
| 1.36 × 10 ⁻³ | 5.47 × 10 ⁻² | 40 | 3.11 × 10 ¹ |

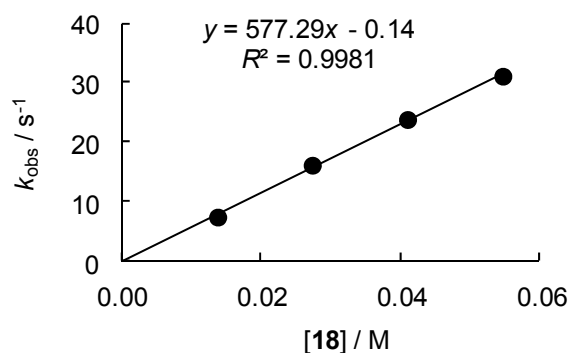
$$k_2 = 5.77 \times 10^2 \text{ M}^{-1} \text{ s}^{-1}$$


Table 5.32. Rate constants for the reactions of acetic anhydride (**3**) with *n*-butylamine (**19**) in CH₃CN (stopped-flow technique, 20 °C, conductimetry).

| [3] ₀ /M | [19] ₀ /M | [19] ₀ /[3] ₀ | <i>k</i> _{obs} /s ⁻¹ |
|------------------------------|-------------------------------|---|--|
| 1.37 × 10 ⁻³ | 1.38 × 10 ⁻² | 10 | 9.55 |
| 1.37 × 10 ⁻³ | 2.76 × 10 ⁻² | 20 | 1.83 × 10 ¹ |
| 1.37 × 10 ⁻³ | 4.14 × 10 ⁻² | 30 | 2.95 × 10 ¹ |
| 1.37 × 10 ⁻³ | 5.75 × 10 ⁻² | 42 | 4.13 × 10 ¹ |
| 1.37 × 10 ⁻³ | 6.91 × 10 ⁻² | 50 | 4.97 × 10 ¹ |

$k_2 = 7.35 \times 10^2 \text{ M}^{-1} \text{ s}^{-1}$

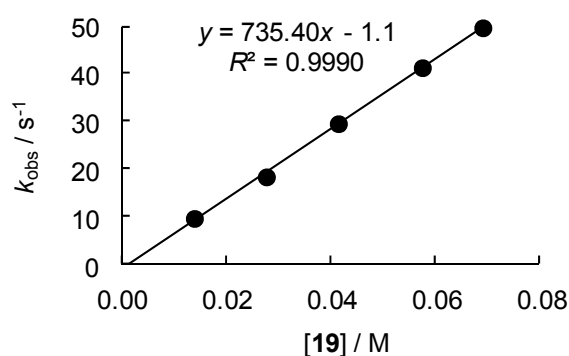


Table 5.33. Rate constants for the reactions of acetic anhydride (**3**) with *N,N*-bis-(2-methoxyethyl)amine (**21**) in CH₃CN (stopped-flow technique, 20 °C, conductimetry).

| [3] ₀ /M | [21] ₀ /M | [21] ₀ /[3] ₀ | <i>k</i> _{obs} /s ⁻¹ |
|------------------------------|-------------------------------|---|--|
| 4.41 × 10 ⁻³ | 8.33 × 10 ⁻² | 19 | 6.53 × 10 ⁻¹ |
| 4.41 × 10 ⁻³ | 1.67 × 10 ⁻¹ | 38 | 1.31 |
| 4.41 × 10 ⁻³ | 2.50 × 10 ⁻¹ | 57 | 1.98 |
| 4.41 × 10 ⁻³ | 3.54 × 10 ⁻¹ | 80 | 2.81 |
| 4.41 × 10 ⁻³ | 4.16 × 10 ⁻¹ | 94 | 3.26 |

$k_2 = 7.88 \text{ M}^{-1} \text{ s}^{-1}$

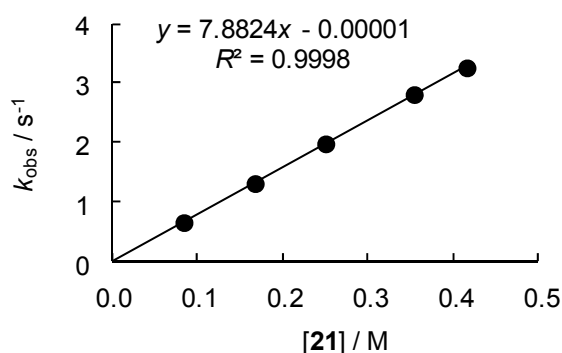


Table 5.34. Rate constants for the reactions of acetic anhydride (**3**) with di-*n*-propylamine (**22**) in CH₃CN (stopped-flow technique, 20 °C, conductimetry).

| [3] ₀ /M | [22] ₀ /M | [22] ₀ /[3] ₀ | <i>k</i> _{obs} /s ⁻¹ |
|------------------------------|-------------------------------|---|--|
| 1.83 × 10 ⁻³ | 1.81 × 10 ⁻² | 10 | 1.02 |
| 1.83 × 10 ⁻³ | 3.63 × 10 ⁻² | 20 | 2.20 |
| 1.83 × 10 ⁻³ | 5.58 × 10 ⁻² | 30 | 3.42 |
| 1.83 × 10 ⁻³ | 7.25 × 10 ⁻² | 40 | 4.56 |
| 1.83 × 10 ⁻³ | 9.20 × 10 ⁻² | 50 | 5.86 |

$k_2 = 6.54 \times 10^1 \text{ M}^{-1} \text{ s}^{-1}$

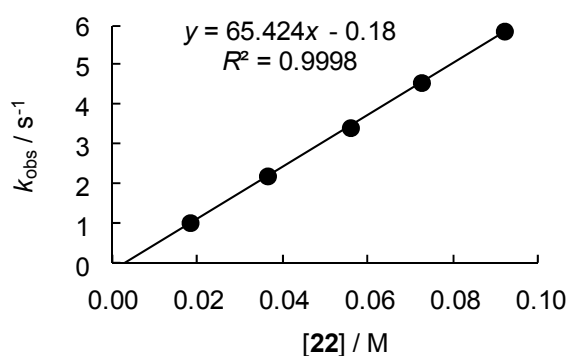


Table 5.35. Rate constants for the reactions of acetic anhydride (**3**) with diethylamine (**23**) in CH₃CN (stopped-flow technique, 20 °C, conductimetry).

| [3] ₀ /M | [23] ₀ /M | [23] ₀ /[3] ₀ | <i>k</i> _{obs} /s ⁻¹ |
|--|-------------------------------|---|--|
| 1.82 × 10 ⁻³ | 1.89 × 10 ⁻² | 10 | 1.35 |
| 1.82 × 10 ⁻³ | 3.57 × 10 ⁻² | 20 | 2.74 |
| 1.82 × 10 ⁻³ | 5.46 × 10 ⁻² | 30 | 4.48 |
| 1.82 × 10 ⁻³ | 9.24 × 10 ⁻² | 51 | 8.04 |
| <i>k</i> ₂ = 9.15 × 10 ¹ M ⁻¹ s ⁻¹ | | | |

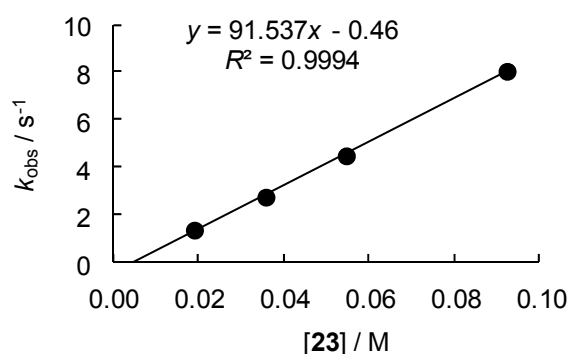
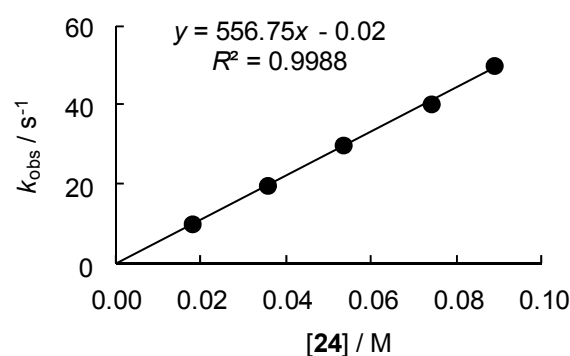


Table 5.36. Rate constants for the reactions of acetic anhydride (**3**) with morpholine (**24**) in CH₃CN (stopped-flow technique, 20 °C, conductimetry).

| [3] ₀ /M | [24] ₀ /M | [24] ₀ /[3] ₀ | <i>k</i> _{obs} /s ⁻¹ |
|--|-------------------------------|---|--|
| 1.83 × 10 ⁻³ | 1.78 × 10 ⁻² | 10 | 9.98 |
| 1.83 × 10 ⁻³ | 3.55 × 10 ⁻² | 19 | 1.97 × 10 ¹ |
| 1.83 × 10 ⁻³ | 5.33 × 10 ⁻² | 29 | 2.99 × 10 ¹ |
| 1.83 × 10 ⁻³ | 7.40 × 10 ⁻² | 40 | 4.03 × 10 ¹ |
| 1.83 × 10 ⁻³ | 8.88 × 10 ⁻² | 49 | 5.00 × 10 ¹ |
| <i>k</i> ₂ = 5.57 × 10 ² M ⁻¹ s ⁻¹ | | | |



Kinetics of the reactions of benzoyl chloride (4) with amines in CH₃CN

Table 5.37. Rate constants for the reactions of benzoyl chloride (**4**) with *tert*-butylamine (**13**) in CH₃CN (stopped-flow technique, 20 °C, conductimetry).

| [4] ₀ /M | [13] ₀ /M | [13] ₀ /[4] ₀ | <i>k</i> _{obs} /s ⁻¹ |
|--|-------------------------------|---|--|
| 2.58 × 10 ⁻⁴ | 5.10 × 10 ⁻³ | 20 | 3.25 |
| 2.58 × 10 ⁻⁴ | 1.02 × 10 ⁻² | 40 | 6.31 |
| 2.58 × 10 ⁻⁴ | 1.57 × 10 ⁻² | 61 | 9.93 |
| 2.58 × 10 ⁻⁴ | 2.04 × 10 ⁻² | 79 | 1.28 × 10 ¹ |
| <i>k</i> ₂ = 6.28 × 10 ² M ⁻¹ s ⁻¹ | | | |

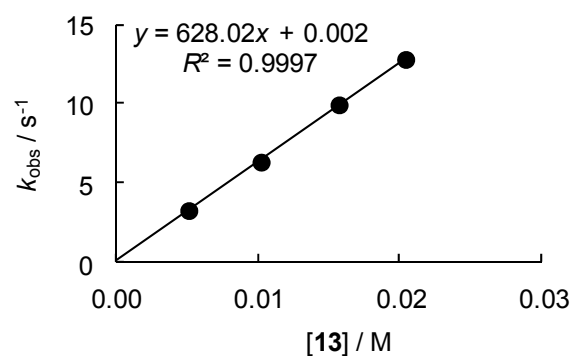


Table 5.38. Rate constants for the reactions of benzoyl chloride (**4**) with isopropylamine (**14**) in CH₃CN (stopped-flow technique, 20 °C, conductimetry).

| [4] ₀ /M | [14] ₀ /M | [14] ₀ /[4] ₀ | <i>k</i> _{obs} /s ⁻¹ |
|--|-------------------------------|---|--|
| 4.51 × 10 ⁻⁵ | 6.77 × 10 ⁻⁴ | 15 | 7.54 |
| 4.51 × 10 ⁻⁵ | 9.30 × 10 ⁻⁴ | 21 | 1.01 × 10 ¹ |
| 4.51 × 10 ⁻⁵ | 1.10 × 10 ⁻³ | 24 | 1.19 × 10 ¹ |
| 4.51 × 10 ⁻⁵ | 1.61 × 10 ⁻³ | 36 | 1.69 × 10 ¹ |
| <i>k</i> ₂ = 1.00 × 10 ⁴ M ⁻¹ s ⁻¹ | | | |

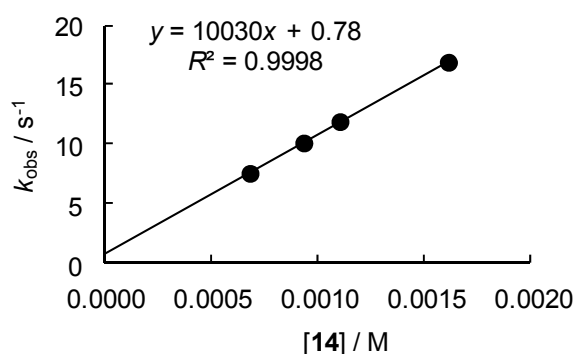


Table 5.39. Rate constants for the reactions of benzoyl chloride (**4**) with benzylamine (**15**) in CH₃CN (stopped-flow technique, 20 °C, conductimetry).

| [4] ₀ /M | [15] ₀ /M | [15] ₀ /[4] ₀ | <i>k</i> _{obs} /s ⁻¹ |
|--|-------------------------------|---|--|
| 4.51 × 10 ⁻⁵ | 7.05 × 10 ⁻⁴ | 16 | 1.01 × 10 ¹ |
| 4.51 × 10 ⁻⁵ | 9.17 × 10 ⁻⁴ | 20 | 1.25 × 10 ¹ |
| 4.51 × 10 ⁻⁵ | 1.13 × 10 ⁻³ | 25 | 1.49 × 10 ¹ |
| 4.51 × 10 ⁻⁵ | 1.34 × 10 ⁻³ | 30 | 1.74 × 10 ¹ |
| 4.51 × 10 ⁻⁵ | 1.55 × 10 ⁻³ | 34 | 1.97 × 10 ¹ |
| <i>k</i> ₂ = 1.14 × 10 ⁴ M ⁻¹ s ⁻¹ | | | |

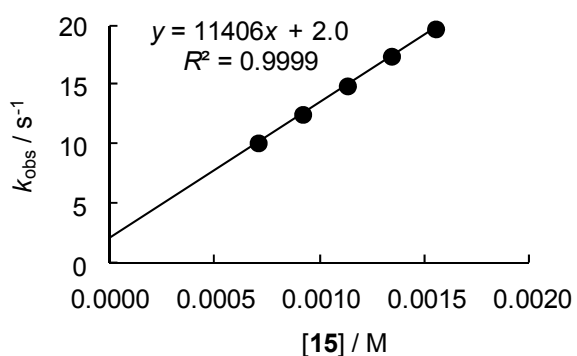


Table 5.40. Rate constants for the reactions of benzoyl chloride (**4**) with allylamine (**16**) in CH₃CN (stopped-flow technique, 20 °C, conductimetry).

| [4] ₀ /M | [16] ₀ /M | [16] ₀ /[4] ₀ | <i>k</i> _{obs} /s ⁻¹ |
|--|-------------------------------|---|--|
| 4.94 × 10 ⁻⁵ | 7.15 × 10 ⁻⁴ | 14 | 1.36 × 10 ¹ |
| 4.94 × 10 ⁻⁵ | 9.53 × 10 ⁻⁴ | 19 | 1.72 × 10 ¹ |
| 4.94 × 10 ⁻⁵ | 1.19 × 10 ⁻³ | 24 | 2.12 × 10 ¹ |
| 4.94 × 10 ⁻⁵ | 1.49 × 10 ⁻³ | 30 | 2.62 × 10 ¹ |
| <i>k</i> ₂ = 1.63 × 10 ⁴ M ⁻¹ s ⁻¹ | | | |

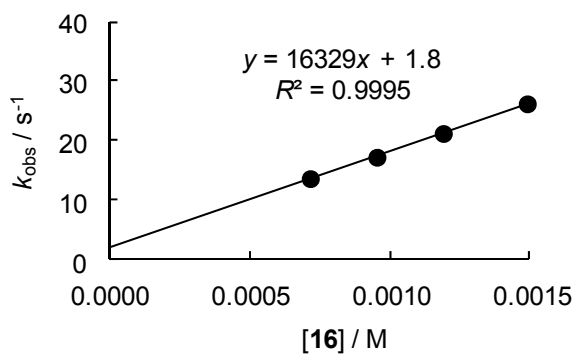


Table 5.41. Rate constants for the reactions of benzoyl chloride (**4**) with *n*-propylamine (**18**) in CH₃CN (stopped-flow technique, 20 °C, conductimetry).

| [4] ₀ /M | [18] ₀ /M | [18] ₀ /[4] ₀ | <i>k</i> _{obs} /s ⁻¹ |
|--|-------------------------------|---|--|
| 2.47 × 10 ⁻⁵ | 4.65 × 10 ⁻⁴ | 19 | 3.02 × 10 ¹ |
| 2.47 × 10 ⁻⁵ | 6.20 × 10 ⁻⁴ | 25 | 3.69 × 10 ¹ |
| 2.47 × 10 ⁻⁵ | 7.75 × 10 ⁻⁴ | 31 | 4.33 × 10 ¹ |
| 2.47 × 10 ⁻⁵ | 8.53 × 10 ⁻⁴ | 35 | 4.82 × 10 ¹ |
| <i>k</i> ₂ = 4.53 × 10 ⁴ M ⁻¹ s ⁻¹ | | | |

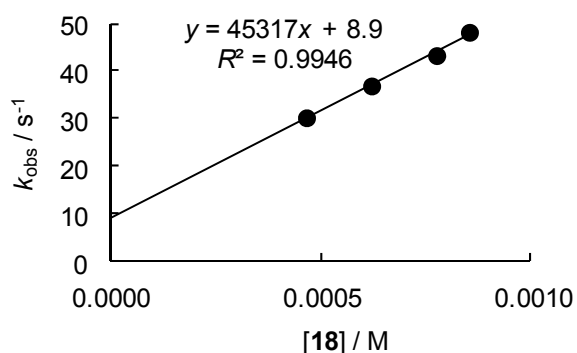


Table 5.42. Rate constants for the reactions of benzoyl chloride (**4**) with *N,N*-bis-(2-methoxyethyl)amine (**21**) in CH₃CN (stopped-flow technique, 20 °C, conductimetry).

| [4] ₀ /M | [21] ₀ /M | [21] ₀ /[4] ₀ | <i>k</i> _{obs} /s ⁻¹ |
|--|-------------------------------|---|--|
| 2.58 × 10 ⁻⁴ | 4.88 × 10 ⁻³ | 19 | 2.32 × 10 ¹ |
| 2.58 × 10 ⁻⁴ | 9.76 × 10 ⁻³ | 38 | 4.62 × 10 ¹ |
| 2.58 × 10 ⁻⁴ | 1.46 × 10 ⁻² | 57 | 6.56 × 10 ¹ |
| 2.58 × 10 ⁻⁴ | 1.95 × 10 ⁻² | 76 | 8.46 × 10 ¹ |
| 2.58 × 10 ⁻⁴ | 2.44 × 10 ⁻² | 95 | 1.05 × 10 ² |
| <i>k</i> ₂ = 4.14 × 10 ³ M ⁻¹ s ⁻¹ | | | |

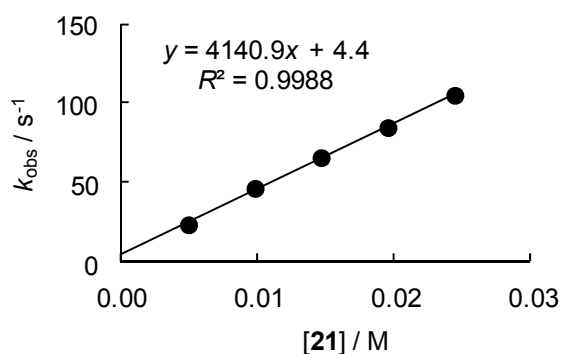


Table 5.43. Rate constants for the reactions of benzoyl chloride (**4**) with di-*n*-propylamine (**22**) in CH₃CN (stopped-flow technique, 20 °C, conductimetry).

| [4] ₀ /M | [22] ₀ /M | [22] ₀ /[4] ₀ | <i>k</i> _{obs} /s ⁻¹ |
|--|-------------------------------|---|--|
| 9.43 × 10 ⁻⁵ | 1.43 × 10 ⁻³ | 15 | 3.84 × 10 ¹ |
| 9.43 × 10 ⁻⁵ | 1.89 × 10 ⁻³ | 20 | 5.26 × 10 ¹ |
| 9.43 × 10 ⁻⁵ | 2.35 × 10 ⁻³ | 25 | 6.67 × 10 ¹ |
| 9.43 × 10 ⁻⁵ | 2.87 × 10 ⁻³ | 30 | 7.94 × 10 ¹ |
| <i>k</i> ₂ = 2.86 × 10 ⁴ M ⁻¹ s ⁻¹ | | | |

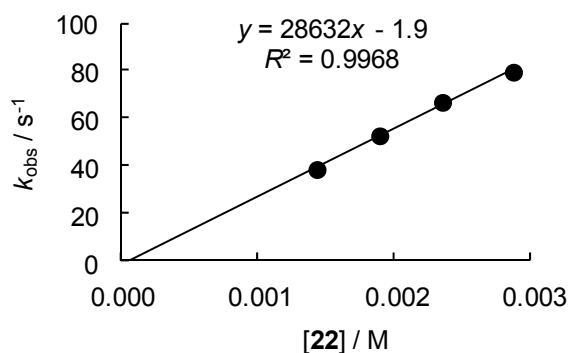


Table 5.44. Rate constants for the reactions of benzoyl chloride (**4**) with diethylamine (**23**) in CH₃CN (stopped-flow technique, 20 °C, conductimetry).

| [4] ₀ /M | [23] ₀ /M | [23] ₀ /[4] ₀ | <i>k</i> _{obs} /s ⁻¹ |
|--|-------------------------------|---|--|
| 9.15 × 10 ⁻⁵ | 9.36 × 10 ⁻⁴ | 10 | 2.80 × 10 ¹ |
| 9.15 × 10 ⁻⁵ | 1.37 × 10 ⁻³ | 15 | 4.29 × 10 ¹ |
| 9.15 × 10 ⁻⁵ | 1.87 × 10 ⁻³ | 20 | 5.76 × 10 ¹ |
| 9.15 × 10 ⁻⁵ | 2.31 × 10 ⁻³ | 25 | 7.04 × 10 ¹ |
| 9.15 × 10 ⁻⁵ | 2.75 × 10 ⁻³ | 30 | 8.20 × 10 ¹ |
| <i>k</i> ₂ = 2.96 × 10 ⁴ M ⁻¹ s ⁻¹ | | | |

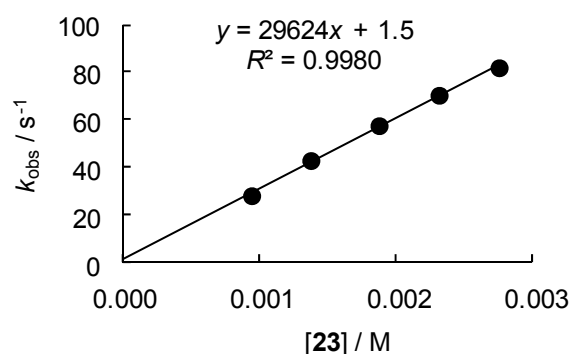
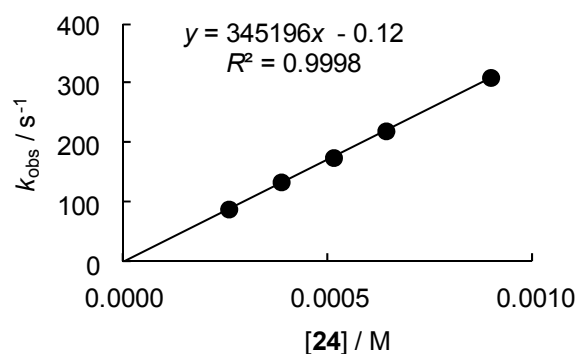


Table 5.45. Rate constants for the reactions of benzoyl chloride (**4**) with morpholine (**24**) in CH₃CN (stopped-flow technique, 20 °C, conductimetry).

| [4] ₀ /M | [24] ₀ /M | [24] ₀ /[4] ₀ | <i>k</i> _{obs} /s ⁻¹ |
|--|-------------------------------|---|--|
| 2.74 × 10 ⁻⁵ | 2.56 × 10 ⁻⁴ | 9 | 8.83 × 10 ¹ |
| 2.74 × 10 ⁻⁵ | 3.84 × 10 ⁻⁴ | 14 | 1.34 × 10 ² |
| 2.74 × 10 ⁻⁵ | 5.12 × 10 ⁻⁴ | 19 | 1.75 × 10 ² |
| 2.74 × 10 ⁻⁵ | 6.40 × 10 ⁻⁴ | 23 | 2.20 × 10 ² |
| 2.74 × 10 ⁻⁵ | 8.96 × 10 ⁻⁴ | 33 | 3.10 × 10 ² |
| <i>k</i> ₂ = 3.45 × 10 ⁵ M ⁻¹ s ⁻¹ | | | |



Kinetics of the reactions of 1-benzoyl-4-(dimethylamino)pyridinium chloride (5) with amines in CH₃CN

Table 5.46. Rate constants for the reactions of isopropylamine (**14**) with 1-benzoyl-4-(dimethylamino)pyridinium chloride (**5**) generated from benzoyl chloride (**4**) with 0.99 equiv. DMAP in CH₃CN (stopped-flow technique, 20 °C, λ = 317 nm).

| [5] ₀ /M | [14] ₀ /M | [14] ₀ /[5] ₀ | <i>k</i> _{obs} /s ⁻¹ |
|--|-------------------------------|---|--|
| 4.24 × 10 ⁻⁵ | 1.05 × 10 ⁻³ | 25 | 2.65 × 10 ⁻¹ |
| 4.24 × 10 ⁻⁵ | 1.84 × 10 ⁻³ | 43 | 4.83 × 10 ⁻¹ |
| 4.24 × 10 ⁻⁵ | 2.63 × 10 ⁻³ | 61 | 7.16 × 10 ⁻¹ |
| 4.24 × 10 ⁻⁵ | 3.42 × 10 ⁻³ | 80 | 9.19 × 10 ⁻¹ |
| <i>k</i> ₂ = 2.78 × 10 ² M ⁻¹ s ⁻¹ | | | |

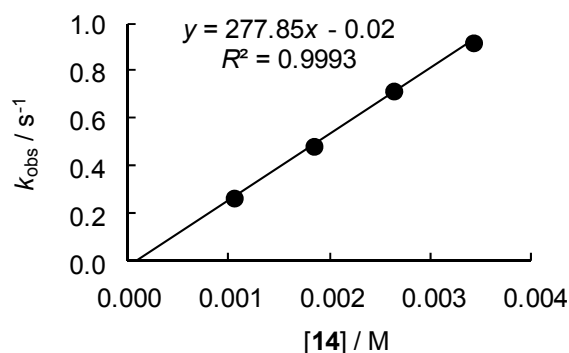


Table 5.47. Rate constants for the reactions of benzylamine (**15**) with 1-benzoyl-4-(dimethylamino)pyridinium chloride (**5**) generated in CH₃CN (stopped-flow technique, 20 °C, λ = 318 nm).

| [5] ₀ /M | [15] ₀ /M | [15] ₀ /[5] ₀ | <i>k</i> _{obs} /s ⁻¹ |
|--|-------------------------------|---|--|
| 7.53 × 10 ⁻⁵ | 1.57 × 10 ⁻³ | 21 | 7.10 × 10 ⁻¹ |
| 7.53 × 10 ⁻⁵ | 3.06 × 10 ⁻³ | 41 | 1.40 |
| 7.53 × 10 ⁻⁵ | 4.55 × 10 ⁻³ | 60 | 2.11 |
| 7.53 × 10 ⁻⁵ | 6.11 × 10 ⁻³ | 81 | 2.81 |
| 7.53 × 10 ⁻⁵ | 7.53 × 10 ⁻³ | 100 | 3.55 |
| <i>k</i> ₂ = 4.73 × 10 ² M ⁻¹ s ⁻¹ | | | |

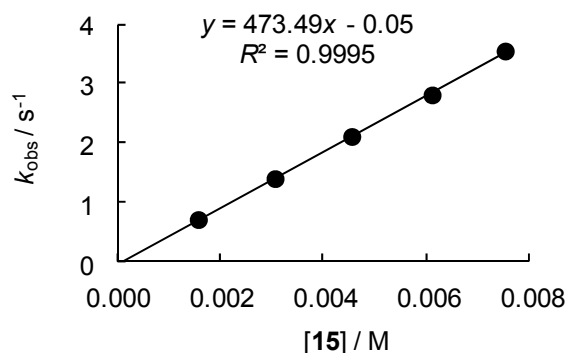


Table 5.48. Rate constants for the reactions of benzylamine (**15**) with 1-benzoyl-4-(dimethylamino)pyridinium chloride (**5**) generated from benzoyl chloride (**4**) with 1.0 equiv. DMAP in CH₃CN (stopped-flow technique, 20 °C, λ = 317 nm).

| [5] ₀ /M | [15] ₀ /M | [15] ₀ /[5] ₀ | <i>k</i> _{obs} /s ⁻¹ |
|--|-------------------------------|---|--|
| 7.53 × 10 ⁻⁵ | 1.48 × 10 ⁻³ | 20 | 6.71 × 10 ⁻¹ |
| 7.53 × 10 ⁻⁵ | 3.04 × 10 ⁻³ | 40 | 1.36 |
| 7.53 × 10 ⁻⁵ | 4.52 × 10 ⁻³ | 60 | 2.15 |
| 7.53 × 10 ⁻⁵ | 6.08 × 10 ⁻³ | 81 | 2.87 |
| 7.53 × 10 ⁻⁵ | 7.64 × 10 ⁻³ | 101 | 3.63 |
| <i>k</i> ₂ = 4.84 × 10 ² M ⁻¹ s ⁻¹ | | | |

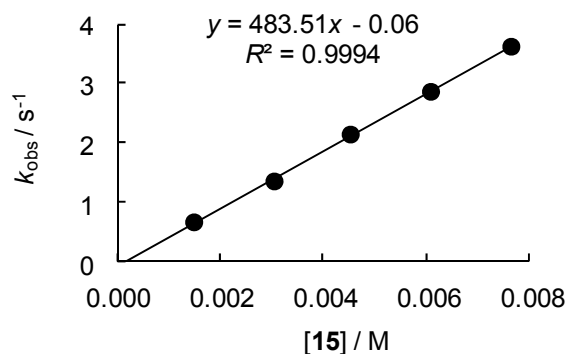


Table 5.49. Rate constants for the reactions of allylamine (**16**) with 1-benzoyl-4-(dimethylamino)pyridinium chloride (**5**) generated from benzoyl chloride (**4**) with 1.0 equiv. DMAP in CH₃CN (stopped-flow technique, 20 °C, λ = 317 nm).

| [5] ₀ /M | [16] ₀ /M | [16] ₀ /[5] ₀ | <i>k</i> _{obs} /s ⁻¹ |
|--|-------------------------------|---|--|
| 3.73 × 10 ⁻⁵ | 7.38 × 10 ⁻⁴ | 20 | 4.58 × 10 ⁻¹ |
| 3.73 × 10 ⁻⁵ | 1.48 × 10 ⁻³ | 40 | 9.44 × 10 ⁻¹ |
| 3.73 × 10 ⁻⁵ | 2.21 × 10 ⁻³ | 59 | 1.44 |
| 3.73 × 10 ⁻⁵ | 2.95 × 10 ⁻³ | 79 | 1.94 |
| 3.73 × 10 ⁻⁵ | 3.69 × 10 ⁻³ | 99 | 2.38 |
| <i>k</i> ₂ = 6.56 × 10 ² M ⁻¹ s ⁻¹ | | | |

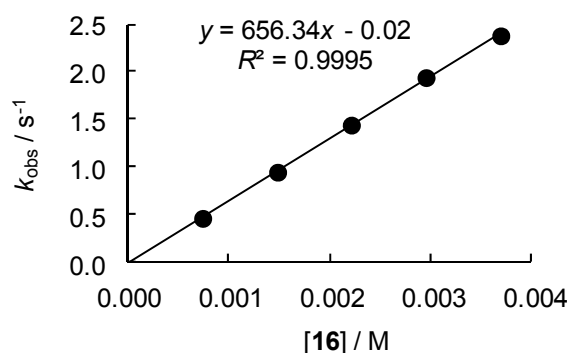


Table 5.50. Rate constants for the reactions of ethanolamine (**17**) with 1-benzoyl-4-(dimethylamino)pyridinium chloride (**5**) generated from benzoyl chloride (**4**) with 1.0 equiv. DMAP in CH₃CN (stopped-flow technique, 20 °C, $\lambda = 317$ nm).

| [5] ₀ /M | [17] ₀ /M | [17] ₀ /[5] ₀ | $k_{\text{obs}}/\text{s}^{-1}$ |
|--|-------------------------------|---|--------------------------------|
| 3.73×10^{-5} | 8.09×10^{-4} | 22 | 1.23 |
| 3.73×10^{-5} | 1.48×10^{-3} | 40 | 2.25 |
| 3.73×10^{-5} | 2.29×10^{-3} | 61 | 3.49 |
| 3.73×10^{-5} | 2.97×10^{-3} | 80 | 4.48 |
| 3.73×10^{-5} | 3.78×10^{-3} | 101 | 5.81 |
| $k_2 = 1.53 \times 10^3 \text{ M}^{-1} \text{ s}^{-1}$ | | | |

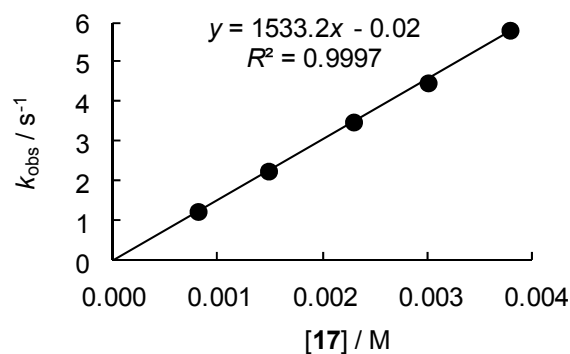


Table 5.51. Rate constants for the reactions of *n*-butylamine (**19**) with 1-benzoyl-4-(dimethylamino)pyridinium chloride (**5**) generated from benzoyl chloride (**4**) with 0.99 equiv. DMAP in CH₃CN (stopped-flow technique, 20 °C, $\lambda = 317$ nm).

| [5] ₀ /M | [19] ₀ /M | [19] ₀ /[5] ₀ | $k_{\text{obs}}/\text{s}^{-1}$ |
|--|-------------------------------|---|--------------------------------|
| 4.24×10^{-5} | 8.55×10^{-4} | 20 | 3.36 |
| 4.24×10^{-5} | 1.71×10^{-3} | 40 | 7.03 |
| 4.24×10^{-5} | 2.52×10^{-3} | 59 | 1.04×10^1 |
| 4.24×10^{-5} | 3.42×10^{-3} | 80 | 1.43×10^1 |
| 4.24×10^{-5} | 4.33×10^{-3} | 101 | 1.82×10^1 |
| $k_2 = 4.27 \times 10^3 \text{ M}^{-1} \text{ s}^{-1}$ | | | |

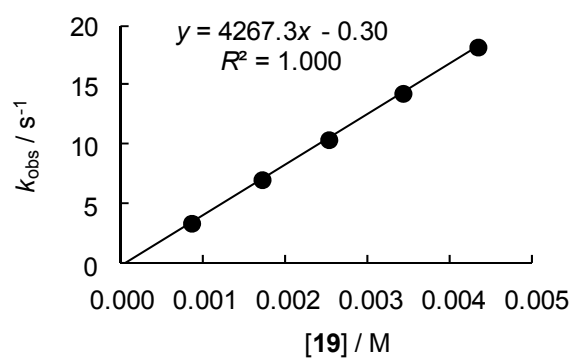


Table 5.52. Rate constants for the reactions of hydrazine (**20**) with 1-benzoyl-4-(dimethylamino)pyridinium chloride (**5**) generated from benzoyl chloride (**4**) with 1.0 equiv. DMAP in CH₃CN (stopped-flow technique, 20 °C, λ = 317 nm).

| [5] ₀ /M | [20] ₀ /M | [20] ₀ /[5] ₀ | <i>k</i> _{obs} /s ⁻¹ |
|--|-------------------------------|---|--|
| 3.62 × 10 ⁻⁵ | 3.69 × 10 ⁻⁴ | 10 | 5.64 |
| 3.62 × 10 ⁻⁵ | 7.38 × 10 ⁻⁴ | 20 | 1.29 × 10 ¹ |
| 3.62 × 10 ⁻⁵ | 1.11 × 10 ⁻³ | 31 | 2.01 × 10 ¹ |
| 3.62 × 10 ⁻⁵ | 1.48 × 10 ⁻³ | 41 | 2.60 × 10 ¹ |
| 3.62 × 10 ⁻⁵ | 1.85 × 10 ⁻³ | 51 | 3.26 × 10 ¹ |
| <i>k</i> ₂ = 1.81 × 10 ⁴ M ⁻¹ s ⁻¹ | | | |

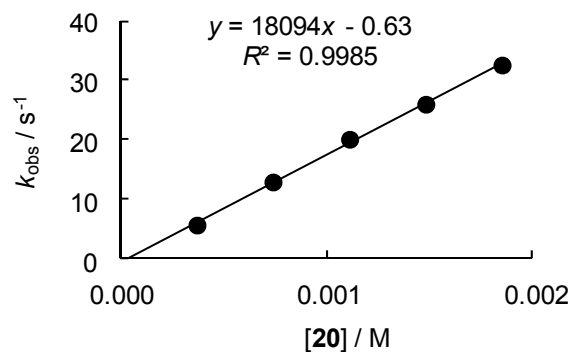


Table 5.53. Rate constants for the reactions of *N,N*-bis-(2-methoxyethyl)amine (**21**) with 1-benzoyl-4-(dimethylamino)pyridinium chloride (**5**) in CH₃CN (diode array spectrophotometer, 20 °C, λ = 317 nm).

| [5] ₀ /M | [21] ₀ /M | [21] ₀ /[5] ₀ | <i>k</i> _{obs} /s ⁻¹ |
|--|-------------------------------|---|--|
| 6.54 × 10 ⁻⁵ | 1.35 × 10 ⁻³ | 21 | 2.45 × 10 ⁻³ |
| 6.52 × 10 ⁻⁵ | 2.59 × 10 ⁻³ | 40 | 4.05 × 10 ⁻³ |
| 6.55 × 10 ⁻⁵ | 3.86 × 10 ⁻³ | 59 | 6.99 × 10 ⁻³ |
| 6.49 × 10 ⁻⁵ | 5.16 × 10 ⁻³ | 80 | 1.09 × 10 ⁻² |
| 6.49 × 10 ⁻⁵ | 6.50 × 10 ⁻³ | 100 | 1.27 × 10 ⁻² |
| <i>k</i> ₂ = 2.13 M ⁻¹ s ⁻¹ | | | |

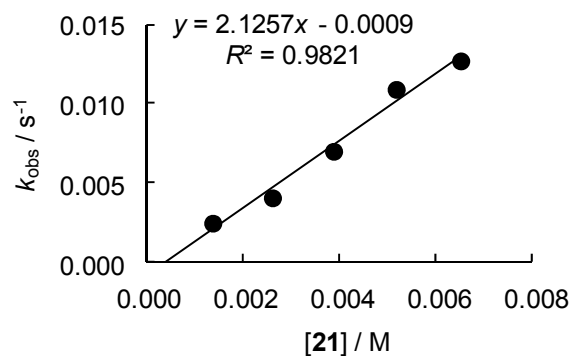


Table 5.54. Rate constants for the reactions of di-*n*-propylamine (**22**) with 1-benzoyl-4-(dimethylamino)pyridinium chloride (**5**) in CH₃CN (diode array spectrophotometer, 20 °C, λ = 317 nm).

| [5] ₀ /M | [22] ₀ /M | [22] ₀ /[5] ₀ | <i>k</i> _{obs} /s ⁻¹ |
|--|-------------------------------|---|--|
| 7.58 × 10 ⁻⁵ | 1.50 × 10 ⁻³ | 20 | 3.72 × 10 ⁻² |
| 7.61 × 10 ⁻⁵ | 2.31 × 10 ⁻³ | 30 | 5.91 × 10 ⁻² |
| 7.55 × 10 ⁻⁵ | 2.96 × 10 ⁻³ | 39 | 7.47 × 10 ⁻² |
| 7.43 × 10 ⁻⁵ | 4.51 × 10 ⁻³ | 61 | 1.18 × 10 ⁻¹ |
| <i>k</i> ₂ = 2.68 × 10 ¹ M ⁻¹ s ⁻¹ | | | |

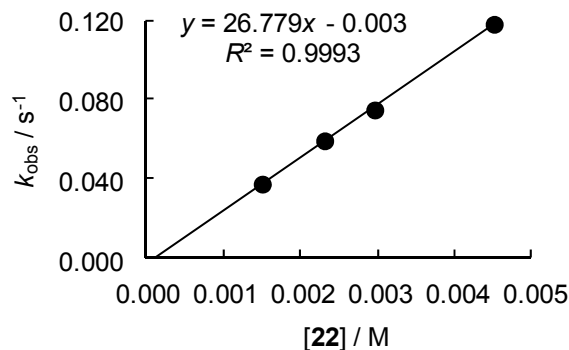


Table 5.55. Rate constants for the reactions of diethylamine (**23**) with 1-benzoyl-4-(dimethylamino)pyridinium chloride (**5**) in CH₃CN (diode array spectrophotometer, 20 °C, λ = 317 nm).

| [5] ₀ /M | [23] ₀ /M | [23] ₀ /[5] ₀ | <i>k</i> _{obs} /s ⁻¹ |
|--|-------------------------------|---|--|
| 4.91 × 10 ⁻⁵ | 4.68 × 10 ⁻⁴ | 10 | 2.60 × 10 ⁻² |
| 5.26 × 10 ⁻⁵ | 1.00 × 10 ⁻³ | 19 | 5.93 × 10 ⁻² |
| 5.09 × 10 ⁻⁵ | 1.62 × 10 ⁻³ | 32 | 9.53 × 10 ⁻² |
| 4.96 × 10 ⁻⁵ | 2.84 × 10 ⁻³ | 57 | 1.72 × 10 ⁻¹ |
| <i>k</i> ₂ = 6.14 × 10 ¹ M ⁻¹ s ⁻¹ | | | |

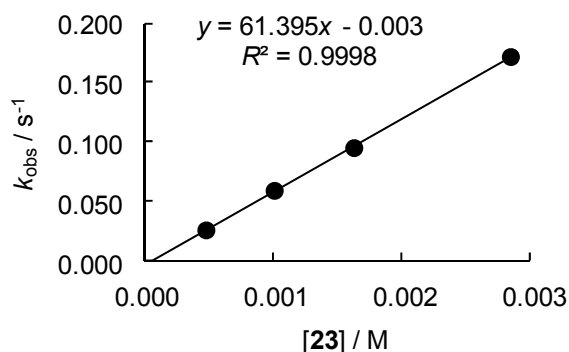


Table 5.56. Rate constants for the reactions of morpholine (**24**) with 1-benzoyl-4-(dimethylamino)pyridinium chloride (**5**) in CH₃CN (stopped-flow technique, 20 °C, λ = 317 nm).

| [5] ₀ /M | [24] ₀ /M | [24] ₀ /[5] ₀ | <i>k</i> _{obs} /s ⁻¹ |
|--|-------------------------------|---|--|
| 4.97 × 10 ⁻⁵ | 9.54 × 10 ⁻⁴ | 19 | 5.34 × 10 ⁻¹ |
| 4.97 × 10 ⁻⁵ | 2.03 × 10 ⁻³ | 41 | 1.13 |
| 4.97 × 10 ⁻⁵ | 2.98 × 10 ⁻³ | 60 | 1.70 |
| 4.97 × 10 ⁻⁵ | 3.94 × 10 ⁻³ | 79 | 2.23 |
| 4.97 × 10 ⁻⁵ | 5.01 × 10 ⁻³ | 101 | 2.84 |
| <i>k</i> ₂ = 5.70 × 10 ² M ⁻¹ s ⁻¹ | | | |

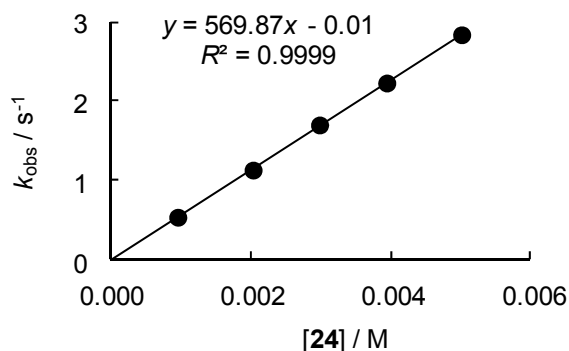


Table 5.57. Rate constants for the reactions of piperidine (**25**) with 1-benzoyl-4-(dimethylamino)pyridinium chloride (**5**) generated from benzoyl chloride (**4**) with 1.0 equiv. DMAP in CH₃CN (stopped-flow technique, 20 °C, λ = 317 nm).

| [5] ₀ /M | [25] ₀ /M | [25] ₀ /[5] ₀ | <i>k</i> _{obs} /s ⁻¹ |
|--|-------------------------------|---|--|
| 3.85 × 10 ⁻⁵ | 7.64 × 10 ⁻⁴ | 20 | 1.12 × 10 ¹ |
| 3.85 × 10 ⁻⁵ | 1.53 × 10 ⁻³ | 40 | 2.22 × 10 ¹ |
| 3.85 × 10 ⁻⁵ | 2.29 × 10 ⁻³ | 60 | 3.33 × 10 ¹ |
| 3.85 × 10 ⁻⁵ | 3.06 × 10 ⁻³ | 79 | 4.44 × 10 ¹ |
| 3.85 × 10 ⁻⁵ | 3.82 × 10 ⁻³ | 99 | 5.49 × 10 ¹ |
| <i>k</i> ₂ = 1.43 × 10 ⁴ M ⁻¹ s ⁻¹ | | | |

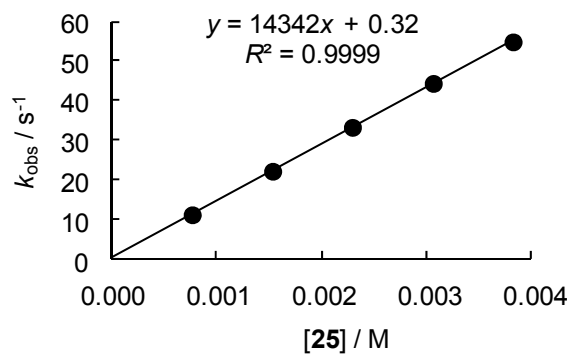


Table 5.58. Rate constants for the reactions of pyrrolidine (**26**) with 1-benzoyl-4-(dimethylamino)pyridinium chloride (**5**) in CH₃CN (stopped-flow technique, 20 °C, λ = 317 nm).

| [5] ₀ /M | [26] ₀ /M | [26] ₀ /[5] ₀ | <i>k</i> _{obs} /s ⁻¹ |
|--|-------------------------------|---|--|
| 4.01 × 10 ⁻⁵ | 4.02 × 10 ⁻⁴ | 10 | 7.34 × 10 ¹ |
| 4.01 × 10 ⁻⁵ | 6.03 × 10 ⁻⁴ | 15 | 1.10 × 10 ² |
| 4.01 × 10 ⁻⁵ | 8.04 × 10 ⁻⁴ | 20 | 1.49 × 10 ² |
| 4.01 × 10 ⁻⁵ | 1.01 × 10 ⁻³ | 25 | 1.81 × 10 ² |
| 4.01 × 10 ⁻⁵ | 1.21 × 10 ⁻³ | 30 | 2.20 × 10 ² |
| <i>k</i> ₂ = 1.80 × 10 ⁵ M ⁻¹ s ⁻¹ | | | |

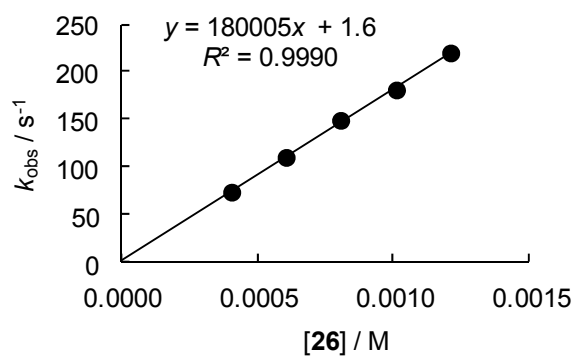


Table 5.59. Rate constants for the reactions of 1,2-dimethylhydrazine (**27**) with 1-benzoyl-4-(dimethylamino)pyridinium chloride (**5**) in CH₃CN (stopped-flow technique, 20 °C, $\lambda = 317$ nm).

| [5] ₀ /M | [27] ₀ /M | [27] ₀ /[5] ₀ | $k_{\text{obs}}/\text{s}^{-1}$ |
|--|-------------------------------|---|--------------------------------|
| 3.97×10^{-5} | 8.32×10^{-4} | 21 | 2.79×10^{-1} |
| 3.97×10^{-5} | 1.54×10^{-3} | 39 | 4.69×10^{-1} |
| 3.97×10^{-5} | 2.38×10^{-3} | 60 | 6.38×10^{-1} |
| 3.97×10^{-5} | 3.21×10^{-3} | 81 | 9.09×10^{-1} |
| 3.97×10^{-5} | 3.92×10^{-3} | 99 | 1.19 |
| $k_2 = 2.87 \times 10^2 \text{ M}^{-1} \text{ s}^{-1}$ | | | |

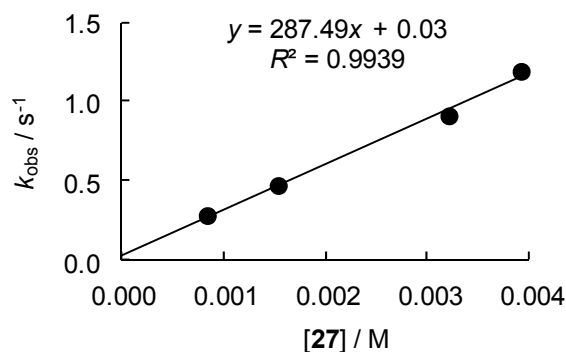
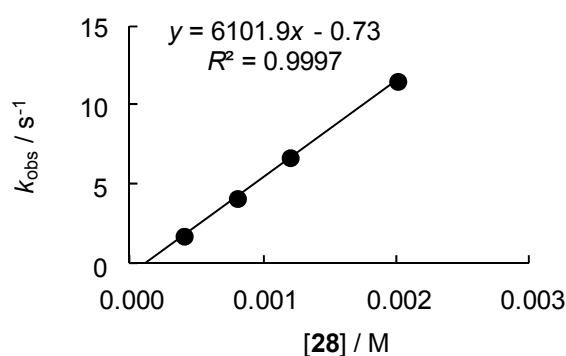


Table 5.60. Rate constants for the reactions of methylhydrazine (**28**) with 1-benzoyl-4-(dimethylamino)pyridinium chloride (**5**) in CH₃CN (stopped-flow technique, 20 °C, $\lambda = 317$ nm).

| [5] ₀ /M | [28] ₀ /M | [28] ₀ /[5] ₀ | $k_{\text{obs}}/\text{s}^{-1}$ |
|--|-------------------------------|---|--------------------------------|
| 3.97×10^{-5} | 4.02×10^{-4} | 10 | 1.72 |
| 3.97×10^{-5} | 8.03×10^{-4} | 20 | 4.10 |
| 3.97×10^{-5} | 1.20×10^{-3} | 30 | 6.68 |
| 3.97×10^{-5} | 2.01×10^{-3} | 51 | 1.15×10^1 |
| $k_2 = 6.10 \times 10^3 \text{ M}^{-1} \text{ s}^{-1}$ | | | |



Kinetics of the reactions of 1-benzoyl-4-(dimethylamino)pyridinium chloride (5) with carboxylates in CH₃CN

Table 5.61. Rate constants for the reactions of tetra-*n*-butylammonium benzoate (**29**) with 1-benzoyl-4-(dimethylamino)pyridinium chloride (**5**) in CH₃CN (stopped-flow technique, 20 °C, λ = 317 nm).

| [5] ₀ /M | [29] ₀ /M | [29] ₀ /[5] ₀ | <i>k</i> _{obs} /s ⁻¹ |
|--|-------------------------------|---|--|
| 2.47 × 10 ⁻⁵ | 1.98 × 10 ⁻⁴ | 8 | 2.38 × 10 ² |
| 2.47 × 10 ⁻⁵ | 2.22 × 10 ⁻⁴ | 9 | 2.69 × 10 ² |
| 2.47 × 10 ⁻⁵ | 2.46 × 10 ⁻⁴ | 10 | 2.97 × 10 ² |
| 2.47 × 10 ⁻⁵ | 2.70 × 10 ⁻⁴ | 11 | 3.26 × 10 ² |
| 2.47 × 10 ⁻⁵ | 3.00 × 10 ⁻⁴ | 12 | 3.60 × 10 ² |
| <i>k</i> ₂ = 1.19 × 10 ⁶ M ⁻¹ s ⁻¹ | | | |

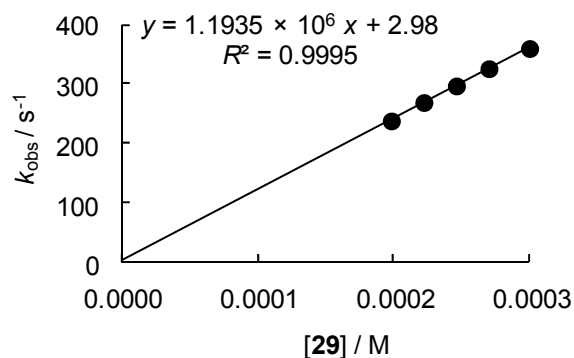
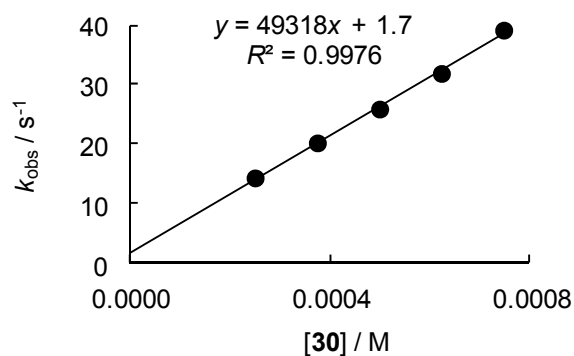


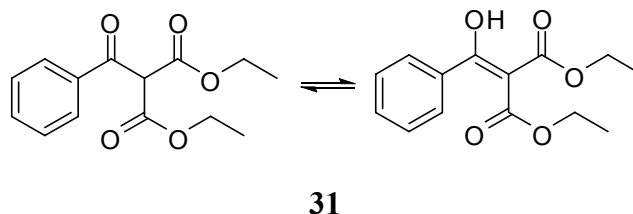
Table 5.62. Rate constants for the reactions of tetra-*n*-butylammonium 4-nitrobenzoate (**30**) with 1-benzoyl-4-(dimethylamino)pyridinium chloride (**5**) in CH₃CN (stopped-flow technique, 20 °C, λ = 317 nm).

| [5] ₀ /M | [30] ₀ /M | [30] ₀ /[5] ₀ | <i>k</i> _{obs} /s ⁻¹ |
|--|-------------------------------|---|--|
| 2.47 × 10 ⁻⁵ | 2.49 × 10 ⁻⁴ | 10 | 1.43 × 10 ¹ |
| 2.47 × 10 ⁻⁵ | 3.74 × 10 ⁻⁴ | 15 | 2.02 × 10 ¹ |
| 2.47 × 10 ⁻⁵ | 4.99 × 10 ⁻⁴ | 20 | 2.59 × 10 ¹ |
| 2.47 × 10 ⁻⁵ | 6.23 × 10 ⁻⁴ | 25 | 3.19 × 10 ¹ |
| 2.47 × 10 ⁻⁵ | 7.48 × 10 ⁻⁴ | 30 | 3.92 × 10 ¹ |
| <i>k</i> ₂ = 4.93 × 10 ⁴ M ⁻¹ s ⁻¹ | | | |



5.4.3 Product Characterization

Diethyl 2-benzoylmalonate (**31**)



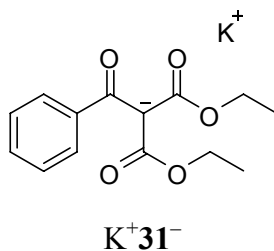
A solution of 4-nitrophenyl benzoate (**1**, 827 mg, 3.40 mmol) in DMSO (20 mL) was added to a stirred solution of potassium diethyl malonate (**7**, 1.35 g, 6.81 mmol) in DMSO (40 mL) at 20 °C and stirred for 2 h. After addition of 4-toluenesulfonic acid monohydrate (1.29 g, 6.78 mmol), water (40 mL) was added, and the solution was extracted with Et₂O (3 × 100 mL). The combined organic layers were dried (Na₂SO₄), filtered, and evaporated under reduced pressure. The crude product was purified by column chromatography on silica gel (ether/pentane): **31** (571 mg, 2.16 mmol, 64 %) was obtained as a colorless oil in a 9:1 ratio of the keto and enol (marked with *) form in CDCl₃.^[37]

¹H NMR (600 MHz, CDCl₃): δ = 13.40 (s br, 1 H, OH*), 7.88–7.90 (m, 2 H, 2 × H_{ar}), 7.57–7.60 (m, 1 H, H_{ar}), 7.54–7.56 (m, 2 H, 2 × H_{ar}*), 7.43–7.78 (m, 2 H and 1 H, 2 × H_{ar}, H_{ar}* superimposed), 7.37–7.39 (m, 2 H, 2 × H_{ar}*), 5.28 (s, 1 H, CH), 4.32 (q, *J* = 7.2 Hz, 2 H, CH₂*), 4.21–4.29 (m, *J* = 4 Hz, 2 × CH₂), 4.05 (q, *J* = 7.2 Hz, 2 H, CH₂*), 1.33 (t, *J* = 7.1 Hz, 3 H, CH₃*), 1.23 (t, *J* = 7.1 Hz, 6 H, 2 × CH₃), 1.01 (t, *J* = 7.2 Hz, 3 H, CH₃*).

¹³C-NMR (150 MHz, CDCl₃): δ = 189.1 (s), 175.4 (s*), 171.1 (s*), 166.3 (s*), 165.0 (s), 135.5 (s), 134.1 (d), 131.3 (d*), 130.2 (s*), 129.0 (d), 128.6 (d), 128.4 (d*), 127.7 (d*), 100.4 (s*), 62.5 (t), 62.0 (d), 61.8 (t*), 61.4 (t*), 14.2 (q*), 14.0 (q), 13.7 (q*).

HR-MS (EI, positive): *m/z* calcd. for C₁₄H₁₆O₅⁺: 264.0992, found 264.0992.

Potassium diethyl 2-benzoylmalonate ($\text{K}^+\mathbf{31}^-$)



Diethyl 2-benzoylmalonate (**31**, 50 mg, 0.19 mmol) was added to a solution of $\text{KO}t\text{Bu}$ (21 mg, 0.19 mmol) in d_6 -DMSO (1 mL). The product ($\text{K}^+\mathbf{31}^-$) was immediately analyzed by NMR spectroscopy.

^1H NMR (400 MHz, d_6 -DMSO): δ = 7.18–7.28 (m, 5 H, H_{Ar}), 3.73 (q, J = 7.1 Hz, 4 H, $2 \times \text{CH}_2$), 0.87 (t, J = 7.1 Hz, 6 H, $2 \times \text{CH}_3$).

^{13}C -NMR (100 MHz, d_6 -DMSO): δ = 188.8 (s), 169.6 (s), 146.9 (s), 127.3 (d), 126.9 (d), 126.7 (d), 90.7 (s), 56.9 (t), 14.3 (q).

5.5 References

- [1] a) J. P. Guthrie, in: *Reviews of Reactive Intermediate Chemistry* (Eds.: M. S. Platz, R. A. Moss, M. Jones, Jr.), Wiley-Interscience, Hoboken, **2007**, pp. 3–45; b) D. P. N. Satchell, R. S. Satchell, in: *Supplement B: The Chemistry of Acid Derivatives, Vol. 2* (Ed.: S. Patai), John Wiley & Sons, New York, **1992**, pp. 748–802.
- [2] Selected examples: a) T. W. Bentley, G. Llewellyn, J. A. McAlister, *J. Org. Chem.* **1996**, *61*, 7927–7932; b) A. Williams, *Acc. Chem. Res.* **1989**, *22*, 387–392; c) B. C. Lee, J. H. Yoon, C. G. Lee, I. Lee, *J. Phys. Org. Chem.* **1994**, *7*, 273–279.
- [3] Reviews: a) C. D. Ritchie, *Can. J. Chem.* **1986**, *64*, 2239–2250; b) C. D. Ritchie, *Pure Appl. Chem.* **1978**, *50*, 1281–1290; c) C. D. Ritchie, *Acc. Chem. Res.* **1972**, *5*, 348–354.
- [4] C. D. Ritchie, *J. Am. Chem. Soc.* **1975**, *97*, 1170–1179.
- [5] a) H. Mayr, A. R. Ofial, *Pure Appl. Chem.* **2005**, *77*, 1807–1821; b) H. Mayr, B. Kempf, A. R. Ofial, *Acc. Chem. Res.* **2003**, *36*, 66–77; c) R. Lucius, R. Loos, H. Mayr, *Angew. Chem.* **2002**, *114*, 97–102; *Angew. Chem. Int. Ed.* **2002**, *41*, 91–95; d) H. Mayr, T. Bug, M. F. Gotta, N. Hering, B. Irrgang, B. Janker, B. Kempf, R. Loos, A. R. Ofial,

- G. Remennikov, H. Schimmel, *J. Am. Chem. Soc.* **2001**, *123*, 9500–9512; e) H. Mayr, M. Patz, *Angew. Chem.* **1994**, *106*, 990–1010; *Angew. Chem. Int. Ed. Engl.* **1994**, *33*, 938–957; f) For a comprehensive listing of nucleophilicity parameters (N , s_N) and electrophilicity parameters (E) see <http://www.cup.uni-muenchen.de/oc/mayr/DBintro.html>.
- [6] R. Appel, H. Mayr, *J. Am. Chem. Soc.* **2011**, *133*, 8240–8251.
- [7] Selected examples: a) J. Isaad, A. Perwuelz, *Tetrahedron Lett.* **2010**, *51*, 5328–5332; b) I.-H. Um, K.-H. Kim, H.-R. Park, M. Fujio, Y. Tsuno, *J. Org. Chem.* **2004**, *69*, 3937–3942; c) H. J. Koh, H. C. Lee, H. W. Lee, I. Lee, *Bull. Korean Chem. Soc.* **1995**, *16*, 839–844; d) M. Jedrzejczak, R. E. Motie, D. P. N. Satchell, R. S. Satchell, W. N. Wassef, *J. Chem. Soc. Perkin Trans. 2* **1994**, *65*, 1471–1479; e) D. J. Palling, W. P. Jencks, *J. Am. Chem. Soc.* **1984**, *106*, 4869–4876.
- [8] a) F. E. Condon, *J. Org. Chem.* **1972**, *37*, 3608–3615; b) W. J. Theuer, J. A. Moore, *J. Org. Chem.* **1964**, *29*, 3734–3735.
- [9] R. L. Hinman, D. Fulton, *J. Am. Chem. Soc.* **1958**, *80*, 1895–1900.
- [10] a) K. Too, D. M. Brown, E. Bongard, V. Yarley, L. Vivas, D. Loakes, *Bioorg. Med. Chem.* **2007**, *15*, 5551–5562; b) K. Banert, M. Hagedorn, J. Schlott, *Chem. Lett.* **2003**, *32*, 360–361; c) C. Gibson, S. L. Goodman, D. Hahn, G. Hölzermann, H. Kessler, *J. Org. Chem.* **1999**, *64*, 7388–7394; d) T. Ryckmans, H.-G. Viehe, J. Feneau-Dupont, B. Tinant, J.-P. Declercq, *Tetrahedron* **1997**, *53*, 1729–1734; e) C. L. Branch, A. W. Guest, S. C. Finch (Beecham Group p.l.c), US5275816, **1994**; f) A. W. Guest, R. G. Adams, M. J. Basker, E. G. Brain, C. L. Branch, F. P. Harrington, J. E. Neale, M. J. Pearson, I. I. Zomaya, *J. Antibiot.* **1993**, *46*, 1279–1288; g) H. Hilpert, A. S. Dreiding, *Helv. Chim. Acta* **1984**, *67*, 1547–1561; h) D. L. Trepanier, K. L. Shriver, J. N. Eble, *J. Med. Chem.* **1969**, *12*, 257–260; i) M. Busch, E. Opfermann, H. H. Walther, *Ber. Dtsch. Chem. Ges.* **1904**, *37*, 2318–2333.
- [11] T. A. Nigst, A. Antipova, H. Mayr, *J. Org. Chem.* **2012**, *77*, 8142–8155.
- [12] N. E. Kayaleh, R. C. Gupta, F. Johnson, *J. Org. Chem.* **2000**, *65*, 4515–4522.
- [13] a) L. Claisen, *Justus Liebigs Ann. Chem.* **1896**, *291*, 25–137; b) L. Claisen, *Justus Liebigs Ann. Chem.* **1893**, *277*, 162–206; c) J. U. Nef, *Justus Liebigs Ann. Chem.* **1893**, *277*, 59–78.
- [14] a) J.-C. Jung, E. B. Watkins, M. A. Avery, *Heterocycles* **2005**, *65*, 77–94; b) A. Michael, O. Eckstein, *Ber. Dtsch. Chem. Ges.* **1905**, *38*, 50–53.

- [15] a) B. C. Kraybill, L. L. Elkin, J. D. Blethrow, D. O. Morgan, K. M. Shokat, *J. Am. Chem. Soc.* **2002**, *124*, 12118–12128; b) H. Graboyes, G. E. Jaffe, I. J. Pachter, J. P. Rosenbloom, A. J. Villani, J. W. Wilson, J. Weinstock, *J. Med. Chem.* **1968**, *11*, 568–573.
- [16] a) A. Riahi, M. Shkooor, O. Fatunsin, M. A. Yawer, I. Hussain, C. Fischer, P. Langer, *Tetrahedron* **2009**, *65*, 9300–9315; b) A. Riahi, M. Shkooor, R. A. Khera, H. Reinke, P. Langer, *Tetrahedron Lett.* **2009**, *50*, 3017–3019.
- [17] O. Kaumanns, R. Appel, T. Lemek, F. Seeliger, H. Mayr, *J. Org. Chem.* **2009**, *74*, 75–81.
- [18] T. Bug, T. Lemek, H. Mayr, *J. Org. Chem.* **2004**, *69*, 7565–7576.
- [19] T. Lemek, H. Mayr, *J. Org. Chem.* **2003**, *68*, 6880–6886.
- [20] T. B. Phan, C. Nolte, S. Kobayashi, A. R. Ofial, H. Mayr, *J. Am. Chem. Soc.* **2009**, *131*, 11392–11401.
- [21] T. Kanzian, T. A. Nigst, A. Maier, S. Pichl, H. Mayr, *Eur. J. Org. Chem.* **2009**, 6379–6385.
- [22] S. Minegishi, H. Mayr, *J. Am. Chem. Soc.* **2003**, *125*, 286–295.
- [23] I.-H. Um, S.-E. Jeon, J.-A. Seok, *Chem. Eur. J.* **2006**, *12*, 1237–1243.
- [24] T. B. Phan, H. Mayr, *Can. J. Chem.* **2005**, *83*, 1554–1560.
- [25] J.-A. Seo, S.-I. Kim, Y. J. Hong, I.-H. Um, *Bull. Korean Chem. Soc.* **2010**, *31*, 303–308.
- [26] I.-H. Um, J.-Y. Lee, S.-Y. Bae, E. Buncl, *Can. J. Chem.* **2005**, *83*, 1365–1371.
- [27] M. S. Wolfe, *Synthetic Commun.* **1997**, *27*, 2975–2984.
- [28] T. A. Nigst, *Diplomarbeit*, Ludwig-Maximilians-Universität München, **2007**.
- [29] T. A. Nigst, J. Ammer, H. Mayr, *Angew. Chem.* **2012**, *124*, 1381–1385; *Angew. Chem. Int. Ed.* **2012**, *51*, 1353–1356.
- [30] H. F. Schaller, A. A. Tishkov, X. Feng, H. Mayr, *J. Am. Chem. Soc.* **2008**, *130*, 3012–3022.
- [31] J. F. Coetzee, G. R. Padmanabhan, *J. Am. Chem. Soc.* **1965**, *87*, 5005–5010.
- [32] a) J. W. Bunting, J. M. Mason, C. K. M. Heo, *J. Chem. Soc. Perkin Trans 2* **1994**, 2291–2300; b) C. K. M. Heo, J. W. Bunting, *J. Chem. Soc. Perkin Trans. 2* **1994**, 2279–2290; c) Bell, R. P. *The Proton in Chemistry*, Methuen, London, **1959**, p. 159.
- [33] a) E. Buncl, I.-H. Um, *Tetrahedron* **2004**, *60*, 7801–7825; b) A. P. Grekov, V. Y. Veselov, *Russ. Chem. Rev.* **1978**, *47*, 631–648; c) N. J. Fina, J. O. Edwards, *Int. J. Chem. Kinet.* **1973**, *5*, 1–26.

- [34] T. C. Bruice, A. Donzel, R. W. Huffman, A. R. Butler, *J. Am. Chem. Soc.* **1967**, *89*, 2106–2121.
- [35] a) I. Cumpstey, *Org. Biomol. Chem.* **2012**, *10*, 2503–2508; b) C. Perrin, *Tetrahedron* **1995**, *51*, 11901–11935; c) P. P. Graczyk, M. Mikołajczyk, in: *Topics in Stereochemistry, Vol. 21* (Eds.: E. L. Eliel, S. H. Wilen), John Wiley & Sons, New York, **1994**, pp. 159–349; d) E. Juaristi, G. Cuevas, *Tetrahedron* **1992**, *48*, 5019–5087.
- [36] I. Zenz, H. Mayr, *J. Org. Chem.* **2011**, *76*, 9370–9378.
- [37] Analytic data have been published previously: Q. Shen, W. Huang, J. Wang, X. Zhou, *Org. Lett.* **2007**, *9*, 4491–4494.

Chapter 6

REACTIVITIES OF PYRIDINES AND *N*-ACYLPYRIDINIUM IONS: KINETICS OF MODEL REACTIONS OF AN ORGANOCATALYTIC CYCLE

Tobias A. Nigst, Raman Tandon, Hendrik Zipse and Herbert Mayr, manuscript in preparation.
The results obtained by R. Tandon are not listed in the Experimental Section.

6.1 Introduction

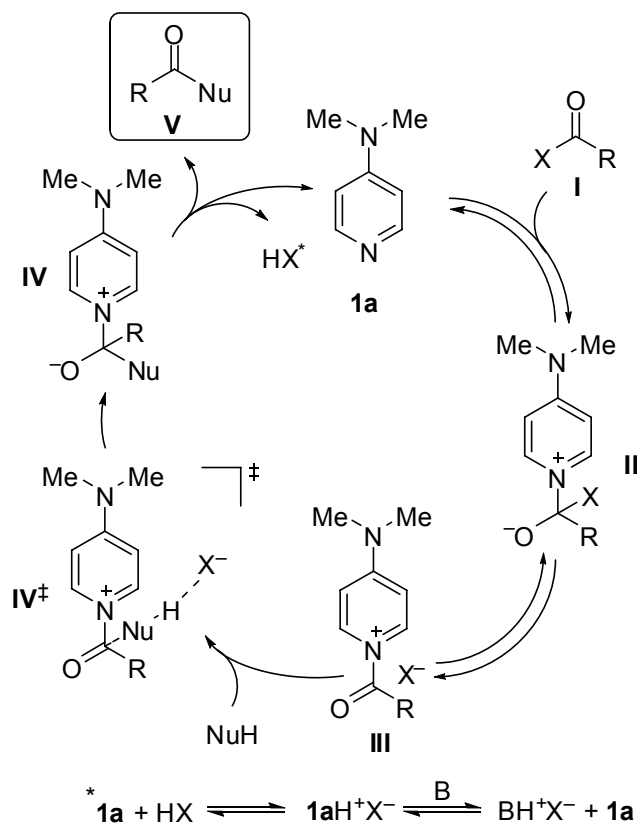
Acylation belongs to the most essential reactions in organic chemistry. In particular esterifications are not only important in the laboratory, but also in nature, as they provide a way for biological systems to handle energy transport and to build up complex molecules.^[1] Numerous catalysts were designed to improve the efficiencies of these reactions with respect to enantioselectivities^[1] and reactivities.^[2]

Already in 1898, pyridine was found by Einhorn and Hollandt to catalyze acylation reactions of alcohols and phenols.^[3] Litvinenko and Kirichenko as well as Steglich and Höfle demonstrated that catalytic amounts of 4-(dimethylamino)pyridine (DMAP) promoted the transfer of acyl groups 6000 times more efficiently than pyridine.^[4] Until today, DMAP and related pyridines are commonly used as nucleophilic catalysts for acylation reactions of sterically hindered alcohols and amines of low reactivity.^[1,2,5] In order to increase the rates of esterification reactions, chemists tried to employ more nucleophilic pyridines. In these investigations, 4-(pyrrolidino)pyridine (PPY) turned out to be three times more efficient than DMAP.^[6] In 2003, Mayr, Steglich, Zipse and co-workers showed that the conformational fixation of the lone pair of the 4-amino group by bridging the substituents in 3,4- and 3,4,5-position of the pyridine ring further increased the rates for esterifications of tertiary alcohols.^[7] Thus, 9-azajulolidine (TCAP) was found to accelerate the acylation of sterically hindered alcohols up to 10 times more than DMAP. Based on this concept, Han and David developed syntheses of new DMAP derivatives, such as 3,4-dialkylaminopyridine derivatives^[8] and 3,4,5-trialkylaminopyridines, the so called “superDMAPs”,^[9,10] which

showed outstanding nucleophilicities. However, despite the higher catalytic activities of these highly electron-rich pyridines, for most purposes DMAP is still the best choice in terms of cost-benefit ratio.

Besides the numerous attempts to develop more active catalysts, only few researchers investigated the complex mechanisms of pyridine-catalyzed acylation reactions.^[2,11,12]

The commonly accepted simplified mechanism^[2,11] (Scheme 6.1) comprises the reversible formation of the *N*-acylpyridinium salt **III** by addition of DMAP (**1a**) to the acyl donor (**I**) which proceeds either concertedly or via the tetrahedral intermediate **II**. Subsequent addition of the nucleophile NuH, for example an alcohol or an amine, to **III** leads to the product **IV** through transition state **IV[‡]**, in which the attack of the nucleophile is assisted by a proton transfer to the counterion X⁻. The formation of the product **V** by elimination of the catalyst is accompanied by the generation of HX which has to be trapped by an auxiliary base (B) in order to avoid deactivation of the catalyst. This mechanism has been supported by Zipse and co-workers who investigated the intermediates of the DMAP-catalyzed acetylation of *tert*-butanol with acetic anhydride by means of DFT calculations in the gas phase and in several chlorinated solvents.^[12]



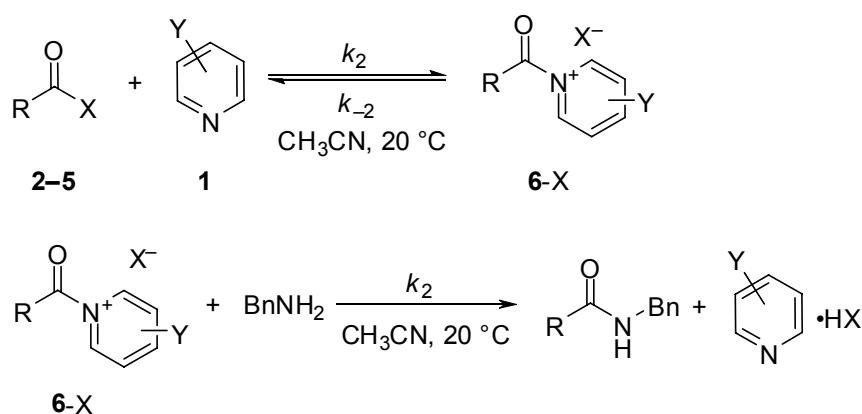
Scheme 6.1. Simplified mechanism for the DMAP-catalyzed acylation reaction.

The kinetics of the reaction of 1-propargylcyclohexanol with acetic anhydride and triethylamine has widely been used as a benchmark to characterize the activities of different catalysts.^[10] Zipse and co-workers showed that the stabilities of the *N*-acylpyridinium ions, which were calculated via isodesmic acyl-transfer reactions, provided a reasonable prediction of the catalysts' activities by computational methods.^[13]

Previously, we have characterized the nucleophilicities of various substituted pyridines,^[14,15] including 3,4,5-triaminopyridines,^[10] towards benzhydrylium ions according to the linear free energy relationship [Eq. (6.1)], where electrophiles are characterized by one parameter (electrophilicity *E*) and nucleophiles are characterized by two parameters (nucleophilicity *N* and sensitivity *s_N*).^[16]

$$\log k_2(20\text{ }^\circ\text{C}) = s_N(N + E) \quad (6.1)$$

In order to obtain more insight into the pyridine-catalyzed acylation reactions, we have now systematically investigated the kinetics of two model reactions, which are related to the catalytic cycle of Scheme 6.1, namely the reactions of the substituted pyridines **1a–q** (Figure 6.1) with the acylating agents **2–5** (Figure 6.2), and the subsequent reactions of the resulting *N*-acylpyridinium ions **6–X** with benzylamine as reference nucleophile in acetonitrile at 20 °C (Scheme 6.2).



Scheme 6.2. Reactions investigated in this study.

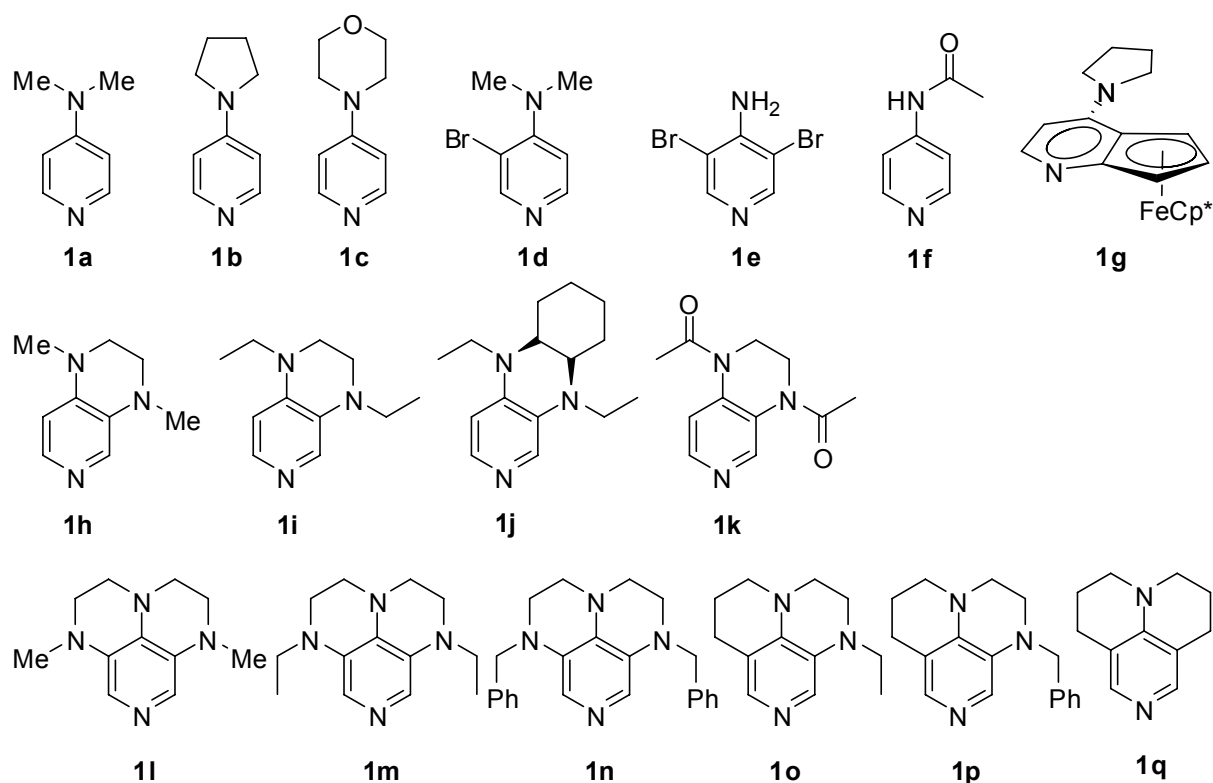


Figure 6.1. Pyridines used in this study.

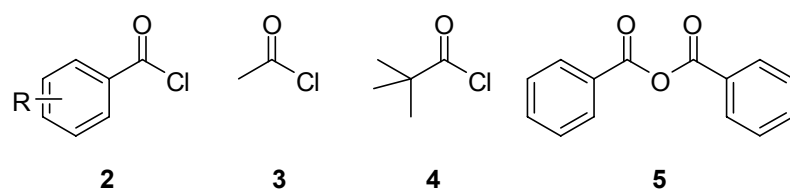


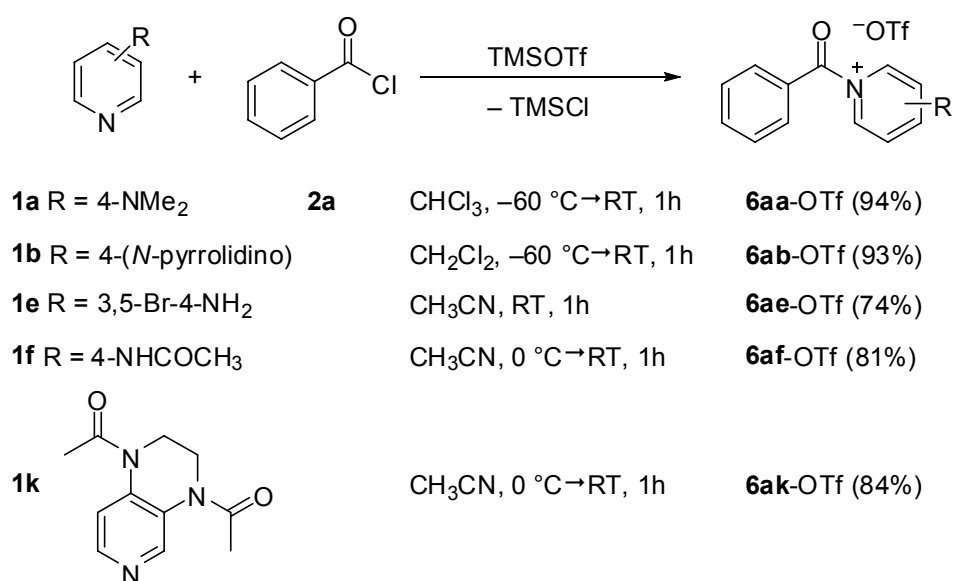
Figure 6.2. Acylating agents used in this study.

6.2 Results and Discussion

6.2.1 Synthesis of *N*-Acylpyridinium Ions

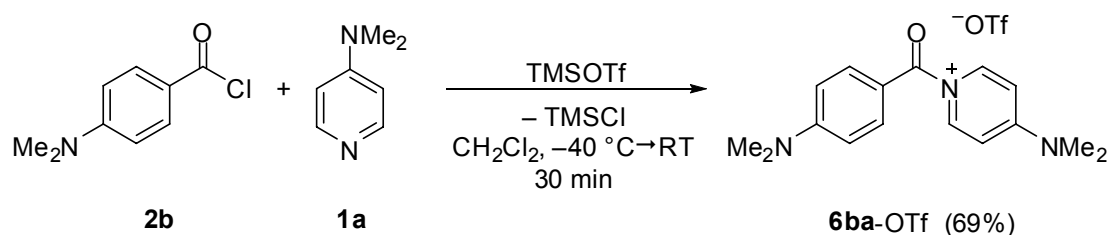
Following a procedure described by Wolfe, benzoyl chloride (**2a**) was combined with DMAP (**1a**) in dichloromethane at ambient temperature to form the *N*-benzoylpyridinium chloride **6aa-Cl**, which precipitated upon addition of ether.^[17] Pyridines of lower basicities react with benzoyl chloride (**2a**) reversibly. Yamaguchi *et al.* showed that the addition of AgOTf, NaOTf, LiOTf, AgBF₄, and TMSOTf significantly enhanced the yields of the reactions of

chloroformates with allysilanes and quinolines or isoquinolines.^[18] In line with these results, ¹H NMR spectroscopic studies by Wanner and co-workers showed that the addition of silyl triflates to mixtures of substituted pyridines and pivaloyl chloride shifts the equilibrium to the side of the *N*-acylpyridinium ions, even when electron acceptor-substituted pyridines were used.^[19] Accordingly, *N*-benzoyl-4-(dimethylamino)pyridinium triflate (**6aa**-OTf) was synthesized by adding one equivalent of TMSOTf to an equimolar mixture of benzoyl chloride (**2a**) and DMAP (**1a**; Scheme 6.3). Analogously, the amino-substituted pyridines **1b**, **1e**, **1f**, and **1k** reacted with benzoyl chloride (**2a**) and TMSOTf to form the corresponding *N*-benzoylpyridinium triflates **6**-OTf in good yields (Scheme 6.3). Remarkably, **1e** formed a stable *N*-benzoylpyridinium triflate with **2a** despite its NH₂ substituent, which provides an alternative reaction center that might also be acylated as previously observed for 4-aminopyridine.^[20] Obviously, the two bromo substituents shield the amino group sufficiently that the reaction at the amino group is highly retarded.



Scheme 6.3. Products of the reaction of benzoyl chloride (**2a**) with pyridines **1a,b,e,f,k** and TMSOTf.

The same method was applied for the synthesis of *N*-acylpyridinium triflates generated from 4-(dimethylamino)benzoyl chloride (**2b**) or pivaloyl chloride (**4**),^[21] DMAP (**1a**) and TMSOTf (Scheme 6.4).



Scheme 6.4. Products of the reactions of 4-(dimethylamino)benzoyl chloride (**2b**) or pivaloyl chloride (**4**) with DMAP (**1a**) and TMSOTf.

6.2.2 Kinetics of the Reactions of the Benzoyl Chlorides **2a–n** with the Pyridines **1a–q**

N-Benzoylpyridinium chlorides **6-Cl**, generated from benzoyl chloride (**2a**) and donor-substituted pyridines **1a–q** showed intensive UV/Vis-absorptions at $\lambda = 280\text{--}430$ nm, which were bathochromically shifted compared to the pyridines. Increasing the electron-donating abilities of the substituents usually shifted the absorption maxima to higher wave lengths (Table 6.1). In the series of the bridged pyridines **1h–q** the absorption maxima increased in the following order: 3,5-dialkyl-4-alkylamino < 3,4-diacetyl < 3,4-dialkylamino \approx 5-alkyl-3,4-dialkylamino < 3,4,5-trialkylamino. The distinct absorbances of the *N*-benzoylpyridinium chlorides **6-Cl** allowed the spectrophotometric determination of the rates of the reactions of benzoyl chloride (**2a**) with the pyridines **1a–q** in acetonitrile at 20 °C using stopped-flow methods as described previously.^[16] Either the benzoyl chlorides or the pyridines were used in large excess (usually over 10 equiv. relative to the other) to ensure first-order conditions.

Highly reactive pyridines, that is, those with 4-alkylamino substituents (**1a–d,g–j,l–q**), reacted quantitatively with benzoyl chloride (**2a**) as verified by the similar end absorbances when the concentrations of the compound used in excess were varied. For the reactions of **2a** with those pyridines, monoexponential increases of the absorbances of the *N*-benzoylpyridinium chlorides **6-Cl** were observed, and the first-order rate constants k_{obs} were obtained by least-squares fitting of the exponential function $A = A_0(1 - e^{-k_{\text{obs}}t}) + C$ to the time-dependent absorbances; a typical example is shown in Figure 6.3. Plots of k_{obs} versus the concentration of the compound in excess were linear and the second-order rate constants k_2 (Table 6.1) were obtained as the slopes of these plots [Eqs. (6.2) and (6.3)]. The intercepts of the plots were close to zero, in line with the quantitative progress of these reactions.

$$\text{for } [1]_0 \gg [2]_0 \rightarrow k_{\text{obs}} = k_2[1] \quad (6.2)$$

$$\text{for } [2]_0 \gg [1]_0 \rightarrow k_{\text{obs}} = k_2[2] \quad (6.3)$$

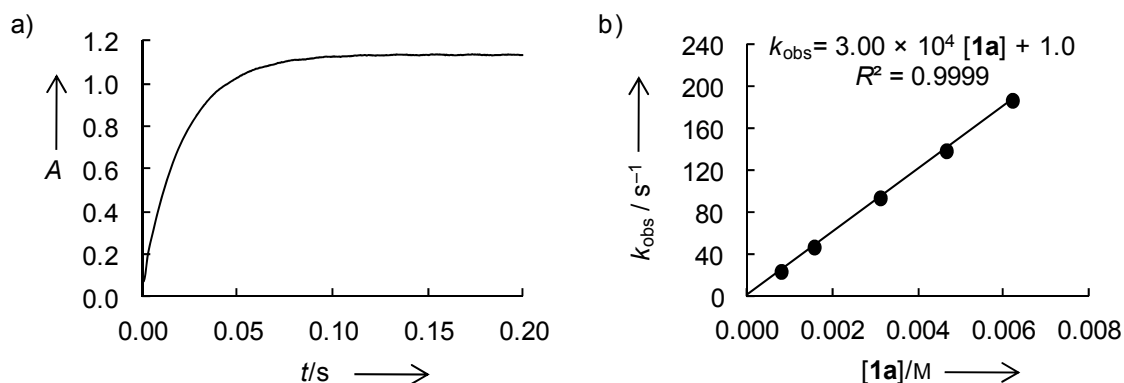


Figure 6.3. a) Exponential increase of the absorbance at 317 nm during the reaction of benzoyl chloride ($[2a] = 7.72 \times 10^{-5} \text{ M}$) with DMAP ($[1a] = 1.54 \times 10^{-3} \text{ M}$; $k_{\text{obs}} = 4.74 \times 10^1 \text{ s}^{-1}$) in acetonitrile at 20 °C. b) A plot of k_{obs} versus $[1a]$ yields the second-order rate constant $k_2 = 3.00 \times 10^4 \text{ M}^{-1} \text{ s}^{-1}$ as the slope of the correlation line.^[21]

For the reactions of benzoyl chloride (**2a**) with 4-(*N*-pyrrolidino)pyridine (PPY, **1b**) and 4-(*N*-morpholino)pyridine (**1c**) it was demonstrated, that both **2a** as well as **1b** or **1c** can be used as compounds in excess. The reactions followed a second-order rate law in both cases, first order in each of the reactants, and the second-order rate constants obtained by the different methods differed by less than 5%.

For the reactions of **2a** with **1a** or **1b** also the influence of the solvent on the kinetics was probed. A decrease of the second-order rate constant by a factor of approximately three was observed for both reactions when changing the solvent from acetonitrile to dichloromethane and by another factor of approximately three when going to chloroform. For the reaction of **1a** with **2a** in dichloromethane it was also demonstrated that the same second-order rate constants were determined regardless which of the compounds was used in excess (Figure 6.4).

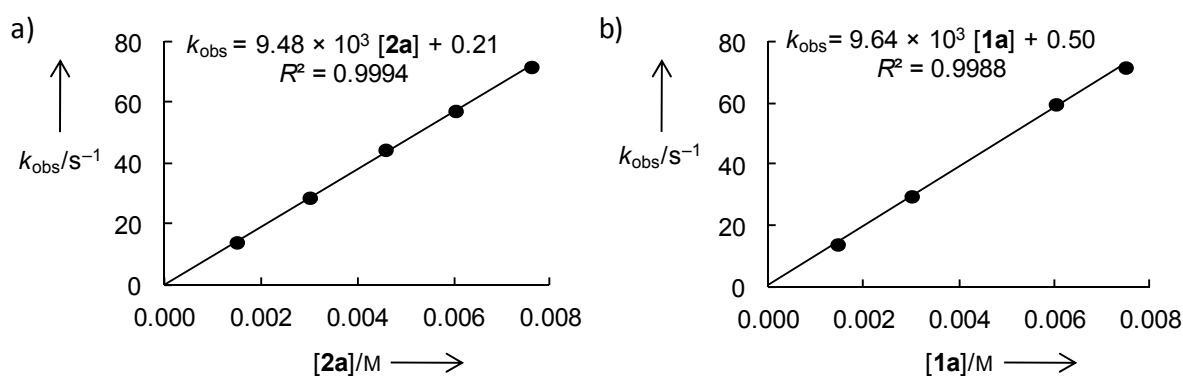
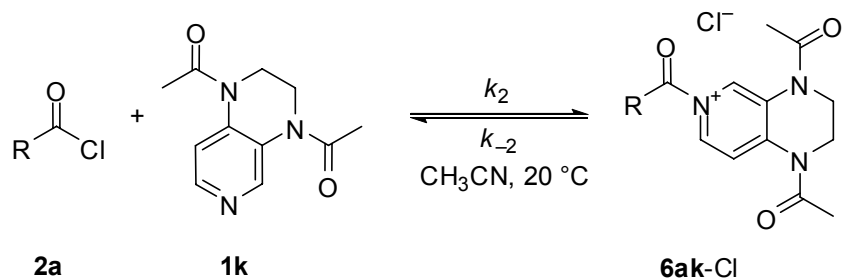


Figure 6.4. a) A plot of k_{obs} versus $[2\mathbf{a}]$ yields the second-order rate constant $k_2 = 9.48 \times 10^3 \text{ M}^{-1} \text{ s}^{-1}$ for the reaction of benzoyl chloride ($2\mathbf{a}$) with DMAP ($[1\mathbf{a}] = 7.60 \times 10^{-5} \text{ M}$) in CH_2Cl_2 at 20°C . b) A plot of k_{obs} versus $[1\mathbf{a}]$ yields the second-order rate constant $k_2 = 9.64 \times 10^3 \text{ M}^{-1} \text{ s}^{-1}$ for the reaction of DMAP ($1\mathbf{a}$) with benzoyl chloride ($[2\mathbf{a}] = 7.49 \times 10^{-5} \text{ M}$) in CH_2Cl_2 at 20°C .

The less reactive 3,5-dibromo-4-aminopyridine ($1\mathbf{e}$) and the acylamido-substituted pyridines $1\mathbf{f}, \mathbf{k}$ did not react quantitatively with benzoyl chloride ($2\mathbf{a}$). When $1\mathbf{k}$ was combined with different concentrations of $2\mathbf{a}$ (Scheme 6.5), the final absorbance of the *N*-benzoylpyridinium chloride $6\mathbf{ak}\text{-Cl}$ increased with the concentration of $2\mathbf{a}$ (Figure 6.5a). In the reaction of $1\mathbf{k}$ with 20 equivalents of benzoyl chloride ($[2\mathbf{a}] = 5.88 \times 10^{-3} \text{ M}$) the time-dependent absorbance of the *N*-benzoylpyridinium chloride $6\mathbf{ak}\text{-Cl}$ deviated significantly from a monoexponential fit. However, the difference between the observed absorbances and the monoexponential fits decreases with increasing concentration of $2\mathbf{a}$. Finally, at $[2\mathbf{a}] = 4.17 \times 10^{-2} \text{ M}$ (140 equiv. excess relative to the pyridine), an almost monoexponential increase of the absorbance was observed. As the differences between the observed absorbances and the monoexponential fits were small at higher concentrations of the electrophile, the second-order rate constant k_2 was determined as the slope of the linear correlation k_{obs} versus $[2\mathbf{a}]$ (Figure 6.5b, Table 6.1).



Scheme 6.5. Reaction of the benzoyl chloride (**2a**) with the pyridine **1k**.

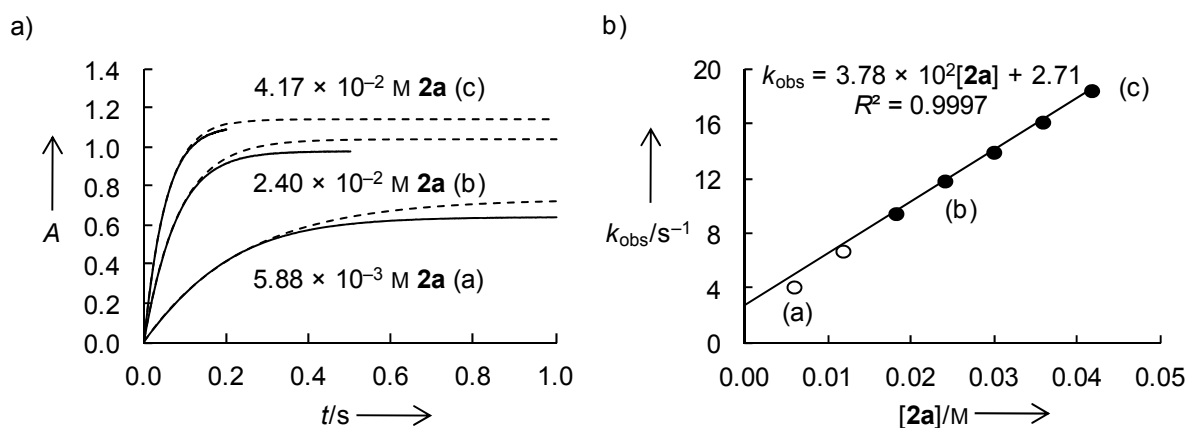


Figure 6.5. a) Increase of the absorbance at 345 nm during the reaction of benzoyl chloride (**2a**) with **1k** ($[\mathbf{1k}] = 2.98 \times 10^{-4} \text{ M}$) in acetonitrile at 20 °C. Dashed lines: Monoexponential fits of the time-dependent absorbances. b) A plot of k_{obs} versus $[\mathbf{2a}]$ yields the second-order rate constant $k_2 = 3.78 \times 10^2 \text{ M}^{-1} \text{ s}^{-1}$ (open symbols refer to rate constants, which were not used for determination of the regression line).

This behavior can be explained by a rate law containing a second-order back-reaction of the *N*-benzoylpyridinium ion **6ak** with the chloride ion according to Equation (6.4), which neglects ion-pairing.

$$\frac{d[\mathbf{6ak}]}{dt} = k_2[\mathbf{1k}][\mathbf{2a}] - k_{-2}[\mathbf{6ak}][\text{Cl}^-] = k_2[\mathbf{1k}][\mathbf{2a}] - k_{-2}[\mathbf{6ak}]^2 \quad (6.4)$$

In contrast to the incompletely proceeding reactions of pyridines with benzhydrylium ions,^[14] where a first-order back-reaction was observed, the rate law for the reactions with benzoyl chloride (**2a**) could not be integrated analytically.

However, by addition of an excess of external chloride ions to the reaction mixture, the chloride ion concentration remains almost constant during the reaction, and the second-order back-reaction is converted into a first-order reaction which simplifies the evaluation of the kinetics according to Equation (6.5).

$$\frac{d[\mathbf{6ak}]}{dt} = k_2[\mathbf{1k}][\mathbf{2a}] - k_{-1\psi}[\mathbf{6ak}] \quad (6.5)$$

When benzoylchloride (**2a**) is used in excess relative to the pyridine **1k**, integration of Equation (6.5) with the constraint $[\mathbf{1k}]_0 = [\mathbf{1k}] + [\mathbf{6ak}]$ yields Equation (6.6), that is, the obtained rate law leads to a monoexponential increase of the concentration of the formed *N*-benzoylpyridinium ion.^[22]

$$k_{\text{obs}} = k_2[\mathbf{2a}] + k_{-1\psi} \quad (6.6)$$

When we added 2 equivalents of *n*-Bu₄N⁺ Cl⁻ to a solution of **1k** and benzoyl chloride (**2a**) in CH₃CN, we indeed observed a monoexponential increase of the absorbance (Figure 6.6a) different from the situation in the absence of *n*-Bu₄N⁺ Cl⁻ (Figure 6.5). The observed rate constants correlated linearly with the concentration of **1k** and the thus determined second-order rate constant k_2 was in good accordance to the rate constant determined in the absence of *n*-Bu₄N⁺ Cl⁻ (Figure 6.6b, Table 6.1). The lower final absorbances observed in the presence of *n*-Bu₄N⁺ Cl⁻ can be rationalized by the more pronounced back reaction.

Similarly, addition of two equivalents of *n*-Bu₄N⁺ Cl⁻ turned out to be sufficient to convert the complex kinetics of the reaction of 3,5-dibromo-4-aminopyridine (**1e**) with benzoyl chloride (**2a**) to first-order kinetics. As the differences between the time-dependent absorbances and the monoexponential fits were very small for the reaction of *N*-acetyl-4-aminopyridine (**1f**) with benzoyl chloride (**2a**) we determined the kinetics without the addition of *n*-Bu₄N⁺ Cl⁻.

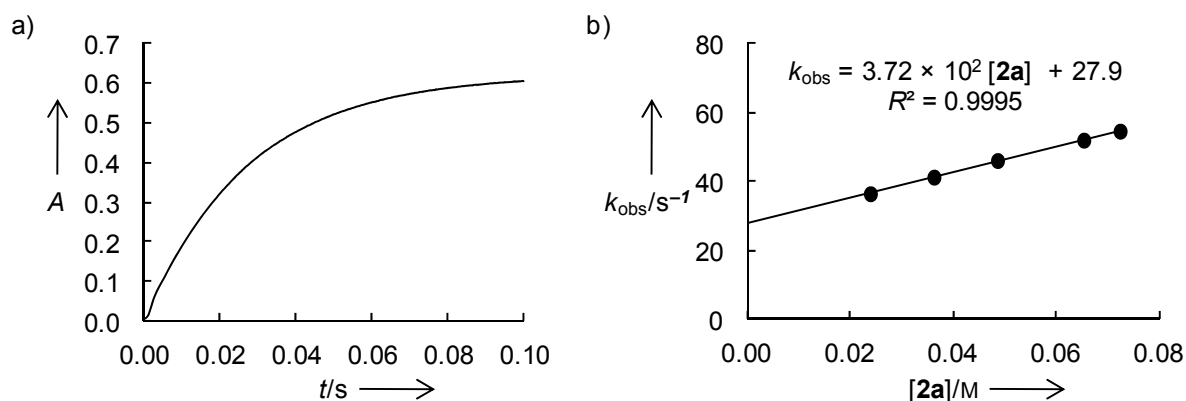


Figure 6.6. a) Increase of the absorbance at 345 nm during the reaction of benzoyl chloride ($[\mathbf{2a}] = 2.38 \times 10^{-2} \text{ M}$) with **1k** ($[\mathbf{1k}] = 6.05 \times 10^{-4} \text{ M}$) in presence of $n\text{-Bu}_4\text{N}^+ \text{Cl}^-$ ($1.21 \times 10^{-3} \text{ M}$). b) A plot of k_{obs} versus $[\mathbf{2a}]$ yields the second-order rate constant $k_2 = 3.72 \times 10^2 \text{ M}^{-1} \text{ s}^{-1}$.

Due to the more pronounced back-reactions, the addition of chloride anions is problematic for the determination of the kinetics of the reactions of benzoyl chloride (**2a**) with pyridines of low Lewis basicity, like the parent compound or nitropyridines. In such cases the low conversions in the absence of additional chloride ions would be further decreased to a point at which the evaluation fails due to the limited accuracy of the absorbancies of the benzoylpyridinium ions.

Table 6.1. Second-order rate constants k_2 for the reactions of benzoyl chloride (**2a**) with the pyridines **1a–q** in acetonitrile at 20 °C and absorption maxima of the generated *N*-benzoylpyridinium chloride **6-Cl**.

| Pyridine | $\lambda_{\text{max}}/\text{nm}$ | $k_2/\text{M}^{-1} \text{ s}^{-1}$ |
|-----------|----------------------------------|---|
| 1a | 317 | 3.00×10^4 [a,b] |
| | 318 | $9.64 \times 10^3 (\text{CH}_2\text{Cl}_2)$ [b,c] |
| | | $9.49 \times 10^3 (\text{CH}_2\text{Cl}_2)$ [c,d] |

Table 6.1 (continued).

| Pyridine | $\lambda_{\text{max}}/\text{nm}$ | $k_2/\text{M}^{-1} \text{s}^{-1}$ |
|-----------|----------------------------------|---|
| 1b | 321 | 4.28×10^4 [b] |
| | | 4.09×10^4 [d] |
| | | 1.48×10^4 (CH_2Cl_2) [b] |
| | | 5.08×10^3 (CHCl_3) [d] |
| 1c | 319 | 1.12×10^4 [b] |
| | | 1.09×10^4 [d] |
| 1d | 334 | 3.28×10^2 [d] |
| 1e | 283 | 5.46×10^1 [d,e] |
| 1f | 297 | 9.69×10^2 [b] |
| 1g | 325 | 1.73×10^4 [d] |
| 1h | 380 | 8.27×10^4 [d] |
| 1i | 390 | 1.23×10^5 [f] |
| 1j | 390 | 1.40×10^5 [d] |
| | | 3.77×10^2 [d] |
| 1k | 345 | 3.73×10^2 [d,e] |
| | | 1.37×10^5 [d] |
| 1l | 417 | 1.37×10^5 [d] |
| 1m | 427 | 1.62×10^5 [d] |
| 1n | 424 | 1.97×10^5 [d] |
| 1o | 390 | 1.68×10^5 [d] |
| 1p | 386 | 1.92×10^5 [d] |
| 1q | 335 | 1.27×10^5 [d] |

[a] From Ref. [21]. [b] The pyridine **1** was used in excess. [c] Re-evaluated from Ref. [21]. [d] Benzoyl chloride (**2a**) was used in excess. [e] Measured in presence of *n*-Bu₄N⁺ Cl⁻. [f] Determined using equal concentrations of the nucleophile and the electrophile and second-order kinetic analysis.

A plot of $(\log k_2)/S_N$ for the reactions of **2a** with pyridines **1** versus the nucleophilicity parameters *N* of the pyridines **1**^[10,15] is linear with a slope close to unity (Figure 6.7). Similarly to the reactivities of primary and secondary amines towards 1-benzoyl-4-(dimethylamino)pyridinium chloride (**6aa-Cl**), which follow separate correlation lines,^[23]

the reactions of **2a** with pyridines are well described by the nucleophilicity parameters *N* which were derived from their reactions with benzhydrylium ions.

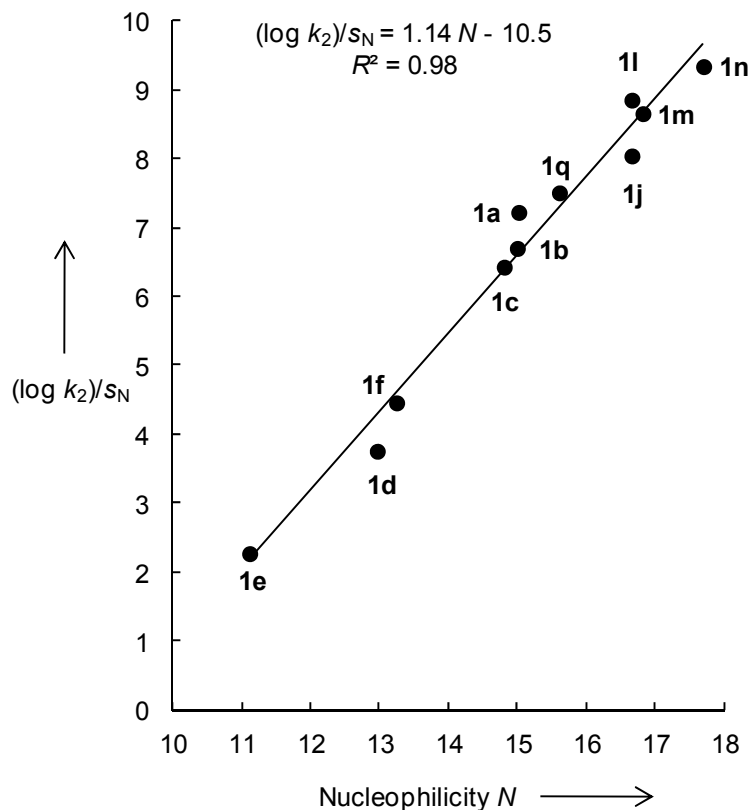


Figure 6.7. Correlation of $(\log k_2)/S_N$ against the nucleophilicity parameters *N* of the pyridines **1** for their reactions with benzoyl chloride (**2a**).^[a,b]

[a] Nucleophilicity parameters *N* from Ref. [10,15]. [b] For the determination of the nucleophilicity parameters of **1b,j,q** see Experimental Section.

In general, the reactivities of the pyridines **1** towards benzoyl chloride (**2a**) increase with electron-donating substituents in 4-position of the pyridine ring. For example, PPY (**1b**) is 1.4 times more reactive than DMAP (**1a**), which is again 2.7 times more reactive than 4-morpholinopyridine (**1c**). An electron-withdrawing bromo-substituent in 3-position (**1d**) decreases the reactivity of DMAP by a factor of 90.

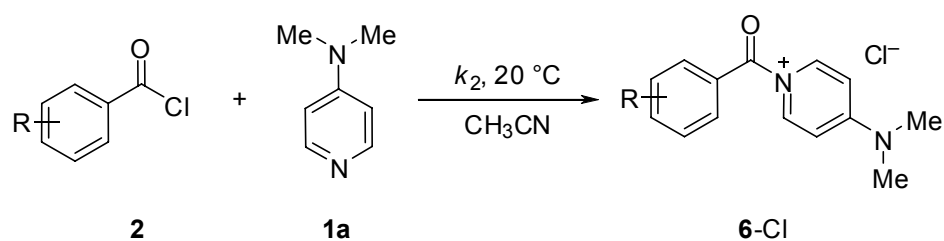
As observed for the nucleophilicities of pyridines towards benzhydrylium ions,^[10] bridging of the substituents in 3,4- or 3,4,5- position of the pyridine rings increases their reactivities by conformational fixation of the lone pairs at the amino groups.^[7] The lowest reactivity within the series is found for the methyl-substituted 3,4-dialkylaminopyridine **1h**. The exchange of the methyl groups by ethyl groups results in a 1.5-fold increase of reactivity (**1i/1h**). No

further increase of the reactivity is observed by fusing the alkyl bridge of **1i** with a cyclohexyl ring (**1j**). The tricyclic 3,4,5-alkylaminopyridines **1l,m** were found to be 1.3–1.7 times more reactive than the analogously substituted bicyclic 3,4-dialkylaminopyridines **1h,i**. In analogy to the nucleophilicities towards benzhydrylium ions,^[10] the benzyl-substituted superDMAP **1n** shows the highest reactivity in this reaction series. While substitution of one alkylamino group in **1m,n** by a carbon atom (\rightarrow **1o,p**) does not affect the nucleophilic reactivity, TCAP (**1q**) was found to be 1.3 to 1.5 times less reactive than the 3,4,5-trialkylaminopyridines and is therefore comparable to **1i**.

As expected from the low nucleophilicities of the acetylated pyridine **1f** towards benzhydrylium ions,^[10,15] **1f** and **1k** react considerably slower with benzoyl chloride (**2a**) than DMAP (**1a**) or **1i** ($1a/1f = 31$, $1i/1k = 3.3 \times 10^2$). The chiral catalyst **1g** developed by Fu for asymmetric reactions and for the kinetic resolution of alcohols and amines,^[24] reacts 1.7 times more slowly than DMAP (**1a**).

6.2.3 Kinetics of the Reactions of DMAP (**2a**) with Other Acyl Chlorides and Anhydrides

The second-order rate constants (Table 6.2) for the reactions of DMAP (**1a**) with substituted benzoyl chlorides **2b–n** (Scheme 6.6) were determined spectrophotometrically at the absorption maxima of the *N*-acylpyridinium ions using the same method as described above.



Scheme 6.6. Reactions of substituted benzoyl chlorides **2b–n** with DMAP (**1a**) in acetonitrile at 20°C .

Table 6.2. Second-order rate constants k_2 for the reactions of DMAP (**1a**) with substituted benzoyl chlorides **2a–n** in acetonitrile at 20 °C.^[a]

| Benzoyl Chloride | $\lambda_{\text{max}}/\text{nm}$ | $k_2/\text{M}^{-1} \text{ s}^{-1}$ |
|------------------------------------|----------------------------------|------------------------------------|
| 4-NMe ₂ 2b | 370 | 1.91×10^2 |
| 4-OMe 2c | 320 | 4.33×10^3 |
| 4-Me 2d | 319 | 1.32×10^4 |
| 3,4,5-(OMe) ₃ 2e | 320 | 1.95×10^4 |
| H 2a | 317 | 3.00×10^4 ^[b] |
| 4-F 2f | 317 | 3.47×10^4 |
| 4-Cl 2g | 320 | 6.82×10^4 |
| 4-Br 2h | 319 | 7.64×10^4 |
| 4-Cl 2i | 330 | 1.01×10^5 |
| 3-F 2j | 325 | 1.14×10^5 |
| <i>o</i> -Br 2k | 320 | 1.23×10^5 |
| 3-Br 2l | 325 | 1.47×10^5 |
| 3,5-F 2m | 325 | 4.71×10^5 |
| 2,3,4,5,6-F ₅ 2n | 325 | 5.43×10^5 |

[a] DMAP (**1a**) was used in excess. [b] From Ref. [21].

When the logarithms of the second-order rate constants were plotted against the Hammett substituent parameters σ ,^[25] a curved plot was obtained, showing that the electron-donating substituents decrease the reactivities to a greater extent than expected from their σ parameters (Figure 6.8a). By employing the Yukawa-Tsuno equation [Eq. (6.7)],^[26] a linear correlation with a slope of $\rho = 1.7$ was obtained for $r = 0.53$ (Figure 6.8b).

$$\lg \frac{k_2(\mathbf{2a-m})}{k_2(\mathbf{2a})} = \rho(\sigma_x + r(\sigma_x^+ - \sigma_x)) \quad (6.7)$$

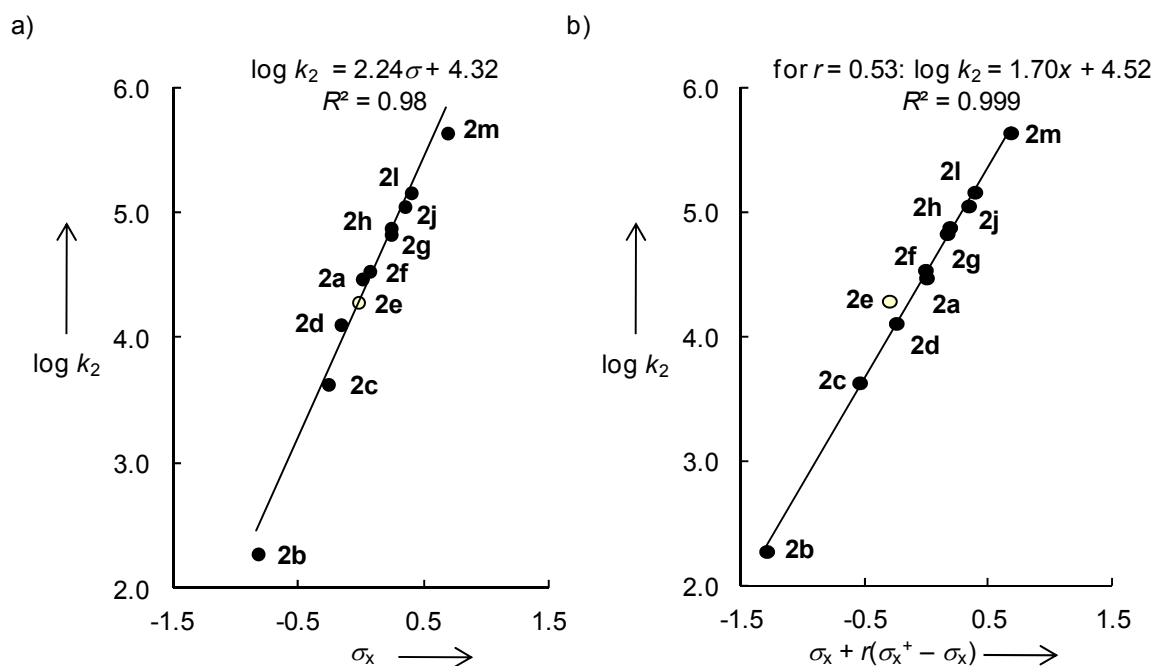
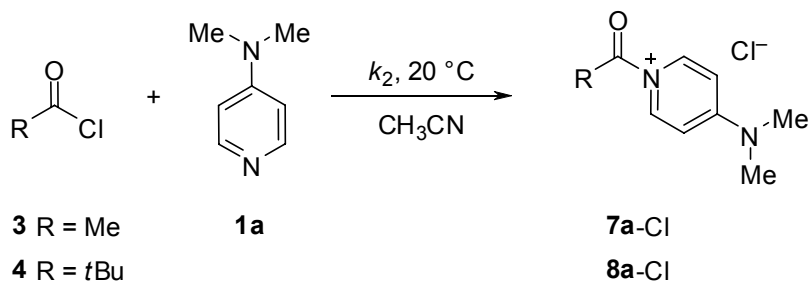


Figure 6.8. a) Hammett plot for the reactions of DMAP (**1a**) with substituted benzoyl chlorides **2**. b) Yukawa-Tsuo plot for the reactions of DMAP (**1a**) with substituted benzoyl chlorides **2** for $r = 0.53$.^[a]

^[a] Open symbols refer to rate constants which were not used for the calculation of the correlation lines.

Acetyl chloride (**3**) was found to react 3.8 times faster with DMAP (**1a**) than benzoyl chloride (**2a**), and a decrease of the second-order rate constant by a factor of 9.5 was observed when the methyl group of acetyl chloride (**3**) was exchanged by the sterically demanding *tert*-butyl group (\rightarrow **4**; Scheme 6.7, Table 6.3).



Scheme 6.7. Reactions of acetyl chloride (**3**) and pivaloyl chloride (**4**) with DMAP (**1a**) in acetonitrile at 20°C .

Table 6.3. Second-order rate constants k_2 for the reactions of DMAP (**1a**) with different acyl derivatives in acetonitrile at 20 °C.

| Acyl Derivative | | $\lambda_{\text{max}}/\text{nm}$ | $k_2/\text{M}^{-1} \text{ s}^{-1}$ |
|-------------------|-----------|----------------------------------|------------------------------------|
| acetyl chloride | 3 | 312 | 1.15×10^5 |
| pivaloyl chloride | 4 | 320 | 1.12×10^4 [a] |
| benzoyl chloride | 2a | 317 | 3.00×10^4 [b] |
| benzoic anhydride | 5 | | 3.8×10^1 [c] |

[a] From Ref. [21]. [b] Re-evaluated from Ref. [21]. [c] Method of initial rate, see Experimental Section.

As anhydrides are commonly used as electrophiles in DMAP-catalyzed acylation reactions, we also determined the kinetics of the reaction of DMAP (**1a**) with benzoic anhydride (**5**) in acetonitrile at 20 °C. From the plots of the time-dependent absorbances of the *N*-benzoylpyridinium ion **6aa**-OBz at different concentrations of **1a**, it can be concluded that the reaction is incomplete even at a high concentration of DMAP (Figure 6.9).^[21] The absorbances at $t = 0$, which increase with the concentration of **1a** are caused by a tail of the absorption band of DMAP. Similar to the reaction of **1e** or **1k** with **2a**, a non-exponential increase of the absorbance was observed. However, even at the highest concentration of DMAP studied ($[\mathbf{1a}] = 0.05 \text{ M}$), the time-dependent increase of absorbance still deviated significantly from an exponential fit of the first two half-lives of the reaction as shown by the dashed line in Figure 6.9. In contrast to the reactions of **2a** with **1e** or **1k**, the addition of the counter anion, that is, benzoate ions, cannot be used as method to simplify the kinetics, because the reactions would become too fast to be followed by the stopped-flow systems, and the resulting absorbances would be below the detection limit. Assuming that the counterions benzoate or chloride do not affect the absorption coefficient of the *N*-benzoyl-4-(dimethylamino)pyridinium ion (for Cl^- : $\varepsilon = 1.57 \times 10^4 \text{ M}^{-1} \text{ cm}^{-1}$), we can calculate the concentrations of the product **6aa**-OBz. The conversions obtained in the reaction, ranged from 4–12%.

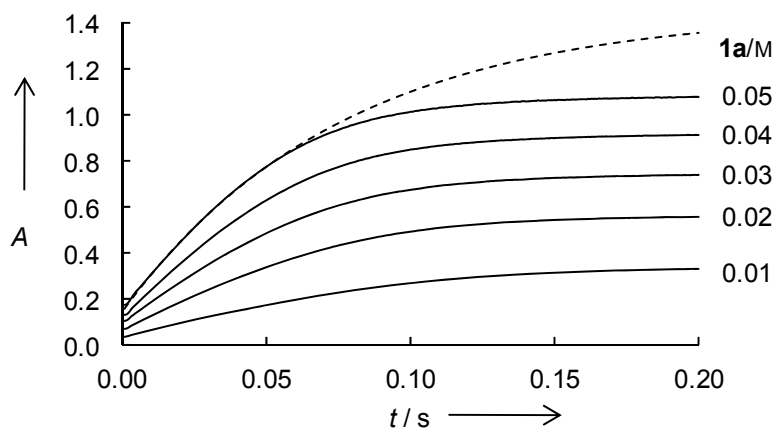


Figure 6.9. Increase of the absorbance at 316 nm during the reaction of benzoic anhydride ($[5] = 4.99 \times 10^{-4}$ M) with DMAP ($[1a]$ is specified at the curves) in acetonitrile at 20 °C. Dashed line: monoexponential fit of the first two half-lives for $[1a] = 0.05$ M.^[21]

For the evaluation of the kinetics of the forward reaction, the method of initial rate was used, which yielded a second-order rate law with a rate constant of $k_2 = 3.8 \times 10^1 \text{ M}^{-1} \text{ s}^{-1}$ (for details see Experimental Section). Consequently, benzoic anhydride (**5**) is approximately 800 times less reactive towards DMAP than benzoyl chloride (**2a**).

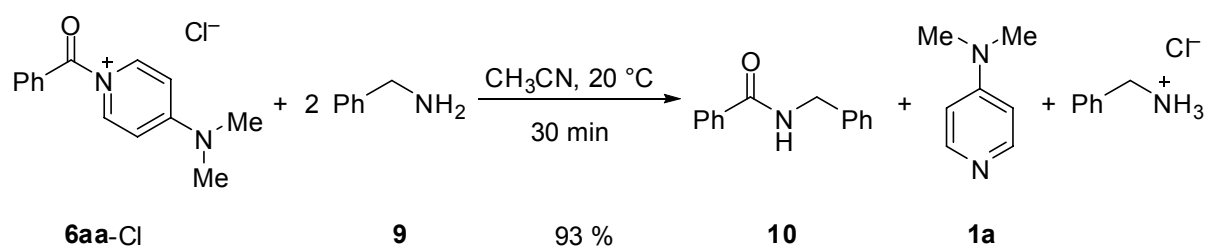
In order to determine the complete rate law for the reaction, we have also studied the back-reaction of the *N*-benzoylpyridinium chloride **6aa**-Cl with benzoate ions kinetically. Therefore, we followed the time-dependent UV/Vis absorbance decay of **6aa** during its reaction with an excess of $n\text{-Bu}_4\text{N}^+ \text{BzO}^-$ in acetonitrile at 20 °C.^[25] Again, first-order decays were observed and the observed rate constants k_{obs} correlated linearly with the concentration of the benzoate salt ($k_{-2} = 1.11 \times 10^6 \text{ M}^{-1} \text{ s}^{-1}$). Equation (6.8) results as rate-law for the reaction of benzoylchloride (**2a**) with benzoic anhydride (**5**).

$$\frac{d[6aa]}{dt} = k_2 \cdot [2a][5] - k_{-2}[6aa][\text{BzO}^-] \quad (6.8)$$

However, if the values for the equilibrium constant for the reaction are determined from the final absorbances of the individual experiments, discrepancies up to a factor of 6 are observed compared to the ratio of the rate constants for the forward and the backward reactions, which shows that the simple rate law of Equation (6.8) does not describe the reaction completely, as for example, effects of ion pairing are not included.

6.2.4 Kinetics of the Reactions of *N*-Acylpyridinium ions with Benzylamine (**9**)

Combination of *N*-benzoylpyridinium chloride **6aa-Cl** with benzylamine (**9**) in acetonitrile at 20 °C yielded the amide **10**, DMAP (**1a**) and benzylammonium chloride which precipitated from the reaction solution (Scheme 6.8).^[21]



Scheme 6.8. Reaction of **6aa-Cl** with benzylamine (**9**) in acetonitrile at 20 °C.^[21]

For the determination of the electrophilic reactivities of *N*-acylpyridinium ions mainly those electrophiles were chosen, which do not have α -hydrogen atoms, in order to exclude the formation of ketenes in a side reaction. Benzylamine (**9**) was used as reference nucleophile in high excess to ensure first-order conditions.

During the reaction of *N*-(4-dimethylamino)benzoyl-4-(dimethylamino)pyridinium chloride (**6ba-Cl**) with benzylamine (**9**) the absorption band of **6ba-Cl** at 370 nm decreased (Figure 6.10). As neither the formed amide, DMAP, benzylammonium, nor protonated DMAP ions absorb above 350 nm, the absorbance was directly proportional to the concentration of **6ba-Cl**, and the complete decay of the absorbance showed the irreversibility of the reaction. Furthermore, an isosbestic point at 301 nm was observed, which proved that no long-lived UV-active intermediate was formed during the reaction.

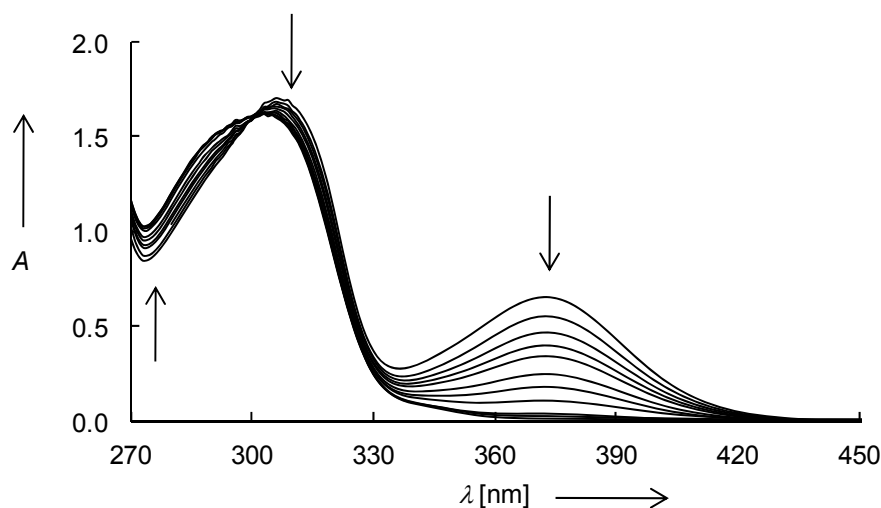


Figure 6.10. UV/Vis spectra during the reaction of 1-(4-dimethylamino)benzoyl 4-(dimethylamino)pyridinium chloride (**6ba-Cl**) with benzylamine (**9**) after $t = 0, 5, 10, 15, 20, 30, 40, 60, 90, 120$ and 180 s.

Similarly, the other *N*-benzoylpyridinium ions **6** reacted irreversibly with benzylamine (**9**) and the kinetics of the reactions were determined spectrophotometrically in acetonitrile at $20\text{ }^{\circ}\text{C}$ at the absorption bands of the *N*-benzoylpyridinium ions. For all reactions, monoexponential decays of the absorbances were observed (fit functions: $A = A_0e^{-k_{\text{obs}}t} + C$), and the second-order rate constants k_2 (Tables 6.4 and 6.5) were obtained as the slopes of the linear plots of k_{obs} versus [**9**]. The *N*-benzoylpyridinium chlorides **6-Cl** were either used as isolated salts or generated by mixing equal amounts of the benzoyl chlorides and the pyridine; as demonstrated for the reaction of **6aa-Cl** with benzylamine (**9**) both methods gave rate constants, which differed by less than 3%.^[25] As the reactions of **1e** and **1k** with **2a** were reversible, the isolated triflates **6ae-OTf** and **6ak-OTf** were used in these cases.

Table 6.4. Second-order rate constants k_2 for the reactions of benzylamine (**9**) with substituted 1-benzoyl-4-(dimethylamino)pyridinium chlorides **6-Cl**^[a] in acetonitrile at 20 °C.

| Substituent | | $k_2 / \text{M}^{-1} \text{s}^{-1}$ |
|--------------------------|---------------|-------------------------------------|
| H | 6aa-Cl | 4.78×10^2 ^[b] |
| 4-NMe ₂ | 6ba-Cl | 5.44 |
| 4-OMe | 6ca-Cl | 8.92×10^1 |
| 4-Me | 6da-Cl | 2.39×10^2 |
| 3,4,5-(OMe) ₃ | 6ea-Cl | 3.91×10^2 |
| 4-F | 6fa-Cl | 4.88×10^2 |
| 4-Br | 6ha-Cl | 8.65×10^2 |
| 3-F | 6ja-Cl | 1.40×10^3 |
| 2-Br | 6ka-Cl | 4.98×10^1 |
| 3-Br | 6la-Cl | 1.44×10^3 |
| 3,5-F ₂ | 6ma-Cl | 4.17×10^3 |

[a] Generated by mixing the benzoyl chloride **2a-m** with DMAP (**1a**). [b] From Ref. [25].

Table 6.5. Second-order rate constants k_2 for the reactions of *N*-acylpyridinium ions **6-8**^[a] with benzylamine (**9**) in acetonitrile at 20 °C.

| Electrophile | $k_2 / \text{M}^{-1} \text{s}^{-1}$ |
|-------------------------------|---|
| 6aa-OTf ^[b] | 4.03×10^2 |
| 6ab-Cl | 2.79×10^2 |
| 6ab-Cl | 3.66×10^4 (CHCl ₃) |
| 6ac-Cl | 8.99×10^2 |
| 6ad-Cl | 9.59×10^3 |
| 6ah-Cl | 2.72×10^2 |
| 6ai-Cl | 2.04×10^2 |
| 6aj-Cl | 1.62×10^2 |
| 6ak-OTf ^[c] | 1.57×10^5 |
| 6al-Cl | 1.41×10^2 |
| 6am-Cl | 1.28×10^2 |

Table 6.5 (continued).

| Electrophile | $k_2/\text{M}^{-1} \text{s}^{-1}$ |
|---------------|-----------------------------------|
| 6an-Cl | 1.98×10^2 |
| 6ao-Cl | 8.36×10^1 |
| 6ap-Cl | 1.18×10^2 |
| 6aq-Cl | 6.66×10^1 |
| 7a-Cl | 7.39×10^2 |
| 8a-Cl | 6.24×10^3 |

[a] Generated by mixing the acyl chloride **2a**, **3** or **4** and the pyridine **1a–q**. [b] Re-evaluated from Ref. [21]. [c] The isolated triflate salt **6-OTf** was used.

In order to determine whether the counterion influences the reactivity of the *N*-benzoylpyridinium ions **6**, we compared the reaction of benzylamine (**9**) with **6aa-Cl** and **6aa-OTf**. The latter was found to react approximately 20 % more slowly than the chloride salt. Thus, it can be concluded that the deprotonation of the ammonium nitrogen atom by triflate or chloride cannot occur in the rate determining step of the reaction. The determination of the kinetics of reactions of *N*-benzoylpyridinium ions **6** with more basic counter ions, like acetate or benzoate, which can be presumed to enhance the reactivities to a far greater extent, was impossible by this methodology, as these ions reacted reversibly with the *N*-benzoylpyridinium ions to form acid anhydrides. Therefore, the amination reactions of the *N*-benzoylpyridinium chlorides and triflates in acetonitrile are concluded to proceed either concerted^[27] or by formation of tetrahedral intermediates, which are rapidly deprotonated in a subsequent reaction. The mechanism neither involves a second amine molecule acting as general base nor the rate-determining formation of acylium ions as demonstrated by the linear dependence of the rates on the concentrations of benzylamine (**9**).

In analogy to the reactions of substituted benzoyl chlorides with DMAP (**1a**), electron-withdrawing groups in the benzoyl moiety also increase the reactivities of the *N*-benzoylpyridinium chlorides **6-Cl**. A slightly curved plot was obtained, when the second-order rate constants were correlated with the Hammett substituent parameters σ_x (Figure 6.12a). Again, the application of the Yukawa-Tsuno equation [Eq. (6.7)] resulted in a linear correlation with

a slope of $\rho = 1.34$ for $r = 0.68$ (Figure 6.11b), showing that the degree of resonance interaction is greater than for the reactions of benzoyl chlorides with DMAP (see above).

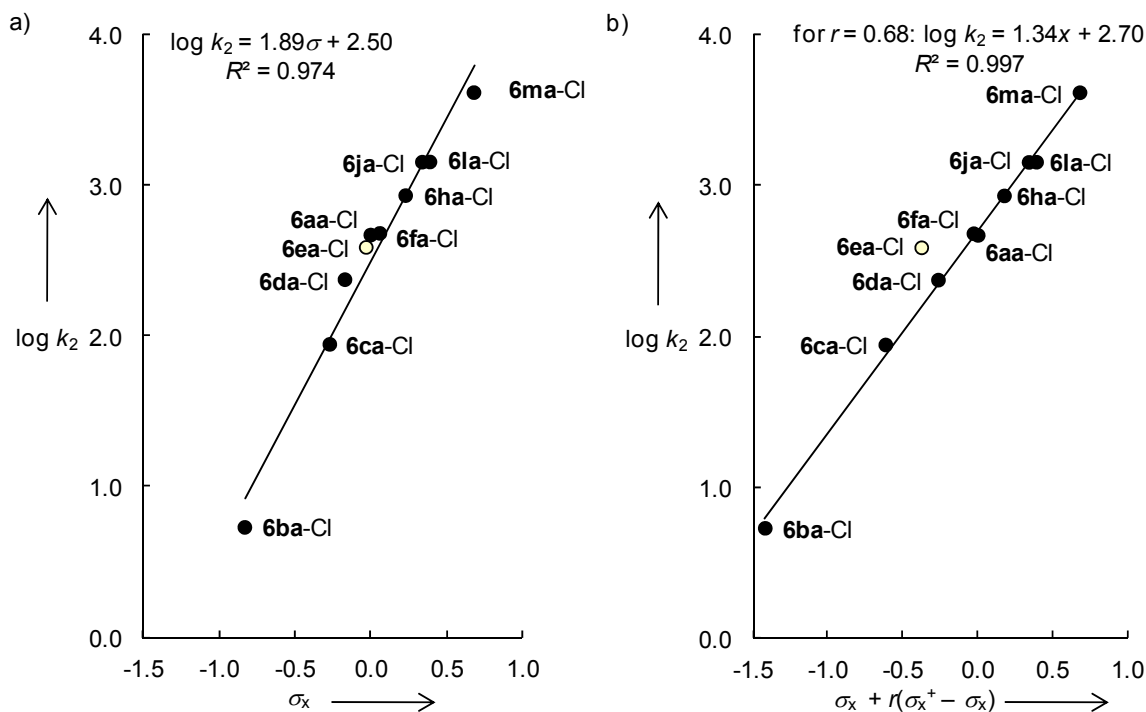


Figure 6.12. a) Hammett-plot for the reactions of benzylamine (**9**) with substituted 1-benzoyl-4-(dimethylamino)pyridinium chlorides **6-Cl**. b) Yukawa-Tsuno-plot for the reactions of benzylamine (**9**) with substituted 1-benzoyl 4-(dimethylamino)pyridinium chlorides **6-Cl** with $r = 0.68$.^[a]

[a] Open symbols refer to rate constants which were not used for the calculation of the correlation lines.

When the rate constants for the pyridinolysis reactions of substituted benzoyl chlorides were plotted versus the rate constants of the aminolysis reaction of the thus formed 1-benzoyl-4-(dimethylamino)pyridinium chlorides **6-Cl**, a linear correlation was obtained, which showed that the effect of the substituents is slightly greater in the pyridinolysis reaction (Figure 6.12). Only substituents in *ortho*-position affected the two reactions in different manners, as evident by the fact that aminolysis reaction of **6ka-Cl** is 30 times slower than expected from the rate of its formation from DMAP (**1a**) and **2k**.

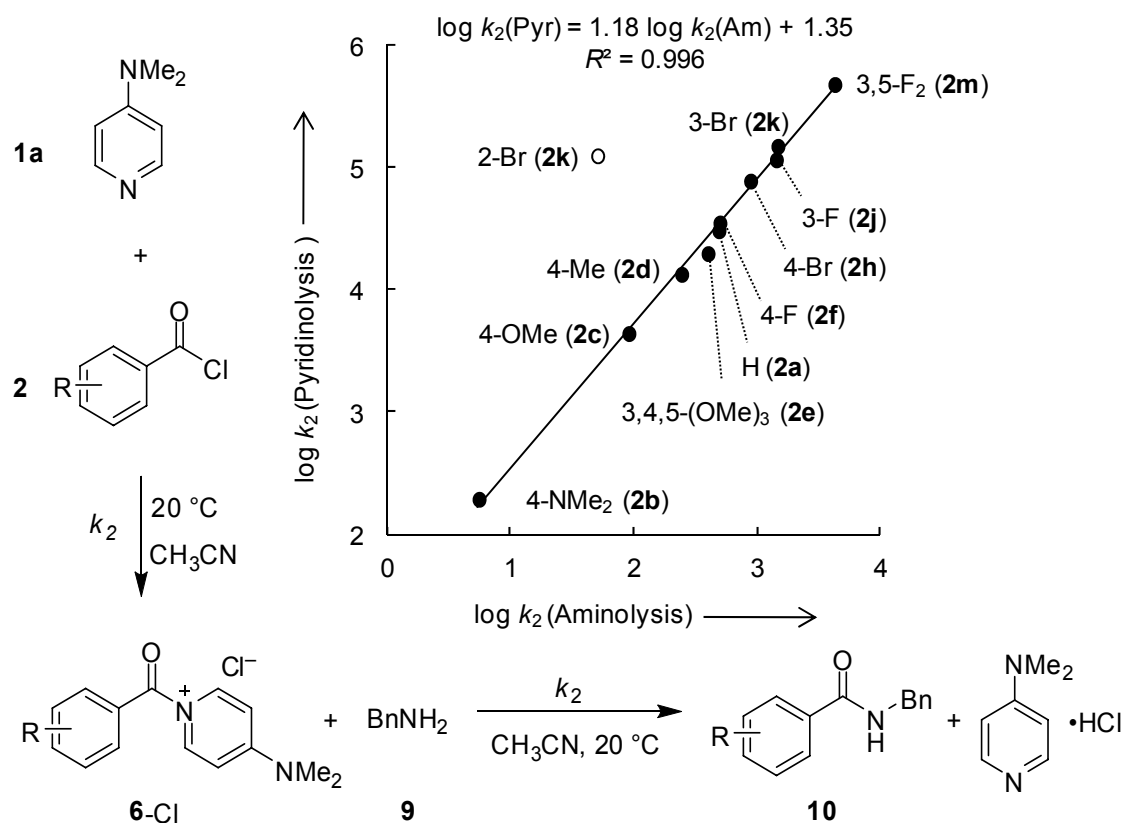


Figure 6.12. Correlation between the rate of the aminolysis reaction of substituted 1-benzoyl-4-(dimethylamino)pyridinium chlorides **6-Cl** with benzylamine (**9**; “Am”) and the rate of the pyridinolysis reactions of the corresponding benzoyl chlorides **2** (“Pyr”).

While the reactivities of the acyl chlorides towards DMAP (**1a**) increase in the order pivaloyl chloride (**4**) < benzoyl chloride (**2a**) < acetyl chloride (**3**), the reactivities of the corresponding *N*-acylpyridinium ions (Figure 6.13) increase in the order **6aa-Cl** < **7a-Cl** < **8a-Cl**. The remarkably high reactivity of the pivaloyl-substituted *N*-acylpyridinium ion **8a-Cl**, which is even 8.5 times more reactive than **7a-Cl**, is presumably caused by enhanced twisting of the pyridine ring out of the carbonyl plane.

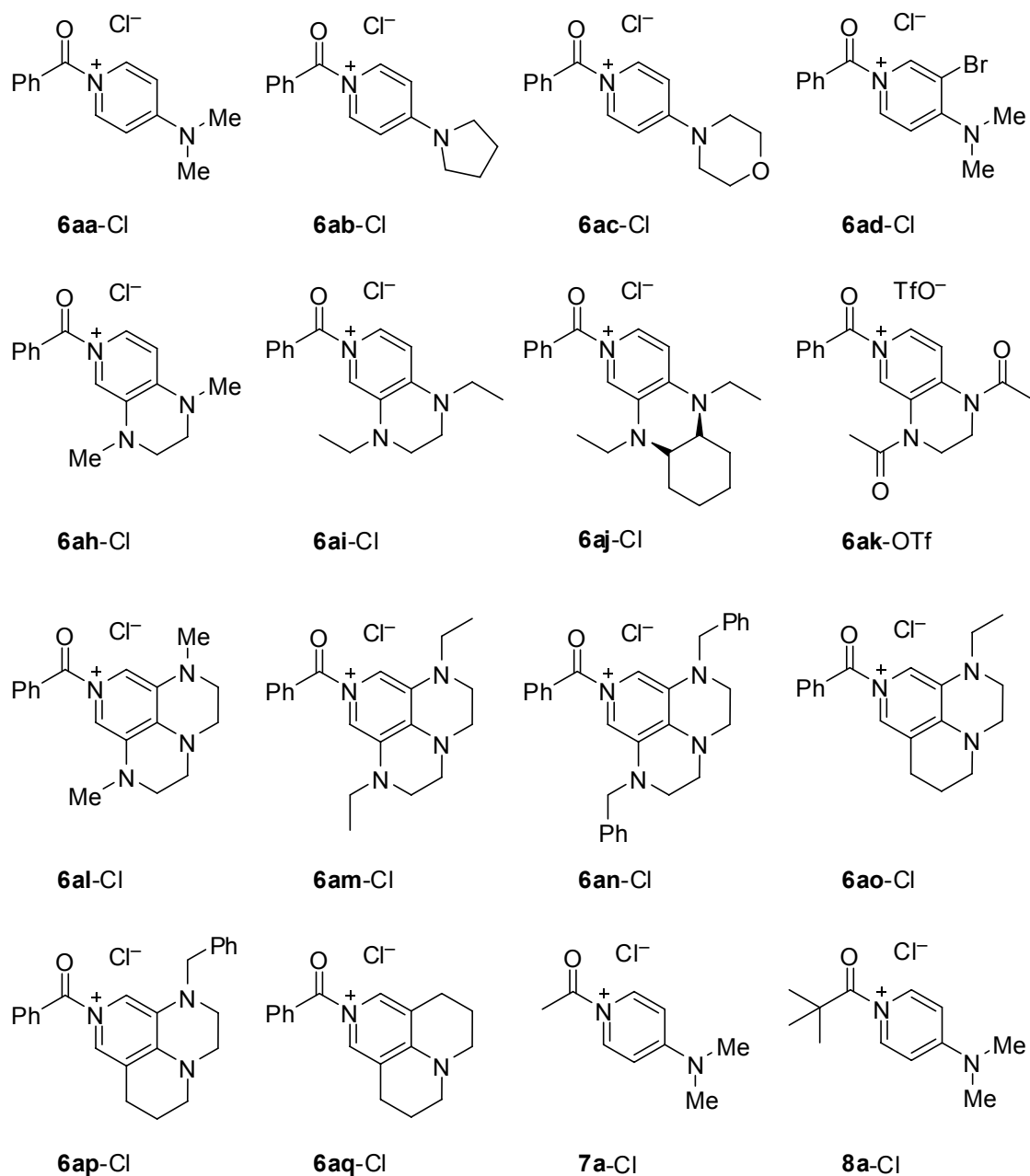


Figure 6.13. Structures of *N*-acylpyridinium salts **6–8**.

While electron-donating groups in the pyridines (**1**) increase their reactivities towards benzoyl chloride (**2a**), electron donors in the pyridines decrease the reactivities of *N*-benzoylpyridinium ions **6**. In general, the more nucleophilic pyridines give rise to *N*-benzoylpyridinium ions of lower electrophilic reactivity.

Figure 6.14 shows a plot of the second-order rate constants of the amination reaction of **6** versus the second-order rate constant of the pyridinolysis reaction of benzoyl chloride (**2a**). A

linear correlation with a slope of -1.33 was observed for 4-dialkylamino-substituted pyridines, which demonstrates that the formation of *N*-benzoylpyridinium ions is more sensitive to the electron-donating ability of the substituents in the pyridine than the corresponding aminolysis reactions with benzylamine (**9**). In the region of the highly nucleophilic pyridines (**1h–q**) the scatter of the correlation is higher, which shows that the bridging of substituents in pyridines affects the nucleophilicities of the pyridines and the electrophilicities of the *N*-acylpyridinium ions in different ways. For example, the benzyl-substituted superDMAP (**1n**) is more nucleophilic than the ethyl-substituted analogue **1m**, and at the same time the benzyl-substituted *N*-benzoylpyridinium chloride **6an-Cl** is also more reactive than the ethyl-substituted one (**6am-Cl**). The *N*-benzoylpyridinium chlorides generated from the 5-alkyl-3,4-dialkylaminopyridines **1o,p** react much slower with benzylamine (**9**) than the *N*-benzoylpyridinium chlorides generated from the analogous 3,4,5-trialkylaminopyridines **1m,n** despite the similar nucleophilicities of the pyridines towards benzoyl chloride (**2a**).

Although **1d** and **1k** are similarly reactive towards benzoyl chloride (**2a**), the reaction of **1k** was found to be reversible while **1d** reacted quantitatively. In contrast, the reactivities of the *N*-benzoylpyridinium ions **6ad-Cl** and **6ak-OTf** differed by a factor of 16. Consequently, the intrinsic barrier for the reaction of the acyl-substituted pyridine **1k** with benzoyl chloride (**2a**) has to be smaller than for the reaction with **1d**. Thus, the reorganization energies in the reactions of benzoyl chloride with **1k** is lower than for reactions with alkyl amino-substituted pyridines.

The reaction of **6ab-Cl** with benzylamine (**9**) was also investigated in chloroform, a common solvent for DMAP-catalyzed acylation reactions. In the less polar solvent CHCl_3 , the reaction of the *N*-benzoylpyridinium chloride **6ab-Cl** is 130 times faster than in acetonitrile, while its formation from benzoyl chloride (**2a**) and PPY (**1b**) was only 8.4 times slower in CHCl_3 .

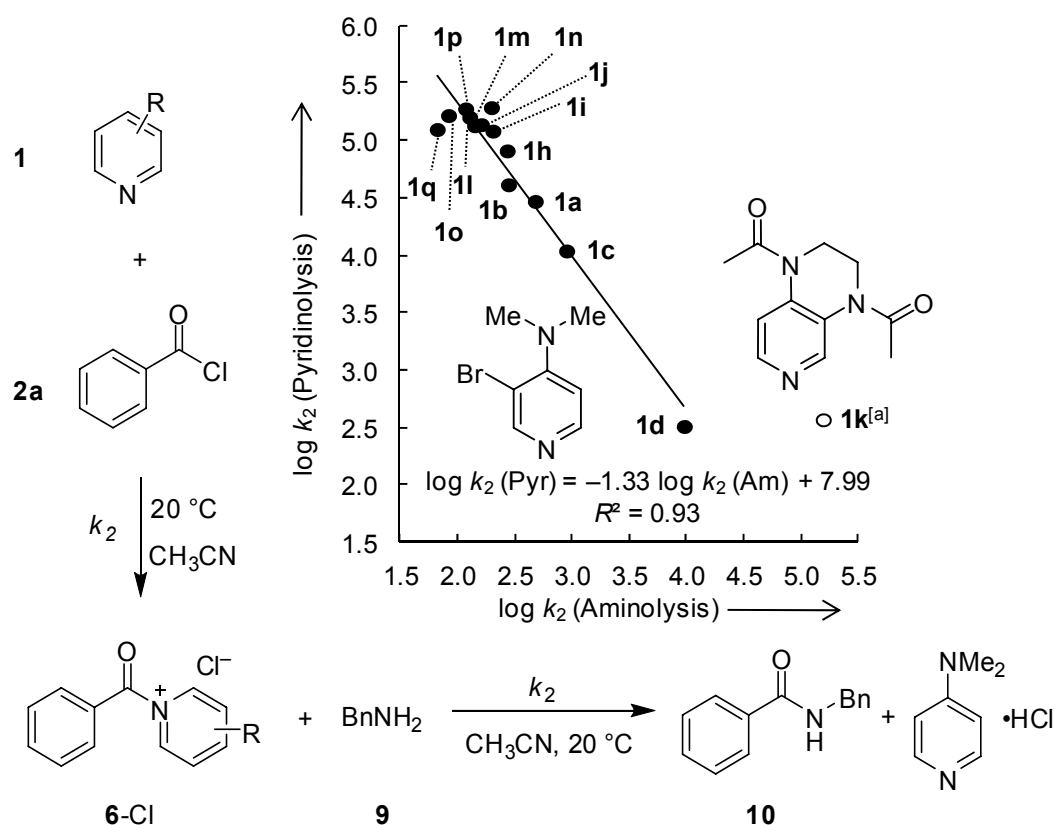


Figure 6.14. Correlation between the rate of the aminolysis reaction of *N*-benzoylpyridinium chlorides **6-Cl** with benzylamine (**9**; “Am”) and the rate of the pyridinolysis reaction of corresponding benzoyl chloride (**2a**; “Pyr”).

[a] Counterion for **6ak**: OTf⁻.

6.3 Conclusion

In summary, we have determined the kinetics of the formation of *N*-acylpyridinium ions and their consumption by benzylamine and evaluated substitution effects in both the acyl and the pyridine moiety.

While electron-withdrawing groups in the benzoyl moiety accelerate both the reactivities of benzoyl chlorides and of the *N*-benzoylpyridinium ions, the electrophilities of *N*-benzoylpyridinium ions decrease with increasing nucleophilicities of the pyridines. The rates of the formation of the *N*-benzoylpyridinium ions from benzoyl chloride and substituted pyridines is more sensitive to the electron-donating ability of the substituents in the pyridine than their aminolysis reactions.

With these kinetic data in hand, we can now derive which amination reactions can be catalyzed by pyridines. Therefore several requirements have to be met by the reaction partners.

(1) The pyridines have to be more nucleophilic than the amines. Therefore, reactions of highly reactive amines, like propylamine or piperidine, with any acylation agent cannot be catalyzed by pyridines, because in these reactions the back-ground reaction would be faster than the catalyzed reaction (Figure 6.15).

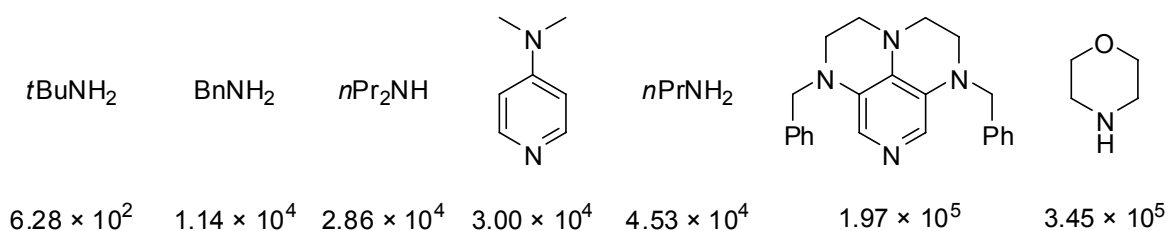


Figure 6.15. Second-order rate constants k_2 ($\text{M}^{-1} \text{s}^{-1}$) for the reactions of amines and pyridines with benzoyl chloride in CH_3CN at 20°C .^[23]

(2) The formed *N*-acylpyridinium ions have to be more electrophilic than the original acylation agents, meaning that, for example, reactions of the highly electrophilic benzoyl chloride with amines cannot be catalyzed.

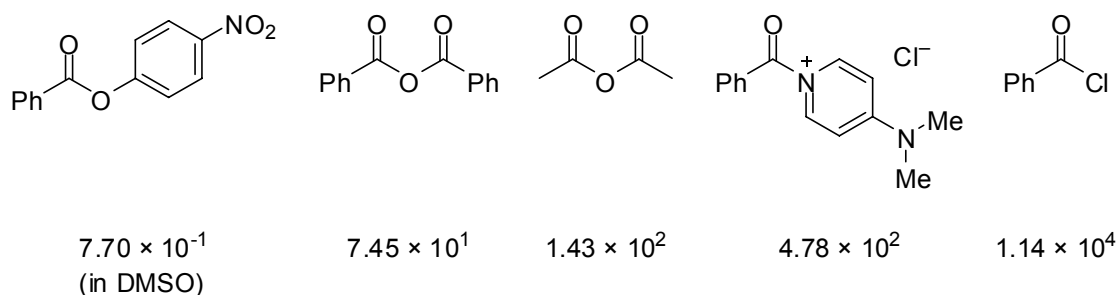


Figure 6.16. Second-order rate constants k_2 ($\text{M}^{-1} \text{s}^{-1}$) for the reactions of benzylamine with acylating agents in CH_3CN at 20°C .^[23]

Apart from the requirements concerning reactivities, the Lewis basicity of the catalyst is also crucial for efficient catalysis as a high concentration of the intermediate *N*-acylpyridinium

ions is required. However, the nucleofugalities of the pyridines must not be too poor as the rate determining step could change otherwise.

6.4 Experimental Section

6.4.1 General Comment

Materials. The pyridines **1a–c,g,q**, benzoyl chlorides **2a–n**, acetyl chloride (**3**), pivaloyl chloride (**4**), benzoic anhydride (**5**), and trimethylsilyl triflate were purchased and used without further purification. Benzylamine (**9**) was purchased and purified by distillation prior to use

The pyridines **1d–f**^[15] and **1n**^[10] were synthesized as described previously.

Acetonitrile (> 99.9%, extra dry) and chloroform (> 99.9%, extra dry) were purchased and used without further purification. Dichloromethane (p.a. grade) was subsequently treated with concentrated sulfuric acid, water, 10% NaHCO₃ solution, and again water. After predrying with anhydrous CaCl₂, it was freshly distilled over CaH₂.

Analytics. In the ¹H and ¹³C NMR spectra the chemical shifts in ppm refer the solvent residual signals as internal standard: CD₃CN ($\delta_{\text{H}} = 1.94$, $\delta_{\text{C}} = 1.32$) The following abbreviations were used for signal multiplicities: s = singlet, d = doublet, t = triplet, q = quartet, m = multiplet, br = broad. For reasons of simplicity, the ¹H NMR signals of AA'BB'-spin systems of *p*-substituted aromatic rings were treated as doublets.

IR spectra were recorded with a FT-IR-BX with a ATR probe. The following abbreviations were used for signal intensities: s = strong, m = medium, w = weak.

HRMS-ESI spectra were obtained with a Thermo Finnigan LTQ FT Ultra (IonMax ion source, 4 kV). HRMS-FAB spectra were obtained with a Thermo Finnigan MAT 95 oder a Jeol MStation (xenon atoms, 8 kV, in 2-nitrobenzylalcohol or glycerine matrix).

Elementary analyses were obtained with a Vario El at the microanalytic laboratory at the LMU München.

Kinetic Experiments. The kinetics of the reactions investigated were followed by UV/Vis spectrophotometry by using working stations similar to those described previously.^[16]

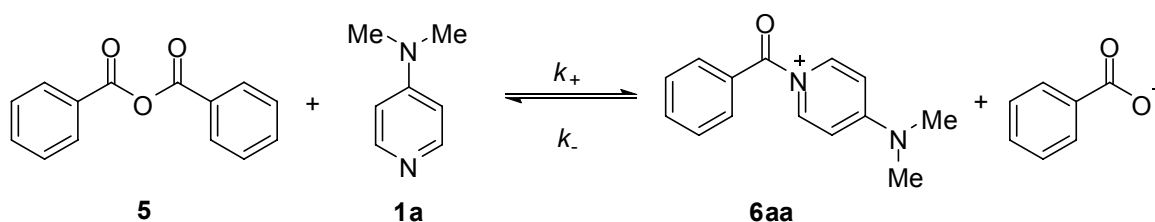
For slow reactions ($\tau_{1/2} > 10$ s), the spectra were collected at different times by using a J&M TIDAS diode array spectrophotometer that was connected to a Hellma 661.502-QX quartz Suprasil immersion probe (5 mm light path) by fiber optic cables with standard SMA connectors. All kinetic measurements were carried out in Schlenk glassware under exclusion of moisture. The temperature of the solutions during the kinetic studies was maintained at $20\text{ }^{\circ}\text{C} \pm 0.1\text{ }^{\circ}\text{C}$ and monitored with a thermo-couple probe that was inserted into the reaction mixture.

Stopped-flow spectrophotometer systems (Applied Photophysics SX.18MV-R or Hi-Tech SF-61DX2) were used for the investigation of faster reactions ($10\text{ ms} < \tau_{1/2} < 10$ s). The kinetic runs were initiated by mixing equal volumes of the solutions of the nucleophiles and the electrophiles.

Either the nucleophiles or the electrophiles were used in large excess (over 8 equivalents relative to the other) to ensure first-order conditions with $k_{\text{obs}} = k_2[\text{Nu}]_0 + k_0$. The first-order rate constants k_{obs} (s^{-1}) were obtained by least-squares fitting of the single-exponential curve $A_t = A_0 e^{-k_{\text{obs}}t} + C$ to the decays of the absorbances at λ_{max} , or the exponential increase function $A_t = A_0(1 - e^{-k_{\text{obs}}t} + C)$, respectively. The slopes of the plots of k_{obs} versus the concentrations of the excess compound yielded the second-order rate constants k_2 ($\text{M}^{-1}\text{ s}^{-1}$).

From the linear plots of the second-order rate constants k_2 against the previously reported electrophilicity parameters E of the benzhydrylium ions **Ea–f** the nucleophile-specific parameters N and s_N for the pyridines **1b,j,q** were determined according to Equation (6.1).

Method of Initial Rate. To evaluate the rate constants for the reaction of benzoic anhydride (**5**) with DMAP (**1a**), the method of initial rate was used. Therefore we set up a general rate law, in which we assume a forward-reaction which is dependent on the concentrations of DMAP (**1a**) and benzoic anhydride (**5**) and a backward-reaction depending exclusively on the concentrations of the *N*-acylpyridinium ion **6aa** and the benzoate ion (Scheme 6.9, Equation (6.9)).



Scheme 6.9. Equilibrium reaction of benzoic anhydride (**5**) with DMAP (**1a**).

$$\frac{d[\mathbf{6aa}]}{dt} = k_+[\mathbf{1a}]^u[\mathbf{5}]^v - k_-[\mathbf{6aa}]^w[\text{BzO}^-]^x \quad (6.9)$$

At $t = 0$, the rate law is simplified to Equation (6.10) as the initial concentrations of **6aa** and BzO^- equal zero.

$$\frac{d[\mathbf{6aa}]}{dt_0} = k_+[\mathbf{1a}]_0^u \cdot [\mathbf{5}]_0^v \quad (6.10)$$

In our experiments, we calculated the concentrations of the *N*-acylpyridinium ion **6aa** from the absorption coefficients of the chloride salt ($\varepsilon = 1.57 \times 10^4 \text{ M}^{-1} \text{ cm}^{-1}$) and plotted them versus the time. In the time range from 5 ms to 20 ms of the reaction, we then determined the first derivative of these curves numerically. An extrapolation of the first derivative to $t = 0$ results in the initial rate ($d[\mathbf{6aa}]/dt_0$) for the reaction.

In order to obtain the coefficients u of the rate law, the sensitivity of the initial rates on the concentrations of DMAP (**1a**) was studied. By taking the logarithm of Equation (6.10), Equation (6.11) is obtained, which can be rewritten as Equation (6.12).

$$\log\left(\frac{d[\mathbf{6aa}]}{dt_0}\right) = \log(k_+) + \log([\mathbf{1a}]_0^u) + \log([\mathbf{5}]_0^v) \quad (6.11)$$

$$\log\left(\frac{d[\mathbf{6aa}]}{dt_0}\right) = \log(k_+) + u \log([\mathbf{1a}]_0) + \log([\mathbf{5}]_0^v) \quad (6.12)$$

According to Equation (6.12), the coefficient u can be obtained as the slope of the linear plot of $\log([\mathbf{1a}]_0)$ versus the logarithm of the initial rate (Figure 6.15a). Analogously, the coefficient v can be determined from plots of $\log([\mathbf{5}]_0)$ versus the logarithm of the initial rate, when the concentration of $[\mathbf{5}]$ is varied (Figure 6.15b).

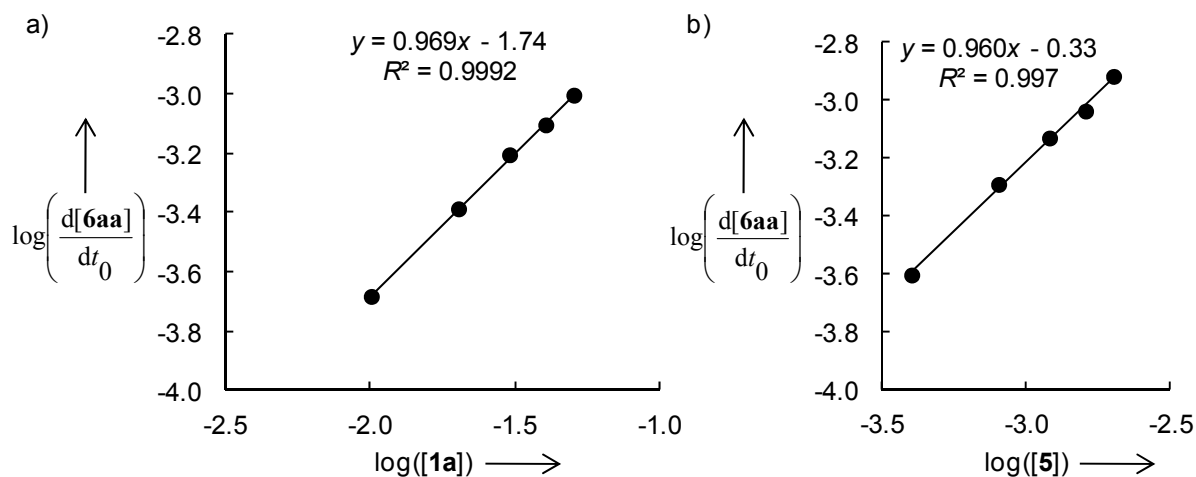


Figure 6.15. a) A plot of the logarithm of the initial rate of the reaction of **1a** with **5** versus $\log([\mathbf{1a}])$ yields the reaction order in DMAP ($u = 1$). b) A plot of the logarithm of the initial rate of the reaction of **1a** with **5** versus $\log([\mathbf{5}])$ yields the reaction order in benzoic anhydride ($v = 1$).

From these plots, it can be concluded that the forward-reaction is first-order in both $[\mathbf{1a}]$ and $[\mathbf{5}]$, and second-order overall [Eq. (6.13)].

$$\frac{d[\mathbf{6aa}]}{dt_0} = k_2[\mathbf{1a}]_0 \cdot [\mathbf{5}]_0 \quad (6.13)$$

The second-order rate constant k_2 were finally determined from the linear plots of $\frac{d[\mathbf{6aa}]}{dt_0} \cdot \frac{1}{[\mathbf{5}]_0}$ versus $[\mathbf{1a}]$ and $\frac{d[\mathbf{6aa}]}{dt_0} \cdot \frac{1}{[\mathbf{1a}]_0}$ versus $[\mathbf{5}]$ respectively (Figure 6.16), which are in good accordance with each other.

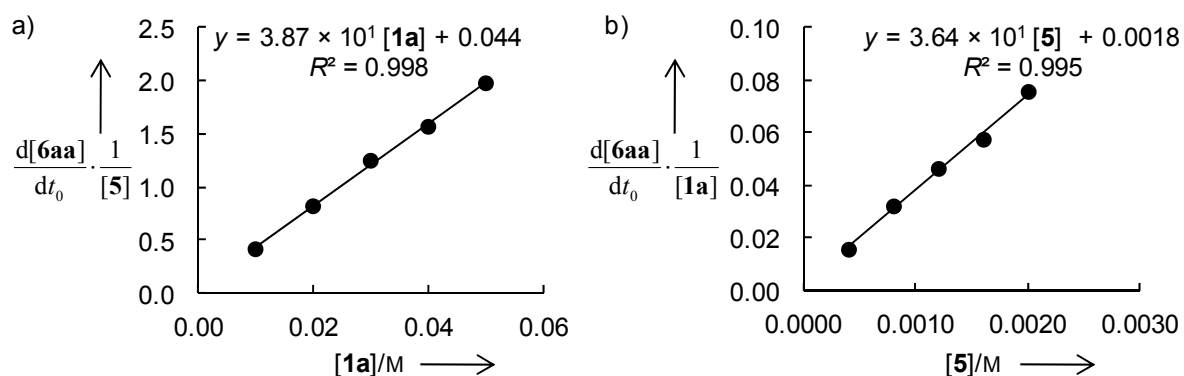


Figure 6.16. a) A plot of the initial rate of the reaction of **1a** with **5** divided by **[5]** versus **[1a]** yields the second-order rate constant $k_2 = 3.87 \times 10^1 \text{ M}^{-1}\text{s}^{-1}$. b) A plot of the initial rate of the reaction of **1a** with **5** divided by **[1a]** versus **[5]** yields the second-order rate constant $k_2 = 3.64 \times 10^1 \text{ M}^{-1}\text{s}^{-1}$.

6.4.2 Kinetic Experiments

Kinetics of the reactions of pyridines (1) with benzoyl chlorides (2)

Table 6.6. Rate constants for the reactions of 4-dimethylaminopyridine (**1a**) with benzoyl chloride (**2a**) in CH_2Cl_2 (stopped-flow technique, 20 °C, $\lambda = 318 \text{ nm}$).

| $[2a]_0/M$ | $[1a]_0/M$ | $[1a]_0/[2a]_0$ | k_{obs}/s^{-1} |
|--|-----------------------|-----------------|-------------------------|
| 7.49×10^{-5} | 1.46×10^{-3} | 19 | 1.41×10^1 |
| 7.49×10^{-5} | 3.01×10^{-3} | 40 | 2.98×10^1 |
| 7.49×10^{-5} | 6.03×10^{-3} | 81 | 5.98×10^1 |
| 7.49×10^{-5} | 7.49×10^{-3} | 100 | 7.18×10^1 |
| $k_2 = 9.64 \times 10^3 \text{ M}^{-1} \text{ s}^{-1}$ | | | |

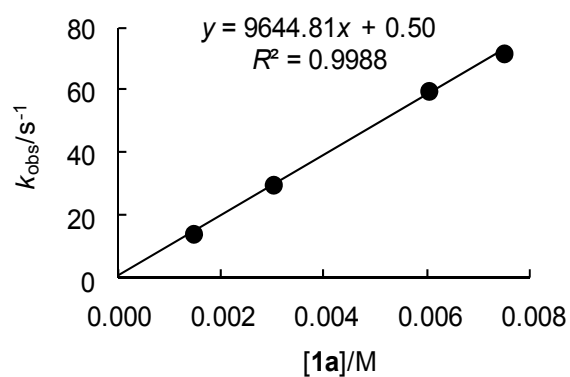


Table 6.7. Rate constants for the reactions of 4-dimethylaminopyridine (**1a**) with benzoyl chloride (**2a**) in CH₂Cl₂ (stopped-flow technique, 20 °C, λ = 318 nm).

| [1a] ₀ /M | [2a] ₀ /M | [2a] ₀ /[1a] ₀ | <i>k</i> _{obs} /s ⁻¹ |
|-------------------------------|-------------------------------|--|--|
| 7.60 × 10 ⁻⁵ | 1.51 × 10 ⁻³ | 20 | 1.41 × 10 ¹ |
| 7.60 × 10 ⁻⁵ | 3.02 × 10 ⁻³ | 40 | 2.88 × 10 ¹ |
| 7.60 × 10 ⁻⁵ | 4.59 × 10 ⁻³ | 60 | 4.46 × 10 ¹ |
| 7.60 × 10 ⁻⁵ | 6.04 × 10 ⁻³ | 79 | 5.74 × 10 ¹ |
| 7.60 × 10 ⁻⁵ | 7.61 × 10 ⁻³ | 100 | 7.19 × 10 ¹ |

$k_2 = 9.48 \times 10^3 \text{ M}^{-1} \text{ s}^{-1}$

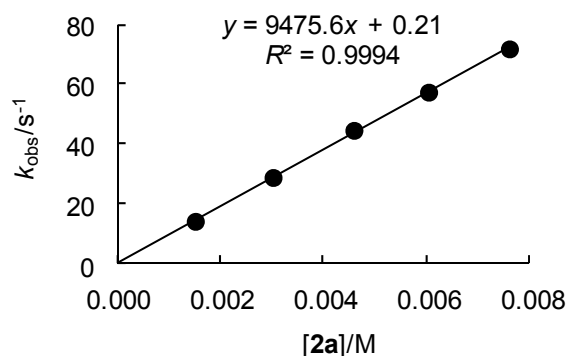


Table 6.8. Rate constants for the reactions of 4-(1-pyrrolidinyl)pyridine (**1b**) with benzoyl chloride (**2a**) in CH₃CN (stopped-flow technique, 20 °C, λ = 321 nm).

| [2a] ₀ /M | [1b] ₀ /M | [1b] ₀ /[2a] ₀ | <i>k</i> _{obs} /s ⁻¹ |
|-------------------------------|-------------------------------|--|--|
| 7.53 × 10 ⁻⁵ | 7.49 × 10 ⁻⁴ | 10 | 3.29 × 10 ¹ |
| 7.53 × 10 ⁻⁵ | 1.50 × 10 ⁻³ | 20 | 6.55 × 10 ¹ |
| 7.53 × 10 ⁻⁵ | 3.04 × 10 ⁻³ | 40 | 1.28 × 10 ² |
| 7.53 × 10 ⁻⁵ | 4.54 × 10 ⁻³ | 60 | 1.96 × 10 ² |

$k_2 = 4.28 \times 10^4 \text{ M}^{-1} \text{ s}^{-1}$

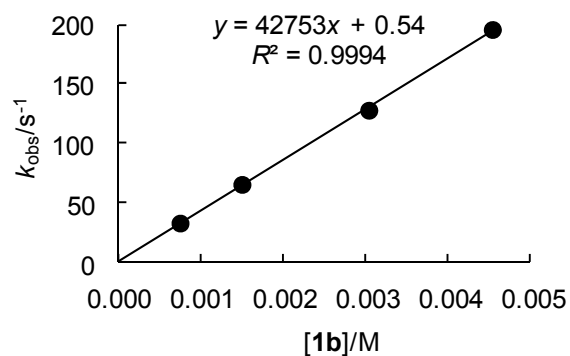


Table 6.9. Rate constants for the reactions of 4-(1-pyrrolidinyl)pyridine (**1b**) with benzoyl chloride (**2a**) in CH₃CN (stopped-flow technique, 20 °C, λ = 321 nm).

| [1b] ₀ /M | [2a] ₀ /M | [2a] ₀ /[1b] ₀ | <i>k</i> _{obs} /s ⁻¹ |
|-------------------------------|-------------------------------|--|--|
| 5.05 × 10 ⁻⁵ | 4.91 × 10 ⁻⁴ | 10 | 2.14 × 10 ¹ |
| 5.05 × 10 ⁻⁵ | 7.36 × 10 ⁻⁴ | 15 | 3.32 × 10 ¹ |
| 5.05 × 10 ⁻⁵ | 1.31 × 10 ⁻³ | 26 | 5.65 × 10 ¹ |
| 5.05 × 10 ⁻⁵ | 2.05 × 10 ⁻³ | 41 | 8.75 × 10 ¹ |
| 5.05 × 10 ⁻⁵ | 3.11 × 10 ⁻³ | 62 | 1.29 × 10 ² |

$k_2 = 4.09 \times 10^4 \text{ M}^{-1} \text{ s}^{-1}$

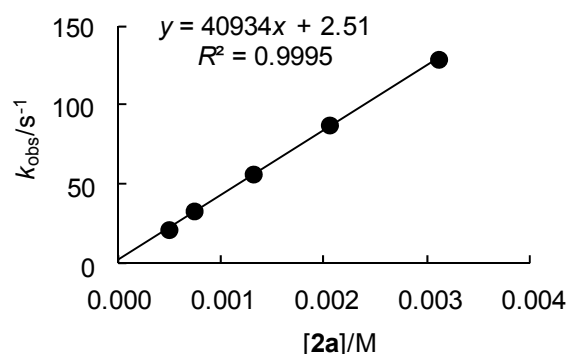


Table 6.10. Rate constants for the reactions of 4-(1-pyrrolidiny)pyridine (**1b**) with benzoyl chloride (**2a**) in CH₂Cl₂ (stopped-flow technique, 20 °C, λ = 321 nm).

| [2a] ₀ /M | [1b] ₀ /M | [1b] ₀ /[2a] ₀ | <i>k</i> _{obs} /s ⁻¹ |
|-------------------------------|-------------------------------|--|--|
| 5.31 × 10 ⁻⁵ | 1.07 × 10 ⁻³ | 20 | 1.44 × 10 ¹ |
| 5.31 × 10 ⁻⁵ | 2.14 × 10 ⁻³ | 40 | 3.16 × 10 ¹ |
| 5.31 × 10 ⁻⁵ | 3.21 × 10 ⁻³ | 60 | 4.95 × 10 ¹ |
| 5.31 × 10 ⁻⁵ | 4.25 × 10 ⁻³ | 80 | 6.36 × 10 ¹ |
| 5.31 × 10 ⁻⁵ | 5.32 × 10 ⁻³ | 100 | 7.67 × 10 ¹ |

$k_2 = 1.48 \times 10^4 \text{ M}^{-1} \text{ s}^{-1}$

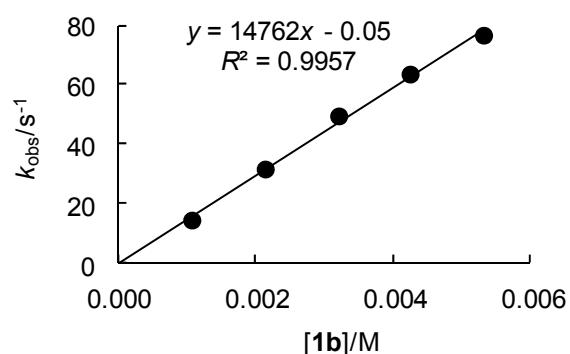


Table 6.11. Rate constants for the reactions of 4-(1-pyrrolidiny)pyridine (**1b**) with benzoyl chloride (**2a**) in CH₂Cl₃ (stopped-flow technique, 20 °C, λ = 321 nm).

| [1b] ₀ /M | [2a] ₀ /M | [2a] ₀ /[1b] ₀ | <i>k</i> _{obs} /s ⁻¹ |
|-------------------------------|-------------------------------|--|--|
| 7.50 × 10 ⁻⁵ | 1.54 × 10 ⁻³ | 21 | 6.92 |
| 7.50 × 10 ⁻⁵ | 2.99 × 10 ⁻³ | 40 | 1.36 × 10 ¹ |
| 7.50 × 10 ⁻⁵ | 4.52 × 10 ⁻³ | 60 | 2.17 × 10 ¹ |
| 7.50 × 10 ⁻⁵ | 5.97 × 10 ⁻³ | 80 | 2.88 × 10 ¹ |
| 7.50 × 10 ⁻⁵ | 7.51 × 10 ⁻³ | 100 | 3.72 × 10 ¹ |

$k_2 = 5.08 \times 10^3 \text{ M}^{-1} \text{ s}^{-1}$

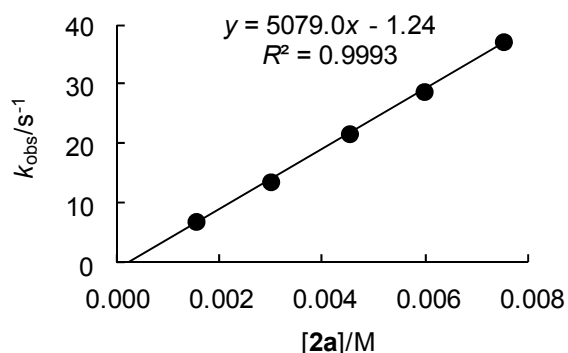


Table 6.12. Rate constants for the reactions of 4-(1-morpholinyl)pyridine (**1c**) with benzoyl chloride (**2a**) in CH₃CN (stopped-flow technique, 20 °C, λ = 319 nm).

| [2a] ₀ /M | [1c] ₀ /M | [1c] ₀ /[2a] ₀ | <i>k</i> _{obs} /s ⁻¹ |
|-------------------------------|-------------------------------|--|--|
| 5.25 × 10 ⁻⁵ | 5.11 × 10 ⁻⁴ | 10 | 5.20 |
| 5.25 × 10 ⁻⁵ | 7.66 × 10 ⁻⁴ | 15 | 7.96 |
| 5.25 × 10 ⁻⁵ | 1.30 × 10 ⁻³ | 25 | 1.38 × 10 ¹ |
| 5.25 × 10 ⁻⁵ | 2.04 × 10 ⁻³ | 39 | 2.22 × 10 ¹ |
| 5.25 × 10 ⁻⁵ | 3.06 × 10 ⁻³ | 58 | 3.37 × 10 ² |

$k_2 = 1.12 \times 10^4 \text{ M}^{-1} \text{ s}^{-1}$

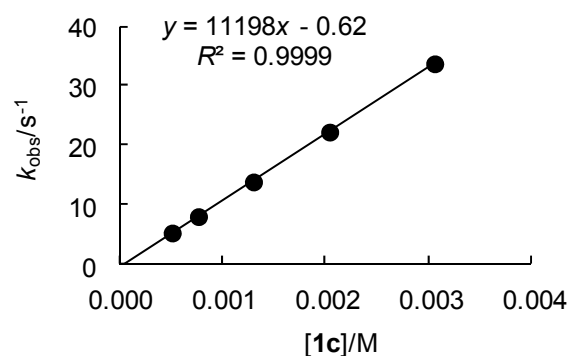


Table 6.13. Rate constants for the reactions of 4-(1-morpholinyl)pyridine (**1c**) with benzoyl chloride (**2a**) in CH₃CN (stopped-flow technique, 20 °C, λ = 319 nm).

| [1c] ₀ /M | [2a] ₀ /M | [2a] ₀ /[1c] ₀ | <i>k</i> _{obs} /s ⁻¹ |
|--|-------------------------------|--|--|
| 4.42 × 10 ⁻⁵ | 8.49 × 10 ⁻⁴ | 19 | 8.09 |
| 4.42 × 10 ⁻⁵ | 1.77 × 10 ⁻³ | 40 | 1.88 × 10 ¹ |
| 4.42 × 10 ⁻⁵ | 2.62 × 10 ⁻³ | 59 | 2.77 × 10 ¹ |
| 4.42 × 10 ⁻⁵ | 3.54 × 10 ⁻³ | 80 | 3.82 × 10 ¹ |
| 4.42 × 10 ⁻⁵ | 4.38 × 10 ⁻³ | 99 | 4.67 × 10 ² |
| <i>k</i> ₂ = 1.09 × 10 ⁴ M ⁻¹ s ⁻¹ | | | |

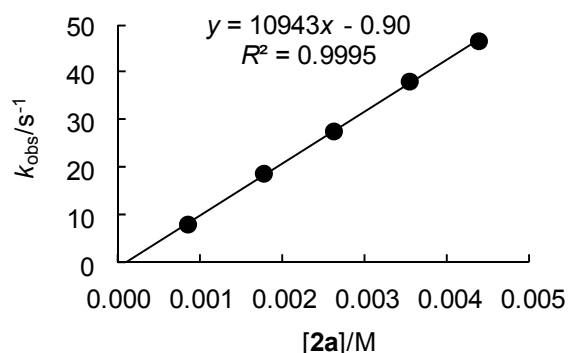


Table 6.14. Rate constants for the reactions of 3-bromo-4-dimethylaminopyridine (**1d**) with benzoyl chloride (**2a**) in CH₃CN (stopped-flow technique, 20 °C, λ = 334 nm).

| [2a] ₀ /M | [1d] ₀ /M | [1d] ₀ /[2a] ₀ | <i>k</i> _{obs} /s ⁻¹ |
|--|-------------------------------|--|--|
| 9.64 × 10 ⁻⁵ | 2.05 × 10 ⁻³ | 21 | 6.92 × 10 ⁻¹ |
| 9.64 × 10 ⁻⁵ | 3.84 × 10 ⁻³ | 40 | 1.26 |
| 9.64 × 10 ⁻⁵ | 5.62 × 10 ⁻³ | 58 | 1.86 |
| 9.64 × 10 ⁻⁵ | 7.67 × 10 ⁻³ | 80 | 2.53 |
| 9.64 × 10 ⁻⁵ | 9.72 × 10 ⁻³ | 101 | 3.20 |
| <i>k</i> ₂ = 3.28 × 10 ² M ⁻¹ s ⁻¹ | | | |

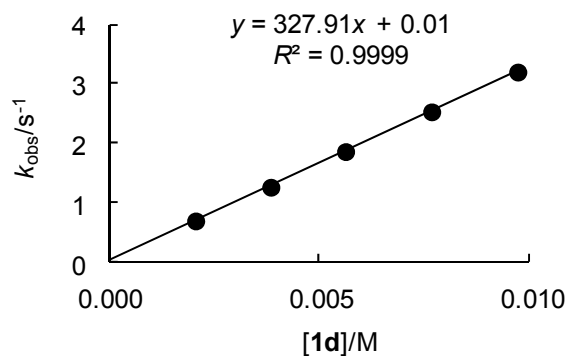


Table 6.15. Rate constants for the reactions of 4-amino-3,5-dibromopyridine (**1e**) with benzoyl chloride (**2a**) and *n*-Bu₄N⁺Cl⁻ (3.97 × 10⁻⁴ M) in CH₃CN (stopped-flow technique, 20 °C, λ = 310 nm).

| [2a] ₀ /M | [1e] ₀ /M | [1e] ₀ /[2a] ₀ | <i>k</i> _{obs} /s ⁻¹ |
|--|-------------------------------|--|--|
| 1.98 × 10 ⁻⁴ | 8.11 × 10 ⁻³ | 41 | 5.40 |
| 1.98 × 10 ⁻⁴ | 1.20 × 10 ⁻² | 60 | 5.63 |
| 1.98 × 10 ⁻⁴ | 1.58 × 10 ⁻² | 80 | 5.80 |
| 1.98 × 10 ⁻⁴ | 2.01 × 10 ⁻² | 101 | 6.13 |
| 1.98 × 10 ⁻⁴ | 2.82 × 10 ⁻² | 142 | 6.48 |
| <i>k</i> ₂ = 5.46 × 10 ² M ⁻¹ s ⁻¹ | | | |

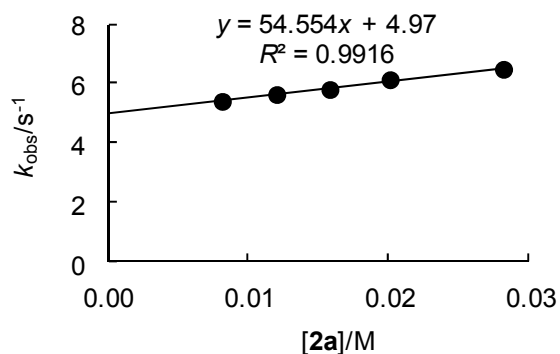


Table 6.16. Rate constants for the reactions of *N*-acetyl-4-aminopyridine (**1f**) with benzoyl chloride (**2a**) in CH₃CN (stopped-flow technique, 20 °C, λ = 296 nm).

| [2a] ₀ /M | [1f] ₀ /M | [1f] ₀ /[2a] ₀ | <i>k</i> _{obs} /s ⁻¹ |
|--|-------------------------------|--|--|
| 1.01 × 10 ⁻⁴ | 9.93 × 10 ⁻⁴ | 10 | 1.21 |
| 1.01 × 10 ⁻⁴ | 2.07 × 10 ⁻³ | 21 | 2.26 |
| 1.01 × 10 ⁻⁴ | 4.14 × 10 ⁻³ | 41 | 4.29 |
| 1.01 × 10 ⁻⁴ | 6.13 × 10 ⁻³ | 61 | 6.18 |
| <i>k</i> ₂ = 9.69 × 10 ² M ⁻¹ s ⁻¹ | | | |

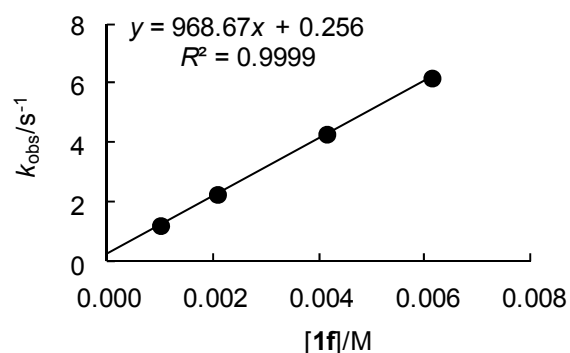


Table 6.17. Rate constants for the reactions of (S)-(-)-4-dimethylaminopyrindinyl-(pentaphenylcyclopentadienyl)iron (**1g**) with benzoyl chloride (**2a**) in CH₃CN (stopped-flow technique, 20 °C, λ = 325 nm).

| [1g] ₀ /M | [2a] ₀ /M | [2a] ₀ /[1g] ₀ | <i>k</i> _{obs} /s ⁻¹ |
|--|-------------------------------|--|--|
| 1.49 × 10 ⁻⁴ | 2.23 × 10 ⁻³ | 15 | 4.35 × 10 ¹ |
| 1.49 × 10 ⁻⁴ | 2.98 × 10 ⁻³ | 20 | 5.73 × 10 ¹ |
| 1.49 × 10 ⁻⁴ | 3.72 × 10 ⁻³ | 25 | 6.95 × 10 ¹ |
| 1.49 × 10 ⁻⁴ | 4.47 × 10 ⁻³ | 30 | 8.29 × 10 ¹ |
| 1.49 × 10 ⁻⁴ | 5.21 × 10 ⁻³ | 35 | 9.51 × 10 ¹ |
| <i>k</i> ₂ = 1.73 × 10 ⁴ M ⁻¹ s ⁻¹ | | | |

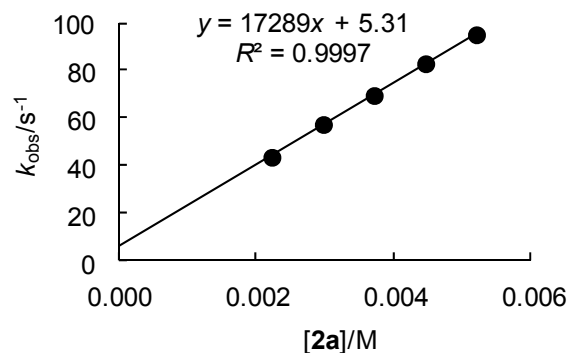


Table 6.18. Rate constants for the reactions of 1,4-dimethyl-1,2,3,4-tetrahydropyrido[3,4-*b*]pyrazine (**1h**) with benzoyl chloride (**2a**) in CH₃CN (stopped-flow technique, 20 °C, λ = 380 nm).

| [1h] ₀ /M | [2a] ₀ /M | [2a] ₀ /[1h] ₀ | <i>k</i> _{obs} /s ⁻¹ |
|--|-------------------------------|--|--|
| 1.00 × 10 ⁻⁴ | 9.16 × 10 ⁻⁴ | 9 | 7.72 × 10 ¹ |
| 1.00 × 10 ⁻⁴ | 1.20 × 10 ⁻³ | 12 | 9.97 × 10 ¹ |
| 1.00 × 10 ⁻⁴ | 1.48 × 10 ⁻³ | 15 | 1.22 × 10 ² |
| 1.00 × 10 ⁻⁴ | 1.69 × 10 ⁻³ | 17 | 1.37 × 10 ² |
| 1.00 × 10 ⁻⁴ | 2.04 × 10 ⁻³ | 20 | 1.70 × 10 ² |
| <i>k</i> ₂ = 8.27 × 10 ⁴ M ⁻¹ s ⁻¹ | | | |

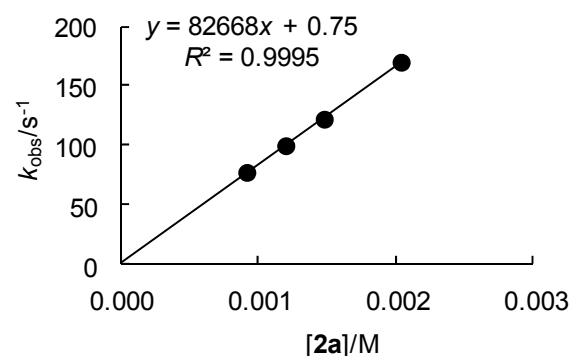


Table 6.19. Rate constants for the reactions of 1,4-diethyl-1,2,3,4-tetrahydropyrido[3,4-*b*]pyrazine (**1i**) with benzoyl chloride (**2a**) in CH₃CN (stopped-flow technique, 20 °C, λ = 390 nm).^[a]

| [1i] ₀ /M | [2a] ₀ /M | [2a] ₀ /[1i] ₀ | <i>k</i> _{obs} /s ⁻¹ |
|--|-------------------------------|--|--|
| 1.97 × 10 ⁻⁴ | 1.99 × 10 ⁻⁴ | 1.0 | 24.4 |
| <i>k</i> ₂ = 1.23 × 10 ⁵ M ⁻¹ s ⁻¹ | | | |

[a] The first-order rate constants *k*_{obs} was obtained by least-squares fitting of the function $A = -A_0/(1 - k_{\text{obs}}A_0t) + C$ to the absorbance increase.

Table 6.20. Rate constants for the reactions of 5,10-diethyl-5,5a,6,7,8,9,9a,10-octahydropyrido[3,4-*b*]quinoxaline (**1j**) with benzoyl chloride (**2a**) in CH₃CN (stopped-flow technique, 20 °C, λ = 390 nm).

| [1j] ₀ /M | [2a] ₀ /M | [2a] ₀ /[1j] ₀ | <i>k</i> _{obs} /s ⁻¹ |
|--|-------------------------------|--|--|
| 7.50 × 10 ⁻⁵ | 7.39 × 10 ⁻⁴ | 10 | 1.13 × 10 ² |
| 7.50 × 10 ⁻⁵ | 1.13 × 10 ⁻³ | 15 | 1.68 × 10 ² |
| 7.50 × 10 ⁻⁵ | 1.48 × 10 ⁻³ | 20 | 2.16 × 10 ² |
| 7.50 × 10 ⁻⁵ | 1.87 × 10 ⁻³ | 25 | 2.72 × 10 ² |
| <i>k</i> ₂ = 1.40 × 10 ⁵ M ⁻¹ s ⁻¹ | | | |

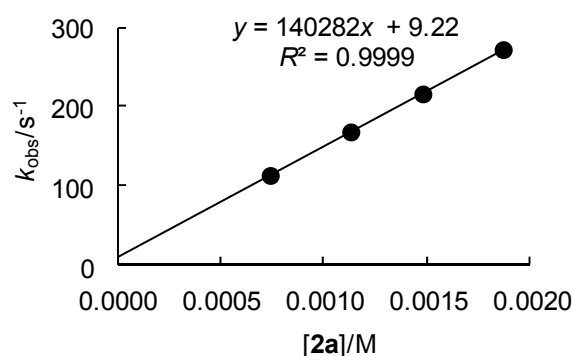
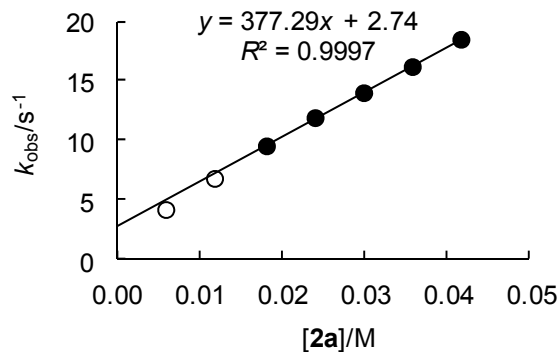


Table 6.21. Rate constants for the reactions of 1,1'-(2,3-dihydropyrido[3,4-*b*]pyrazine-1,4-diyl)diethanone (**1k**) with benzoyl chloride (**2a**) in CH₃CN (stopped-flow technique, 20 °C, $\lambda = 345$ nm).^[a]

| [1k] ₀ /M | [2a] ₀ /M | [2a] ₀ /[1k] ₀ | $k_{\text{obs}}/\text{s}^{-1}$ |
|--|-------------------------------|--|--------------------------------|
| 2.98×10^{-4} | 5.88×10^{-3} | 20 | 4.16 |
| 2.98×10^{-4} | 1.18×10^{-2} | 39 | 6.78 |
| 2.98×10^{-4} | 1.81×10^{-2} | 61 | 9.52 |
| 2.98×10^{-4} | 2.40×10^{-2} | 81 | 1.19×10^1 |
| 2.98×10^{-4} | 2.99×10^{-2} | 100 | 1.40×10^1 |
| 2.98×10^{-4} | 3.58×10^{-2} | 120 | 1.62×10^1 |
| 2.98×10^{-4} | 4.17×10^{-2} | 140 | 1.85×10^1 |
| $k_2 = 3.77 \times 10^2 \text{ M}^{-1} \text{ s}^{-1}$ | | | |



[a] Open data points were not used for the determination of the regression line.

Table 6.22. Rate constants for the reactions of 1-(4-acetyl-3,4-dihydro-2*H*-pyrido[3,4-*b*]pyrazin-1-yl)ethanone (**1k**) with benzoyl chloride (**2a**) and *n*-Bu₄N⁺Cl⁻ (1.22×10^{-4} M) in CH₃CN (stopped-flow technique, 20 °C, $\lambda = 345$ nm).

| [1k] ₀ /M | [2a] ₀ /M | [2a] ₀ /[1k] ₀ | $k_{\text{obs}}/\text{s}^{-1}$ |
|--|-------------------------------|--|--------------------------------|
| 6.05×10^{-5} | 2.38×10^{-2} | 39 | 3.66×10^1 |
| 6.05×10^{-5} | 3.61×10^{-2} | 60 | 4.14×10^1 |
| 6.05×10^{-5} | 4.85×10^{-2} | 80 | 4.62×10^1 |
| 6.05×10^{-5} | 6.52×10^{-2} | 108 | 5.22×10^1 |
| 6.05×10^{-5} | 7.23×10^{-2} | 119 | 5.47×10^1 |
| $k_2 = 3.73 \times 10^2 \text{ M}^{-1} \text{ s}^{-1}$ | | | |

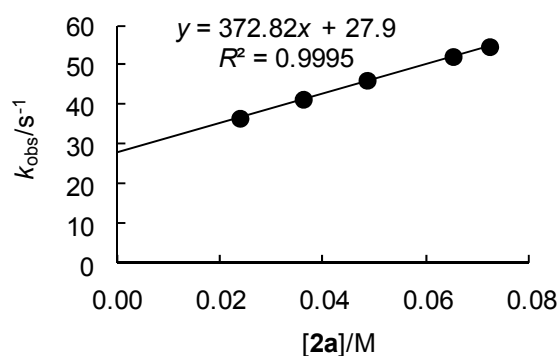


Table 6.23. Rate constants for the reactions of 1,6-dimethyl-2,3,5,6-tetrahydro-1*H*,4*H*-1,3a,6,8-tetraaza-phenalene (**1l**) with benzoyl chloride (**2a**) in CH₃CN (stopped-flow technique, 20 °C, λ = 417 nm).

| [1l] ₀ /M | [2a] ₀ /M | [2a] ₀ /[1l] ₀ | <i>k</i> _{obs} /s ⁻¹ |
|--|-------------------------------|--|--|
| 3.70 × 10 ⁻⁵ | 5.63 × 10 ⁻⁴ | 15 | 8.37 × 10 ¹ |
| 3.70 × 10 ⁻⁵ | 7.39 × 10 ⁻⁴ | 20 | 1.10 × 10 ² |
| 3.70 × 10 ⁻⁵ | 9.51 × 10 ⁻⁴ | 26 | 1.39 × 10 ² |
| 3.70 × 10 ⁻⁵ | 1.13 × 10 ⁻³ | 30 | 1.62 × 10 ² |
| 3.70 × 10 ⁻⁵ | 1.30 × 10 ⁻³ | 35 | 1.85 × 10 ² |
| <i>k</i> ₂ = 1.37 × 10 ⁵ M ⁻¹ s ⁻¹ | | | |

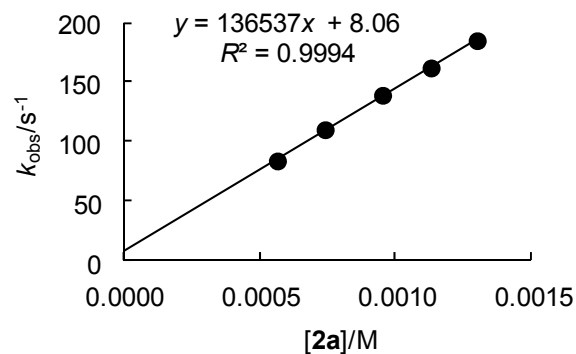


Table 6.24. Rate constants for the reactions of 1,6-diethyl-2,3,5,6-tetrahydro-1*H*,4*H*-1,3a,6,8-tetraaza-phenalene (**1m**) with benzoyl chloride (**2a**) in CH₃CN (stopped-flow technique, 20 °C, λ = 427 nm).

| [1m] ₀ /M | [2a] ₀ /M | [2a] ₀ /[1m] ₀ | <i>k</i> _{obs} /s ⁻¹ |
|--|-------------------------------|--|--|
| 3.83 × 10 ⁻⁵ | 7.70 × 10 ⁻⁴ | 20 | 1.23 × 10 ² |
| 3.83 × 10 ⁻⁵ | 9.76 × 10 ⁻⁴ | 25 | 1.57 × 10 ² |
| 3.83 × 10 ⁻⁵ | 1.13 × 10 ⁻³ | 30 | 1.80 × 10 ² |
| 3.83 × 10 ⁻⁵ | 1.49 × 10 ⁻³ | 39 | 2.40 × 10 ² |
| <i>k</i> ₂ = 1.62 × 10 ⁵ M ⁻¹ s ⁻¹ | | | |

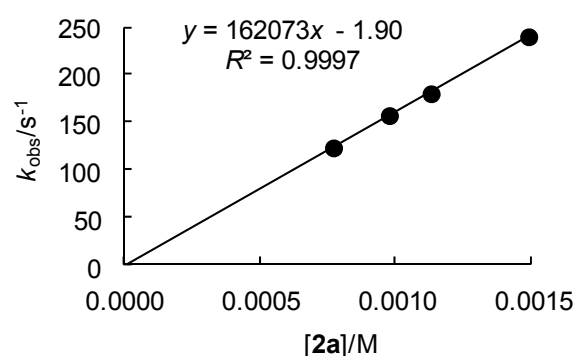


Table 6.25. Rate constants for the reactions of 1,6-dibenzyl-2,3,5,6-tetrahydro-1*H*,4*H*-1,3a,6,8-tetraaza-phenalene (**1n**) with benzoyl chloride (**2a**) in CH₃CN (stopped-flow technique, 20 °C, λ = 424 nm).

| [1n] ₀ /M | [2a] ₀ /M | [2a] ₀ /[1n] ₀ | <i>k</i> _{obs} /s ⁻¹ |
|--|-------------------------------|--|--|
| 3.80 × 10 ⁻⁵ | 7.70 × 10 ⁻⁴ | 20 | 1.57 × 10 ² |
| 3.80 × 10 ⁻⁵ | 9.76 × 10 ⁻⁴ | 26 | 1.99 × 10 ² |
| 3.80 × 10 ⁻⁵ | 1.13 × 10 ⁻³ | 30 | 2.31 × 10 ² |
| 3.80 × 10 ⁻⁵ | 1.49 × 10 ⁻³ | 39 | 2.99 × 10 ² |
| <i>k</i> ₂ = 1.97 × 10 ⁵ M ⁻¹ s ⁻¹ | | | |

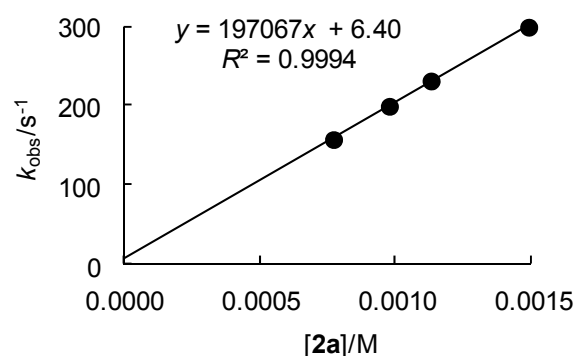


Table 6.26. Rate constants for the reactions of 1-ethyl-2,3,5,6-tetrahydro-1*H*,4*H*-1,3*a*,8-tetraaza-phenalene (**1o**) with benzoyl chloride (**2a**) in CH₃CN (stopped-flow technique, 20 °C, λ = 390 nm).

| [1o] ₀ /M | [2a] ₀ /M | [2a] ₀ /[1o] ₀ | <i>k</i> _{obs} /s ⁻¹ |
|--|-------------------------------|--|--|
| 3.73 × 10 ⁻⁵ | 5.63 × 10 ⁻⁴ | 15 | 1.02 × 10 ² |
| 3.73 × 10 ⁻⁵ | 7.39 × 10 ⁻⁴ | 20 | 1.32 × 10 ² |
| 3.73 × 10 ⁻⁵ | 9.51 × 10 ⁻⁴ | 25 | 1.69 × 10 ² |
| 3.73 × 10 ⁻⁵ | 1.13 × 10 ⁻³ | 30 | 1.97 × 10 ² |
| <i>k</i> ₂ = 1.68 × 10 ⁵ M ⁻¹ s ⁻¹ | | | |

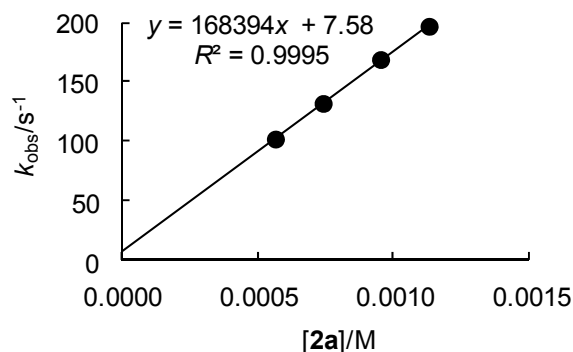


Table 6.27. Rate constants for the reactions of 1-benzyl-2,3,5,6-tetrahydro-1*H*,4*H*-1,3*a*,8-tetraaza-phenalene (**1p**) with benzoyl chloride (**2a**) in CH₃CN (stopped-flow technique, 20 °C, λ = 386 nm).

| [1p] ₀ /M | [2a] ₀ /M | [2a] ₀ /[1p] ₀ | <i>k</i> _{obs} /s ⁻¹ |
|--|-------------------------------|--|--|
| 3.20 × 10 ⁻⁵ | 6.56 × 10 ⁻⁴ | 21 | 1.30 × 10 ² |
| 3.20 × 10 ⁻⁵ | 9.85 × 10 ⁻⁴ | 31 | 1.90 × 10 ² |
| 3.20 × 10 ⁻⁵ | 1.26 × 10 ⁻³ | 39 | 2.41 × 10 ² |
| 3.20 × 10 ⁻⁵ | 1.59 × 10 ⁻³ | 50 | 3.10 × 10 ² |
| <i>k</i> ₂ = 1.92 × 10 ⁵ M ⁻¹ s ⁻¹ | | | |

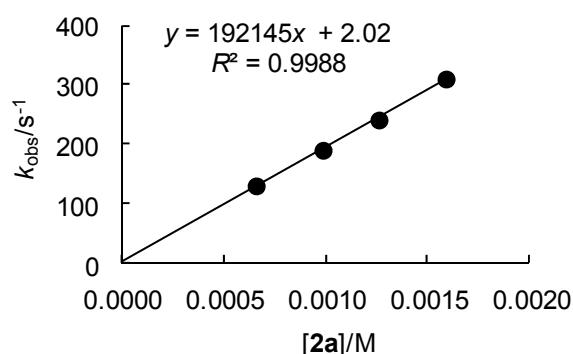


Table 6.28. Rate constants for the reactions of 9-azajulolidine (**1q**) with benzoyl chloride (**2a**) in CH₃CN (stopped-flow technique, 20 °C, λ = 335 nm).

| [1q] ₀ /M | [2a] ₀ /M | [2a] ₀ /[1q] ₀ | <i>k</i> _{obs} /s ⁻¹ |
|--|-------------------------------|--|--|
| 4.00 × 10 ⁻⁵ | 5.99 × 10 ⁻⁴ | 15 | 8.24 × 10 ¹ |
| 4.00 × 10 ⁻⁵ | 8.10 × 10 ⁻⁴ | 20 | 1.10 × 10 ² |
| 4.00 × 10 ⁻⁵ | 9.86 × 10 ⁻⁴ | 25 | 1.32 × 10 ² |
| 4.00 × 10 ⁻⁵ | 1.20 × 10 ⁻³ | 30 | 1.59 × 10 ² |
| 4.00 × 10 ⁻⁵ | 1.37 × 10 ⁻³ | 34 | 1.81 × 10 ² |
| <i>k</i> ₂ = 1.27 × 10 ⁵ M ⁻¹ s ⁻¹ | | | |

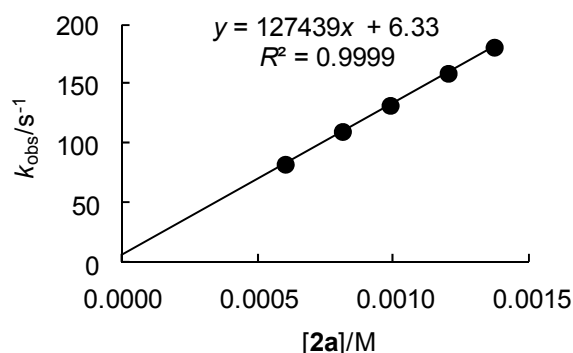


Table 6.29. Rate constants for the reactions of 4-dimethylaminopyridine (**1a**) with 4-dimethylaminobenzoyl chloride (**2b**) in CH₃CN (stopped-flow technique, 20 °C, λ = 370 nm).

| [2b] ₀ /M | [1a] ₀ /M | [1a] ₀ /[2b] ₀ | <i>k</i> _{obs} /s ⁻¹ |
|--|-------------------------------|--|--|
| 9.02 × 10 ⁻⁵ | 8.98 × 10 ⁻⁴ | 10 | 1.62 × 10 ⁻¹ |
| 9.02 × 10 ⁻⁵ | 1.35 × 10 ⁻³ | 15 | 2.47 × 10 ⁻¹ |
| 9.02 × 10 ⁻⁵ | 1.73 × 10 ⁻³ | 19 | 3.20 × 10 ⁻¹ |
| 9.02 × 10 ⁻⁵ | 2.25 × 10 ⁻³ | 25 | 4.19 × 10 ⁻¹ |
| 9.02 × 10 ⁻⁵ | 2.69 × 10 ⁻³ | 30 | 5.05 × 10 ⁻¹ |
| <i>k</i> ₂ = 1.91 × 10 ² M ⁻¹ s ⁻¹ | | | |

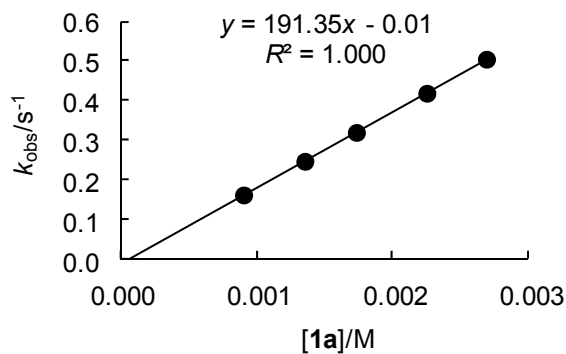


Table 6.30. Rate constants for the reactions of 4-dimethylaminopyridine (**1a**) with 4-methoxybenzoyl chloride (**2c**) in CH₃CN (stopped-flow technique, 20 °C, λ = 320 nm).

| [2c] ₀ /M | [1a] ₀ /M | [1a] ₀ /[2c] ₀ | <i>k</i> _{obs} /s ⁻¹ |
|--|-------------------------------|--|--|
| 3.52 × 10 ⁻⁵ | 3.52 × 10 ⁻⁴ | 10 | 1.55 |
| 3.52 × 10 ⁻⁵ | 7.04 × 10 ⁻⁴ | 20 | 3.00 |
| 3.52 × 10 ⁻⁵ | 1.06 × 10 ⁻³ | 30 | 4.50 |
| 3.52 × 10 ⁻⁵ | 1.41 × 10 ⁻³ | 40 | 6.10 |
| 3.52 × 10 ⁻⁵ | 1.76 × 10 ⁻³ | 50 | 7.62 |
| <i>k</i> ₂ = 4.33 × 10 ³ M ⁻¹ s ⁻¹ | | | |

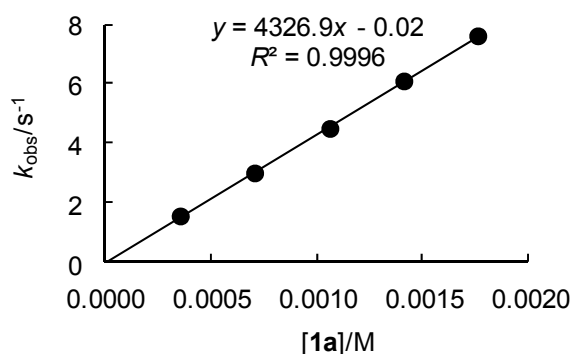


Table 6.31. Rate constants for the reactions of 4-dimethylaminopyridine (**1a**) with 4-methylbenzoyl chloride (**2d**) in CH₃CN (stopped-flow technique, 20 °C, λ = 319 nm).

| [2d] ₀ /M | [1a] ₀ /M | [1a] ₀ /[2d] ₀ | <i>k</i> _{obs} /s ⁻¹ |
|--|-------------------------------|--|--|
| 1.90 × 10 ⁻⁵ | 1.94 × 10 ⁻⁴ | 10 | 2.43 |
| 1.90 × 10 ⁻⁵ | 2.82 × 10 ⁻⁴ | 15 | 3.57 |
| 1.90 × 10 ⁻⁵ | 3.78 × 10 ⁻³ | 20 | 4.84 |
| 1.90 × 10 ⁻⁵ | 4.75 × 10 ⁻³ | 25 | 6.14 |
| <i>k</i> ₂ = 1.32 × 10 ⁴ M ⁻¹ s ⁻¹ | | | |

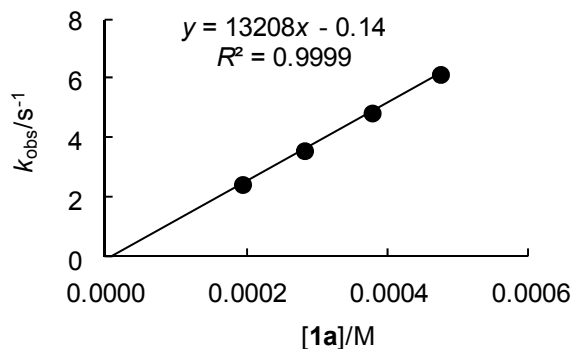


Table 6.32. Rate constants for the reactions of 4-dimethylaminopyridine (**1a**) with 3,4,5-trimethoxybenzoyl chloride (**2e**) in CH₃CN (stopped-flow technique, 20 °C, λ = 320 nm).

| [2e] ₀ /M | [1a] ₀ /M | [1a] ₀ /[2e] ₀ | <i>k</i> _{obs} /s ⁻¹ |
|--|-------------------------------|--|--|
| 3.10 × 10 ⁻⁵ | 3.02 × 10 ⁻⁴ | 10 | 5.81 |
| 3.10 × 10 ⁻⁵ | 6.28 × 10 ⁻⁴ | 20 | 1.22 × 10 ¹ |
| 3.10 × 10 ⁻⁵ | 9.30 × 10 ⁻⁴ | 30 | 1.84 × 10 ¹ |
| 3.10 × 10 ⁻⁵ | 1.23 × 10 ⁻³ | 40 | 2.41 × 10 ¹ |
| 3.10 × 10 ⁻⁵ | 1.56 × 10 ⁻³ | 50 | 3.03 × 10 ¹ |
| <i>k</i> ₂ = 1.95 × 10 ⁴ M ⁻¹ s ⁻¹ | | | |

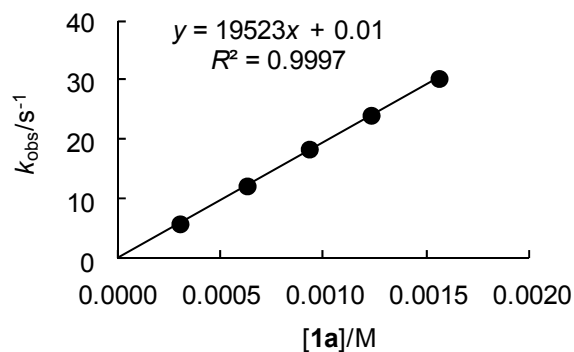


Table 6.33. Rate constants for the reactions of 4-dimethylaminopyridine (**1a**) with 4-fluorobenzoyl chloride (**2f**) in CH₃CN (stopped-flow technique, 20 °C, λ = 317 nm).

| [2f] ₀ /M | [1a] ₀ /M | [1a] ₀ /[2f] ₀ | <i>k</i> _{obs} /s ⁻¹ |
|--|-------------------------------|--|--|
| 3.34 × 10 ⁻⁵ | 3.26 × 10 ⁻⁴ | 10 | 1.13 × 10 ¹ |
| 3.34 × 10 ⁻⁵ | 6.71 × 10 ⁻⁴ | 20 | 2.39 × 10 ¹ |
| 3.34 × 10 ⁻⁵ | 9.97 × 10 ⁻⁴ | 30 | 3.53 × 10 ¹ |
| 3.34 × 10 ⁻⁵ | 1.34 × 10 ⁻³ | 40 | 4.72 × 10 ¹ |
| 3.34 × 10 ⁻⁵ | 1.67 × 10 ⁻³ | 50 | 5.79 × 10 ¹ |
| <i>k</i> ₂ = 3.47 × 10 ⁴ M ⁻¹ s ⁻¹ | | | |

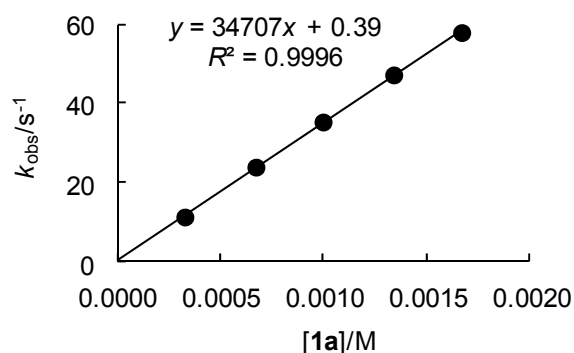


Table 6.34. Rate constants for the reactions of 4-dimethylaminopyridine (**1a**) with 4-chlorobenzoyl chloride (**2g**) in CH₃CN (stopped-flow technique, 20 °C, λ = 320 nm).

| [2g] ₀ /M | [1a] ₀ /M | [1a] ₀ /[2g] ₀ | <i>k</i> _{obs} /s ⁻¹ |
|--|-------------------------------|--|--|
| 3.74 × 10 ⁻⁵ | 7.58 × 10 ⁻⁴ | 20 | 5.37 × 10 ¹ |
| 3.74 × 10 ⁻⁵ | 1.48 × 10 ⁻³ | 40 | 1.05 × 10 ² |
| 3.74 × 10 ⁻⁵ | 2.24 × 10 ⁻³ | 60 | 1.59 × 10 ² |
| 3.74 × 10 ⁻⁵ | 2.97 × 10 ⁻³ | 79 | 2.08 × 10 ² |
| 3.74 × 10 ⁻⁵ | 3.69 × 10 ⁻³ | 99 | 2.53 × 10 ² |
| <i>k</i> ₂ = 6.82 × 10 ⁴ M ⁻¹ s ⁻¹ | | | |

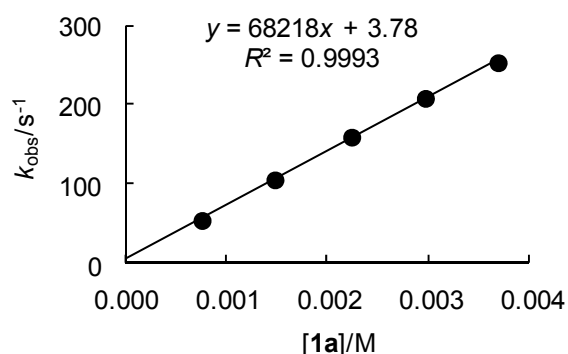


Table 6.35. Rate constants for the reactions of 4-dimethylaminopyridine (**1a**) with 4-bromobenzoyl chloride (**2h**) in CH₃CN (stopped-flow technique, 20 °C, λ = 319 nm).

| [2h] ₀ /M | [1a] ₀ /M | [1a] ₀ /[2h] ₀ | <i>k</i> _{obs} /s ⁻¹ |
|--|-------------------------------|--|--|
| 2.90 × 10 ⁻⁵ | 2.90 × 10 ⁻⁴ | 10 | 2.35 × 10 ¹ |
| 2.90 × 10 ⁻⁵ | 5.80 × 10 ⁻⁴ | 20 | 4.67 × 10 ¹ |
| 2.90 × 10 ⁻⁵ | 8.70 × 10 ⁻⁴ | 30 | 6.95 × 10 ¹ |
| 2.90 × 10 ⁻⁵ | 1.16 × 10 ⁻³ | 40 | 9.12 × 10 ¹ |
| 2.90 × 10 ⁻⁵ | 1.45 × 10 ⁻³ | 50 | 1.12 × 10 ² |
| <i>k</i> ₂ = 7.64 × 10 ⁴ M ⁻¹ s ⁻¹ | | | |

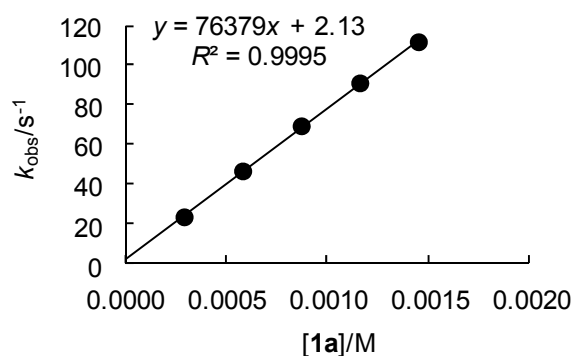


Table 6.36. Rate constants for the reactions of 4-dimethylaminopyridine (**1a**) with 2-chlorobenzoyl chloride (**2i**) in CH₃CN (stopped-flow technique, 20 °C, λ = 330 nm).

| [2i] ₀ /M | [1a] ₀ /M | [1a] ₀ /[2i] ₀ | <i>k</i> _{obs} /s ⁻¹ |
|--|-------------------------------|--|--|
| 3.70 × 10 ⁻⁵ | 7.25 × 10 ⁻⁴ | 20 | 7.35 × 10 ¹ |
| 3.70 × 10 ⁻⁵ | 1.48 × 10 ⁻³ | 40 | 1.47 × 10 ² |
| 3.70 × 10 ⁻⁵ | 2.24 × 10 ⁻³ | 61 | 2.22 × 10 ² |
| 3.70 × 10 ⁻⁵ | 2.97 × 10 ⁻³ | 80 | 3.01 × 10 ² |
| 3.70 × 10 ⁻⁵ | 3.62 × 10 ⁻³ | 98 | 3.64 × 10 ² |
| <i>k</i> ₂ = 1.01 × 10 ⁵ M ⁻¹ s ⁻¹ | | | |

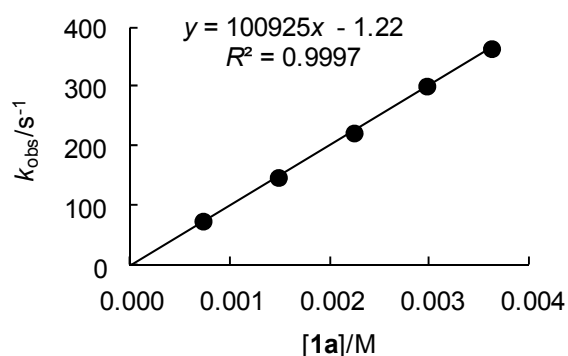


Table 6.37. Rate constants for the reactions of 4-dimethylaminopyridine (**1a**) with 3-fluorobenzoyl chloride (**2j**) in CH₃CN (stopped-flow technique, 20 °C, λ = 325 nm).

| [2j] ₀ /M | [1a] ₀ /M | [1a] ₀ /[2j] ₀ | <i>k</i> _{obs} /s ⁻¹ |
|--|-------------------------------|--|--|
| 3.78 × 10 ⁻⁵ | 3.77 × 10 ⁻⁴ | 10 | 4.64 × 10 ¹ |
| 3.78 × 10 ⁻⁵ | 7.53 × 10 ⁻⁴ | 20 | 9.13 × 10 ¹ |
| 3.78 × 10 ⁻⁵ | 1.13 × 10 ⁻³ | 30 | 1.36 × 10 ² |
| 3.78 × 10 ⁻⁵ | 1.51 × 10 ⁻³ | 40 | 1.78 × 10 ² |
| 3.78 × 10 ⁻⁵ | 1.93 × 10 ⁻³ | 51 | 2.23 × 10 ² |
| <i>k</i> ₂ = 1.14 × 10 ⁵ M ⁻¹ s ⁻¹ | | | |

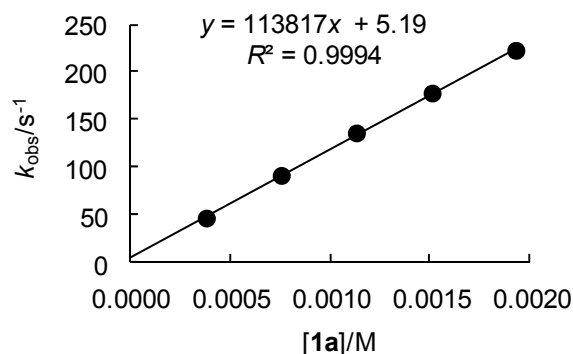


Table 6.38. Rate constants for the reactions of 4-dimethylaminopyridine (**1a**) with 2-bromobenzoyl chloride (**2k**) in CH₃CN (stopped-flow technique, 20 °C, λ = 320 nm).

| [2k] ₀ /M | [1a] ₀ /M | [1a] ₀ /[2k] ₀ | <i>k</i> _{obs} /s ⁻¹ |
|--|-------------------------------|--|--|
| 3.86 × 10 ⁻⁵ | 4.09 × 10 ⁻⁴ | 11 | 5.43 × 10 ¹ |
| 3.86 × 10 ⁻⁵ | 7.89 × 10 ⁻⁴ | 20 | 1.02 × 10 ² |
| 3.86 × 10 ⁻⁵ | 1.17 × 10 ⁻³ | 30 | 1.48 × 10 ² |
| 3.86 × 10 ⁻⁵ | 1.58 × 10 ⁻³ | 41 | 1.98 × 10 ² |
| <i>k</i> ₂ = 1.23 × 10 ⁵ M ⁻¹ s ⁻¹ | | | |

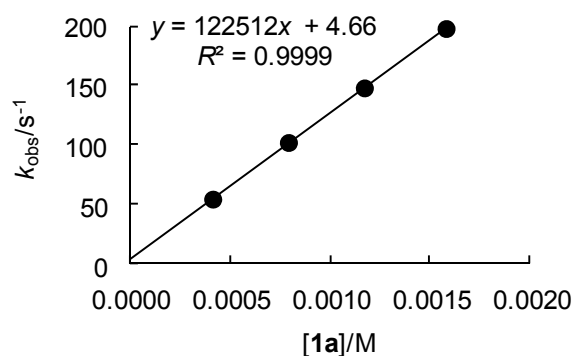


Table 6.39. Rate constants for the reactions of 4-dimethylaminopyridine (**1a**) with 3-bromobenzoyl chloride (**2l**) in CH₃CN (stopped-flow technique, 20 °C, λ = 325 nm).

| [2l] ₀ /M | [1a] ₀ /M | [1a] ₀ /[2l] ₀ | <i>k</i> _{obs} /s ⁻¹ |
|--|-------------------------------|--|--|
| 3.85 × 10 ⁻⁵ | 3.77 × 10 ⁻⁴ | 10 | 5.73 × 10 ¹ |
| 3.85 × 10 ⁻⁵ | 7.77 × 10 ⁻⁴ | 20 | 1.14 × 10 ² |
| 3.85 × 10 ⁻⁵ | 1.15 × 10 ⁻³ | 30 | 1.68 × 10 ² |
| 3.85 × 10 ⁻⁵ | 1.53 × 10 ⁻³ | 40 | 2.22 × 10 ² |
| 3.85 × 10 ⁻⁵ | 1.93 × 10 ⁻³ | 50 | 2.86 × 10 ² |
| <i>k</i> ₂ = 1.47 × 10 ⁵ M ⁻¹ s ⁻¹ | | | |

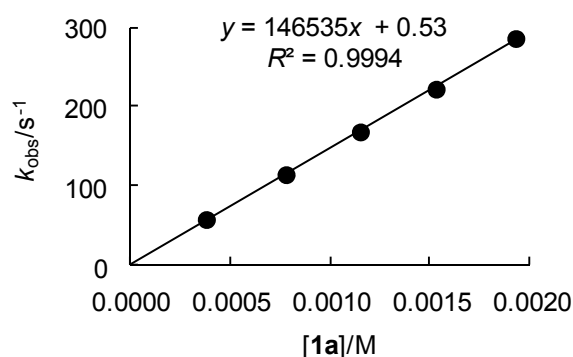


Table 6.40. Rate constants for the reactions of 4-dimethylaminopyridine (**1a**) with 3,5-difluorobenzoyl chloride (**2m**) in CH₃CN (stopped-flow technique, 20 °C, λ = 325 nm).

| [2m] ₀ /M | [1a] ₀ /M | [1a] ₀ /[2m] ₀ | <i>k</i> _{obs} /s ⁻¹ |
|--|-------------------------------|--|--|
| 2.58 × 10 ⁻⁵ | 1.65 × 10 ⁻⁴ | 6 | 7.77 × 10 ¹ |
| 2.58 × 10 ⁻⁵ | 2.12 × 10 ⁻⁴ | 8 | 9.87 × 10 ¹ |
| 2.58 × 10 ⁻⁵ | 2.59 × 10 ⁻⁴ | 10 | 1.21 × 10 ² |
| 2.58 × 10 ⁻⁵ | 3.06 × 10 ⁻⁴ | 12 | 1.44 × 10 ² |
| <i>k</i> ₂ = 4.71 × 10 ⁵ M ⁻¹ s ⁻¹ | | | |

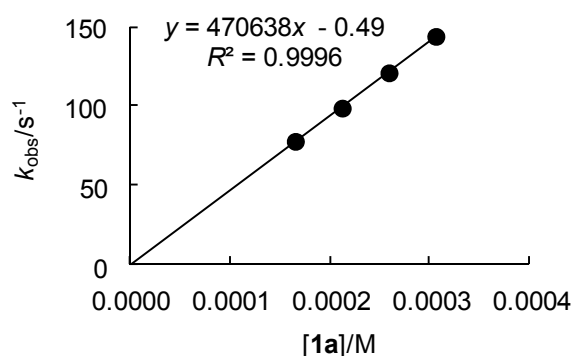
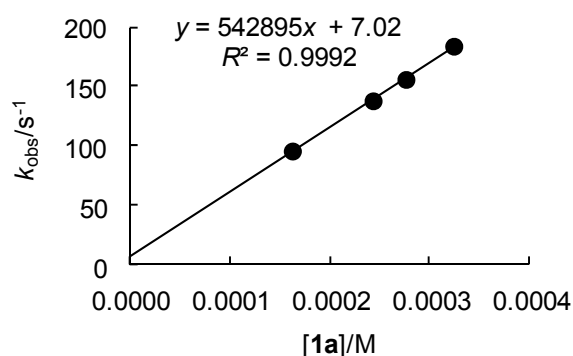


Table 6.41. Rate constants for the reactions of 4-dimethylaminopyridine (**1a**) with pentafluorobenzoyl chloride (**2n**) in CH₃CN (stopped-flow technique, 20 °C, λ = 325 nm).

| [2n] ₀ /M | [1a] ₀ /M | [1a] ₀ /[2n] ₀ | <i>k</i> _{obs} /s ⁻¹ |
|--|-------------------------------|--|--|
| 2.01 × 10 ⁻⁵ | 1.62 × 10 ⁻⁴ | 8 | 9.57 × 10 ¹ |
| 2.01 × 10 ⁻⁵ | 2.43 × 10 ⁻⁴ | 12 | 1.38 × 10 ² |
| 2.01 × 10 ⁻⁵ | 2.76 × 10 ⁻⁴ | 14 | 1.56 × 10 ² |
| 2.01 × 10 ⁻⁵ | 3.24 × 10 ⁻⁴ | 16 | 1.84 × 10 ² |
| <i>k</i> ₂ = 5.43 × 10 ⁵ M ⁻¹ s ⁻¹ | | | |



Kinetics of the reactions of DMAP (**1a**) with other acyl derivatives

Table 6.42. Rate constants for the reactions of 4-dimethylaminopyridine (**1a**) with acetyl chloride (**3**) in CH₃CN (stopped-flow technique, 20 °C, λ = 312 nm).

| [3] ₀ /M | [1a] ₀ /M | [1a] ₀ /[3] ₀ | <i>k</i> _{obs} /s ⁻¹ |
|--|-------------------------------|---|--|
| 7.42 × 10 ⁻⁵ | 8.95 × 10 ⁻⁴ | 12 | 1.19 × 10 ² |
| 7.42 × 10 ⁻⁵ | 1.07 × 10 ⁻³ | 14 | 1.42 × 10 ² |
| 7.42 × 10 ⁻⁵ | 1.21 × 10 ⁻³ | 16 | 1.55 × 10 ² |
| 7.42 × 10 ⁻⁵ | 1.34 × 10 ⁻³ | 18 | 1.71 × 10 ² |
| <i>k</i> ₂ = 1.15 × 10 ⁵ M ⁻¹ s ⁻¹ | | | |

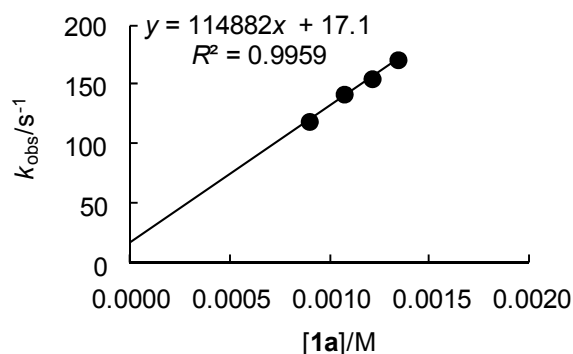


Table 6.43. Rate constants for the reactions of 4-dimethylaminopyridine (**1a**) with pivaloyl chloride (**4**) in CH₃CN (stopped-flow technique, 20 °C, λ = 320 nm).

| [4] ₀ /M | [1a] ₀ /M | [1a] ₀ /[4] ₀ | <i>k</i> _{obs} /s ⁻¹ |
|------------------------------|-------------------------------|---|--|
| 7.55 × 10 ⁻⁵ | 1.52 × 10 ⁻³ | 20 | 1.51 × 10 ¹ |
| 7.55 × 10 ⁻⁵ | 3.04 × 10 ⁻³ | 40 | 3.17 × 10 ¹ |
| 7.55 × 10 ⁻⁵ | 4.56 × 10 ⁻³ | 60 | 4.90 × 10 ¹ |
| 7.55 × 10 ⁻⁵ | 6.08 × 10 ⁻³ | 80 | 6.54 × 10 ¹ |
| 7.55 × 10 ⁻⁵ | 7.60 × 10 ⁻³ | 101 | 8.37 × 10 ¹ |

$k_2 = 1.12 \times 10^4 \text{ M}^{-1} \text{ s}^{-1}$

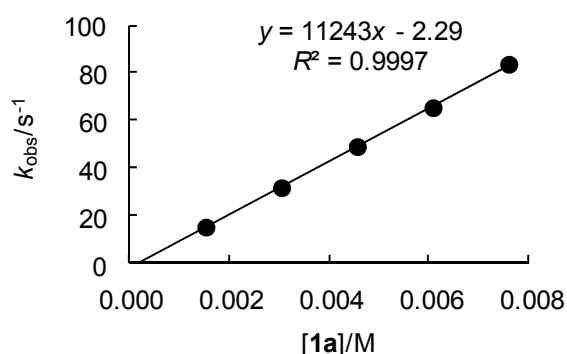


Table 6.44. Rate constants for the reactions of 4-dimethylaminopyridine (**1a**) with benzoic anhydride (**5**) in CH₃CN (stopped-flow technique, 20 °C, λ = 317 nm).

| [5] ₀ /M | [1a] ₀ /M | [1a] ₀ /[5] ₀ | <i>k</i> _{initial} /M ⁻¹ s ⁻¹ |
|------------------------------|-------------------------------|---|--|
| 4.99 × 10 ⁻⁴ | 1.00 × 10 ⁻² | 20 | 2.07 × 10 ⁻⁴ |
| 4.99 × 10 ⁻⁴ | 2.00 × 10 ⁻² | 40 | 4.09 × 10 ⁻⁴ |
| 4.99 × 10 ⁻⁴ | 3.00 × 10 ⁻² | 60 | 6.23 × 10 ⁻⁴ |
| 4.99 × 10 ⁻⁴ | 4.00 × 10 ⁻² | 80 | 7.85 × 10 ⁻⁴ |
| 4.99 × 10 ⁻⁴ | 5.01 × 10 ⁻² | 100 | 9.89 × 10 ⁻⁴ |

$k_2 = 3.87 \times 10^1 \text{ M}^{-1} \text{ s}^{-1}$

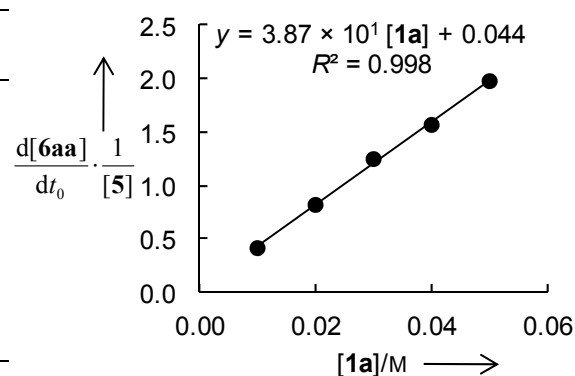
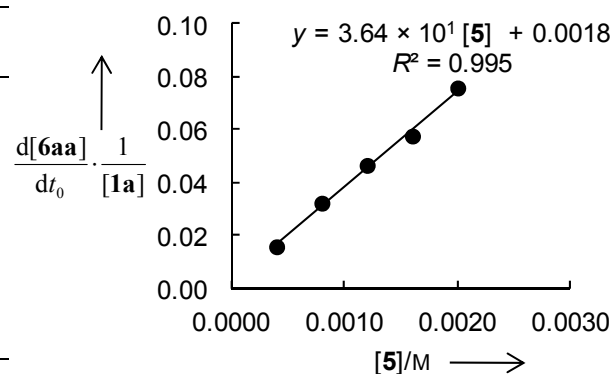


Table 6.45. Rate constants for the reactions of 4-dimethylaminopyridine (**1a**) with benzoic anhydride (**5**) in CH₃CN (stopped-flow technique, 20 °C, λ = 317 nm).

| [1a] ₀ /M | [5] ₀ /M | [1a] ₀ /[5] ₀ | <i>k</i> _{initial} /M ⁻¹ s ⁻¹ |
|-------------------------------|------------------------------|---|--|
| 1.60 × 10 ⁻² | 4.00 × 10 ⁻⁴ | 40 | 2.50 × 10 ⁻⁴ |
| 1.60 × 10 ⁻² | 8.00 × 10 ⁻⁴ | 20 | 5.13 × 10 ⁻⁴ |
| 1.60 × 10 ⁻² | 1.20 × 10 ⁻³ | 13 | 7.42 × 10 ⁻⁴ |
| 1.60 × 10 ⁻² | 1.60 × 10 ⁻³ | 10 | 9.19 × 10 ⁻⁴ |
| 1.60 × 10 ⁻² | 2.00 × 10 ⁻³ | 8 | 1.21 × 10 ⁻³ |

$k_2 = 3.64 \times 10^1 \text{ M}^{-1} \text{ s}^{-1}$



Kinetics of the reactions of N-acylpyridinium ions with benzylamine (9)

Table 6.46. Rate constants for the reactions of 1-benzoyl-4-(dimethylamino)pyridinium triflate (**6aa**-OTf) with benzylamine (**9**) in CH₃CN (stopped-flow technique, 20 °C, λ = 316 nm).

| [6aa] ₀ /M | [9] ₀ /M | [9] ₀ /[6aa] ₀ | <i>k</i> _{obs} /s ⁻¹ |
|--|------------------------------|--|--|
| 7.51 × 10 ⁻⁵ | 1.51 × 10 ⁻³ | 20 | 5.86 × 10 ⁻¹ |
| 7.51 × 10 ⁻⁵ | 3.01 × 10 ⁻³ | 40 | 1.17 |
| 7.51 × 10 ⁻⁵ | 6.02 × 10 ⁻³ | 80 | 2.38 |
| 7.51 × 10 ⁻⁵ | 6.84 × 10 ⁻³ | 91 | 2.74 |
| <i>k</i> ₂ = 4.03 × 10 ² M ⁻¹ s ⁻¹ | | | |

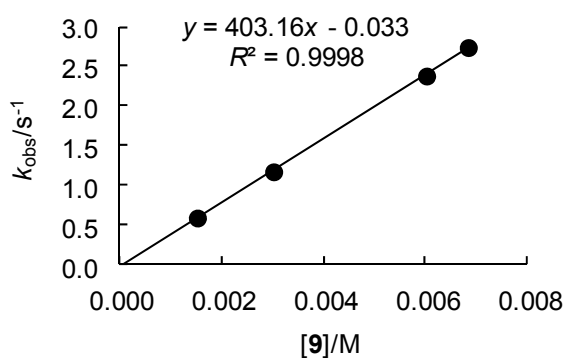


Table 6.47. Rate constants for the reactions of benzylamine (**9**) with 1-benzoyl-4-(pyrrolidin-1-yl)pyridinium chloride (**6ab**-Cl) generated from 4-(1-pyrrolidinyl)pyridine (**1b**) with 1.00 equiv. of benzoyl chloride (**2a**) in CH₃CN (stopped-flow technique, 20 °C, λ = 321 nm).

| [6ab] ₀ /M | [9] ₀ /M | [9] ₀ /[6ab] ₀ | <i>k</i> _{obs} /s ⁻¹ |
|--|------------------------------|--|--|
| 3.83 × 10 ⁻⁵ | 7.40 × 10 ⁻⁴ | 19 | 1.95 × 10 ⁻¹ |
| 3.83 × 10 ⁻⁵ | 1.55 × 10 ⁻³ | 40 | 4.19 × 10 ⁻¹ |
| 3.83 × 10 ⁻⁵ | 2.29 × 10 ⁻³ | 60 | 6.35 × 10 ⁻¹ |
| 3.83 × 10 ⁻⁵ | 3.70 × 10 ⁻³ | 97 | 1.02 |
| <i>k</i> ₂ = 2.79 × 10 ² M ⁻¹ s ⁻¹ | | | |

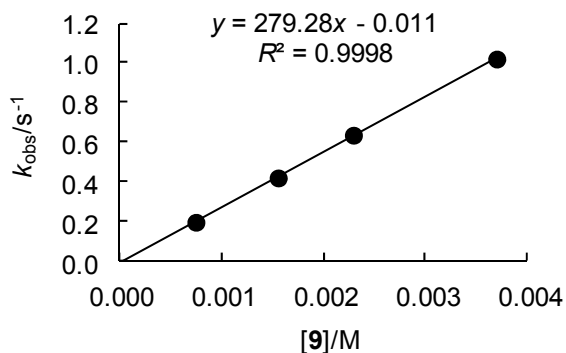


Table 6.48. Rate constants for the reactions of benzylamine (**9**) with 1-benzoyl-4-(pyrrolidin-1-yl)pyridinium chloride (**6ab-Cl**) generated from 4-(1-pyrrolidinyl)pyridine (**1b**) with 0.67 equiv. of benzoyl chloride (**2a**) in CH₃Cl (stopped-flow technique, 20 °C, λ = 321 nm).

| [6ab] ₀ /M | [9] ₀ /M | [9] ₀ /[6ab] ₀ | <i>k</i> _{obs} /s ⁻¹ |
|--|------------------------------|--|--|
| 3.86 × 10 ⁻⁵ | 5.70 × 10 ⁻⁴ | 15 | 2.24 × 10 ¹ |
| 3.86 × 10 ⁻⁵ | 7.98 × 10 ⁻⁴ | 21 | 3.08 × 10 ¹ |
| 3.86 × 10 ⁻⁵ | 9.69 × 10 ⁻⁴ | 25 | 3.67 × 10 ¹ |
| 3.86 × 10 ⁻⁵ | 1.14 × 10 ⁻³ | 30 | 4.34 × 10 ¹ |
| <i>k</i> ₂ = 3.66 × 10 ⁴ M ⁻¹ s ⁻¹ | | | |

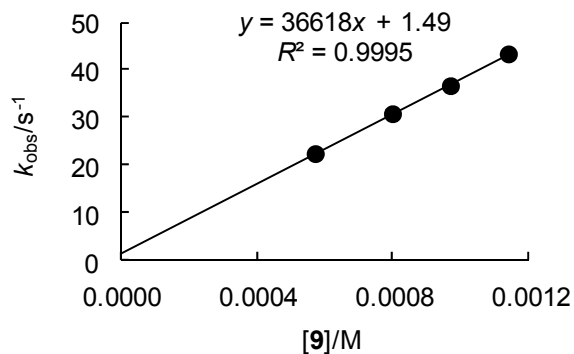


Table 6.49. Rate constants for the reactions of benzylamine (**9**) with 1-benzoyl-3-bromo-4-(morpholin-1-yl)pyridinium chloride (**6ac-Cl**) generated from 4-(1-morpholinyl)pyridine (**1c**) with 0.65 equiv. of benzoyl chloride (**2a**) in CH₃CN (stopped-flow technique, 20 °C, λ = 319 nm).

| [6ac] ₀ /M | [9] ₀ /M | [9] ₀ /[6ac] ₀ | <i>k</i> _{obs} /s ⁻¹ |
|--|------------------------------|--|--|
| 3.40 × 10 ⁻⁵ | 6.95 × 10 ⁻⁴ | 20 | 6.25 × 10 ⁻¹ |
| 3.40 × 10 ⁻⁵ | 1.39 × 10 ⁻³ | 41 | 1.24 |
| 3.40 × 10 ⁻⁵ | 2.01 × 10 ⁻³ | 59 | 1.79 |
| 3.40 × 10 ⁻⁵ | 2.70 × 10 ⁻³ | 79 | 2.41 |
| 3.40 × 10 ⁻⁵ | 3.40 × 10 ⁻³ | 100 | 3.06 |
| <i>k</i> ₂ = 8.99 × 10 ² M ⁻¹ s ⁻¹ | | | |

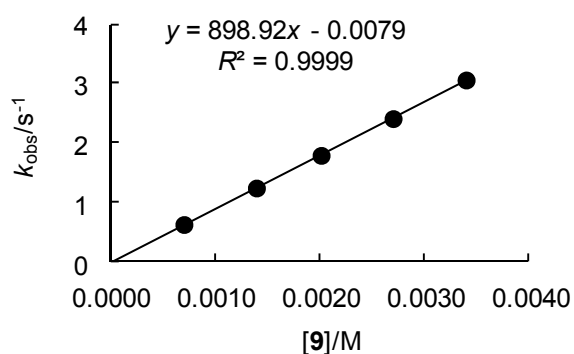


Table 6.50. Rate constants for the reactions of benzylamine (**9**) with 1-benzoyl-4-(dimethylamino)pyridinium chloride (**6ad-Cl**) generated from 3-bromo-4-dimethylaminopyridine (**1d**) with 0.99 equiv. of benzoyl chloride (**2a**) in CH₃CN (stopped-flow technique, 20 °C, λ = 334 nm).

| [6ad] ₀ /M | [9] ₀ /M | [9] ₀ /[6ad] ₀ | <i>k</i> _{obs} /s ⁻¹ |
|--|------------------------------|--|--|
| 7.35 × 10 ⁻⁵ | 1.55 × 10 ⁻³ | 21 | 1.58 × 10 ¹ |
| 7.35 × 10 ⁻⁵ | 2.87 × 10 ⁻³ | 39 | 2.83 × 10 ¹ |
| 7.35 × 10 ⁻⁵ | 4.42 × 10 ⁻³ | 60 | 4.29 × 10 ¹ |
| 7.35 × 10 ⁻⁵ | 5.96 × 10 ⁻³ | 81 | 5.77 × 10 ¹ |
| 7.35 × 10 ⁻⁵ | 7.51 × 10 ⁻³ | 102 | 7.31 × 10 ¹ |
| <i>k</i> ₂ = 8.99 × 10 ² M ⁻¹ s ⁻¹ | | | |

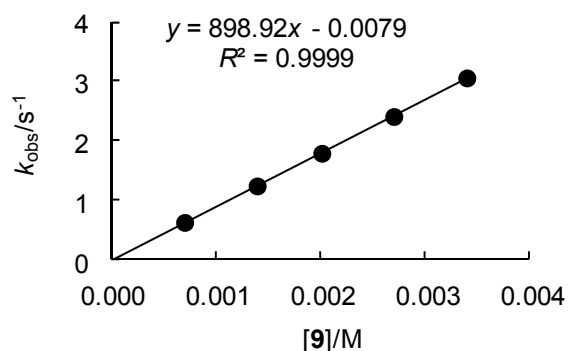


Table 6.51. Rate constants for the reactions of benzylamine (**9**) with 6-benzoyl-1,4-dimethyl-1,2,3,4-tetrahydropyrido[3,4-*b*]pyrazin-6-ium chloride (**6ah-Cl**) generated from 1,4-dimethyl-1,2,3,4-tetrahydropyrido[3,4-*b*]pyrazine (**1h**) with 0.99 equiv. of benzoyl chloride (**2a**) in CH₃CN (stopped-flow technique, 20 °C, λ = 380 nm).

| [6ah] ₀ /M | [9] ₀ /M | [9] ₀ /[6ah] ₀ | <i>k</i> _{obs} /s ⁻¹ |
|--|------------------------------|--|--|
| 1.41 × 10 ⁻⁴ | 2.93 × 10 ⁻³ | 21 | 7.57 × 10 ⁻¹ |
| 1.41 × 10 ⁻⁴ | 5.67 × 10 ⁻³ | 40 | 1.47 |
| 1.41 × 10 ⁻⁴ | 8.40 × 10 ⁻³ | 60 | 2.19 |
| 1.41 × 10 ⁻⁴ | 1.13 × 10 ⁻² | 81 | 3.02 |
| 1.41 × 10 ⁻⁴ | 1.41 × 10 ⁻² | 100 | 3.79 |
| <i>k</i> ₂ = 2.72 × 10 ² M ⁻¹ s ⁻¹ | | | |

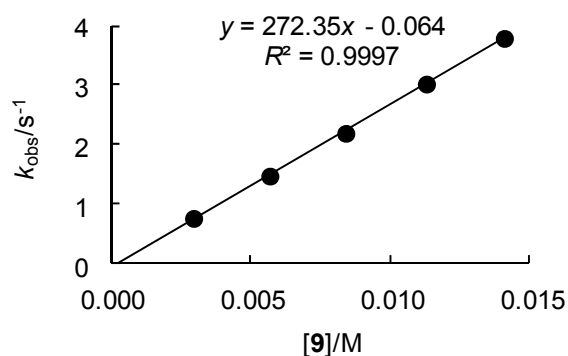


Table 6.52. Rate constants for the reactions of benzylamine (**9**) with 6-benzoyl-1,4-diethyl-1,2,3,4-tetrahydropyrido[3,4-*b*]pyrazin-6-ium chloride (**6ai**-Cl) generated from 1,4-diethyl-1,2,3,4-tetrahydropyrido[3,4-*b*]pyrazine (**1i**) with 0.67 equiv. of benzoyl chloride (**2a**) in CH₃CN (stopped-flow technique, 20 °C, λ = 390 nm).

| [6ai] ₀ /M | [9] ₀ /M | [9] ₀ /[6ai] ₀ | <i>k</i> _{obs} /s ⁻¹ |
|--------------------------------|------------------------------|--|--|
| 1.02 × 10 ⁻⁴ | 2.01 × 10 ⁻³ | 20 | 4.11 × 10 ⁻¹ |
| 1.02 × 10 ⁻⁴ | 4.02 × 10 ⁻³ | 39 | 8.08 × 10 ⁻¹ |
| 1.02 × 10 ⁻⁴ | 6.18 × 10 ⁻³ | 61 | 1.25 |
| 1.02 × 10 ⁻⁴ | 7.72 × 10 ⁻³ | 76 | 1.57 |
| 1.02 × 10 ⁻⁴ | 1.02 × 10 ⁻² | 100 | 2.08 |

$k_2 = 2.04 \times 10^2 \text{ M}^{-1} \text{ s}^{-1}$

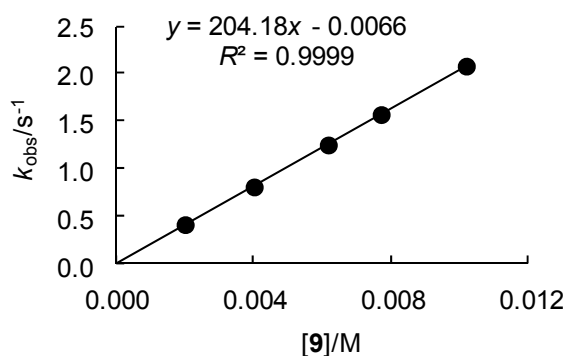


Table 6.53. Rate constants for the reactions of benzylamine (**9**) with 2-benzoyl-5,10-diethyl-5,5a,6,7,8,9,9a,10-octahydropyrido[3,4-*b*]quinoxalin-2-ium chloride (**6aj**-Cl) generated from 5,10-diethyl-5,5a,6,7,8,9,9a,10-octahydropyrido[3,4-*b*]quinoxaline (**1j**) with 0.51 equiv. of benzoyl chloride (**2a**) in CH₃CN (stopped-flow technique, 20 °C, λ = 390 nm).

| [6aj] ₀ /M | [9] ₀ /M | [9] ₀ /[6aj] ₀ | <i>k</i> _{obs} /s ⁻¹ |
|--------------------------------|------------------------------|--|--|
| 6.16 × 10 ⁻⁵ | 1.20 × 10 ⁻³ | 19 | 1.99 × 10 ⁻¹ |
| 6.16 × 10 ⁻⁵ | 2.39 × 10 ⁻³ | 39 | 3.93 × 10 ⁻¹ |
| 6.16 × 10 ⁻⁵ | 3.76 × 10 ⁻³ | 61 | 6.16 × 10 ⁻¹ |
| 6.16 × 10 ⁻⁵ | 4.95 × 10 ⁻³ | 80 | 8.15 × 10 ⁻¹ |
| 6.16 × 10 ⁻⁵ | 6.15 × 10 ⁻³ | 100 | 1.00 |

$k_2 = 1.62 \times 10^2 \text{ M}^{-1} \text{ s}^{-1}$

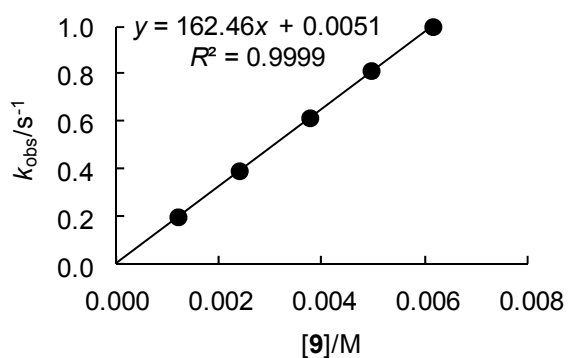


Table 6.54. Rate constants for the reactions of benzylamine (**9**) with 1,4-diacetyl-6-benzoyl-1,2,3,4-tetrahydropyrido[3,4-*b*]pyrazin-6-ium triflate (**6ak**-OTf) in CH₃CN (stopped-flow technique, 20 °C, $\lambda = 345$ nm).

| [6ak] ₀ /M | [9] ₀ /M | [9] ₀ /[6ak] ₀ | $k_{\text{obs}}/\text{s}^{-1}$ |
|--|------------------------------|--|--------------------------------|
| 8.11×10^{-5} | 7.91×10^{-4} | 10 | 1.22×10^2 |
| 8.11×10^{-5} | 9.50×10^{-4} | 12 | 1.48×10^2 |
| 8.11×10^{-5} | 1.11×10^{-3} | 14 | 1.74×10^2 |
| 8.11×10^{-5} | 1.27×10^{-3} | 16 | 1.98×10^2 |
| 8.11×10^{-5} | 1.42×10^{-3} | 18 | 2.21×10^2 |
| $k_2 = 1.57 \times 10^5 \text{ M}^{-1} \text{ s}^{-1}$ | | | |

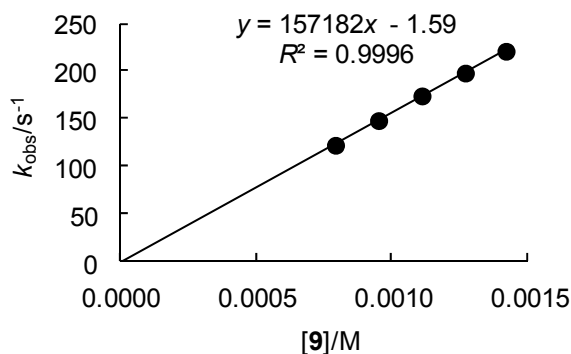


Table 6.55. Rate constants for the reactions of benzylamine (**9**) with 8-benzoyl-1,6-dimethyl-2,3,5,6-tetrahydro-1*H*,4*H*-1,3*a*,6,8-tetraaza-phenalen-8-ium chloride (**6al**-Cl) generated from 1,6-dimethyl-2,3,5,6-tetrahydro-1*H*,4*H*-1,3*a*,6,8-tetraaza-phenalene (**11**) with 1.00 equiv. of benzoyl chloride (**2a**) in CH₃CN (stopped-flow technique, 20 °C, $\lambda = 417$ nm).

| [6al] ₀ /M | [9] ₀ /M | [9] ₀ /[6al] ₀ | $k_{\text{obs}}/\text{s}^{-1}$ |
|--|------------------------------|--|--------------------------------|
| 8.80×10^{-5} | 1.73×10^{-3} | 20 | 2.34×10^{-1} |
| 8.80×10^{-5} | 3.53×10^{-3} | 40 | 4.85×10^{-1} |
| 8.80×10^{-5} | 5.26×10^{-3} | 60 | 7.26×10^{-1} |
| 8.80×10^{-5} | 7.06×10^{-3} | 80 | 9.82×10^{-1} |
| 8.80×10^{-5} | 8.80×10^{-3} | 100 | 1.23 |
| $k_2 = 1.41 \times 10^2 \text{ M}^{-1} \text{ s}^{-1}$ | | | |

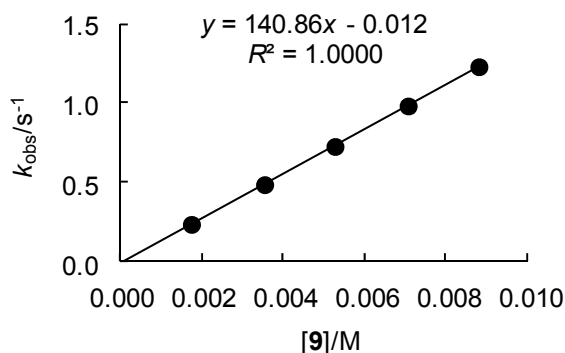


Table 6.56. Rate constants for the reactions of benzylamine (**9**) with 8-benzoyl-1,6-diethyl-2,3,5,6-tetrahydro-1*H*,4*H*-1,3a,6,8-tetraaza-phenalen-8-ium chloride (**6am**-Cl) generated from 1,6-diethyl-2,3,5,6-tetrahydro-1*H*,4*H*-1,3a,6,8-tetraaza-phenalene (**1m**) with 1.00 equiv. of benzoyl chloride (**2a**) in CH₃CN (stopped-flow technique, 20 °C, λ = 427 nm).

| [6am] ₀ /M | [9] ₀ /M | [9] ₀ /[6am] ₀ | <i>k</i> _{obs} /s ⁻¹ |
|--------------------------------|------------------------------|--|--|
| 7.19 × 10 ⁻⁵ | 1.43 × 10 ⁻³ | 20 | 1.90 × 10 ⁻¹ |
| 7.19 × 10 ⁻⁵ | 2.86 × 10 ⁻³ | 40 | 3.76 × 10 ⁻¹ |
| 7.19 × 10 ⁻⁵ | 4.30 × 10 ⁻³ | 60 | 5.62 × 10 ⁻¹ |
| 7.19 × 10 ⁻⁵ | 5.73 × 10 ⁻³ | 80 | 7.47 × 10 ⁻¹ |
| 7.19 × 10 ⁻⁵ | 7.16 × 10 ⁻³ | 100 | 9.24 × 10 ⁻¹ |

$k_2 = 1.28 \times 10^2 \text{ M}^{-1} \text{ s}^{-1}$

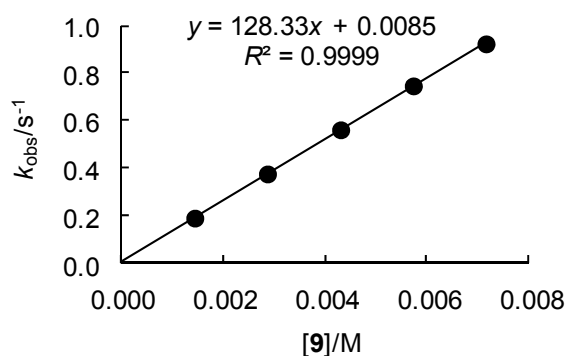


Table 6.57. Rate constants for the reactions of benzylamine (**9**) with 8-benzoyl-1,6-dibenzyl-2,3,5,6-tetrahydro-1*H*,4*H*-1,3a,6,8-tetraaza-phenalen-8-ium chloride (**6an**-Cl) generated from 1,6-dibenzyl-2,3,5,6-tetrahydro-1*H*,4*H*-1,3a,6,8-tetraaza-phenalene (**1n**) with 1.00 equiv. of benzoyl chloride (**2a**) in CH₃CN (stopped-flow technique, 20 °C, λ = 424 nm).

| [6an] ₀ /M | [9] ₀ /M | [9] ₀ /[6an] ₀ | <i>k</i> _{obs} /s ⁻¹ |
|--------------------------------|------------------------------|--|--|
| 7.19 × 10 ⁻⁵ | 1.43 × 10 ⁻³ | 20 | 2.99 × 10 ⁻¹ |
| 7.19 × 10 ⁻⁵ | 2.86 × 10 ⁻³ | 40 | 5.81 × 10 ⁻¹ |
| 7.19 × 10 ⁻⁵ | 4.30 × 10 ⁻³ | 60 | 8.69 × 10 ⁻¹ |
| 7.19 × 10 ⁻⁵ | 5.73 × 10 ⁻³ | 80 | 1.16 |
| 7.19 × 10 ⁻⁵ | 7.16 × 10 ⁻³ | 100 | 1.43 |

$k_2 = 1.98 \times 10^2 \text{ M}^{-1} \text{ s}^{-1}$

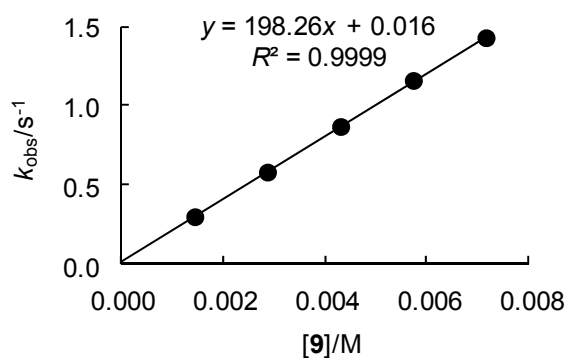


Table 6.58. Rate constants for the reactions of benzylamine (**9**) with 1-benzoyl-4-ethyl-4,5,6,8,9,10-hexahydropyrazino[3,2,1-*de*][1,5]naphthyridin-1-ium chloride (**6ao-Cl**) generated from 1-ethyl-2,3,5,6-tetrahydro-1*H*,4*H*-1,3a,8-tetraaza-phenalene (**1o**) with 1.00 equiv. of benzoyl chloride (**2a**) in CH₃CN (stopped-flow technique, 20 °C, λ = 417 nm).

| [6ao] ₀ /M | [9] ₀ /M | [9] ₀ /[6ao] ₀ | <i>k</i> _{obs} /s ⁻¹ |
|--|------------------------------|--|--|
| 8.80 × 10 ⁻⁵ | 1.73 × 10 ⁻³ | 20 | 1.43 × 10 ⁻¹ |
| 8.80 × 10 ⁻⁵ | 3.53 × 10 ⁻³ | 40 | 2.93 × 10 ⁻¹ |
| 8.80 × 10 ⁻⁵ | 5.26 × 10 ⁻³ | 60 | 4.37 × 10 ⁻¹ |
| 8.80 × 10 ⁻⁵ | 7.06 × 10 ⁻³ | 80 | 5.88 × 10 ⁻¹ |
| 8.80 × 10 ⁻⁵ | 8.80 × 10 ⁻³ | 100 | 7.34 × 10 ⁻¹ |
| <i>k</i> ₂ = 8.36 × 10 ¹ M ⁻¹ s ⁻¹ | | | |

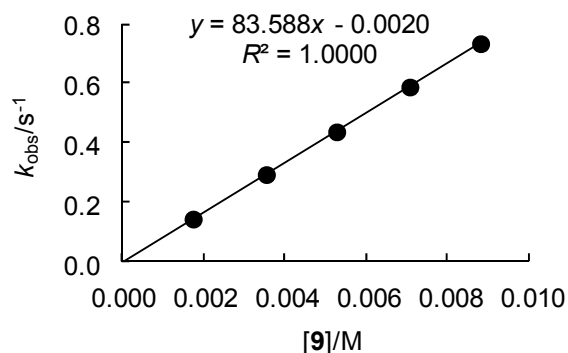


Table 6.59. Rate constants for the reactions of benzylamine (**9**) with 1-benzoyl-4-benzyl-4,5,6,8,9,10-hexahydropyrazino[3,2,1-*de*][1,5]naphthyridin-1-ium chloride (**6ap-Cl**) generated from 1-benzyl-2,3,5,6-tetrahydro-1*H*,4*H*-1,3a,8-tetraaza-phenalene (**1p**) with 1.00 equiv. of benzoyl chloride (**2a**) in CH₃CN (stopped-flow technique, 20 °C, λ = 386 nm).

| [6ap] ₀ /M | [9] ₀ /M | [9] ₀ /[6ap] ₀ | <i>k</i> _{obs} /s ⁻¹ |
|--|------------------------------|--|--|
| 8.75 × 10 ⁻⁵ | 1.75 × 10 ⁻³ | 20 | 2.07 × 10 ⁻¹ |
| 8.75 × 10 ⁻⁵ | 3.49 × 10 ⁻³ | 40 | 4.03 × 10 ⁻¹ |
| 8.75 × 10 ⁻⁵ | 5.14 × 10 ⁻³ | 59 | 6.03 × 10 ⁻¹ |
| 8.75 × 10 ⁻⁵ | 6.99 × 10 ⁻³ | 80 | 8.18 × 10 ⁻¹ |
| 8.75 × 10 ⁻⁵ | 8.73 × 10 ⁻³ | 100 | 1.03 |
| <i>k</i> ₂ = 1.18 × 10 ² M ⁻¹ s ⁻¹ | | | |

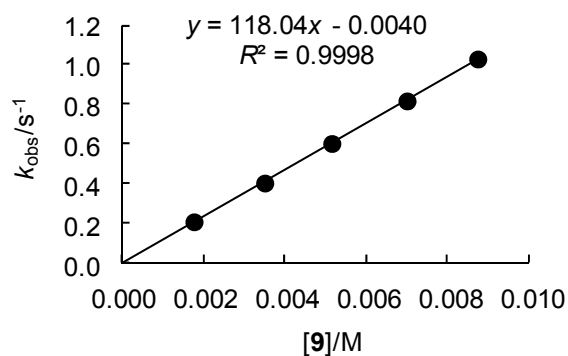


Table 6.60. Rate constants for the reactions of benzylamine (**9**) with 1-benzoyl-4,5,6,8,9,10-hexahydropyrido[3,2,1-*de*][1,5]naphthyridin-1-ium chloride (**6aq-Cl**) generated from 9-azajulolidine (**1q**) with 1.00 equiv. of benzoyl chloride (**2a**) in CH₃CN (stopped-flow technique, 20 °C, $\lambda = 335$ nm).

| [6aq] ₀ /M | [9] ₀ /M | [9] ₀ /[6aq] ₀ | $k_{\text{obs}}/\text{s}^{-1}$ |
|--|------------------------------|--|--------------------------------|
| 4.23×10^{-5} | 8.70×10^{-4} | 21 | 5.58×10^{-2} |
| 4.23×10^{-5} | 1.67×10^{-3} | 39 | 1.10×10^{-1} |
| 4.23×10^{-5} | 2.54×10^{-3} | 60 | 1.67×10^{-1} |
| 4.23×10^{-5} | 3.41×10^{-3} | 81 | 2.26×10^{-1} |
| 4.23×10^{-5} | 4.21×10^{-3} | 100 | 2.78×10^{-1} |
| $k_2 = 6.66 \times 10^1 \text{ M}^{-1} \text{ s}^{-1}$ | | | |

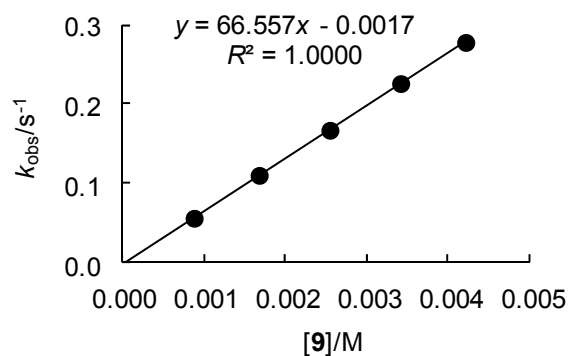


Table 6.61. Rate constants for the reactions of benzylamine (**9**) with (4-dimethylamino)-1-(4-(dimethylamino)benzoyl)pyridinium chloride (**6ba-Cl**) generated from 4-dimethylaminopyridine (**1a**) with 0.96 equiv. of 4-dimethylaminobenzoyl chloride (**2b**) in CH₃CN (diode array spectrophotometer, 20 °C, $\lambda = 370$ nm).

| [6ba] ₀ /M | [9] ₀ /M | [9] ₀ /[6ba] ₀ | $k_{\text{obs}}/\text{s}^{-1}$ |
|--|------------------------------|--|--------------------------------|
| 1.55×10^{-4} | 1.60×10^{-3} | 10 | 7.63×10^{-3} |
| 1.64×10^{-4} | 2.86×10^{-3} | 17 | 1.45×10^{-2} |
| 1.61×10^{-4} | 4.79×10^{-3} | 30 | 2.52×10^{-2} |
| 1.52×10^{-4} | 6.09×10^{-3} | 40 | 3.26×10^{-2} |
| 1.69×10^{-4} | 8.54×10^{-3} | 51 | 4.52×10^{-2} |
| $k_2 = 5.44 \text{ M}^{-1} \text{ s}^{-1}$ | | | |

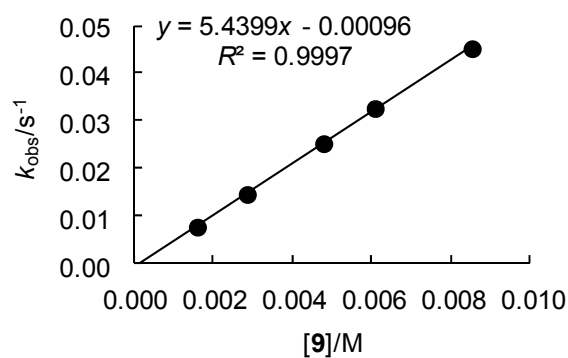


Table 6.62. Rate constants for the reactions of benzylamine (**9**) with (4-dimethylamino)-1-(4-methoxybenzoyl)pyridinium chloride (**6ca-Cl**) generated from 4-dimethylaminopyridine (**1a**) with 0.95 equiv. of 4-methoxybenzoyl chloride (**2c**) in CH₃CN (stopped-flow technique, 20 °C, $\lambda = 320$ nm).

| [6ca] ₀ /M | [9] ₀ /M | [9] ₀ /[6ca] ₀ | $k_{\text{obs}}/\text{s}^{-1}$ |
|--|------------------------------|--|--------------------------------|
| 3.67×10^{-5} | 7.91×10^{-4} | 22 | 6.79×10^{-2} |
| 3.67×10^{-5} | 1.45×10^{-3} | 40 | 1.28×10^{-1} |
| 3.67×10^{-5} | 2.24×10^{-3} | 61 | 1.98×10^{-1} |
| 3.67×10^{-5} | 2.90×10^{-3} | 79 | 2.56×10^{-1} |
| 3.67×10^{-5} | 3.69×10^{-3} | 101 | 3.27×10^{-1} |
| $k_2 = 8.92 \times 10^1 \text{ M}^{-1} \text{ s}^{-1}$ | | | |

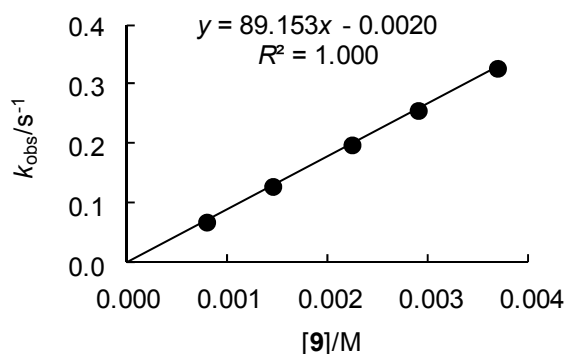


Table 6.63. Rate constants for the reactions of benzylamine (**9**) with (4-dimethylamino)-1-(4-methylbenzoyl)pyridinium chloride (**6da-Cl**) generated from 4-dimethylaminopyridine (**1a**) with 0.97 equiv. of 4-methylbenzoyl chloride (**2d**) in CH₃CN (stopped-flow technique, 20 °C, $\lambda = 317$ nm).

| [6da] ₀ /M | [9] ₀ /M | [9] ₀ /[6da] ₀ | $k_{\text{obs}}/\text{s}^{-1}$ |
|--|------------------------------|--|--------------------------------|
| 2.99×10^{-5} | 6.83×10^{-4} | 23 | 1.37×10^{-1} |
| 2.99×10^{-5} | 1.19×10^{-3} | 40 | 2.57×10^{-1} |
| 2.99×10^{-5} | 1.71×10^{-3} | 57 | 3.88×10^{-1} |
| 2.99×10^{-5} | 2.39×10^{-3} | 80 | 5.44×10^{-1} |
| 2.99×10^{-5} | 3.07×10^{-3} | 103 | 7.09×10^{-1} |
| $k_2 = 2.39 \times 10^2 \text{ M}^{-1} \text{ s}^{-1}$ | | | |

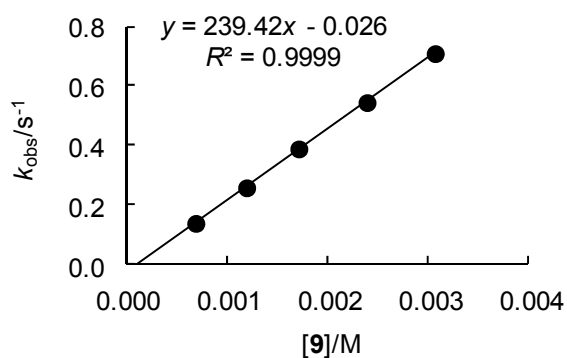


Table 6.64. Rate constants for the reactions of benzylamine (**9**) with (4-dimethylamino)-1-(3,4,5-trimethoxybenzoyl)pyridinium chloride (**6ea-Cl**) generated from 4-dimethylaminopyridine (**1a**) with 0.95 equiv. of 3,4,5-trimethoxybenzoyl chloride (**2e**) in CH₃CN (stopped-flow technique, 20 °C, $\lambda = 320$ nm).

| [6ea] ₀ /M | [9] ₀ /M | [9] ₀ /[6ea] ₀ | $k_{\text{obs}}/\text{s}^{-1}$ |
|--------------------------------|------------------------------|--|--------------------------------|
| 3.66×10^{-5} | 7.12×10^{-4} | 19 | 2.79×10^{-1} |
| 3.66×10^{-5} | 1.49×10^{-3} | 41 | 5.78×10^{-1} |
| 3.66×10^{-5} | 2.21×10^{-3} | 60 | 8.62×10^{-1} |
| 3.66×10^{-5} | 2.92×10^{-3} | 80 | 1.14 |
| 3.66×10^{-5} | 3.56×10^{-3} | 97 | 1.39 |

$k_2 = 3.91 \times 10^2 \text{ M}^{-1} \text{ s}^{-1}$

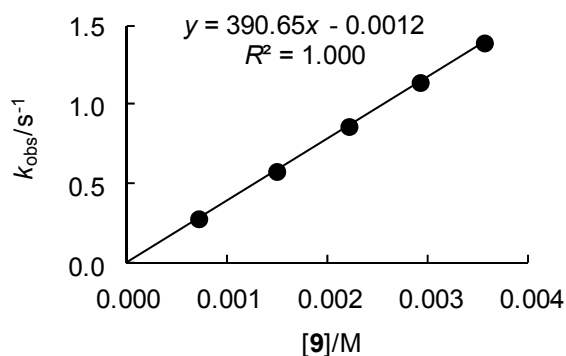


Table 6.65. Rate constants for the reactions of benzylamine (**9**) with (4-dimethylamino)-1-(4-fluorobenzoyl)pyridinium chloride (**6fa-Cl**) generated from 4-dimethylaminopyridine (**1a**) with 0.95 equiv. of 4-fluorobenzoyl chloride (**2f**) in CH₃CN (stopped-flow technique, 20 °C, $\lambda = 320$ nm).

| [6fa] ₀ /M | [9] ₀ /M | [9] ₀ /[6fa] ₀ | $k_{\text{obs}}/\text{s}^{-1}$ |
|--------------------------------|------------------------------|--|--------------------------------|
| 3.58×10^{-5} | 6.79×10^{-4} | 19 | 3.26×10^{-1} |
| 3.58×10^{-5} | 1.36×10^{-3} | 38 | 6.48×10^{-1} |
| 3.58×10^{-5} | 2.17×10^{-3} | 61 | 1.05 |
| 3.58×10^{-5} | 2.71×10^{-3} | 76 | 1.32 |
| 3.58×10^{-5} | 3.53×10^{-3} | 99 | 1.71 |

$k_2 = 4.88 \times 10^2 \text{ M}^{-1} \text{ s}^{-1}$

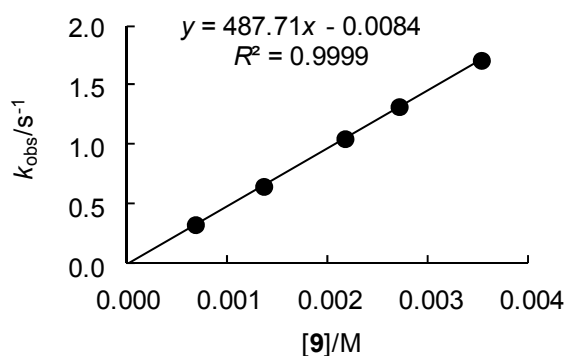


Table 6.66. Rate constants for the reactions of benzylamine (**9**) with (4-dimethylamino)-1-(4-bromobenzoyl)pyridinium chloride (**6ha-Cl**) generated from 4-dimethylaminopyridine (**1a**) with 0.95 equiv. of 4-bromobenzoyl chloride (**2h**) in CH₃CN (stopped-flow technique, 20 °C, λ = 320 nm).

| [6ha] ₀ /M | [9] ₀ /M | [9] ₀ /[6ha] ₀ | <i>k</i> _{obs} /s ⁻¹ |
|--|------------------------------|--|--|
| 3.68 × 10 ⁻⁵ | 7.12 × 10 ⁻⁴ | 19 | 6.03 × 10 ⁻¹ |
| 3.68 × 10 ⁻⁵ | 1.49 × 10 ⁻³ | 41 | 1.26 |
| 3.68 × 10 ⁻⁵ | 2.21 × 10 ⁻³ | 60 | 1.89 |
| 3.68 × 10 ⁻⁵ | 2.92 × 10 ⁻³ | 79 | 2.49 |
| 3.68 × 10 ⁻⁵ | 3.56 × 10 ⁻³ | 97 | 3.07 |
| <i>k</i> ₂ = 8.65 × 10 ² M ⁻¹ s ⁻¹ | | | |

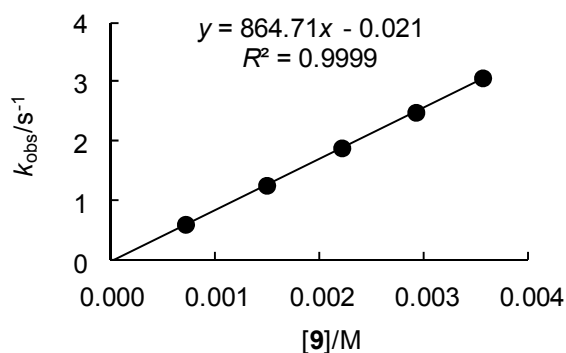


Table 6.67. Rate constants for the reactions of benzylamine (**9**) with (4-dimethylamino)-1-(3-fluorobenzoyl)pyridinium chloride (**6ja-Cl**) generated from 4-dimethylaminopyridine (**1a**) with 0.95 equiv. of 3-fluorobenzoyl chloride (**2j**) in CH₃CN (stopped-flow technique, 20 °C, λ = 325 nm).

| [6ja] ₀ /M | [9] ₀ /M | [9] ₀ /[6ja] ₀ | <i>k</i> _{obs} /s ⁻¹ |
|--|------------------------------|--|--|
| 3.79 × 10 ⁻⁵ | 7.91 × 10 ⁻⁴ | 21 | 1.06 |
| 3.79 × 10 ⁻⁵ | 1.58 × 10 ⁻³ | 42 | 2.17 |
| 3.79 × 10 ⁻⁵ | 2.24 × 10 ⁻³ | 59 | 3.07 |
| 3.79 × 10 ⁻⁵ | 3.03 × 10 ⁻³ | 80 | 4.21 |
| 3.79 × 10 ⁻⁵ | 3.82 × 10 ⁻³ | 101 | 5.45 |
| <i>k</i> ₂ = 1.40 × 10 ³ M ⁻¹ s ⁻¹ | | | |

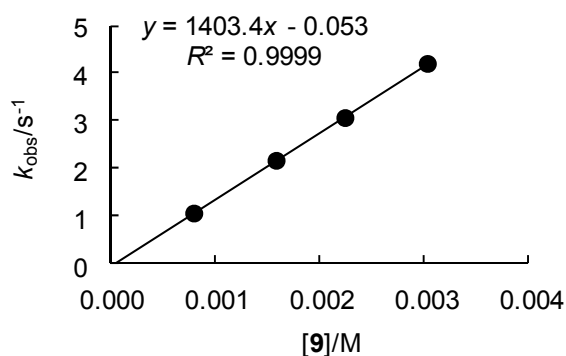


Table 6.68. Rate constants for the reactions of benzylamine (**9**) with (4-dimethylamino)-1-(2-bromobenzoyl)pyridinium chloride (**6ka-Cl**) generated from 4-dimethylaminopyridine (**1a**) with 0.95 equiv. of 2-bromobenzoyl chloride (**2k**) in CH₃CN (stopped-flow technique, 20 °C, $\lambda = 330$ nm).

| [6ka] ₀ /M | [9] ₀ /M | [9] ₀ /[6ka] ₀ | $k_{\text{obs}}/\text{s}^{-1}$ |
|--|------------------------------|--|--------------------------------|
| 3.50×10^{-5} | 6.90×10^{-4} | 20 | 3.99×10^{-2} |
| 3.50×10^{-5} | 1.38×10^{-3} | 39 | 7.46×10^{-2} |
| 3.50×10^{-5} | 2.07×10^{-3} | 59 | 1.09×10^{-1} |
| 3.50×10^{-5} | 2.76×10^{-3} | 79 | 1.42×10^{-1} |
| 3.50×10^{-5} | 3.45×10^{-3} | 99 | 1.78×10^{-1} |
| $k_2 = 4.98 \times 10^1 \text{ M}^{-1} \text{ s}^{-1}$ | | | |

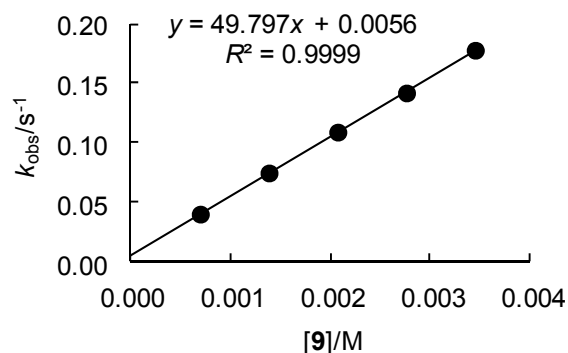


Table 6.69. Rate constants for the reactions of benzylamine (**9**) with (4-dimethylamino)-1-(3-bromobenzoyl)pyridinium chloride (**6la-Cl**) generated from 4-dimethylaminopyridine (**1a**) with 0.95 equiv. of 3-bromobenzoyl chloride (**2l**) in CH₃CN (stopped-flow technique, 20 °C, $\lambda = 325$ nm).

| [6la] ₀ /M | [9] ₀ /M | [9] ₀ /[6la] ₀ | $k_{\text{obs}}/\text{s}^{-1}$ |
|--|------------------------------|--|--------------------------------|
| 3.66×10^{-5} | 7.85×10^{-4} | 21 | 1.09 |
| 3.66×10^{-5} | 1.48×10^{-3} | 40 | 2.12 |
| 3.66×10^{-5} | 2.18×10^{-3} | 60 | 3.13 |
| 3.66×10^{-5} | 2.97×10^{-3} | 81 | 4.24 |
| 3.66×10^{-5} | 3.66×10^{-3} | 100 | 5.26 |
| $k_2 = 1.44 \times 10^3 \text{ M}^{-1} \text{ s}^{-1}$ | | | |

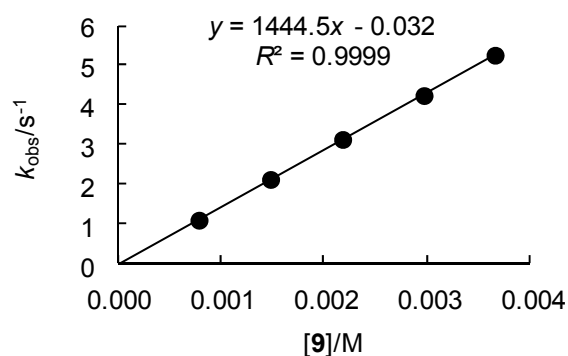


Table 6.70. Rate constants for the reactions of benzylamine (**9**) with (4-dimethylamino)-1-(3,5-difluorobenzoyl)pyridinium chloride (**6ma-Cl**) generated from 4-dimethylaminopyridine (**1a**) with 0.95 equiv. of 3,5-difluorobenzoyl chloride (**2m**) in CH₃CN (stopped-flow technique, 20 °C, $\lambda = 325$ nm).

| [6ma] ₀ /M | [9] ₀ /M | [9] ₀ /[6ma] ₀ | $k_{\text{obs}}/\text{s}^{-1}$ |
|--------------------------------|------------------------------|--|--------------------------------|
| 3.75×10^{-5} | 7.37×10^{-4} | 20 | 3.03 |
| 3.75×10^{-5} | 1.52×10^{-3} | 40 | 6.33 |
| 3.75×10^{-5} | 2.29×10^{-3} | 61 | 9.76 |
| 3.75×10^{-5} | 3.03×10^{-3} | 81 | 1.28×10^1 |
| 3.75×10^{-5} | 3.77×10^{-3} | 100 | 1.56×10^1 |

$k_2 = 4.17 \times 10^3 \text{ M}^{-1} \text{ s}^{-1}$

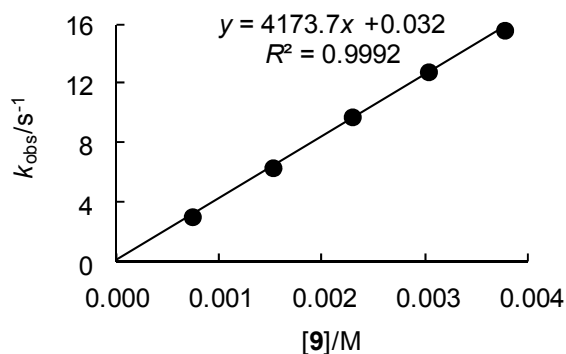


Table 6.71. Rate constants for the reactions of 1-acetyl-4-(dimethylamino)pyridinium chloride (**7a-Cl**) with benzylamine (**9**) generated from 4-dimethylaminopyridine (**1a**) with 0.95 equiv. of acetyl chloride (**3**) in CH₃CN (stopped-flow technique, 20 °C, $\lambda = 312$ nm).

| [7a] ₀ /M | [9] ₀ /M | [9] ₀ /[7a] ₀ | $k_{\text{obs}}/\text{s}^{-1}$ |
|-------------------------------|------------------------------|---|--------------------------------|
| 3.61×10^{-5} | 7.11×10^{-4} | 20 | 5.03×10^{-1} |
| 3.61×10^{-5} | 1.42×10^{-3} | 39 | 1.01 |
| 3.61×10^{-5} | 2.19×10^{-3} | 61 | 1.58 |
| 3.61×10^{-5} | 2.90×10^{-3} | 80 | 2.09 |
| 3.61×10^{-5} | 3.55×10^{-3} | 98 | 2.61 |

$k_2 = 7.39 \times 10^2 \text{ M}^{-1} \text{ s}^{-1}$

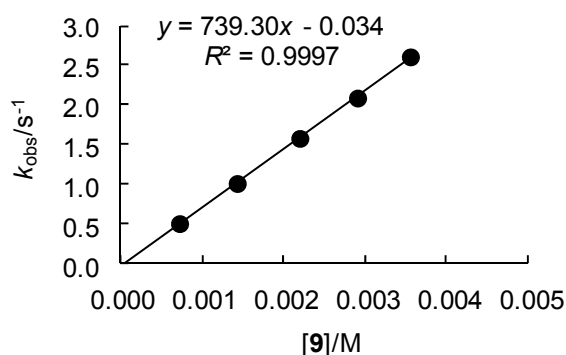
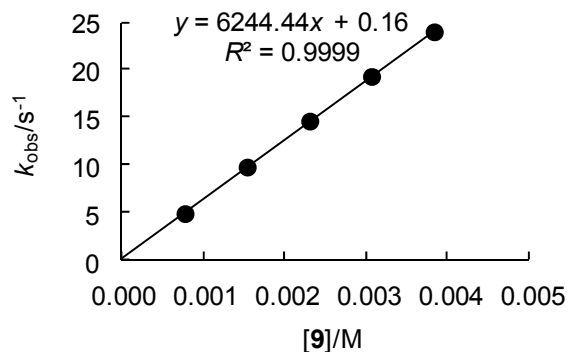


Table 6.72. Rate constants for the reactions of 4-(dimethylamino)-1-pivaloylpyridinium chloride (**8a-Cl**) with benzylamine (**9**) generated from 4-dimethylaminopyridine (**1a**) with 0.96 equiv. of pivaloyl chloride (**4**) in CH₃CN (stopped-flow technique, 20 °C, λ = 312 nm).

| [8a] ₀ /M | [9] ₀ /M | [9] ₀ /[8a] ₀ | <i>k</i> _{obs} /s ⁻¹ |
|--|------------------------------|---|--|
| 3.82 × 10 ⁻⁵ | 7.66 × 10 ⁻⁴ | 20 | 4.86 |
| 3.82 × 10 ⁻⁵ | 1.53 × 10 ⁻³ | 40 | 9.76 |
| 3.82 × 10 ⁻⁵ | 2.30 × 10 ⁻³ | 60 | 1.46 × 10 ¹ |
| 3.82 × 10 ⁻⁵ | 3.06 × 10 ⁻³ | 80 | 1.93 × 10 ¹ |
| 3.82 × 10 ⁻⁵ | 3.83 × 10 ⁻³ | 100 | 2.40 × 10 ¹ |
| <i>k</i> ₂ = 6.24 × 10 ³ M ⁻¹ s ⁻¹ | | | |



Kinetics of the reactions of 4-(1-pyrrolidinyl)pyridine (1b) with benzhydrylium ions (E)^[28]

Table 6.73. Rate constants for the reactions of 4-(1-pyrrolidinyl)pyridine (**1b**) with (lil)₂CH⁺ BF₄⁻ (**Ea**) in CH₃CN (stopped-flow, 20 °C, λ = 631 nm).

| [Ea] ₀ /M | [1b] ₀ /M | [1b] ₀ /[Ea] ₀ | <i>k</i> _{obs} /s ⁻¹ |
|--|-------------------------------|--|--|
| 7.51 × 10 ⁻⁶ | 1.51 × 10 ⁻⁴ | 20 | 5.02 × 10 ⁻¹ |
| 7.51 × 10 ⁻⁶ | 3.02 × 10 ⁻⁴ | 40 | 9.01 × 10 ⁻¹ |
| 7.51 × 10 ⁻⁶ | 4.52 × 10 ⁻⁴ | 60 | 1.28 |
| 7.51 × 10 ⁻⁶ | 6.03 × 10 ⁻⁴ | 80 | 1.73 |
| 7.51 × 10 ⁻⁶ | 7.54 × 10 ⁻⁴ | 100 | 2.14 |
| <i>k</i> ₂ = 2.72 × 10 ³ M ⁻¹ s ⁻¹ | | | |

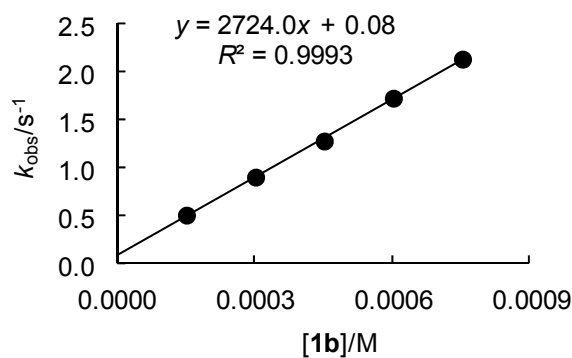


Table 6.74. Rate constants for the reactions of 4-(1-pyrrolidinyl)pyridine (**1b**) with (ind)₂CH⁺ BF₄⁻ (**Ec**) in CH₃CN (stopped-flow, 20 °C, λ = 616 nm).

| [Ec] ₀ /M | [1b] ₀ /M | [1b] ₀ /[Ec] ₀ | k _{obs} /s ⁻¹ |
|--|-------------------------|--------------------------------------|-----------------------------------|
| 7.55 × 10 ⁻⁶ | 1.51 × 10 ⁻⁴ | 20 | 2.93 |
| 7.55 × 10 ⁻⁶ | 3.02 × 10 ⁻⁴ | 40 | 5.76 |
| 7.55 × 10 ⁻⁶ | 4.52 × 10 ⁻⁴ | 60 | 8.56 |
| 7.55 × 10 ⁻⁶ | 6.03 × 10 ⁻⁴ | 80 | 1.15 × 10 ¹ |
| $k_2 = 1.89 \times 10^4 \text{ M}^{-1} \text{ s}^{-1}$ | | | |

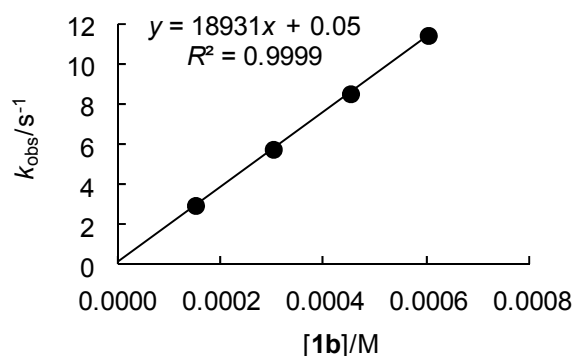


Table 6.75. Rate constants for the reactions of 4-(1-pyrrolidinyl)pyridine (**1b**) with (pyr)₂CH⁺ BF₄⁻ (**Ee**) in CH₃CN (stopped-flow, 20 °C, λ = 616 nm).

| [Ee] ₀ /M | [1b] ₀ /M | [1b] ₀ /[Ee] ₀ | k _{obs} /s ⁻¹ |
|--|-------------------------|--------------------------------------|-----------------------------------|
| 7.65 × 10 ⁻⁶ | 1.50 × 10 ⁻⁴ | 20 | 2.32 × 10 ¹ |
| 7.65 × 10 ⁻⁶ | 2.25 × 10 ⁻⁴ | 29 | 3.41 × 10 ¹ |
| 7.65 × 10 ⁻⁶ | 3.01 × 10 ⁻⁴ | 39 | 4.51 × 10 ¹ |
| 7.65 × 10 ⁻⁶ | 3.76 × 10 ⁻⁴ | 49 | 5.50 × 10 ¹ |
| 7.65 × 10 ⁻⁶ | 4.51 × 10 ⁻⁴ | 59 | 6.58 × 10 ¹ |
| $k_2 = 1.41 \times 10^5 \text{ M}^{-1} \text{ s}^{-1}$ | | | |

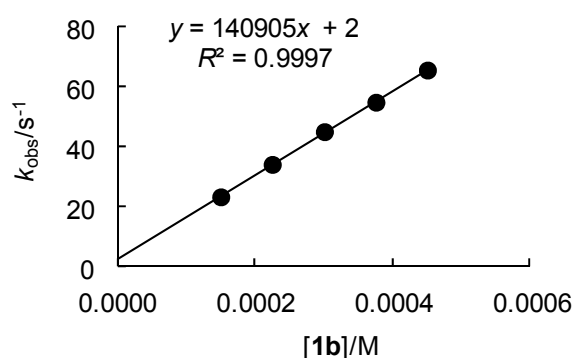


Table 6.76. Rate constants for the reactions of 4-(1-pyrrolidinyl)pyridine (**1b**) with (dma)₂CH⁺ BF₄⁻ (**Ef**) in CH₃CN (stopped-flow, 20 °C, λ = 605 nm).

| [Ef] ₀ /M | [1b] ₀ /M | [1b] ₀ /[Ef] ₀ | k _{obs} /s ⁻¹ |
|--|-------------------------|--------------------------------------|-----------------------------------|
| 7.64 × 10 ⁻⁶ | 1.50 × 10 ⁻⁴ | 20 | 5.01 × 10 ¹ |
| 7.64 × 10 ⁻⁶ | 2.25 × 10 ⁻⁴ | 29 | 7.54 × 10 ¹ |
| 7.64 × 10 ⁻⁶ | 3.01 × 10 ⁻⁴ | 39 | 9.88 × 10 ¹ |
| 7.64 × 10 ⁻⁶ | 3.76 × 10 ⁻⁴ | 49 | 1.19 × 10 ² |
| 7.64 × 10 ⁻⁶ | 4.51 × 10 ⁻⁴ | 59 | 1.40 × 10 ² |
| $k_2 = 2.97 \times 10^5 \text{ M}^{-1} \text{ s}^{-1}$ | | | |

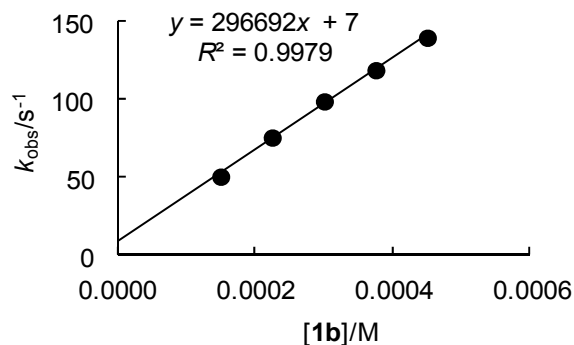
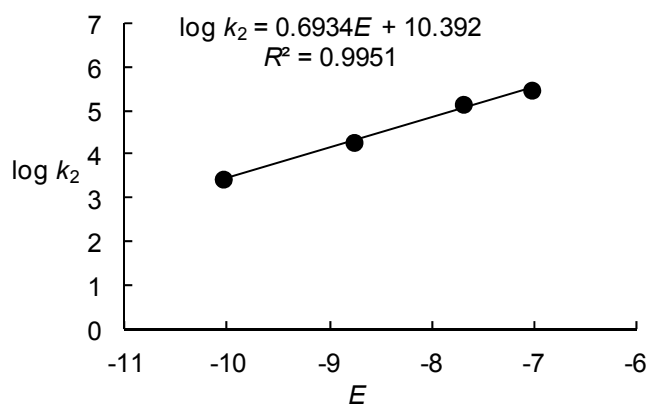


Table 6.77. Determination of the nucleophilicity parameters N and s_N for the 4-(1-pyrrolidinyl)pyridine (**1b**) in CH_3CN .

| Electrophile (E) | $k_2/\text{M}^{-1} \text{s}^{-1}$ | $\log k_2$ |
|------------------------------|-----------------------------------|------------|
| Ea $(-10.04)^{[16c]}$ | 2.72×10^3 | 3.43 |
| Ec $(-8.76)^{[16c]}$ | 1.89×10^4 | 4.28 |
| Ee $(-7.69)^{[16c]}$ | 1.41×10^5 | 5.15 |
| Ef $(-7.02)^{[16c]}$ | 2.97×10^5 | 5.47 |
| $N = 14.99, s_N = 0.69$ | | |



Kinetics of the reactions of 5,10-diethyl-5,5a,6,7,8,9,9a,10-octahydropyrido[3,4-b]quinoxaline (1j) with benzhydrylium ions (E)^[28]

Table 6.78. Rate constants for the reactions of 5,10-diethyl-5,5a,6,7,8,9,9a,10-octahydropyrido[3,4-*b*]quinoxaline (**1j**) with $(\text{lil})_2\text{CH}^+ \text{BF}_4^-$ (**Ea**) in CH_3CN (stopped-flow, 20 °C, $\lambda = 631 \text{ nm}$).

| $[\text{Ea}]_0/\text{M}$ | $[\mathbf{1j}]_0/\text{M}$ | $[\mathbf{1j}]_0/[\text{Ea}]_0$ | $k_{\text{obs}}/\text{s}^{-1}$ |
|--|----------------------------|---------------------------------|--------------------------------|
| 7.45×10^{-6} | 1.52×10^{-4} | 20 | 2.73 |
| 7.45×10^{-6} | 3.05×10^{-4} | 41 | 5.34 |
| 7.45×10^{-6} | 4.70×10^{-4} | 63 | 8.20 |
| 7.45×10^{-6} | 5.97×10^{-4} | 80 | 1.05×10^1 |
| 7.45×10^{-6} | 7.49×10^{-4} | 101 | 1.31×10^1 |
| $k_2 = 1.74 \times 10^4 \text{ M}^{-1} \text{ s}^{-1}$ | | | |

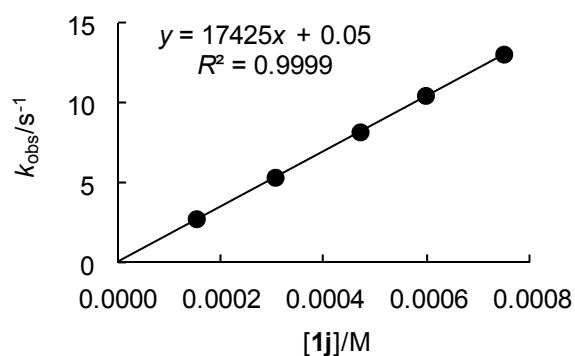


Table 6.79. Rate constants for the reactions of 5,10-diethyl-5,5a,6,7,8,9,9a,10-octahydropyrido[3,4-*b*]quinoxaline (**1j**) with (jul)₂CH⁺ BF₄⁻ (**Eb**) in CH₃CN (stopped-flow, 20 °C, λ = 631 nm).

| [Eb] ₀ /M | [1j] ₀ /M | [1j] ₀ /[Eb] ₀ | <i>k</i> _{obs} /s ⁻¹ |
|--|-------------------------------|--|--|
| 7.43 × 10 ⁻⁶ | 1.52 × 10 ⁻⁴ | 20 | 7.88 |
| 7.43 × 10 ⁻⁶ | 3.05 × 10 ⁻⁴ | 41 | 1.52 × 10 ¹ |
| 7.43 × 10 ⁻⁶ | 4.70 × 10 ⁻⁴ | 63 | 2.33 × 10 ¹ |
| 7.43 × 10 ⁻⁶ | 5.97 × 10 ⁻⁴ | 80 | 2.95 × 10 ¹ |
| 7.43 × 10 ⁻⁶ | 7.49 × 10 ⁻⁴ | 101 | 3.71 × 10 ¹ |
| <i>k</i> ₂ = 4.89 × 10 ⁴ M ⁻¹ s ⁻¹ | | | |

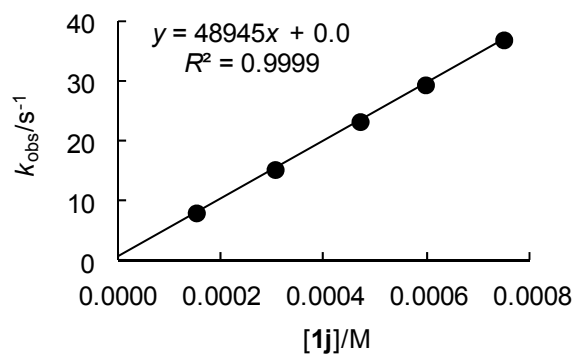


Table 6.80. Rate constants for the reactions of 5,10-diethyl-5,5a,6,7,8,9,9a,10-octahydropyrido[3,4-*b*]quinoxaline (**1j**) with (ind)₂CH⁺ BF₄⁻ (**Ec**) in CH₃CN (stopped-flow, 20 °C, λ = 616 nm).

| [Ec] ₀ /M | [1j] ₀ /M | [1j] ₀ /[Ec] ₀ | <i>k</i> _{obs} /s ⁻¹ |
|--|-------------------------------|--|--|
| 7.14 × 10 ⁻⁶ | 1.43 × 10 ⁻⁴ | 20 | 1.46 × 10 ¹ |
| 7.14 × 10 ⁻⁶ | 2.86 × 10 ⁻⁴ | 40 | 2.90 × 10 ¹ |
| 7.14 × 10 ⁻⁶ | 4.42 × 10 ⁻⁴ | 62 | 4.40 × 10 ¹ |
| 7.14 × 10 ⁻⁶ | 5.85 × 10 ⁻⁴ | 82 | 5.74 × 10 ¹ |
| 7.14 × 10 ⁻⁶ | 7.41 × 10 ⁻⁴ | 104 | 7.29 × 10 ¹ |
| <i>k</i> ₂ = 9.70 × 10 ⁴ M ⁻¹ s ⁻¹ | | | |

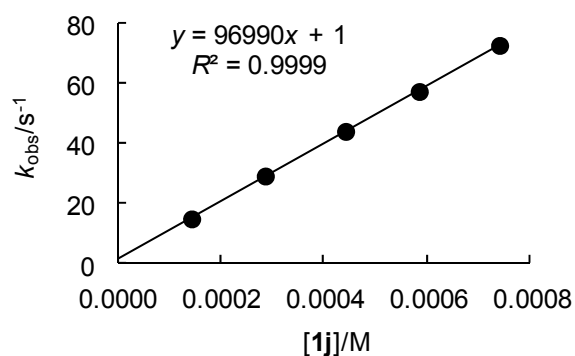


Table 6.81. Rate constants for the reactions of 5,10-diethyl-5,5a,6,7,8,9,9a,10-octahydropyrido[3,4-*b*]quinoxaline (**1j**) with (thq)₂CH⁺ BF₄⁻ (**Ed**) in CH₃CN (stopped-flow, 20 °C, λ = 619 nm).

| [Ed] ₀ /M | [1j] ₀ /M | [1j] ₀ /[Ed] ₀ | <i>k</i> _{obs} /s ⁻¹ |
|--|-------------------------------|--|--|
| 7.34 × 10 ⁻⁶ | 1.43 × 10 ⁻⁴ | 19 | 4.03 × 10 ¹ |
| 7.34 × 10 ⁻⁶ | 2.86 × 10 ⁻⁴ | 39 | 8.06 × 10 ¹ |
| 7.34 × 10 ⁻⁶ | 4.42 × 10 ⁻⁴ | 60 | 1.20 × 10 ² |
| 7.34 × 10 ⁻⁶ | 5.85 × 10 ⁻⁴ | 80 | 1.53 × 10 ² |
| 7.34 × 10 ⁻⁶ | 7.41 × 10 ⁻⁴ | 101 | 2.01 × 10 ² |
| <i>k</i> ₂ = 2.67 × 10 ⁵ M ⁻¹ s ⁻¹ | | | |

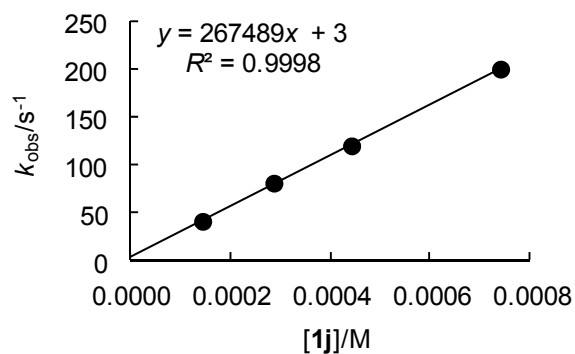


Table 6.82. Rate constants for the reactions of 5,10-diethyl-5,5a,6,7,8,9,9a,10-octahydropyrido[3,4-*b*]quinoxaline (**1j**) with (pyr)₂CH⁺ BF₄⁻ (**Ee**) in CH₃CN (stopped-flow, 20 °C, λ = 616 nm).

| [Ee] ₀ /M | [1j] ₀ /M | [1j] ₀ /[Ee] ₀ | <i>k</i> _{obs} /s ⁻¹ |
|--|-------------------------------|--|--|
| 7.75 × 10 ⁻⁶ | 5.55 × 10 ⁻⁵ | 7 | 3.98 × 10 ¹ |
| 7.75 × 10 ⁻⁶ | 1.11 × 10 ⁻⁴ | 14 | 7.77 × 10 ¹ |
| 7.75 × 10 ⁻⁶ | 1.57 × 10 ⁻⁴ | 20 | 1.10 × 10 ² |
| 7.75 × 10 ⁻⁶ | 2.13 × 10 ⁻⁴ | 27 | 1.45 × 10 ² |
| 7.75 × 10 ⁻⁶ | 2.59 × 10 ⁻⁴ | 33 | 1.77 × 10 ² |
| <i>k</i> ₂ = 6.71 × 10 ⁵ M ⁻¹ s ⁻¹ | | | |

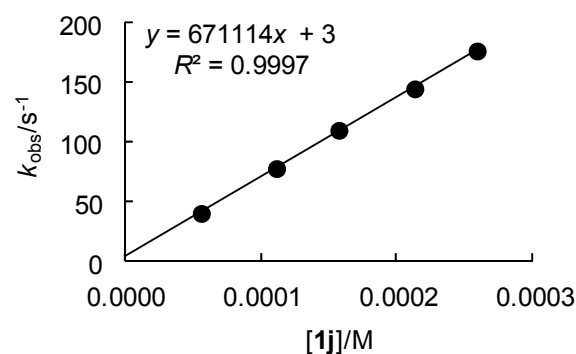


Table 6.83. Rate constants for the reactions of 5,10-diethyl-5,5a,6,7,8,9,9a,10-octahydropyrido[3,4-*b*]quinoxaline (**1j**) with (dma)₂CH⁺ BF₄⁻ (**Ef**) in CH₃CN (stopped-flow, 20 °C, λ = 613 nm).

| [Ef] ₀ /M | [1j] ₀ /M | [1j] ₀ /[Ef] ₀ | <i>k</i> _{obs} /s ⁻¹ |
|-------------------------------|-------------------------------|--|--|
| 8.70 × 10 ⁻⁶ | 5.55 × 10 ⁻⁵ | 6 | 8.52 × 10 ¹ |
| 8.70 × 10 ⁻⁶ | 6.48 × 10 ⁻⁵ | 7 | 1.01 × 10 ² |
| 8.70 × 10 ⁻⁶ | 8.33 × 10 ⁻⁵ | 10 | 1.27 × 10 ² |
| 8.70 × 10 ⁻⁶ | 9.25 × 10 ⁻⁵ | 11 | 1.40 × 10 ² |
| 8.70 × 10 ⁻⁶ | 1.57 × 10 ⁻⁴ | 18 | 2.37 × 10 ² |

$k_2 = 1.49 \times 10^6 \text{ M}^{-1} \text{ s}^{-1}$

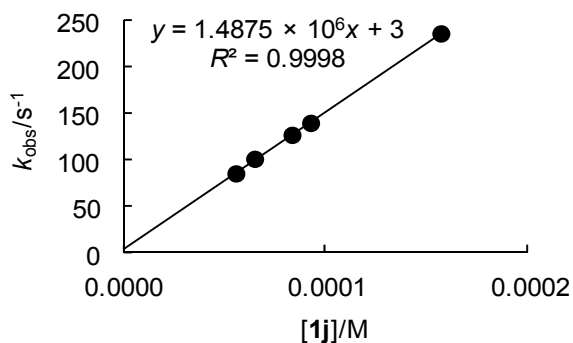
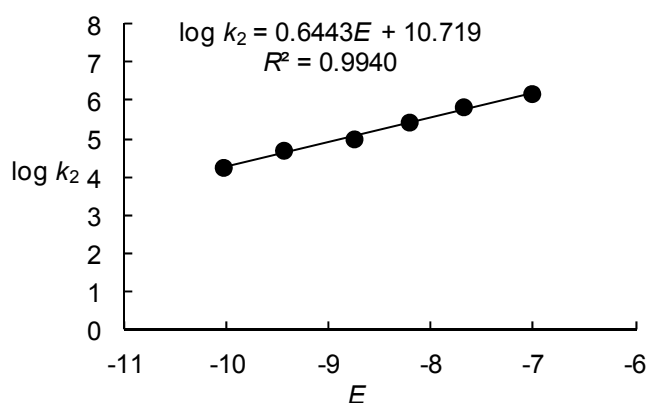


Table 6.84. Determination of the nucleophilicity parameters *N* and *s*_N for 5,10-diethyl-5,5a,6,7,8,9,9a,10-octahydropyrido[3,4-*b*]quinoxaline (**1j**) in CH₃CN.

| Electrophile (<i>E</i>) | <i>k</i> ₂ /M ⁻¹ s ⁻¹ | log <i>k</i> ₂ |
|-------------------------------------|--|---------------------------|
| Ea (-10.04) ^[16c] | 1.74 × 10 ⁴ | 4.24 |
| Eb (-9.45) ^[16c] | 4.89 × 10 ⁴ | 4.69 |
| Ec (-8.76) ^[16c] | 9.70 × 10 ⁴ | 4.99 |
| Ed (-8.22) ^[16c] | 2.67 × 10 ⁵ | 5.43 |
| Ee (-7.69) ^[16c] | 6.71 × 10 ⁵ | 5.83 |
| Ef (-7.02) ^[16c] | 1.49 × 10 ⁶ | 6.17 |

$N = 16.64, s_N = 0.64$



Kinetics of the reactions of 9-azajulolidine (**1q**) with benzhydrylium ions (**E**)^[28]

Table 6.85. Rate constants for the reactions of 9-azajulolidine (**1q**) with (lil)₂CH⁺ BF₄⁻ (**Ea**) in CH₃CN (stopped-flow, 20 °C, λ = 631 nm).

| [Ea] ₀ /M | [1q] ₀ /M | [1q] ₀ /[Ea] ₀ | <i>k</i> _{obs} /s ⁻¹ |
|--|-------------------------------|--|--|
| 6.92 × 10 ⁻⁶ | 1.36 × 10 ⁻⁴ | 20 | 8.33 × 10 ⁻¹ |
| 6.92 × 10 ⁻⁶ | 2.73 × 10 ⁻⁴ | 39 | 1.70 |
| 6.92 × 10 ⁻⁶ | 4.09 × 10 ⁻⁴ | 59 | 2.52 |
| 6.92 × 10 ⁻⁶ | 5.58 × 10 ⁻⁴ | 81 | 3.47 |
| 6.92 × 10 ⁻⁶ | 6.94 × 10 ⁻⁴ | 100 | 4.36 |
| <i>k</i> ₂ = 6.30 × 10 ³ M ⁻¹ s ⁻¹ | | | |

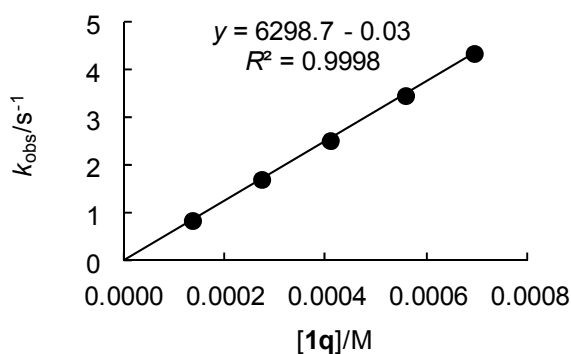


Table 6.86. Rate constants for the reactions of 9-azajulolidine (**1q**) with (ind)₂CH⁺ BF₄⁻ (**Ec**) in CH₃CN (stopped-flow, 20 °C, λ = 616 nm).

| [Ec] ₀ /M | [1q] ₀ /M | [1q] ₀ /[Ec] ₀ | <i>k</i> _{obs} /s ⁻¹ |
|--|-------------------------------|--|--|
| 7.17 × 10 ⁻⁶ | 1.36 × 10 ⁻⁴ | 19 | 6.00 |
| 7.17 × 10 ⁻⁶ | 2.73 × 10 ⁻⁴ | 38 | 1.20 × 10 ¹ |
| 7.17 × 10 ⁻⁶ | 4.09 × 10 ⁻⁴ | 57 | 1.75 × 10 ¹ |
| 7.17 × 10 ⁻⁶ | 5.58 × 10 ⁻⁴ | 78 | 2.36 × 10 ¹ |
| 7.17 × 10 ⁻⁶ | 6.94 × 10 ⁻⁴ | 97 | 2.94 × 10 ¹ |
| <i>k</i> ₂ = 4.17 × 10 ⁴ M ⁻¹ s ⁻¹ | | | |

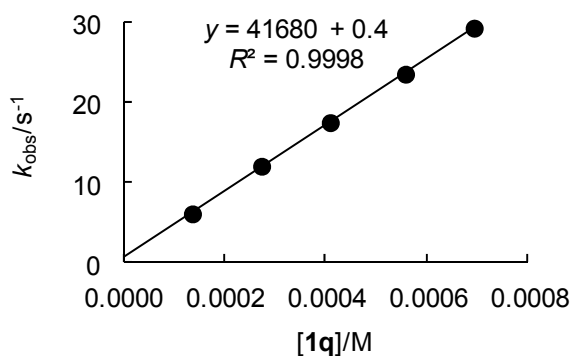


Table 6.87. Rate constants for the reactions of 9-azajulolidine (**1q**) with (pyr)₂CH⁺ BF₄⁻ (**Ee**) in CH₃CN (stopped-flow, 20 °C, λ = 611 nm).

| [Ee] ₀ /M | [1q] ₀ /M | [1q] ₀ /[Ee] ₀ | k _{obs} /s ⁻¹ |
|-------------------------|-------------------------|--------------------------------------|-----------------------------------|
| 7.17 × 10 ⁻⁶ | 6.92 × 10 ⁻⁵ | 10 | 2.18 × 10 ¹ |
| 7.17 × 10 ⁻⁶ | 1.04 × 10 ⁻⁴ | 15 | 3.23 × 10 ¹ |
| 7.17 × 10 ⁻⁶ | 1.44 × 10 ⁻⁴ | 20 | 4.45 × 10 ¹ |
| 7.17 × 10 ⁻⁶ | 1.73 × 10 ⁻⁴ | 24 | 5.34 × 10 ² |
| 7.17 × 10 ⁻⁶ | 2.13 × 10 ⁻⁴ | 30 | 6.52 × 10 ² |

$k_2 = 3.03 \times 10^5 \text{ M}^{-1} \text{ s}^{-1}$

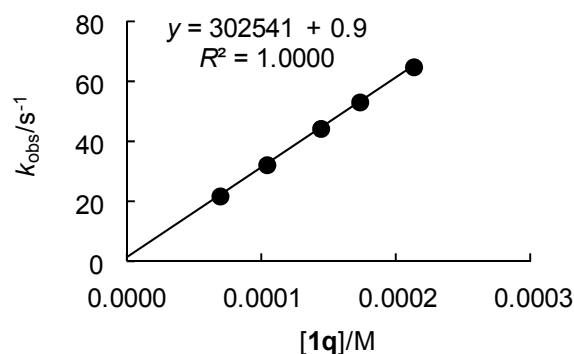


Table 6.88. Rate constants for the reactions of 9-azajulolidine (**1q**) with (dma)₂CH⁺ BF₄⁻ (**Ef**) in CH₃CN (stopped-flow, 20 °C, λ = 605 nm).

| [Ef] ₀ /M | [1q] ₀ /M | [1q] ₀ /[Ef] ₀ | k _{obs} /s ⁻¹ |
|-------------------------|-------------------------|--------------------------------------|-----------------------------------|
| 7.06 × 10 ⁻⁶ | 6.92 × 10 ⁻⁵ | 10 | 4.63 × 10 ¹ |
| 7.06 × 10 ⁻⁶ | 1.04 × 10 ⁻⁴ | 15 | 7.01 × 10 ¹ |
| 7.06 × 10 ⁻⁶ | 1.44 × 10 ⁻⁴ | 20 | 9.55 × 10 ¹ |
| 7.06 × 10 ⁻⁶ | 1.73 × 10 ⁻⁴ | 25 | 1.14 × 10 ² |
| 7.06 × 10 ⁻⁶ | 2.13 × 10 ⁻⁴ | 30 | 1.39 × 10 ² |

$k_2 = 6.43 \times 10^5 \text{ M}^{-1} \text{ s}^{-1}$

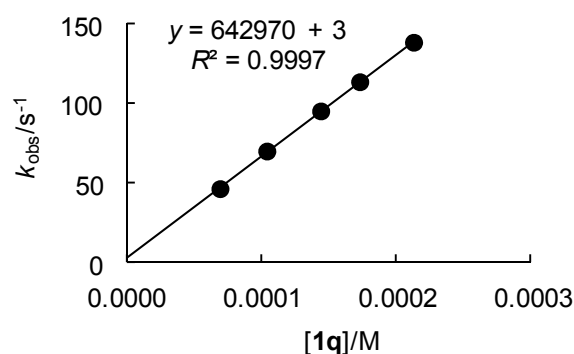
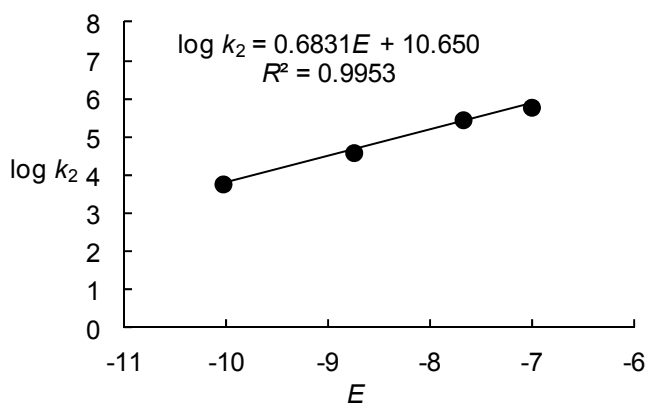


Table 6.89. Determination of the nucleophilicity parameters *N* and *s_N* for 9-azajulolidine (**1q**) in CH₃CN.

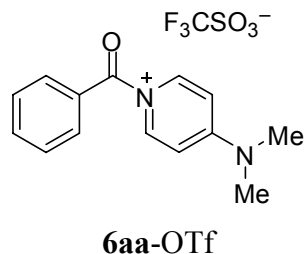
| Electrophile (<i>E</i>) | k ₂ /M ⁻¹ s ⁻¹ | log k ₂ |
|-------------------------------------|---|--------------------|
| Ea (-10.04) ^[16c] | 6.30 × 10 ³ | 3.80 |
| Ec (-8.76) ^[16c] | 4.17 × 10 ⁴ | 4.62 |
| Ee (-7.69) ^[16c] | 3.03 × 10 ⁵ | 5.48 |
| Ef (-7.02) ^[16c] | 6.43 × 10 ⁵ | 5.81 |

$N = 15.59, s_N = 0.68$



6.4.3 Product Characterization

1-Benzoyl-4-(dimethylamino)pyridinium trifluoromethanesulfonate (**6aa**-OTf)



Benzoyl chloride (**2a**, 2.34 mL, 2.85 g, 20.3 mmol) and trimethylsilyl triflate (3.65 mL, 4.48 g, 20.2 mmol) were added to a solution of 4-dimethylaminopyridine (**1a**, 2.44 g, 20.0 mmol) in CHCl₃ (10 mL) at -60 °C. The solution was warmed to RT over 1h, and the colorless precipitate was filtered off and dried under reduced pressure: **6aa**-OTf (7.04 g, 18.7 mmol, 94%).

¹H NMR (400 MHz, CD₃CN): δ = 3.34 (s, 6 H, 2 \times CH₃), 6.98 (d, J = 8.2 Hz, 2 H, H_{Ar}), 7.62–7.67 (m, 2 H, H_{Ar}), 7.76–7.82 (m, 3 H, H_{Ar}), 8.38 (d, J = 8.3 Hz, 2 H, H_{Ar}).

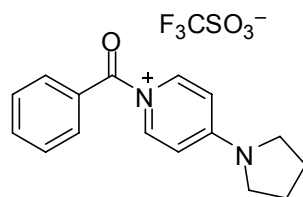
¹³C NMR (100 MHz, CD₃CN): δ = 41.7 (q), 108.1 (d), 122.1 (q, ¹ $J_{C,F}$ = 320 Hz), 129.9 (s), 130.2 (d), 131.7 (d), 135.5 (d), 139.4 (d), 159.5 (s), 168.9 (s).

IR (ATR): $\tilde{\nu}$ /cm⁻¹ = 3076 (w), 1719 (m), 1641 (s), 1593 (m), 1344 (w), 1262 (s), 1210 (m), 1147 (m), 1113 (s), 1030 (s), 999 (w), 928 (m), 837 (w), 804 (m), 763 (m), 755 (m), 727 (s), 708 (s), 633 (m).

HRMS (ESI, positive) m/z calcd. for C₁₄H₁₅N₂O⁺: 227.1179, found: 227.1178.

Anal. calcd for C₁₅H₁₅F₃N₂O₄S (376.35): C, 47.87; H, 4.02; N, 7.44; S, 8.52; found: C, 47.56; H, 4.08; N, 7.52; S, 8.67.

1-Benzoyl-4-(pyrrolidin-1-yl)pyridinium trifluoromethanesulfonate (**6ab**-OTf)



6ab-OTf

Benzoyl chloride (**2a**, 1.17 mL, 1.5 g, 10.2 mmol) and trimethylsilyl triflate (1.83 mL, 2.25 g, 10.1 mmol) were added to a solution of 4-(1-pyrrolidinyl)pyridine (**1b**, 1.48 g, 9.99 mmol) in CH₂Cl₂ (20 mL) at -60 °C. The solution was warmed to RT over 1h, and Et₂O (40 mL) was added dropwise. The colorless precipitate was filtered off and dried under reduced pressure: **6ab**-OTf (3.73 g, 9.27 mmol, 93%).

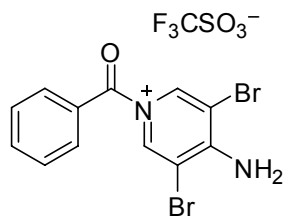
¹H NMR (400 MHz, CD₃CN): δ = 2.09–2.13 (m, 4 H, 2 \times CH₂), 3.66–3.69 (m, 4 H, 2 \times NCH₂), 6.83 (d, J = 8.2 Hz, 2 H, H_{Ar}), 7.62–7.67 (m, 2 H, H_{Ar}), 7.76–7.83 (m, 3 H, H_{Ar}), 8.36 (d, J = 8.2 Hz, 2 H, H_{Ar}).

¹³C NMR (100 MHz, CD₃CN): δ = 25.6 (t), 50.9 (t), 108.9 (d), 122.2 (q, ¹ $J_{C,F}$ = 321 Hz), 130.0 (s), 130.2 (d), 131.6 (d), 135.5 (d), 139.3 (d), 156.5 (s), 169.1 (s).

HRMS (ESI, positive) m/z calcd. for C₁₆H₁₇N₂O⁺: 253.1335, found: 253.1335.

Anal. calcd for C₁₇H₁₇F₃N₂O₄S (402.39): C, 50.74; H, 4.26; N, 6.96; S, 7.97; found: C, 50.62; H, 4.27; N, 6.94; S, 8.13.

4-Amino-1-benzoyl-3,5-dibromopyridinium trifluoromethanesulfonate (**6ae**-OTf)



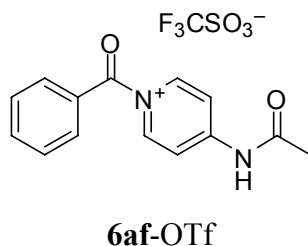
6ae-OTf

Benzoyl chloride (**2a**, 122 μL , 149. mg, 1.06 mmol) and trimethylsilyl triflate (181 μL , 222 mg, 1.00 mmol) were added to a solution of 4-amino-3,5-dibromopyridine (**1e**, 252 mg, 1.00 mmol) in CH_3CN (10 mL) at RT. The formed precipitate dissolved within one minute and the solution was stirred for 1h at RT. Et_2O (20 mL) was added dropwise, and the colorless precipitate was filtered off and dried under reduced pressure: **6ae-OTf** (376 mg, 0.743 mmol, 74%).

^1H NMR (400 MHz, CD_3CN): δ = 7.64–7.70 (m, 2 H, H_{Ar}), 7.82–7.89 (m, 3 H, H_{Ar}), 8.01 (s br, 2 H, NH_2), 8.75 (s, 2 H, H_{Ar}).

^{13}C NMR (100 MHz, CD_3CN): δ = 104.7 (s), 122.1 (q, $^1J_{\text{C,F}} = 321$ Hz), 128.4 (s), 130.6 (d), 132.4 (d), 136.7 (d), 141.4 (d), 158.9 (s), 166.9 (s).

4-Acetamido-1-benzoylpyridinium trifluoromethanesulfonate (**6af-OTf**)

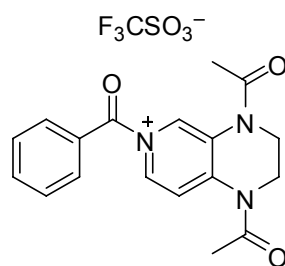


Benzoyl chloride (**2a**, 232 μL , 283 mg, 2.01 mmol) and trimethylsilyl triflate (361 μL , 0.443 mg, 1.99 mmol) were added to a solution of *N*-acetyl-4-aminopyridine (**1f**, 272 mg, 2.00 mmol) in CH_3CN (20 mL) at 0 $^\circ\text{C}$. The solution was stirred for 1h at RT, and Et_2O (40 mL) was added dropwise. The colorless precipitate was filtered off and dried under reduced pressure: **6af-OTf** (636 mg, 1.63 mmol, 81%).

^1H NMR (400 MHz, CD_3CN): δ = 2.30 (s, 3 H, CH_3), 7.66–7.72 (m, 2 H, H_{Ar}), 7.84–7.91 (m, 3 H, H_{Ar}), 8.15 (d br, $J = 6.5$ Hz, 2 H, H_{Ar}), 8.82 (d, $J = 7.8$ Hz, 2 H, H_{Ar}), 10.30 (s br, 1 H, NH).

^{13}C NMR (100 MHz, CD_3CN): δ = 25.3 (t), 114.6 (d), 122.0 (q, $^1J_{\text{C,F}} = 320$ Hz), 128.4 (s), 130.5 (d), 132.7 (d), 136.8 (d), 143.9 (d), 158.0 (s), 168.2 (s), 172.3 (s).

1,4-Diacetyl-6-benzoyl-1,2,3,4-tetrahydropyrido[3,4-*b*]pyrazin-6-ium trifluoromethanesulfonate (**6ak-OTf**)



6ak-OTf

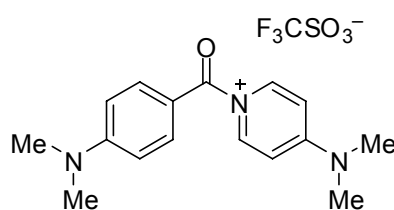
Benzoyl chloride (**2a**, 105 μ L, 128 mg, 0.911 mmol) and trimethylsilyl triflate (160 μ L, 200 mg, 0.901 mmol) were added to a solution of 1,1'-(2,3-dihydropyrido[3,4-*b*]pyrazine-1,4-diyl)diethanone (**1k**, 186 mg, 0.848 mmol) in CH₃CN (10 mL) at 0 °C. The solution was stirred for 1h at RT, and Et₂O (40 mL) was added dropwise. The yellow precipitate was filtered off and dried under reduced pressure: **6ak-OTf** (336 mg, 0.710 mmol, 84%).

¹H NMR (400 MHz, CD₃CN): δ = 2.30 (s, 3 H, CH₃), 2.46 (s, 3 H, CH₃), 3.98–4.02 (m, 2 H, CH₂), 4.10–4.14 (m, 2 H, CH₂), 7.66–7.72 (m, 2 H, H_{Ar}), 7.86–7.93 (m, 3 H, H_{Ar}), 8.61 (dd, J = 7.8, 2.0 Hz, 1 H, H_{Ar}), 8.88(d, J = 7.7 Hz, 1 H, H_{Ar}), 8.15 (s br, 1 H, H_{Ar}).

¹³C NMR (100 MHz, CD₃CN):^[a] δ = 23.1 (q), 25.4 (q), 48.1 (t), 116.9 (d), 122.0 (q, ¹ $J_{C,F}$ = 320 Hz), 128.2 (d), 130.3 (s), 130.4 (d), 130.5 (s), 132.8 (d), 136.9 (d), 137.4 (d), 167.9 (s), 174.0 (s).

[a] one quaternary carbon is superimposed.

(4-Dimethylamino)-1-(4-dimethylaminobenzoyl)pyridinium trifluoromethanesulfonate (**6ba-OTf**)



6ba-OTf

4-Dimethylaminobenzoyl chloride (**2b**, 210 mg, 1.14 mmol) and trimethylsilyl triflate (207 μ L, 0.254 mg, 1.14 mmol) were added to a solution of 4-dimethylaminopyridine (**1a**, 134 mg, 1.10 mmol) in CH₂Cl₂ (20 mL) at -40 °C. The solution was warmed to RT over 30 min, and Et₂O (40 mL) was added dropwise. The yellow precipitate was filtered off and dried under reduced pressure: **6ba**-OTf (119 mg, 0.761 mmol, 69%).

¹H NMR (400 MHz, CD₃CN): δ = 3.11 (s, 6 H, 2 \times CH₃), 3.31 (s, 6 H, 2 \times CH₃), 6.81 (d, *J* = 9.2 Hz, 2 H, H_{Ar}), 6.93 (d, *J* = 8.1 Hz, 2 H, H_{Ar}), 7.64 (d, *J* = 9.3 Hz, 2 H, H_{Ar}), 8.34 (d, *J* = 8.1 Hz, 2 H, H_{Ar}).

¹³C NMR (100 MHz, CD₃CN): δ = 40.4 (q), 41.4 (q), 107.7 (d), 112.2 (d), 114.0 (s), 122.2 (q, ¹*J*_{C,F} = 320 Hz), 134.8 (d), 140.1 (d), 156.0 (s), 159.3 (s), 167.7 (s).

HRMS (ESI, positive) *m/z* calcd. for C₁₆H₂₀N₃O⁺: 270.1601, found: 270.1592.

6.5 References

- [1] C. E. Müller, P. R. Schreiner, *Angew. Chem.* **2011**, *123*, 6136–6167; *Angew. Chem. Int. Ed.* **2011**, *50*, 6012–6042.
- [2] N. De Rycke, F. Couty, O. R. P. David, *Chem. Eur. J.* **2011**, *17*, 12852–12871.
- [3] A. Einhorn, F. Hollandt, *Liebigs Ann. Chem.* **1898**, *301*, 95–115.
- [4] a) G. Höfle, W. Steglich, H. Vorbrüggen, *Angew. Chem.* **1969**, *81*, 1001; *Angew. Chem. Int. Ed. Engl.* **1969**, *8*, 981. b) L. M. Litvinenko, A. I. Kirichenko, *Dokl. Akad. Nauk SSSR, Ser. Khim.* **1967**, *176*, 97–100.
- [5] R. Murugan, E. F. V. Scriven, *Aldrichimica Acta* **2003**, *36*, 21–27.
- [6] W. Steglich, G. Höfle, *Tetrahedron Lett.* **1970**, *11*, 4727–4730.
- [7] M. R. Heinrich, H. S. Klisa, H. Mayr, W. Steglich, H. Zipse, *Angew. Chem.* **2003**, *115*, 4975–4977; *Angew. Chem. Int. Ed.* **2003**, *42*, 4826–4828.
- [8] I. Held, S. Xu, H. Zipse, *Synthesis* **2007**, *8*, 1185–1196.
- [9] S. Singh, G. Das, O. V. Singh, H. Han, *Org. Lett.* **2007**, *9*, 401–404.
- [10] N. De Rycke, G. Berionni, F. Couty, H. Mayr, R. Goumont, O. R. P. David, *Org. Lett.* **2011**, *13*, 530–533.
- [11] A. C. Spivey, S. Arseniyadis, *Angew. Chem.* **2004**, *116*, 5552–5557; *Angew. Chem. Int. Ed.* **2004**, *43*, 5436–5441 and references cited therein.

- [12] a) S. Xu, I. Held, B. Kempf, H. Mayr, W. Steglich, H. Zipse, *Chem. Eur. J.* **2005**, *11*, 4751–4757.
- [13] I. Held, A. Villinger, H. Zipse, *Synthesis* **2005**, 1425–1430.
- [14] F. Brotzel, B. Kempf, T. Singer, H. Zipse, H. Mayr, *Chem. Eur. J.* **2007**, *13*, 336–345.
- [15] T. A. Nigst, J. Ammer, H. Mayr, *J. Phys. Chem. A* **2012**, *116*, 8494–8499.
- [16] a) H. Mayr, B. Kempf, A. R. Ofial, *Acc. Chem. Res.* **2003**, *36*, 66–77; b) R. Lucius, R. Loos, H. Mayr, *Angew. Chem.* **2002**, *114*, 97–102; *Angew. Chem. Int. Ed.* **2002**, *41*, 91–95; c) H. Mayr, T. Bug, M. F. Gotta, N. Hering, B. Irrgang, B. Janker, B. Kempf, R. Loos, A. R. Ofial, G. Remennikov, H. Schimmel, *J. Am. Chem. Soc.* **2001**, *123*, 9500–9512; d) H. Mayr, M. Patz, *Angew. Chem.* **1994**, *106*, 990–1010; *Angew. Chem. Int. Ed. Engl.* **1994**, *33*, 938–957; e) for a comprehensive listing of nucleophilicity parameters N , s_N and electrophilicity parameters, E , see <http://www.cup.uni-muenchen.de/oc/mayr/DBintro.html>.
- [17] M. S. Wolfe, *Synthetic Commun.* **1997**, *27*, 2975–2984.
- [18] a) R. Yamaguchi, B. Hatano, T. Nakayasu, S. Kozima, *Tetrahedron Lett.* **1997**, *38*, 403–406; b) R. Yamaguchi, Y. Omoto, M. Miyake, K. Fujita, *Chem. Lett.* **1998**, 547–548.
- [19] J. Pabel, C. E. Hösl, M. Maurus, M. Ege, K. T. Wanner, *J. Org. Chem.* **2000**, *65*, 9272–9275.
- [20] R. A. Jonas, A. R. Katritzky, *J. Chem. Soc.* **1959**, 1317–1323.
- [21] T. A. Nigst, *Diplomarbeit*, Ludwig-Maximilians-Universität München, **2007**.
- [22] R. Schmid, V. N. Sapunov, *Non-formal kinetics*, Verlag Chemie, Weinheim, **1981**.
- [23] T. A. Nigst, H. Mayr, manuscript in preparation.
- [24] a) R. P. Wurz, E. C. Lee, J. C. Ruble, G. C. Fu, *Adv. Synth. Catal.* **2007**, *349*, 2345–2352; b) E. Bappert, P. Mueller, G. C. Fu, *Chem. Commun.* **2006**, 2604–2606; c) G. C. Fu, *Acc. Chem. Res.* **2004**, *37*, 542–547; d) S. Arai, S. Bellemin-Laponnaz, G. C. Fu, *Angew. Chem.* **2001**, *113*, 240–242; *Angew. Chem. Int. Ed.* **2001**, *40*, 234–236.
- [25] C. Hansch, A. Leo, R. W. Taft, *Chem. Rev.* **1991**, *91*, 165–195.
- [26] Y. Tsuno, M. Fujio, *Chem. Soc. Rev.* **1996**, *25*, 129–139.
- [27] a) D. P. N. Satchell, R. S. Satchell in *Supplement B: The chemistry of acid derivatives*, Vol. 2 (Ed.: S. Patai), John Wiley & Sons, New York, **1992**, pp. 748–802; b) A. Williams, *Acc. Chem. Res.* **1989**, *22*, 387–392.
- [28] For abbreviations of benzhydrylium ions see: Ref. [16c].

Chapter 7

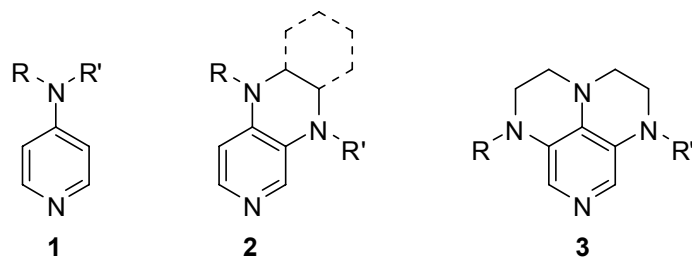
INDUCTIVE EFFECTS THROUGH ALKYL GROUPS — HOW LONG IS LONG ENOUGH?

Raman Tandon, Tobias A. Nigst, and Hendrik Zipse, manuscript in preparation.

The results obtained by R. Tandon are not listed in the Experimental Section.

7.1 Introduction

The influence of alkyl groups of variable length on ground state properties of organic molecules and on their reaction rates in unimolecular and bimolecular transformations has been discussed in terms of steric and electronic substituent effects.^[1] The latter of these may be divided further into inductive (through-bond) and field (through-space) components. A strict separation of these components is difficult. In recent efforts to develop nucleophilic catalysts of enhanced reactivity and selectivity, we^[2] and others^[3] explored the performance of alkyl-substituted aminopyridines of general formula **1**, **2**, and **3** in pyridine-catalyzed acylation reactions of tertiary alcohols (Figure 7.1). These compounds are highly active nucleophilic catalysts with small alkyl substituents such as R = methyl or ethyl, and the question arose whether if the catalytic efficiency can be increased by elongation of the alkyl groups.



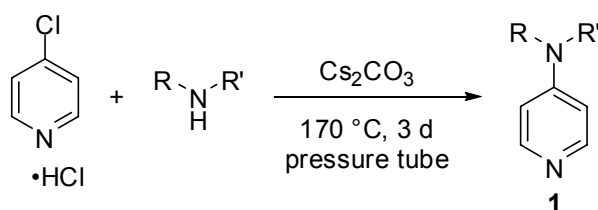
R, R' = **a** Me, Me; **b** Me, Et; **c** Et, Et; **d** *n*Bu, *n*Bu; **e** *n*Bu, *n*Bu;
f *n*Pent, *n*Pent; **g** *n*Hex, *n*Hex; **h** *n*Oct, *n*Oct

Figure 7.1. Structures of pyridine derivatives used as nucleophilic catalysts.

In more general terms this poses the question of the chain length dependence of inductive effects in general. We report here the effects of chain elongation of the alkyl groups on 4-alkylaminopyridines on the rates of pyridine-catalyzed acylations of alcohols, the benzylation of the pyridines, the reactions of *N*-benzoylpyridinium ions with benzylamine, and theoretically calculated acetylation enthalpies to provide a quantitative answer.

7.2 Results and Discussion

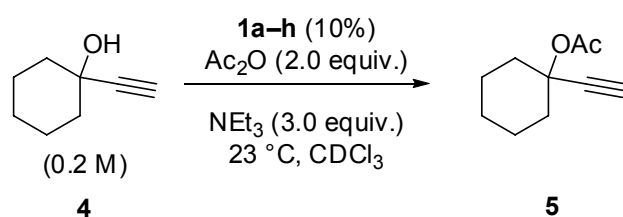
The aminopyridines **1a–h** were synthesized by treatment of 4-chloropyridine with the corresponding dialkylamines following established procedures in the literature (Scheme 7.1).^[4]



R, R' = **a** Me, Me; **b** Me, Et; **c** Et, Et; **d** *n*Bu, *n*Bu; **e** *n*Bu, *n*Bu;
f *n*Pent, *n*Pent; **g** *n*Hex, *n*Hex; **h** *n*Oct, *n*Oct

Scheme 7.1 Synthesis of pyridine derivatives **1a–h**.

The catalytic potential of these catalysts has been explored by an ¹H NMR spectroscopic investigation of the acetylation of the tertiary alcohol **4** with acetic anhydride (Scheme 7.2). All reactions eventually proceeded to full conversion, and the rates of the reactions were thus characterized by the reaction half-life $\tau_{1/2}$ using the approach described previously (Table 7.1).^[2b]



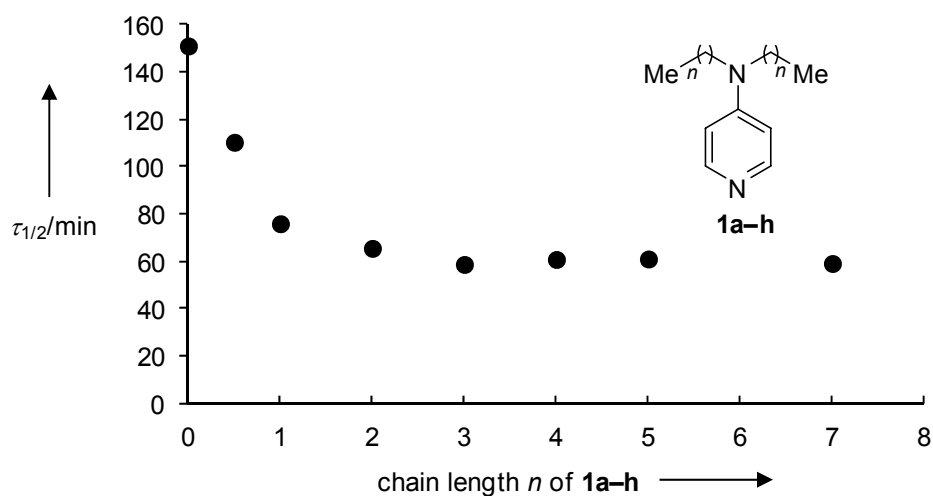
Scheme 7.2 ¹H NMR benchmark reaction in CDCl₃.

Table 7.1. Half-lives for the pyridine catalyzed reactions of **4** with acetic anhydride.

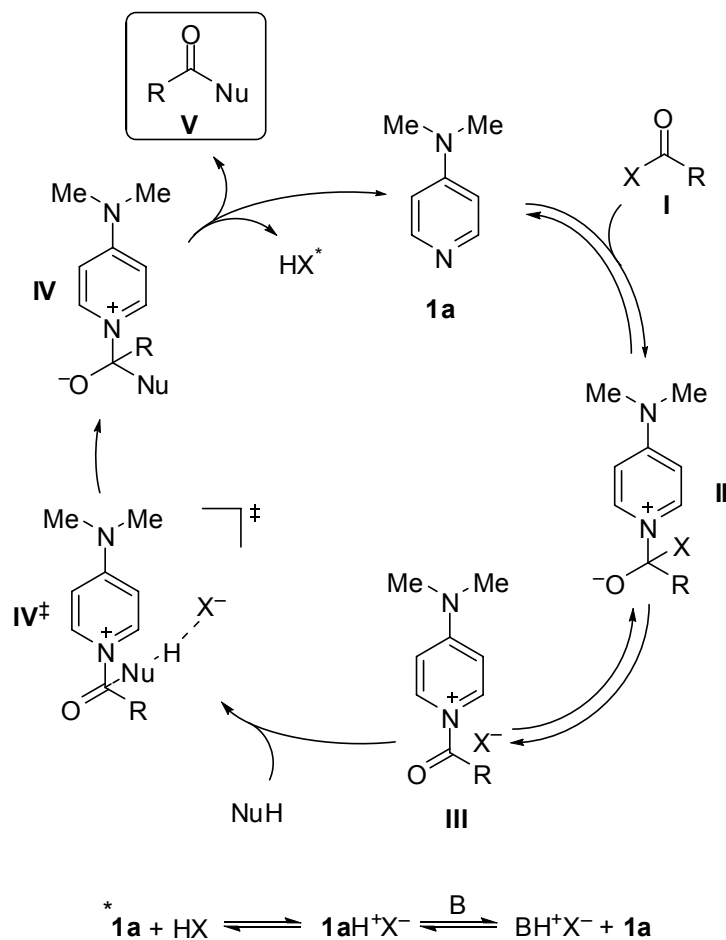
| Catalyst | $\tau_{1/2}/\text{min}$ |
|-----------|-------------------------|
| 1a | $151.0 \pm 1.7^{[a]}$ |
| 1b | 110.3 ± 0.2 |
| 1c | 74.9 ± 0.6 |
| 1d | 65.5 ± 0.4 |
| 1e | 58.7 ± 1.6 |
| 1f | 60.8 ± 0.3 |
| 1g | 61.0 ± 0.2 |
| 1h | 59.1 ± 0.5 |

[a] From Ref. [2b].

In the above mentioned benchmark reaction, the catalytic activity increases with the chain length of the alkyl substituents on the 4-amino group by a factor of 2.6 from DMAP (**1a**) to 4-di-*n*-octylaminopyridine (**1h**), which has an activity comparable to that of 4-(pyrrolidino)pyridine or **2c**.^[2d] R = butyl is the optimum choice between chain length and activity, since elongation of the chain from butyl to octyl did not lead to increased activities. The perfect fit of **1b** with the data of the symmetrically substituted aminopyridines shows that the inductive effects on the 4-amino group are cumulative (Figure 7.2).

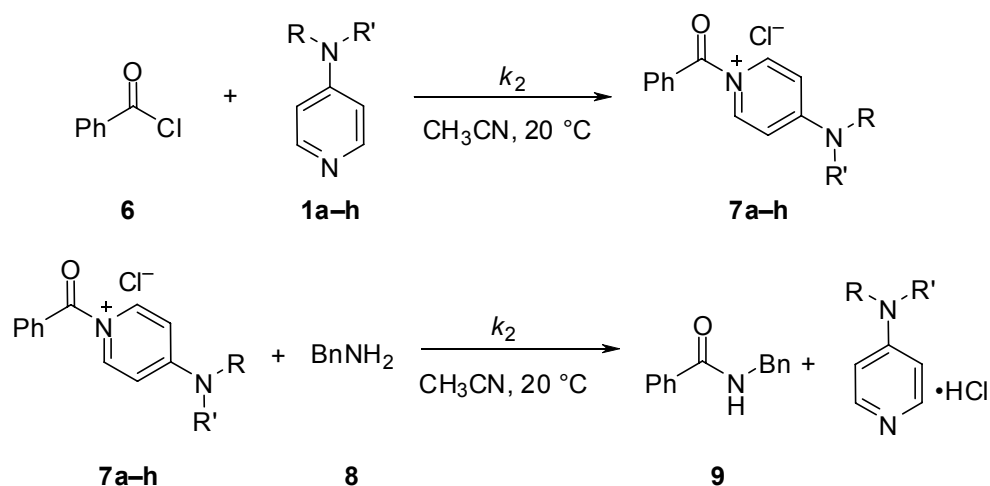
**Figure 7.2.** Correlation of the half-life times versus the length of the *N*-alkyl chains of **1a-1h**.

N-Acylpyridinium ions have been proposed as the key intermediates of the catalytic cycle for the acylation reactions described above (Scheme 7.2).^[5]



Scheme 7.2. Simplified mechanism for the DMAP-catalyzed acylation reaction.

In a first step the nucleophilic catalyst reacts with the acyl donor in a fast pre-equilibrium to form an *N*-acylpyridinium ion **III**. In the rate-determining, second step the acylated catalyst reacts with the alcohol to form the acylated product **V** after elimination of DMAP (**1a**). Herein we will report the kinetics of two model reactions for the individual steps of a pyridine-catalyzed acylation reaction (Scheme 7.3).



Scheme 7.3. Reaction of benzoyl chloride (**6**) with pyridines **1a–h** and aminolysis reactions of the thus formed *N*-benzoylpyridinium chlorides **7a–h** with benzylamine (**8**) in acetonitrile.

The kinetics of the model reactions were followed by UV/Vis spectrophotometry under first order conditions monitoring the absorbances of the *N*-benzoylpyridinium chloride **7a–h** as described previously.^[6] For all reactions monoexponential increases or decays of the absorbances **7a–h** were observed and the first-order rate constants k_{obs} were obtained by least-squares fitting of the exponential functions $A = A_0(1 - e^{-k_{\text{obs}}t}) + C$ or $A = A_0e^{-k_{\text{obs}}t} + C$ to the time-dependent absorbances. Plots of k_{obs} versus the concentration of the compound in excess (**6** or **8**, respectively) were linear and the second-order rate constants k_2 (Table 7.2) were obtained as the slopes of these plots. The intercepts of the plots were close to zero, in line with the quantitative courses of the reaction.

While the reactivities of the pyridines **1a–h** towards benzoyl chloride (**6**) increase with the chain length of the alkyl groups by a factor of 1.5, a decrease of the reactivities of the *N*-benzoylpyridinium ions **7a–h** by a factor of 1.3 was observed. Similar to the pyridine-catalyzed acylation reactions of **4**, saturation of the inductive effects of the alkyl groups are observed already at R = butyl (Figures 7.3 and 7.4).

Table 7.2. Second-order rate constants for the reactions of benzoyl chloride (**6**) with pyridines **1a–h** and *N*-benzoylpyridinium chlorides **7a–h** with benzylamine (**8**) in acetonitrile at 20 °C.

| | $k_2/\text{M}^{-1} \text{s}^{-1}$ | $k_2/\text{M}^{-1} \text{s}^{-1}$ |
|-----------|-----------------------------------|-----------------------------------|
| 1a | 3.00×10^4 [a] | 7a 4.78×10^2 [b] |
| 1b | 3.36×10^4 | 7b 4.11×10^2 |
| 1c | 4.06×10^4 | 7c 3.78×10^2 |
| 1e | 4.14×10^4 | 7e 3.68×10^2 |
| 1g | 4.13×10^4 | 7g 3.53×10^2 |
| 1h | 4.37×10^4 | 7h 3.69×10^2 |

[a] From Ref. [7]. [b] From Ref. [6].

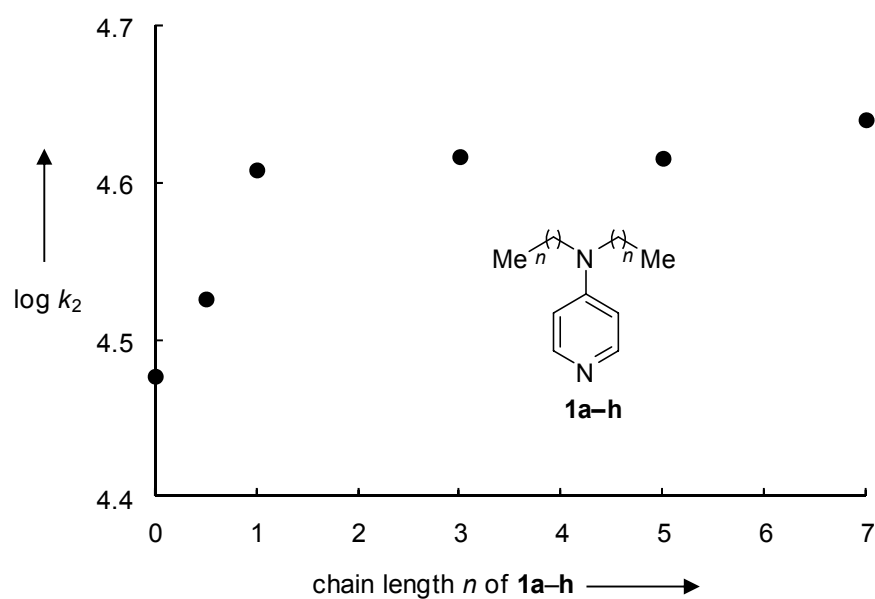


Figure 7.3. Correlation of the second-order rate constants k_2 for the reactions of **1a–h** with benzoyl chloride (**6**) versus the length of the *N*-alkyl chains of **1a–h**.

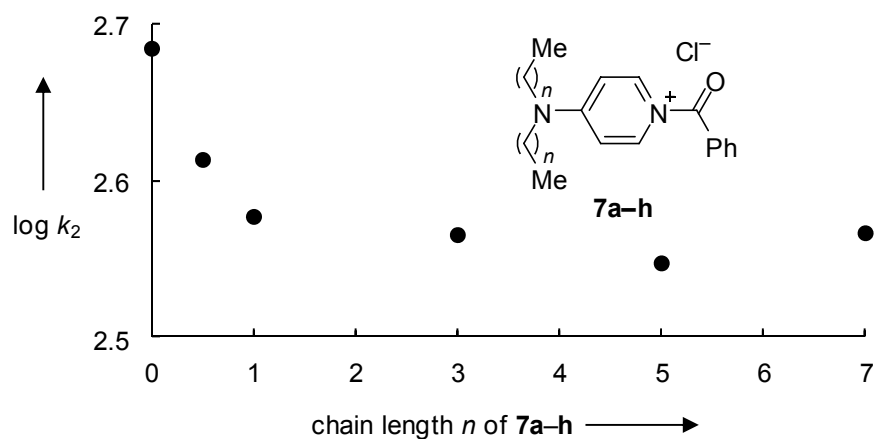
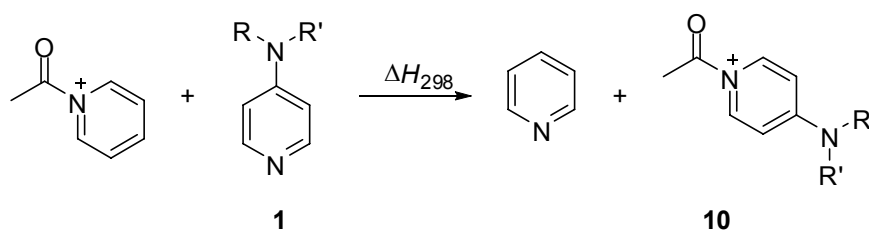


Figure 7.4. Correlation of the second-order rate constants k_2 for the reactions of **7a-h** with benzylamine (**8**) versus the length of the *N*-alkyl chains of **7a-h**.

It has been noted before that the stabilities of the acyl intermediates can be used as a quantitative indicator for the catalytic performance of the respective pyridines.^[2b] Thus, relative acetylation enthalpies for **1a-1h** were calculated at the MP2(FC)/6-31+G(2d,p)//B98/6-31G(d) level according to the isodesmic reaction depicted in Scheme 7.4.



Scheme 7.4. Isodesmic reaction for the calculation of acetylation enthalpies.

For the catalysts **1a-d** all possible conformers within a 30 kJ range were taken into account. Conformers for catalysts **1e-1h** were generated from **1d** by adding the required number of CH₂-groups all staggered. The Boltzmann distribution was used to calculate the statistical weight of the individual conformers and averaged energies were used for the calculation of the acetylation enthalpies (ΔH_{298} averaged). Additionally, acetylation enthalpies were computed for the most favored conformers of **1a-h** and the corresponding acylated conformers, even if the latter were not energetically favored (ΔH_{298} selected).

Table 7.3 shows a summary of the calculated reaction enthalpies for catalysts **1a–h** for the Boltzmann averaged conformers (second and third column), the best conformers (fourth and fifth column, Figure 7.5) and selected conformers (sixth and seventh column).

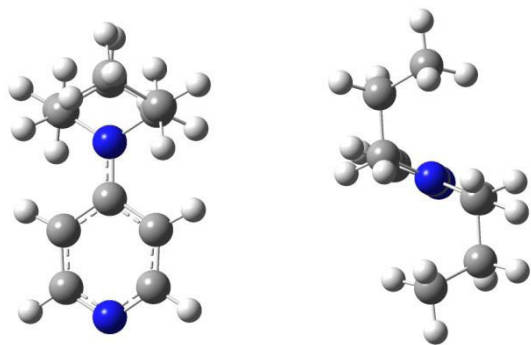


Figure 7.5. Best conformer of **1d** from front view (left) and top view (right).

Table 7.3. Acetylation enthalpies (kJ/mol) for **1a–h** according to Scheme 7.4 for the Boltzmann averaged, selected and best conformers calculated at MP2-5 and level of theory or G3MP2B3 in the gas phase and in CHCl₃ solution.

| catalyst | ΔH_{298} averaged | | ΔH_{298} best | | ΔH_{298} selected | | ΔH_{298} G3MP2B3 |
|-----------|------------------------------|-----------|--------------------------|-----------|------------------------------|-----------|-----------------------------|
| | gas phase | solvation | gas phase | solvation | gas phase | solvation | gas phase |
| 1a | -77.1 | -61.2 | -77.1 | -61.2 | -77.1 | -61.2 | -81.8 |
| 1b | -81.6 | -63.3 | -81.9 | -63.6 | -81.3 | -62.9 | -86.6 |
| 1c | -87.6 | -67.1 | -88.2 | -67.8 | -88.2 | -67.7 | -92.6 |
| 1d | -90.1 | -66.1 | -90.6 | -66.1 | -88.9 | -65.5 | -93.9 |
| 1e | -93.2 | -67.9 | -92.2 | -67.1 | -92.1 | -67.1 | -97.3 |
| 1f | -94.1 | -67.8 | -93.2 | -67.6 | -93.2 | -67.1 | -98.6 |
| 1g | -94.8 | -68.1 | -94.2 | -67.4 | -94.2 | -67.4 | -99.6 |
| 1h | -96.7 | -68.5 | -95.0 | -68.2 | -95.0 | -67.4 | – |

The plots of the Boltzmann averaged and best acetylation enthalpies versus the number of C-atoms in **1a–h** do not show a saturation effect similar to that discussed above (triangles in Figure 7.6). Due to the huge possible numbers of conformers in **1e–h** a big part of the

conformational space might not be covered by the restrictions made for the generation of conformers.

In order to account for solvent effects, the acetylation enthalpies were also calculated in chloroform using the PCM approach at the HF/6-31G(d) level with UAHF radii. When the solvation energies are included for the correlation, the plot of the acetylation enthalpies versus the number of C-atoms exhibits the experimentally observed saturation effect beyond four C-atoms (circles in Figure 7.6). As the acylation enthalpies obtained for the selected conformers at the G3MP2B3 level of theory resembled those at the MP2-5 level of theory, we omitted to analyse of the full conformational space at the higher level of theory.

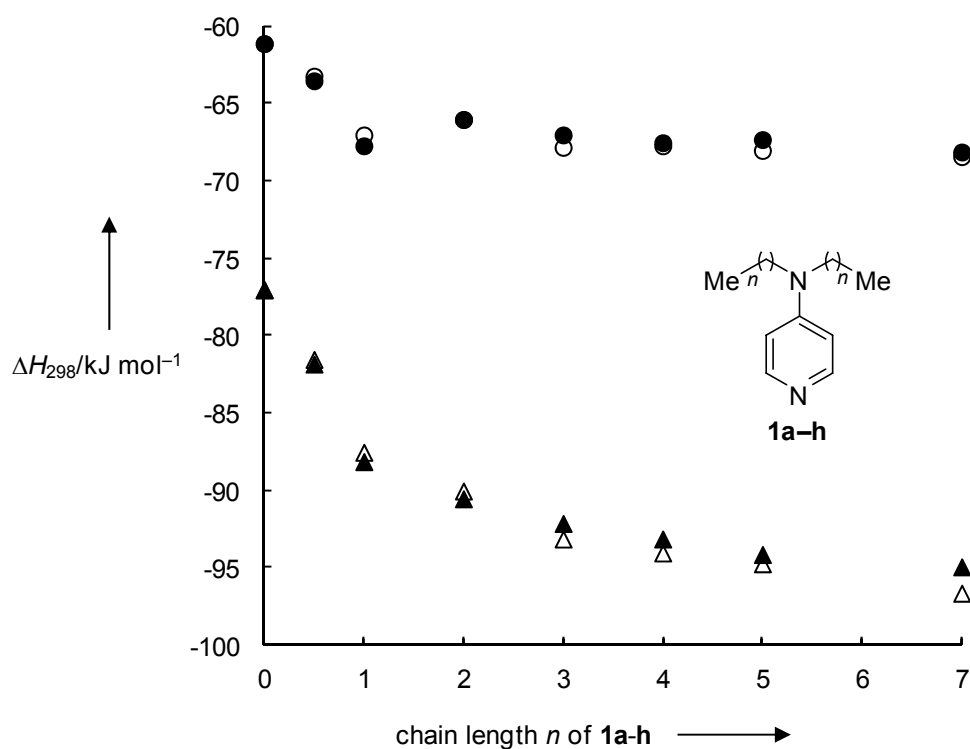


Figure 7.6. Enthalpies for the isodesmic reaction of Scheme 7.4 versus the length of the *N*-alkyl chains of **1a–h** (open symbols: ΔH_{298} averaged; closed symbols: ΔH_{298} best; triangles: in gas phase; circles: in chloroform solution)

Analysis of the structures of the best conformers of the acetylated pyridines showed that the inductive effects also affect the bond lengths between the reacting centers (Table 7.4), that is,

the pyridine nitrogen and the carbonyl group, which decreased with increasing nucleophilicity of the pyridines (Figure 7.7).

Table 7.4. N-C bond lengths of the acylated catalysts **10a–h**.

| Acylated Catalyst | N-C Bond Length/pm |
|-------------------|--------------------|
| 10a | 148.288 |
| 10b | 148.081 |
| 10c | 147.861 |
| 10d | 147.685 |
| 10e | 147.644 |
| 10f | 147.531 |
| 10g | 147.535 |
| 10h | 147.481 |

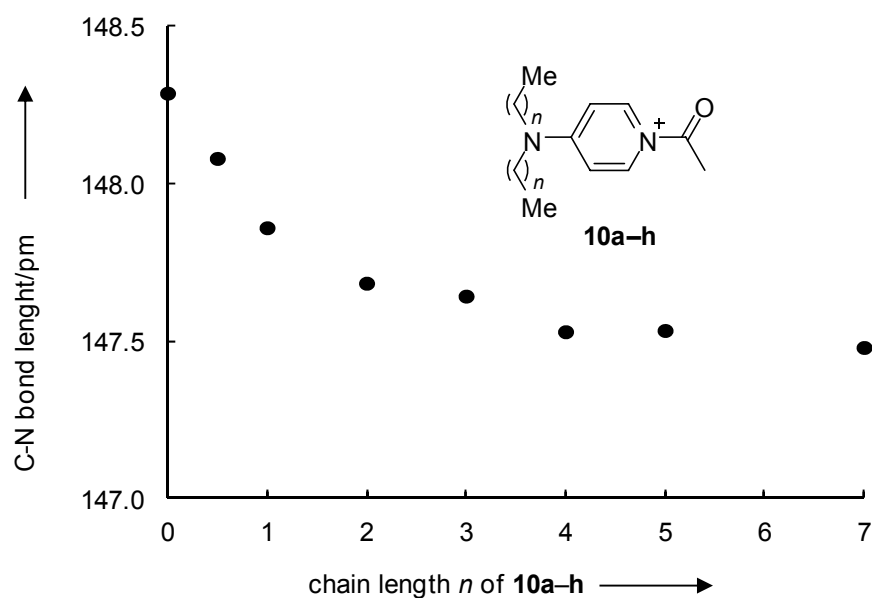


Figure 7.7. Correlation of the N-C bond lengths of the best conformers of **10a–h** versus the length of the N -alkyl chains of **10a–h**.

7.3 Conclusion

In summary, numerous properties of alkylaminopyridines show a saturation of substituent effects with the alkyl group chain lengths beyond four carbon atoms. We believe this to be a general result in situations lacking direct steric effects between alkyl substituents and the respective reaction centers.

7.4 Experimental Section

7.4.1 General Comment

Materials. Benzoyl chloride (**6**) and benzylamine (**8**) were purchased and purified by distillation prior to use.

Acetonitrile (> 99.9%, extra dry) was purchased and used without further purification.

Kinetics. The kinetics of the reactions of the pyridines **1b–h** with benzoyl chloride (**6**) and that of *N*-benzoylpyridinium chlorides **7b–h** with benzylamine (**8**) in acetonitrile at 20 °C were monitored by UV/Vis spectroscopy.

The stock solutions of the *N*-benzoylpyridinium chlorides **7b–h** were prepared by mixing benzoyl chloride (**6**) with 1.0 equivalents of the pyridines **1b–h** in acetonitrile.

Stopped-flow spectrophotometer systems (Applied Photophysics SX.18MV-R or Hi-Tech SF-61DX2) were used for the investigation of the reactions. The kinetic runs were initiated by mixing equal volumes of acetonitrile solutions of the electrophiles and the nucleophiles. The temperature of the solutions during the kinetic studies was maintained to 20 °C within ± 0.1 °C by using circulating bath cryostats.

Benzoyl chloride (**6**) was used in large excess (over 8 equivalents) relative to the pyridines **1b–h** to ensure first-order conditions with $k_{\text{obs}} = k_2[\text{Nu}]_0 + k_0$. For the reactions of *N*-benzoylpyridinium chlorides **7b–h** with benzylamine (**8**), the latter was used in excess. The first-order rate constants k_{obs} (s^{-1}) were obtained by least-squares fitting of the single-exponential curve $A_t = A_0 e^{-k_{\text{obs}} t} + C$ to the absorbances of the *N*-benzoylpyridinium chlorides **7b–h** at or close to λ_{max} . The slopes of the plot of k_{obs} versus the concentrations yielded the second order rate constant k_2 ($\text{M}^{-1} \text{s}^{-1}$).

7.4.2 Kinetic Experiments

Kinetics of the reactions of pyridines (1b–h) with benzoyl chloride (6) in CH₃CN

Table 7.5. Rate constants for the reactions of 4-(ethylmethylamino)pyridine (**1b**) with benzoyl chloride (**6**) in CH₃CN (20 °C, $\lambda = 320$ nm).

| [1b] ₀ /M | [6] ₀ /M | [6] ₀ /[1b] ₀ | $k_{\text{obs}}/\text{s}^{-1}$ |
|--|------------------------------|---|--------------------------------|
| 3.69×10^{-5} | 7.75×10^{-4} | 21 | 2.92×10^1 |
| 3.69×10^{-5} | 1.10×10^{-3} | 30 | 3.94×10^1 |
| 3.69×10^{-5} | 1.49×10^{-3} | 40 | 5.30×10^1 |
| 3.69×10^{-5} | 1.87×10^{-3} | 51 | 6.57×10^1 |
| 3.69×10^{-5} | 2.26×10^{-3} | 61 | 7.89×10^1 |
| $k_2 = 3.36 \times 10^4 \text{ M}^{-1} \text{ s}^{-1}$ | | | |

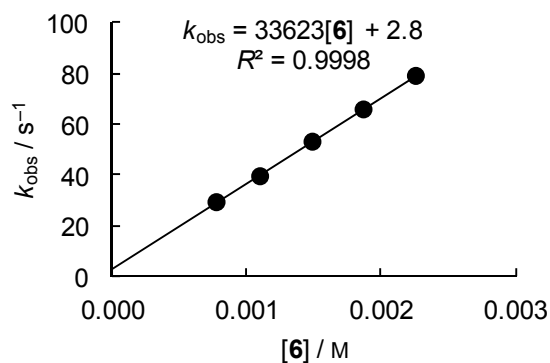


Table 7.6. Rate constants for the reactions of 4-(diethylamino)pyridine (**1c**) with benzoyl chloride (**6**) in CH₃CN (20 °C, $\lambda = 320$ nm).

| [1c] ₀ /M | [6] ₀ /M | [6] ₀ /[1c] ₀ | $k_{\text{obs}}/\text{s}^{-1}$ |
|--|------------------------------|---|--------------------------------|
| 3.71×10^{-5} | 7.75×10^{-4} | 21 | 3.46×10^1 |
| 3.71×10^{-5} | 1.10×10^{-3} | 30 | 4.71×10^1 |
| 3.71×10^{-5} | 1.49×10^{-3} | 40 | 6.32×10^1 |
| 3.71×10^{-5} | 1.87×10^{-3} | 50 | 7.79×10^1 |
| 3.71×10^{-5} | 2.26×10^{-3} | 61 | 9.51×10^1 |
| $k_2 = 4.06 \times 10^4 \text{ M}^{-1} \text{ s}^{-1}$ | | | |

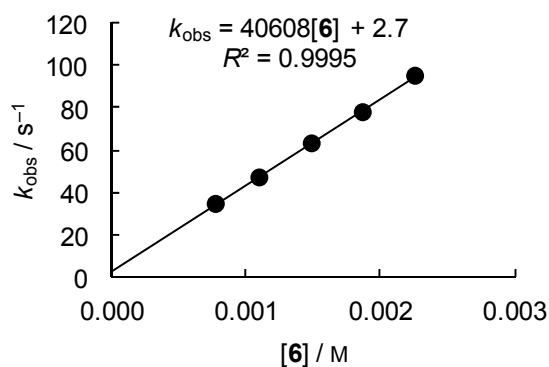
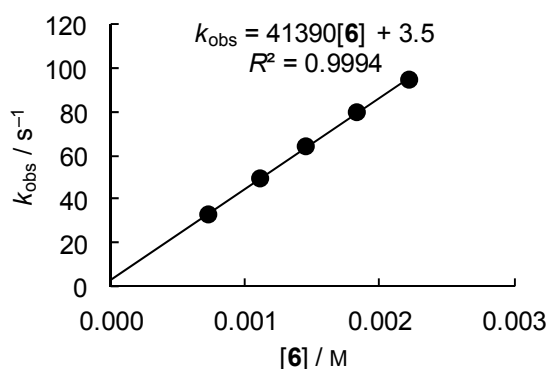
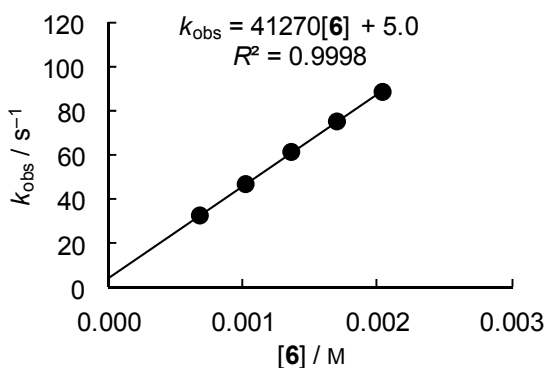


Table 7.7. Rate constants for the reactions of 4-(di-*n*-butylamino)pyridine (**1e**) with benzoyl chloride (**6**) in CH₃CN (20 °C, $\lambda = 320$ nm).

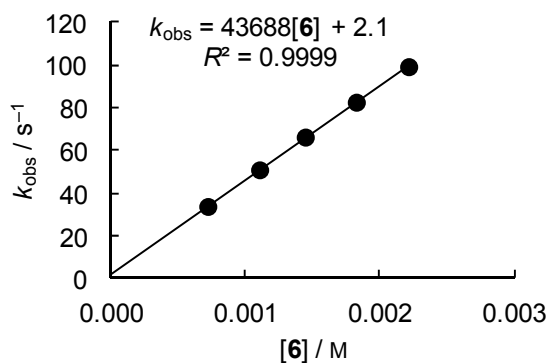
| [1e] ₀ /M | [6] ₀ /M | [6] ₀ /[1e] ₀ | $k_{\text{obs}}/\text{s}^{-1}$ |
|--|------------------------------|---|--------------------------------|
| 3.42×10^{-5} | 7.24×10^{-4} | 21 | 3.30×10^1 |
| 3.42×10^{-5} | 1.11×10^{-3} | 32 | 4.95×10^1 |
| 3.42×10^{-5} | 1.45×10^{-3} | 42 | 6.42×10^1 |
| 3.42×10^{-5} | 1.83×10^{-3} | 54 | 7.98×10^1 |
| 3.42×10^{-5} | 2.22×10^{-3} | 65 | 9.47×10^1 |
| $k_2 = 4.14 \times 10^4 \text{ M}^{-1} \text{ s}^{-1}$ | | | |

**Table 7.8.** Rate constants for the reactions of 4-(di-*n*-hexylamino)pyridine (**1g**) with benzoyl chloride (**6**) in CH₃CN (20 °C, $\lambda = 320$ nm).

| [1g] ₀ /M | [6] ₀ /M | [6] ₀ /[1g] ₀ | $k_{\text{obs}}/\text{s}^{-1}$ |
|--|------------------------------|---|--------------------------------|
| 3.40×10^{-5} | 6.79×10^{-4} | 20 | 3.28×10^1 |
| 3.40×10^{-5} | 1.02×10^{-3} | 30 | 4.70×10^1 |
| 3.40×10^{-5} | 1.36×10^{-3} | 40 | 6.16×10^1 |
| 3.40×10^{-5} | 1.70×10^{-3} | 50 | 7.54×10^1 |
| 3.40×10^{-5} | 2.04×10^{-3} | 60 | 8.88×10^1 |
| $k_2 = 4.13 \times 10^4 \text{ M}^{-1} \text{ s}^{-1}$ | | | |

**Table 7.9.** Rate constants for the reactions of 4-(di-*n*-oktylamino)pyridine (**1h**) with benzoyl chloride (**6**) in CH₃CN (20 °C, $\lambda = 320$ nm).

| [1h] ₀ /M | [6] ₀ /M | [6] ₀ /[1h] ₀ | $k_{\text{obs}}/\text{s}^{-1}$ |
|--|------------------------------|---|--------------------------------|
| 3.70×10^{-5} | 7.24×10^{-4} | 20 | 3.35×10^1 |
| 3.70×10^{-5} | 1.11×10^{-3} | 30 | 5.06×10^1 |
| 3.70×10^{-5} | 1.45×10^{-3} | 39 | 6.59×10^1 |
| 3.70×10^{-5} | 1.83×10^{-3} | 49 | 8.22×10^1 |
| 3.70×10^{-5} | 2.22×10^{-3} | 60 | 9.88×10^1 |
| $k_2 = 4.37 \times 10^4 \text{ M}^{-1} \text{ s}^{-1}$ | | | |



Kinetics of the reactions of N-benzoylpyridinium chlorides 7b–h with benzylamine (8) in CH₃CN

Table 7.10. Rate constants for the reactions of 1-benzoyl-4-(ethylmethylamino)pyridinium chloride (7b) generated from benzoyl chloride (6) and 4-(ethylmethylamino)pyridine (1b, 1.0 equiv.) with benzylamine (8) in CH₃CN (20 °C, λ = 320 nm).

| [7b] ₀ /M | [8] ₀ /M | [8] ₀ /[7b] ₀ | k _{obs} /s ⁻¹ |
|--|-------------------------|-------------------------------------|-----------------------------------|
| 3.32 × 10 ⁻⁵ | 6.41 × 10 ⁻⁴ | 19 | 2.69 × 10 ⁻¹ |
| 3.32 × 10 ⁻⁵ | 1.28 × 10 ⁻³ | 39 | 5.29 × 10 ⁻¹ |
| 3.32 × 10 ⁻⁵ | 1.92 × 10 ⁻³ | 58 | 7.89 × 10 ⁻¹ |
| 3.32 × 10 ⁻⁵ | 2.56 × 10 ⁻³ | 77 | 1.06 |
| 3.32 × 10 ⁻⁵ | 3.20 × 10 ⁻³ | 96 | 1.32 |
| $k_2 = 4.11 \times 10^2 \text{ M}^{-1} \text{ s}^{-1}$ | | | |

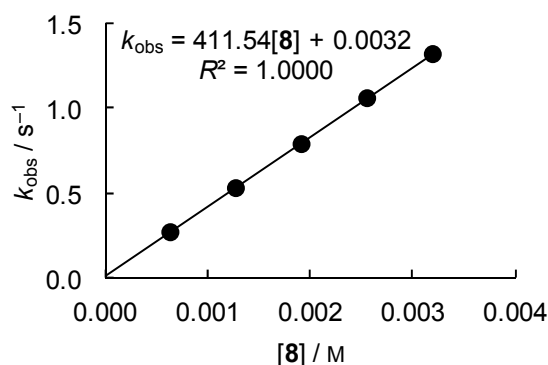


Table 7.11. Rate constants for the reactions of 1-benzoyl-4-(diethylamino)pyridinium chloride (7c) generated from benzoyl chloride (6) and 4-(diethylamino)pyridine (1c, 1.0 equiv.) with benzylamine (8) in CH₃CN (20 °C, λ = 320 nm).

| [7c] ₀ /M | [8] ₀ /M | [8] ₀ /[7c] ₀ | k _{obs} /s ⁻¹ |
|--|-------------------------|-------------------------------------|-----------------------------------|
| 3.23 × 10 ⁻⁵ | 6.41 × 10 ⁻⁴ | 20 | 2.53 × 10 ⁻¹ |
| 3.23 × 10 ⁻⁵ | 1.28 × 10 ⁻³ | 40 | 4.89 × 10 ⁻¹ |
| 3.23 × 10 ⁻⁵ | 1.92 × 10 ⁻³ | 59 | 7.26 × 10 ⁻¹ |
| 3.23 × 10 ⁻⁵ | 2.56 × 10 ⁻³ | 79 | 9.72 × 10 ⁻¹ |
| 3.23 × 10 ⁻⁵ | 3.20 × 10 ⁻³ | 99 | 1.22 |
| $k_2 = 3.78 \times 10^2 \text{ M}^{-1} \text{ s}^{-1}$ | | | |

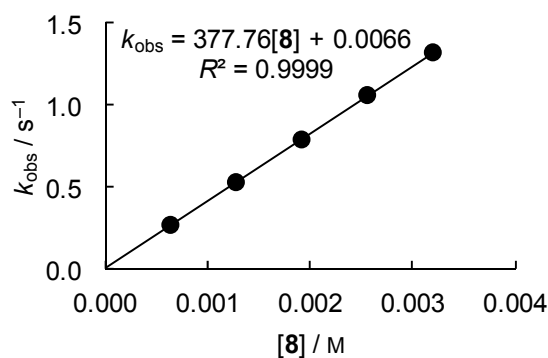


Table 7.12. Rate constants for the reactions of 1-benzoyl-4-(di-*n*-butylamino)pyridinium chloride (**7e**) generated from benzoyl chloride (**6**) and 4-(di-*n*-butylamino)pyridine (**1e**, 1.0 equiv.) with benzylamine (**8**) in CH₃CN (20 °C, λ = 320 nm).

| [7e] ₀ /M | [8] ₀ /M | [8] ₀ /[7e] ₀ | <i>k</i> _{obs} /s ⁻¹ |
|--|------------------------------|---|--|
| 3.28 × 10 ⁻⁵ | 6.26 × 10 ⁻⁴ | 19 | 2.28 × 10 ⁻¹ |
| 3.28 × 10 ⁻⁵ | 1.25 × 10 ⁻³ | 38 | 4.64 × 10 ⁻¹ |
| 3.28 × 10 ⁻⁵ | 1.88 × 10 ⁻³ | 57 | 6.95 × 10 ⁻¹ |
| 3.28 × 10 ⁻⁵ | 2.51 × 10 ⁻³ | 77 | 9.27 × 10 ⁻¹ |
| 3.28 × 10 ⁻⁵ | 3.13 × 10 ⁻³ | 95 | 1.15 |
| <i>k</i> ₂ = 3.68 × 10 ² M ⁻¹ s ⁻¹ | | | |

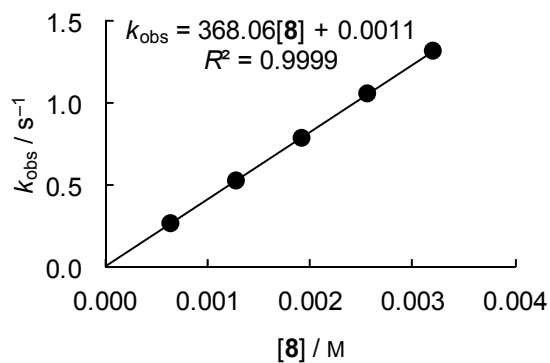


Table 7.13. Rate constants for the reactions of 1-benzoyl-4-(di-*n*-hexylamino)pyridinium chloride (**7g**) generated from benzoyl chloride (**6**) and 4-(di-*n*-hexylamino)pyridine (**1g**, 1.0 equiv.) with benzylamine (**8**) in CH₃CN (20 °C, λ = 320 nm).

| [7g] ₀ /M | [8] ₀ /M | [8] ₀ /[7g] ₀ | <i>k</i> _{obs} /s ⁻¹ |
|--|------------------------------|---|--|
| 3.40 × 10 ⁻⁵ | 6.92 × 10 ⁻⁴ | 20 | 2.47 × 10 ⁻¹ |
| 3.40 × 10 ⁻⁵ | 1.39 × 10 ⁻³ | 41 | 4.96 × 10 ⁻¹ |
| 3.40 × 10 ⁻⁵ | 2.08 × 10 ⁻³ | 61 | 7.37 × 10 ⁻¹ |
| 3.40 × 10 ⁻⁵ | 2.67 × 10 ⁻³ | 79 | 9.48 × 10 ⁻¹ |
| 3.40 × 10 ⁻⁵ | 3.36 × 10 ⁻³ | 99 | 1.19 |
| <i>k</i> ₂ = 3.53 × 10 ² M ⁻¹ s ⁻¹ | | | |

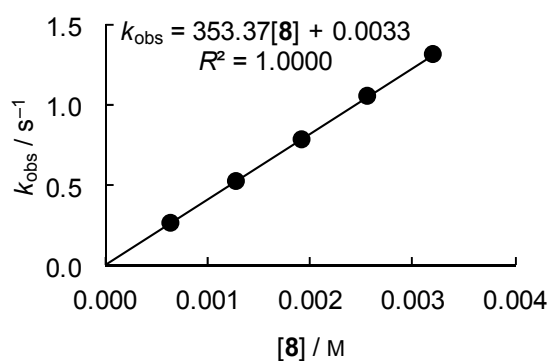
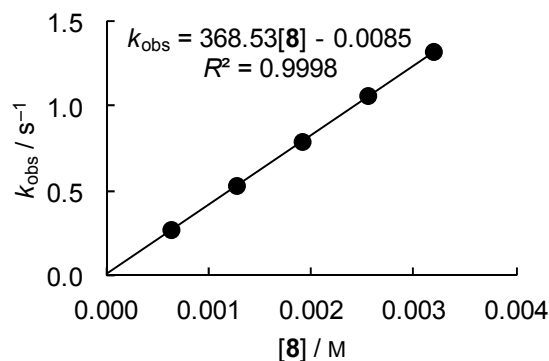


Table 7.14. Rate constants for the reactions of 1-benzoyl-4-(di-*n*-oktylamino)pyridinium chloride (**7h**) generated from benzoyl chloride (**6**) and 4-(di-*n*-oktylamino)pyridine (**1h**, 1.0 equiv.) with benzylamine (**8**) in CH₃CN (20 °C, λ = 320 nm).

| [7h] ₀ /M | [8] ₀ /M | [8] ₀ /[7h] ₀ | <i>k</i> _{obs} /s ⁻¹ |
|-------------------------------|------------------------------|---|--|
| 3.28 × 10 ⁻⁵ | 6.26 × 10 ⁻⁴ | 19 | 2.23 × 10 ⁻¹ |
| 3.28 × 10 ⁻⁵ | 1.25 × 10 ⁻³ | 38 | 4.53 × 10 ⁻¹ |
| 3.28 × 10 ⁻⁵ | 1.88 × 10 ⁻³ | 57 | 6.85 × 10 ⁻¹ |
| 3.28 × 10 ⁻⁵ | 2.51 × 10 ⁻³ | 77 | 9.09 × 10 ⁻¹ |
| 3.28 × 10 ⁻⁵ | 3.13 × 10 ⁻³ | 95 | 1.15 |

$$k_2 = 3.69 \times 10^2 \text{ M}^{-1} \text{ s}^{-1}$$


7.5 References

- [1] a) O. Exner, *J. Phys. Org. Chem.* **1999**, *12*, 265–274; b) M. Charton, *J. Phys. Org. Chem.* **1999**, *12*, 275–282; c) V. Galkin, *J. Phys. Org. Chem.* **1999**, *12*, 283–288; d) O. Exner, M. Charton, V. Galkin, *J. Phys. Org. Chem.* **1999**, *12*, 289.
- [2] a) V. D'Elia, Y.-H. Liu, H. Zipse, *Eur. J. Org. Chem.* **2011**, 1527–1533; b) I. Held, E. Larionov, C. Bozler, F. Wagner, H. Zipse, *Synthesis* **2009**, 2267–2277; c) I. Held, P. von den Hoff, D. S. Stephenson, H. Zipse, *Adv. Synth. Catal.* **2008**, *350*, 1891–1900; d) I. Held, S. Xu, H. Zipse, *Synthesis* **2007**, 1185–1196; e) M. R. Heinrich, H. S. Klisa, H. Mayr, W. Steglich, H. Zipse, *Angew. Chem.* **2003**, *115*, 4975–4977; *Angew. Chem. Int. Ed.* **2003**, *42*, 4826–4828.
- [3] N. De Rycke, F. Couty, O. R.P. David, *Chem. Eur. J.* **2011**, *17*, 12852–12871 and references cited therein.
- [4] C. Pedersen, *Synthesis* **1978**, 844–845.
- [5] S. Xu, I. Held, B. Kempf, H. Mayr, W. Steglich, H. Zipse, *Chem. Eur. J.* **2005**, *11*, 4751–4757.
- [6] T. A. Nigst R. Tandon, H. Mayr, H. Zipse, manuscript in preparation.
- [7] T. A. Nigst, *Diplomarbeit*, Ludwig-Maximilians-Universität München, **2007**.

Chapter 8

PHOTOGENERATION OF BENZHYDRYL CATIONS BY NEAR-UV LASER FLASH PHOTOLYSIS OF PYRIDINIUM SALTS

Tobias A. Nigst, Johannes Ammer, and Herbert Mayr in *J. Phys. Chem. A* **2012**, *116*, 8494–8499.

The results obtained by J. Ammer are not listed in the Experimental Section.

8.1 Introduction

Pyridinium salts have a rich photochemistry^[1] which includes their use as photoinitiators in cationic polymerizations.^[2-4] However, the heterolytic cleavage of the exocyclic C–N bond of *N*-alkylated pyridinium ions was only found in few cases.^[4] The observation that photolyses of related onium salts, such as phosphonium^[5,6] or ammonium salts,^[7,8] gave excellent yields of carbocations thus prompted us to investigate substituted pyridinium salts as precursors for the carbocations. The use of highly substituted aminopyridines as photo-leaving groups promised a good wavelength tunability, which would be interesting for applications as photoinitiators^[9,10] and for kinetic investigations of carbocation reactivities.

Many bimolecular reactions of carbocations proceed on a time scale from nanoseconds to microseconds, which requires short pump pulses for time-resolved measurements. The most common and most affordable source of light pulses with pulse widths of a few nanoseconds is the Nd/YAG laser.^[11] Its fundamental emission in the infrared region (1064 nm) can be converted to the second, third, or fourth harmonics to generate laser pulses in the visible (532 nm) or UV range (355 or 266 nm). In the following discussion, we used the Nd/YAG laser as an example to address some problems related to the choice of excitation wavelength in laser flash photolysis experiments, but similar problems will also be encountered with other types of lasers (including tunable lasers). In previous investigations, we have generated benzhydryl cations **1** and other carbocations by heterolytic photocleavage of precursor molecules such as arylmethyl halides^[12] or arylmethyl triarylphosphonium salts^[6] which have significant UV absorbances at 266 nm, but not at 355 nm (Scheme 8.1). Typically, the

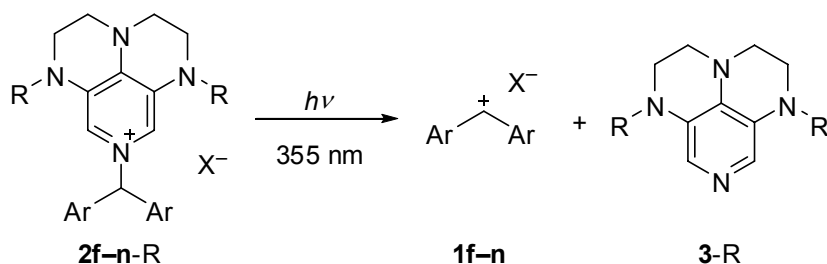
carbocations were obtained by irradiating precursor solutions with $A_{266\text{ nm}} \approx 0.1$ to 1.0 with a 266 nm laser pulse; subsequently, the UV/Vis absorption decays of the carbocations were monitored in the presence of the nucleophilic reaction partners.^[8,13]



Scheme 8.1. Photo-heterolysis of substrates R-PLG (photo-leaving group $\text{PLG}^- = \text{Cl}^-$, PR'_3 , etc.) and subsequent trapping of the generated carbocations R^+ by nucleophiles Nu.

This procedure is problematic when the reaction partners also have considerable absorbances at the excitation wavelength of 266 nm. In this case, the laser pulse may also generate reactive intermediates from the nucleophilic reaction partner and we can no longer be sure which process is causing the decay of the carbocation. In the usual experimental setup^[11] featuring a 90 degree angle between pump and probe light, the opacity of the sample solutions for the 266 nm pump pulse also prevents sufficient excitation of the precursor molecules to generate the carbocations. The same problems do not only occur when the nucleophilic reaction partner absorbs at 266 nm but also when experiments are carried out in solvents with a high UV cutoff such as *N,N*-dimethylformamide (DMF), dimethyl sulfoxide (DMSO), or acetone.

In such cases, the third harmonic of the Nd/YAG laser (355 nm) would be suitable as pump, but onium salts do not usually absorb at this wavelength. The use of photosensitizers, a common strategy for photoinitiator systems,^[9,10] cannot be employed for kinetic studies, because the diffusion-limited bimolecular excitation transfer is too slow. It was therefore, desirable to develop a carbocation precursor that can be irradiated at 355 nm. For this purpose, we took advantage of the fact that amino-substitution of pyridinium salts causes red-shifts of the UV absorptions.^[1a] In this work, we report the generation of benzhydryl cations **1(f-n)** by 355 nm irradiation of benzhydrylpyridinium salts **2(f-n)-R** derived from 3,4,5-triamino-substituted pyridines **3-R**, the so-called superDMAPs^[14,15] (Scheme 8.2).



Scheme 8.2. Generation of benzhydrylium ions **1(f-n)** by 355 nm laser flash photolysis of pyridinium ions **2(f-n)-R** with different substituents R on the pyridine moiety.^[a]

[a] For Substitution Patterns **f-n** of the Benzhydryl Moiety, see Table 8.1. Counteranion $X^- = Cl^-$ or BF_4^- .

For testing our approach, we measured the rate constants of the reactions of benzhydrylium ions **1** (Table 8.1) with pyridines **4–8** (Figure 8.1). Pyridines have strong UV absorptions below 300 nm and are known to undergo photoisomerizations via azaprefulvenes or Dewar-pyridines upon ~ 254 nm irradiation.^[16] Therefore, their reactivities cannot be characterized readily with a method that uses 266 nm pump pulses. Rate constants of the reactions of photolytically generated carbocations with pyridines could previously only be determined, when the employed precursors incorporated a highly conjugated π -system which absorbed at $\lambda > 300$ nm.^[17] The reactivity data acquired in this study will subsequently be employed to determine the nucleophilicity parameters N and s_N for the pyridines **4–8** according to the linear free energy relationship [Eq. (8.1)], which allows us to predict second-order rate constants k_2 for polar organic reactions with one electrophile-specific parameter E and two solvent-dependent nucleophile-specific parameters N and s_N .^[18]

$$\lg k_2 = s_N(N + E) \quad (8.1)$$

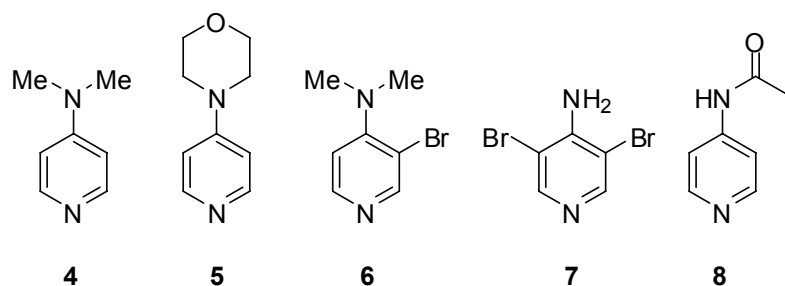
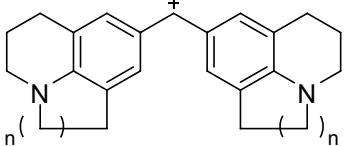
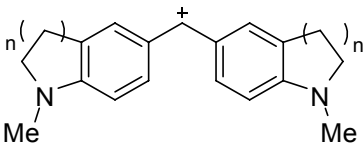
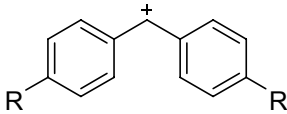
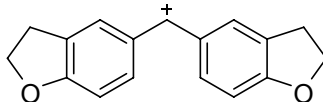
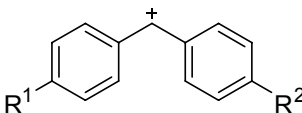


Figure 8.1. Pyridines employed as nucleophiles in this study.

Table 8.4. List of the reference electrophiles **1** used in this study.

| Reference Electrophile | $E^{[a]}$ |
|---|---|
|  $n = 1$ | 1a -10.04 |
| $n = 2$ | 1b -9.45 |
|  $n = 1$ | 1c -8.76 |
| $n = 2$ | 1d -8.22 |
|  | R = <i>N</i> -pyrrolidino 1e -7.69 |
| | R = NMe ₂ 1f -7.02 |
| | R = N(Me)Ph 1g -5.89 |
| | R = <i>N</i> -morpholino 1h -5.53 |
| | R = N(Me)CH ₂ CF ₃ 1i -3.85 |
|  | 1j -1.36 |
|  | R ¹ = R ² = OMe 1k 0.00 |
| | R ¹ = OMe, R ² = H 1l 2.11 |
| | R ¹ = R ² = Me 1m 3.63 |
| | R ¹ = Me, R ² = H 1n 4.43 ^[b] |
| | R ¹ = R ² = H 1o 5.47 ^[b] |

[a] Electrophilicity parameters E were taken from Ref. [18a] unless noted otherwise. [b] From Ref. [6b].

8.2 Results and Discussion

8.2.1 Photo-generation of Benzhydrylium Ions

Since the photo-electrofuges (that is, the carbocations-to-be) do not absorb at 355 nm, the excitation must occur at the photo-nucleofuge (that is, the PLG moiety in Scheme 8.1). Our recent investigation of 3,4,5-triamino-substituted pyridines **3-R** (Figure 8.2) showed that these

compounds are strong Lewis bases and that the pyridinium ions **2-R**, that is their adducts with benzhydrylium ions **1**, show UV absorptions around 355 nm.^[15]

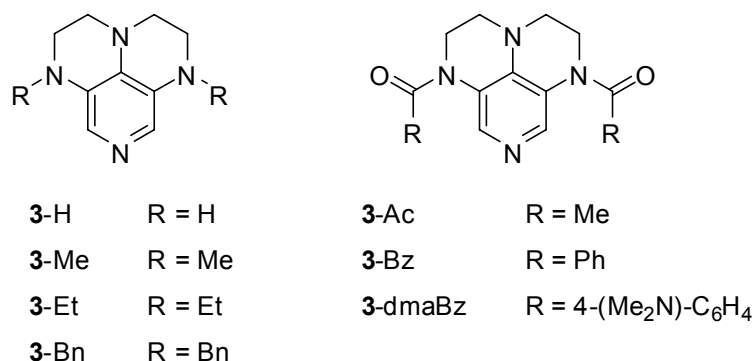


Figure 8.2. Pyridines employed as photo-leaving groups in this study (dmaBz = 4-(dimethylamino)benzoyl).

The pyridines **3-R** were obtained in four to six steps from 4-pyridone as described by David *et al.*^[15] In order to use the costly materials efficiently, we did not isolate the benzhydrylpyridinium tetrafluoroborates **2(f-j)-R** ($X^- = \text{BF}_4^-$) but generated them in solution by combining the pyridines **3-R** with solutions of the isolated^[18a] benzhydrylium tetrafluoroborates **1f-j** BF_4^- (that is, reverse of the reaction depicted in Scheme 8.2). The formation of the pyridinium salts **2(f-j)-R** was indicated by the immediate disappearance of the color of **1f-j** and the appearance of UV/Vis absorption bands at 340–380 nm. The benzhydrylpyridinium chlorides **2(j-o)-R** ($X^- = \text{Cl}^-$) were obtained from reactions of **3-R** with the corresponding benzhydryl chlorides $\text{Ar}_2\text{CH}-\text{Cl}$. The syntheses of **2n-R** and **2o-R** by this method required longer reaction times of 2 h or overnight, as revealed by the full development of the pyridinium bands in the UV/Vis spectrum.

Figure 8.3 shows the UV/Vis absorption spectra of several 1-benzhydrylpyridinium salts **2l-R** derived from the pyridines **3-R**. The parent compound **2l-H** (not shown) and the *N*-alkyl-substituted derivatives **2l-Bn**, **2l-Me** (Figure 8.3), and **2l-Et** (not shown) have absorption maxima near 355 nm. The absorption maxima of the *N*-acyl-substituted compounds **2l-Ac** and **2l-Bz** (not shown) are too far in the UV but can be red-shifted by the introduction of the NMe_2 substituent on the benzoyl group (\rightarrow **2l-dmaBz**, Figure 8.3). In agreement with previous reports,^[1a] the absorption maximum of the pyridinium salts does not depend on the substituent at the pyridine nitrogen atom.

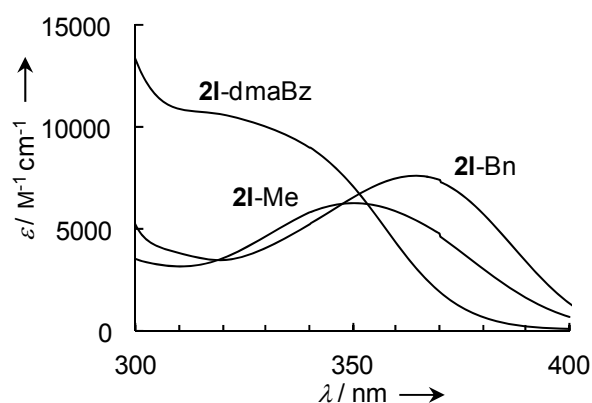


Figure 8.3. UV/Vis absorption spectra of pyridinium salts **2I-R** ($X^- = Cl^-$) with different substituents.

When we irradiated $\sim 1.2 \times 10^{-4}$ M solutions of the parent pyridinium salt **2(i-l)-H** or the *N*-alkyl derivatives **2(i-l)-Bn**, **2(i-l)-Me**, or **2(i-l)-Et** in CH_3CN with a 7-ns laser pulse from the frequency-tripled Nd/YAG laser ($\lambda_{exc} = 355$ nm, ~ 50 mJ/pulse), we detected the previously described^[12] UV/Vis absorption bands of the moderately stabilized benzhydrylium ions **1i-l** at $\lambda_{max} = 450$ – 600 nm in the transient spectra, and observed the disappearance (bleaching) of the pyridinium salts **2(i-l)-R** at ~ 350 – 370 nm. Figure 8.4 shows the transient spectra obtained by irradiation of the *N*-benzyl-substituted pyridinium salts **2(f-n)-Bn** with different substituents on the benzhydryl moiety. The different absorbances of the benzhydrylium ions **1(f-n)** in Figures 8.4a–d are mostly due to the different absorption coefficients and correspond to concentrations of the benzhydrylium ions of $(0.6$ – $2.3) \times 10^{-6}$ M. The spectrum obtained by irradiation of **2n-Bn** ($X^- = Cl^-$) additionally shows a small band at ~ 338 nm, which we assign to the phenyl(*p*-tolyl)methyl radical by comparison with its previously published spectrum.^[12] More electrophilic carbocations such as the parent benzhydrylium ion **1o** could not be obtained in concentrations which were sufficient for kinetic investigations; in these cases we mainly observed the benzhydryl radicals.

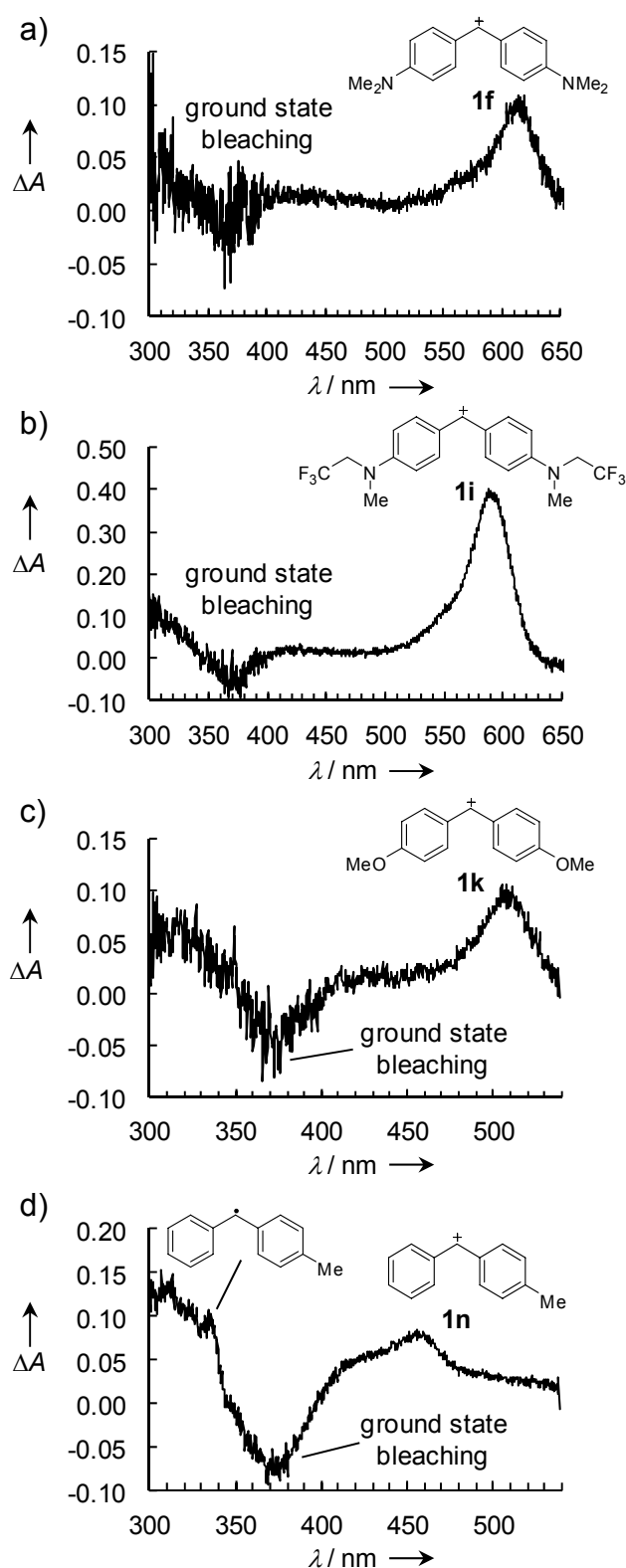


Figure 8.4. Transient UV/Vis spectra obtained by irradiation of 1.2×10^{-4} M solutions of **2f**-Bn ($X^- = \text{BF}_4^-$) (a), **2i**-Bn ($X^- = \text{BF}_4^-$) (b), **2k**-Bn ($X^- = \text{Cl}^-$) (c), or **2n**-Bn ($X^- = \text{Cl}^-$) (d) in acetonitrile with a 7-ns laser pulse ($\lambda_{\text{exc}} = 355$ nm).

The yields and lifetimes of the carbocations **1i–l** obtained by photolysis of the parent pyridinium salts **2(i–l)-H** and the *N*-alkylated derivatives **2(i–l)-Bn**, **2(i–l)-Me**, and **2(i–l)-Et** were almost independent of the nature of the photo-nucleofuge **3-R**. Irradiation of the *N*-acyl derivative **2l-dmaBz** however, did not yield any carbocations **1l**. For our kinetic investigations, we selected the *N*-benzyl derivatives **2-Bn** because the pyridine **3-Bn** has the highest Lewis basicity in the series^[15] and, therefore, forms the most stable pyridinium ions (see below).

In the photolyses of benzhydryl triphenylphosphonium salts, the yields and lifetimes of the benzhydryl cations greatly depend on the counter-anion of the precursor salt.^[6a] The generation of benzhydryl radicals by electron transfer in electronically excited phosphonium chloride and bromide ion pairs was described, but this process is unimportant at low concentrations of the precursor salts in CH₃CN, as the phosphonium halides are mostly unpaired under these conditions.^[6a] However, the lifetimes of the photo-generated benzhydryl cations are reduced significantly by the diffusion-controlled reactions with the halide counter-anions.^[6a] Therefore, we also investigated the influence of the counter-anion in the photolysis of **2j-Bn** on the lifetime of the photo-generated carbocation **1j**. When we irradiated a 1.2×10^{-4} M solution of the pyridinium halide **2j-Bn** ($X^- = \text{Cl}^-$), we observed a monoexponential decay of the benzhydryl cation **1j** with a rate constant of $k_{\text{obs}} = 1.9 \times 10^6 \text{ s}^{-1}$, which corresponds to a second-order rate constant of $1.6 \times 10^{10} \text{ M}^{-1} \text{ s}^{-1}$ for the reaction of **1j** with **2j-Bn** Cl^- . As this value is slightly larger than the previously reported value of $9.39 \times 10^9 \text{ M}^{-1} \text{ s}^{-1}$ for the reaction of **1j** with Cl^- in acetonitrile,^[19] one might assign this decay to the combination of **1j** with chloride ions. On the other hand, when we employed the pyridinium tetrafluoroborate **2j-Bn** ($X^- = \text{BF}_4^-$) as precursor, the decay of the benzhydryl cation **1j** was not monoexponential and we found an initial fast decay with a rate constant comparable to that obtained with **2j-Bn** Cl^- , which was followed by a slower decay on the microsecond time scale. We explain this behavior by a fast reversible reaction of **1j** with the tertiary amine functions of the precursor salt **2j-Bn**, which is followed by a slower unidentified subsequent reaction. This behavior is analogous to other tertiary amines where we also observed fast reversible reactions followed by slower decays due to unknown subsequent reactions.^[8] Due to the high nucleophilic reactivity of the tertiary amine centers of the precursors **2-Bn**, the choice of the counter-anion X^- is thus not so important and we did not convert the chlorides **2(j–n)-Bn** ($X^- = \text{Cl}^-$) to the tetrafluoroborates. Because of the proximity of the diffusion limit, the reactions of **1j–n** with chloride^[19] or tertiary amines^[8]

proceed with almost the same rate constants and we observed similar decay rates for all investigated benzhydrylium ions obtained from different precursors **2(j–n)**-Bn ($X^- = \text{Cl}^-$ or BF_4^-).

8.2.2 Kinetic Investigations

With a method at hand to generate the benzydrylium ions **1** using 355 nm laser pulses, we determined rate constants of reactions of **1** with nucleophiles. After irradiation of the pyridinium salts **2(f–l)**-Bn (approximately 1.2×10^{-4} M) in the presence of a large excess of added nucleophiles (7×10^{-4} to 1×10^{-1} M), we observed monoexponential decays of the absorbances A of the photo-generated benzhydrylium ions **1f–l**, as illustrated in Figure 8.5 for the reaction of **1h** with DMAP (**4**). The decays of the absorbances were fitted with the exponential function $A(t) = A_0 e^{-k_{\text{obs}} t} + C$ to obtain the pseudo-first-order rate constants k_{obs} (s^{-1}). Plots of k_{obs} versus the nucleophile concentrations were linear in all cases, and the slopes of these plots provided the second-order rate constants k_2 ($\text{M}^{-1} \text{s}^{-1}$) for the reactions of **1f–l** with the nucleophiles.

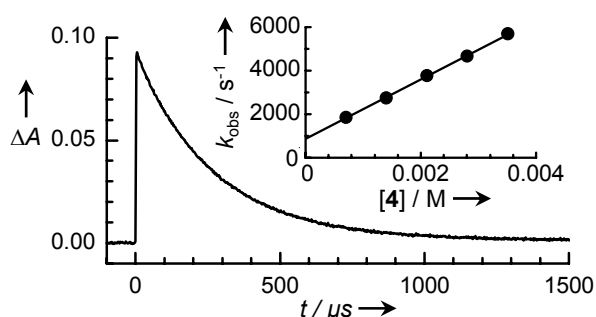


Figure 8.5. Plot of the absorbance decay of **1h** at $\lambda = 612$ nm observed after irradiation of **2h**-Bn (1.2×10^{-4} M, $X^- = \text{BF}_4^-$) with a 7-ns laser pulse ($\lambda_{\text{exc}} = 355$ nm, ~ 50 mJ/pulse) in the presence of 4-(dimethylamino)pyridine ($[4] = 2.12 \times 10^{-3}$ M). Inset: Plot of k_{obs} versus $[4]$; $k_{\text{obs}} = 1.37 \times 10^6 [4] + 857$ ($R^2 = 0.9996$).

In order to study some systems of known reactivity, we measured the second-order rate constants k_2 for the reactions of some benzhydrylium ions **1** with 4-(dimethylamino)pyridine (DMAP, **4**) in acetonitrile (Table 8.2). The second-order rate constant for the reaction of **4**

with **1f** was previously determined with the stopped-flow method,^[20] and we wanted to reproduce this measurement with our new method.

Table 8.2. Second-order rate constants k_2 for the reactions of the reference electrophiles **1** with the pyridines **4–8** at 20 °C and resulting N and s_N parameters.

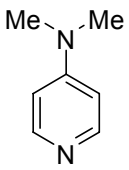
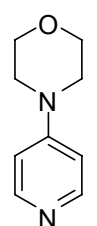
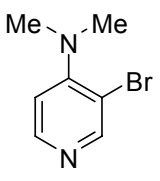
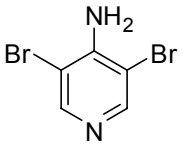
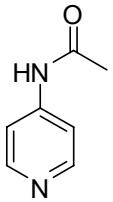
| Pyridine | N | s_N | Ar ₂ CH ⁺ | $k_2^{[a]}/\text{M}^{-1} \text{s}^{-1}$ |
|---|------------------------|-------|---------------------------------|---|
| 4 in CH ₃ CN  | 15.51 | 0.62 | 1a | 2.11×10^3 [b,c] |
| | | | 1b | 5.30×10^3 [b,c] |
| | | | 1c | 1.29×10^4 [b,c] |
| | | | 1d | 3.32×10^4 [b,c] |
| | | | 1f | 2.31×10^5 [b,c,d] |
| | | | 1f | 2.97×10^5 [d] |
| | | | 1h | 1.37×10^6 |
| | | | 1i | 1.33×10^7 |
| | | | 4 in DMSO | |
| 1i | 5.62×10^6 [e] | | | |
| 4 in DMF | | | 1f | 2.04×10^5 [b,c] |
| | | | 1i | 7.97×10^6 [e] |
| 4 in acetone | | | 1i | 2.50×10^7 [e] |
| 5 in CH ₃ CN  | 14.80 | 0.63 | 1a | 7.27×10^2 [b] |
| | | | 1c | 5.72×10^3 [b] |
| | | | 1e | 4.42×10^4 [b] |
| | | | 1f | 9.28×10^4 [b,d] |
| | | | 1f | 1.36×10^5 [d] |
| | | | 1h | 6.30×10^5 |
| | | | 1i | 6.39×10^6 |

Table 8.2 (continued).

| Pyridine | N | s_N | Ar_2CH^+ | $k_2^{[a]}/\text{M}^{-1} \text{s}^{-1}$ |
|---|-------|-------|--------------------------|---|
| 6 in CH_3CN  | 12.96 | 0.67 | 1e | 4.04×10^3 [b] |
| | | | 1f | 1.00×10^4 [b] |
| | | | 1g | 7.02×10^4 [b] |
| | | | 1h | 5.76×10^4 [b] |
| | | | 1i | 6.45×10^5 [b] |
| | | | 1j | 8.20×10^7 |
| 7 in CH_3CN  | 11.11 | 0.75 | 1h | 1.63×10^4 [b] |
| | | | 1i | 1.96×10^5 [b] |
| | | | 1j | 4.97×10^7 |
| | | | 1k | 1.31×10^8 |
| 8 in CH_3CN  | 13.24 | 0.67 | 1d | 2.38×10^3 [b] |
| | | | 1e | 6.30×10^3 [b] |
| | | | 1f | 1.76×10^4 [b] |
| | | | 1h | 1.07×10^5 [b] |
| | | | 1i | 1.36×10^6 |
| | | | 1j | 1.28×10^8 |

[a] Laser flash photolysis of **2-Bn** unless noted otherwise. [b] Stopped-flow UV/Vis measurement. [c] From Ref. [20]. [d] The average of both rate constants from laser flash photolysis and stopped-flow measurements was used for the correlation analysis. [e] With <1% acetonitrile as cosolvent.

However, due to the similar electrofugalities of **1f** ($E_f = 4.84$) and **1c** ($E_f = 4.83$),^[21] the formation of **1f** by thermal dissociation of **2f-Bn** in acetonitrile solutions is expected to occur with a rate constant similar to that reported for the dissociation of **2c-Bn** ($9.6 \times 10^{-2} \text{ s}^{-1}$).^[15] In the presence of high concentrations of DMAP (**4**), the benzhydrylium ions **1f** will then be trapped by **4** to give a pyridinium salt with no absorption at 355 nm. As a consequence, we had to work quickly and keep the nucleophile concentration below ca. $5 \times 10^{-3} \text{ M}$ in order to maintain a sufficient concentration of **2f-Bn**, which is needed to generate the carbocation **1f** with the 355 nm laser pulse. The rate constant for the reaction of **4** with **1f** ($2.97 \times 10^5 \text{ M}^{-1} \text{ s}^{-1}$)

determined in this way is in fair agreement with the previously reported value from stopped-flow experiments ($2.31 \times 10^5 \text{ M}^{-1} \text{ s}^{-1}$).^[20]

The rate constants for the reactions of **4** with **1h** and **1i** are too fast for the stopped-flow method and could not be measured with the established laser flash photolytic method using 266 nm laser pulses because **4** absorbs at the excitation wavelength. These rate constants could now be determined by laser flash photolysis of **2-Bn** at 355 nm (Table 8.2), and Figure 8.6 shows that these rate constants extend the correlation line for $\lg k_2$ (**1a–d**), which was determined by stopped-flow experiments. If all available data are used to calculate the nucleophilicity parameters of **4** we obtain $N = 15.51$ and $s_N = 0.62$ (Table 8.2), which deviate only slightly from the previously published values.^[20]

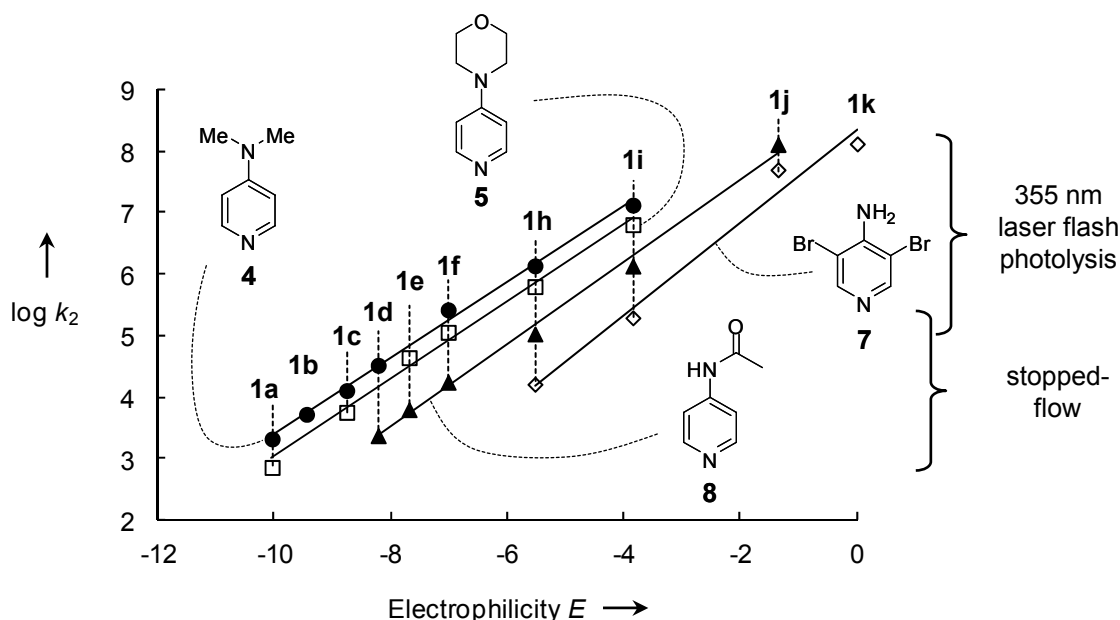


Figure 8.6. Plot of $\lg k_2$ for reactions of benzhydrylium ions **1** with substituted pyridines **4–8** versus the electrophilicity parameters E of the benzhydrylium ions. The plot for **6** is not shown because it overlaps with **8**; it is shown in the Experimental Section.

Encouraged by the results with **4**, we determined second-order rate constants $k_2 > 10^5 \text{ M}^{-1} \text{ s}^{-1}$ for the reactions of **1f–k** with the substituted pyridines **5–8** (Table 8.2) in acetonitrile with the 355 nm laser flash photolytic method.^[22] These data are supplemented with rate constants for slower reactions ($k_2 < 10^6 \text{ M}^{-1} \text{ s}^{-1}$), which were determined with the stopped-flow method under first-order conditions by using the nucleophiles in a large excess (over 10 equiv.

relative to the benzhydrylium tetrafluoroborates **1a–i**) as described previously^[18a] (Table 8.2). Again we observed good linear correlations of $\lg k_2$ versus E (Figure 8.6) for the data from both methods. As previously observed, **1g**^[8,23a,b] (not shown) and **1j**^[23c] always react somewhat faster in acetonitrile solution than expected from their E parameters which have been determined in CH_2Cl_2 solutions.

In the case of **7**, only the reactions with **1h** and **1i** can be followed with the stopped-flow method, as the better stabilized carbocations show no conversion in reactions with **7** due to its low Lewis basicity. We have now been able to characterize the nucleophilicity of **7** over a wider reactivity range by including the data determined by the laser flash photolysis method. From the correlations in Figure 8.6 we derived the nucleophilicity parameters of **4–8** listed in Table 8.2. As expected, the nucleophilicities of the 4-amino-substituted pyridines **4–7** decrease with the electron-withdrawing character of the substituents (Table 8.2 and Figure 8.6). The *N*-acetyl-4-aminopyridine (**8**) is of similar reactivity as the 3-bromo-substituted DMAP **6**.

To demonstrate the applicability of the method in solvents with high UV cutoff, we also measured the second-order rate constants for the reactions of **1i** with **4** in DMSO, DMF and acetone (Table 8.2). The order of reactivity (acetone > acetonitrile > DMF > DMSO) agrees with that previously reported for the reactions of **4** with **1f**.^[20] Furthermore, we determined first-order rate constants for the reactions of **1l** with 80% and 90% aqueous acetone (Table 8.3) and found good agreement between the experimental rate constants and the values calculated from Equation (8.1) and the solvent nucleophilicity parameters N_1 and s_N of the acetone/water mixtures.^[24]

Table 8.3. Comparison of experimental and calculated first-order rate constants (s^{-1}) for reactions of **1l** with acetone/water mixtures.

| solvent ^[a] | $k_1^{[b]}/\text{s}^{-1}$ | $k_{\text{calc}}^{[c]}/\text{s}^{-1}$ | k_2/k_{calc} |
|------------------------|---------------------------|---------------------------------------|-----------------------|
| 90A10W | 6.23×10^6 | 4.35×10^6 | 1.43 |
| 80A20W | 6.61×10^6 | 7.17×10^6 | 0.92 |

[a] Solvent mixtures given in v/v (A = acetone, W = water). [b] Laser flash photolysis of **2l**-Bn. [c] Calculated from Equation (7.1) using the previously published N_1 and s_N parameters of acetone/water mixtures (90A10W: $N_1 = 5.70$, $s_N = 0.85$; 80A20W: $N_1 = 5.77$, $s_N = 0.87$).^[24]

8.3 Conclusion

We have demonstrated that the 355 nm laser flash photolysis of pyridinium salts **2-Bn** is a suitable method for the generation of benzhydrylium ions **1** in the presence of reactants or solvents that absorb at 266 nm. The scope of carbocations which can be generated is more restricted than in the 266 nm photolyses of quaternary phosphonium salts.^[6,8] Highly reactive carbocations such as **1o** cannot be generated efficiently, and the precursors **2-Bn** of carbocations which are less Lewis-acidic than **1f** are not stable in the presence of nucleophiles which trap the small concentrations of benzhydrylium ions, which exist in solutions of **2(a-f)-Bn** in the dark. Nevertheless, we could generate benzhydrylium ions **1f-n** covering more than ten orders of reactivity and investigate the rates of their reactions with nucleophiles. We employed this method to characterize the nucleophilic reactivities of the electron-rich pyridines **5-8**, which will be used for further studies in our group. Moreover, we have demonstrated that the third harmonic of the Nd/YAG laser (355 nm) can be employed to generate benzhydrylium ions **1** in solvents with high UV cutoff such as acetone (cutoff: 330 nm)^[25] which is opaque to the quadrupled Nd/YAG laser (266 nm) and the XeCl excimer laser (308 nm). Laser flash photolysis of substituted pyridinium salts at 355 nm thus supplements the established kinetic methods and is particularly useful for characterizing nucleophiles which do not react with stabilized carbocations for thermodynamic reasons and which cannot be studied with 266 nm laser flash photolytically generated carbocations due to the absorbance of the sample solutions.

8.4 Experimental Section

8.4.1 General Comment

Materials. Acetonitrile (> 99.9%, extra dry), DMSO (> 99.5%, extra dry), DMF (> 99.8%, extra dry), and acetone (> 99.9%, extra dry) were purchased and used without further purification. Water was distilled and passed through a Milli-Q water purification system. 4-(Dimethylamino)pyridine (**4**) and 4-(morpholino)pyridine (**5**) were purchased and purified by recrystallization prior to use. The 3,4,5-triaminopyridines **3**,^[15] 3-bromo-4-

(dimethylamino)pyridine (**6**),^[26] 3,5-dibromo-4-aminopyridine (**7**)^[27] and *N*-acetyl-4-aminopyridine (**8**)^[28] were synthesized according to literature procedures.

Analytics. In the ¹H and ¹³C NMR spectra the chemical shifts in ppm refer to the solvent residual signals as internal standard: CD₃CN ($\delta_{\text{H}} = 1.94$, $\delta_{\text{C}} = 1.32$). The following abbreviations were used for signal multiplicities: brs = broad singlet, s = singlet, d = doublet, q = quartet. For reasons of simplicity, the ¹H NMR signals of AA'BB'-spin systems of *p*-substituted aromatic rings are treated as doublets.

Kinetics. The kinetics of the reactions of the benzhydrylium ions **1** (for abbreviations see Ref. [18a]) with the pyridines **4–8** or solvents were followed by UV/Vis spectroscopy in acetonitrile, DMSO, DMF, acetone or water acetone mixtures at 20 °C.

Stopped-flow spectrophotometer systems (Applied Photophysics SX.18MV-R or Hi-Tech SF-61DX2) were used for the investigation of reactions with $10 \text{ ms} < \tau_{1/2} < 10 \text{ s}$. The kinetic runs were initiated by mixing equal volumes of the solutions of the pyridines **4–8** and the benzhydrylium tetrafluoroborates **1** in the given solvents.

Reactions with $\tau_{1/2} < 10 \text{ ms}$ were analyzed by laser flash photolytic generation of **1f–o** from benzhydrylpyridinium ions **2(f–o)-R** in the presence of excess nucleophile. Solutions of the carbocation precursors were irradiated with a 7-ns pulse from the third harmonic of a Nd:YAG laser (355 nm, ~50 mJ/pulse), and a xenon lamp was used as probe light for UV/Vis detection. The system was equipped with a fluorescence flow cell and a synchronized pump system which allowed the complete exchange of the sample volume between subsequent laser pulses. For each concentration, ≥ 50 individual measurements were averaged.

The pyridines **4–8** were used in large excess (over 10 equiv.) relative to the electrophiles **1** to ensure first-order conditions with $k_{\text{obs}} = k_2[\text{Nu}]_0 + k_0$. From the exponential decays of the absorbances at λ_{max} of **1**, the first-order rate constants k_{obs} [s⁻¹] were obtained by least-squares fitting of the single-exponential function $A_t = A_0 e^{-k_{\text{obs}} t} + C$ to the absorbances. The slopes of plots of k_{obs} versus the concentrations of the nucleophiles yielded the second-order rate constants

k_2 [M⁻¹ s⁻¹].

8.4.2 Kinetic Experiments

Kinetics of the reactions of 4-(dimethylamino)pyridine (4) with benzhydrylium ions (1)

Table 8.4. Rate constants for the reactions of 4-(dimethylamino)pyridine (4) with (dma)₂CH⁺ BF₄⁻ (1f) generated from 2f-Bn in CH₃CN (laser flash photolysis, 20 °C, λ = 605 nm).

| [2f-Bn] ₀ /M | [4] ₀ /M | k _{obs} /s ⁻¹ |
|-------------------------|-------------------------|-----------------------------------|
| 1.21 × 10 ⁻⁴ | 8.16 × 10 ⁻⁴ | 3.82 × 10 ² |
| 1.21 × 10 ⁻⁴ | 1.63 × 10 ⁻³ | 6.86 × 10 ² |
| 1.21 × 10 ⁻⁴ | 2.45 × 10 ⁻³ | 9.36 × 10 ² |
| 1.21 × 10 ⁻⁴ | 3.26 × 10 ⁻³ | 1.15 × 10 ³ |
| 1.21 × 10 ⁻⁴ | 4.08 × 10 ⁻³ | 1.36 × 10 ³ |

$k_2 = 2.97 \times 10^5 \text{ M}^{-1} \text{ s}^{-1}$

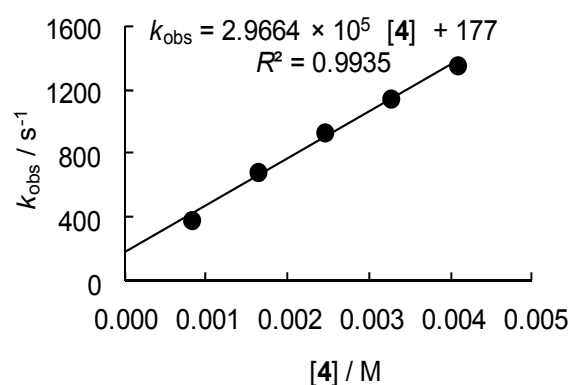


Table 8.5. Rate constants for the reactions of 4-(dimethylamino)pyridine (4) with (mor)₂CH⁺ BF₄⁻ (1h) generated from 2h-Bn in CH₃CN (laser flash photolysis, 20 °C, λ = 612 nm).

| [2h-Bn] ₀ /M | [4] ₀ /M | k _{obs} /s ⁻¹ |
|-------------------------|-------------------------|-----------------------------------|
| 1.20 × 10 ⁻⁴ | 7.02 × 10 ⁻⁴ | 1.83 × 10 ³ |
| 1.20 × 10 ⁻⁴ | 1.40 × 10 ⁻³ | 2.75 × 10 ³ |
| 1.20 × 10 ⁻⁴ | 2.11 × 10 ⁻³ | 3.77 × 10 ³ |
| 1.20 × 10 ⁻⁴ | 2.81 × 10 ⁻³ | 4.66 × 10 ³ |
| 1.20 × 10 ⁻⁴ | 3.51 × 10 ⁻³ | 5.68 × 10 ³ |

$k_2 = 1.37 \times 10^6 \text{ M}^{-1} \text{ s}^{-1}$

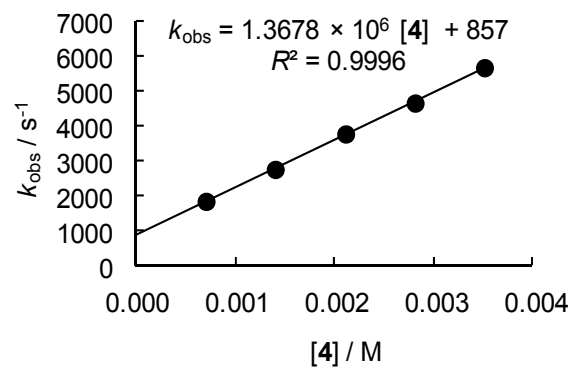


Table 8.6. Rate constants for the reactions of 4-(dimethylamino)pyridine (**4**) with (mfa)₂CH⁺BF₄⁻ (**1i**) generated from **2i**-Bn in CH₃CN (laser flash photolysis, 20 °C, λ = 586 nm).

| [2i -Bn] ₀ /M | [4] ₀ /M | k _{obs} /s ⁻¹ |
|----------------------------------|------------------------------|-----------------------------------|
| 1.20 × 10 ⁻⁴ | 7.10 × 10 ⁻⁴ | 1.15 × 10 ⁴ |
| 1.20 × 10 ⁻⁴ | 1.42 × 10 ⁻³ | 2.10 × 10 ⁴ |
| 1.20 × 10 ⁻⁴ | 2.13 × 10 ⁻³ | 3.04 × 10 ⁴ |
| 1.20 × 10 ⁻⁴ | 2.84 × 10 ⁻³ | 4.00 × 10 ⁴ |
| 1.20 × 10 ⁻⁴ | 3.55 × 10 ⁻³ | 4.91 × 10 ⁴ |

$k_2 = 1.33 \times 10^7 \text{ M}^{-1} \text{ s}^{-1}$

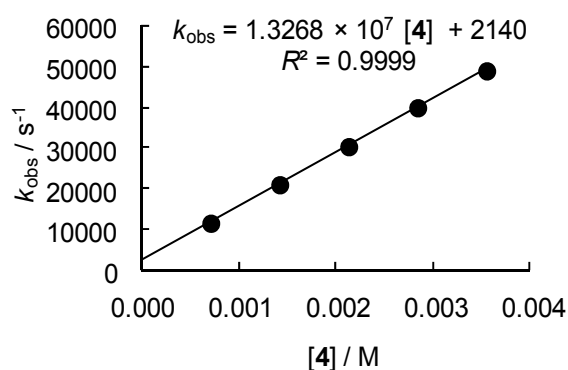
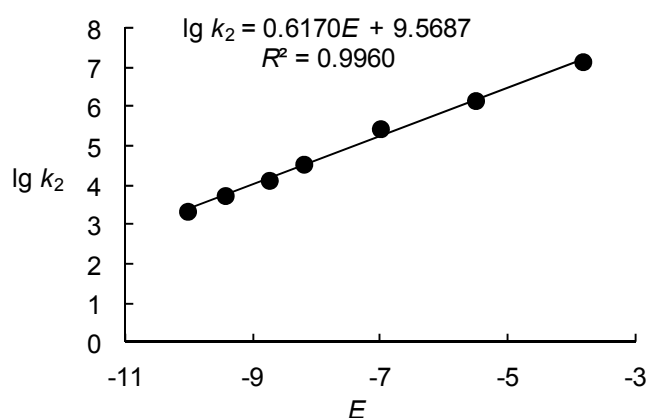


Table 8.7. Determination of the nucleophilicity parameters N and s_N for 4-(dimethylamino)-pyridine (**4**) in CH₃CN.

| Electrophile (E) | $k_2/\text{M}^{-1} \text{ s}^{-1}$ | $\lg k_2$ |
|----------------------|------------------------------------|-----------|
| 1a (-10.04) | 2.11×10^3 [a] | 3.32 |
| 1b (-9.45) | 5.30×10^3 [a] | 3.72 |
| 1c (-8.76) | 1.29×10^4 [a] | 4.11 |
| 1d (-8.22) | 3.32×10^4 [a] | 4.52 |
| 1f (-7.02) | 2.64×10^5 [b] | 5.42 |
| 1h (-5.53) | 1.37×10^6 | 6.14 |
| 1i (-3.85) | 1.33×10^7 | 7.12 |

$N = 15.51, s_N = 0.62$



[a] Rate constants taken from Ref. [20] [b] Mean value of the independently determined second-order rate constants obtained by using the stopped-flow technique^[20] ($2.31 \times 10^5 \text{ M}^{-1} \text{ s}^{-1}$) and the laser flash photolysis ($2.97 \times 10^5 \text{ M}^{-1} \text{ s}^{-1}$).

Table 8.8. Rate constants for the reactions of 4-(dimethylamino)pyridine (**4**) with (mfa)₂CH⁺ BF₄⁻ (**1i**) generated from **2i**-Bn BF₄⁻ in DMSO (laser flash photolysis, 20 °C, λ = 589 nm).

| [2i -Bn] ₀ /M | [4] ₀ /M | k _{obs} /s ⁻¹ |
|--|------------------------------|-----------------------------------|
| 8.50 × 10 ⁻⁵ | 8.16 × 10 ⁻⁴ | 5.12 × 10 ³ |
| 8.50 × 10 ⁻⁵ | 1.63 × 10 ⁻³ | 9.60 × 10 ³ |
| 8.50 × 10 ⁻⁵ | 2.45 × 10 ⁻³ | 1.40 × 10 ⁴ |
| 8.50 × 10 ⁻⁵ | 3.26 × 10 ⁻³ | 1.87 × 10 ⁴ |
| 8.50 × 10 ⁻⁵ | 4.08 × 10 ⁻³ | 2.35 × 10 ⁴ |
| $k_2 = 5.62 \times 10^6 \text{ M}^{-1} \text{ s}^{-1}$ | | |

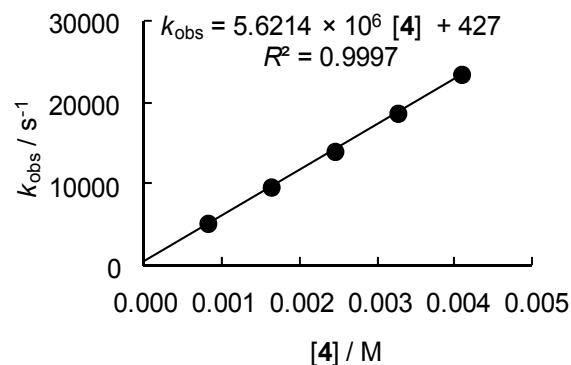


Table 8.9. Rate constants for the reactions of 4-(dimethylamino)pyridine (**4**) with (mfa)₂CH⁺ BF₄⁻ (**1i**) generated from **2i**-Bn BF₄⁻ in DMF (laser flash photolysis, 20 °C, λ = 589 nm).

| [2i -Bn] ₀ /M | [4] ₀ /M | k _{obs} /s ⁻¹ |
|--|------------------------------|-----------------------------------|
| 8.50 × 10 ⁻⁵ | 2.03 × 10 ⁻² | 2.19 × 10 ⁵ |
| 8.50 × 10 ⁻⁵ | 2.67 × 10 ⁻² | 2.72 × 10 ⁵ |
| 8.50 × 10 ⁻⁵ | 3.34 × 10 ⁻² | 3.28 × 10 ⁵ |
| 8.50 × 10 ⁻⁵ | 4.45 × 10 ⁻² | 4.14 × 10 ⁵ |
| 8.50 × 10 ⁻⁵ | 5.11 × 10 ⁻² | 4.65 × 10 ⁵ |
| $k_2 = 7.97 \times 10^6 \text{ M}^{-1} \text{ s}^{-1}$ | | |

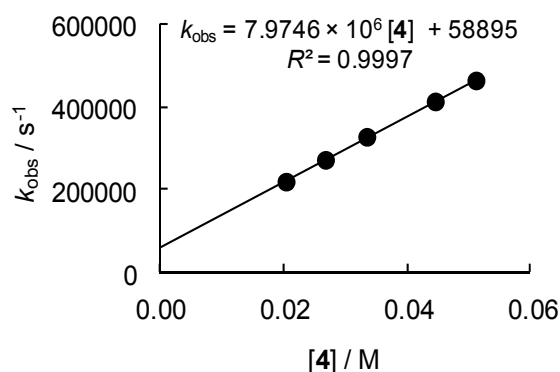
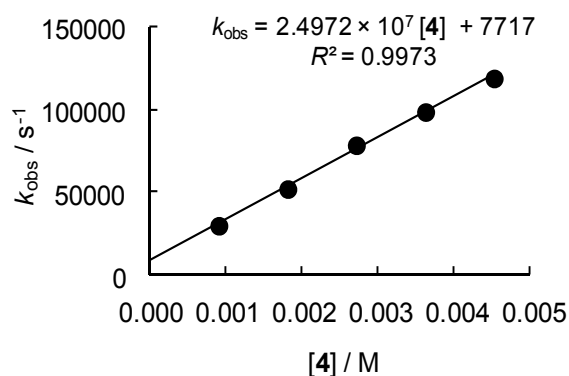


Table 8.10. Rate constants for the reactions of 4-(dimethylamino)pyridine (**4**) with (mfa)₂CH⁺ BF₄⁻ (**1i**) generated from **2i**-Bn BF₄⁻ in acetone (laser flash photolysis, 20 °C, λ = 593 nm).

| [2i -Bn] ₀ /M | [4] ₀ /M | k _{obs} /s ⁻¹ |
|--|------------------------------|-----------------------------------|
| 8.50 × 10 ⁻⁵ | 9.04 × 10 ⁻⁴ | 2.95 × 10 ⁴ |
| 8.50 × 10 ⁻⁵ | 1.81 × 10 ⁻³ | 5.18 × 10 ⁴ |
| 8.50 × 10 ⁻⁵ | 2.71 × 10 ⁻³ | 7.84 × 10 ⁴ |
| 8.50 × 10 ⁻⁵ | 3.62 × 10 ⁻³ | 9.86 × 10 ⁴ |
| 8.50 × 10 ⁻⁵ | 4.52 × 10 ⁻³ | 1.19 × 10 ⁵ |
| $k_2 = 2.50 \times 10^7 \text{ M}^{-1} \text{ s}^{-1}$ | | |



Kinetics of the reactions of 4-(morpholino)pyridine (5) with benzhydrylium ions (1)

Table 8.11. Rate constants for the reactions of 4-(morpholino)pyridine (5) with $(\text{il})_2\text{CH}^+ \text{BF}_4^-$ (1a) in CH_3CN (stopped-flow technique, 20 °C, $\lambda = 631 \text{ nm}$).

| $[\mathbf{1a}]_0/\text{M}$ | $[\mathbf{5}]_0/\text{M}$ | $[\mathbf{5}]_0/[\mathbf{1a}]_0$ | $k_{\text{obs}}/\text{s}^{-1}$ |
|----------------------------|---------------------------|----------------------------------|--------------------------------|
| 1.49×10^{-5} | 4.10×10^{-4} | 27 | 5.99×10^{-1} |
| 1.49×10^{-5} | 8.20×10^{-4} | 55 | 8.98×10^{-1} |
| 1.49×10^{-5} | 1.19×10^{-3} | 80 | 1.16 |
| 1.49×10^{-5} | 1.60×10^{-3} | 107 | 1.47 |
| 1.49×10^{-5} | 2.01×10^{-3} | 134 | 1.76 |

$k_2 = 7.27 \times 10^2 \text{ M}^{-1} \text{ s}^{-1}$

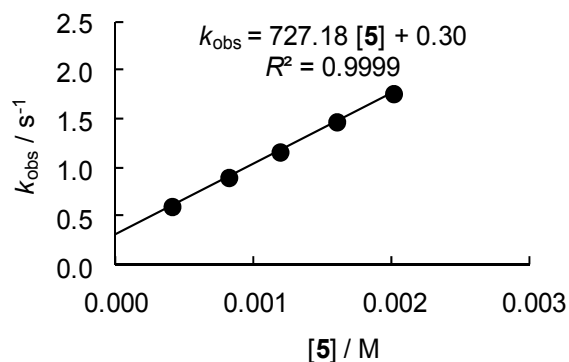


Table 8.12. Rate constants for the reactions of 4-(morpholino)pyridine (5) with $(\text{ind})_2\text{CH}^+ \text{BF}_4^-$ (1c) in CH_3CN (stopped-flow technique, 20 °C, $\lambda = 616 \text{ nm}$).

| $[\mathbf{1c}]_0/\text{M}$ | $[\mathbf{5}]_0/\text{M}$ | $[\mathbf{5}]_0/[\mathbf{1c}]_0$ | $k_{\text{obs}}/\text{s}^{-1}$ |
|----------------------------|---------------------------|----------------------------------|--------------------------------|
| 1.81×10^{-5} | 3.71×10^{-4} | 21 | 2.09 |
| 1.81×10^{-5} | 7.19×10^{-4} | 40 | 3.97 |
| 1.81×10^{-5} | 1.09×10^{-3} | 60 | 5.97 |
| 1.81×10^{-5} | 1.44×10^{-3} | 180 | 8.14 |
| 1.81×10^{-5} | 1.81×10^{-3} | 100 | 1.03×10^1 |

$k_2 = 5.72 \times 10^3 \text{ M}^{-1} \text{ s}^{-1}$

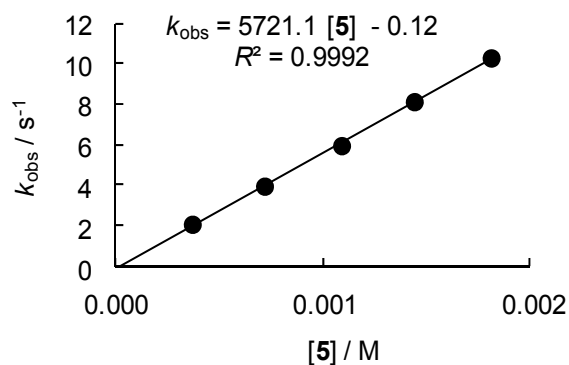
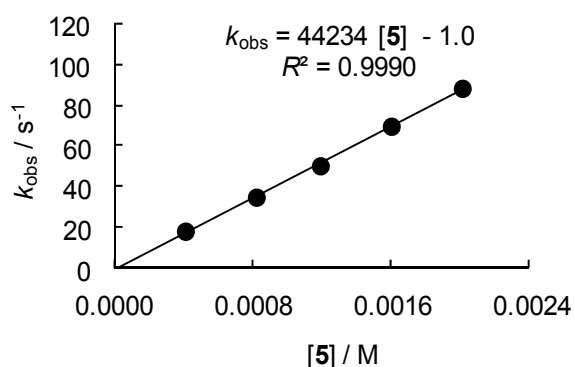


Table 8.13. Rate constants for the reactions of 4-(morpholino)pyridine (**5**) with (pyr)₂CH⁺ BF₄⁻ (**1e**) in CH₃CN (stopped-flow technique, 20 °C, λ = 611 nm).

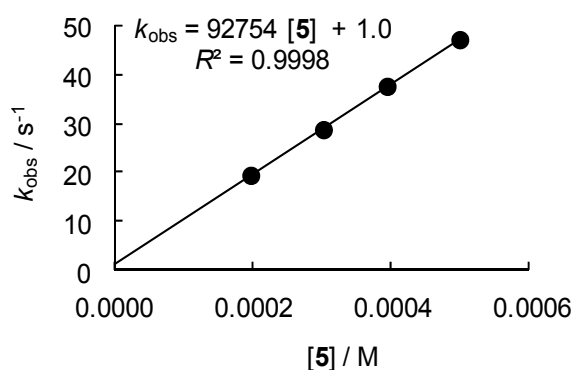
| [1e] ₀ /M | [5] ₀ /M | [5] ₀ /[1e] ₀ | <i>k</i> _{obs} /s ⁻¹ |
|-------------------------------|------------------------------|---|--|
| 1.50 × 10 ⁻⁵ | 4.10 × 10 ⁻⁴ | 27 | 1.80 × 10 ¹ |
| 1.50 × 10 ⁻⁵ | 8.20 × 10 ⁻⁴ | 55 | 3.48 × 10 ¹ |
| 1.50 × 10 ⁻⁵ | 1.19 × 10 ⁻³ | 80 | 5.03 × 10 ¹ |
| 1.50 × 10 ⁻⁵ | 1.60 × 10 ⁻³ | 106 | 6.98 × 10 ¹ |
| 1.50 × 10 ⁻⁵ | 2.01 × 10 ⁻³ | 134 | 8.85 × 10 ¹ |

$k_2 = 4.42 \times 10^4 \text{ M}^{-1} \text{ s}^{-1}$


Table 8.14. Rate constants for the reactions of 4-(morpholino)pyridine (**5**) with (dma)₂CH⁺ BF₄⁻ (**1f**) in CH₃CN (stopped-flow technique, 20 °C, λ = 605 nm).

| [1f] ₀ /M | [5] ₀ /M | [5] ₀ /[1f] ₀ | <i>k</i> _{obs} /s ⁻¹ |
|-------------------------------|------------------------------|---|--|
| 1.99 × 10 ⁻⁵ | 1.97 × 10 ⁻⁴ | 10 | 1.94 × 10 ¹ |
| 1.99 × 10 ⁻⁵ | 3.02 × 10 ⁻⁴ | 15 | 2.88 × 10 ¹ |
| 1.99 × 10 ⁻⁵ | 3.94 × 10 ⁻⁴ | 20 | 3.77 × 10 ¹ |
| 1.99 × 10 ⁻⁵ | 4.99 × 10 ⁻⁴ | 25 | 4.73 × 10 ¹ |

$k_2 = 9.28 \times 10^4 \text{ M}^{-1} \text{ s}^{-1}$


Table 8.15. Rate constants for the reactions of 4-(morpholino)pyridine (**5**) with (dma)₂CH⁺ BF₄⁻ (**1f**) generated from **2f**-Bn BF₄⁻ in CH₃CN (laser flash photolysis, 20 °C, λ = 605 nm).

| [2f -Bn] ₀ /M | [4] ₀ /M | <i>k</i> _{obs} /s ⁻¹ |
|----------------------------------|------------------------------|--|
| 1.21 × 10 ⁻⁴ | 6.74 × 10 ⁻⁴ | 1.56 × 10 ² |
| 1.21 × 10 ⁻⁴ | 1.35 × 10 ⁻³ | 2.54 × 10 ² |
| 1.21 × 10 ⁻⁴ | 2.02 × 10 ⁻³ | 3.41 × 10 ² |
| 1.21 × 10 ⁻⁴ | 2.70 × 10 ⁻³ | 4.28 × 10 ² |
| 1.21 × 10 ⁻⁴ | 3.37 × 10 ⁻³ | 5.28 × 10 ² |

$k_2 = 1.36 \times 10^5 \text{ M}^{-1} \text{ s}^{-1}$

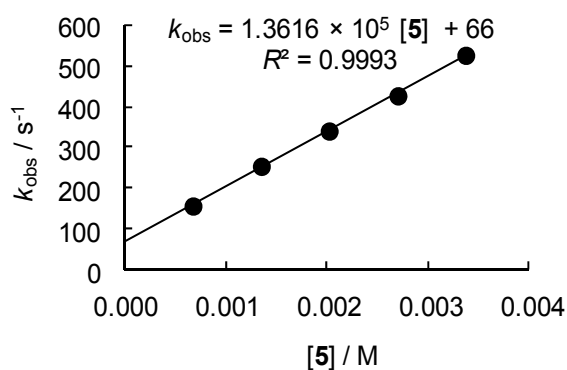


Table 8.16. Rate constants for the reactions of 4-(morpholino)pyridine (**5**) with (mor)₂CH⁺ BF₄⁻ (**1h**) generated from **2h**-Bn BF₄⁻ in CH₃CN (laser flash photolysis, 20 °C, λ = 612 nm).

| [2h -Bn] ₀ /M | [5] ₀ /M | <i>k</i> _{obs} /s ⁻¹ |
|----------------------------------|------------------------------|--|
| 1.20 × 10 ⁻⁴ | 2.48 × 10 ⁻³ | 2.16 × 10 ³ |
| 1.20 × 10 ⁻⁴ | 4.13 × 10 ⁻³ | 3.24 × 10 ³ |
| 1.20 × 10 ⁻⁴ | 5.78 × 10 ⁻³ | 4.33 × 10 ³ |
| 1.20 × 10 ⁻⁴ | 7.43 × 10 ⁻³ | 5.33 × 10 ³ |
| 1.20 × 10 ⁻⁴ | 9.08 × 10 ⁻³ | 6.31 × 10 ³ |

$k_2 = 6.30 \times 10^5 \text{ M}^{-1} \text{ s}^{-1}$

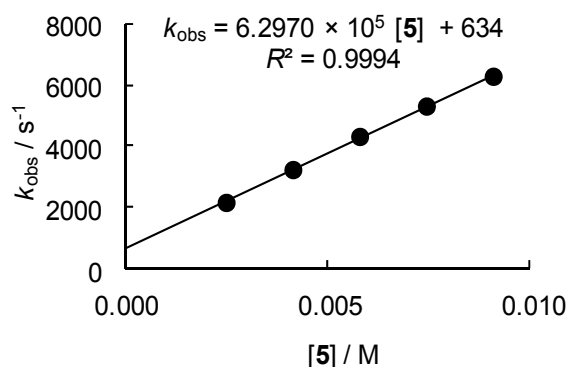


Table 8.17. Rate constants for the reactions of 4-(morpholino)pyridine (**5**) with (mfa)₂CH⁺ BF₄⁻ (**1i**) generated from **2i**-Bn BF₄⁻ in CH₃CN (laser flash photolysis, 20 °C, λ = 586 nm).

| [2i -Bn] ₀ /M | [5] ₀ /M | <i>k</i> _{obs} /s ⁻¹ |
|----------------------------------|------------------------------|--|
| 1.21 × 10 ⁻⁴ | 1.73 × 10 ⁻³ | 1.32 × 10 ⁴ |
| 1.21 × 10 ⁻⁴ | 2.88 × 10 ⁻³ | 2.04 × 10 ⁴ |
| 1.21 × 10 ⁻⁴ | 4.03 × 10 ⁻³ | 2.78 × 10 ⁴ |
| 1.21 × 10 ⁻⁴ | 5.19 × 10 ⁻³ | 3.53 × 10 ⁴ |
| 1.21 × 10 ⁻⁴ | 6.34 × 10 ⁻³ | 4.26 × 10 ⁴ |

$k_2 = 6.39 \times 10^6 \text{ M}^{-1} \text{ s}^{-1}$

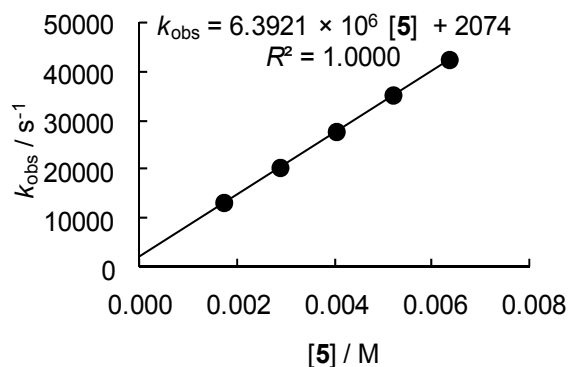
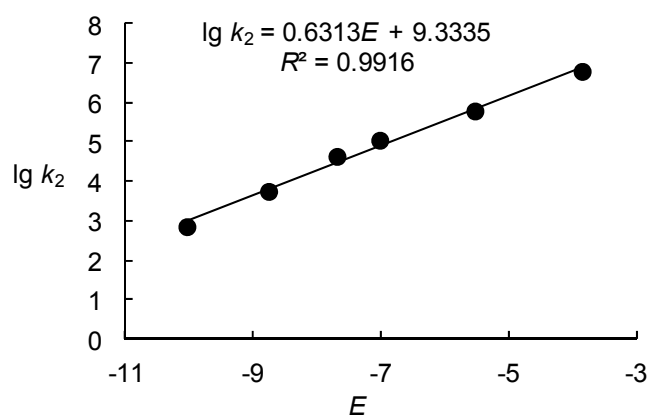


Table 8.18. Determination of the nucleophilicity parameters N and s_N for 4-(morpholino)-pyridine (**5**) in CH_3CN .

| Electrophile (E) | $k_2/\text{M}^{-1} \text{s}^{-1}$ | $\lg k_2$ |
|----------------------|-----------------------------------|-----------|
| 1a (-10.04) | 7.27×10^2 | 2.86 |
| 1c (-8.76) | 5.72×10^3 | 3.76 |
| 1e (-7.69) | 4.42×10^4 | 4.65 |
| 1f (-7.02) | 1.14×10^5 [a] | 5.06 |
| 1h (-5.53) | 6.30×10^5 | 5.80 |
| 1i (-3.85) | 6.39×10^6 | 6.81 |

$N = 14.80, s_N = 0.63$



[a] Mean value of the independently determined second-order rate constants obtained by using the stopped-flow technique ($9.28 \times 10^4 \text{M}^{-1} \text{s}^{-1}$) and the laser flash photolysis ($1.36 \times 10^5 \text{M}^{-1} \text{s}^{-1}$).

Kinetics of the reactions of 3-bromo-4-(dimethylamino)pyridine (6) with benzhydrylium ions (1)

Table 8.19. Rate constants for the reactions of 3-bromo-4-(dimethylamino)pyridine (**6**) with $(\text{pyr})_2\text{CH}^+ \text{BF}_4^-$ (**1e**) in CH_3CN (stopped-flow technique, 20°C , $\lambda = 611 \text{nm}$).

| $[\mathbf{1e}]_0/\text{M}$ | $[\mathbf{6}]_0/\text{M}$ | $[\mathbf{6}]_0/[\mathbf{1e}]_0$ | $k_{\text{obs}}/\text{s}^{-1}$ |
|----------------------------|---------------------------|----------------------------------|--------------------------------|
| 1.80×10^{-5} | 9.04×10^{-4} | 50 | 1.62×10^1 |
| 1.80×10^{-5} | 1.81×10^{-3} | 101 | 1.98×10^1 |
| 1.80×10^{-5} | 2.71×10^{-3} | 151 | 2.35×10^1 |
| 1.80×10^{-5} | 3.62×10^{-3} | 201 | 2.71×10^1 |
| 1.80×10^{-5} | 4.52×10^{-3} | 251 | 3.08×10^1 |

$k_2 = 4.04 \times 10^3 \text{M}^{-1} \text{s}^{-1}$

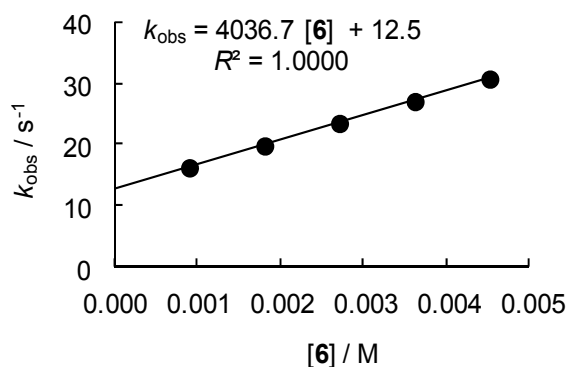
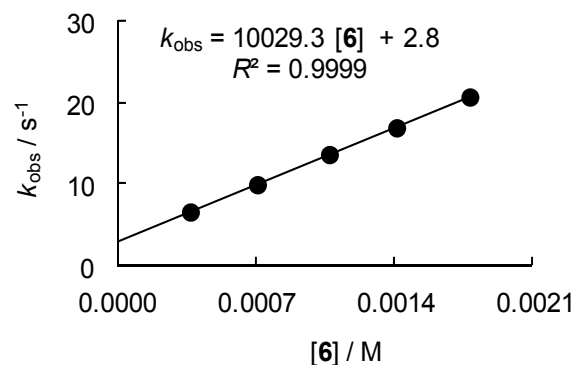
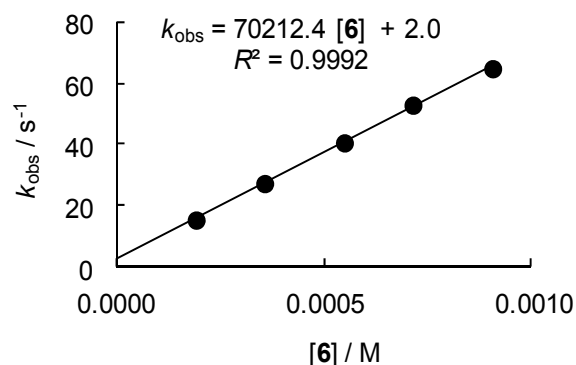


Table 8.20. Rate constants for the reactions of 3-bromo-4-(dimethylamino)pyridine (**6**) with (dma)₂CH⁺ BF₄⁻ (**1f**) in CH₃CN (stopped-flow technique, 20 °C, λ = 605 nm).

| [1f] ₀ /M | [6] ₀ /M | [6] ₀ /[1f] ₀ | <i>k</i> _{obs} /s ⁻¹ |
|--|------------------------------|---|--|
| 1.80 × 10 ⁻⁵ | 3.67 × 10 ⁻⁴ | 21 | 6.51 |
| 1.80 × 10 ⁻⁵ | 7.06 × 10 ⁻⁴ | 40 | 9.88 |
| 1.80 × 10 ⁻⁵ | 1.07 × 10 ⁻³ | 60 | 1.36 × 10 ¹ |
| 1.80 × 10 ⁻⁵ | 1.41 × 10 ⁻³ | 79 | 1.69 × 10 ¹ |
| 1.80 × 10 ⁻⁵ | 1.78 × 10 ⁻³ | 100 | 2.07 × 10 ¹ |
| <i>k</i> ₂ = 1.00 × 10 ⁴ M ⁻¹ s ⁻¹ | | | |


Table 8.21. Rate constants for the reactions of 3-bromo-4-(dimethylamino)pyridine (**6**) with (mpa)₂CH⁺ BF₄⁻ (**1g**) in CH₃CN (stopped-flow technique, 20 °C, λ = 612 nm).

| [1g] ₀ /M | [6] ₀ /M | [6] ₀ /[1g] ₀ | <i>k</i> _{obs} /s ⁻¹ |
|--|------------------------------|---|--|
| 9.00 × 10 ⁻⁶ | 1.92 × 10 ⁻⁴ | 21 | 1.52 × 10 ¹ |
| 9.00 × 10 ⁻⁶ | 3.57 × 10 ⁻⁴ | 40 | 2.72 × 10 ¹ |
| 9.00 × 10 ⁻⁶ | 5.49 × 10 ⁻⁴ | 61 | 4.06 × 10 ¹ |
| 9.00 × 10 ⁻⁶ | 7.14 × 10 ⁻⁴ | 79 | 5.30 × 10 ¹ |
| 9.00 × 10 ⁻⁶ | 9.06 × 10 ⁻⁴ | 101 | 6.50 × 10 ¹ |
| <i>k</i> ₂ = 7.02 × 10 ⁴ M ⁻¹ s ⁻¹ | | | |


Table 8.22. Rate constants for the reactions of 3-bromo-4-(dimethylamino)pyridine (**6**) with (mor)₂CH⁺ BF₄⁻ (**1h**) in CH₃CN (stopped-flow technique, 20 °C, λ = 611 nm).

| [1h] ₀ /M | [6] ₀ /M | [6] ₀ /[1h] ₀ | <i>k</i> _{obs} /s ⁻¹ |
|--|------------------------------|---|--|
| 7.26 × 10 ⁻⁶ | 2.70 × 10 ⁻⁴ | 37 | 1.74 × 10 ¹ |
| 7.26 × 10 ⁻⁶ | 5.73 × 10 ⁻⁴ | 79 | 3.45 × 10 ¹ |
| 7.26 × 10 ⁻⁶ | 8.42 × 10 ⁻⁴ | 116 | 5.03 × 10 ¹ |
| 7.26 × 10 ⁻⁶ | 1.15 × 10 ⁻³ | 158 | 6.81 × 10 ¹ |
| 7.26 × 10 ⁻⁶ | 1.42 × 10 ⁻³ | 195 | 8.35 × 10 ¹ |
| <i>k</i> ₂ = 5.76 × 10 ⁴ M ⁻¹ s ⁻¹ | | | |

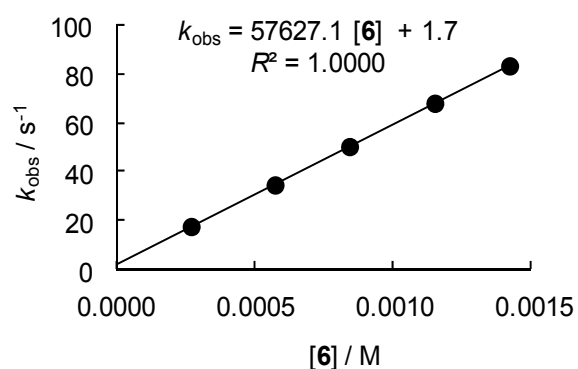


Table 8.23. Rate constants for the reactions of 3-bromo-4-(dimethylamino)pyridine (**6**) with (mfa)₂CH⁺ BF₄⁻ (**1i**) in CH₃CN (stopped-flow technique, 20 °C, λ = 586 nm).

| [1i] ₀ /M | [6] ₀ /M | [6] ₀ /[1i] ₀ | <i>k</i> _{obs} /s ⁻¹ |
|-------------------------------|------------------------------|---|--|
| 9.01 × 10 ⁻⁶ | 1.37 × 10 ⁻⁴ | 15 | 9.81 × 10 ¹ |
| 9.01 × 10 ⁻⁶ | 1.92 × 10 ⁻⁴ | 21 | 1.36 × 10 ² |
| 9.01 × 10 ⁻⁶ | 2.20 × 10 ⁻⁴ | 24 | 1.51 × 10 ² |
| 9.01 × 10 ⁻⁶ | 2.75 × 10 ⁻⁴ | 30 | 1.89 × 10 ² |
| 9.01 × 10 ⁻⁶ | 3.29 × 10 ⁻⁴ | 37 | 2.22 × 10 ² |

$k_2 = 6.45 \times 10^5 \text{ M}^{-1} \text{ s}^{-1}$

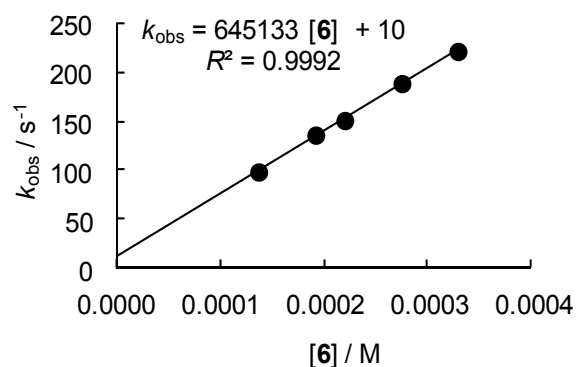


Table 8.24. Rate constants for the reactions of 3-bromo-4-(dimethylamino)pyridine (**6**) with (fur)₂CH⁺ BF₄⁻ (**1j**) generated from **2j**-Bn Cl⁻ in CH₃CN (laser flash photolysis, 20 °C, λ = 523 nm).

| [2j -Bn] ₀ /M | [6] ₀ /M | <i>k</i> _{obs} /s ⁻¹ |
|----------------------------------|------------------------------|--|
| 1.20 × 10 ⁻⁴ | 2.57 × 10 ⁻² | 2.71 × 10 ⁶ |
| 1.20 × 10 ⁻⁴ | 3.13 × 10 ⁻² | 3.14 × 10 ⁶ |
| 1.20 × 10 ⁻⁴ | 4.81 × 10 ⁻² | 4.40 × 10 ⁶ |
| 1.20 × 10 ⁻⁴ | 5.49 × 10 ⁻² | 5.12 × 10 ⁶ |
| 1.20 × 10 ⁻⁴ | 6.80 × 10 ⁻² | 6.17 × 10 ⁶ |

$k_2 = 8.20 \times 10^7 \text{ M}^{-1} \text{ s}^{-1}$

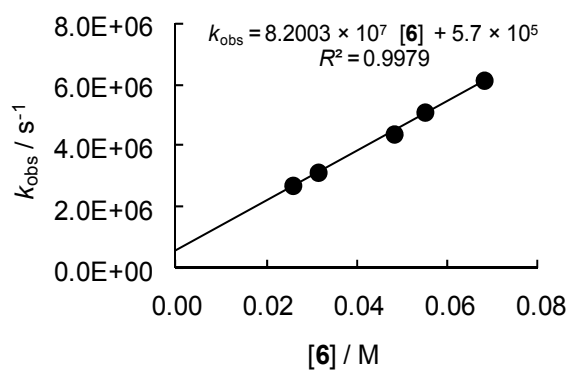
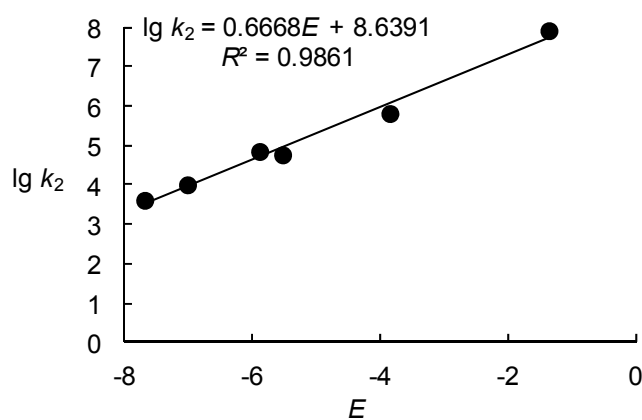


Table 8.25. Determination of the nucleophilicity parameters N and s_N for 3-bromo-4-(dimethylamino)pyridine (**6**) in CH_3CN

| Electrophile (E) | $k_2/\text{M}^{-1} \text{s}^{-1}$ | $\lg k_2$ |
|----------------------|-----------------------------------|-----------|
| 1e (-7.69) | 4.04×10^3 | 3.61 |
| 1f (-7.02) | 1.00×10^4 | 4.00 |
| 1g (-5.89) | 7.02×10^4 | 4.85 |
| 1h (-5.53) | 5.76×10^4 | 4.76 |
| 1i (-3.85) | 6.45×10^5 | 5.81 |
| 1j (-1.36) | 8.20×10^7 | 7.91 |

$N = 12.96, s_N = 0.67$



Kinetics of the reactions of 3,5-dibromo-4-aminopyridine (7) with benzhydrylium ions (1)

Table 8.26. Rate constants for the reactions of 3,5-dibromo-4-aminopyridine (**7**) with $(\text{mor})_2\text{CH}^+ \text{BF}_4^-$ (**1h**) in CH_3CN (stopped-flow technique, 20°C , $\lambda = 611 \text{ nm}$).

| $[\mathbf{1h}]_0/\text{M}$ | $[\mathbf{7}]_0/\text{M}$ | $[\mathbf{7}]_0/[\mathbf{1h}]_0$ | $k_{\text{obs}}/\text{s}^{-1}$ |
|----------------------------|---------------------------|----------------------------------|--------------------------------|
| 1.91×10^{-5} | 3.77×10^{-4} | 20 | 9.88 |
| 1.91×10^{-5} | 7.53×10^{-4} | 40 | 1.62×10^1 |
| 1.91×10^{-5} | 1.13×10^{-3} | 60 | 2.24×10^1 |
| 1.91×10^{-5} | 1.51×10^{-3} | 80 | 2.84×10^1 |
| 1.91×10^{-5} | 1.88×10^{-3} | 100 | 3.45×10^1 |

$k_2 = 1.63 \times 10^4 \text{ M}^{-1} \text{ s}^{-1}$

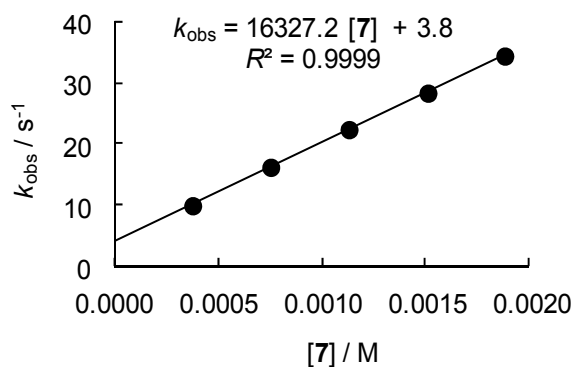


Table 8.27. Rate constants for the reactions of 3,5-dibromo-4-aminopyridine (**7**) with $(\text{mfa})_2\text{CH}^+ \text{BF}_4^-$ (**1i**) in CH_3CN (stopped-flow technique, 20 °C, $\lambda = 586 \text{ nm}$).

| $[\mathbf{1i}]_0/\text{M}$ | $[\mathbf{7}]_0/\text{M}$ | $[\mathbf{7}]_0/[\mathbf{1i}]_0$ | $k_{\text{obs}}/\text{s}^{-1}$ |
|----------------------------|---------------------------|----------------------------------|--------------------------------|
| 1.78×10^{-5} | 1.83×10^{-4} | 10 | 3.74×10^1 |
| 1.78×10^{-5} | 2.74×10^{-4} | 15 | 5.34×10^1 |
| 1.78×10^{-5} | 3.65×10^{-4} | 21 | 7.20×10^1 |
| 1.78×10^{-5} | 4.57×10^{-4} | 26 | 9.04×10^1 |
| 1.78×10^{-5} | 5.25×10^{-4} | 29 | 1.04×10^2 |

$k_2 = 1.96 \times 10^5 \text{ M}^{-1} \text{ s}^{-1}$

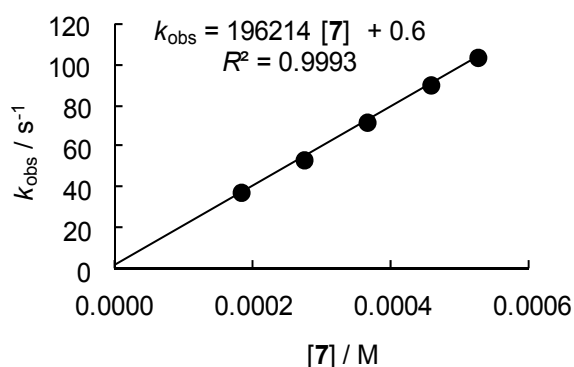


Table 8.28. Rate constants for the reactions of 3,5-dibromo-4-aminopyridine (**7**) with $(\text{fur})_2\text{CH}^+ \text{BF}_4^-$ (**1j**) generated from **2j**-Bn Cl^- in CH_3CN (laser flash photolysis, 20 °C, $\lambda = 523 \text{ nm}$).

| $[\mathbf{2j-Bn}]_0/\text{M}$ | $[\mathbf{7}]_0/\text{M}$ | $k_{\text{obs}}/\text{s}^{-1}$ |
|-------------------------------|---------------------------|--------------------------------|
| 1.11×10^{-4} | 2.63×10^{-2} | 3.38×10^6 |
| 1.11×10^{-4} | 3.81×10^{-2} | 3.90×10^6 |
| 1.11×10^{-4} | 5.19×10^{-2} | 4.46×10^6 |
| 1.11×10^{-4} | 6.05×10^{-2} | 4.89×10^6 |
| 1.11×10^{-4} | 9.85×10^{-2} | 6.76×10^6 |

$k_2 = 4.97 \times 10^7 \text{ M}^{-1} \text{ s}^{-1}$

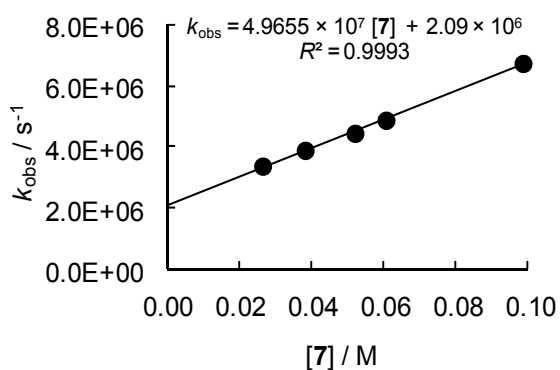


Table 8.29. Rate constants for the reactions of 3,5-dibromo-4-aminopyridine (**7**) with $(\text{ani})_2\text{CH}^+ \text{BF}_4^-$ (**1k**) generated from **2k**-Bn Cl^- in CH_3CN (laser flash photolysis, 20 °C, $\lambda = 508 \text{ nm}$).

| $[\mathbf{2k}\text{-Bn}]_0/\text{M}$ | $[\mathbf{7}]_0/\text{M}$ | $k_{\text{obs}}/\text{s}^{-1}$ |
|--|---------------------------|--------------------------------|
| 1.19×10^{-4} | 1.23×10^{-2} | 5.38×10^6 |
| 1.19×10^{-4} | 2.04×10^{-2} | 6.02×10^6 |
| 1.19×10^{-4} | 2.71×10^{-2} | 7.03×10^6 |
| 1.19×10^{-4} | 3.49×10^{-2} | 7.77×10^6 |
| 1.19×10^{-4} | 4.31×10^{-2} | 9.49×10^6 |
| $k_2 = 1.31 \times 10^8 \text{ M}^{-1} \text{ s}^{-1}$ | | |

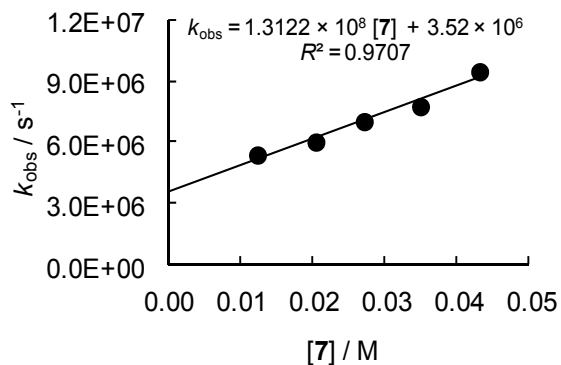
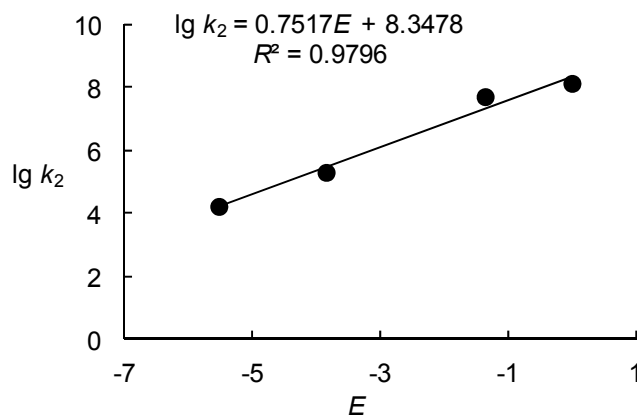


Table 8.30. Determination of the nucleophilicity parameters N and s_N for 3,5-dibromo-4-aminopyridine (**7**) in CH_3CN .

| Electrophile (E) | $k_2/\text{M}^{-1} \text{ s}^{-1}$ | $\lg k_2$ |
|-------------------------|------------------------------------|-----------|
| 1h (-5.53) | 1.63×10^4 | 4.21 |
| 1i (-3.85) | 1.96×10^5 | 5.29 |
| 1j (-1.36) | 4.97×10^7 | 7.67 |
| 1k (0.00) | 1.31×10^8 | 8.12 |
| $N = 11.11, s_N = 0.75$ | | |



Kinetics of the reactions of N-acetyl-4-aminopyridine (8) with benzhydrylium ions (1)

Table 8.31. Rate constants for the reactions of N-acetyl-4-aminopyridine (8) with (thq)₂CH⁺ BF₄⁻ (1d) in CH₃CN (stopped-flow technique, 20 °C, λ = 619 nm).

| [1d] ₀ /M | [8] ₀ /M | [8] ₀ /[1d] ₀ | k _{obs} /s ⁻¹ |
|--|-------------------------|-------------------------------------|-----------------------------------|
| 1.50 × 10 ⁻⁵ | 1.72 × 10 ⁻³ | 115 | 2.63 × 10 ¹ |
| 1.50 × 10 ⁻⁵ | 2.29 × 10 ⁻³ | 153 | 2.79 × 10 ¹ |
| 1.50 × 10 ⁻⁵ | 2.86 × 10 ⁻³ | 191 | 2.87 × 10 ¹ |
| 1.50 × 10 ⁻⁵ | 3.43 × 10 ⁻³ | 229 | 3.03 × 10 ¹ |
| 1.50 × 10 ⁻⁵ | 4.01 × 10 ⁻³ | 267 | 3.19 × 10 ¹ |
| $k_2 = 2.38 \times 10^3 \text{ M}^{-1} \text{ s}^{-1}$ | | | |

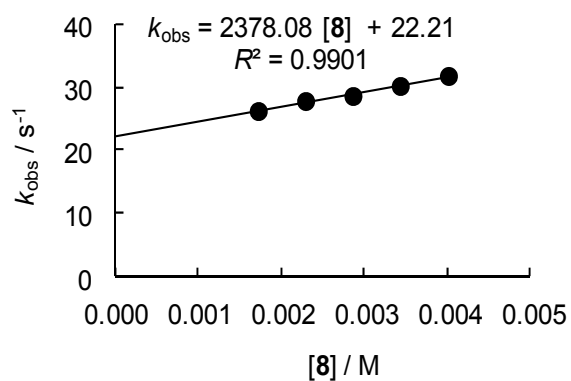


Table 8.32. Rate constants for the reactions of N-acetyl-4-aminopyridine (8) with (pyr)₂CH⁺ BF₄⁻ (1e) in CH₃CN (stopped-flow technique, 20 °C, λ = 611 nm).

| [1e] ₀ /M | [8] ₀ /M | [8] ₀ /[1e] ₀ | k _{obs} /s ⁻¹ |
|--|-------------------------|-------------------------------------|-----------------------------------|
| 1.42 × 10 ⁻⁵ | 2.70 × 10 ⁻⁴ | 19 | 2.08 × 10 ¹ |
| 1.42 × 10 ⁻⁵ | 5.40 × 10 ⁻⁴ | 38 | 2.30 × 10 ¹ |
| 1.42 × 10 ⁻⁵ | 8.10 × 10 ⁻⁴ | 57 | 2.51 × 10 ¹ |
| 1.42 × 10 ⁻⁵ | 1.08 × 10 ⁻³ | 76 | 2.60 × 10 ¹ |
| 1.42 × 10 ⁻⁵ | 1.35 × 10 ⁻³ | 95 | 2.78 × 10 ¹ |
| $k_2 = 6.30 \times 10^3 \text{ M}^{-1} \text{ s}^{-1}$ | | | |

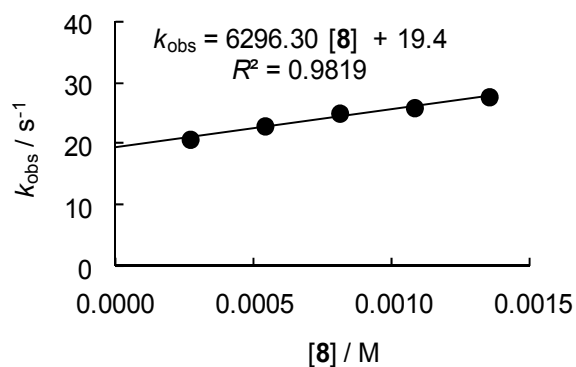
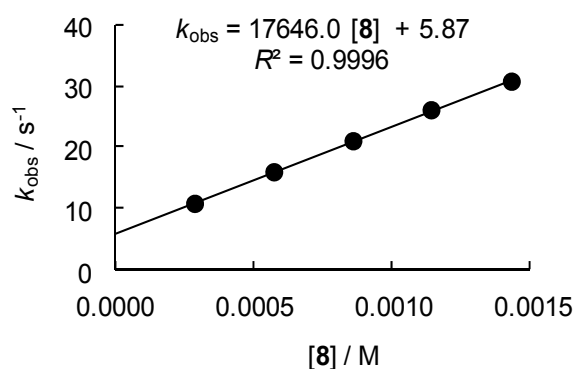
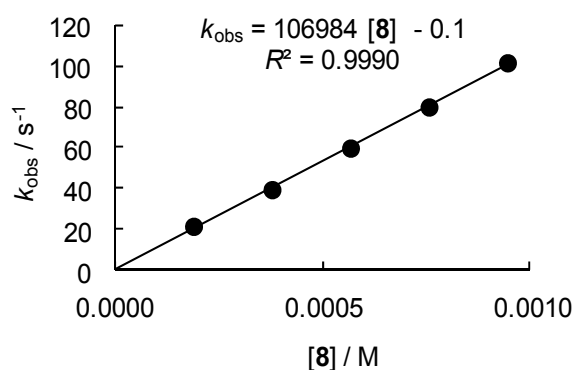


Table 8.33. Rate constants for the reactions of *N*-acetyl-4-aminopyridine (**8**) with (dma)₂CH⁺ BF₄⁻ (**1f**) in CH₃CN (stopped-flow technique, 20 °C, λ = 605 nm).

| [1f] ₀ /M | [8] ₀ /M | [8] ₀ /[1f] ₀ | <i>k</i> _{obs} /s ⁻¹ |
|--|------------------------------|---|--|
| 1.47 × 10 ⁻⁵ | 2.86 × 10 ⁻⁴ | 20 | 1.08 × 10 ¹ |
| 1.47 × 10 ⁻⁵ | 5.72 × 10 ⁻⁴ | 39 | 1.60 × 10 ¹ |
| 1.47 × 10 ⁻⁵ | 8.58 × 10 ⁻⁴ | 59 | 2.11 × 10 ¹ |
| 1.47 × 10 ⁻⁵ | 1.14 × 10 ⁻³ | 78 | 2.62 × 10 ¹ |
| 1.47 × 10 ⁻⁵ | 1.43 × 10 ⁻³ | 98 | 3.09 × 10 ¹ |
| <i>k</i> ₂ = 1.76 × 10 ⁴ M ⁻¹ s ⁻¹ | | | |


Table 8.34. Rate constants for the reactions of *N*-acetyl-4-aminopyridine (**8**) with (mor)₂CH⁺ BF₄⁻ (**1h**) in CH₃CN (stopped-flow technique, 20 °C, λ = 611 nm).

| [1h] ₀ /M | [8] ₀ /M | [8] ₀ /[1h] ₀ | <i>k</i> _{obs} /s ⁻¹ |
|--|------------------------------|---|--|
| 1.90 × 10 ⁻⁵ | 1.89 × 10 ⁻⁴ | 10 | 2.13 × 10 ¹ |
| 1.90 × 10 ⁻⁵ | 3.78 × 10 ⁻⁴ | 20 | 3.94 × 10 ¹ |
| 1.90 × 10 ⁻⁵ | 5.67 × 10 ⁻⁴ | 30 | 5.99 × 10 ¹ |
| 1.90 × 10 ⁻⁵ | 7.56 × 10 ⁻⁴ | 40 | 8.02 × 10 ¹ |
| 1.90 × 10 ⁻⁵ | 9.45 × 10 ⁻⁴ | 50 | 1.02 × 10 ² |
| <i>k</i> ₂ = 1.07 × 10 ⁵ M ⁻¹ s ⁻¹ | | | |


Table 8.35. Rate constants for the reactions of *N*-acetyl-4-aminopyridine (**8**) with (mfa)₂CH⁺ BF₄⁻ (**1i**) generated from **2i**-Bn BF₄⁻ in CH₃CN (laser flash photolysis, 20 °C, λ = 586 nm).

| [2i -Bn] ₀ /M | [8] ₀ /M | <i>k</i> _{obs} /s ⁻¹ |
|--|------------------------------|--|
| 1.21 × 10 ⁻⁴ | 1.76 × 10 ⁻² | 2.72 × 10 ⁴ |
| 1.21 × 10 ⁻⁴ | 3.08 × 10 ⁻² | 4.56 × 10 ⁴ |
| 1.21 × 10 ⁻⁴ | 4.57 × 10 ⁻² | 6.62 × 10 ⁴ |
| 1.21 × 10 ⁻⁴ | 5.89 × 10 ⁻² | 8.54 × 10 ⁴ |
| 1.21 × 10 ⁻⁴ | 7.59 × 10 ⁻² | 1.06 × 10 ⁵ |
| <i>k</i> ₂ = 1.36 × 10 ⁶ M ⁻¹ s ⁻¹ | | |

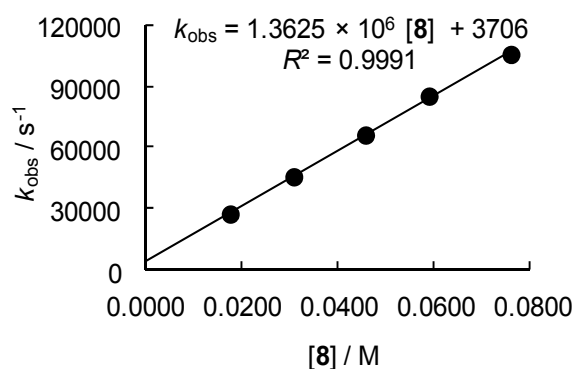


Table 8.36. Rate constants for the reactions of *N*-acetyl-4-aminopyridine (**8**) with (fur)₂CH⁺ BF₄⁻ (**1j**) generated from **2j**-Bn Cl⁻ in CH₃CN (laser flash photolysis, 20 °C, λ = 523 nm).

| [2j -Bn] ₀ /M | [8] ₀ /M | <i>k</i> _{obs} /s ⁻¹ |
|----------------------------------|------------------------------|--|
| 1.20 × 10 ⁻⁴ | 3.89 × 10 ⁻² | 5.44 × 10 ⁶ |
| 1.20 × 10 ⁻⁴ | 4.79 × 10 ⁻² | 6.78 × 10 ⁶ |
| 1.20 × 10 ⁻⁴ | 5.58 × 10 ⁻² | 7.51 × 10 ⁶ |
| 1.20 × 10 ⁻⁴ | 7.78 × 10 ⁻² | 1.03 × 10 ⁷ |
| 1.20 × 10 ⁻⁴ | 8.89 × 10 ⁻² | 1.20 × 10 ⁷ |

$k_2 = 1.28 \times 10^8 \text{ M}^{-1} \text{ s}^{-1}$

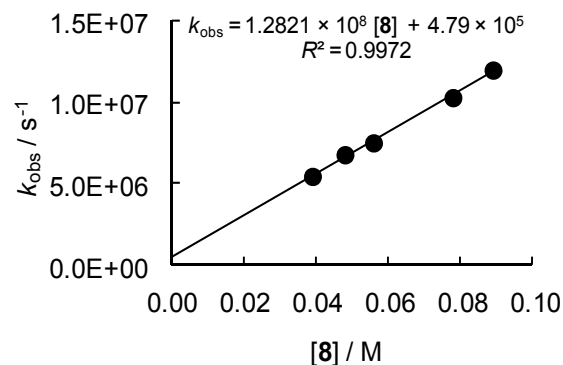
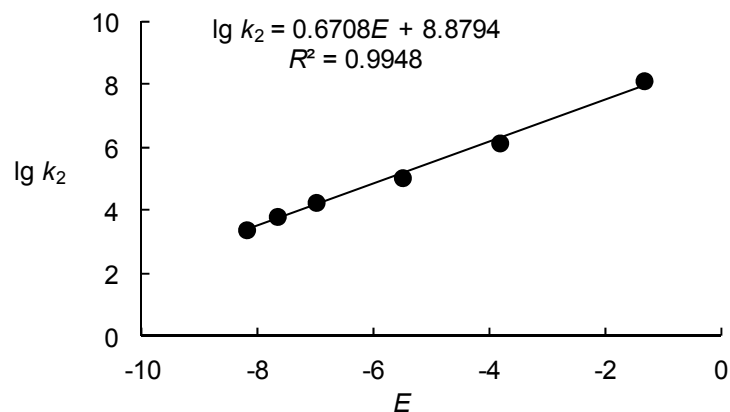


Table 8.37. Determination of the nucleophilicity parameters *N* and *s*_N for *N*-acetyl-4-aminopyridine (**8**) in CH₃CN.

| Electrophile (<i>E</i>) | <i>k</i> ₂ /M ⁻¹ s ⁻¹ | lg <i>k</i> ₂ |
|---------------------------|--|--------------------------|
| 1d (-8.22) | 2.38 × 10 ³ | 3.38 |
| 1e (-7.69) | 6.30 × 10 ³ | 3.80 |
| 1f (-7.02) | 1.76 × 10 ⁴ | 4.25 |
| 1h (-5.53) | 1.07 × 10 ⁵ | 5.03 |
| 1i (-3.85) | 1.36 × 10 ⁶ | 6.18 |
| 1j (-1.36) | 1.28 × 10 ⁸ | 8.11 |

$N = 13.24, s_N = 0.67$



Kinetics of the reactions of benzhydrylium ions (I) with aqueous acetone

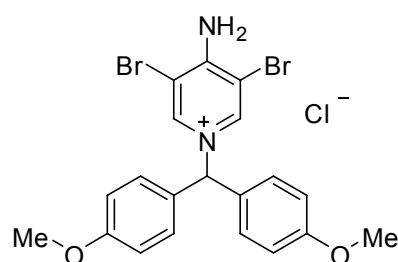
Table 8.38. First order rate constants for the reaction of $\text{ani(Ph)CH}^+ \text{BF}_4^-$ (**11**) generated from **21-Bn** Cl^- with aqueous acetone (laser flash photolysis, 20°C, $\lambda = 455 \text{ nm}$) and comparison with the calculated rate constant.

| solvent ^[a] | [21-Bn] ₀ /M | k_1 ^[b] /s ⁻¹ | k_{calc} ^[c] /s ⁻¹ | k_1/k_{calc} |
|------------------------|----------------------------------|---------------------------------------|---|-----------------------|
| 90A10W | 8.00×10^{-5} | 6.23×10^6 | 4.35×10^6 | 1.43 |
| 80A20W | 8.00×10^{-5} | 6.61×10^6 | 7.17×10^6 | 0.92 |

[a] Solvent mixtures given in v/v (A = acetone, W = water). [b] Laser flash photolysis of **21-Bn**. [c] Calculated from Equation (8.1) using the previously published N_1 and s_N parameters of acetone/water mixtures (90A10W: $N_1 = 5.70$, $s_N = 0.85$; 80A20W: $N_1 = 5.77$, $s_N = 0.87$).^[24]

8.4.3 Product Characterization

[Bis(4-methoxyphenyl)methyl]-3,5-dibromo-4-aminopyridinium chloride



3,5-Dibromo-4-aminopyridine (**7**, 45 mg, 0.18 mmol) was added to a solution of 4,4'-dimethoxybenzhydryl chloride (**1k-Cl**, 47 mg, 0.18 mmol) in CD_3CN (1 mL), stirred for 5 min at RT, and analyzed by NMR spectroscopy.

¹H NMR (300 MHz, CD_3CN): $\delta = 3.77$ (s, 6 H, OCH_3), 6.93 (d, $J = 8.9 \text{ Hz}$, 4 H, H_{ar}), 7.19 (d, $J = 8.6 \text{ Hz}$, 4 H, H_{ar}), 7.59 (s, 1 H, Ar_2CH), 7.89 (brs, 2 H, NH_2), 8.70 (s, 2 H, CH_{pyr}).

¹³C-NMR (75 MHz, CD_3CN): $\delta = 56.1$ (q), 73.9 (d, Ar_2CH), 105.3 (s), 115.4 (d), 129.3 (s), 131.2 (d), 143.4 (d), 155.7 (s), 161.2 (s).

NMR signal assignments were based on additional 2D-NMR experiments (HSQC, and HMBC). The attack of the pyridine nitrogen is evident from the ³J coupling between Ar_2CH and CH_{pyr} in the HMBC spectrum.

8.5 References

- [1] Reviews: a) M. I. Knyazhanskii, Y. R. Tymyanskii, V. M. Feigelman, A. R. Katritzky, *Heterocycles* **1987**, *26*, 2963–2982; b) P. S. Mariano in *CRC Handbook of Organic Photochemistry and Photobiology* (Ed.: W. Horspool, F. Lenci), *2nd ed.*, CRC Press, Boca Raton, **2004**, pp. 100–1 – 100–10; c) T. Damiano, D. Morton, A. Nelson, *Org. Biomol. Chem.* **2007**, *5*, 2735–2752; d) J. Zou, P. S. Mariano, *Photochem. Photobiol. Sci.* **2008**, *7*, 393–404.
- [2] Review: W. Schnabel, *Macromol. Rapid Commun.* **2000**, *21*, 628–642.
- [3] General reviews on photoinitiators in cationic polymerizations: a) R. Lazauskaite, J. V. Grazulevicius in *Handbook of Photochemistry and Photobiology, Vol. 2* (Ed.: H. S. Nalwa.) American Scientific Publishers, Stevenson Ranch (CA), **2003**, pp. 335–392; b) Y. Yagci, S. Jockusch, N. J. Turro, *Macromolecules* **2010**, *43*, 6245–6260; c) K. Suyama, M. Shirai, *Prog. Polym. Sci.* **2009**, *34*, 194–209.
- [4] a) F. Kasapoglu, M. Aydin, N. Arsu, Y. Yagci, *J. Photochem. Photobiol., A* **2003**, *159*, 151–159; b) N. Yonet, N. Bicak, M. Yurtsever, Y. Yagci, *Polym. Int.* **2007**, *56*, 525–531.
- [5] a) E. O. Alonso, L. J. Johnston, J. C. Scaiano, V. G. Toscano, *Can. J. Chem.* **1992**, *70*, 1784–1794; b) C. Imrie, T. A. Modro, E. R. Rohwer, C. C. P. Wagener, *J. Org. Chem.* **1993**, *58*, 5643–5649.
- [6] a) J. Ammer, C. F. Sailer, E. Riedle, H. Mayr, *J. Am. Chem. Soc.* **2012**, *134*, 11481–11494; b) J. Ammer, C. Nolte, H. Mayr, *J. Am. Chem. Soc.* **2012**, *134*, 13902–13911.
- [7] R. A. McClelland, C. Chan, F. L. Cozens, A. Modro, S. Steenken, *Angew. Chem.* **1991**, *103*, 1389–1391; *Angew. Chem. Int. Ed. Engl.* **1991**, *30*, 1337–1339.
- [8] J. Ammer, M. Baidya, S. Kobayashi, H. Mayr, *J. Phys. Org. Chem.* **2010**, *23*, 1029–1035.
- [9] Review on wavelength tunability in photoinitiated cationic polymerization: B. Aydogan, B. Gacal, A. Yildirim, N. Yonet, Y. Yuksel, Y. Yagci in *Photochemistry and UV Curing: New Trends* (Ed.: J.-P. Fouassier), Research Signpost, Kerala, **2006**, pp. 187–201.
- [10] Review on photoacid generation with tailored wavelengths: J. V. Crivello, *J. Photopolym. Sci. Technol.* **2008**, *21*, 493–497.

- [11] a) J. C. Scaiano, in: *Reactive Intermediate Chemistry* (Eds.: R. A. Moss, M. S. Platz, M. J. Jones), Wiley, Hoboken, NJ, **2004**, pp. 847–871; b) N. P. Schepp, F. L. Cozens, in: *Lasers in Chemistry, Vol. 2* (Ed.: M. Lackner), Wiley-VCH, Weinheim, **2008**, pp. 1073–1091.
- [12] J. Bartl, S. Steenken, H. Mayr, R. A. McClelland, *J. Am. Chem. Soc.* **1990**, *112*, 6918–6928.
- [13] Further recent examples: a) J. Ammer, H. Mayr, *Macromolecules* **2010**, *43*, 1719–1723; b) M. Baidya, S. Kobayashi, H. Mayr, *J. Am. Chem. Soc.* **2010**, *132*, 4796–4805; c) N. Streidl, R. Branzan, H. Mayr, *Eur. J. Org. Chem.* **2010**, 4205–4210; d) T. Kanzian, S. Lakhdar, H. Mayr, *Angew. Chem.* **2010**, *122*, 9717–9720; *Angew. Chem. Int. Ed.* **2010**, *49*, 9526–9529; e) S. Lakhdar, J. Ammer, H. Mayr, *Angew. Chem.* **2011**, *123*, 10127–10130; *Angew. Chem. Int. Ed.* **2011**, *50*, 9953–9956; f) M. Horn, H. Mayr, *Eur. J. Org. Chem.* **2011**, 6470–6475; g) K. Troshin, C. Schindele, H. Mayr, *J. Org. Chem.* **2011**, *76*, 9391–9408; h) T. A. Nigst, J. Ammer, H. Mayr, *Angew. Chem.* **2011**, *124*, 1381–1385; *Angew. Chem. Int. Ed.* **2011**, *51*, 1353–1356; i) C. Nolte, J. Ammer, H. Mayr, *J. Org. Chem.* **2012**, *77*, 3325–3335.
- [14] a) S. Singh, G. Das, O. V. Singh, H. Han, *Org. Lett.* **2007**, *9*, 401–404; b) C. Lindner, R. Tandon, Y. Liu, B. Maryasin, H. Zipse, *Org. Biomol. Chem.* **2012**, *10*, 3210–3218; c) N. De Rycke, F. Couty, O. R. P. David, *Chem. Eur. J.* **2011**, *17*, 12852–12871.
- [15] N. De Rycke, G. Berionni, F. Couty, H. Mayr, R. Goumont, O. R. P. David, *Org. Lett.* **2011**, *13*, 530–533.
- [16] a) Review: J. W. Pavlik, in: *CRC Handbook of Organic Photochemistry and Photobiology* (Ed.: W. Horspool, F. Lenci), 2nd ed., CRC Press, Boca Raton, **2004**, pp. 97-1 – 97-22; b) J. W. Pavlik, S. Laohhasurayotin, T. Vongnakorn, *J. Org. Chem.* **2007**, *72*, 7116–7124; c) J. W. Pavlik, S. Laohhasurayotin, *J. Org. Chem.* **2008**, *73*, 2746–2752.
- [17] A. Dembinski, Y. Yagci, W. Schnabel, *Polymer* **1993**, *34*, 3738–3740.
- [18] a) H. Mayr, T. Bug, M. F. Gotta, N. Hering, B. Irrgang, B. Janker, B. Kempf, R. Loos, A. R. Ofial, G. Remennikov, H. Schimmel, *J. Am. Chem. Soc.* **2001**, *123*, 9500–9512; b) H. Mayr, B. Kempf, A. R. Ofial, *Acc. Chem. Res.* **2003**, *36*, 66–77; c) For a comprehensive database of nucleophilicity and electrophilicity parameters, see: <http://www.cup.lmu.de/oc/mayr/DBintro.html>.

- [19] S. Minegishi, R. Loos, S. Kobayashi, H. Mayr, *J. Am. Chem. Soc.* **2005**, *127*, 2641–2649.
- [20] F. Brotzel, B. Kempf, T. Singer, H. Zipse, H. Mayr, *Chem. Eur. J.* **2007**, *13*, 336–345.
- [21] N. Streidl, B. Denegri, O. Kronja, H. Mayr, *Acc. Chem. Res.* **2010**, *43*, 1537–1549.
- [22] Attack of the pyridine nitrogen in the reaction of **7** with 4,4'-dimethoxybenzhydryl chloride in CD₃CN was demonstrated by ¹H NMR experiments, see Experimental Section for details.
- [23] a) T. A. Nigst, M. Westermaier, A. R. Ofial, H. Mayr, *Eur. J. Org. Chem.* **2008**, 2369–2374; b) M. Kędziołek, P. Mayer, H. Mayr, *Eur. J. Org. Chem.* **2009**, 1202–1206; c) T. A. Nigst, A. Antipova, H. Mayr, *J. Org. Chem.* **2012**, *77*, 8142–8155.
- [24] B. Denegri, S. Minegishi, O. Kronja, H. Mayr, *Angew. Chem.* **2004**, *116*, 2353–2356; *Angew. Chem. Int. Ed.* **2004**, *43*, 2302–2305.
- [25] T. J. Bruno, P. D. N. Svoronos, *Handbook of Basic Tables for Chemical Analysis*, 2nd ed., CRC Press, Boca Raton, **2003**.
- [26] M. P. Groziak, L. M. Melcher, *Heterocycles* **1987**, *26*, 2905–2910.
- [27] V. Cañibano, J. F. Rodríguez, M. Santos, M. A. Sanz-Tejedor, M. C. Carreño, G. González, J. L. García-Ruano, *Synthesis* **2001**, 2175–2179.
- [28] J. M. Bakke, J. Riha, *J. Heterocycl. Chem.* **1999**, *36*, 1143–1145.

Chapter 9

NUCLEOPHILICITIES AND LEWIS BASICITIES OF ISOTHIIOUREA DERIVATIVES

Biplab Maji, Caroline Joannesse, Tobias A. Nigst, Andrew D. Smith, and Herbert Mayr in *J. Org. Chem.* **2011**, 76, 5104–5112.

The experiments were performed jointly with C. Joannesse. The results obtained by B. Maji are not listed in the Experimental Section.

9.1 Introduction

Lewis bases (that is, **1–17**, Figure 9.1) have the ability to promote the acylation of alcohols and amines.^[1] 4-(Dimethylamino)pyridine^[2] (DMAP, **1**) and *N*-methylimidazole^[3] (NMI, **2**) as well as the amidines 1,8-diazabicyclo[5.4.0]undec-7-ene (DBU, **3**)^[4] or 1,5-diazabicyclo[4.3.0]non-5-ene (DBN, **4**)^[4] are among the most common achiral catalysts used for these reactions. Birman has shown that chiral amidines act as enantioselective catalysts for the kinetic resolution of alcohols.^[5] Recent independent work by the Okamoto and Birman groups has demonstrated that isothioureas are highly active *O*-acylation catalysts.^[6,7] Okamoto found 3,4-dihydro-2*H*-pyrimido[2,1-*b*]benzothiazole (DHPB, **10**) to be remarkably active for catalyzing the acylation of 1-phenylethanol, even more active than the “benchmark” catalyst DMAP (**1**).^[6] Birman’s concurrent investigations of the acylations of primary and secondary alcohols with a series of amidines and isothioureas revealed a significant variation in catalytic activity with ring size. Notably, tetrahydropyrimidine-based isothioureas THTP (**9**) and DHPB (**10**) showed catalytic activity in chloroform similar or slightly higher than that of DMAP, depending on their concentrations.^[7] Subsequent related studies probed the ability of a variety of amidines and isothioureas to catalyze the *O*- to *C*-carboxyl transfer rearrangement of oxazolyl and related heterocyclic carbonates, and the *C*-acylation of silyl ketene acetals, and showed that tetrahydropyrimidine-based DHPB **10** was also the optimal achiral catalyst in Figure 9.1.^[8]

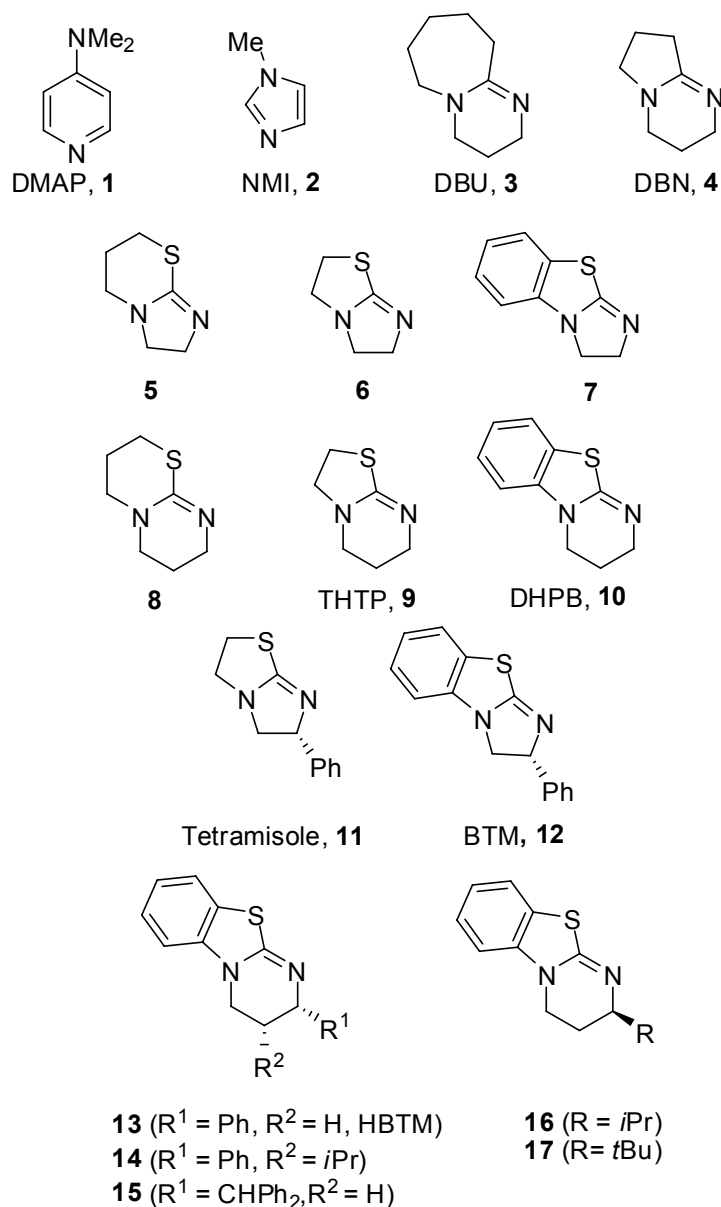
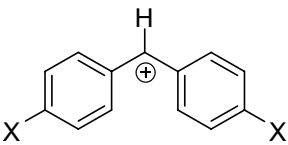


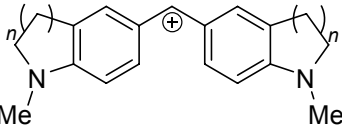
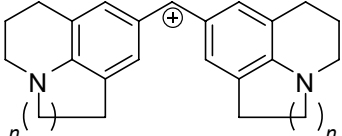
Figure 9.1. Selected nitrogen-containing heterocycles commonly used as acyl transfer catalysts.

Given their promising reactivity profiles, a series of chiral isothioureas have been prepared and utilized in asymmetric catalysis. Pioneering studies by Birman and Li showed that tetramisole (**11**) and its benzannulated analogue BTM (**12**) can catalyze the kinetic resolution of alcohols with exquisite selectivity.^[9] Since the demonstration of this methodology, a range of chiral isothioureas (of which **12–17** are representative) have been successfully utilized in a variety of asymmetric processes including kinetic resolutions,^[10] desymmetrizations,^[11,12] dynamic kinetic resolutions,^[13] and the generation of ammonium enolates from carboxylic

acids,^[14] as well as enantioselective carboxy and acyl group transfer reactions.^[15] The commercial availability of tetramisole (**11**), and the ease of synthesis of chiral isothiouras such as **12–17** from enantiopure amino alcohols, arguably make these derivatives more readily accessible than many common chiral DMAP derivatives.^[16] Notably, in many of these processes the catalytic activity and enantioselectivity vary significantly with ring size and stereodirecting unit. For example, Birman has shown that the incorporation of an additional *syn*-C(3)-methyl group within the HBTM-skeleton (**14**, Me instead of *i*Pr) has a dramatic effect upon both catalytic activity and stereoselectivity in kinetic resolutions of aryl-cycloalkanols,^[17] a similar effect has been noted on the kinetic resolution of aryl alkyl alcohols when introducing a *syn*-C(3)-isopropyl unit (**14**).^[18]

While it may be expected that the organocatalytic activities of these heterocycles will depend on their relative nucleophilicities and Lewis basicities, to date a quantitative comparison of these properties has not been reported. To gain insight into some of the factors that may affect their catalytic activities, we have determined rate and equilibrium constants of the reactions of the isothiourea derivatives **5–10** and **13–17** with stabilized benzhydrylium ions (Table 9.1) and compared these data with those of other nucleophilic organocatalysts such as DMAP (**1**), NMI (**2**), DBU (**3**) and DBN (**4**).^[19,20]

Table 9.1. Abbreviations and electrophilicity parameters for the benzhydrylium ions used for this work.


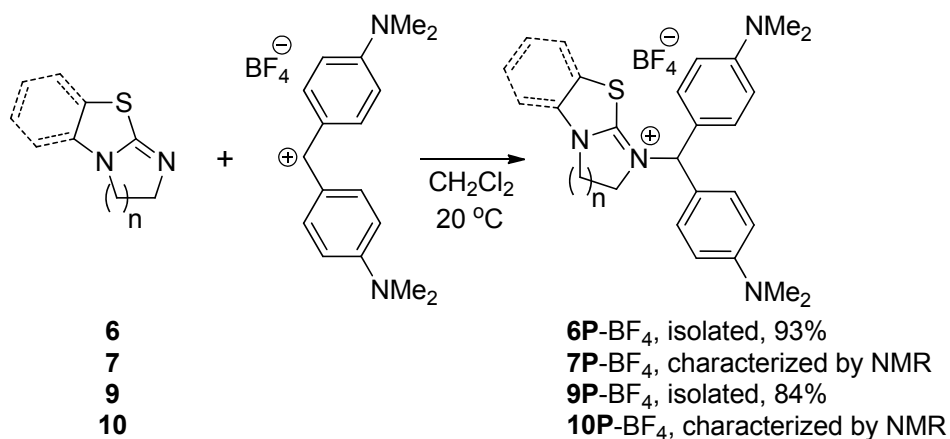
| X | Abbreviations | $E^{[a]}$ |
|---|--|-----------|
| N(CH ₃)CH ₂ CF ₃ | (mfa) ₂ CH ⁺ | -3.85 |
| NPh ₂ | (dpa) ₂ CH ⁺ | -4.72 |
| N(CH ₂ CH ₂) ₂ O | (mor) ₂ CH ⁺ | -5.53 |
| N(Ph)CH ₃ | (mpa) ₂ CH ⁺ | -5.89 |
| N(CH ₃) ₂ | (dma) ₂ CH ⁺ | -7.02 |
| N(CH ₂) ₄ | (pyr) ₂ CH ⁺ | -7.69 |
|  | $n = 2$ (thq) ₂ CH ⁺ | -8.22 |
| | $n = 1$ (ind) ₂ CH ⁺ | -8.76 |
|  | $n = 2$ (jul) ₂ CH ⁺ | -9.45 |
| | $n = 1$ (lil) ₂ CH ⁺ | -10.04 |

[a] Electrophilicity parameters E for benzhydrylium ions from Ref. [19d].

9.2 Results and Discussion

9.2.1 Product Studies

When CH₂Cl₂ solutions of the isothioureas **6** or **9** were added to CH₂Cl₂ solutions of (dma)₂CH⁺BF₄⁻ at room temperature, the thiuronium tetrafluoroborates **6P**-BF₄ and **9P**-BF₄ formed, which were isolated and characterized (Scheme 9.1). The ¹³C NMR spectra show that the benzhydryl carbon, which absorbs at $\delta \approx 160$ ppm in (dma)₂CH⁺, is shifted to $\delta \approx 70$ ppm due to the change in hybridization from sp² to sp³. Since the reactions of the benzannulated isothioureas **7** and **10** with (dma)₂CH⁺BF₄⁻ are highly reversible, the corresponding adducts **7P**-BF₄ and **10P**-BF₄ were not isolated but identified by NMR after mixing the isothioureas **7** and **10** with equimolar amounts of (dma)₂CH⁺BF₄⁻ in deuterated dimethyl sulfoxide.



Scheme 9.1. Products of the reactions of isothioureas with $(\text{dma})_2\text{CH}^+\text{BF}_4^-$.

9.2.2 Kinetics

Using this information, the rates of the reactions of the isothioureas **5-10** and **13-17** with the benzhydrylium ions shown in Table 9.1 were measured photometrically by monitoring the decay of the absorbances of the benzhydrylium ions; conventional or stopped-flow techniques were used as previously described.^[19] By employing the isothioureas in high excess relative to the benzhydrylium ions, first-order conditions were achieved. The first-order rate constants k_{obs} (s^{-1}), obtained by fitting the decay of the absorbances of the benzhydrylium ions to the monoexponential function $A = A_0e^{-k_{\text{obs}}t} + C$ correlated linearly with the nucleophile concentrations (Figure 9.2). The slopes of these correlation lines yielded the second-order rate constants k ($\text{M}^{-1}\text{ s}^{-1}$), which are collected in Table 9.2. The kinetic profiles of the reactions of $(\text{ind})_2\text{CH}^+$ with **7**, **9** and **10** were also studied at variable temperature to determine the Eyring activation parameters which are collected in the footnotes of Table 9.2. The negative activation entropies (-57 to $-68\text{ J mol}^{-1}\text{ K}^{-1}$) are similar to those reported for the reactions of other n -nucleophiles with benzhydrylium ions in CH_2Cl_2 .^[20]

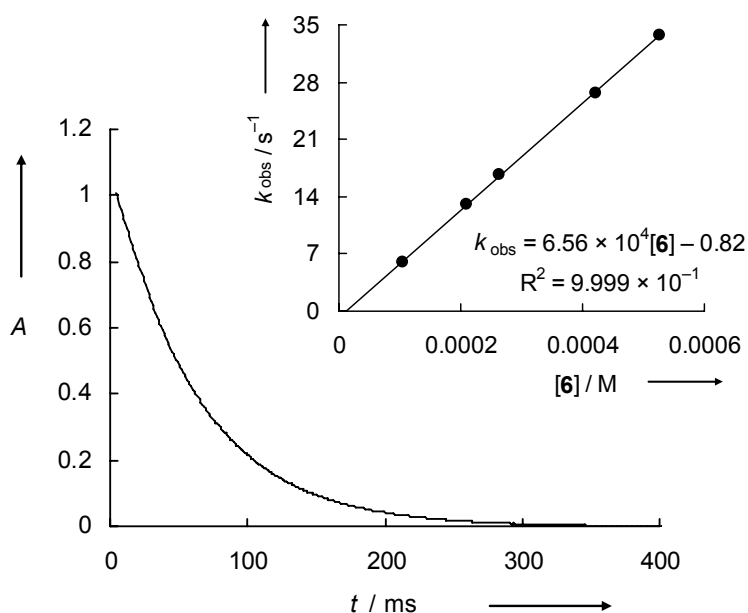


Figure 9.2. Exponential decay of the absorbance at 613 nm during the reaction of **6** (2.11×10^{-4} M) with $(\text{dma})_2\text{CH}^+\text{BF}_4^-$ (1.41×10^{-5} M) at 20 °C in CH_2Cl_2 ($k_{\text{obs}} = 13.0 \text{ s}^{-1}$). Inset: Determination of the second-order rate constant $k = 6.56 \times 10^4 \text{ M}^{-1}\text{s}^{-1}$ from the dependence of k_{obs} on the concentration of **6**.

Table 9.2. Second-order rate constants k for the reactions of the isothiourea derivatives **5–10** and **13–17** with the benzhydrylium ions (Ar_2CH^+ , Table 9.1) in CH_2Cl_2 at 20 °C.

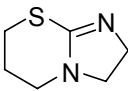
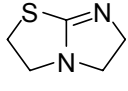
| Isothiourea | $N, s_N^{[a]}$ | Ar_2CH^+ | $k \text{ (M}^{-1}\text{s}^{-1}\text{)}$ |
|---|----------------|-----------------------------|--|
|  5 | 13.00, 0.83 | $(\text{dma})_2\text{CH}^+$ | 9.16×10^4 |
| | | $(\text{pyr})_2\text{CH}^+$ | 2.55×10^4 |
| | | $(\text{thq})_2\text{CH}^+$ | 7.72×10^3 |
| | | $(\text{ind})_2\text{CH}^+$ | 3.54×10^3 |
|  6 | 12.98, 0.81 | $(\text{dma})_2\text{CH}^+$ | 6.56×10^4 |
| | | $(\text{pyr})_2\text{CH}^+$ | 1.93×10^4 |
| | | $(\text{thq})_2\text{CH}^+$ | 5.86×10^3 |
| | | $(\text{ind})_2\text{CH}^+$ | 2.79×10^3 |

Table 9.2 (continued).

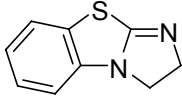
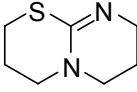
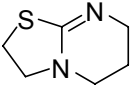
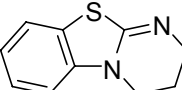
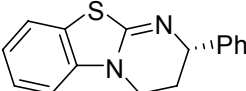
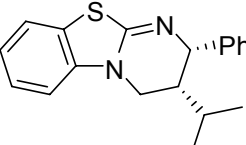
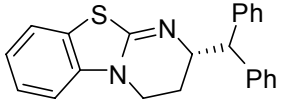
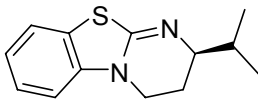
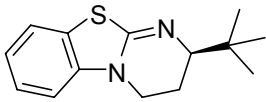
| Isothiourea | N, s_N | Ar_2CH^+ | k ($\text{M}^{-1}\text{s}^{-1}$) |
|--|-------------|-----------------------------|--------------------------------------|
|  7 | 13.42, 0.73 | $(\text{dma})_2\text{CH}^+$ | 4.76×10^4 |
| | | $(\text{pyr})_2\text{CH}^+$ | 1.46×10^4 |
| | | $(\text{thq})_2\text{CH}^+$ | 5.83×10^3 |
| | | $(\text{ind})_2\text{CH}^+$ | 2.60×10^3 [b] |
|  8 | 14.10, 0.82 | $(\text{thq})_2\text{CH}^+$ | 5.88×10^4 |
| | | $(\text{ind})_2\text{CH}^+$ | 2.76×10^4 |
| | | $(\text{jul})_2\text{CH}^+$ | 4.85×10^3 |
| | | $(\text{lil})_2\text{CH}^+$ | 2.27×10^3 |
|  THTP, 9 | 14.45, 0.78 | $(\text{thq})_2\text{CH}^+$ | 7.09×10^4 |
| | | $(\text{ind})_2\text{CH}^+$ | 3.68×10^4 [c] |
| | | $(\text{jul})_2\text{CH}^+$ | 6.69×10^3 |
| | | $(\text{lil})_2\text{CH}^+$ | 3.15×10^3 |
|  DHPB, 10 | 13.86, 0.78 | $(\text{dma})_2\text{CH}^+$ | 2.29×10^5 |
| | | $(\text{pyr})_2\text{CH}^+$ | 7.49×10^4 |
| | | $(\text{thq})_2\text{CH}^+$ | 2.07×10^4 |
| | | $(\text{ind})_2\text{CH}^+$ | 1.11×10^4 [d] |
|  13 | 13.45, 0.72 | $(\text{mor})_2\text{CH}^+$ | 3.80×10^5 |
| | | $(\text{mpa})_2\text{CH}^+$ | 2.91×10^5 |
| | | $(\text{dma})_2\text{CH}^+$ | 5.15×10^4 |
| | | $(\text{pyr})_2\text{CH}^+$ | 1.40×10^4 |
| | | $(\text{thq})_2\text{CH}^+$ | 4.60×10^3 |
|  14 | 14.96, 0.64 | $(\text{mpa})_2\text{CH}^+$ | 5.28×10^5 |
| | | $(\text{dma})_2\text{CH}^+$ | 1.26×10^5 |
| | | $(\text{pyr})_2\text{CH}^+$ | 4.06×10^4 |
| | | $(\text{thq})_2\text{CH}^+$ | 1.76×10^4 |
| | | $(\text{ind})_2\text{CH}^+$ | 8.59×10^3 |

Table 9.2 (continued).

| Isothiourea | N, s_N | Ar_2CH^+ | $k (M^{-1}s^{-1})$ |
|---|-------------|---------------|--------------------|
|  15 | 15.30, 0.55 | $(dpa)_2CH^+$ | 6.09×10^5 |
| | | $(mor)_2CH^+$ | 2.22×10^5 |
| | | $(mpa)_2CH^+$ | 1.37×10^5 |
| | | $(dma)_2CH^+$ | 3.38×10^4 |
|  16 | 16.50, 0.48 | $(dpa)_2CH^+$ | 4.48×10^5 |
| | | $(mor)_2CH^+$ | 1.57×10^5 |
| | | $(mpa)_2CH^+$ | 1.05×10^5 |
| | | $(dma)_2CH^+$ | 3.73×10^4 |
| | | $(pyr)_2CH^+$ | 1.53×10^4 |
|  17 | 12.95, 0.58 | $(mfa)_2CH^+$ | 2.51×10^5 |
| | | $(dpa)_2CH^+$ | 4.57×10^4 |
| | | $(mor)_2CH^+$ | 2.06×10^4 |
| | | $(mpa)_2CH^+$ | 1.58×10^4 |

[a] Parameters as defined by Equation (9.1). [b] Eyring activation parameters: $\Delta H^\ddagger = 32.6 \pm 1.3 \text{ kJ mol}^{-1}$, $\Delta S^\ddagger = -68.0 \pm 4.7 \text{ J mol}^{-1} \text{ K}^{-1}$. [c] Eyring activation parameters: $\Delta H^\ddagger = 29.3 \pm 0.7 \text{ kJ mol}^{-1}$, $\Delta S^\ddagger = -57.3 \pm 2.5 \text{ J mol}^{-1} \text{ K}^{-1}$. [d] Eyring activation parameters: $\Delta H^\ddagger = 30.6 \pm 1.8 \text{ kJ mol}^{-1}$, $\Delta S^\ddagger = -63.0 \pm 6.3 \text{ J mol}^{-1} \text{ K}^{-1}$.

9.2.3 Correlation Analysis

In previous publications, we have shown that the rates of the reactions of carbocations and Michael acceptors with n , π , and σ -nucleophiles can be described by the linear free energy relationship [Eq. (9.1)], where electrophiles are characterized by the electrophilicity parameter E , nucleophiles are characterized by the nucleophilicity parameter N and the nucleophile-dependent sensitivity parameter s_N (previously termed s). On the basis of Equation (9.1) it was possible to develop the most comprehensive nucleophilicity scale presently available.¹⁹

$$\log k_{20^\circ\text{C}} = s_N(N + E) \quad (9.1)$$

Figure 9.3 shows linear correlations between the second-order rate constants k and the previously published electrophilicity parameters E , as required by Equation (9.1). The slopes

of the correlation lines yield the nucleophile-specific sensitivity parameters s_N and the intercepts on the abscissa give the nucleophilicity parameters N which are tabulated in Table 9.2.

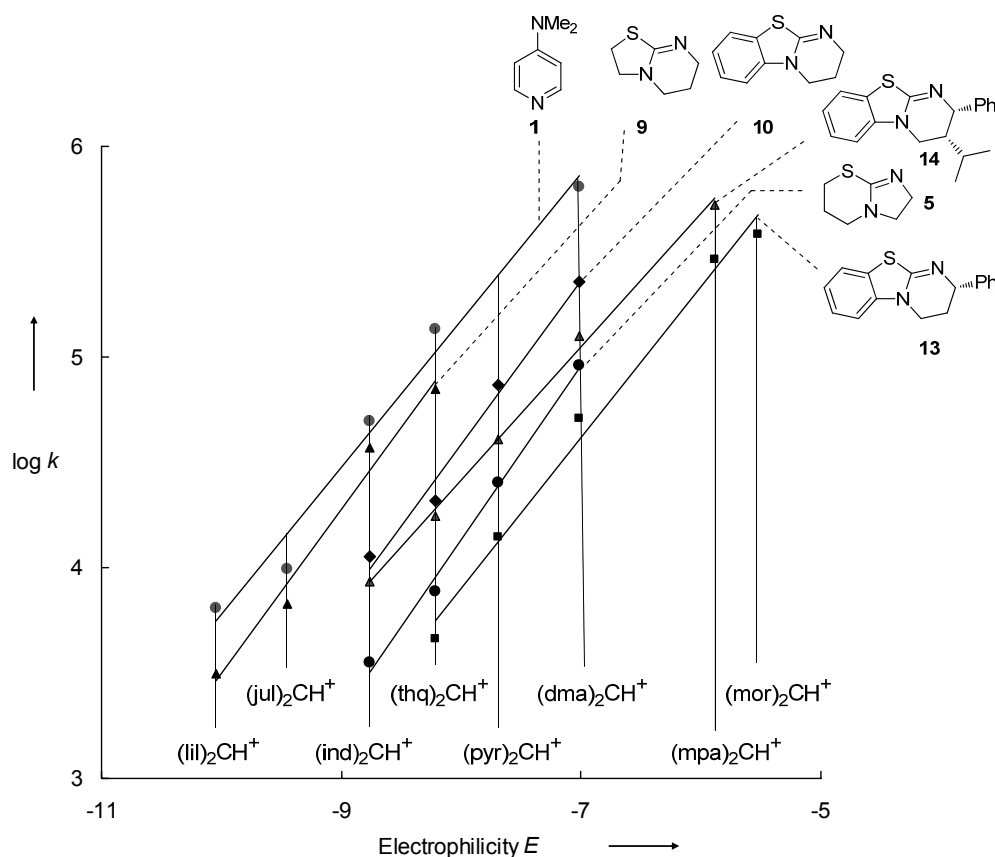


Figure 9.3. Plots of $\log k$ for the reactions of some isothioureas with benzhydrylium ions versus their electrophilicity parameters E in CH_2Cl_2 at 20°C . Rate constants for DMAP were taken from Ref. [20b].

The almost equal slopes ($0.73 < s_N < 0.83$) of the correlation lines for the isothioureas **5–10** (unsubstituted at C-2) indicate that their relative nucleophilicities are almost independent of the reactivity of the electrophilic reaction partner. In contrast, the chiral derivatives **13–17** have somewhat lower, variable, s_N parameters reflecting the dependence of their relative nucleophilicities on the reaction partner.

9.2.4 Lewis Basicities and Intrinsic Reactivities of Isothioureas

Brønsted basicities, which have often been used for a first screening of potential nucleophilic organocatalysts, have been reported for only a few isothioureas.^[21] As Lewis basicities are more relevant for their reactions with carbon electrophiles, we have now studied the equilibrium constants of the reactions of several isothioureas with benzhydrylium ions.

The reactions of **7**, **9**, and **10**, and of the C(2)-substituted chiral isothioureas **13–17** with several colored amino-substituted benzhydrylium ions proceed incompletely, allowing the measurement of the equilibrium constants for these reactions by UV/Vis spectroscopy. Assuming proportionality between the absorbances and the concentrations of the benzhydrylium ions (as for the evaluation of the kinetic experiments), the equilibrium constants for the reactions [Eq. (9.2)] can be determined from the initial absorbances (A_0) of the benzhydrylium ions and the absorbances at equilibrium (A) according to Equation (9.3) and results are listed in Table 9.3.



$$K = \frac{[\text{Ar}_2\text{CH-Nu}^+]}{[\text{Ar}_2\text{CH}^+][\text{Nu}]} = \frac{A_0 - A}{A[\text{Nu}]} \quad (9.3)$$

Table 9.3. Equilibrium constants K , activation free energies ΔG^\ddagger , reaction free energies ΔG^0 , and intrinsic barriers ΔG_0^\ddagger for the reactions of isothioureas with benzhydrylium ions (Ar_2CH^+) in CH_2Cl_2 at 20 °C, as well as rate constants (k_{\leftarrow}) and nucleofugality parameters N_f for the reverse reactions.

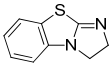
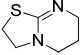
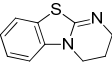
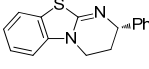
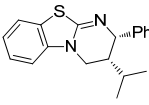
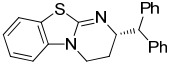
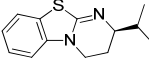
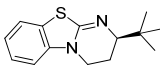
| Isothioureas | Ar_2CH^+ | K [M^{-1}] | ΔG^\ddagger ^[a] [kJ mol ⁻¹] | ΔG^0 ^[b] [kJ mol ⁻¹] | ΔG_0^\ddagger ^[c] [kJ mol ⁻¹] | k_{\leftarrow} ^[d] [s ⁻¹] | N_f ^[e] |
|---|------------------------------------|-----------------------------------|---|--|---|---|----------------------|
| | | | | | | | |
|  7 | (thq) ₂ CH ⁺ | 2.56×10^4 | 50.6 | -24.7 | 62.3 | 2.28×10^{-1} | -5.79 |
| | (ind) ₂ CH ⁺ | 2.00×10^4 ^[f] | 52.6 | -24.1 ^[f] | 64.1 | 1.30×10^{-1} | |
|  THTP 9 | (ind) ₂ CH ⁺ | 1.90×10^6 ^[g] | 46.1 | -35.2 ^[g] | 62.5 | 1.94×10^{-2} | -6.49 |
| | (jul) ₂ CH ⁺ | 6.16×10^4 | 50.3 | -26.9 | 63.0 | 1.09×10^{-1} | |
| | (lil) ₂ CH ⁺ | 6.27×10^4 | 52.1 | -26.9 | 64.9 | 5.02×10^{-2} | |
|  DHPB 10 | (pyr) ₂ CH ⁺ | 7.73×10^4 | 44.4 | -27.4 | 57.3 | 9.69×10^{-1} | -5.26 |
| | (thq) ₂ CH ⁺ | 2.75×10^4 | 47.5 | -24.9 | 59.3 | 7.53×10^{-1} | |
| | (ind) ₂ CH ⁺ | 2.02×10^4 ^[h] | 49.0 | -24.2 ^h | 60.5 | 5.50×10^{-1} | |
|  HBTM 13 | (mpa) ₂ CH ⁺ | 5.95×10^5 | 41.1 | -32.4 | 56.1 | 4.89×10^{-1} | -3.98 |
| | (dma) ₂ CH ⁺ | 1.07×10^4 | 45.3 | -22.6 | 56.0 | 4.81 | |
| | (pyr) ₂ CH ⁺ | 8.96×10^2 | 48.5 | -16.6 | 56.5 | 1.56×10^1 | |
| | (thq) ₂ CH ⁺ | 3.32×10^2 | 51.2 | -14.1 | 58.0 | 1.39×10^1 | |
| | (ind) ₂ CH ⁺ | 1.98×10^2 ^[i] | 52.8 ^[j] | -12.9 ^[i] | 59.1 | 1.20×10^1 | |
|  14 | (dma) ₂ CH ⁺ | 5.54×10^4 | 43.1 | -26.6 | 55.6 | 2.27 | -4.24 |
| | (pyr) ₂ CH ⁺ | 3.88×10^3 | 45.9 | -20.1 | 55.5 | 1.05×10^1 | |
| | (thq) ₂ CH ⁺ | 1.67×10^3 | 47.9 | -18.1 | 56.6 | 1.05×10^1 | |
| | (ind) ₂ CH ⁺ | 1.17×10^3 | 49.7 | -17.2 | 58.0 | 7.34 | |
|  15 | (mpa) ₂ CH ⁺ | 4.66×10^4 | 42.9 | -26.2 | 55.2 | 2.94 | -3.15 |
| | (dma) ₂ CH ⁺ | 9.95×10^2 | 46.3 | -16.8 | 54.4 | 3.40×10^1 | |
|  16 | (mpa) ₂ CH ⁺ | 1.01×10^5 | 43.6 | -28.1 | 56.8 | 1.04 | -3.57 |
| | (dma) ₂ CH ⁺ | 2.70×10^3 | 46.1 | -19.3 | 55.3 | 1.38×10^1 | |

Table 9.3 (continued).

| Isothiureas | Ar ₂ CH ⁺ | <i>K</i> [M ⁻¹] | Δ <i>G</i> [‡] [a] [kJ mol ⁻¹] | Δ <i>G</i> ⁰ [b] [kJ mol ⁻¹] | Δ <i>G</i> ₀ [‡] [c] [kJ mol ⁻¹] | <i>k</i> _← ^[d] [s ⁻¹] | <i>N</i> _f ^[e] |
|--|------------------------------------|--------------------------------|--|--|---|--|--------------------------------------|
|  17 | (mor) ₂ CH ⁺ | 1.36 × 10 ⁴ | 47.5 | -23.2 | 58.5 | 1.51 | -2.75 |
| | (mpa) ₂ CH ⁺ | 2.45 × 10 ³ | 48.2 | -19.0 | 57.3 | 6.45 | |
| DMAP 1 ^[k] | (thq) ₂ CH ⁺ | 2.81 × 10 ⁵ | 42.9 | -30.6 | 57.2 | 4.80 × 10 ⁻¹ | -5.32 ^[l] |
| | (ind) ₂ CH ⁺ | 1.71 × 10 ⁵ | 45.4 | -29.4 | 59.2 | 2.90 × 10 ⁻¹ | |

[a] From rate constants in Table 9.2 using the Eyring equation. [b] From equilibrium constants *K* in this table ($-RT \ln K$). [c] From Equation (9.4). [d] $k_{\leftarrow} = k/K$. [e] From Equation (9.5) assuming $s_f = 1$. [f] $\Delta H^\circ = -49.8 \text{ kJ mol}^{-1}$, $\Delta S^\circ = -87.7 \text{ J mol}^{-1} \text{ K}^{-1}$. [g] $\Delta H^\circ = -63.9 \text{ kJ mol}^{-1}$, $\Delta S^\circ = -97.9 \text{ J mol}^{-1} \text{ K}^{-1}$. [h] $\Delta H^\circ = -50.2 \text{ kJ mol}^{-1}$, $\Delta S^\circ = -88.7 \text{ J mol}^{-1} \text{ K}^{-1}$. [i] Equilibrium constant extrapolated from a van't Hoff plot from measurements at lower temperatures. $\Delta H^\circ = -44.2 \text{ kJ mol}^{-1}$, $\Delta S^\circ = -106.9 \text{ J mol}^{-1} \text{ K}^{-1}$. [j] Calculated using Equation (9.1) and reactivity parameters from Table 9.1 and Table 9.3. [k] Data for DMAP was taken from Ref. [20b]. [l] From Ref. [24].

Substitution of the activation free energies ΔG^\ddagger and Gibbs free energies ΔG^0 into the Marcus equation [Eq. (9.4)]^[22] yields the intrinsic barriers ΔG_0^\ddagger (that is, the barriers of the corresponding reactions with $\Delta G^0 = 0$) which are also listed in Table 9.3.

$$\Delta G^\ddagger = \Delta G_0^\ddagger + 0.5 \Delta G^0 + ((\Delta G^0)^2 / 16 \Delta G_0^\ddagger) \quad (9.4)$$

With ΔG_0^\ddagger between 54 and 65 kJ mol⁻¹, the intrinsic barriers are of similar magnitude as previously reported for the reactions of benzhydrylium ions with pyridines^[20a,b] and azoles.^[20c] Table 9.3 shows also that the dependence of the intrinsic barriers ΔG_0^\ddagger on the structures of the benzhydrylium ions mirrors previously observed patterns. In particular, the intrinsic barriers for the reactions of the five-membered ring compounds (ind)₂CH⁺ and (lil)₂CH⁺ are always 1–2 kJ mol⁻¹ higher than those of the corresponding six-membered ring-analogues (thq)₂CH⁺ and (jul)₂CH⁺, respectively, resulting in a breakdown of rate-equilibrium relationships.^[23,24]

9.2.5 Structure Reactivity Relationships

From the observation that the isothiureas **5**, **6**, and **8**, (like the amidines DBU (**3**) and DBN (**4**)) react quantitatively with all benzhydrylium tetrafluoroborates investigated, it can be derived that they have Lewis basicities higher than those of the isothiureas listed in Table 9.3.

As Figure 9.3 shows that the relative reactivities of isothiureas are somewhat dependent on the reactivity of the benzhydrylium ion used as the reaction partner, we will first consider the rate and equilibrium constants for the reactions with $(\text{ind})_2\text{CH}^+$, for which directly measured rate and equilibrium constants are available for most isothiureas (Figure 9.4).

Comparison of the imidazoline derivatives **5–7** shows that their nucleophilic reactivities are only slightly affected by the nature of the annelated sulfur-containing heterocycle. The benzannulation in compound **7** accelerates the reverse reaction k_{\leftarrow} , however, with the consequence that the equilibrium constant for adduct formation becomes measurable for the reaction of $(\text{ind})_2\text{CH}^+$ with **7**.

A comparable trend was observed for the tetrahydropyrimidine series **8–10** (line 2 of Figure 9.4) which are approximately one order of magnitude more nucleophilic than their lower homologues **5–7** ($k(\mathbf{8})/k(\mathbf{5}) \approx 8$; $k(\mathbf{9})/k(\mathbf{6}) \approx 13$; $k(\mathbf{10})/k(\mathbf{7}) \approx 4$). Also in this series, variation of the annelated sulfur heterocycle had a relatively small effect ($k(\mathbf{9})/k(\mathbf{10}) \approx 3$) on the nucleophilic reactivity but a large effect on Lewis basicity ($K(\mathbf{9})/K(\mathbf{10}) \approx 10^2$). Thus lines 1 and 2 of Figure 9.4 show the same trend that benzannulation has a much larger effect on Lewis basicity than on nucleophilicity.

Introduction of the phenyl group in the 2-position of **10** (\rightarrow **13**) reduces the nucleophilic reactivity by a factor of 4.5 but the Lewis basicity by a factor of 100. Remarkably, an additional syn-C(3)-isopropyl group in **14** (relative to HBTM (**13**)) increases its Lewis basicity (by a factor of 6) and nucleophilicity (by a factor of 3.6). Though there is no direct correlation between these data, it is notable that this trend corresponds with the experimentally observed beneficial effect of an additional syn-3-substituent to **13** (\rightarrow **14**) in kinetic resolution reactions in terms of catalytic activity and enantioselectivity.^[17,18] The last entry of Figure 9.4 shows that both, nucleophilicities and Lewis basicities of the tetrahydropyrimidine derivatives **9** and **10**, are comparable to those of DMAP (**1**).

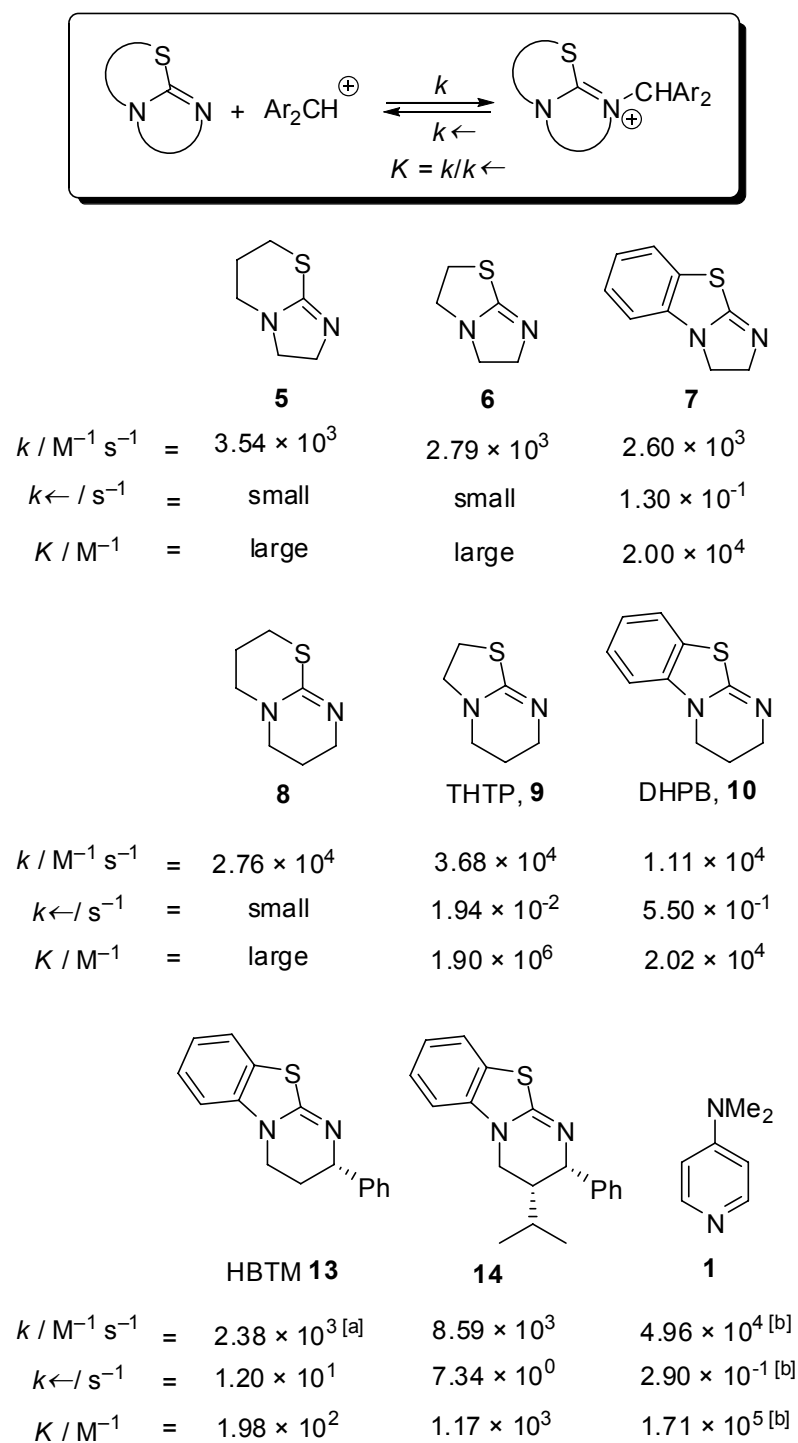


Figure 4. Second-order rate constants k , reverse rate constants k_{\leftarrow} , and equilibrium constants K for the reactions of the isothiourea derivatives **5–10** with $(\text{ind})_2\text{CH}^+\text{BF}_4^-$ in CH_2Cl_2 at 20°C .

[a] Rate constant calculated by using Equation (9.1) from the E value of $(\text{ind})_2\text{CH}^+$ (Table 9.1), and the N and s_N value of **13** from Table 9.2. [b] Data for **1** was taken from Ref. [20b].

The influence of the substituent at C-2 can be derived from the rate and equilibrium constants of its reactions with $(\text{dma})_2\text{CH}^+$ (Table 9.4). As in the comparisons of Figure 9.4, variation of the substituents affects the equilibrium constants much more than the rate constants. While the change from phenyl to *tert*-butyl reduces nucleophilicity by approximately one order of magnitude, the equilibrium constant decreases by more than two orders of magnitude.

Table 9.4. Second-order rate constants k , reverse rate constants k_{\leftarrow} , and equilibrium constants K for the reactions of the isothioureas **13**, **15–17** with $(\text{dma})_2\text{CH}^+\text{BF}_4^-$ in CH_2Cl_2 .

| R | $k/\text{M}^{-1} \text{s}^{-1}$ | $k_{\leftarrow}/\text{s}^{-1}$ | K/M^{-1} |
|---------------------------------|---------------------------------|--------------------------------|-----------------------------|
| Ph (13) | 5.15×10^4 | 4.81×10^0 | 1.07×10^4 |
| CHPh ₂ (15) | 3.38×10^4 | 3.40×10^1 | 9.95×10^2 |
| <i>i</i> Pr (16) | 3.73×10^4 | 1.38×10^1 | 2.70×10^3 |
| <i>t</i> Bu (17) | 2.8×10^3 [a] | $\approx 5 \times 10^1$ | $\approx 6 \times 10^1$ [a] |

[a] Rate constant calculated by using Equation (9.1) as in Figure 9.4, the E value of $(\text{dma})_2\text{CH}^+$, and the N and s_N values of **17**. [b] Estimated by dividing $K[(\text{mpa})_2\text{CH}^+]$ by 40, the ratio derived from equilibrium constants of **15** and **16** with $(\text{mpa})_2\text{CH}^+$ and $(\text{dma})_2\text{CH}^+$.

9.2.6 Nucleofugalities of Isothioureas

In analogy to Equation (9.1),^[19] which has been used to construct a comprehensive nucleophilicity scale, Equation (9.5)^[24] has recently been suggested as the basis for a comprehensive nucleofugality scale. Benzhydrylium ions of variable electrofugality (characterized by E_f) have been employed as reference electrofuges for characterizing the nucleofugalities of leaving groups in different solvents.

$$\log k_{\leftarrow}(25\text{ }^\circ\text{C}) = s_f(N_f + E_f) \quad (9.5)$$

In general, the nucleofugality parameters N_f and the nucleofuge-specific sensitivity parameters s_f are obtained from the linear plots of $\log k_{\leftarrow}$ (25 °C) versus the previously reported^[24] electrofugality parameters E_f of the benzhydrylium ions analogously to the procedure used in Figure 9.3 for determining the nucleophile-specific parameters N and s_N . It has been suggested, however, to assume $s_f = 1.0$ if only heterolysis rate constants of low precision and/or referring to benzhydrylium ions of similar electrofugality are known. This is the case for the k_{\leftarrow} values given in Table 9.3, which are obtained indirectly as the ratios of k/K and furthermore refer to 20 °C. Neglecting the small difference in temperature, we have therefore calculated the N_f parameters of isothioureas (listed in Table 9.3) from Equation (9.5) setting the s_f parameter to 1.0.

Due to the high Lewis basicities of DBU (**3**), DBN (**4**), and the isothioureas **5**, **6**, and **8** equilibrium constants could not be measured, indicating that they are poor nucleofuges. The trends in N_f shown in Table 9.3 are equivalent to the trends in k_{\leftarrow} discussed for Figure 9.4 and Table 9.4.

It is the benefit of the N_f values in Table 9.3 that they allow a comparison of the leaving group abilities in CH_2Cl_2 of isothioureas with those of other nucleofuges. Thus, comparison with N_f values listed in Ref. [24] shows that the nucleofugalities of **7**, **9** and **10** are comparable to those of DMAP (**1**) ($N_f = -5.32$), or *N*-methylimidazole (**2**) ($N_f = -6.29$ in CH_3CN) and *N*-phenylimidazole ($N_f = -5.59$ in CH_3CN), or tris(*p*-tolyl)phosphane ($N_f = -5.20$) and tris(*p*-anisyl)phosphane ($N_f = -5.91$). The nucleofugalities of **13** and **14** are comparable to that of triphenylphosphane ($N_f = -4.44$) and N_f of the *tert*-butyl-substituted compound **17** is similar to that of 4-methoxypyridine ($N_f = -2.80$) and isoquinoline ($N_f = -3.04$ in CH_3CN).

9.3 Conclusion

In a systematic study Birman *et al.* observed that the relative catalytic activities of DMAP (**1**) and THTP (**9**) in the acylation of alcohols with $\text{Ac}_2\text{O}/i\text{Pr}_2\text{NEt}$ in chloroform vary dramatically and can be reversed when the concentration of the catalyst and/or the nature of the alcohols are altered.^[7] One must, therefore, conclude that there is not a single, best acylation catalyst. Thus the nucleophilicities and Lewis basicities of isothioureas reported in this work are two important but not the only factors controlling catalytic activities.

As the reactions of isothioureas with benzhydrylium ions have been found to follow the linear free energy relationship [Eq. (9.1)] it was possible to determine the nucleophilicity parameters for the isothioureas **5–10** and **13–17** and to include these compounds into our comprehensive nucleophilicity scale. Figure 9.5 shows that the nucleophilicities N of the investigated isothioureas are in between those of the classical organocatalysts DMAP (**1**) and NMI (**2**).

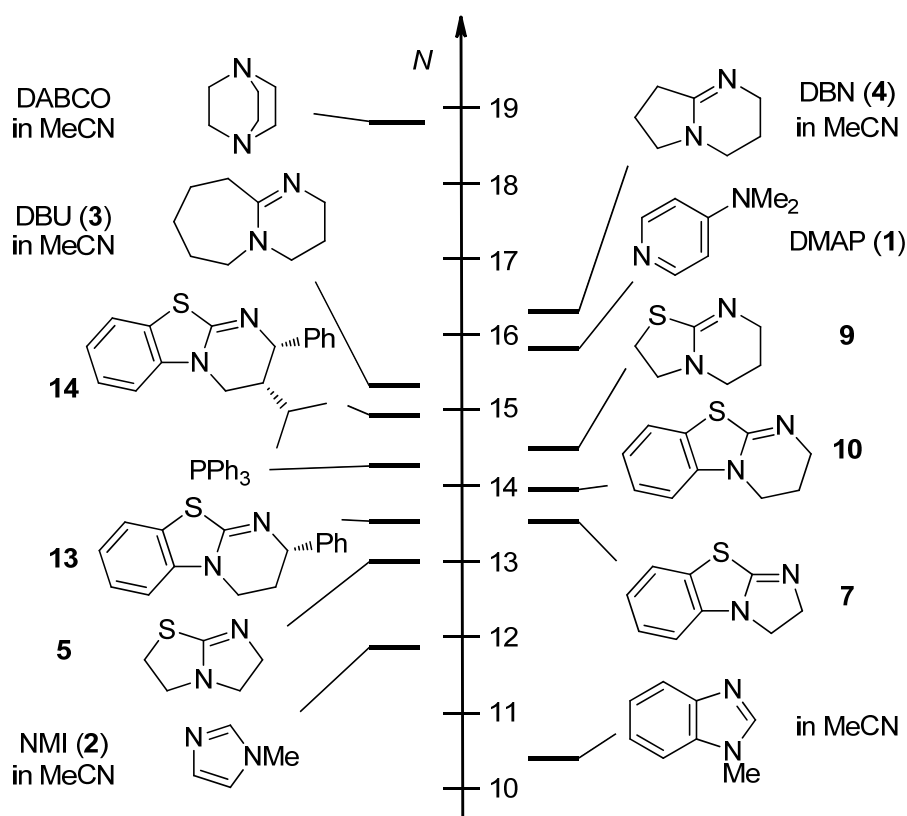


Figure 9.5. Comparison of the nucleophilicities N of isothioureas with other nucleophilic organocatalysts (solvent is CH_2Cl_2 unless stated otherwise).^[a]

[a] Nucleophilicity parameters N from Ref. [20].

The availability of rate and equilibrium constants for the reactions of these nucleophiles with the benzhydrylium ion $(\text{ind})_2\text{CH}^+$ furthermore allows us to construct the quantitative energy profile diagrams as depicted for some reactions in Figure 9.6. It is thus found that imidazoles are less nucleophilic as well as less Lewis basic than isothioureas. Although the kinetic and thermodynamic properties of most isothioureas investigated are comparable to those of DMAP, DABCO is a stronger nucleophile than all isothioureas investigated, while its Lewis basicity is comparable to those of the least basic isothioureas.

In future work we will examine the relevance of these kinetic and thermodynamic data for various organocatalytic transformations.

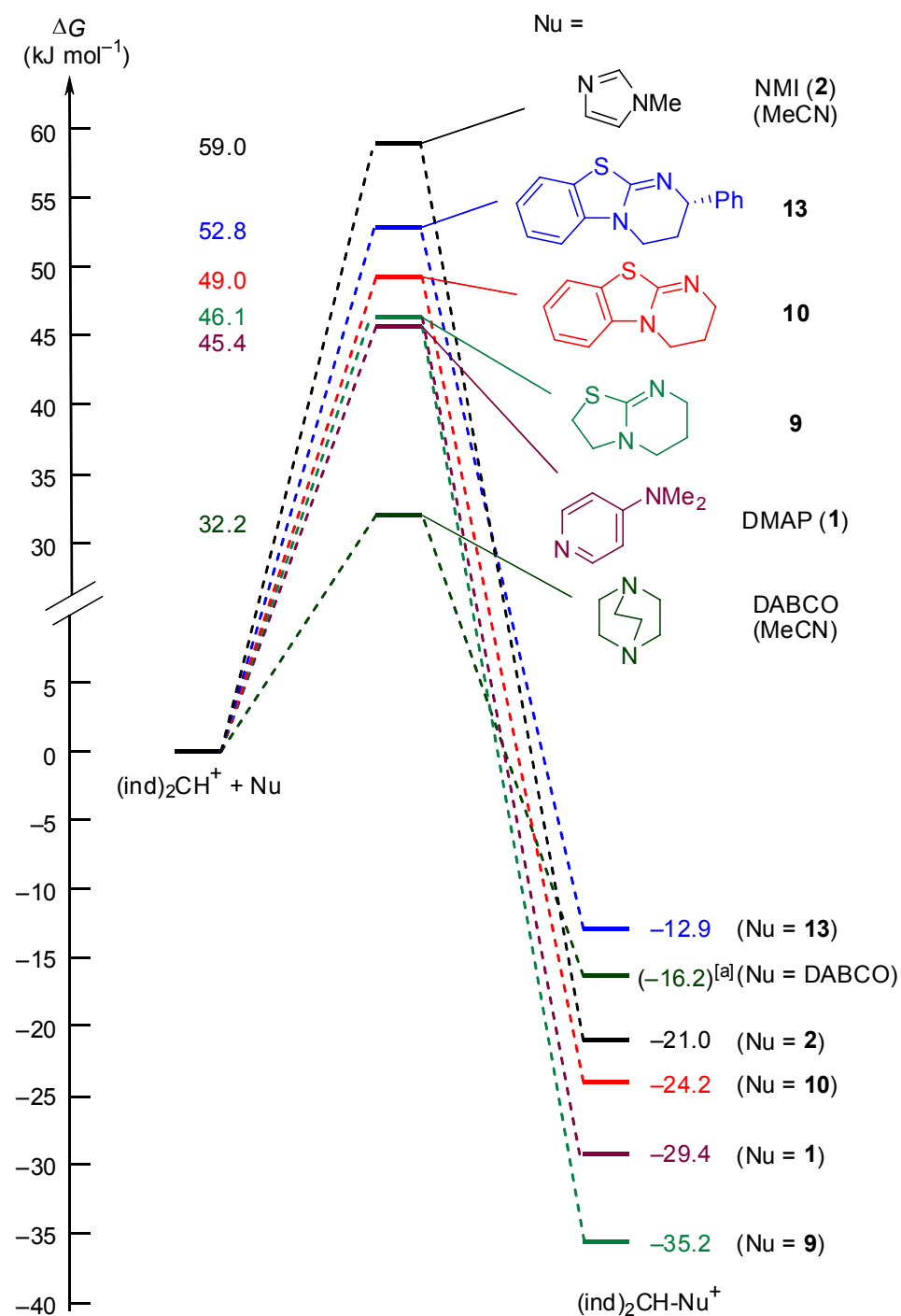


Figure 9.6. Gibbs energy profiles for the reactions of various nucleophilic organocatalysts with the benzhydrylium ion $(\text{ind})_2\text{CH}^+$ in CH_2Cl_2 at 20°C (ΔG^\ddagger and ΔG^0 values from Table 9.3 or from Ref. [20]).

[a] ΔG^0 was estimated in Ref. [20e].

9.4 Experimental Section

9.4.1 General Comment

Materials. CH₂Cl₂ (p.a. grade) was subsequently treated with concentrated sulfuric acid, water, 10% NaHCO₃ solution, and again water. After predrying with anhydrous CaCl₂, it was freshly distilled over CaH₂. Isothioureas were synthesized according to literature procedures.^[15,18] All other chemicals were purchased from commercial sources and (if necessary) purified by recrystallization or distillation prior to use.

Kinetics. The reactions of isothioureas with the colored benzhydrylium ions (Ar₂CH⁺) were followed photometrically at or close to the absorption maxima of (Ar₂CH⁺) by UV/Vis spectroscopy as described previously.^[19] Slow reactions ($\tau_{1/2} > 10$ s) were determined by using conventional UV/Vis spectrophotometers. Stopped-flow techniques were used for the investigation of rapid reactions ($\tau_{1/2} < 10$ s). The temperature of solutions was kept constant at 20.0 ± 0.1 °C during all kinetic studies by using a circulating bath thermostat. The first-order rate constants k_{obs} (s⁻¹) were obtained by least-squares fitting of the absorbances to the monoexponential function $A = A_0 e^{-k_{\text{obs}} t} + C$. The second-order rate constants k (M⁻¹ s⁻¹) were obtained from the slopes of the linear plots of k_{obs} against the nucleophile concentrations.

Determination of Equilibrium Constants. In some cases where initially generated adducts underwent slow subsequent reactions, the equilibrium constants were determined by UV/Vis spectroscopy using a stopped-flow instrument in CH₂Cl₂. In these cases different concentrations of nucleophiles were mixed with solutions of the electrophiles. The end absorbances were obtained by least-squares fitting of the exponential absorbance decay to the mono-exponential function $A = A_0 e^{-k_{\text{obs}} t} + C$, that is, $A = C$.

Assuming a proportionality between the absorbances and the concentrations of the benzhydrylium ions, the equilibrium constants (K) can be expressed by the absorbances of the benzhydrylium ions before (A_0) and after (A) the addition of isothioureas using Equation (9.3).

The temperature of the solutions during all equilibrium studies was kept constant at (20.0 ± 0.1) °C using a circulating bath thermostat.

9.4.2 Kinetics of the reactions of isothiureas with benzhydrylium ions (Ar_2CH^+)**Table 9.5.** Kinetics of the reactions of **13** with $(\text{Ar})_2\text{CH}^+$ in CH_2Cl_2 at 20 °C.

| $[(\text{mor})_2\text{CH}^+]$ (mol L ⁻¹) | [13] (mol L ⁻¹) | k_{obs} (s ⁻¹) | $\lambda = 620 \text{ nm}$ | k (M ⁻¹ s ⁻¹) |
|---|---------------------------------------|--|----------------------------|---|
| 7.53×10^{-6} | 7.61×10^{-5} | 3.39×10^1 | | 3.80×10^5 |
| | 1.52×10^{-4} | 6.35×10^1 | | |
| | 1.90×10^{-4} | 7.81×10^1 | | |
| | 3.04×10^{-4} | 1.24×10^2 | | |
| | 3.80×10^{-4} | 1.48×10^2 | | |
| $[(\text{mpa})_2\text{CH}^+]$ (mol L ⁻¹) | [13] (mol L ⁻¹) | k_{obs} (s ⁻¹) | $\lambda = 620 \text{ nm}$ | k (M ⁻¹ s ⁻¹) |
| 1.98×10^{-5} | 1.33×10^{-4} | 3.43×10^1 | | 2.91×10^5 |
| | 2.22×10^{-4} | 5.85×10^1 | | |
| | 2.88×10^{-4} | 7.97×10^1 | | |
| | 3.99×10^{-4} | 1.10×10^2 | | |
| | 4.87×10^{-4} | 1.31×10^2 | | |
| | 6.20×10^{-4} | 1.78×10^2 | | |
| $[(\text{dma})_2\text{CH}^+]$ (mol L ⁻¹) | [13] (mol L ⁻¹) | k_{obs} (s ⁻¹) | $\lambda = 613 \text{ nm}$ | k (M ⁻¹ s ⁻¹) |
| 2.76×10^{-5} | 3.99×10^{-4} | 2.39×10^1 | | 5.15×10^4 |
| | 7.97×10^{-4} | 4.24×10^1 | | |
| | 1.20×10^{-3} | 6.22×10^1 | | |
| | 1.60×10^{-3} | 8.35×10^1 | | |
| | 1.99×10^{-3} | 1.06×10^2 | | |

Table 9.5. (continued)

| $[(\text{pyr})_2\text{CH}^+]$ (mol L ⁻¹) | [13] (mol L ⁻¹) | k_{obs} (s ⁻¹) | $\lambda = 620 \text{ nm}$ | k (M ⁻¹ s ⁻¹) |
|--|--------------------------------|--|----------------------------|---|
| 1.96×10^{-5} | 3.99×10^{-4} | 2.16×10^1 | | 1.40×10^4 |
| | 7.97×10^{-4} | 2.74×10^1 | | |
| | 1.20×10^{-3} | 3.26×10^1 | | |
| | 1.60×10^{-3} | 3.83×10^1 | | |
| | 1.99×10^{-3} | 4.41×10^1 | | |
| $[(\text{thq})_2\text{CH}^+]$ (mol L ⁻¹) | [13] (mol L ⁻¹) | k_{obs} (s ⁻¹) | $\lambda = 628 \text{ nm}$ | k (M ⁻¹ s ⁻¹) |
| 1.41×10^{-5} | 8.38×10^{-4} | 1.95×10^1 | | 4.60×10^3 |
| | 1.26×10^{-3} | 2.16×10^1 | | |
| | 1.68×10^{-3} | 2.37×10^1 | | |
| | 2.09×10^{-3} | 2.56×10^1 | | |
| | 2.51×10^{-3} | 2.71×10^1 | | |
| Reactivity parameters for 13 in CH ₂ Cl ₂ | | | | |
| Ar ₂ CH ⁺ | <i>E</i> | k (M ⁻¹ s ⁻¹) | | $N = 13.45$ $s_N = 0.72$ |
| (mor) ₂ CH ⁺ | -5.53 | 3.80×10^5 | | |
| (mpa) ₂ CH ⁺ | -5.89 | 2.91×10^5 | | |
| (dma) ₂ CH ⁺ | -7.02 | 5.15×10^4 | | |
| (pyr) ₂ CH ⁺ | -7.69 | 1.40×10^4 | | |
| (thq) ₂ CH ⁺ | -8.22 | 4.60×10^3 | | |

Table 9.6. Kinetics of the reactions of **14** with (Ar)₂CH⁺ in CH₂Cl₂ at 20°C.

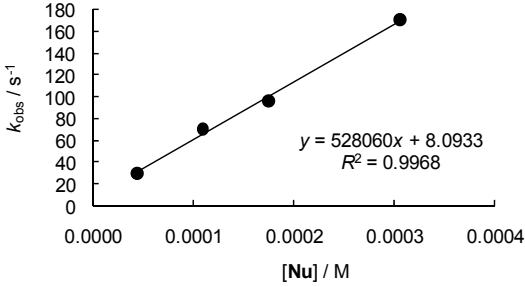
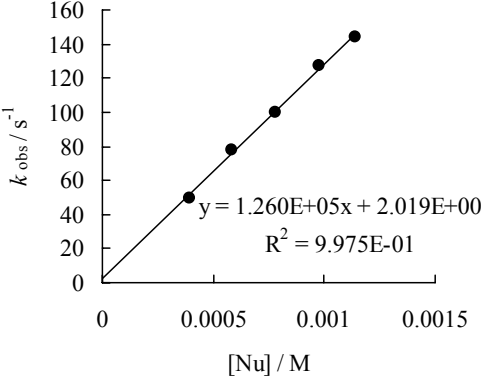
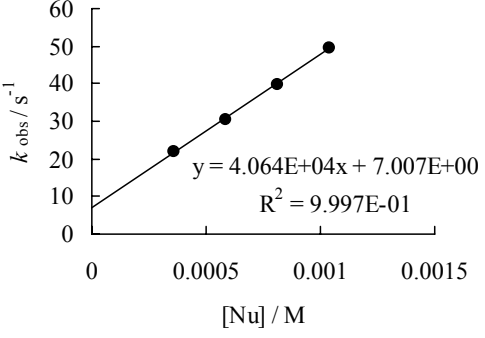
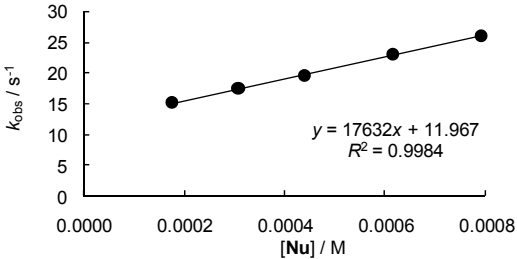
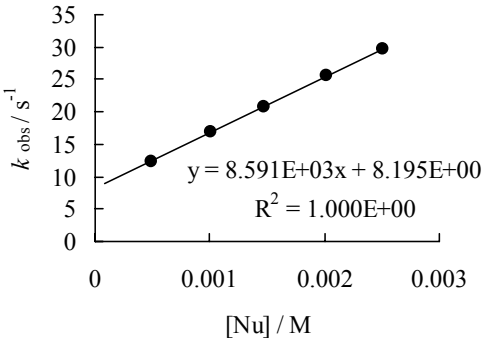
| $[(\text{mpa})_2\text{CH}^+]$ (mol L ⁻¹) | [14] (mol L ⁻¹) | k_{obs} (s ⁻¹) | $\lambda = 622 \text{ nm}$ | k (M ⁻¹ s ⁻¹) |
|---|---------------------------------------|--|--|---|
| 5.17×10^{-6} | 4.38×10^{-5} | 2.99×10^1 |  | 5.28×10^5 |
| | 1.10×10^{-4} | 7.02×10^1 | | |
| | 1.75×10^{-4} | 9.70×10^1 | | |
| | 3.07×10^{-4} | 1.71×10^2 | | |
| $[(\text{dma})_2\text{CH}^+]$ (mol L ⁻¹) | [14] (mol L ⁻¹) | k_{obs} (s ⁻¹) | $\lambda = 613 \text{ nm}$ | k (M ⁻¹ s ⁻¹) |
| 1.92×10^{-5} | 3.91×10^{-4} | 4.96×10^1 |  | 1.26×10^5 |
| | 5.86×10^{-4} | 7.80×10^1 | | |
| | 7.82×10^{-4} | 1.00×10^2 | | |
| | 9.77×10^{-4} | 1.27×10^2 | | |
| | 1.14×10^{-3} | 1.44×10^1 | | |
| $[(\text{pyr})_2\text{CH}^+]$ (mol L ⁻¹) | [14] (mol L ⁻¹) | k_{obs} (s ⁻¹) | $\lambda = 620 \text{ nm}$ | k (M ⁻¹ s ⁻¹) |
| 2.03×10^{-5} | 3.57×10^{-4} | 2.17×10^1 |  | 4.06×10^4 |
| | 5.84×10^{-4} | 3.05×10^1 | | |
| | 8.11×10^{-4} | 3.99×10^1 | | |
| | 1.04×10^{-3} | 4.94×10^1 | | |

Table 9.6. (continued)

| $[(\text{thq})_2\text{CH}^+]$ (mol L ⁻¹) | [14] (mol L ⁻¹) | k_{obs} (s ⁻¹) | $\lambda = 628 \text{ nm}$ | k (M ⁻¹ s ⁻¹) |
|---|--------------------------------|--|--|---|
| 5.40×10^{-6} | 1.75×10^{-4} | 1.51×10^1 |  | 1.76×10^4 |
| | 3.07×10^{-4} | 1.75×10^1 | | |
| | 4.38×10^{-4} | 1.94×10^1 | | |
| | 6.14×10^{-4} | 2.29×10^1 | | |
| | 7.89×10^{-4} | 2.59×10^1 | | |

| $[(\text{ind})_2\text{CH}^+]$ (mol L ⁻¹) | [14] (mol L ⁻¹) | k_{obs} (s ⁻¹) | $\lambda = 625 \text{ nm}$ | k (M ⁻¹ s ⁻¹) |
|---|--------------------------------|--|---|---|
| 1.50×10^{-5} | 4.89×10^{-4} | 1.24×10^1 |  | 8.59×10^3 |
| | 1.01×10^{-3} | 1.69×10^1 | | |
| | 1.47×10^{-3} | 2.08×10^1 | | |
| | 2.02×10^{-3} | 2.55×10^1 | | |
| | 2.51×10^{-3} | 2.98×10^1 | | |

Reactivity parameters for 14 in CH₂Cl₂

| Ar ₂ CH ⁺ | E | k (M ⁻¹ s ⁻¹) |
|------------------------------------|-------|--|
| (mpa) ₂ CH ⁺ | -5.89 | 5.28×10^5 |
| (dma) ₂ CH ⁺ | -7.02 | 1.26×10^5 |
| (pyr) ₂ CH ⁺ | -7.69 | 4.06×10^4 |
| (thq) ₂ CH ⁺ | -8.22 | 1.76×10^4 |
| (ind) ₂ CH ⁺ | -8.76 | 8.59×10^3 |

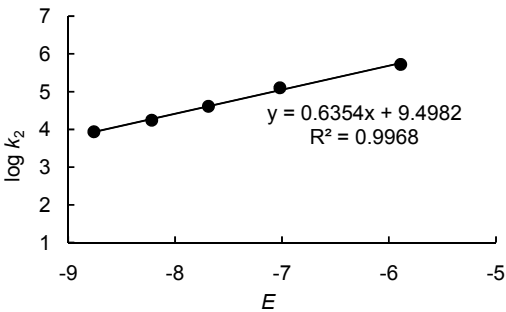
| | |
|--|-----------------------------|
|  | $N = 14.96$ $s_N = 0.64$ |
|--|-----------------------------|

Table 9.7. Kinetics of the reactions of **15** with (Ar)₂CH⁺ in CH₂Cl₂ at 20°C.

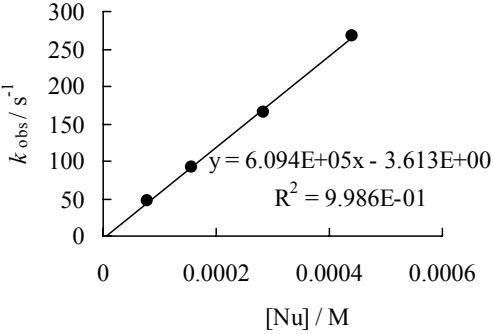
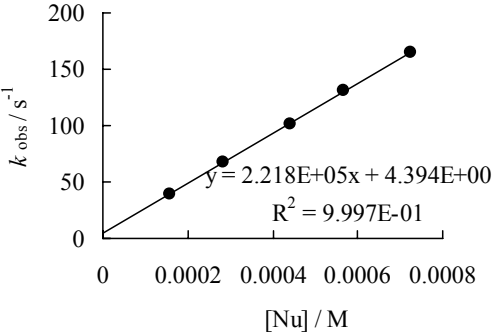
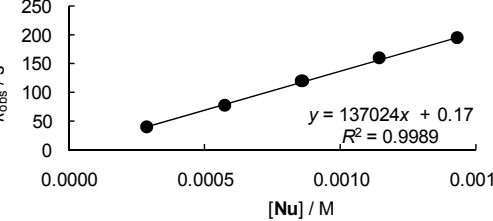
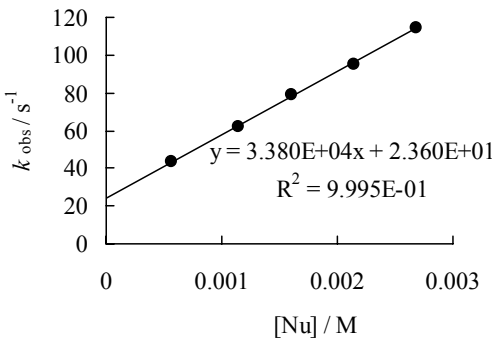
| [(dpa) ₂ CH ⁺] (mol L ⁻¹) | [15] (mol L ⁻¹) | <i>k</i> _{obs} (s ⁻¹) | λ = 672 nm | <i>k</i> (M ⁻¹ s ⁻¹) |
|---|---|---|--|--|
| 1.44 × 10 ⁻⁵ | 7.88 × 10 ⁻⁵ | 4.75 × 10 ¹ |  | 6.09 × 10 ⁵ |
| | 1.58 × 10 ⁻⁴ | 9.12 × 10 ¹ | | |
| | 2.84 × 10 ⁻⁴ | 1.65 × 10 ² | | |
| | 4.41 × 10 ⁻⁴ | 2.68 × 10 ² | | |
| [(mor) ₂ CH ⁺] (mol L ⁻¹) | [15] (mol L ⁻¹) | <i>k</i> _{obs} (s ⁻¹) | λ = 620 nm | <i>k</i> (M ⁻¹ s ⁻¹) |
| 7.64 × 10 ⁻⁶ | 1.58 × 10 ⁻⁴ | 3.93 × 10 ¹ |  | 2.22 × 10 ⁵ |
| | 2.84 × 10 ⁻⁴ | 6.80 × 10 ¹ | | |
| | 4.41 × 10 ⁻⁴ | 1.01 × 10 ² | | |
| | 5.67 × 10 ⁻⁴ | 1.31 × 10 ² | | |
| | 7.25 × 10 ⁻⁴ | 1.65 × 10 ² | | |
| [(mpa) ₂ CH ⁺] (mol L ⁻¹) | [15] (mol L ⁻¹) | <i>k</i> _{obs} (s ⁻¹) | λ = 622 nm | <i>k</i> (M ⁻¹ s ⁻¹) |
| 1.97 × 10 ⁻⁵ | 2.86 × 10 ⁻⁴ | 3.93 × 10 ¹ |  | 1.37 × 10 ⁵ |
| | 5.71 × 10 ⁻⁴ | 7.62 × 10 ¹ | | |
| | 8.57 × 10 ⁻⁴ | 1.20 × 10 ² | | |
| | 1.14 × 10 ⁻³ | 1.58 × 10 ² | | |
| | 1.43 × 10 ⁻³ | 1.94 × 10 ² | | |

Table 9.7. (continued)

| $[(\text{dma})_2\text{CH}^+]$ (mol L ⁻¹) | [15] (mol L ⁻¹) | k_{obs} (s ⁻¹) | $\lambda = 613 \text{ nm}$ | k (M ⁻¹ s ⁻¹) |
|---|---|--|--|---|
| 3.52×10^{-5} | 5.71×10^{-4} | 4.23×10^1 |  | 3.38×10^4 |
| | 1.14×10^{-3} | 6.24×10^1 | | |
| | 1.60×10^{-3} | 7.89×10^1 | | |
| | 2.14×10^{-3} | 9.53×10^1 | | |
| | 2.68×10^{-3} | 1.14×10^2 | | |

Reactivity parameters for **15** in CH₂Cl₂

| Ar ₂ CH ⁺ | E | k (M ⁻¹ s ⁻¹) | $N = 15.30$ $s_N = 0.55$ |
|------------------------------------|-------|--|-----------------------------|
| (dpa) ₂ CH ⁺ | -4.72 | 6.09×10^5 | |
| (mor) ₂ CH ⁺ | -5.53 | 2.22×10^5 | |
| (mpa) ₂ CH ⁺ | -5.89 | 1.37×10^5 | |
| (dma) ₂ CH ⁺ | -7.02 | 3.38×10^4 | |

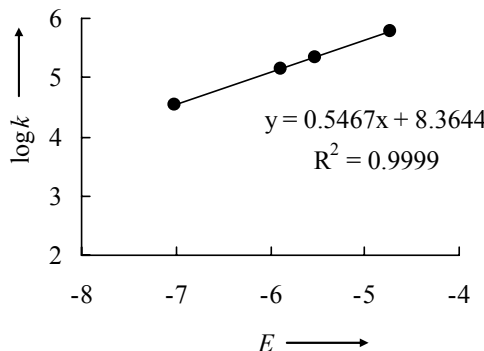


Table 9.8. Kinetics of the reactions of **16** with (Ar)₂CH⁺ in CH₂Cl₂ at 20°C.

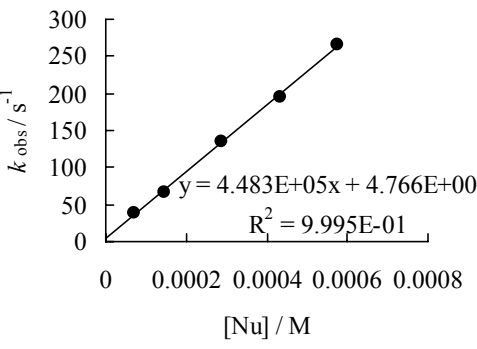
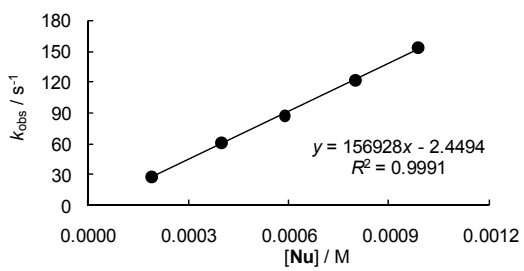
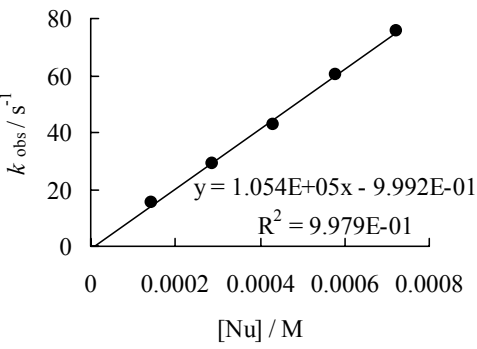
| [(dpa) ₂ CH ⁺] (mol L ⁻¹) | [16] (mol L ⁻¹) | <i>k</i> _{obs} (s ⁻¹) | λ = 672 nm | <i>k</i> (M ⁻¹ s ⁻¹) |
|---|---|---|--|--|
| 1.57 × 10 ⁻⁵ | 7.21 × 10 ⁻⁵ | 3.85 × 10 ¹ |  | 4.48 × 10 ⁵ |
| | 1.44 × 10 ⁻⁴ | 6.75 × 10 ¹ | | |
| | 2.89 × 10 ⁻⁴ | 1.36 × 10 ² | | |
| | 4.33 × 10 ⁻⁴ | 1.96 × 10 ² | | |
| | 5.77 × 10 ⁻⁴ | 2.65 × 10 ² | | |
| [(mor) ₂ CH ⁺] (mol L ⁻¹) | [16] (mol L ⁻¹) | <i>k</i> _{obs} (s ⁻¹) | λ = 620 nm | <i>k</i> (M ⁻¹ s ⁻¹) |
| 1.99 × 10 ⁻⁵ | 1.89 × 10 ⁻⁴ | 2.80 × 10 ¹ |  | 1.57 × 10 ⁵ |
| | 3.99 × 10 ⁻⁴ | 6.09 × 10 ¹ | | |
| | 5.88 × 10 ⁻⁴ | 8.73 × 10 ¹ | | |
| | 7.98 × 10 ⁻⁴ | 1.23 × 10 ² | | |
| | 9.87 × 10 ⁻⁴ | 1.54 × 10 ² | | |
| [(mpa) ₂ CH ⁺] (mol L ⁻¹) | [16] (mol L ⁻¹) | <i>k</i> _{obs} (s ⁻¹) | λ = 622 nm | <i>k</i> (M ⁻¹ s ⁻¹) |
| 6.54 × 10 ⁻⁶ | 1.44 × 10 ⁻⁴ | 1.51 × 10 ¹ |  | 1.05 × 10 ⁵ |
| | 2.89 × 10 ⁻⁴ | 2.93 × 10 ¹ | | |
| | 4.33 × 10 ⁻⁴ | 4.28 × 10 ¹ | | |
| | 5.77 × 10 ⁻⁴ | 6.03 × 10 ¹ | | |
| | 7.21 × 10 ⁻⁴ | 7.56 × 10 ¹ | | |

Table 9.8. (continued)

| $[(\text{dma})_2\text{CH}^+]$ (mol L ⁻¹) | [16] (mol L ⁻¹) | k_{obs} (s ⁻¹) | $\lambda = 613 \text{ nm}$ | k (M ⁻¹ s ⁻¹) |
|---|---|--|----------------------------|---|
| 1.38×10^{-5} | 4.22×10^{-4} | 1.81×10^1 | | 3.73×10^4 |
| | 8.44×10^{-4} | 3.21×10^1 | | |
| | 1.21×10^{-3} | 4.36×10^1 | | |
| | 1.69×10^{-3} | 6.48×10^1 | | |
| | 2.11×10^{-3} | 8.03×10^1 | | |

| $[(\text{pyr})_2\text{CH}^+]$ (mol L ⁻¹) | [16] (mol L ⁻¹) | k_{obs} (s ⁻¹) | $\lambda = 620 \text{ nm}$ | k (M ⁻¹ s ⁻¹) |
|---|---|--|----------------------------|---|
| 6.42×10^{-6} | 8.44×10^{-4} | 3.20×10^1 | | 1.53×10^4 |
| | 2.11×10^{-3} | 5.07×10^1 | | |
| | 2.59×10^{-3} | 5.91×10^1 | | |
| | 3.31×10^{-3} | 6.95×10^1 | | |

Reactivity parameters for **16** in CH₂Cl₂

| Ar ₂ CH ⁺ | E | k (M ⁻¹ s ⁻¹) | |
|------------------------------------|-------|--|--|
| (dpa) ₂ CH ⁺ | -4.72 | 4.50×10^5 | |
| (dma) ₂ CH ⁺ | -5.53 | 1.57×10^5 | |
| (mpa) ₂ CH ⁺ | -5.89 | 1.05×10^5 | |
| (dma) ₂ CH ⁺ | -7.02 | 3.73×10^4 | |
| (pyr) ₂ CH ⁺ | -7.69 | 1.53×10^4 | |

$N = 16.50$
 $s_N = 0.48$

Table 9.9. Kinetics of the reactions of **17** with (Ar)₂CH⁺ in CH₂Cl₂ at 20°C.

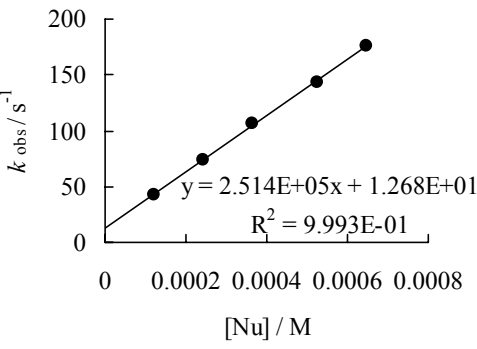
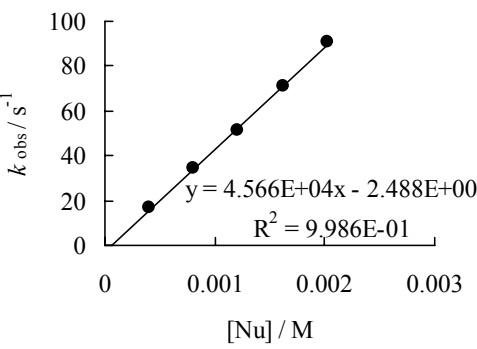
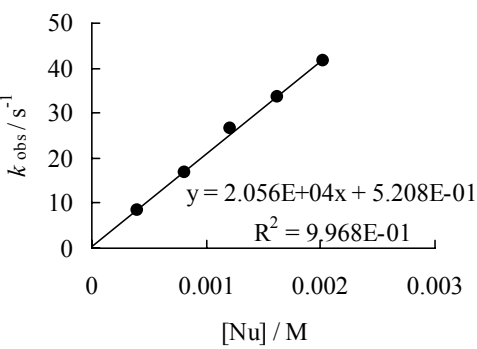
| $[(\text{mfa})_2\text{CH}^+]$ (mol L ⁻¹) | [17] (mol L ⁻¹) | k_{obs} (s ⁻¹) | $\lambda = 593 \text{ nm}$ | k (M ⁻¹ s ⁻¹) |
|---|---------------------------------------|--|--|---|
| 7.39×10^{-6} | 1.21×10^{-4} | 4.25×10^1 |  | 2.51×10^5 |
| | 2.43×10^{-4} | 7.39×10^1 | | |
| | 3.64×10^{-4} | 1.06×10^2 | | |
| | 5.26×10^{-4} | 1.43×10^2 | | |
| | 6.47×10^{-4} | 1.76×10^2 | | |
| $[(\text{dpa})_2\text{CH}^+]$ (mol L ⁻¹) | [17] (mol L ⁻¹) | k_{obs} (s ⁻¹) | $\lambda = 672 \text{ nm}$ | k (M ⁻¹ s ⁻¹) |
| 3.98×10^{-5} | 4.04×10^{-4} | 1.69×10^1 |  | 4.57×10^4 |
| | 8.09×10^{-4} | 3.44×10^1 | | |
| | 1.21×10^{-3} | 5.21×10^1 | | |
| | 1.62×10^{-3} | 7.12×10^1 | | |
| | 2.02×10^{-3} | 9.08×10^1 | | |
| $[(\text{mor})_2\text{CH}^+]$ (mol L ⁻¹) | [17] (mol L ⁻¹) | k_{obs} (s ⁻¹) | $\lambda = 620 \text{ nm}$ | k (M ⁻¹ s ⁻¹) |
| 1.99×10^{-5} | 4.04×10^{-4} | 8.54×10^0 |  | 2.06×10^4 |
| | 8.09×10^{-4} | 1.67×10^1 | | |
| | 1.21×10^{-3} | 2.67×10^1 | | |
| | 1.62×10^{-3} | 3.37×10^1 | | |
| | 2.02×10^{-3} | 4.16×10^1 | | |

Table 9.9. (continued)

| $[(\text{mpa})_2\text{CH}^+]$ (mol L ⁻¹) | [17] (mol L ⁻¹) | k_{obs} (s ⁻¹) | $\lambda = 628 \text{ nm}$ | k (M ⁻¹ s ⁻¹) |
|---|---|--|----------------------------|---|
| 6.82×10^{-6} | 1.31×10^{-4} | 8.53×10^0 | | 1.58×10^4 |
| | 2.61×10^{-4} | 1.02×10^1 | | |
| | 3.92×10^{-4} | 1.23×10^1 | | |
| | 6.10×10^{-4} | 1.60×10^1 | | |
| | 8.27×10^{-4} | 1.93×10^1 | | |

Reactivity parameters for **17** in CH₂Cl₂

| Ar ₂ CH ⁺ | E | k (M ⁻¹ s ⁻¹) | |
|------------------------------------|-------|--|--|
| (mfa) ₂ CH ⁺ | -3.85 | 2.51×10^5 | |
| (dpa) ₂ CH ⁺ | -4.72 | 4.57×10^4 | |
| (dma) ₂ CH ⁺ | -5.53 | 2.06×10^4 | |
| (mpa) ₂ CH ⁺ | -5.89 | 1.58×10^4 | |

9.4.3 Equilibrium constants (K) for the reactions of benzhydrylium ions (Ar_2CH^+) with isothiureas in CH_2Cl_2 .

Table 9.10. Determination of the equilibrium constant for the reaction of $(\text{mpa})_2\text{CH}^+$ and **13** ($\epsilon[(\text{mpa})_2\text{CH}^+$ at 622 nm] = $1.41 \times 10^5 \text{ M}^{-1} \text{ cm}^{-1}$ and $d = 1.0 \text{ cm}$, CH_2Cl_2 at 20.0 °C).

| Entry | $[\mathbf{13}]_0$ (mol L ⁻¹) | A | $[(\text{mpa})_2\text{CH}^+]_{\text{eq}}$ (mol L ⁻¹) | K (L mol ⁻¹) |
|-------|--|-------|--|----------------------------|
| 0 | 0 | 0.813 | 5.77×10^{-6} | |
| 1 | 7.13×10^{-6} | 0.281 | 1.99×10^{-6} | 5.64×10^5 |
| 2 | 1.35×10^{-5} | 0.137 | 9.72×10^{-7} | 5.67×10^5 |
| 3 | 1.98×10^{-5} | 0.077 | 5.46×10^{-7} | 6.55×10^5 |

$$K_{\text{av}}(20 \text{ }^\circ\text{C}) = 5.95 \times 10^5 \text{ L mol}^{-1}$$

Table 9.11. Determination of the equilibrium constant for the reaction of $(\text{dma})_2\text{CH}^+$ and **13** ($\epsilon[(\text{dma})_2\text{CH}^+$ at 613 nm] = $1.70 \times 10^5 \text{ M}^{-1} \text{ cm}^{-1}$ and $d = 0.5 \text{ cm}$, CH_2Cl_2 at 20.0 °C).

| Entry | $[\mathbf{13}]_0$ (mol L ⁻¹) | A | $[(\text{dma})_2\text{CH}^+]_{\text{eq}}$ (mol L ⁻¹) | K (L mol ⁻¹) |
|-------|--|-------|--|----------------------------|
| 0 | 0 | 0.955 | 1.12×10^{-5} | |
| 1 | 1.33×10^{-4} | 0.405 | 4.76×10^{-6} | 1.07×10^4 |
| 2 | 2.22×10^{-4} | 0.279 | 3.28×10^{-6} | 1.13×10^4 |
| 3 | 3.99×10^{-4} | 0.180 | 2.12×10^{-6} | 1.10×10^4 |
| 4 | 7.97×10^{-4} | 0.100 | 1.18×10^{-6} | 1.09×10^4 |
| 5 | 1.20×10^{-3} | 0.072 | 8.47×10^{-7} | 1.03×10^4 |
| 6 | 1.60×10^{-3} | 0.055 | 6.47×10^{-7} | 1.03×10^4 |
| 7 | 1.99×10^{-3} | 0.045 | 5.29×10^{-7} | 1.02×10^4 |

$$K_{\text{av}}(20 \text{ }^\circ\text{C}) = 1.07 \times 10^4 \text{ L mol}^{-1}$$

Table 9.12. Determination of the equilibrium constant for the reaction of $(\text{pyr})_2\text{CH}^+$ and **13** ($\epsilon[(\text{pyr})_2\text{CH}^+$ at 620 nm] = $1.74 \times 10^5 \text{ M}^{-1} \text{ cm}^{-1}$ and $d = 0.5 \text{ cm}$, CH_2Cl_2 at 20.0 °C).

| Entry | $[\mathbf{13}]_0$ (mol L ⁻¹) | A | $[(\text{pyr})_2\text{CH}^+]_{\text{eq}}$ (mol L ⁻¹) | K (L mol ⁻¹) |
|-------|--|-------|--|----------------------------|
| 0 | 0 | 1.58 | 1.82×10^{-5} | |
| 1 | 3.99×10^{-4} | 1.16 | 1.33×10^{-5} | 9.19×10^2 |
| 2 | 7.97×10^{-4} | 0.929 | 1.07×10^{-5} | 8.88×10^2 |
| 3 | 1.20×10^{-3} | 0.772 | 8.87×10^{-6} | 8.79×10^2 |
| 4 | 1.60×10^{-3} | 0.651 | 7.48×10^{-6} | 9.01×10^2 |
| 5 | 1.99×10^{-3} | 0.571 | 6.56×10^{-6} | 8.93×10^2 |

$$K_{\text{av}}(20 \text{ }^\circ\text{C}) = 8.96 \times 10^2 \text{ L mol}^{-1}$$

Table 9.13. Determination of the equilibrium constant for the reaction of $(\text{thq})_2\text{CH}^+$ and **13** ($\epsilon[(\text{thq})_2\text{CH}^+$ at 628 nm] = $1.78 \times 10^5 \text{ M}^{-1} \text{ cm}^{-1}$ and $d = 0.5 \text{ cm}$, CH_2Cl_2 at 20.0 °C).

| Entry | $[\mathbf{13}]_0$ (mol L ⁻¹) | A | $[(\text{thq})_2\text{CH}^+]_{\text{eq}}$ (mol L ⁻¹) | K (L mol ⁻¹) |
|-------|--|-------|--|----------------------------|
| 0 | 0 | 1.18 | 1.33×10^{-5} | |
| 1 | 8.38×10^{-4} | 0.931 | 1.05×10^{-5} | 3.20×10^2 |
| 2 | 1.26×10^{-3} | 0.835 | 9.38×10^{-6} | 3.29×10^2 |
| 3 | 1.68×10^{-3} | 0.753 | 8.46×10^{-6} | 3.39×10^2 |
| 4 | 2.09×10^{-3} | 0.686 | 7.71×10^{-6} | 3.45×10^2 |
| 5 | 2.51×10^{-3} | 0.650 | 7.30×10^{-6} | 3.26×10^2 |

$$K_{\text{av}}(20 \text{ °C}) = 3.32 \times 10^2 \text{ L mol}^{-1}$$

Table 9.14. Determination of the equilibrium constant for the reaction of $(\text{dma})_2\text{CH}^+$ and **14** ($\epsilon[(\text{dma})_2\text{CH}^+$ at 613 nm] = $1.70 \times 10^5 \text{ M}^{-1} \text{ cm}^{-1}$ and $d = 1.0 \text{ cm}$, CH_2Cl_2 at 20.0 °C).

| Entry | $[\mathbf{14}]_0$ (mol L ⁻¹) | A | $[(\text{dma})_2\text{CH}^+]_{\text{eq}}$ (mol L ⁻¹) | K (L mol ⁻¹) |
|-------|--|-------|--|----------------------------|
| 0 | 0 | 0.822 | 5.19×10^{-6} | |
| 1 | 4.23×10^{-5} | 0.309 | 1.82×10^{-6} | 4.76×10^4 |
| 2 | 5.67×10^{-5} | 0.226 | 1.33×10^{-6} | 5.49×10^4 |
| 3 | 7.22×10^{-5} | 0.184 | 1.08×10^{-6} | 5.57×10^4 |
| 4 | 1.03×10^{-4} | 0.122 | 7.18×10^{-7} | 6.32×10^4 |

$$K_{\text{av}}(20 \text{ °C}) = 5.54 \times 10^4 \text{ L mol}^{-1}$$

Table 9.15. Determination of the equilibrium constant for the reaction of $(\text{pyr})_2\text{CH}^+$ and **14** ($\epsilon[(\text{pyr})_2\text{CH}^+$ at 620 nm] = $1.74 \times 10^5 \text{ M}^{-1} \text{ cm}^{-1}$ and $d = 0.5 \text{ cm}$, CH_2Cl_2 at 20.0 °C).

| Entry | $[\mathbf{14}]_0$ (mol L ⁻¹) | A | $[(\text{pyr})_2\text{CH}^+]_{\text{eq}}$ (mol L ⁻¹) | K (L mol ⁻¹) |
|-------|--|-------|--|----------------------------|
| 0 | 0 | 1.41 | 1.62×10^{-5} | |
| 1 | 3.57×10^{-4} | 0.604 | 6.94×10^{-6} | 3.85×10^3 |
| 2 | 5.84×10^{-4} | 0.439 | 5.05×10^{-6} | 3.87×10^3 |
| 3 | 8.11×10^{-4} | 0.338 | 3.89×10^{-6} | 3.98×10^3 |
| 4 | 1.04×10^{-3} | 0.277 | 3.18×10^{-6} | 3.99×10^3 |
| 5 | 1.23×10^{-3} | 0.256 | 2.94×10^{-6} | 3.71×10^3 |

$$K_{\text{av}}(20 \text{ °C}) = 3.88 \times 10^3 \text{ L mol}^{-1}$$

Table 9.16. Determination of the equilibrium constant for the reaction of $(\text{thq})_2\text{CH}^+$ and **14** ($\epsilon[(\text{thq})_2\text{CH}^+$ at 628 nm] = $1.78 \times 10^5 \text{ M}^{-1} \text{ cm}^{-1}$ and $d = 1.0 \text{ cm}$, CH_2Cl_2 at 20.0 °C).

| Entry | $[\mathbf{14}]_0$ (mol L ⁻¹) | A | $[(\text{pyr})_2\text{CH}^+]_{\text{eq}}$ (mol L ⁻¹) | K (L mol ⁻¹) |
|-------|--|-------|--|----------------------------|
| 0 | 0 | 1.08 | 6.07×10^{-6} | |
| 1 | 1.75×10^{-4} | 0.852 | 4.79×10^{-6} | 1.54×10^3 |
| 2 | 3.07×10^{-4} | 0.718 | 4.03×10^{-6} | 1.65×10^3 |
| 3 | 4.38×10^{-4} | 0.626 | 3.52×10^{-6} | 1.67×10^3 |
| 4 | 6.14×10^{-4} | 0.528 | 2.97×10^{-6} | 1.71×10^3 |
| 5 | 7.89×10^{-4} | 0.454 | 2.55×10^{-6} | 1.76×10^3 |

$$K_{\text{av}}(20 \text{ °C}) = 1.67 \times 10^3 \text{ L mol}^{-1}$$

Table 9.17. Determination of the equilibrium constant for the reaction of $(\text{ind})_2\text{CH}^+$ and **14** ($\epsilon[(\text{ind})_2\text{CH}^+$ at 625 nm] = $1.78 \times 10^5 \text{ M}^{-1} \text{ cm}^{-1}$ and $d = 0.5 \text{ cm}$, CH_2Cl_2 at 20.0 °C).

| Entry | $[\mathbf{14}]_0$ (mol L ⁻¹) | A | $[(\text{ind})_2\text{CH}^+]_{\text{eq}}$ (mol L ⁻¹) | K (L mol ⁻¹) |
|-------|--|-------|--|----------------------------|
| 0 | 0 | 1.11 | 1.25×10^{-5} | |
| 1 | 4.89×10^{-4} | 0.712 | 8.00×10^{-6} | 1.15×10^3 |
| 2 | 1.01×10^{-3} | 0.509 | 5.72×10^{-6} | 1.18×10^3 |
| 3 | 1.47×10^{-3} | 0.411 | 4.62×10^{-6} | 1.16×10^3 |
| 4 | 2.02×10^{-3} | 0.331 | 3.72×10^{-6} | 1.17×10^3 |
| 5 | 2.51×10^{-3} | 0.281 | 3.15×10^{-6} | 1.19×10^3 |

$$K_{\text{av}}(20 \text{ °C}) = 1.17 \times 10^3 \text{ L mol}^{-1}$$

Table 9.18. Determination of the equilibrium constant for the reaction of $(\text{mpa})_2\text{CH}^+$ and **15** ($\epsilon[(\text{mpa})_2\text{CH}^+$ at 622 nm] = $1.41 \times 10^5 \text{ M}^{-1} \text{ cm}^{-1}$ and $d = 1.0 \text{ cm}$, CH_2Cl_2 at 20.0 °C).

| Entry | $[\mathbf{15}]_0$ (mol L ⁻¹) | A | $[(\text{mpa})_2\text{CH}^+]_{\text{eq}}$ (mol L ⁻¹) | K (L mol ⁻¹) |
|-------|--|-------|--|----------------------------|
| 0 | 0 | 0.860 | 6.10×10^{-6} | |
| 1 | 6.48×10^{-6} | 0.681 | 4.83×10^{-6} | 5.04×10^4 |
| 2 | 2.00×10^{-5} | 0.485 | 3.44×10^{-6} | 4.46×10^4 |
| 3 | 2.95×10^{-5} | 0.396 | 2.81×10^{-6} | 4.47×10^4 |

$$K_{\text{av}}(20 \text{ °C}) = 4.66 \times 10^4 \text{ L mol}^{-1}$$

Table 9.19. Determination of the equilibrium constant for the reaction of $(\text{dma})_2\text{CH}^+$ and **15** ($\epsilon[(\text{dma})_2\text{CH}^+$ at 613 nm] = $1.70 \times 10^5 \text{ M}^{-1} \text{ cm}^{-1}$ and $d = 0.5 \text{ cm}$, CH_2Cl_2 at 20.0 °C).

| Entry | [15] ₀ (mol L ⁻¹) | <i>A</i> | [(dma) ₂ CH ⁺] _{eq} (mol L ⁻¹) | <i>K</i> (L mol ⁻¹) |
|-------|---|----------|--|---------------------------------|
| 0 | 0 | 0.961 | 1.13×10^{-5} | |
| 1 | 5.71×10^{-4} | 0.640 | 7.53×10^{-6} | 8.84×10^2 |
| 2 | 1.14×10^{-3} | 0.448 | 5.27×10^{-6} | 1.01×10^3 |
| 3 | 1.60×10^{-3} | 0.366 | 4.31×10^{-6} | 1.02×10^3 |
| 4 | 2.14×10^{-3} | 0.301 | 3.54×10^{-6} | 1.03×10^3 |
| 5 | 2.68×10^{-3} | 0.256 | 3.01×10^{-6} | 1.03×10^3 |

$$K_{\text{av}}(20 \text{ °C}) = 9.95 \times 10^2 \text{ L mol}^{-1}$$

Table 9.20. Determination of the equilibrium constant for the reaction of $(\text{mpa})_2\text{CH}^+$ and **16** ($\epsilon[(\text{mpa})_2\text{CH}^+$ at 622 nm] = $1.41 \times 10^5 \text{ M}^{-1} \text{ cm}^{-1}$ and $d = 1.0 \text{ cm}$, CH_2Cl_2 at 20.0 °C).

| Entry | [16] ₀ (mol L ⁻¹) | <i>A</i> | [(mpa) ₂ CH ⁺] _{eq} (mol L ⁻¹) | <i>K</i> (L mol ⁻¹) |
|-------|---|----------|--|---------------------------------|
| 0 | 0 | 0.832 | 5.90×10^{-6} | |
| 1 | 6.63×10^{-6} | 0.568 | 4.03×10^{-6} | 9.77×10^4 |
| 2 | 1.89×10^{-5} | 0.324 | 2.30×10^{-6} | 1.02×10^5 |
| 3 | 3.31×10^{-5} | 0.211 | 1.50×10^{-6} | 1.03×10^5 |

$$K_{\text{av}}(20 \text{ °C}) = 1.01 \times 10^5 \text{ L mol}^{-1}$$

Table 9.21. Determination of the equilibrium constant for the reaction of $(\text{dma})_2\text{CH}^+$ and **16** ($\epsilon[(\text{dma})_2\text{CH}^+$ at 613 nm] = $1.70 \times 10^5 \text{ M}^{-1} \text{ cm}^{-1}$ and $d = 1.0 \text{ cm}$, CH_2Cl_2 at 20.0 °C).

| Entry | [16] ₀ (mol L ⁻¹) | <i>A</i> | [(dma) ₂ CH ⁺] _{eq} (mol L ⁻¹) | <i>K</i> (L mol ⁻¹) |
|-------|---|----------|--|---------------------------------|
| 0 | 0 | 1.22 | 1.44×10^{-5} | |
| 1 | 2.81×10^{-4} | 0.724 | 8.52×10^{-6} | 2.49×10^3 |
| 2 | 5.62×10^{-4} | 0.496 | 5.84×10^{-6} | 2.64×10^3 |
| 3 | 8.43×10^{-4} | 0.369 | 4.34×10^{-6} | 2.77×10^3 |
| 4 | 1.12×10^{-3} | 0.288 | 3.39×10^{-6} | 2.92×10^3 |

$$K_{\text{av}}(20 \text{ °C}) = 2.70 \times 10^3 \text{ L mol}^{-1}$$

Table 9.22. Determination of the equilibrium constant for the reaction of $(\text{mor})_2\text{CH}^+$ and **17** ($\epsilon[(\text{mpa})_2\text{CH}^+$ at 620 nm] = $1.45 \times 10^5 \text{ M}^{-1} \text{ cm}^{-1}$ and $d = 0.5 \text{ cm}$, CH_2Cl_2 at 20.0 °C).

| Entry | [17] ₀ (mol L ⁻¹) | <i>A</i> | $[(\text{mor})_2\text{CH}^+]_{\text{eq}}$ (mol L ⁻¹) | <i>K</i> (L mol ⁻¹) |
|-------|---|----------|--|---------------------------------|
| 0 | 0 | 1.18 | 1.63×10^{-5} | |
| 1 | 4.04×10^{-4} | 0.170 | 2.34×10^{-6} | 1.52×10^4 |
| 2 | 8.09×10^{-4} | 0.097 | 1.34×10^{-6} | 1.41×10^4 |
| 3 | 1.21×10^{-3} | 0.066 | 9.10×10^{-7} | 1.41×10^4 |
| 4 | 1.62×10^{-3} | 0.055 | 7.59×10^{-7} | 1.27×10^4 |
| 5 | 2.02×10^{-3} | 0.047 | 6.48×10^{-7} | 1.20×10^4 |

$$K_{\text{av}}(20 \text{ °C}) = 1.36 \times 10^4 \text{ L mol}^{-1}$$

Table 9.23. Determination of the equilibrium constant for the reaction of $(\text{mpa})_2\text{CH}^+$ and **17** ($\epsilon[(\text{mpa})_2\text{CH}^+$ at 622 nm] = $1.41 \times 10^5 \text{ M}^{-1} \text{ cm}^{-1}$ and $d = 0.5 \text{ cm}$, CH_2Cl_2 at 20.0 °C).

| Entry | [17] ₀ (mol L ⁻¹) | <i>A</i> | $[(\text{mpa})_2\text{CH}^+]_{\text{eq}}$ (mol L ⁻¹) | <i>K</i> (L mol ⁻¹) |
|-------|---|----------|--|---------------------------------|
| 0 | 0 | 0.783 | 1.11×10^{-5} | |
| 1 | 1.31×10^{-4} | 0.558 | 7.91×10^{-6} | 3.15×10^3 |
| 2 | 2.61×10^{-4} | 0.500 | 7.09×10^{-6} | 2.20×10^3 |
| 3 | 3.92×10^{-4} | 0.442 | 6.27×10^{-6} | 1.99×10^3 |
| 4 | 5.66×10^{-4} | 0.375 | 5.32×10^{-6} | 1.94×10^3 |
| 5 | 6.97×10^{-4} | 0.259 | 3.67×10^{-6} | 2.93×10^3 |

$$K_{\text{av}}(20 \text{ °C}) = 2.45 \times 10^3 \text{ L mol}^{-1}$$

9.5 References

- [1] For an excellent review, see: S. E. Denmark, G. L. Beutner, *Angew. Chem.* **2008**, *120*, 1584–1663; *Angew. Chem. Int. Ed.* **2008**, *47*, 1560–1638.
- [2] a) V. Lutz, J. Glatthaar, C. Würtele, M. Serafin, H. Hausmann, P. R. Schreiner, *Chem. Eur. J.* **2009**, *15*, 8548–8557; b) For mechanistic interpretations, see: S. Xu, I. Held, B. Kempf, H. Mayr, W. Steglich, H. Zipse, *Chem. Eur. J.* **2005**, *11*, 4751–4757; c) A. C. Spivey, S. Arseniyadis, *Angew. Chem.* **2004**, *116*, 552–557; *Angew. Chem. Int. Ed.* **2004**, *43*, 5436–5441; d) R. Murugan, E. F. V. Scriven, *Aldrichimica Acta* **2003**, *36*, 21–27; e) G. Höfle, W. Steglich, A. Vorbrüggen, *Angew. Chem.* **1978**, *90*, 602–615; *Angew. Chem. Int. Ed. Engl.* **1978**, *17*, 569–583.

- [3] For a select example, see: K. A. Connors, N. K. Pandit, *Anal. Chem.* **1978**, *50*, 1542–1545.
- [4] For select examples, see: a) J. E. Taylor, M. D. Jones, J. M. J. Williams, S. D. Bull, *Org. Lett.* **2010**, *12*, 5740–5743; b) C. Larrivéé-Aboussafy, B. P. Jones, K. E. Price, M. A. Hardink, R. W. McLaughlin, B. M. Lillie, J. M. Hawkins, R. Vaidyanathan, *Org. Lett.* **2010**, *12*, 324–327; c) K. E. Price, C. Larrivéé-Aboussafy, B. M. Lillie, R. W. McLaughlin, J. Mustakis, K. W. Hettenbach, J. M. Hawkins, R. Vaidyanathan, *Org. Lett.* **2009**, *11*, 2003–2006; d) W. Zhang, M. Shi, *Org. Biomol. Chem.* **2006**, *4*, 1671–1674; e) B. G. G. Lohmeijer, R. C. Pratt, F. Leibfarth, J. W. Logan, D. A. Long, A. P. Dove, F. Nederberg, J. Choi, C. Wade, R. M. Waymouth, J. L. Hedrick, *Macromolecules* **2006**, *39*, 8574–8583; f) W.-C. Shieh, S. Dell, O. Repic, *J. Org. Chem.* **2002**, *67*, 2188–2191.
- [5] a) V. B. Birman, X. Li, H. Jiang, E. W. Uffman, *Tetrahedron* **2006**, *62*, 285–294; b) V. B. Birman, H. Jiang, *Org. Lett.* **2005**, *7*, 3445–3447; c) V. B. Birman, E. W. Uffman, H. Jiang, X. Li, C. J. Kilbane, *J. Am. Chem. Soc.* **2004**, *126*, 12226–12227.
- [6] M. Kobayashi, S. Okamoto, *Tetrahedron Lett.* **2006**, *47*, 4347–4350.
- [7] V. B. Birman, X. Li, Z. Han, *Org. Lett.* **2007**, *9*, 37–40.
- [8] a) P. A. Woods, L. C. Morrill, T. Lebl, A. M. Z. Slawin, R. A. Bragg, A. D. Smith, *Org. Lett.* **2010**, *12*, 2660–2663; b) C. Joannesse, C. Simal, C. Concellón, J. E. Thomson, C. D. Campbell, A. M. Z. Slawin, A. D. Smith, *Org. Biomol. Chem.* **2008**, *6*, 2900–2907.
- [9] V. B. Birman, X. Li, *Org. Lett.* **2006**, *8*, 1351–1354.
- [10] For kinetic resolutions using anhydrides as acylating agents, see reference 9 and: a) Q. Xu, H. Zhou, X. Geng, P. Chen, *Tetrahedron*, **2009**, *65*, 2232–2238; b) X. Yang, V. B. Birman, *Adv. Synth. Catal.* **2009**, *351*, 2301–2304; c) V. B. Birman, X. Li, *Org. Lett.* **2008**, *10*, 1115–1118; d) V. B. Birman, H. Jiang, X. Li, V. Geo, E. W. Uffman, *J. Am. Chem. Soc.* **2006**, *128*, 6536–6537; e) V. B. Birman, L. Geo, *Org. Lett.* **2006**, *8*, 4859–4861; For kinetic resolutions using carboxylic acids as acylating agents utilizing in situ formation of a reactive mixed anhydride, see: f) I. Shiina, K. Ono, K. Nakata, *Chem. Lett.* **2011**, *40*, 147–149.; g) I. Shiina, K. Nakata, K. Ono, M. Sugimoto, A. Sekiguchi, *Chem. Eur. J.* **2010**, *16*, 167–172; h) I. Shiina, K. Nakata, *Heterocycles* **2010**, *80*, 169–175; i) K. Nakata, Y. Onda, K. Ono, I. Shiina, *Tetrahedron Lett.* **2010**, *51*, 5666–5669; j) I. Shiina, K. Nakata, M. Sugimoto, Y. Onda, T. Iizumi, K. Ono, *Heterocycles* **2009**, *77*, 801–810; k) I. Shiina, K. Nakata, *Tetrahedron Lett.* **2007**, *48*, 8314–8317; l) I.

- Shiina, K. Nakata, Y. Onda, *Eur. J. Org. Chem.* **2008**, 5887–5890; m) X. Yang, V. B. Birman, *Adv. Synth. Catal.* 2009, 351, 2301–2304;
- [11] V. B. Birman, H. Jiang, X. Li, *Org. Lett.* **2007**, 9, 3237–3240.
- [12] J. A. Kalow, A. G. Doyle, *J. Am. Chem. Soc.* **2010**, 132, 3268–3269.
- [13] X. Yang, G. Lu, V. B. Birman, *Org. Lett.* **2010**, 12, 892–895.
- [14] a) D. Belmessieri, L. C. Morrill, C. Simal, A. M. Z. Slawin, A. D. Smith, *J. Am. Chem. Soc.* **2011**, 133, 2714–2720; b) C. A. Leverett, V. C. Purohit, D. Romo, *Angew. Chem.* **2010**, 122, 9669–9673; *Angew. Chem. Int. Ed.* **2010**, 49, 9479–9483; c) V. C. Purohit, A. S. Matla, D. Romo, *J. Am. Chem. Soc.* **2008**, 130, 10478–10479. For other Lewis base mediated reactions utilizing carboxylic acids as ammonium enolate precursors, see: d) H. Nguyen, G. Ma, T. Gladysheva, T. Fremgen, D. Romo, *J. Org. Chem.* **2011**, 76, 2–12; e) H. Nguyen, G. Ma, D. Romo, *Chem. Commun.* **2010**, 46, 4803–4805; f) K. A. Morris, K. M. Arendt, S. H. Oh, D. Romo, *Org. Lett.* **2010**, 12, 3764–3767; g) G. Ma, H. Nguyen, D. Romo, *Org. Lett.* **2007**, 9, 2143–2146; h) H. Henry-Riyad, C. Lee, V. C. Purohit, D. Romo, *Org. Lett.* **2006**, 8, 4363–4366; i) S. H. Oh, G. S. Cortez, D. Romo, *J. Org. Chem.* **2005**, 70, 2835–2838; j) G. S. Cortez, R. L. Tennyson, D. Romo, *J. Am. Chem. Soc.* **2001**, 123, 7945–7946; k) G. S. Cortez, S. H. Oh, D. Romo, *Synthesis* **2001**, 1731–1736.
- [15] C. Joannesse, C. P. Johnston, C. Concellón, C. Simal, D. Philp, A. D. Smith, *Angew. Chem.* 2009, 121, 9076–9080; *Angew. Chem. Int. Ed.* **2009**, 48, 8914–8918.
- [16] a) S. A. Shaw, P. Aleman, J. Christy, J. W. Kampf, P. Va, E. Vedejs, *J. Am. Chem. Soc.* **2006**, 128, 925–934; b) H. V. Nguyen, D. C. D. Butler, C. J. Richards, *Org. Lett.* **2006**, 8, 769–772; c) G. C. Fu, *Acc. Chem. Res.* **2004**, 37, 542–547; d) S. A. Shaw, P. Aleman, E. Vedejs, *J. Am. Chem. Soc.* **2003**, 125, 13368–13369; e) G. C. Fu, *Acc. Chem. Res.* **2000**, 33, 412–420;
- [17] Y. Zhang, V. B. Birman, *Adv. Synth. Catal.* 2009, 351, 2525–2529.
- [18] D. Belmessieri, C. Joannesse, P. A. Woods, C. MacGregor, C. Jones, C. D. Campbell, C. P. Johnston, N. Duguet, C. Concellón, R. A. Bragg, A. D. Smith, *Org. Biomol. Chem.* 2011, 9, 559–570.
- [19] Reviews on nucleophilicities: a) H. Mayr, A. R. Ofial, *J. Phys. Org. Chem.* **2008**, 21, 584–595; b) H. Mayr, A. R. Ofial, *Pure Appl. Chem.* **2005**, 77, 1807–1821; c) H. Mayr, B. Kempf, A. R. Ofial, *Acc. Chem. Res.* **2003**, 36, 66–77; d) H. Mayr, T. Bug, M. F. Gotta, N. Hering, B. Irrgang, B. Janker, B. Kempf, R. Loos, A. R. Ofial, G.

- Remennikov, H. Schimmel, *J. Am. Chem. Soc.* **2001**, *123*, 9500–9512; e) For a comprehensive listing of nucleophilicity and electrophilicity parameters, see: <http://www.cup.uni-muenchen.de/oc/mayr/DBintro.html>.
- [20] For pyridines, see: a) N. De Rycke, G. Berionni, F. Couty, H. Mayr, R. Goumont, O. R. P. David, *Org. Lett.* **2011**, *13*, 530–533; b) F. Brotzel, B. Kempf, T. Singer, H. Zipse, H. Mayr, *Chem. Eur. J.* **2007**, *13*, 336–345. For azoles, see: c) M. Baidya, F. Brotzel, H. Mayr, *Org. Biomol. Chem.* **2010**, *8*, 1929–1935. For PPh₃, see: d) B. Kempf, H. Mayr, *Chem. Eur. J.* **2005**, *11*, 917–927. For DBU and DBN, see: e) M. Baidya, H. Mayr, *Chem. Commun.* **2008**, 1792–1794. For DABCO, see: f) M. Baidya, S. Kobayashi, F. Brotzel, U. Schmidhammer, E. Riedle, H. Mayr, *Angew. Chem.* **2007**, *119*, 6288–6292; *Angew. Chem. Int. Ed.* **2007**, *46*, 6176–6179.
- [21] J. Vana, M. Sedlak, J. Hanusek, *J. Org. Chem.* **2010**, *75*, 3729–3736 and references therein.
- [22] a) W. J. Albery, *Annu. Rev. Phys. Chem.* **1980**, *31*, 227–263; b) R. A. Marcus, *J. Phys. Chem.* **1968**, *72*, 891–899.
- [23] H. F. Schaller, A. A. Tishkov, X. Feng, H. Mayr, *J. Am. Chem. Soc.* **2008**, *130*, 3012–3022.
- [24] N. Streidl, B. Denegri, O. Kronja, H. Mayr, *Acc. Chem. Res.* **2010**, *43*, 1537–1549.